

Genetic factors in the autoimmune disease multiple sclerosis

Inaugural-Dissertation

zur
Erlangung des Doktorgrades der
Mathematisch-Naturwissenschaftlichen Fakultät
der Heinrich-Heine-Universität Düsseldorf

vorgelegt von

Robert Goertsches

aus Leverkusen

Januar 2006

Aus dem Institut für Genetik
der Heinrich-Heine Universität Düsseldorf

Gedruckt mit der Genehmigung der
Mathematisch-Naturwissenschaftlichen Fakultät der
Heinrich-Heine-Universität Düsseldorf

Referent: Prof. Dr. E. Knust
Koreferent: PD Dr. M. Beye
Tag der mündlichen Prüfung: 20.04.2006

"Founded on acquired knowledge, a satisfying accomplishment manifest itself almost effortlessly, . . .

however; only whoever has endured in the dark suspecting search, year after year, constantly swaying between conficende and despair, followed by the final breakthrough to the truth, can fully empathize."

A. Einstein

"Im Lichte bereits erlangter Erkenntnis erscheint das glücklich Erreichte fast wie selbstverständlich, . . .

aber das ahnungsvolle, Jahre währende Suchen im Dunkeln mit seiner Abwechslung von Zuversicht und Ermattung und seinem endlichen Durchbrechen zur Wahrheit, das kennt nur, wer es selber erlebt hat."

Acknowledgement

I want to express my thanks to the following persons without whom this work would have been impossible to initiate, manage and complete.

I thank very much the person without whom I never would have gotten into this adventure in the first place, Pablo Villoslada, former member of the UNIC, Barcelona, and now investigating neurologist in Pamplona, at the Neuroimmunology department of the University of Navarra, Spain.

I shall furthermore express my deepest gratitude to Xavier Monatalban and his team of the UNIC, exemplary stating close colleagues and friends such as the always good mooded technician Mireia, the mighty informative, multilingual and cohering manager Josep Graells and his colleague Dunja, the living football bibles Carlos and Hector, the capable blood-drawing nurses Rosalia and Maria Jesus, Hammad, Christina, Montse, Eva, and in particular, for scientific advices and vivid discussions extending basic research, Manolo Comabella. All further members of the department that have not been named here, are thanked as well.

I thank Armand Sanchez from the Department of Animal and Food Science, University Autonoma of Barcelona, for providing me with appropriate tools for DNA quantitations, DNA pool construction and quality testing.

Special thanks goes to the company deCODE in Reykjavik, who showed great hospitality scientificwise (providing with the in-house genetic map) and on the personal level (3 months of teaching genetics and still icelandic friendliness), particularly Aslaug Jonasdottir, Ragnaheidur Fosdal, Theodora Thorlacius, and Jeff Gulcher.

Furthermore I would like to express profound thanks to Jaume Bertranpetit and Arcadi Navarro from the Evolutionary biology department of the University Pompeu Fabra, Barcelona, for regular invitations to genetic meetings and providing access to their high-throughput genotyping facilities (thank you as well, Roger and Anna).

I thank Alastair Compston and Stephen Sawcer, Cambridge (UK), for creating GAMES and for being of scientific help long after.

I thank Sergio Baranzini and Jorge Oksenberg from University of California San Francisco (USA), for proof-reading the dissertation and counselling on genetic questions.

I thank very much my supervisor Elisabeth Knust for her patience and interest in my research field that does not overlap exceedingly well with cell polarity in *Drosophila*. I direct the same to Martin Beye who was so kind in accepting to be co-referee of this dissertation.

I deeply thank my parents Elaine and Klaus for being a constant and sensitive support all through my scientific life, and before!

Finally and above all, I thank my dearest wife Verena, who managed to perform a multitude of important deeds: encouraging throughout this devoted long time, counselling on dissertation design, and - most important – giving birth to our daughter Emily, who I also thank for cheering me up endlessly.

Die hier vorgelegte Dissertation habe ich eigenständig und ohne unerlaubte Hilfe angefertigt. Die Dissertation wurde in der vorgelegten oder in ähnlicher Form noch bei keiner anderen Institution eingereicht. Ich habe bisher keine erfolglosen Promotionsversuche unternommen.

Düsseldorf, den 19.01.2006

(Robert Goertsches)

1 Introduction	1-22
1.1 Autoimmunity	2
1.1.1 Autoimmune disease (AID)	2
1.2 Autoimmune disease multiple sclerosis (MS)	3
1.2.1 Clinical aspects of MS	3
1.2.2 Pathological heterogeneity of MS	5
1.2.3 Immunological heterogeneity of MS	6
1.3 Genetic factors in autoimmune disease	8
1.3.1 Simple genetic traits associated with autoimmunity	8
1.3.2 Genetics of common autoimmune diseases	10
1.3.3 Genetic heterogeneity in autoimmune diseases	10
1.4 Epistatic interaction in complex traits	11
1.5 Model of inheritance of autoimmune disease susceptibility	12
1.6 Common genetic variation in the human genome and their genetic markers	13
1.7 Concept of “Linkage Disequilibrium” and “Haplotype”	14
1.8 Basic approaches toward disease gene identification	16
1.8.1 Identifying disease genes in MS	17
1.8.2 Linkage analysis in MS	18
1.8.3 Association analysis in MS	18
1.9 Genetic heterogeneity, inheritance model and susceptibility genes in MS	18
1.9.1 A model of inheritance for MS	18
1.9.2 The (genetic) epidemiology and etiology of MS	20
1.10 Aim and content of the dissertation	21
2 Material & Methods	23-62
2.1 Genomic DNA extraction from peripheral blood	24
2.2 Determination of DNA concentration and quality	26
2.3 DNA pool construction based on fluorescence quantitation	26
2.3.1 Calibration of TKO 100 Mini-Fluorometer by means of calf thymus DNA	28
2.3.2 DNA sample preparation, quantification and appropriate dilution	29
2.3.3 DNA pool construction	29

2.4 DNA pool genotyping by means of microsatellite markers	30
2.4.1 Storage and preparation of reagents for PCR assay	31
2.4.2 Polymerase amplification and thermal cycling	32
2.4.3 Gel electrophoresis of PCR products	33
2.5 Analysis of microsatellite marker genotyped DNA pools	34
2.5.1 Processing of data	34
2.5.2 Analysis of STR-genotyped DNA pools applying the Single Peak Approach	35
2.6 A sliding-window method for the detection of clusters of markers displaying evidence for association with MS	39
2.6.1 Processing of data	39
2.6.2 Analysis of STR-Genotyped DNA pool data by sliding windows	40
2.7 SNP-Genotyping principle: the 5' Nuclease assay	43
2.7.1 Concepts of 5' Nuclease and Allelic Discrimination Assay	43
2.7.2 Preparation of DNA dilutions for PCR assays: 96- and 384-well plates	45
2.7.3 Preparation of reaction solution for PCR assay	47
2.7.4 Polymerase amplification and thermal cycling and end-point analysis	48
2.8 MS patients and controls	50
2.9 SNP selection for two genomic regions of interest	50
2.10 SNP-Genotyping data handling	53
2.10.1 Allelic discrimination	53
2.10.2 Real-time amplification data	54
2.11 Analytical tools for describing genomic structure and detecting disease association	57
2.11.1 Descriptive analyses	57
2.11.1.1 Establishing Hardy-Weinberg equilibrium (HWE) in population samples	57
2.11.1.2 Linkage Disequilibrium (LD) determination by software Haplovview	58

2.11.2 Case-control association analyses	58
2.11.2.1 Single SNP-disease association analyses	58
2.11.2.2 Haplotype-disease association analyses	59
2.12 Accounting for multiple testing	61

3 Results **63-102**

3.1 Genotyping of DNA Pools with microsatellite markers	64
3.2 Application of sliding windows on DNA pool data	66
3.2.1 Descriptive part	66
3.2.2 Sieving MS candidate regions and genes	71
3.3 Genotyping of individual DNA by means of single nucleotide polymorphism marker	79
3.3.1 Yield of applied 5' Nuclease assay	79
3.3.2 Hardy-Weinberg equilibrium (HWE) in healthy control and multiple sclerosis population samples	81
3.3.3 Linkage Disequilibrium block formation at genomic regions of interest 3p25.3 and 10q22.1	81
3.3.4 Detection of statistical significance derived from allele and single genotype comparisons	84
3.3.5 Correction for multiple testing through Sequential Bonferroni	88
3.4 Single gene inspection: haplotype analysis	89
3.4.1 <i>VGLL4</i> - Transcription cofactor vestigial-like protein	90
3.4.2 <i>PRF1</i> – Perforin	91
3.4.3 <i>ADAMTS14</i> - a disintegrin-like and metalloproteinase domain with thrombospondin type 1 modules 14	92
3.4.4 <i>C10orf27</i> – Chromosome 10 open reading frame 27	96
3.5 Combined gene haplotypes based on ascertained data of <i>ADAMTS14</i> and <i>C10orf27</i>	99

4 Discussion **103-122**

4.1 A whole genome screen employing microsatellite markers and pooled DNA	104
4.2 284 candidate genes detected by “Sliding windows”	107
4.3 3p25.2: <i>Apg7l</i> and <i>VglI4</i>	110
4.4 10q22.1: <i>Perforin</i>, <i>ADAMTS14</i> and <i>C10orf27</i>	111
4.4.1 10q22.1: Intergenic haplotypes <i>ADAMTS14</i> and <i>C10orf27</i>	115
4.5 Pros and Cons on association study design	116
4.5.1 Pros of association studies	116
4.5.2 Cons of association studies	117
4.6 Multiple testing and epistasis	119
4.7 Conclusion and outlook	120

5 Summary **123-124****6 Reference List** **125-146****7 Appendix** **147-280**

Appendix A	
STR-Genotyping of individual DNA samples	148
Appendix B	
STR genotyping data from DNA pools	167
Appendix C	
Sliding window plots and synoptical tables	197
Appendix D	
Genes of interest derived from sliding windows	245
Appendix E	
Allele and genotype frequency distributions and corresponding statistics	249
Appendix F	
Haplotype and haplotype pair frequency distributions and corresponding statistics	259

Abbreviations

°C	degree Celsius
aa (Aa)	amino acids
bp	base pairs
kb	kilobases (kilo base pairs)
cM	centiMorgan
OD	Optical Density
ON	Over night
pH	Proton concentration
rpm	rounds per minute
RT	Room temperature
min	Minutes
s	Seconds
µl	Microliter
ml	Millilitre
M	Molar
PBL	Peripheral Blood Leukocytes
DNA	Deoxyribonucleic acid
RNA	Ribonucleic acid
SNP	Single Nucleotide Polymorphism
STR	Short tandem repeat
PCR	Polymerase chain reaction
AIP	Allele image profile
MHC	Major histocompatibility complex
HLA	Human Leukocyte Antigen
MS	Multiple Sclerosis
HC	Healthy Control
RRMS	Relapsing remitting multiple sclerosis
SPMS	Secondary progressive multiple sclerosis
PPMS	Primary progressive multiple sclerosis
EDSS	Expanded Disability Status Scale
Simplex family	One affected individual per family
Multiplex family	More than one affected individual per family
LOD	Base ₁₀ logarithm of the likelihood of the odds ratio for linkage
NPL	Non-parametric linkage
TDT-Test	Transmission disequilibrium test
SD	Standard deviation
OR	Odds ratio
CI	Confidence Interval

1

INTRODUCTION

1.1 Autoimmunity	2
1.1.1 Autoimmune disease (AID)	2
1.2 Autoimmune disease multiple sclerosis (MS)	3
1.2.1 Clinical aspects of MS	3
1.2.2 Pathological heterogeneity of MS	5
1.2.3 Immunological heterogeneity of MS	6
1.3 Genetic factors in autoimmune disease	8
1.3.1 Simple genetic traits associated with autoimmunity	8
1.3.2 Genetics of common autoimmune diseases	10
1.3.3 Genetic heterogeneity in autoimmune diseases	10
1.4 Epistatic interaction in complex traits	11
1.5 Model of inheritance of autoimmune disease susceptibility	12
1.6 Common genetic variation in the human genome and their genetic markers	13
1.7 Concept of “Linkage Disequilibrium” and “Haplotype”	14
1.8 Basic approaches toward disease gene identification	16
1.8.1 Identifying disease genes in MS	17
1.8.2 Linkage analysis in MS	18
1.8.3 Association analysis in MS	18
1.9 Genetic heterogeneity, inheritance model and susceptibility genes in MS	18
1.9.1 A model of inheritance for MS	18
1.9.2 The (genetic) epidemiology and etiology of MS	20
1.10 Aim and content of the dissertation	21

1.1 Autoimmunity

The main function of the immune system is to distinguish foreign antigens, such as infectious agents, from self components of body tissues. Hence, an immunological self tolerance that reliably discriminates between self and non-self antigens is required to be established and maintained. This is realized during stages of immune system maturation through clonal deletion of autoreactive T lymphocytes in the thymus (central tolerance) and the inhibition of autoreactive T and B lymphocytes in the systemic circulation (peripheral tolerance).^{1,2} Regulatory mechanisms that fulfil disclosed surveillance include the induction of anergy, apoptosis and functional suppression, but are not constantly engaged. This implies that self reactive T and B lymphocytes are present in normal, healthy individuals and, under certain conditions, are capable of producing an autoimmune response.³

Whenever dysfunctions occur in the maintenance of the immunological tolerance to self antigens, pathogenic alterations in the immune system can lead to the manifestation of autoreactive phenomena. Several impaired situations convey an autoimmune response characterized by the activation and clonal expansion of autoreactive lymphocytes and the production of autoantibodies against autologous antigens. Thereby triggered cascades lead to an inflammatory process and tissue injury.³

1.1.1 Autoimmune disease (AID)

It is estimated that autoimmune diseases (AID) occur in 3–5% of the world population^{4–6} and are major causes of morbidity and mortality, thus rendering autoimmunity a crucial health problem in modern medicine. Many of these diseases tend to be difficult or impossible to cure, for the obvious reason that the focus of the immune response – self antigens – cannot be eliminated. Furthermore, the physical, psychological and economic burden is especially devastating because they often set upon young adults.⁶

Autoimmune disease is considered to be the result of a complex combination of genetic and environmental factors that lead to altered immune reactivity.^{5,7,8} Given the complexity of such disorders, no single genetic or environmental factor is expected to be necessary or sufficient to cause the diseases.⁹ Hence, the realization that the development of autoimmunity is in part influenced by inherited DNA sequence variations conveys confidence that understanding the genetics of autoimmune diseases will elucidate about the causal derangements, and possibly lead to new therapeutic strategies.

1.2 Autoimmune disease multiple sclerosis (MS)

Multiple sclerosis (MS) is a chronic autoimmune disease of the central nervous system (CNS) that culminates in neurodegeneration.¹⁰⁻¹³ Among other autoimmune diseases it displays a moderate prevalence rate, but furthermore, a constantly rising degree of incidence.^{6,14,15} MS exhibits several characteristics of a multifactorial etiology common to autoimmune disorders - clinically, pathologically, immunologically and genetically, including polygenic inheritance,¹⁶ partial susceptibility conferred by a human leukocyte antigen (HLA)-associated haplotype,¹⁷ and evidence of undefined environmental exposures.^{18,19}

1.2.1 Clinical aspects of MS

MS is an inflammatory disorder characterized by demyelination (myelin loss) within the CNS. As the name implies, affected individuals exhibit hardened (or "sclerotic") tissue in many (or "multiple") parts of the brain and the spinal cord. Demyelination and the resulting formation of scar tissue (axonal pathology) impair the saltatory conduction along axons which is essential for normal functioning of nerve impulses.

Although the disease has a broad range of age at onset (85% of cases occur between the ages of 14 and 55),²⁰ initial symptoms typically manifest in early adulthood (between ages 20 and 40). MS occurs two to three times more frequently in women than men.^{6,20,21} Common symptoms include visual disturbance, loss of balance and coordination, weakness and spasticity, sensory disturbances and pain, bladder and bowel incontinence, fatigue, and cognitive impairment. MS is a clinically heterogeneous disease that varies according to the location and number of lesions in the CNS and several other (para)-clinical parameter (e.g. cerebrospinal fluid, motor neuron evoked potentials). Histopathological studies of lesions suggests that MS is an overlapping spectrum of related disorders (Tab.1.1).²²⁻²⁴

Table 1.1 | Classifications of supposed multiple sclerosis "subtypes".

Clinical course definitions	Clinically Isolated Syndrome (CIS)	McDonald <i>et al.</i> 2001 ²⁵ Miller <i>et al.</i> 2005 ²⁶
	Relapsing remitting (RRMS) / Secondary progressive (SPMS)	Lublin <i>et al.</i> 1996 ²⁷
	Transitional progressive (TPMS)	Thompson <i>et al.</i> 1997 ²⁸ Stevenson <i>et al.</i> 1999 ²⁹
	Progressive-relapsing (PRMS)	Weinshenker <i>et al.</i> 1995 ³⁰ Lublin <i>et al.</i> 1996 ²⁷
	Primary progressive (PPMS)	Revesz <i>et al.</i> 1994 ³¹ Lublin <i>et al.</i> 1996 ²⁷ Thompson <i>et al.</i> 1997 ²⁸
MS variants/ Borderline forms	Acute Disseminated Encephalomyelitis (ADEM)	Dale <i>et al.</i> 2000 ³² Hartung <i>et al.</i> 2001 ³³
	Baló's concentric inflammatory sclerosis	Baló J, 1927 ³⁴
	Schilder's diffuse inflammatory sclerosis	Schilder PF, 1912 ³⁵
	Optic neuromyelitis (Devic's disease, NMO)	Devic E, 1894 ³⁶
	Marburg's disease	Marburg O, 1906 ³⁷
Clinical severity/ Prognosis	"Benign" MS	Kidd D, 1994 ³⁸
	"Malignant" MS	Marburg O, 1906 ³⁷

The disease course varies considerably among affected individuals. Cases may be episodic or progressive, severe or mild, and disseminated or primarily affecting the spinal cord and optic nerve (Tab. 1.1). The two major subtypes are relapsing remitting (RRMS) and primary progressive MS (PPMS). The relapsing remitting course is more common, characterized by two or more separate episodes of worsening symptoms (recurrent attacks) and subsequent clinical recovery. As the disease progresses, many relapsing remitting cases cease to remit and exhibit progression of at least one symptom in a slow or step-wise manner. This form of the disease is referred to as secondary progressive MS (SPMS) (Fig.1.1).

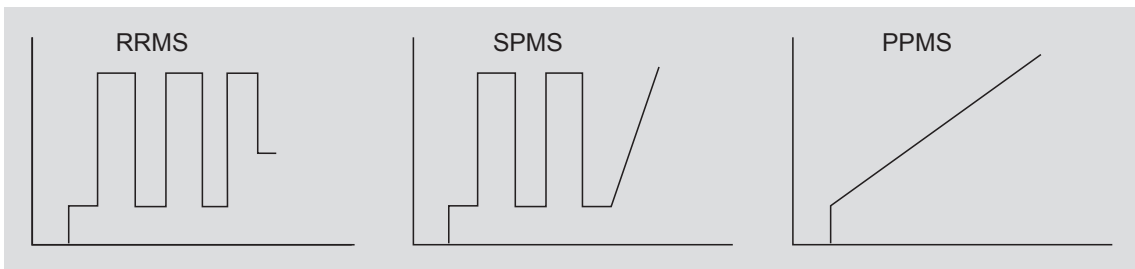


Figure 1.1 | Main clinical courses of multiple sclerosis. Ordinate represents the degree of disability (EDSS); abscissa determines the time; RRMS – relapsing remitting multiple sclerosis, SPMS – secondary progressive multiple sclerosis, PPMS – primary progressive multiple sclerosis (adapted from Lublin *et al.* 1996).

The second major subtype, primary progressive MS, is a less common form characterized by a slow onset and steadily worsening symptoms involving sites of the CNS that do not remit from initial onset. Intermediate phenotypes, such as transitional progressive (TPMS) and progressively relapsing (PRMS), are also common (Tab. 1.1).

As outlined, MS presents a vast range of different symptomatologies and courses, nevertheless, it has been considered as one disease. Hence, a difficulty in establishing a homogenous patients cohort is the differential diagnosis of MS from a number of similar inflammatory demyelinating CNS diseases. The incorrect inclusion of individuals that succumb to a disease outlined in the two lower parts of Table 1.1 would incorporate a strong bias and thus complicate clinical inferences made upon research results.

1.2.2 Pathological heterogeneity of MS

General examination of brain tissue of individuals with MS reveals multiple sharply demarcated plaques in the CNS white matter with a predisposition to the optic nerves and white matter tracts of the periventricular regions, brain stem, and spinal cord.³⁹ As it was recognized early on, substantial axonal injury with axonal transections is abundant throughout active MS lesions.⁴⁰

The inflammatory cell profile of active lesions is characterized by perivascular infiltration of oligoclonal T cells consisting of CD4⁺/CD8⁺ α/β ^{41,42} and γ/δ T cells,⁴³ as well as monocytes with occasional B cells and less frequently plasma cells.⁴⁴ Macrophages are most prominent in the center of the plaques and are seen to contain myelin debris, while oligodendrocyte counts are reduced. Four pathological categories of the disease were defined on the basis of myelin protein loss, the geography and extension of plaques, the patterns of oligodendrocyte destruction, and the immunopathological evidence of complement activation. Two patterns (I and II) showed close similarities to T cell-

mediated or T cell plus antibody- mediated autoimmune encephalomyelitis, respectively. The other patterns (III and IV) were highly suggestive of a vasculopathy or primary oligodendrocyte dystrophy, reminiscent of virus- or toxin-induced demyelination rather than autoimmunity (Fig. 1.2).^{24,45,46}

1.2.3 Immunological heterogeneity of MS

The concepts of MS pathogenesis have been adapted continuously by various research groups.^{10-12,47-49} Although unproven, the current consensus is that MS pathogenesis comprises an initial inflammatory phase, which fulfils the criteria for an autoimmune disease,⁵⁰ followed by a phase of selective demyelination and finally, a neurodegenerative and occasionally in parallel a neuroregenerative phase.^{10,51} Different cells and molecules suggested to be involved in MS are summarized in Figure 1.2. Subjects with genetically determined susceptibility to MS harbor autoreactive T cells that respond more readily to CNS autoantigens.⁵²⁻⁵⁵ Although these can remain dormant for decades, at some point they are activated in the periphery, probably by an exogenous trigger displaying molecular mimicry (e.g. sharing of epitopes that are common to autoantigens and microbial antigens).^{56,57} The pathological activation and clonal expansion of autoreactive T cells is further promoted by underlying immunoregulatory defects, such as decreases of regulatory T cells in the systemic circulation.⁵⁸ It enables activated T cells to migrate through the blood-brain barrier (BBB) to the brain and spinal cord. Reactivated in the CNS, these T cells of either CD4⁺ helper or CD8⁺ cytotoxic phenotype⁵⁹ release pro-inflammatory Th1 cytokines and orchestrate the destruction of the myelin sheath by various types of immune effector cells. Demyelination leads to vulnerable axons that develop altered membrane permeability (Na⁺ and Ca⁺⁺ channels) and increased accessibility for CD8⁺ T cytotoxic cells. Finally, loss of trophic support contributes to the enhanced liability of axon degeneration, which culminates in irreversible axonal loss.⁶⁰ Subsequently, heterogeneous patterns for neurodegeneration can be manifested by a multitude of deregulated elements.

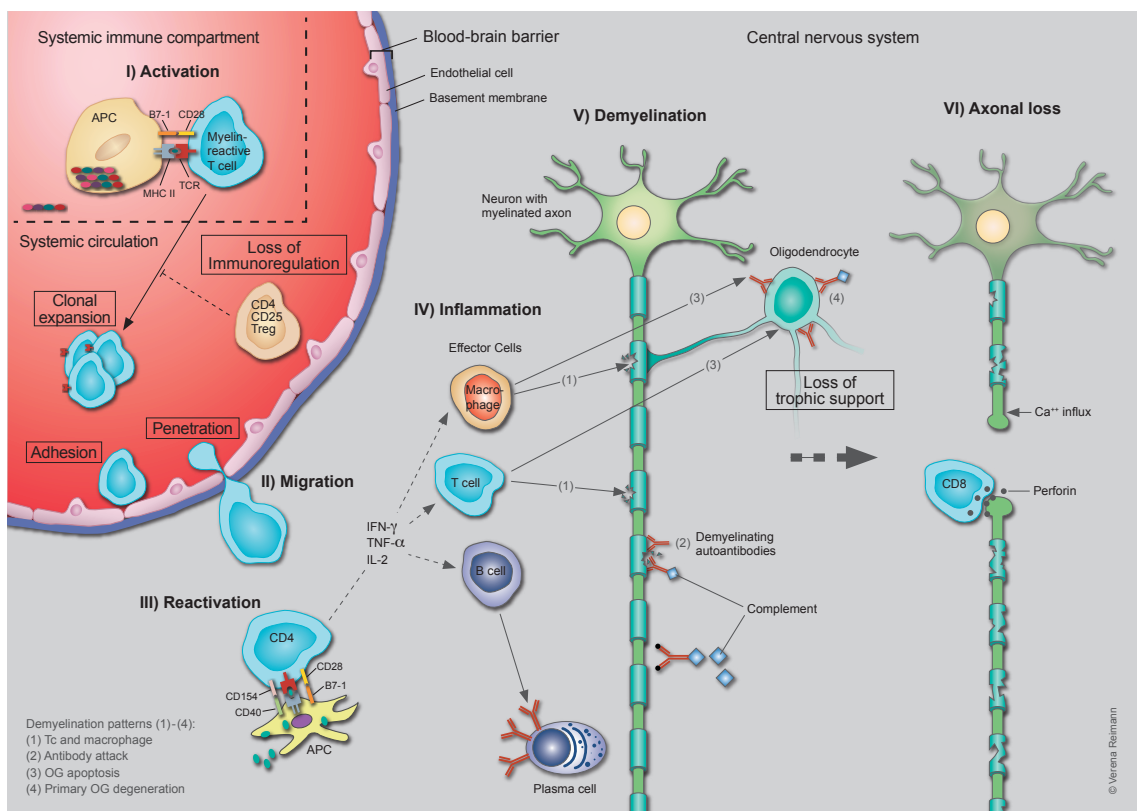


Figure 1.2 | Hypothetical view of mechanisms leading to MS pathogenesis. (I) In a genetically susceptible host, common microbe activated antigen presenting cells (APCs) (Macrophages) contain processed protein sequences cross-reactive with self myelin antigens. In lymphoid organs, peripheral pro-inflammatory T cells, reactive for CNS-myelin, are activated when binding via their T-cell receptor (TCR) to the self-antigen, presented by the major histocompatibility complex class II (MHC II). (II) Activated myelin-reactive T cells undergo clonal expansion profiting from a loss of functional suppression by CD4⁺CD25⁺ regulatory T cells and adhere at and penetrate through the blood–brain barrier (BBB). Stages of transendothelial migration are mediated by adhesion molecules, proteases and chemokines. (III) In the CNS, the T cells recognise antigen presented predominantly by activated microglia, CNS-specific APCs, hence are reactivated. Th1 cytokines (pro-inflammatory), such as Interferon- γ (IFN- γ), Interleukin-2 (IL-2) or Tumor necrosis factor- α (TNF- α), are secreted and an inflammatory cascade is initiated. (IV) Activated macrophages, other T cell types and B cells execute various effector functions including direct attack on the myelin sheaths of axons and the myelin-fabricating oligodendrocytes (OGs). Inflammatory B cells differentiate into plasma cells that secrete demyelinating autoantibodies, which can guide and activate macrophages and additionally ignite the complement cascade. (V)+(VI) Axonal damage takes place as a consequence of extensive demyelination and loss of trophic support. Exposed axons display increased altered permeability followed by enhanced Ca⁺⁺ influx. Disruption of axonal transport alters the cytoskeleton and leads to axonal swelling, lobulation and, finally, disconnection. Demyelination can occur by four different pathological patterns (1–4), as described in the main text.

1.3 Genetic factors in autoimmune disease

In order to determine the evidence of genetic factors in the disease susceptibility, epidemiologists perform population- and family-based studies. Essential tools are surveys that assess population prevalence, recurrence risk, and migration analyses. When carrying out population genetics studies, groups of unrelated individuals afflicted with disease are compared with healthy individuals or persons affected by a distinct disease. In terms of family-based studies, simplex and multiplex families are subject to examinations of the extent of familial clustering (aggregation); the degree to which monozygotic twins are more concordant for the presence of a disease compared with dizygotic twins, and the increased risk that family members of a diseased person will develop same condition compared to an individual from the general population. Such estimate of genetic risk is designated λ_s .

1.3.1 Simple genetic traits associated with autoimmunity

Using λ_s , it becomes obvious that in single-gene disorders, the risk conferred on an individual by a given genetic variant is very high, but the overall impact on the population is minimal because these variants are rare. In these ‘simple’ Mendelian diseases (or traits), the relationship between the causal genetic variant and the disease state is deterministic (Fig. 1.3a). Concrete examples are associations of the gene AIRE (autoimmune regulator) with autoimmune polyendocrine syndrome (APS-1) and CTLA4 with Grave’s disease and type 1 diabetes.⁶¹

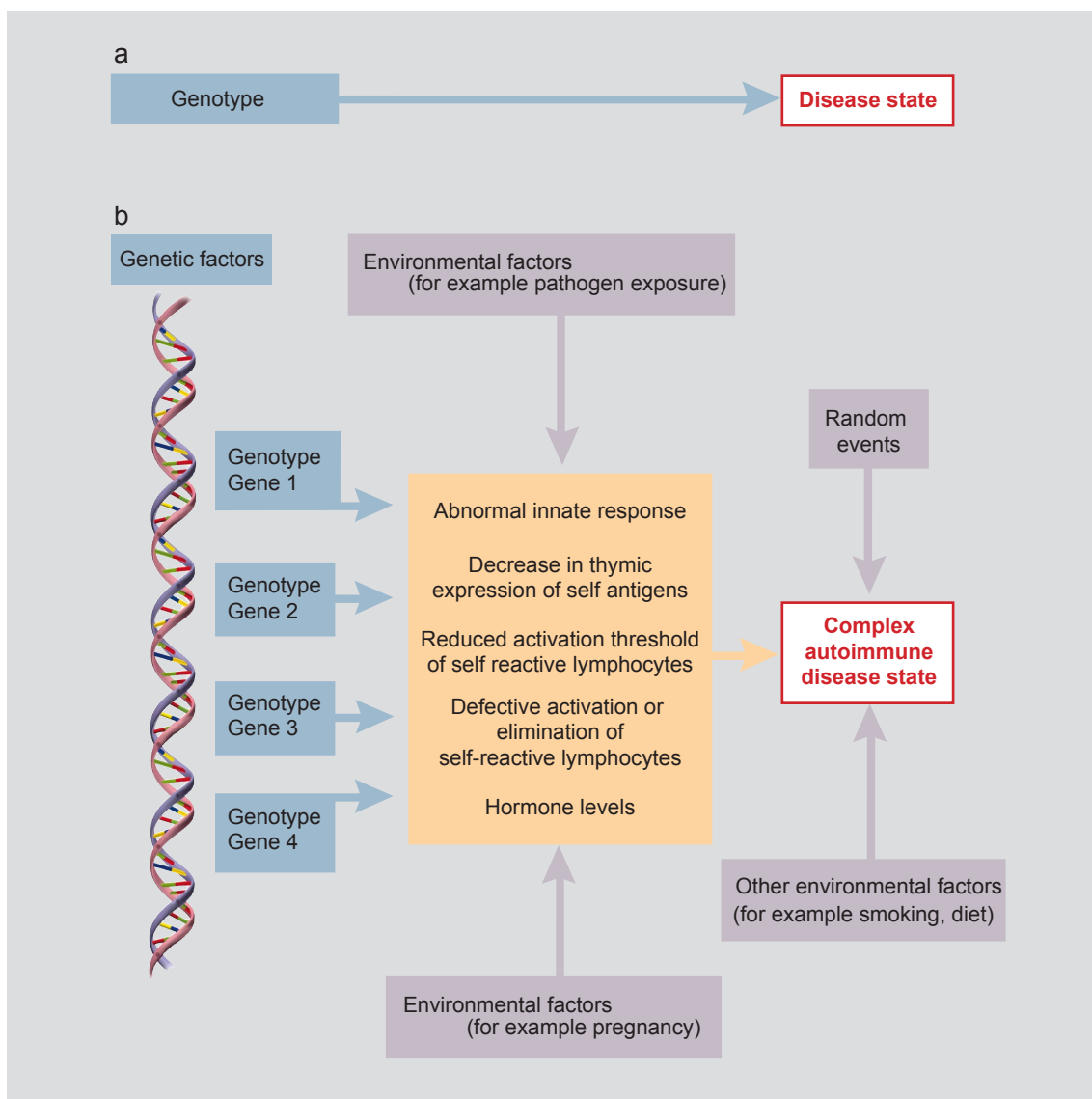


Figure 1.3 | Architecture of single gene disorders versus a model of autoimmune diseases caused by complex traits.

a) In simple Mendelian traits, the relationship between the causal genetic variant (genotype) and the disease state is deterministic. b) In complex traits, the clinically recognized disease state results from interactions between multiple genotypes and the environment. Individual genotypes can affect one or more components of the adaptive or innate immune systems; together these lead to an altered immune response to self antigens. On the basis of current findings, the influence of any individual causal allele is modest, and therefore the relationship between the causal variant(s) and the disease state is probabilistic.

1.3.2 Genetics of common autoimmune diseases

Six of the most common autoimmune diseases are rheumatoid arthritis (RA), Grave's disease, Type I (insulin dependent) diabetes (IDDM), pernicious anemia, systemic lupus erythematosus (SLE), and MS; collectively they represent about 50% of all autoimmune diseases. In contrast to single-gene disorders, common diseases are believed to be dependent on a combination of a number of susceptibility alleles at multiple loci, environmental factors (such as smoking or pathogen exposure and hormone levels), and stochastic events (Fig. 1.3b). In this model, the coexistence of susceptibility genes, each of which contributing only modestly to the disease phenotype, would be mandatory for disease manifestation. There is some debate as to whether common diseases are caused by multiple rare alleles of high penetrance or by common variants of low penetrance (that is, alleles that confer moderate increased risk to disease), stated as the *common disease-common variant hypothesis*.⁶²⁻⁶⁵

In the majority of the acknowledged autoimmune diseases, the major histocompatibility complex (MHC), specifically the class II HLA genes, have been identified as a genetic factor.⁶⁶ Class II MHC molecules normally function to bind and present peptide antigens to antigen-specific T cells, hence even a minimal perturbation in their function can have severe systemic consequences in immune responses, as it is observed in AIDs. Decoding the function of each susceptibility gene and their interactions will help understand the mechanisms of autoimmune pathogenicity.

1.3.3 Genetic heterogeneity in autoimmune diseases

Genetic heterogeneity is a common feature of many genetic systems in both humans and animal models.⁶⁷ It refers to the presence of multiple combinations of genes within the genome that are capable of causing a similar or identical disease phenotype within the same ethnic group. Basically, it reflects the fact that many genes participate in the development of complex phenotypes and that different combinations of genetic abnormalities can lead to a similar outcome.⁶⁸⁻⁷⁰

In AIDs, many aspects of immune function may be affected by these genetic factors. Depending on the individual set of susceptibility alleles, the secretion of proinflammatory cytokines may be enhanced in one and apoptosis or immune regulation disrupted in another, yet leading to the same overall disease type. Furthermore, during disease progression, the contribution of many genes to the quantitative trait implies that individual

patients express different subsets of susceptibility genes at different time points and their respective compositions greatly influence the actual disease phenotype.⁷¹

1.4 Epistatic interaction in complex traits

Epistasis is defined as a genetic interaction in which the genotype at one locus affects the phenotypic expression of the genotype at another locus. Classically, two models have been described in order to explain how genes interact if two or more loci are included in disease predisposition.⁷² In the additive model, the effect of interacting genes is derived by simple addition of each individual effect. The genotype associated penetrance of multiple loci can be modelled like a sum of factors of each genotype in each locus, rendering the global risk λ_R describing formula:

$$\lambda_R = \lambda_{R1} + \lambda_{R2} + \dots + \lambda_R N .$$

In this model, not all susceptibility genes are necessarily needed for the disease to be evident in a given individual.

The second theory corresponds to the multiplicative or epistatic model, where the overall effect of interacting genes is increased in comparison to each single gene's contribution (synergistic effect). For example, two susceptibility alleles would lead to a greater increase in disease severity than would be predicted by simply adding together their individual phenotypes. If the genes that confer disease susceptibility act epistatically, the global risk is equivalent to the product of each value of considered loci:

$$\lambda_R = \lambda_{R1} \times \lambda_{R2} \times \dots \times \lambda_R N .$$

In this case, the lack of one susceptibility gene could have the effect of a complete disease absence or a considerably less severe form.⁷³

A further type of epistasis is a form in which the autoimmune phenotypes of susceptibility alleles are suppressed by epistatic modifiers. Outcomes of animal models indicate that the disease mediated by susceptibility genes can be partially or sometimes completely suppressed by other "modifying" genes in the genome. Despite the presence of potent autoimmune disease alleles, a normal immune phenotype can still develop.⁷⁴ The existence of similar suppressive modifiers in AID in humans has not been demonstrated clearly so far, however it has been reasoned that similar genetic interactions affect disease predisposition.^{75,76}

1.5 Model of inheritance of autoimmune disease susceptibility

The inheritance of multifactorial traits such as AID susceptibility is a complex process. Multifactorial inheritance was first described and modeled as a “threshold liability”.⁷⁷ It was proposed that the penetrance of polygenic, qualitative phenotypes would increase in relation to the number of susceptibility genes present in the genome of an individual.

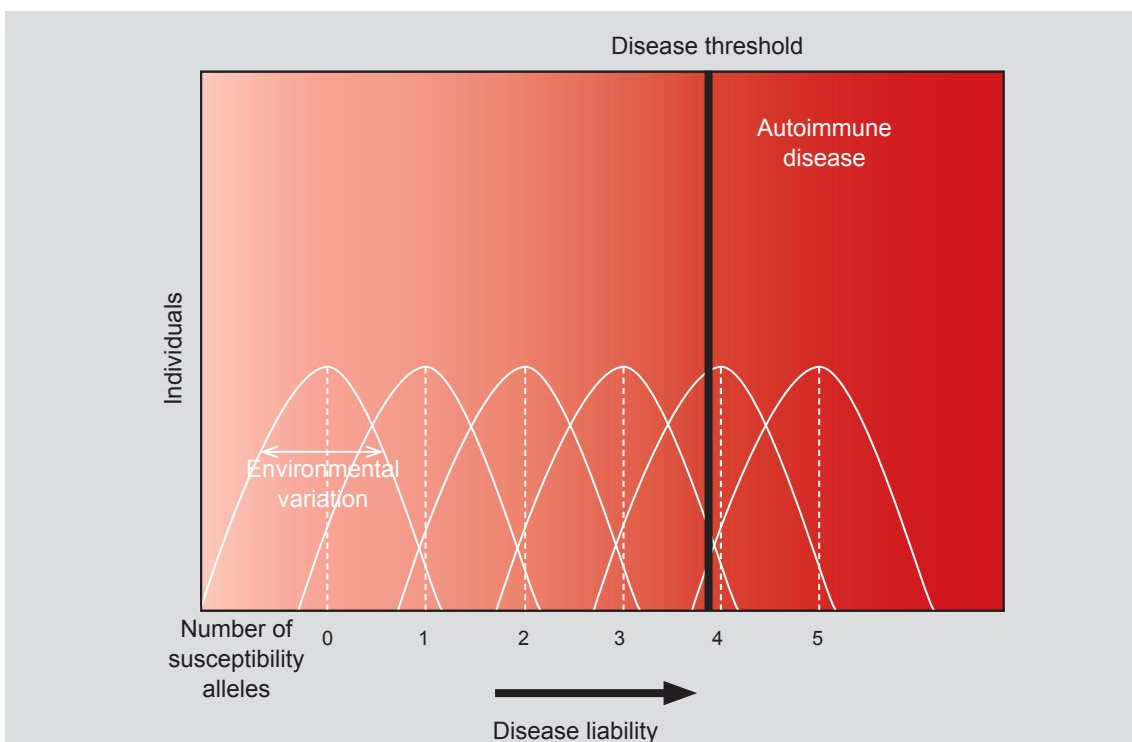


Figure 1.4 | Threshold liabilities in autoimmune disease. In this model, only individuals located to the right of the disease threshold line will develop disease. The abscissa represents increasing liability to disease: individuals being located on the x axis based on the degree of their predisposition to disease. An incremental increase in the number of susceptibility alleles progressively increases liability to disease, resulting in movement toward the disease threshold to the right. The disease liability introduced by environmental and stochastic effects is represented by the normal distribution curve around the location of individuals (with specific degrees of genetic predisposition for disease) (adapted from Wandstrat *et al.* 2001).

A hypothetical model of the inheritance of AID is proposed in Figure 1.4. The abscissa of the graph defines increasing disease liability, the ordinate represents the “threshold”, which delineates the point at which individuals will develop disease. Genetic predisposition places individuals at some point along the abscissa, based on the degree of susceptibility established by their genomes. As denoted in Figure 1.3b, environmental and stochastic

events will then increase or decrease their liability, depending on the individuals' life experience (life style). These environmental factors are arbitrarily depicted as a normal distribution of liability around the mean location (directed by genetic predisposition). The inheritance of susceptibility would then be determined by the cumulative content of disease susceptibility that an individual inherits. This is here presented in a simplistic additive fashion; each additional susceptibility allele incrementally moves an individual the equivalent distance further toward the disease threshold. In reality, the process of inheritance would appear more complex.

As stated before, epistatic interactions could modify the incremental movement of individuals along the abscissa in a complex manner. Thus, the position of an individual along the liability axis would be dependent upon the interactive consequences of all the susceptibility and suppressive modifier alleles present in the person's genome. In this regard, attempts to model the inheritance of AID susceptibility have often focused on distinguishing "additive" inheritance from "multiplicative" models.⁷⁸ Linkage analyses in test crosses of AID-prone animal inbred strains have consistently found that relative risk increases in proportion to the number of active susceptibility genes present in the genome,⁷⁹⁻⁸¹ but the goodness-of-fit for additive versus multiplicative models has not been established.⁸² Given the extensive genetic heterogeneity observed in AID inheritance, it is reasonable to assume that both models exist and function parallel in nature.⁷⁵

1.6 Common genetic variation in the human genome and their genetic markers

The ability to discover as yet unidentified disease alleles has been improved by the expansion of knowledge and understanding regarding the common genetic variation in the human genome.⁸³⁻⁸⁸ Microsatellites are DNA sequences which contain variable numbers of tandem repeats (VNTRs), also termed short tandem repeats (STR) or short tandem sequences (STS). These repetitive sequences can consist of 2, 3, up to 8 bases in length, extending up to 150 bp, encompass 1% of the mammalian genome (occurring every 10,000 bp) and are highly polymorphic.⁸⁸ They were reported to serve as informative genetic markers in 1989.⁸⁹

Recent work has demonstrated though that the majority of genetic variation in the human genome consists of individual bases that exist as either of two alleles (biallelic base-pair substitutions) in the population, known as single nucleotide polymorphisms (SNPs).

SNPs are nucleotide variations, occurring in average every 500 bp⁹⁰ and are thus more frequent than STRs. Approximately ten million SNPs in the human genome have a minor allele frequency greater than 1% and represent about 90% of the genetic variation in the human genome.⁸⁷ Initial efforts to discover and map SNPs to the reference sequence of the human genome have resulted in a public resource (www.ncbi.nlm.nih.gov/SNP) containing most of these common SNPs (currently ~5.8 million).^{87,91-93}

The description of SNPs in the human genome has significantly contributed to the characterization of susceptibility genes in complex diseases.^{84,94} In reference to the structure of the genome, it is of importance to understand the relationships that exist between SNPs. First, by examining a high density of specific areas of the genome,⁹⁵⁻⁹⁷ and then by performing genome-wide surveys,⁹⁸ it has become evident that the alleles of the SNPs form patterns (known as haplotypes) in the genome. Furthermore, the present data and models based on this information suggest that alleles at nearby SNPs are highly correlated with one another (known as linkage disequilibrium) – the same mechanism holds true for all genetic markers including microsatellites – and that recombination “hotspots” exist in the genome.⁹⁷⁻¹⁰⁰

1.7 Concept of “Linkage Disequilibrium” and “Haplotype”

Linkage disequilibrium (LD) is defined, at a population level, as the non-independence of alleles situated at different loci in the genome. In practice, polymorphisms that are positioned relatively close to each other are not inherited at random. The patterns of LD observed in natural populations are the result of a complex interplay between genetic factors, in particular meiotic recombination, and the populations’ demographic history. When a recombination occurs between two loci, it tends to reduce the dependence between the alleles carried at those loci, and thus reduce LD.^{101,102}

The specific set of alleles observed on a single chromosome, or part of a chromosome, is termed a haplotype.¹⁰³ In a single gene, hundreds of SNPs that have been accumulated through the history of a population are found as unique combinations named gene-based haplotypes.¹⁰⁴ However, the range of possible haplotypes (also called haplotype diversity) is not simply a factor of all these polymorphisms but rather tends to be limited with as few as four or five haplotypes predominating in a given population.^{96,97,105,106} Investigations from Gabriel *et al.* (2002),⁹⁸ Daly *et al.* (2001)⁹⁶ and Patil *et al.* (2001)⁹⁵ also indicated that a limited number of SNPs were sufficient to reconstitute most of the common haplotypes;

an optimal collection of SNPs can represent at least 95% of the haplotypes observed in the studied population.¹⁰⁷ These selected SNPs are known as haplotype-tagging SNPs (Fig. 1.5) and function as surrogate markers for all other genetic variation (that is, other SNPs, deletions, insertions and repetitive sequences) found within a given haplotype.

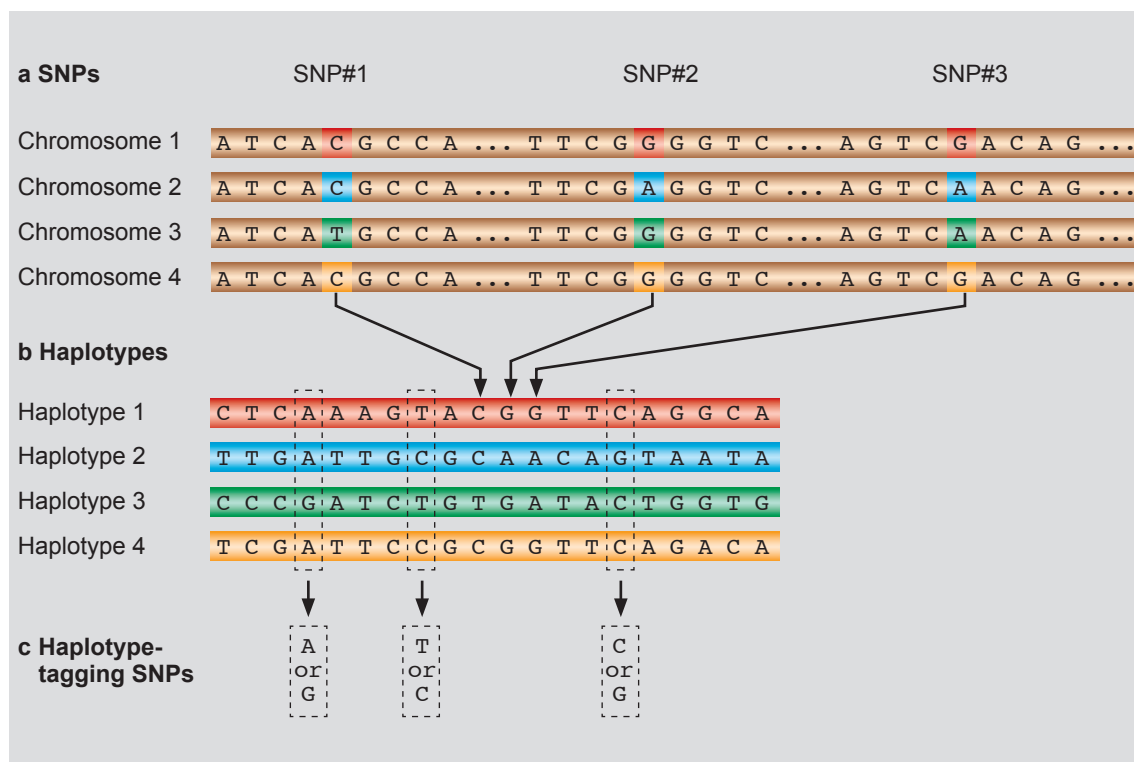


Figure 1.5 | SNPs, haplotypes and haplotype-tagging SNPs. a | Single-nucleotide polymorphisms (SNPs) are shown in a short stretch of DNA in four versions of the same chromosomal region taken from different individuals. Most of the DNA sequence is identical in these chromosomes, but variation is shown to occur at three bases. Each SNP has two possible alleles; the first SNP (SNP#1) has the alleles C and T. b | A haplotype consists of a particular combination of alleles at nearby SNPs. Shown here are the observed genotypes for 20 SNPs that extend across 6,000 bp of DNA. Only the variable bases are shown, including the three SNPs that are shown in panel a. For this region, most of the chromosomes in a population survey have haplotypes 1–4. c | Genotyping of just the 3 haplotype-tagging SNPs out of the 20 SNPs is sufficient to uniquely identify these 4 haplotypes. For example, if a particular chromosome has the sequence A-T-C at these three haplotype-tagging SNPs, this sequence matches the pattern determined for haplotype 1. Note that many chromosomes carry the common haplotypes in the population.

Information from haplotype analyses revealing ‘block’-like structures bears a number of potential advantages for the design of linkage disequilibrium mapping strategies and identification of disease associated candidate genes or genomic regions.^{107,108}

1.8 Basic approaches toward disease gene identification

There are two basic analytic approaches to mapping disease genes: those based on linkage and those based on association. The basic design of the first is by searching for markers that co-segregate with the disease within families (linkage), and the second is by ascertaining marker frequency differences in a series of unrelated cases and a series of demographically ‘matched’ controls (association).

Linkage-based approaches have been widely and successfully applied to Mendelian disorders that display high penetrance.¹⁰⁹ Genome-wide linkage studies attempt to systematically identify genetic markers (and thus a genomic region) where there is more sharing of alleles between individuals with a given trait within families than is statistically expected, applying a transmission disequilibrium test (TDT tests).¹¹⁰ However, for more complex disorders like MS, linkage-based methods are limited by a lack of statistical power; in part because multiple genes are involved in disease susceptibility and most of the risk alleles are presumed to be common, disclosing a low penetrance.⁹⁴ In addition, association studies are statistically more powerful than (genome-wide) linkage analyses.⁶⁹ One can use linkage techniques to identify broad areas that are thought to contain candidate genes and then use linkage disequilibrium techniques to refine these regions. As SNPs display low mutation rates and linkage disequilibrium, they appear ideal for genetic association in case-control studies.^{104,111,112}

Once a promising genomic region of interest has been chosen or identified, two conceptually distinct approaches, the ‘direct’ and the ‘indirect’, can be considered.⁸³ The candidate SNP analysis is a straight forward test of association between a putatively functional variant and disease risk. The alternative, which is referred to as indirect association, is to test a dense map of ‘tag’ SNPs for disease association under the assumption that if a risk polymorphism exists it will either be genotyped directly or be in strong LD with one of the genotyped SNPs.¹¹³ Both direct and indirect association testing can be applied effectively to candidate genes that have been implicated in disease pathogenesis by other means (e.g. based on biological plausibility), as long as common variants have been comprehensively identified in the candidate gene.¹¹⁴

The emerging strategy therefore would be to devise a candidate gene list that is appropriate to a given condition, establish the haplotype structure in the population at risk and define the haplotype frequency for the common variants, identify the polymorphisms that capture that diversity (tagging), and genotype those polymorphisms in a suitably

large case-control group. Figure 1.6 depicts the basic principles of such a study design. Note, that disease predisposing segments (yellow) are present in all individuals including the healthy population.

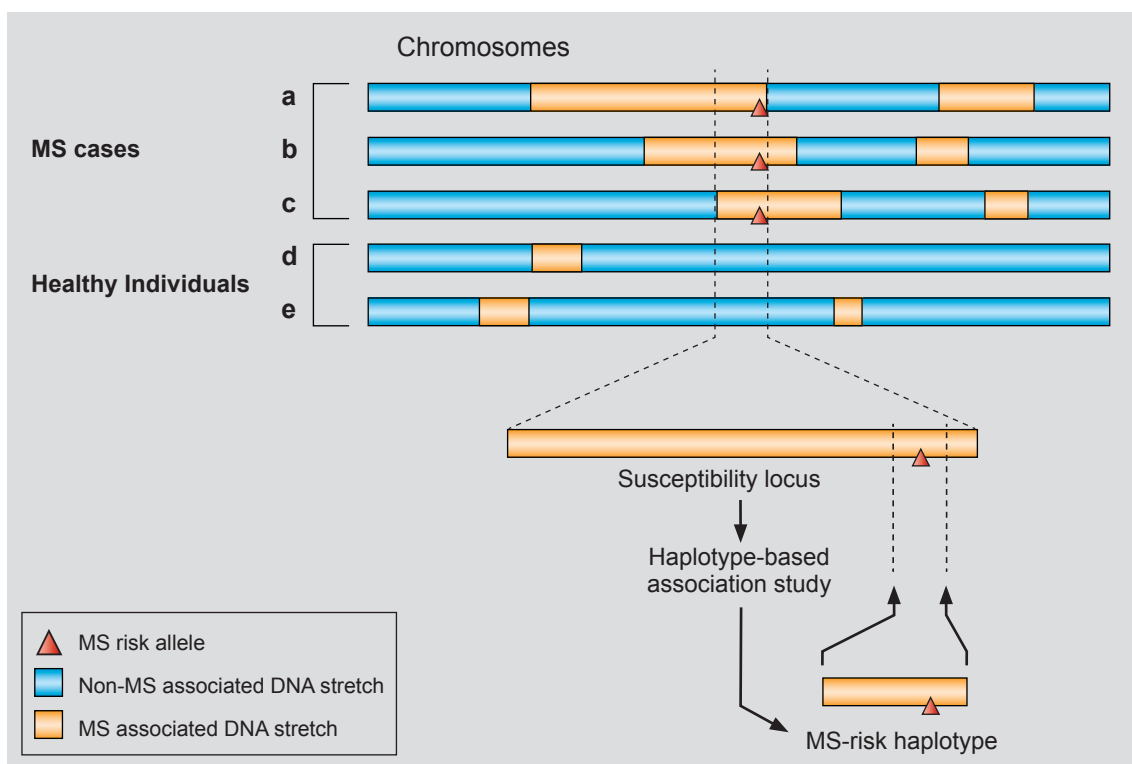


Figure 1.6 | Outline of an association study of MS. Five idealized chromosomes from different individuals are shown (a–e). The first three (a–c) are from patients with multiple sclerosis (MS), and the other two are from healthy control individuals (d, e). The “disease free” chromosomal segments are shown in blue, and those MS associated are shown in yellow. The pink triangle depicts the position of a risk allele that confers susceptibility to MS. Each chromosome has a different proportion of disease association within the chromosomal region being examined. When the location of these segments is compared, one smaller segment has increased MS frequency relative to any other segment among the chromosomes of affected individuals but not among those of healthy control individuals. This is the “susceptibility” locus. The next phase of the analysis then relies on fine-mapping techniques, such as identifying all haplotype blocks within the “susceptibility” locus and testing each haplotype within those blocks for association with MS. This analysis will yield a disease-risk haplotype that contains the disease-risk allele and will be followed by an exhaustive assessment of all genetic variation within the risk haplotype to determine which allele is the risk allele.

1.8.1 Identifying disease genes in MS

In MS research, there has been great interest in testing candidate genomic regions (identified by linkage studies) or candidate genes (selected on the basis of their location under a linkage peak, or their known functional properties, or both) for evidence of

their association with the disease. Most study designs followed a two stage approach, consisting of an initial discovery-driven genome scan and a subsequent validation step employing an increased marker resolution in order to map candidate regions or genes.

1.8.2 Linkage analysis in MS

Several groups have performed a two-stage genomewide screen in DNA samples derived from multiplex families, collected in Canada, the UK, the USA, Finland, and Sardinia testing large sets of microsatellite markers.¹¹⁵⁻¹¹⁹ A fruitful meta-analysis was difficult due to different sets of applied markers.

1.8.3 Association analysis in MS

To date, genomewide screens for association in MS and healthy populations have been realized in the GAMES study¹²⁰ (data from 18 European MS research centers), preceded by their initiators.¹²¹ In these experiments, the groups applied the identical set of microsatellite markers; results from meta-analysis are pending.

Finally, a large number of “suggestive” linkages exist, for which the underlying genetic defect - if it exists - has not been identified so far. Suggestive linkage describes genomic regions with an observed trend toward excess sharing in affected individuals that is not significant after correcting for multiple tests across the genome.^{122,123}

1.9 Genetic heterogeneity, inheritance model and susceptibility genes in MS

1.9.1 A model of inheritance for MS

A simple model of inheritance for all MS subtypes is unlikely and can not account for the nonlinear decrease in disease risk with increasing genetic distance from the MS proband (Fig. 1.7). Concordance estimates in twins and relatives of MS patients differ from prediction based upon a single gene inheritance, and implicates a polygenic etiology for MS.^{16,52}

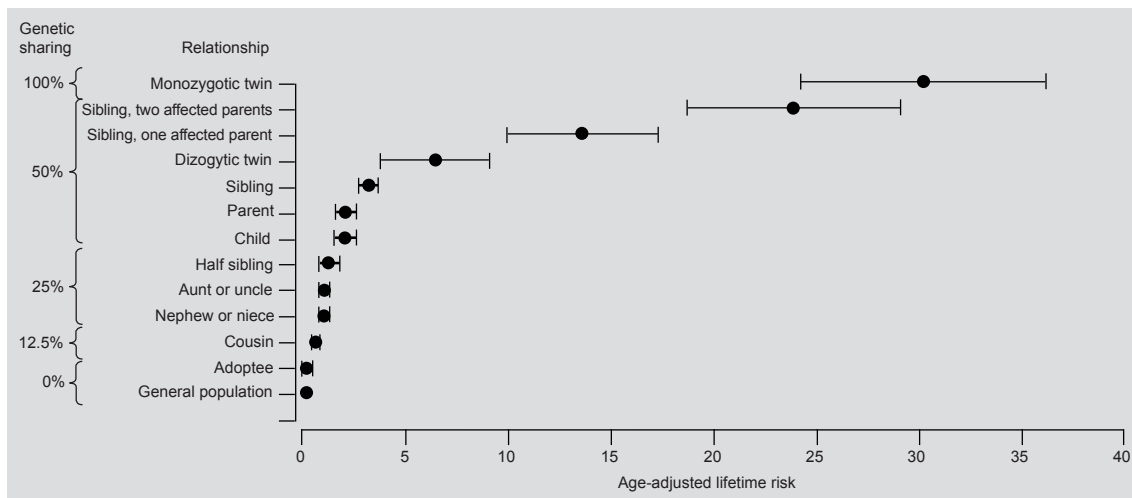


Figure 1.7 | Recurrence risks for multiple sclerosis in families. Age adjusted recurrence risks for different relatives of probands with multiple sclerosis. Pooled data from population based surveys. Estimated 95% confidence intervals are shown.

Correspondingly, amongst several disease causing concepts and hypotheses (Tab. 1.2) the presence of genetic heterogeneity in MS has been proposed and confirmed repeatedly.^{16,79,124-126} The established knowledge informs the MS genetics scientists that the search for genetic factors is comparable to that of a needle in the haystack. Besides the HLA region, it is these presumed many other loci of smaller effect, but which account for the larger portion of the total genetic risk for MS, that researchers seek to identify.

Table 1.2 | Multiple sclerosis as a complex genetic disease.

-
- (1) Etiological heterogeneity
Identical genes, different phenotypes
 - (2) Genetic heterogeneity
Different genes, identical phenotypes
 - (3) Unknown genetic parameters
Single versus multiple genes
Dominant versus recessive mode of inheritance
Incomplete penetrance
 - (4) Gene–gene interactions
 - (5) Post-genomic mechanisms
 - (6) Unidentified non-heritable (environmental) factors
-

1.9.2 The (genetic) epidemiology and etiology of MS

MS population prevalence in Europe is 79/100,000^{15,127} and in Spain 58/100,000.^{15,128}

¹³⁰ Epidemiological studies provide substantial evidence for both environmental and genetic causes of MS while additional indications of a genetic predisposition has been demonstrated in numerous population and family-based studies.

Disparity between prevalence rates cited in distinct population-based studies for MS (values range from 0.9 to 224 per 100,000 inhabitants) revealed that the population prevalence of MS increases with distance from the equator.^{131,132} It was postulated that the distribution can be explained in part by both environmental factors (e.g. diet and vitamin D abnormalities) and population-specific genetics. The importance of genetic background is supported by the differences in the incidence of MS in disparate genetic groups living in the same region. For example, the prevalence of MS among people of Japanese descent living on the Pacific Coast of the USA (6.7/100,000) is considerably lower than that of Caucasians living in California (29.9/100,000). However, individuals of Japanese descent living on the Pacific Coast of the USA have a higher prevalence of MS than Japanese individuals living in Japan (2/100,000), suggesting an additional influencing environmental factor.¹³³ Furthermore, migration studies served to illustrate potential environmental influences on MS prevalence;^{134,135} children born to parents who have migrated from a high-risk area to a low-risk area for MS appear to have a lower lifetime risk than their parents. Conversely, migration of parents from a low-risk area to a high-risk area may confer a higher risk for MS in the children.

A genetic etiology is indicated foremost by both an increased relative risk in siblings of affected individuals compared with the general population (λ_s),¹³⁶ and an enhanced recurrence risk in family members of the affected individual^{137,138} (Fig. 1.7). Studies of half-siblings¹³⁹ and adoptees¹⁴⁰ support the concept that genetic factors are primarily responsible for familial aggregation. Furthermore twin studies from different populations consistently indicate that a monozygotic twin of an MS patient is at higher risk (25–35% concordance rate) for MS than is a dizygotic twin (4–9%),^{141–143} providing additional evidence for a significant, but complex, genetic etiology.

The strongest and most consistent evidence for susceptibility genes lies within the major histocompatibility complex (MHC) on chromosome 6p21.3. Association with the HLA-DR2 haplotype (DRB1*1501 – DQB1*0602) has been repeatedly demonstrated in multiple MS populations.^{53,54,141,144–147} Other HLA associations have also been reported.¹⁴⁸ The total genetic susceptibility attributed to the HLA locus in MS is estimated between 15% and 50%.¹⁴⁹

Other susceptibility alleles seem weakly associated and difficult to identify, but several functionally interesting genes are shared by various autoimmune disorders.^{67,71} A large number of further candidate genes have been suggested but not confirmed. An in-depth listing of MS candidate genes (and their positive and negative outcome, respectively) can be found at http://www.ucsf.edu/msdb/r_ms_candidate_genes.html.

1.10 Aim and content of the dissertation

It is the aim of presented dissertation to identify and elucidate genomic regions and genes in humans which provide unrecognized candidates for MS susceptibility.

Spanish MS patients and healthy individuals are subject of the genetic study. The population based gene mapping strategy based on three stages:

- 1) a primary genomewide association study applying DNA pooling methodology¹⁵⁰ and an evaluation of some obtained results by means of individually genotyping employed DNA,
- 2) an extended analysis of GAMES¹²⁰ data that ground on a heuristic method termed “Sliding windows” which filters candidate genome regions displaying suggestive evidence for association,¹⁵¹ and
- 3) the fine-scale mapping and description of genomic architecture of detected regions of interest containing MS candidate genes.¹⁵²

191 microsatellite markers displayed evidence for association for a genetic predisposition to afflict MS; seven of these were genotyped on individual DNA samples (Appendix A). 284 regions of interest were disclosed by application of the sliding windows approach. Two biologically plausible candidate regions on 3p25.3 and 10q22.1 were fine-mapped by 24 SNPs, their gene-based haplotypes computationally reconstructed and statistical association to MS or a clinical MS subcategory carried out. Tag SNPs and disease-specific haplotypes were ascertained.

2

MATERIAL & METHODS

2.1	Genomic DNA extraction from peripheral blood	24
2.2	Determination of DNA concentration and quality	26
2.3	DNA pool construction based on fluorescence quantitation	26
2.3.1	Calibration of TKO 100 Mini-Fluorometer by means of calf thymus DNA	28
2.3.2	DNA sample preparation, quantification and appropriate dilution	29
2.3.3	DNA pool construction	29
2.4	DNA pool genotyping by means of microsatellite markers	30
2.4.1	Storage and preparation of reagents for PCR assay	31
2.4.2	Polymerase amplification and thermal cycling	32
2.4.3	Gel electrophoresis of PCR products	33
2.5	Analysis of microsatellite marker genotyped DNA pools	34
2.5.1	Processing of data	34
2.5.2	Analysis of STR-genotyped DNA pools applying the Single Peak Approach	35
2.6	A sliding-window method for the detection of clusters of markers displaying evidence for association with MS	39
2.6.1	Processing of data	39
2.6.2	Analysis of STR-Genotyped DNA pool data by sliding windows	40
2.7	SNP-Genotyping principle: the 5' Nuclease assay	43
2.7.1	Concepts of 5' Nuclease and Allelic Discrimination Assay	43
2.7.2	Preparation of DNA dilutions for PCR assays: 96- and 384-well plates	45
2.7.3	Preparation of reaction solution for PCR assay	47
2.7.4	Polymerase amplification and thermal cycling and end-point analysis	48
2.8	MS patients and controls	50
2.9	SNP selection for two genomic regions of interest	50
2.10	SNP-Genotyping data handling	53
2.10.1	Allelic discrimination	53
2.10.2	Real-time amplification data	54
2.11	Analytical tools for describing genomic structure and detecting disease association	57
2.11.1	Descriptive analyses	57
2.11.2	Case-control association analyses	58
2.12	Accounting for multiple testing	61

2.1 Genomic DNA extraction from peripheral blood

Reagents and consumables

Red Blood Cell Lysis (RBCL) Buffer:

144 mM	NH ₄ Cl	Merck
1 mM	NaHCO ₃	Merck
2 mM	Na ₂ EDTA (pH 8.2)	Merck

Nuclei Lysis (NL) Buffer:

400 mM	NaCl	Fluka
10 mM	Tris-HCl (pH 8.2)	Merck
2 mM	Na ₂ EDTA (pH 8.2)	Merck
0.2 %	SDS	Serva
1 mg/ml	Proteinase K	Sigma-Aldrich

Both solutions were filtered, autoclaved and stored at room temperature. Proteinase K (10 mg ml⁻¹) was stored at -20°C and added prior to use (1 ml to 9 ml NLB solution).

Tris-EDTA (TE) buffer	Sigma-Aldrich
Vacutainer SST tubes	BD Diagnostics
50 ml centrifuge tubes	Falcon
Polyethylene Pasteur pipette, 3.5 ml	Genotek, Labclinics
Filter (0.22 mm)	Millipore S.A.
Serological pipettes (5, 10, 25 ml)	Corning
Capillary pipettes, glass	Genotek, Labclinics

Equipment

Autoclave AE dry	SanoClav
Centrifuge RT 6000 D	Sorvall
Rotating shaker	Heidolph
REAX top vortex mixer	Heidolph
Water bath	Boreal
Pipetting aid unit	Roses Scientific

The method to isolate genomic DNA is a modification of the salting out procedure as described by Miller et al.¹⁵³ The obtained high quality DNA is suitable for polymerase chain reaction (PCR) applications.

If not stated otherwise all steps were carried out at room temperature. Venous blood was collected in three 10-ml EDTA vacutainer tubes per individual. After centrifugation for 10 minutes at 700 g (2000 rpm), with a pasteur pipette, most of the plasma was aspirated and discarded. A small remainder of serum, the white blood cells containing “buffy coat” and part of the red blood cell phase constituted approximately 1.5–2 ml per vacutainer tube. This portion was transferred and pooled in one 50 ml conical centrifuge tube (Falcon) for each individual. In order to eliminate most of the contaminating red blood cells, the Falcon tube was filled up to 50 ml with Red Blood Cell Lysis (RBCL) buffer, slowly agitated for 20 minutes on a rotating shaker and then centrifuged with 1700 g (3200 rpm) for 20 minutes. The supernatant was discarded and the cells containing pellet was resuspended with residual volume. A repeated lysis was performed with freshly added 50 ml RBCL buffer and an agitation for 5 minutes. The Falcon tube was centrifuged with 3200 rpm for 10 minutes, the supernatant discarded and the now sufficiently cleaned white blood cell pellet vigorously mixed for 20 seconds. In order to disintegrate cell and nuclear membranes, 10 ml of Nuclei Lysis (NL) buffer supplemented with Proteinase K (1mg ml⁻¹) were added, well agitated and left at 50°C for 2 hours in a water bath, being shaken manually every 20 minutes. Subsequently, for optimal protein precipitation, the sample was kept at 4°C on ice for 10 minutes, 3.5 ml of 7.5 M Ammonium Acetate (4°C) added and the tube vigorously shaken. After additional 15 minutes at 4°C the sample was centrifuged with minimal breaking force 2700 g (4000 rpm) for 10 minutes. The brownish coloured pellet contained dehydrated cleaved protein residues while the supernatant held dissolved uncleaved DNA stretches. In order to precipitate the DNA in the liquid phase the supernatant was poured into a Falcon tube containing 25 ml of 95% Ethanol and was slowly inverted. Following visible DNA strand precipitation (white thread like conglomerate) the sample was centrifuged with 3200 rpm for 10 minutes and washed with 10 ml 95% Ethanol. Rotating the DNA–Ethanol emulsion for 10 minutes desalts the DNA stretches which were thereafter centrifuged with 3200 rpm for 10 minutes. The supernatant was aspirated with a capillary pipette and the tube without cap inverted on paper tissue. Thereby, the remaining ethanol could evaporate for 10 minutes. In order to entirely redissolve the DNA molecules, 4 ml of Tris-EDTA (TE) buffer were added into the tube and kept in a water bath at 50°C over night. When the solution became clear, the optical density was measured and the corresponding DNA concentration ascertained.

2.2 Determination of DNA concentration and quality

Reagents and consumables

1M NaOH	Merck
1M HCl	Merck
Tris-EDTA (TE) buffer	Sigma-Aldrich

Equipment

Spectrophotometer GENEQUANT	Amersham Pharm
Quarz cuvette (10 mm pathlength)	Amersham Pharm
1.5 ml microcentrifuge tube	Eppendorf

Before each usage, the quarz cuvette was treated with 1M NaOH (or 1 M HCl) and thoroughly cleaned with MilliQ water. Adjustment for the spectrophotometer (blank value) was realized by measuring the absorbance of MilliQ water and calibrating the system to zero.

10 µl of dissolved DNA in TE buffer was mixed with 190 µl MilliQ water in a 1.5 ml tube and filled into the such prepared quarz cuvette. The optical density (OD) (that is: absorbance) was measured at wavelength $\lambda=260$ nm and the mean concentration [ng µl⁻¹] was calculated from three determined OD values of the identical sample dilution.

The purity P of the tested DNA sample was ascertained by means of calculating the quotient between wavelengths $\lambda_1=260$ nm and $\lambda_2=280$ nm ($P=\lambda_1/\lambda_2$). DNA samples with a ratio below 1.5 or over 1.9 were excluded from performed experiments or re-precipitated with 7.5 M ammonium acetate and washed in 95% ethanol until the required quality was reached. Samples were aliquoted and stored at -80°C in 1.5 ml tubes at original concentrations (100 to 300 ng µl⁻¹) and at working concentration of 20 ng µl⁻¹.

2.3 DNA pool construction based on fluorescence quantitation

DNA samples from a total number of 200 unrelated affected individuals recruited at two Spanish Neurology centers (Neuroimmunology unit, Vall d'Hebron Hospital, Barcelona and Neurology department, Hospital Clinic, Madrid) were employed in the study applying DNA pooling methodology. Accordingly, the control population comprised of 200 unrelated

individuals which were recruited at both centers in equal proportions to the number of MS patients enrolled in the study, hence served the geographic areas (Tab. 2.1). The study was approved by the Ethics Committees of both University Hospitals and all the subjects involved in the study gave written informed consent.

Table 2.1 | Number of DNA samples collected at two Spanish Multiple Sclerosis centers constituting MS and adjusted control DNA pools. RR: relapsing remitting; SP: secondary progressive; HC: healthy control.

Population	clinical form	Center	
		Barcelona	Madrid
MS	RR	128	41
	SP	31	0
HC		163	37
		322	78

Absorbance readings of a spectrophotometer that is based on monochromatic light dispersion are not satisfactory for an accurate DNA pooling procedure, due to the overlap of the specific absorbance spectra of DNA and RNA ($\lambda=260$ nm) or Protein ($\lambda=280$ nm). A more precise quantification methodology was used here. By means of the fluorescent dye Bisbenzimide, which binds to the minor groove of the DNA strand, a more accurate determination of DNA in an aqueous sample was feasible. The TKO 100 fluorescence assay is based on a relative measurement of emitted light and therefore a calibration reference value needed to be established with a DNA standard solution before DNA concentration could be quantified.

Reagents and consumables

NaCl	Fluka
TrisHCl	Merck
Tris	Merck
EDTA	Merck
Bisbenzimide, fluorescent dye Hoechst 33258	Sigma-Aldrich
Calf thymus DNA standard	Sigma-Aldrich

Hoechst stock solution:

1mg H33258 per 1 ml MilliQ water or TE buffer

The Hoechst stock solution was stored at 2 to 8°C and protected from light.

10X TNE solution:

1 M NaCl	
100 mM TrisHCl	
10 mM EDTA	(pH 7.4)

Working dye solution: 0.1 µg ml⁻¹ H33258 solution in 1X TNE

Hoechst stock solution	10.0 µl
10X TNE	10.0 ml
MilliQ water	90.0 ml

The working dye solution was prepared daily and kept at room temperature.

Calf thymus DNA reference standard (100 µg ml⁻¹):

1 mg ml ⁻¹ calf thymus DNA stock solution	100 µl
10X TNE	100 µl
MilliQ water	800 µl

The calf thymus DNA reference standard solution was stored at 2 to 8°C.

Equipment

TKO 100 Mini-Fluorometer	Hoefer Sci. Instr.
TKO 105 glass fluorometry cuvette	Hoefer Sci. Instr.
Micropipettes (10, 100, 200, 500 µl)	Eppendorff
1.5 ml microcentrifuge tube	Eppendorff
50 ml centrifuge tube	Falcon
REAX Top Vortex Mixer	Heidolph
REAX 2 Overhead Mixer	Heidolph
96 Deepwell™ Plate 1.0 ml	Nunc
Cap for 96 Well Plate (sealing lids)	Nunc

2.3.1 Calibration of TKO 100 Mini-Fluorometer by means of calf thymus DNA

Two milliliter of the working dye solution were filled into the glass fluorometry cuvette, measured for adjustment of the fluorometer and accordingly served as a blank value for the succeeding measuring session.

In order to obtain the reference value 100 ng DNA ml⁻¹, by means of a 10-µl micropipette, 2 µl of DNA reference standard solution were added to the 2 ml working dye solution in the cuvette. Readings not deviating more than 2 units were accepted and adjusted to the value “100”. The cuvette was washed repeatedly with working dye solution, thus the system was prepared for quantification of DNA samples with concentrations ranging between 10 and 500 ng ml⁻¹.

2.3.2 DNA sample preparation, quantification and appropriate dilution

DNA aliquots in 1.5 ml tubes were thawed at room temperature for at least 45 minutes and agitated by means of a Vortex mixer at medium speed for 15 seconds prior to quantification procedure. After the glass cuvette, containing 2 ml working dye solution, was placed in the fluorometer reading chamber, 2 µl of DNA suspension were added. In order to obtain an accurate estimate of the sample concentration, this procedure was repeated three times (triplicate) and the mean value calculated thereby.

After ascertaining the concentration of a DNA suspension, an aliquot of the sample was diluted with TE buffer in a 1.5 ml tube and adjusted to a final 60 ng ml⁻¹ concentration in a 200-µl volume. This dilution was well suspended, its DNA fraction measured and accordingly adjusted in a secondary dilution step, establishing the final concentration of 50 ng ml⁻¹. All samples were read in duplicates; a variation of 2.5 ng ml⁻¹ (5%) from the final 50 ng ml⁻¹ was tolerated. Every result displaying a higher deviation was excluded or remade from its respective stock suspension.

2.3.3 DNA pool construction

One hundred µl of the 50 ng ml⁻¹ concentrated DNA samples were transferred into a 50 ml centrifuge tube; DNA aliquots from MS patients were combined together in a tube denominated “Pool A” and control samples in a further tube labelled “Pool B”, respectively. The 20-ml DNA suspensions were extensively mixed and shaken at 4°C in an overhead mixer for 24 hours. Prior to manually distributing the DNA suspension into a 96 Deepwell plate (400 µl per well) (Tab. 2.2), pools were thoroughly mixed again. Finally, the Deepwell plate was sealed with a lid and stored until use at -80°C.

Table 2.2 | Distribution of DNA pools A (MS patients) and B (healthy controls) across a 96 deepwell plate; 400 µl solution per well; 200 individuals (50ng / µl) per pool.

	1	2	3	4	5	6	7	8	9	10	11	12
A	A	B	A	B	A	B	A	B	A	B	A	B
B	A	B	A	B	A	B	A	B	A	B	A	B
C	A	B	A	B	A	B	A	B	A	B	A	B
D	A	B	A	B	A	B	A	B	A	B	A	B
E	A	B	A	B	A	B	A	B	A	B	A	B
F	A	B	A	B	A	B	A	B	A	B	A	B
G	A	B	A	B	A	B	A	B	A	B	A	B
H	A	B	A	B	A	B	A	B	A	B	A	B

2.4 DNA pool genotyping by means of microsatellite markers

Reagents and consumables

96 Deepwell™ Plate 1.0 ml	Nunc
Cap for 96 Well Plate	Multisorinson Biosci.
384 Well Amplification Plate	Nunc
Optical adhesive covers	Applied Biosystems
20 µl virgin polypropylene tips in 96 rack	Beckman Coulter
20 µl P20 Biomek pipette tips	Beckman
Microsatellite marker (STS)	GAMES collaborative
True Allele™ PCR Premix	Applied Biosystems
Hi-Di™ Formamide	Applied Biosystems
GS400HD ROX labelled size standard	Applied Biosystems
Performance Optimised Polymer 6	Applied Biosystems

Equipment

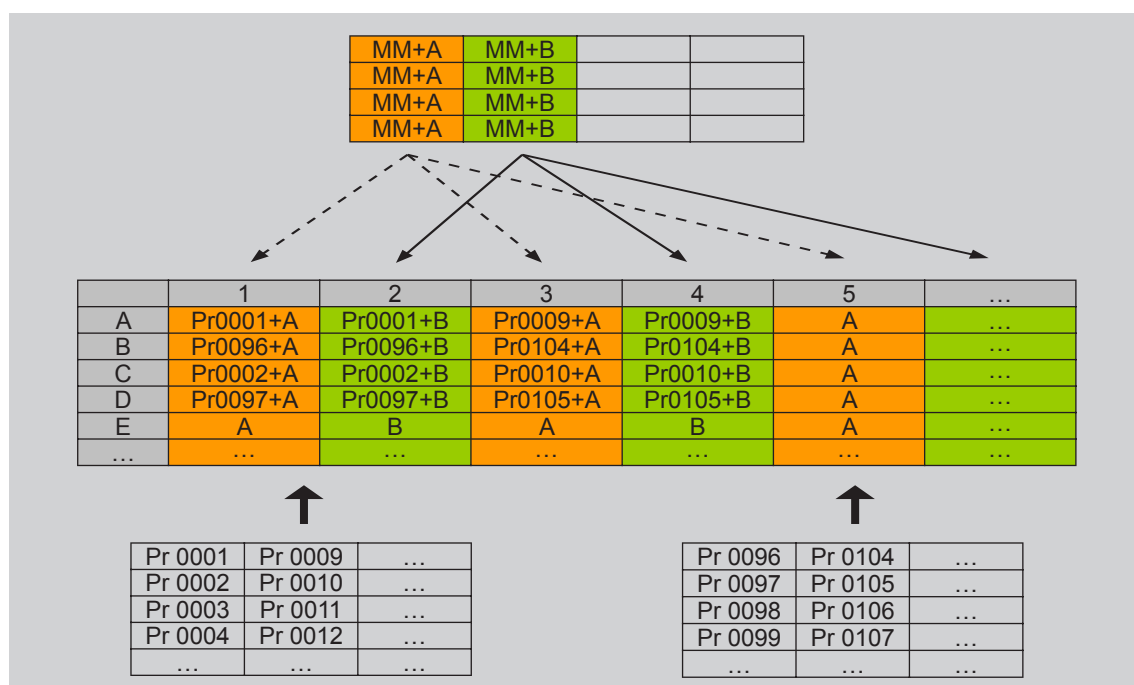
Centrifuge 5810 R	Eppendorf
Multimek™ 96/384-Channel Automated Pipettor	Beckman Coulter
Cyberlab C-400	Gilson
PTV-225 DNA Engine Tetrad™ Cycler	MJ Research
ABI PRISM 3700 High Troughput Sequence Detection System	Applied Biosystems
3700 Genetic Analyser	Applied Biosystems

2.4.1 Storage and preparation of reagents for PCR assay

Specific primer pairs for 5500 microsatellite markers from the GAMES collaborative¹²¹ and 43 from deCODE in-house stock,¹⁵⁴ respectively, were stored in sealed 96 Deepwell plates at -20°C. Preceding each PCR assay preparation, deepwell plates containing DNA-pools or microsatellite primers were thawed at room temperature and quick-spinned in a centrifuge. In order to first dispense primer solutions into a 384 well plate, 2 deepwell plates were successively positioned on a tray of the Multimek Pipettor system. Three µl of each primer pair solution were aspirated and 1.5 µl distributed successively into two adjacent wells of the 384 well plates. Thereby, 2 x 95 microsatellites in duplicates occupied 380 wells, leaving 4 to be filled with MilliQ water (Tab. 2.3). In columns 1 and 2 of a 96 Deepwell plate, pooled DNA suspensions of MS patients (Pool A) and healthy controls (Pool B) were independently admixed to freshly prepared solutions of PCR Premix and MilliQ water (Master Mix).

Both the primer-coated 384 well plate and the 96 well plate containing two Master Mix solutions were positioned in the Cyberlab C-400 system. Mechanically via disposable tips 13.5 µl of each DNA pool-specific Master Mix solutions were transferred to each well of the primer-coated 384 well plate. Such prepared plates were sealed with adhesive covers and placed in the PCR cycler heating blocks.

Table 2.3 | Distribution of DNA pool plus Master Mix (MM) solutions (13.5 µl MM+A/B per well) and microsatellite primer solutions (1.5 µl Pr per well) in a 384 well reaction plate; A: MS patients DNA pool (indicated by orange color); B: healthy controls DNA pool (indicated by green color).



2.4.2 Polymerase amplification and thermal cycling

PCR was performed in 15- μ l final volume reactions using 5 μ l of PCR Premix, 5 pmol of labelled forward primer, 5 pmol of unlabelled reverse primer, 25 ng of template (pooled) DNA and 6.5 μ l of MilliQ water. Thermal cycling was performed on a Tetrad Cycler according to the following protocol: 12 min at 95°C (activation of Taq Gold DNA polymerase); 10 cycles of 94°C for 15 s, 55°C for 15 s and 72°C for 30 s; 20 cycles of 89°C for 15 s, 55°C for 15 s and 72°C for 30 s; and a final step of 72°C for 20 min (Fig. 2.1).

PCR Master Mix (Premix-DNA-MilliQ water solution) for final 15- μ l reaction:

MilliQ water	6.48 μ l	
dNTP (2.0 mmol)	1.9 μ l	
MgCl ₂	1.5 μ l	
10X buffer	1.5 μ l	
Ampli Taq Gold	0.12 μ l	
Pooled DNA (12.5 ng/ μ l)	2.0 μ l	
	<hr/>	
	13.5 μl	
STS Primer Forward	0.75 μ l	
STS Primer Reverse	0.75 μ l	
	<hr/>	
	1.5 μl	
Final reaction volume	15.0 μl	

True Allele™ PCR Premix

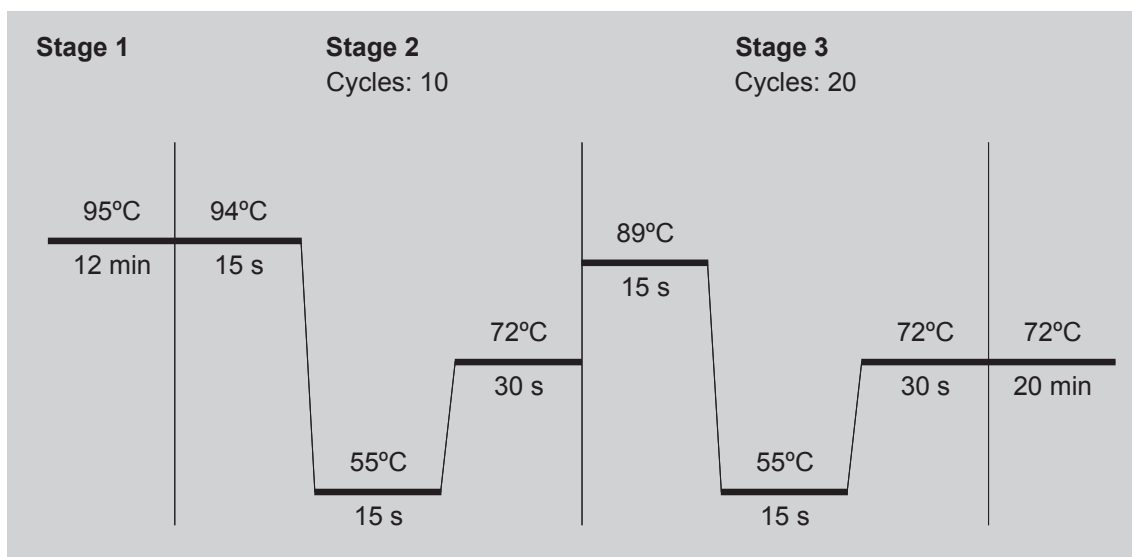


Figure 2.1 | PCR thermal cycling profile of DNA pool and microsatellite marker experiment.

2.4.3 Gel electrophoresis of PCR products

The products from each PCR were electrophoresed twice on a 3700 Genetic Analyser. These two runs generated four sample files (electropherograms) for each marker (2 replicates from the cases pool and 2 replicates from the controls pool). Prior to electrophoresis, 1 µl of PCR product was denatured for 5 minutes at 95°C in combination with 9.55 µl of Hi-Di Formamide and 0.45 µl of GS400HD ROX labelled size standard. Denatured samples were electrokinetically injected with 10 kV applied for 10 s, while capillary electrophoresis used Performance Optimized Polymer 6 (POP6), a cuvette temperature of 35°C, run temperature of 50°C and a run voltage of 6 kV for 75 minutes.

2.5 Analysis of microsatellite marker genotyped DNA pools

Equipment

Software GENESCAN vers. 3.5	Applied Biosystems
Software GENOTYPER vers. 3.6	Applied Biosystems

2.5.1 Processing of data

Each microsatellite marker was amplified once by PCR and electrophoresed twice on different gels thus creating two electropherograms for each sample, indicated as follows:

- “A1” = dilution replicate DNA pool MS patients
- “A2” = dilution replicate DNA pool MS patients
- “B1” = dilution replicate DNA pool Healthy Control
- “B2” = dilution replicate DNA pool Healthy Control

Typing a microsatellite marker in pooled DNA generates an Allele Image Profile (AIP)¹⁵⁵ as depicted in Figure 2.2 consisting of a series of peaks. The peak height pattern of an AIP reflects the underlying allele frequency distribution distorted to an undefined degree by the effects of stutter bands, length-dependent amplification and other artefacts such as Poly-A contamination.

The AIPs from each replicate were visually inspected for PCR artefacts and subsequently analysed using GENESCAN to size-call the alleles and GENOTYPER to define corresponding peak heights. In order to coordinate the results and reduce artefact alleles (monoalleles, “stutter bands”) each profile was compared with a peak determining AIP template, provided by the GAMES initiators. Markers that displayed significant results after statistical AIP examinations were selected for rerun, performing as before described, one PCR reaction and two electrophoresis runs for each marker.

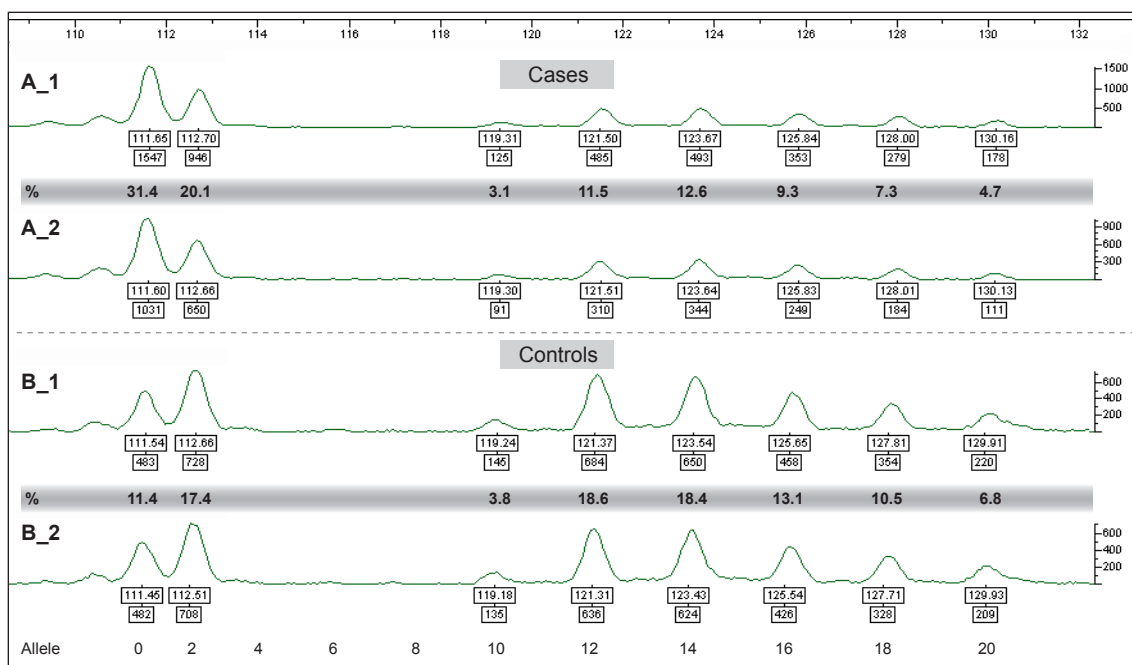


Figure 2.2 | Allele Image Profile (AIP) of dinucleotide microsatellite marker SA-99 (located in MHC III) genotyped with 2 DNA pools constructed from 200 DNA samples of MS patients (Pool A) and 200 healthy controls (Pool B), respectively. A1 and A2 are distinct dilutions of the PCR product from genotyped DNA pool of MS patients; similar for B1 and B2 and healthy controls. Two numbers assigned to each allele indicate product size in length (upper value) and height (lower value). The percentual distributions of mean peak heights for respective pools are highlighted in gray.

2.5.2 Analysis of STR-genotyped DNA pools applying the Single Peak Approach

In order to conduct a conventional χ^2 -test on each allele of a marker comparing the case and control pools (Single Peak Approach, SPA), transformations from independent AIP peak height values to more useful statistics were performed as follows:

Peak height values from GENOTYPER output files (Fig. 2.2) were introduced into a Microsoft Excel spreadsheet that was prepared with an algorithm as shown in the right part of Table 2.4. The increasing numeration beginning at cell B2 represents the peak order from the initial (shortest) allele of the AIP to the final (longest) allele, definitions of which were based on the provided AIP templates for each marker. Peak values of the AIP corresponding to each replicate ("A1", "A2", "B1", and "B2") were introduced in according cells (compare between Fig. 2.2 and Tab. 2.4). If a GENOTYPER file did not generate an useful image to analyse, for example in the case of an empty or only partly readable result for "B2", peak values of "B1" were copied into the corresponding Excel row for "B2".

Table 2.4 | Algorithm of Allele Image Profile (AIP) analysis from microsatellite marker SA-99. Numbers in column B3 to B6 are measured peak height values of "Allele 0" as seen in Figure 2.2 and numbers from B8 to B38 relate to column N formulae; the same holds true for peak heights introduced from cells C3 to L6. Rows 3+4: peak heights of first (A1) and second (A2) dilution replicate DNA pool MS patients; rows 5+6: peak heights of first (B1) and second (B2) dilution replicate DNA pool healthy control; rows 2 and 7: peak and allele numerations, respectively; row 8: calculated length dependent amplification correction factors; rows 11 to 14: corrected peak values; rows 17 to 20: relative peak heights due to 400 alleles per DNA pool; rows 21+22: coefficient of variation (CV) values for each peak pair per pool; rows 23+24: arithmetic means for estimated relative peak heights of each pool; row 26: average of mean values (rows 23+24); rows 28 to 31: see text for details; rows 33+34: chi square value and respective p-value based on one degree of freedom (df=1) of peak comparison Pool A vs. Pool B; B36: microsatellite specific length dependent amplification (LDA) correction factor; B38: microsatellite specific weighting factor; D38: number of alleles per pool.

	A	B	C	D	E	F	G	H	I	J	K	L	M	N
1	SA-99													
2	Peak order	1	2	3	4	5	6	7	8	9	10	11		1
3	A1	1547	946	0	0	0	125	485	493	353	279	178		1547
4	A2	1031	650	0	0	0	91	310	344	249	184	111		1031
5	B1	483	728	0	0	0	145	684	650	458	354	220		483
6	B2	482	708	0	0	0	135	636	624	426	328	209		482
7	Allele	0	2	4	6	8	10	12	14	16	18	20		0
8		0,971	0,943	0,915	0,889	0,863	0,838	0,814	0,790	0,767	0,745	0,723		POWER(1-\$B36:B2)
9														
10	CORRECTED PEAKS													
11	A1	1593	1003	0	0	0	149	596	624	460	374	246		B3/B8
12	A2	1062	689	0	0	0	109	381	435	325	247	153		B4/B8
13	B1	497	772	0	0	0	173	840	823	597	475	304		B5/B8
14	B2	496	751	0	0	0	161	781	790	555	440	289		B6/B8
15														
16	RELATIVE PEAK HEIGHTS:													
17	A1	126,3	79,5	0	0	0	11,8	47,2	49,5	36,5	29,7	19,5		(B11/SUM(\$B11:\$L11))*\$D38
18	A2	124,9	81,1	0	0	0	12,8	44,8	51,2	38,2	29,0	18,0		(B12/SUM(\$B12:\$L12))*\$D38
19	B1	44,4	68,9	0	0	0	15,4	75,0	73,4	53,3	42,4	27,1		(B13/SUM(\$B13:\$L13))*\$D38
20	B2	46,6	70,4	0	0	0	15,1	73,3	74,1	52,1	41,3	27,1		(B14/SUM(\$B14:\$L14))*\$D38
21	CV A1/A2	0,01	0,01				0,05	0,04	0,02	0,03	0,02	0,05		SD / MEAN A1/A2
22	CV B1/B2	0,03	0,02				0,02	0,02	0,01	0,02	0,02	0,00		SD / MEAN B1/B2
23	Arith mean A	125,6	80,3				12,3	46,0	50,3	37,3	29,4	18,8		MEAN (B17:B18)
24	Arith mean B	45,5	69,7				15,3	74,2	73,7	52,7	41,9	27,1		MEAN (B19:B20)
25														
26	(ar.A+ar.B) / 2	85,5	75,0				13,8	60,1	62,0	45,0	35,6	22,9		(B23+B24)/2
27														
28		274,4	319,7				387,7	354,0	349,7	362,7	370,6	381,2		400-B23
29		314,5	325,0				386,2	339,9	338,0	355,0	364,4	377,1		400-B26
30	chi 1	18,76	0,38				0,16	3,29	2,21	1,31	1,09	0,76		(ABS(B23-B26)^2)/B26
31	chi 2	5,10	0,09				0,01	0,58	0,41	0,17	0,11	0,05		(ABS(B28-B29)^2)/B29
32														
33	chi	47,71	0,93				0,33	7,75	5,23	2,95	2,40	1,61		B30*2+B31*2
34	p-value	4,9E-12	0,336				0,564	0,005	0,022	0,086	0,121	0,204		CHIVERT(B33;1)
35	Allele	0	2	4	6	8	10	12	14	16	18	20		0
36	LDA:	0,029												0,029
37														
38	Weight:	1		400										1
39														

At first, peak heights had to be corrected for a length dependent amplification (LDA). This was carried out by combining a mean LDA factor (0.029), provided by Yeo *et al.*,¹⁵⁶ with the index number of the allele being analyzed. The employed value can be modified based on further marker-specific evidence, such as the feature of a di-, tri- or tetranucleotide repeat. The correction factor formula reads $(1 - \text{LDA})^i$ and incorporates for each allele the positional value of its corresponding peak (*i*) displayed in row 2. The application of this result refinement can be seen in row 8 of the excel file (Tab. 2.4), e.g .
 $(1 - 0.029)^1 = 0.971$; $(1 - 0.029)^2 = 0.943$; $(1 - 0.029)^3 = 0.915$; and so forth.

The corrected peaks were estimated by means of dividing the original peak value by its corresponding LDA correction factor (cells B11:L14).

Example allele 0: $1547 / 0.971 = 1593$.

The relative peak heights were calculated and normalized according to the total number of chromosomes in the pools (400 in each) in the following way: A single corrected peak value was divided by the sum of all peak heights in the AIP and multiplied by the total amount of alleles for this marker, equivalent to two alleles per individual in a pool of 200 individuals.

$(\text{Corrected peak value} / \sum \text{Corrected peak values of corresponding AIP}) * \sum \text{Marker-specific allele in pool}$.

Example allele 0: $(1593.2 / 5046.1) * 400 = 126.3$.

In order to determine the accuracy of two readings of identical PCR product, the coefficient of variation (CV= standard deviation divided by arithmetic mean) was calculated for each peak pair. In case of an exceeding value over 10%, the marker was excluded from further analysis.

Example allele 0: CV "A 1 / 2" = $1.00 / 125.6 = 0.01$ (1%);
 CV "B 1 / 2" = $1.54 / 45.5 = 0.03$ (3%) .

Next, the arithmetic mean for estimated relative peak heights of each pool was computed (B23 and B24 respectively) and the average of these mean values was estimated (B26). Introducing the basic concept of the χ^2 -test of observed (O) and expected (E) values, the mean of the MS patients pool at peak 1 ("A"; B23) was subtracted from the sum of marker-specific alleles present in the pool,

$$\text{B28: } 400 - 125.6 = 274.4 ,$$

and the average of both pool means ("arithmetic A"+ "arithmetic B" divided by 2; B26) from the sum of marker-specific alleles respectively,

$$\text{B29: } 400 - 85.5 = 314.5 .$$

Then, the difference of average means A and B subtracted from mean A was squared and divided by average means A and B

$$\text{B30: } (125.6 - 85.5)^2 / 85.5 = 18.8 ,$$

and the second computation contained the squared difference of terms B28 and B29 divided by B29.

$$\text{B31: } (274.4 - 314.5)^2 / 314.5 = 5.1 .$$

These ultimate fractions B30 and B31 were both multiplied by two, summed (B33) as the final χ^2 value and transferred with one degree of freedom into the corresponding probability term “p” (B34). Finally, the microsatellite tested in both pools was compared allele by allele and the allele with the lowest p-value was used as a representative for the corresponding marker, with the exclusion of peaks below 5% in allele frequency. The MS related¹⁵⁴ marker SA-99 was tested first and functioned as a positive control for applied technique. For a small subset of markers the final p-value was further weighted (B38) according to evidence determined at the Cambridge lab supervised by S. Sawcer, but the final adaptions were negligible. For detailed description, the Yeo *et al.*¹⁵⁶ publication shall serve.

The presented method of calculating a statistic did not operate with actual numbers of occurrence, as the focus was not to conduct a formal test of association indicating the statistical significance of observed differences. Hence, the estimated statistic was denominated “empirical p-value”. Furthermore, the pooling method introduces non-sampling errors into the data, which were corrected by adapting factors for length dependent amplification and weighting factors,¹⁵⁶ but not completely removed. On the basis of the generated empirical p-values, all results were ranked due to evidence of association. Results of markers with an empirical p-value below 0.05 that satisfied in their PCR achievement and AIP appearance were selected for a rerun under described conditions (Section 2.4). The resulting degree of replication served as a further criteria for confirmation of acquired results in the first screen. Moreover, when evaluating results the proportional distribution of significant alleles (“A”>“B” or “A”<“B”) was pivotal. For example, if after the second genotyping of marker “SA-99” the AIPs would have displayed inverse frequency of allele 12 in Pool “A” compared to Pool “B”, the results of this marker would have been classified unstable and excluded from further analysis. At this stage of the study – being non-hypothesis driven and explorative – it was renounced to adjust for multiple testing.

2.6 A sliding-window method for the detection of clusters of markers displaying evidence for association with MS

Equipment

Sliding windows software	Univ. Pompeu i Fabra, Barcelona, Spain
SA6 genome assembly	deCODE genetics, Reykjavik, Iceland
Genome Browser (version hg17)	UC Santa Cruz, USA

The scan GAMES analyzed a large set of genetic markers across the genome in order to detect regions associated to the complex trait MS. After completion of the screen the determined statistics (empirical p-value) were ranked according to their evidence of association ($p<0.05$).

A supplementary tool to ranking results based on p-values was devised.¹⁵¹ The method takes into account genomic information such as the recombinatorial landscape and the density of markers. For example, in dense studies one would expect that true associations should appear in clusters with higher frequency than markers with spurious positive associations. Therefore, a simple tool was applied implementing a heuristic method that helps to detect potentially interesting candidate regions by exploiting the distribution of associated markers. Genetic map distances were used instead of the physical distance, since this generated windows of comparable recombination size, and thus took better into account the structure of haplotype blocks in the human genome.^{98,106}

2.6.1 Processing of data

Tested markers were considered informative when unique genomic positions could be assigned. The program was applied on results from 4851 informative markers of the Spanish GAMES study. The analysis proceeded chromosome by chromosome. Starting at every marker (Appendix B), alternatively a 0.5, 1.0, 1.5, 2.0, 2.5, and a 3.0 centi Morgan (cM) window was defined. For every window, the total number of markers on a chromosome and the respective sum of markers showing significant ($p<0.05$) association with MS were computed. Then, the proportion of significant markers in the chromosome under study was used to predict the number of significant markers expected in each window under the hypothesis of an independent distribution of significant markers. A window was considered to contain a cluster of associated markers when the probability of getting a number of significantly associated markers equal or superior to the observed number was smaller than 0.05.

The probability was estimated by means of the binomial distribution:

$$P(s_w) = \sum_{i=s_w}^{m_w} \binom{m_w}{i} \left(\frac{s}{m_c}\right)^i \left(1 - \frac{s}{m_c}\right)^{m_w-i}$$

where,

- m_c indicates the total number of markers in a chromosome,
- s indicates the number of significant markers in the chromosome,
- m_w indicates the total number of markers in a window,
- s_w indicates the number of significant markers in a window.

The formula was devised from the binomial law

$$p(k) = n! / k!(n-k)! * \pi^k (1 - \pi)^{n-k}.$$

Here, the “set of elements n” was replaced by “the total number of markers in a window” (m_w) and the “number of elements k from n” correspond to “the number of significant markers in the window” (s_w). The parameter “proportion π ” was substituted with the ratio of the variables “significant markers in the chromosome” and “total number of markers in the chromosome”, hence s/m_c .

2.6.2 Analysis of STR-Genotyped DNA pool data by sliding windows

As a demonstration of the applied method, computations for a significant window on chromosome 1 are elucidated in detail (compare Appendix B and C). From a total of 534 tested markers in samples of pooled DNA at chromosome 1, 39 markers showed significant association with MS. The first detected 0.5 cM window that contained an elevated number of markers with significant association served as an example of how the formula was implemented. Starting with marker D1S2770 at the genetic position 86.810 cM extending 0.5 cM to 87.310 cM, the window comprised five markers. Two of these (D1S1643, D1S2737) displayed significant differences between MS cases and healthy controls (Appendix B). With respect to the binomial density function, the computed probability of having two or more markers showing association within a window of five markers was the sum of selfsame. So that

$$p = p(2) + p(3) + p(4) + p(5).$$

Corresponding values applied into formula generated:

$$P(2) = \binom{5!}{2! \cdot 3!} \left(\frac{39}{534}\right)^2 \left(1 - \frac{39}{534}\right)^3 = 10 \cdot 0.0054 \cdot 0.7958 = 0.04277$$

$$P(3) = \binom{5!}{3! \cdot 2!} \left(\frac{39}{534}\right)^3 \left(1 - \frac{39}{534}\right)^2 = 10 \cdot 0.0004 \cdot 0.8588 = 0.00338$$

$$P(4) = \binom{5!}{4! \cdot 1!} \left(\frac{39}{534}\right)^4 \left(1 - \frac{39}{534}\right)^1 = 5 \cdot 2.89 \cdot 10^{-5} \cdot 0.9267 = 1.3 \cdot 10^{-4}$$

$$P(5) = \binom{5!}{5! \cdot 0!} \left(\frac{39}{534}\right)^5 \left(1 - \frac{39}{534}\right)^0 = 1 \cdot 2.12 \cdot 10^{-6} \cdot 1 = 2.12 \cdot 10^{-6}$$

resulting in a final “window p”:

$$p = 0.04222 + 0.00335 + 1.32 \cdot 10^{-4} + 2.08 \cdot 10^{-6} = 0.0457 \text{ (Appendix C).}$$

Thereafter, beginning with the subsequent marker (D1S2873) as the initial starting point for the contiguous window encompassing the range 86.841 to 87.341 cM, this region contained four markers (D1S2873, D1S1643, D1S203, D1S2737) including two of them displaying significant association with MS (presented in bold).

Therefore, the equation must read

$$p = p(2) + p(3) + (p4)$$

and corresponding values generated:

$$P(2) = \binom{4!}{2! \cdot 2!} \left(\frac{39}{534}\right)^2 \left(1 - \frac{39}{534}\right)^2 = 6 \cdot 0.0054 \cdot 0.8588 = 0.02769$$

$$P(3) = \binom{4!}{3! \cdot 1!} \left(\frac{39}{534}\right)^3 \left(1 - \frac{39}{534}\right)^1 = 4 \cdot 0.0004 \cdot 0.9267 = 0.00146$$

$$P(4) = \binom{4!}{4! \cdot 0!} \left(\frac{39}{534}\right)^4 \left(1 - \frac{39}{534}\right)^0 = 1 \cdot 2.89 \cdot 10^{-5} \cdot 1 = 2.89 \cdot 10^{-5}$$

resulting in a final “window p”:

$$p = 0.02750 + 0.00144 + 2.89 \cdot 10^{-5} = 0.0290 .$$

Then, the following contiguous window would cover the range 87.173 to 87.673 cM and comprise again four markers (D1S1643; D1S203; D1S2737; D1S2822) including two that are significantly associated. Naturally, the subsequently calculated window p-value was identical to the degree of significance estimated in the previous window.

In summary, three contiguous windows were detected harboring an excess of associated markers (p-values 0.0463, 0.0292, and 0.0292) and covering a total distance (region) of 0.778 cM or 1.574121 Mb. This region was classified as a region of interest.

By means of this procedure, all chromosomes were screened using various window lengths and region-specific probabilities were determined for each window. An illustration of window distributions for all 23 tested chromosomes are plotted in Appendix C. Here, a mere qualitative comparison between different window sizes, the relative window locations (in cM) on the respective chromosome as well as corresponding degrees of significance can be observed and taken into consideration when studying the summarized result tables on the lower end.

2.7 SNP-Genotyping principle: the 5' Nuclease assay

In order to detect genetic variation in a bi-allelic system such as single nucleotide polymorphisms (SNPs) in the human genome, fluorogenic TaqMan® probes and the 5' Nuclease assay for allelic discrimination were employed.

2.7.1 Concepts of 5' Nuclease and Allelic Discrimination Assay

In the 5' nuclease PCR assay, a hybridization probe included in the PCR is cleaved by the 5' nuclease activity of Taq DNA polymerase only if the probe target is being amplified. The probe consists of an oligonucleotide labeled with both a fluorescent reporter dye at the 5' end of the probe and a fluorescence quencher at the 3' end. In the intact probe, proximity of the quencher causes Förster resonance energy transfer (FRET, also called fluorescence resonance energy transfer)¹⁵⁷ and thus reduces the fluorescence from the reporter dye. Cleavage of the fluorogenic probe during the PCR assay liberates the reporter dye, causing an increase in fluorescence intensity (Fig. 2.3).

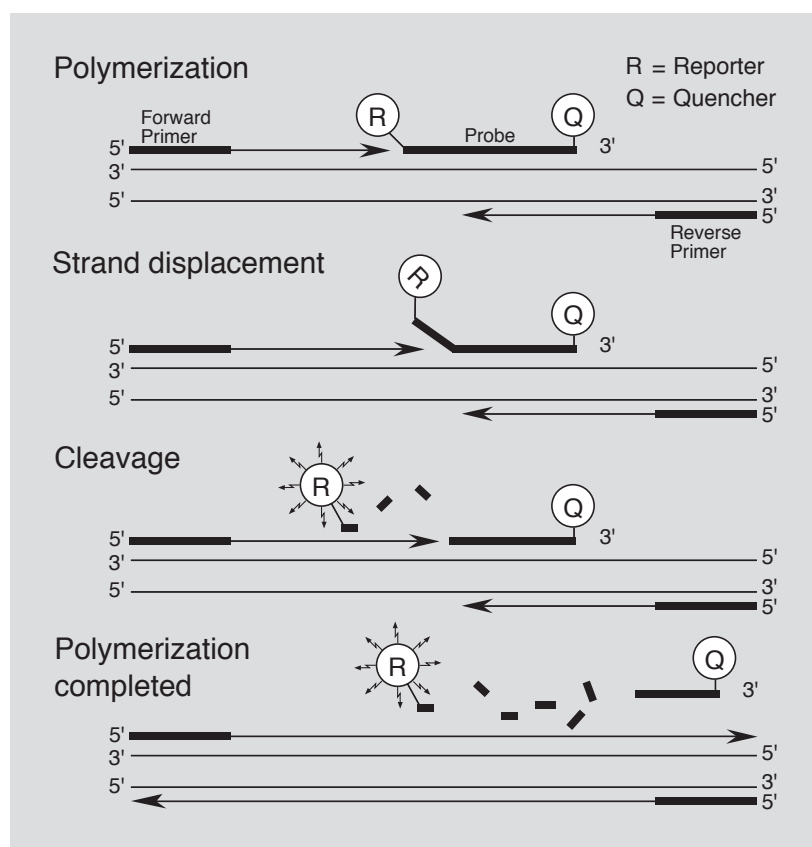


Figure 2.3 | PCR amplification and detection with fluorogenic probes in the 5'-nuclease assay. The main steps in the reaction sequence are polymerisation, strand displacement and cleavage. Two dyes, a fluorescent reporter (R) and a quencher (Q), are attached to the fluorogenic probe. When both dyes are attached to the probe, reporter dye emission is quenched. During each extension cycle, the DNA polymerase cleaves the reporter dye from the probe. Once separated from the quencher, the reporter dye fluoresces.

Figure 2.4 diagrams how fluorescent probes and the 5' nuclease assay are used for allelic discrimination. For a bi-allelic system, probes specific for each allele are included in the PCR assay. The probes can be distinguished because they are labeled with different fluorescent reporter dyes (FAM™ dye and VIC™ dye). A fully hybridized probe remains bound during strand displacement, resulting in efficient probe cleavage by Taq DNA polymerase and release of the reporter dye. A mismatch between probe and target greatly reduces the efficiency of probe hybridization leading to dissociation of the intact probe including reporter and quencher. Thus, substantial increase in FAM or VIC dye fluorescence indicates homozygosity for the FAM- or VIC-specific allele whereas an increase in both signals indicates heterozygosity. The accumulation of PCR products is detected directly by monitoring the increase in fluorescence of the reporter dye in an amplification plot (see section results).

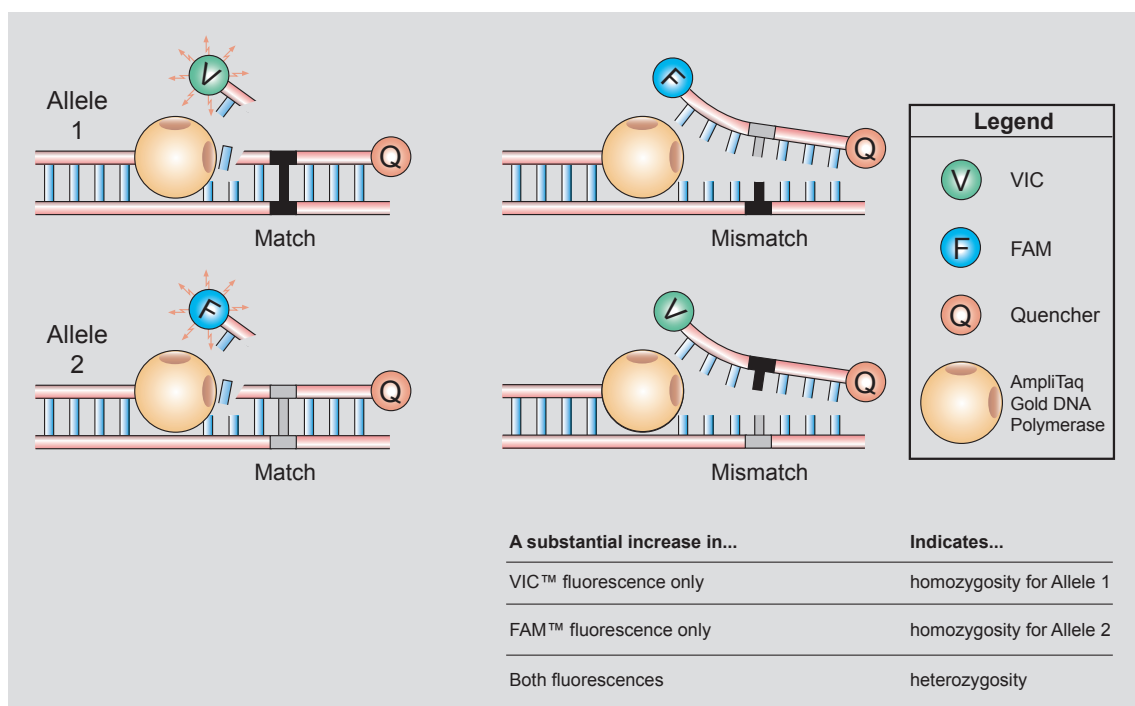


Figure 2.4 | Design strategy for allelic discrimination assay with fluorescent probes in the 5' nuclease assay. The presence of a mismatch between probe and target destabilizes probe binding during strand displacement, reducing the efficiency of probe cleavage. The possible results of the example allelic discrimination assay are summarized above.

Reagents and consumables

50ml TaqMan® Universal PCR MasterMix, no Ung	Applied Biosystems
Assay-on-demand, SNP products/probes	Applied Biosystems
96 well cell culture plate	Nunc
Cap for 96 Well Plate	Multisorinson Biosci.
96 Deepwell™ Plate 1.0 ml	Nunc
384 well clear optical reaction plate	Applied Biosystems
Optical adhesive covers	Applied Biosystems
20 µl virgin-polypropylene tips in 96 rack	Beckman Coulter
20 µl P20 Biomek pipette tips	Beckman
1.5 ml microcentrifuge tubes	Eppendorf

Equipment

Centrifuge 5810 R	Eppendorf
ABI PRISM® 7900 High Troughput Sequence Detection System	Applied Biosystems
Software SDS 2.1	Applied Biosystems
Gene Amp PCR System 9700	Applied Biosystems
Biomek FX	Beckman Coulter
Biomek 2000 (Laboratory Automation Workstation)	Beckman

2.7.2 Preparation of DNA dilutions for PCR assays: 96- and 384-well plates

Construction of master DNA 96 well plates

192 MSRR, 96 MSPP and 286 HC single genomic DNA samples of 20 ng µl⁻¹ concentration in 70-µl volumen were manually distributed into six 96 well plates, sealed with lids in order to avoid evaporation, and stored at -20°C (Tab. 2.5).

Table 2.5 | DNA sample distribution of healthy control (HC1-3), relapsing remitting (RR1;2) and primary progressive (PP) MS individuals in 96 well plates. White wells indicate MS samples whereas blue indicate healthy controls, respectively.

RR 1	1	2	3	4	5	6	7	8	9	10	11	12
A	459	501	529	565	610	638	646	715	755	779	851	914
B	468	508	541	568	615	639	647	720	757	781	863	940
C	471	511	544	577	631	640	650	723	763	785	868	964
D	474	514	547	588	632	641	686	725	767	812	880	977
E	477	517	550	591	633	642	688	726	768	814	884	1008
F	480	520	553	594	634	643	695	732	769	830	890	1017
G	489	523	556	597	635	644	701	735	771	839	903	1028
H	492	526	559	601	636	645	710	745	775	848	906	1047

RR 2	1	2	3	4	5	6	7	8	9	10	11	12
A	1182	1316	1409	1475	1528	1684	1704	1728	1829	770	878	976
B	1188	1319	1412	1483	652	1690	1705	1729	1860	788	897	444
C	1208	1322	1416	1491	1150	1691	1709	1731	1830	791	915	1527
D	1236	1332	1419	1492	1596	1692	1715	1732	691	806	922	1551
E	1279	1397	1434	1498	1612	1699	1716	1733	742	808	925	1863
F	1283	1404	1436	1340	1650	1701	1717	1736	749	817	930	1868
G	1302	1407	1437	1487	1658	1702	1722	1757	752	860	933	1918
H	1307	1408	1445	1497	1665	1703	1725	1790	756	864	950	1951

HC 1	1	2	3	4	5	6	7	8	9	10	11	12
A	C10	C34	C47	C58	C74	C86	C94	C105	C114	C124	C144	C153
B	C15	C37	C49	C60	C75	C87	C95	C106	C115	C129	C146	C154
C	C20	C38	C50	C61	C76	C88	C96	C107	C116	C130	C147	C155
D	C23	C41	C53	C62	C77	C89	C97	C108	C117	C132	C148	C156
E	C27	C42	C54	C67	C78	C90	C98	C109	C118	C135	C149	C157
F	C28	C43	C55	C68	C81	C91	C100	C110	C119	C136	C150	C158
G	C31	C44	C56	C70	C82	C92	C102	C112	C121	C138	C151	C159
H	C32	C46	C57	C72	C84	C93	C103	C113	C123	C142	C152	C160

HC 2	1	2	3	4	5	6	7	8	9	10	11	12
A	C161	C169	C179	C188	C199	C208	C217	C232	H2O	C276	C306	C335
B	C162	C172	C180	C190	C200	C209	C220	C233	C264	C282	C307	C336
C	C163	C173	C181	C191	C201	C210	C226	C234	C265	C284	C319	C337
D	C164	C174	C182	C193	C202	C211	C227	C237	C266	C287	C323	C338
E	C165	C175	C183	C194	C203	C212	C228	C249	C269	C295	C325	C339
F	C166	C176	C185	C195	C204	C213	C229	C251	C270	C298	C326	C341
G	C167	C177	C186	C196	C205	C214	C230	C258	C271	C301	C327	C342
H	C168	C178	C187	C197	C206	C216	C231	C260	C274	C302	C328	C343

HC 3	1	2	3	4	5	6	7	8	9	10	11	12
A	C235	C250	C268	C280	C297	C310	C348	C356	H2O	C371	C379	C387
B	C236	C252	C269	C283	C299	C311	C349	C357	C364	C372	C380	C388
C	C241	C253	C272	C285	C300	C312	C350	C358	C365	C373	C381	C389
D	C243	C256	C273	C286	C303	C314	C351	C359	C366	C374	C382	C390
E	C244	C259	C275	C288	C304	C344	C352	C360	C367	C375	C383	C391
F	C245	C261	C277	C289	C305	C345	C353	C361	C368	C376	C384	C392
G	C246	C263	C278	C293	C308	C346	C354	C362	C369	C377	C385	C393
H	C248	C267	C279	C294	C309	C347	C355	C363	C370	C378	C386	C394

Construction of master DNA 384 well plates

Prior to transfer of DNA dilution into 384 well reaction plates, sealed 96 well plates were thawed at RT, vigorously agitated, briefly spun down in a centrifuge and placed in corresponding positions in the Biomek FX robot. Applying the automated technology, 1 µl of each sample dilution was dispensed into a specified position of a 384 well reaction plate. Table 2.6 illustrates the distribution of 574 DNA dilutions representing the genomes of 192 MSRR and 191 HC individuals (plates 1 to 4 in Tab. 2.5) in plate one (P1) and of 96 MSPP and 95 HC individuals (plates 5 and 6 in Tab. 2.5) in plate two (P2). All pre-coated plates were sealed with optical adhesive covers and stored at -20°C.

Table 2.6 | 384 well reaction plates P1 and P2 containing together 574 different DNA samples. P2 carries 191 DNA samples in duplicates. White wells indicate MS samples whereas blue indicate healthy controls, respectively.

P1	1	2	3	4	5	6	7	8	9	10	11	12	13	14	15	16	17	18	19	20	21	22	23	24
A	459	C10	501	C34	529	C47	565	C58	610	C74	638	C86	646	C94	715	C105	755	C114	779	C124	851	C144	914	C153
B	1182	C161	1316	C169	1409	C179	1475	C188	1528	C199	1684	C208	1704	C217	1728	C232	1829	H20	770	C276	878	C306	976	C335
C	468	C15	508	C37	541	C49	568	C60	615	C75	639	C87	647	C95	720	C106	757	C115	781	C129	863	C146	940	C154
D	1188	C162	1319	C172	1412	C180	1483	C190	652	C200	1690	C209	1705	C220	1729	C233	1860	C264	788	C282	897	C307	444	C336
E	471	C20	511	C38	544	C50	577	C61	631	C76	640	C88	650	C96	723	C107	763	C116	785	C130	868	C147	964	C155
F	1208	C163	1322	C173	1416	C181	1491	C191	1150	C201	1691	C210	1709	C226	1731	C234	1830	C265	791	C284	915	C319	1527	C337
G	474	C23	514	C41	547	C53	588	C62	632	C77	641	C89	686	C97	725	C108	767	C117	812	C132	880	C148	977	C156
H	1236	C164	1332	C174	1419	C182	1492	C193	1596	C202	1692	C211	1715	C227	1732	C237	691	C266	806	C287	922	C323	1551	C338
I	477	C27	517	C42	550	C54	591	C67	633	C78	642	C90	688	C98	726	C109	768	C118	814	C135	884	C149	1008	C157
J	1279	C165	1397	C175	1434	C183	1498	C194	1612	C203	1699	C212	1716	C228	1733	C249	742	C269	808	C295	925	C325	1863	C339
K	480	C28	520	C43	553	C55	594	C68	634	C81	643	C91	695	C100	732	C110	769	C119	830	C136	890	C150	1017	C158
L	1283	C166	1404	C176	1436	C185	1340	C195	1650	C204	1701	C213	1717	C229	1736	C251	749	C270	817	C298	930	C326	1868	C341
M	489	C31	523	C44	556	C56	597	C70	635	C82	644	C92	701	C102	735	C112	771	C121	839	C138	903	C151	1028	C159
N	1302	C167	1407	C177	1437	C186	1487	C196	1658	C205	1702	C214	1722	C230	1757	C258	752	C271	860	C301	933	C327	1918	C342
O	492	C32	526	C46	559	C57	601	C72	636	C84	645	C93	710	C103	745	C113	775	C123	848	C142	906	C152	1047	C160
P	1307	C168	1408	C178	1445	C187	1497	C197	1665	C206	1703	C216	1725	C231	1790	C260	756	C274	864	C302	950	C328	1951	C343

P2	1	2	3	4	5	6	7	8	9	10	11	12	13	14	15	16	17	18	19	20	21	22	23	24	
A	462	462	1011	1139	1139	1203	1203	1431	1431	1534	1534	1567	1567	1578	1578	1604	1604	1633	1633	1710	1710	1840	1840		
B	C235	C235	C250	C250	C250	C268	C268	C280	C280	C297	C297	C310	C310	C348	C348	C356	C356	H20	H20	C371	C371	C379	C379	C387	C387
C	599	599	1013	1013	1140	1140	1204	1204	1472	1472	1550	1550	1568	1568	1588	1588	1606	1606	1649	1649	1711	1711	1841	1841	
D	C236	C236	C252	C252	C252	C269	C269	C283	C283	C299	C299	C311	C311	C349	C349	C357	C357	C364	C364	C372	C372	C380	C380	C388	C388
E	699	699	1014	1014	1151	1151	1206	1206	1473	1473	1553	1553	1569	1569	1589	1589	1608	1608	1654	1654	1718	1718	1842	1842	
F	C241	C241	C253	C253	C253	C272	C272	C285	C285	C300	C300	C312	C312	C350	C350	C358	C358	C365	C365	C373	C373	C381	C381	C389	C389
G	800	800	1015	1015	1159	1159	1209	1209	1482	1482	1554	1554	1570	1570	1597	1597	1609	1609	1656	1656	1730	1730	1846	1846	
H	C243	C243	C256	C256	C256	C273	C273	C286	C286	C303	C303	C314	C314	C351	C351	C359	C359	C366	C366	C374	C374	C382	C382	C390	C390
I	982	982	1040	1040	1168	1168	1218	1218	1490	1490	1557	1557	1571	1571	1600	1600	1610	1610	1657	1657	1734	1734	1886	1886	
J	C244	C244	C259	C259	C275	C275	C288	C288	C304	C304	C344	C344	C352	C352	C360	C360	C367	C367	C375	C375	C383	C383	C391	C391	
K	1005	1005	1134	1134	1184	1184	1231	1231	1500	1500	1562	1562	1573	1573	1601	1601	1613	1613	1659	1659	1825	1825	1934	1934	
L	C245	C245	C261	C261	C277	C277	C289	C289	C305	C305	C345	C345	C353	C353	C361	C361	C368	C368	C376	C376	C384	C384	C392	C392	
M	1006	1006	1135	1135	1195	1195	1240	1240	1526	1526	1563	1563	1576	1576	1602	1602	1615	1615	1660	1660	1833	1833	1974	1974	
N	C246	C246	C263	C263	C278	C278	C293	C293	C308	C308	C346	C346	C354	C354	C362	C362	C369	C369	C377	C377	C385	C385	C393	C393	
O	1007	1007	1138	1138	1198	1198	1328	1328	1530	1530	1565	1565	1577	1577	1603	1603	1631	1631	1663	1663	999	999	1992	1992	
P	C248	C248	C267	C267	C279	C279	C294	C294	C309	C309	C347	C347	C355	C355	C363	C363	C370	C370	C378	C378	C386	C386	C394	C394	

2.7.3 Preparation of reaction solution for PCR assay

The final 5-µl assay volume contained 1 µl of aqueous DNA sample and 4 µl of a solution including the SNP specific probe (stored at -20°C), TaqMan® Universal PCR MasterMix (MM, stored at 4°C) and MilliQ water. Due to variation of fluid dispersion by the utilized technology, reaction solutions were always prepared with 10% excess. In 1.5 ml tubes following components in µl were added as presented in Table 2.7.

Table 2.7 | Overview of preparative steps to create reaction solutions for 5' Nuclease TaqMan PCR assay. N: number of DNA samples to be tested; MM: TaqMan Universal PCR MasterMix; Probe: fluorogenic probe containing reporter and quencher dye; H₂O: MilliQwater. All volumes in [µl].

N	MM	Probe	H ₂ O	+ 10%	MM	Probe	H ₂ O	Final Vol.
2.5	0.25	1.25	X 0.10		2.75	0.28	1.38	4.41 µl
384	960	96	480	X 0.10	1056	105.6	528	1689.6 µl*
192	480	48	240	X 0.10	528	52.8	264	844.8 µl

* If final volume exceeded 1.5 ml, half parts of each assay constituent (MM, probe, MilliQ) were distributed in two microcentrifuge tubes.

Charging DNA-coated 384 well reaction plate with 384 assay solutions

Reaction solutions containing Master Mix, probe and MilliQ water in a final volume of 1689.6 µl were distributed in a column of a 96 Deepwell plate, 211.2 µl each, and positioned in the Biomek 2000, which transferred 4 µl of the reaction solution to each specified well of the DNA-coated 384 well reaction plate (Tab. 2.6, P1). The plates were sealed, briefly spun down and positioned on the tray of the ABI PRISM® 7900.

Charging DNA-coated 384 well reaction plate with 192 assay solutions twice

Reaction solutions containing Master Mix, probe and MilliQ water in a final volume of 844.8 µl were distributed in a column of a 96 Deepwell plate, 105.6 µl each, and positioned in the Biomek 2000. The robot transferred 4 µl of reaction solution to the DNA-coated 384 well reaction plate in an alternating manner, beginning with wells of column 1 and proceeding with entire columns 3, 5, 7, and so forth until column 23 (Tab. 2.6, P2). This procedure was repeated with a further reaction solution containing a different probe, beginning with wells of column 2 and proceeding respectively with columns 4, 6, 8, until 24. The plates were sealed, briefly spun down and positioned on the tray of the ABI PRISM® 7900.

2.7.4 Polymerase amplification and thermal cycling and end-point analysis

PCR in 384 well reaction plates loaded with 5-µl final reaction volume were performed on an ABI PRISM® 7900 under specified conditions: 50°C for 2 and 95°C for 10 min, 40 cycles each of 95°C for 15 sec and 60°C for 1 min. Final extension time was 10 min at 72°C (Fig. 2.5).

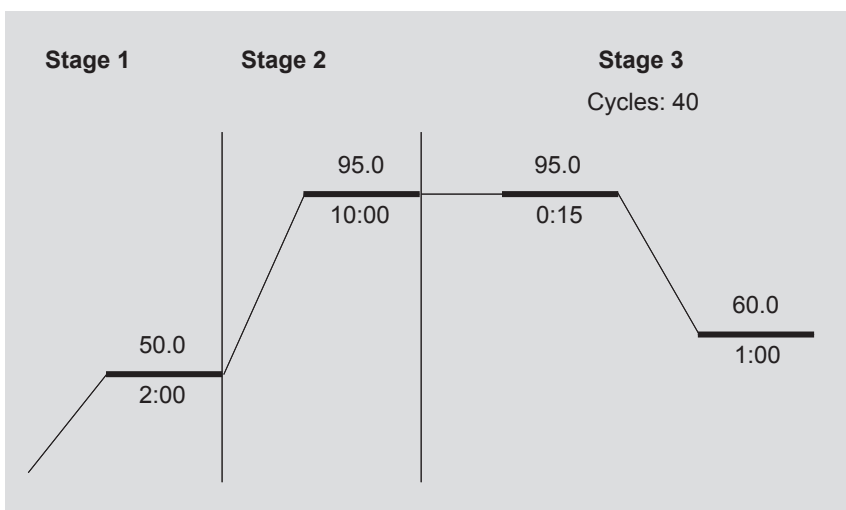


Figure 2.5 | 5' nuclease assay PCR thermal cycling profile.

End-point PCR analysis of 5' Nuclease assay

SNP variation was assessed using the allelic discrimination assay employing the software package SDS 2.1. Genotype-calls were determined visually by inspection of the XY scatter plot. When performing the allelic discrimination task, the auto-call feature of the SDS software was not enabled.

If ambiguous SNP results emerged, such as a data points being visual outliers and not ascribable to clusters of dots, the real-time data (kinetics) of the corresponding samples were examined in the absolute quantification diagram (amplification plot) and either received a definite call or were excluded from further analysis. In case of latter, the DNA concentrations in the master plate were re-measured and correspondingly diluted or concentrated to $20 \text{ ng } \mu\text{l}^{-1}$ and then re-tested in a second PCR. Finally, approved genotype results from SDS software were exported into an Excel spreadsheet. Sample positions on plates were aligned with DNA IDs and clinical forms relapsing remitting or primary progressive MS and healthy controls, respectively.

2.8 MS patients and controls

A total number of 287 unrelated affected individuals were included in the study. All subjects were of Spanish origin and satisfied Poser criteria for clinically definite MS.¹⁵⁸ There were 192 patients with relapsing-remitting MS (RRMS) and 95 with primary-progressive MS (PPMS). The control population comprised of 285 unrelated individuals recruited at the Vall d'Hebron hospital transfusion centre, which serves the geographic area from where the patients were enrolled. The study was approved by the Ethics Committee of Vall d'Hebron University Hospital and all the subjects involved in the study gave written informed consent. A summary of demographic and baseline clinical characteristics of MS patients and healthy controls is shown in Table 2.8.

Table 2.8 | Demographic and baseline clinical characteristics of MS patients and healthy controls used in the SNP genotyping.

Characteristics	HC (n = 285)	MS (n = 287)	RRMS (n = 192)	PPMS (n = 95)
Female/male (% women)	169/116 (59.3)	169/118 (58.9)	120/72 (62.5)	49/46 (51.6)
Age (years) ^a	40.3 (11.4)	43.0 (12.3)	37.8 (10.1)	53.5 (9.5)
Duration of disease (years) ^a	–	11.4 (7.1)	10.4 (6.4)	13.4 (8.0)
Age at disease onset (years) ^a	–	31.6 (10.8)	27.4 (8.8)	40.3 (9.3)
EDSS ^b	–	3.5 (4.0)	2.0 (2.0)	6.0 (3.0)

^aData are expressed as mean (SD). ^bData are expressed as median (interquartile range).

2.9 SNP selection for two genomic regions of interest

In order to validate candidate genes mapping to significant windows (see section 3.2), two genomic regions of interest on chromosome 3 and 10 were selected. The approach consisted of an indirect two-stage strategy, namely a screen by means of evenly spaced SNP markers and in the case of a subsequent detection of associative evidence with MS, an implementation of additional SNP markers in the vicinity of significant SNPs, applied on an increased sample size. This should enhance the marker density and hence further limit specified sequence range linked with potential disease causing variant(s) in the genome.

Table 2.9 | Details of 24 TaqMan® 5' Nuclease assays, commercially available through the Assay-On-Demand service (Applied Biosystems). SNP numeration was arbitrarily.

#SNP	Chr.	Cytogenetic Band	Location Celera Assembly	Context Sequence	Design Strand	Gene Symbol	Gene Name	NCBI Gene Reference	NCBI SNP Reference	Celera ID	SNP Type	MAF - Cauc
3	3	3p25.3	11.549.296	...GAGATGT[C/G]GTTAGCA...	Reverse	APG7L	ubiquitin activating enzyme E1-like protein (Interim)	NM_006395	rs2447605	hCV3008178	Intron	.11
5	3	3p25.3	11.556.076	...CTTGGGT[G/T]GTTCTGA...	Forward	APG7L	ubiquitin activating enzyme E1-like protein (Interim)	NM_006395	rs2616538	hCV3008180	Intron	.20
7	3	3p25.3	11.582.235	...GGTGAGA[C/G]AGTCAGC...	Forward	VGLL-4	Transcription cofactor vestigial-like protein 4	NM_014667	rs892937	hCV3008193	Intron	.38
24	3	3p25.3	11.585.729	...ATTACCC[A/G]TGGAAGT...	Forward	VGLL-4	Transcription cofactor vestigial-like protein 4	NM_014667	rs730178	hCV626612	Intron	.20
3	3	3p25.3	11.587.807	...GAATGCC[A/G]CCACAGC...	Forward	VGLL-4	Transcription cofactor vestigial-like protein 4	NM_014667	rs7622409	hCV3008198	Intron	.48
20	3	3p25.3	11.599.211	...GAAGGCA[A/C]GATGCAT...	Forward	VGLL-4	Transcription cofactor vestigial-like protein 4	NM_014667	rs892932	hCV3008207	Intron	.13
11	3	3p25.3	11.626.896	...AAAAGCC[C/G]TGACGTG...	Forward	VGLL-4	Transcription cofactor vestigial-like protein 4	NM_014667		hCV3008220	Intron	.38
**										hCV7990454	Intergenic / Unknown	.34
14	3	3p25.3	11.695.000	...AGTGGCT[C/T]TTGCTTA...	Forward							
**												
15	3	3p25.3	11.708.124	...GTCTTACI[A/C]GTGGCTG...	Reverse				rs2030066	hCV2720039	Intergenic / Unknown	.40
2	3	3p25.3	11.738.001	...TTAAAGC[C/T]CGGAAGG...	Reverse					hCV2720058	Intergenic / Unknown	.35
4	10	10q22.1	71.690.663	...CACCTAT[G/T]CTTAGCT...	Forward					hCV1799188	Intergenic / Unknown	.33
16	10	10q22.1	71.703.180	...CTTCCGA[A/G]TGCGCCT...	Forward	PRF1	perforin 1 (pore forming protein)	NM_005041, BC047695, X13224, M28393	rs885822	hCV1799201	Silent mutation	.38
1	10	10q22.1	71.704.641	...ATTGGAG[A/G]ACTCTGC...	Forward	PRF1	perforin 1 (pore forming protein)	NM_005041		hCV1799202	Intron	.28
**												
6	10	10q22.1	71.786.645	...TCCAGTG[C/T]CACTCTG...	Forward	ADAMTS14	a disintegrin-like and metalloprotease *	NM_139155, NM_080722		hCV1229664	Intron	.19
19	10	10q22.1	71.794.022	...GATGATG[A/G]CATTGCG...	Forward	ADAMTS14	a disintegrin-like and metalloprotease *	NM_139155, AF358666, AF366351, AJ345098	rs4747075	hCV1229671	Intron	.30
8	10	10q22.1	71.801.641	...TGGCAA[C/G]GTAGGCT...	Forward	ADAMTS14	a disintegrin-like and metalloprotease *	NM_139155, NM_080722	rs7081273	hCV1229684	Intron	.29
23	10	10q22.1	71.808.365	...TAGGCGT[G/A]CCTGTCT...	Forward	ADAMTS14	a disintegrin-like and metalloprotease *	NM_080722, NM_139155, AF358666, AF366351, AJ345098		hCV11453368	Intron	.21
10	10	10q22.1	71.815.810	...GCGCGTG[A/G]AGAAATT...	Reverse	ADAMTS14	a disintegrin-like and metalloprotease *	NM_139155, NM_080722		hCV1229703	Intron	.26
21	10	10q22.1	71.821.387	...ATCTATA[C/T]TGGGTCA...	Reverse	ADAMTS14	a disintegrin-like and metalloprotease *	NM_080722, NM_139155, AF358666, AF366351, AJ345098	rs4746060	hCV11453336	Intron	.13
12	10	10q22.1	71.853.444	...GCTGAGG[A/G]CACCAAG...	Forward	ADAMTS14	a disintegrin-like and metalloprotease *	NM_139155, NM_080722		hCV1229765	Intron	.50
22	10	10q22.1	71.861.562	...TCAGAGT[A/T]AGAGTGG...	Reverse	ADAMTS14	a disintegrin-like and metalloprotease *	NM_080722, NM_139155, AF358666, AF366351, AJ345098		hCV1229794	Intron	.35
13	10	10q22.1	71.876.300	...CTCTTCTT[A/G]CACCCAT...	Forward	C10ORF27	chr 10 open reading frame 27	NM_139155, NM_080722, NM_152710	rs2791196	hCV1229824	Intron	.35
17	10	10q22.1	71.879.610	...CAGGATC[C/T]GACACAG...	Reverse	C10ORF27	chr 10 open reading frame 27	NM_152710, AK057382	rs2254174	hCV9709031	Mis-sense mutation	.13
18	10	10q22.1	71.880.525	...CTCCCA[G/A]AGGTCGG...	Forward	C10ORF27	chr 10 open reading frame 27	NM_152710, AK057382		hCV229116	Intron	.29

* (reprolysin type) with thrombospondin type 1 motif, 14

** Location microsatellite marker in genome: D3S3714 – 11,643,609 bp; D3S3680 – 11,700,958 bp; D10S537 – 71,739,931 bp; D10S1685 – 71,823,494 bp

In total, the screen stage was performed with 15 SNPs (#1 to 15) on 383 DNA samples (Fig. 2.6a; 2.7a) and the second stage was completed with additional 9 SNPs (#16 to 24) and 189 samples, reaching a final 24 SNP markers tested on 383 and 16 SNPs of those on 572 individuals, respectively (Tab. 2.9 and Fig. 2.6b and 2.7b).

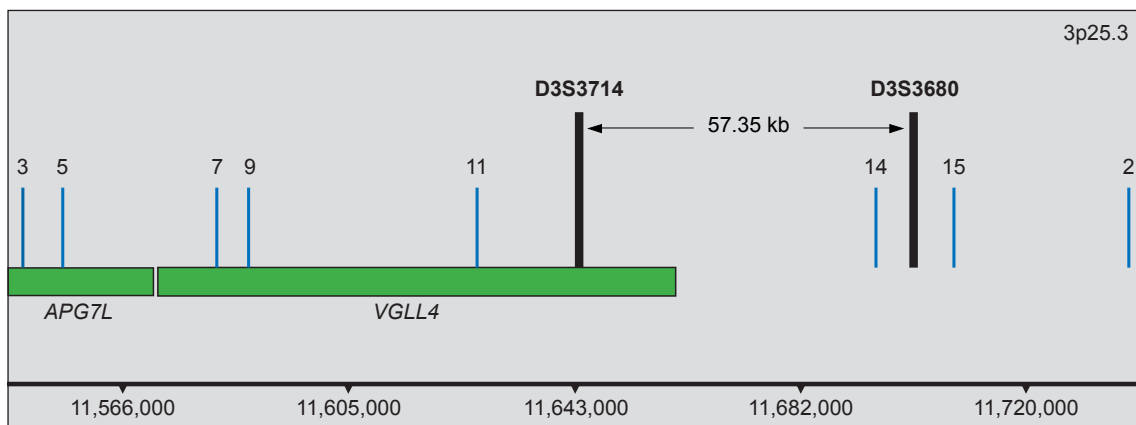


Figure 2.6a | Genomic region 3p25.3 covered with 2 microsatellite and 8 SNP markers; former tested with 400 DNA samples in 2 pools and latter individually in 383 DNA samples. (D3S3714: 11,643,609 bp; D3S3680: 11,700,958 bp)

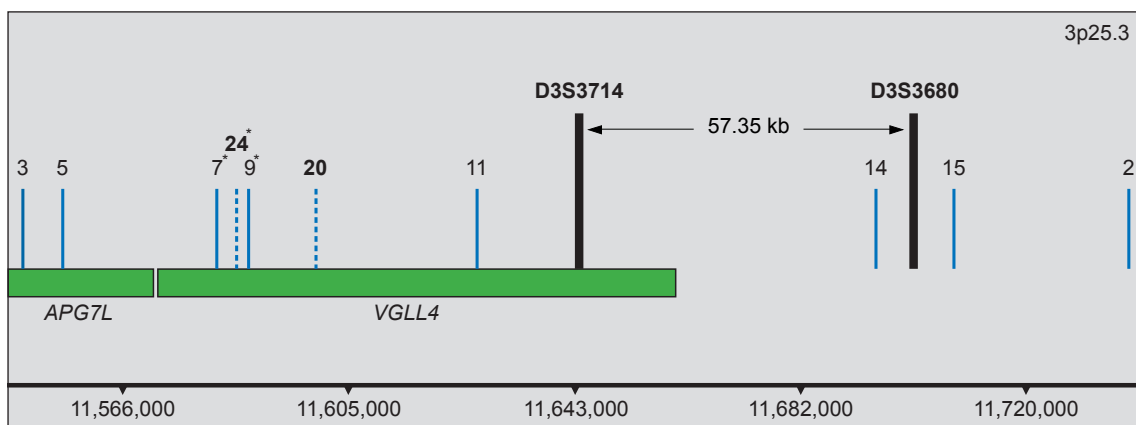


Figure 2.6b | Genomic region 3p25.3 covered with 2 microsatellite and 10 SNP markers; former tested with 400 DNA samples in 2 pools and latter individually in 383 DNA samples; SNPs #7, 24 and 9 in 572 DNA samples, indicated with an asterisk. (D3S3714: 11,643,609 bp; D3S3680: 11,700,958 bp)

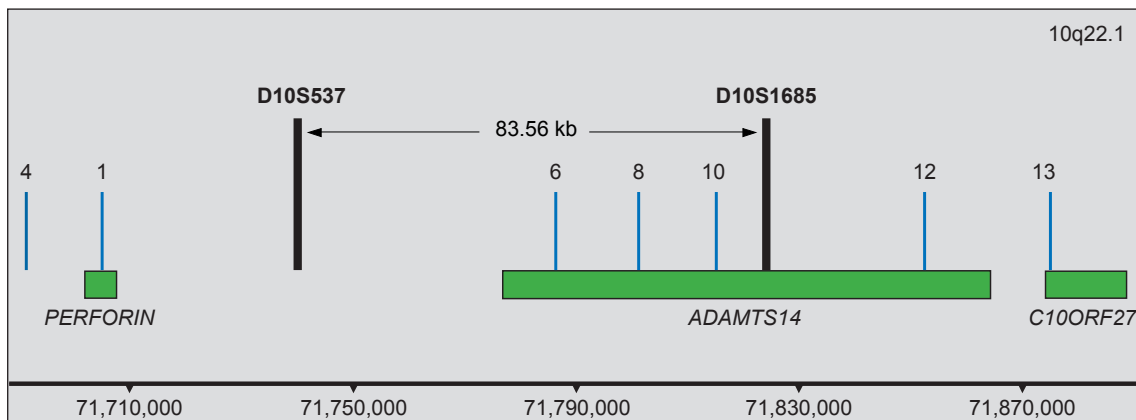


Figure 2.7a | Genomic region 10q22.1 covered with 2 microsatellite and 7 SNP markers; former tested with 400 DNA samples in 2 pools and latter individually in 383 DNA samples. (D10S537: 71,739,931 bp; D10S1685: 71,823,494 bp)

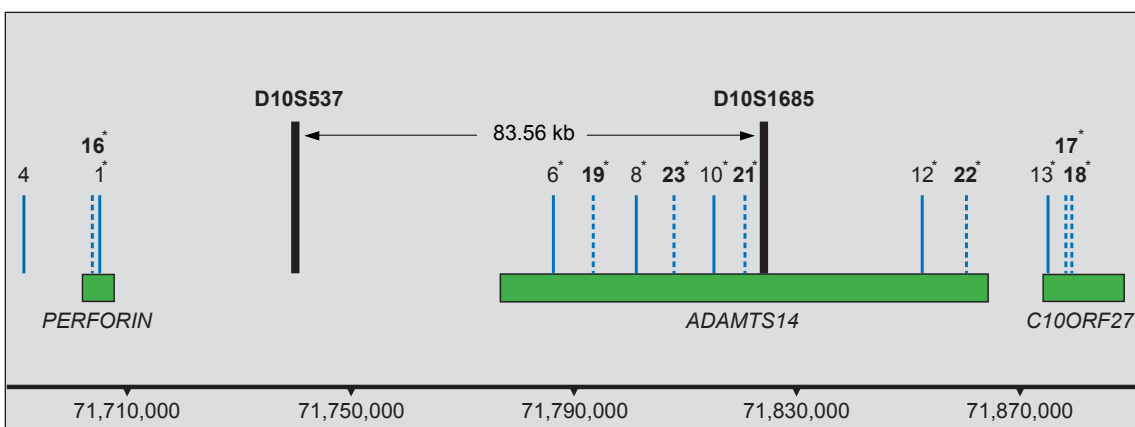


Figure 2.7b | Genomic region 10q22.1 covered with 2 microsatellite and 14 SNP markers; former tested with 400 DNA samples in 2 pools and latter individually in 383 DNA samples; apart from SNP #4, all SNPs were tested in 572 DNA samples, indicated with an asterisk. (D10S537: 71,739,931 bp; D10S1685: 71,823,494 bp)

Figures 2.6 and 2.7 depict both microsatellite marker and SNP localizations. Solid black and blue bars indicate the microsatellite (D3S3714: 11,643,609 bp; D3S3680: 11,700,958 bp; D10S537: 71,739,931 bp; D10S1685: 71,823,494 bp) and SNP positions, respectively, based on the NCBI built 34 and the Celera Discovery System™ SNP data. Dotted blue bars (SNPs 16 to 24) represent SNP markers of the second stage. SNP markers indicated with an asterisk were typed with 572 individual DNA samples.

2.10 SNP-Genotyping data handling

2.10.1 Allelic discrimination

The end-point PCR analysis of a 5' Nuclease assay incorporates the concept of genotypic segregation of samples within the allele plot (allelic discrimination).

A scatter plot of the assay results for SNP19 is shown in Figure 2.8. This plot represents the results of 384 assay reactions derived from 383 individuals and one control reaction without nucleic acid. For SNP 19, the allele G-specific probe was labeled with the fluorescent reporter dye FAM, and the allele A-specific probe was labeled with fluorescent reporter dye VIC. FAM intensity is measured on the Y-axis (vertical) and VIC intensity is measured on the X-axis (horizontal). Four distinct clusters of dots are evident. G/G homozygotes are clustered along the Y-axis, A/A homozygotes are clustered along the X-axis and the cluster within the center of the plot corresponds to A/G heterozygotes. The fourth cluster near the origin either corresponds to the well for which no DNA was

added as a control for DNA contamination or wells for which DNA samples were added but the PCR failed.

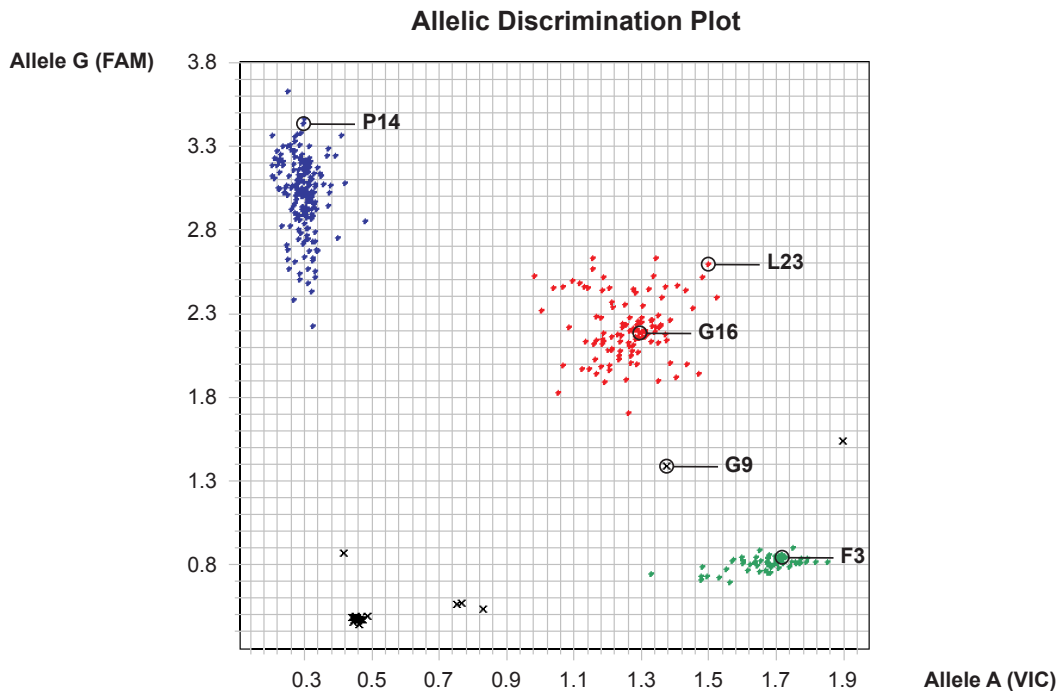


Figure 2.8 | Scatter-plot of 5' nuclease assay output for SNP 19 in intron 2 of ADAMTS14. Blue dots Allele G homozygotes (G/G), green dots Allele A homozygotes (A/A), red dots Heterozygotes (A/G), black square No-template control, black crosses Ambiguous output (outlier). Homozygotes for allele G showed an increased emission of the FAM dye along the Y-axis, due to cleavage of the reporter dye (FAM) into solution. Conversely, allele A homozygotes showed increased VIC dye emission along the X-axis, and heterozygotes, which underwent cleavage of both reporter dyes, are positioned between the two homozygote clusters in the center of the plot. Visual outlier did not cluster with neither of the 4 groups and were scrutinized by means of inspecting the kinetic characteristics of their corresponding real-time amplification curves.

2.10.2 Real-time amplification data

Examples of amplification plots of the 5' nuclease assay for SNP19 are shown in Figures 2.9, 2.10, and 2.11. Here, the amplification kinetics during the entire PCR are depicted. Baseline subtracted reporter dye (ΔRn) signal intensity is measured on the Y-axis and PCR cycle numbers are aligned on the X-axis. Each line in the plot represents the amplification curve of the reporter dyes FAM (blue) or VIC (green). In described data analysis only the characteristical kinetics of the curves during the geometrical (exponential) phases of the amplification were of concern.

Figure 2.9 displays the amplification curves of a typical homozygous G/G SNP result (#P14). Mainly the reporter dye FAM generates fluorescent emission whereas the probe constructed with the dye VIC is not cleaved into solution. This is due to non-existence of its specific allele, consequently it contributes merely with a minimal fluorescence signal. Conversely, figure 2.10 illustrates the reverse ratio of the reporter dyes in the homozygous A/A SNP outcome (#F3). The amplification curves exhibit increased fluorescence for reporter dye VIC in comparison to the course of the FAM curve, which displays a delayed rise in fluorescence and a less emitted signal on the whole.

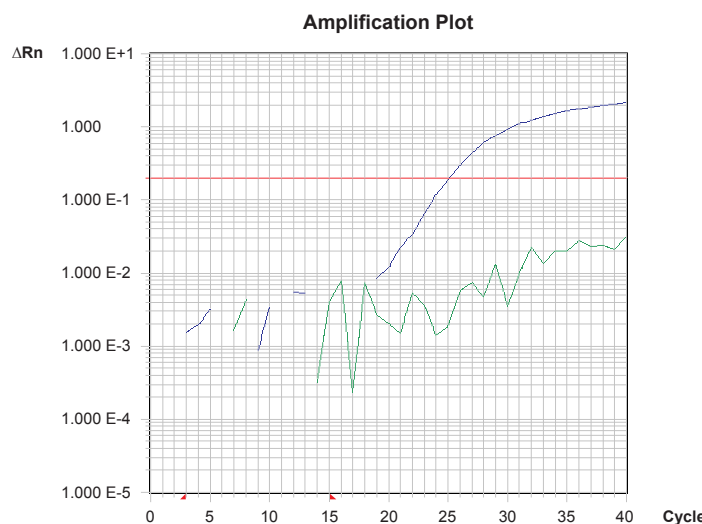


Figure 2.9 | Real-time amplification curves of Individual #P14 for intronic SNP19 in ADAMTS14. Blue: Reporter dye FAM, Green: Reporter dye VIC.

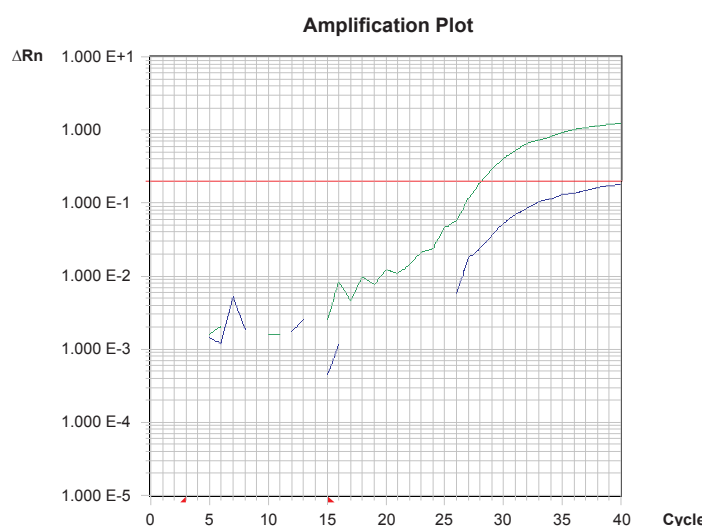


Figure 2.10 | Real-time amplification curves of Individual #F3 for intronic SNP19 in ADAMTS14. Blue: Reporter dye FAM, Green: Reporter dye VIC.

Finally, figure 2.11 delineates three pairs of curves corresponding to fluorescence signals of both reporter dyes from #L23, #G16, and #G9, determinating the heterozygous A/G status. Of these three assays, sample #L23 beared the highest initial DNA concentration as fewer PCR cycles were required to arrive at the threshold setting (red horizontal line). Then follows #G16 and ultimately #G9, latter was an outlier in the scatter plot (Fig. 2.8), but exhibited apparent similar kinetic aspects consisting of two parallel amplification curves for both reporter dyes during the real time progression of the PCR.

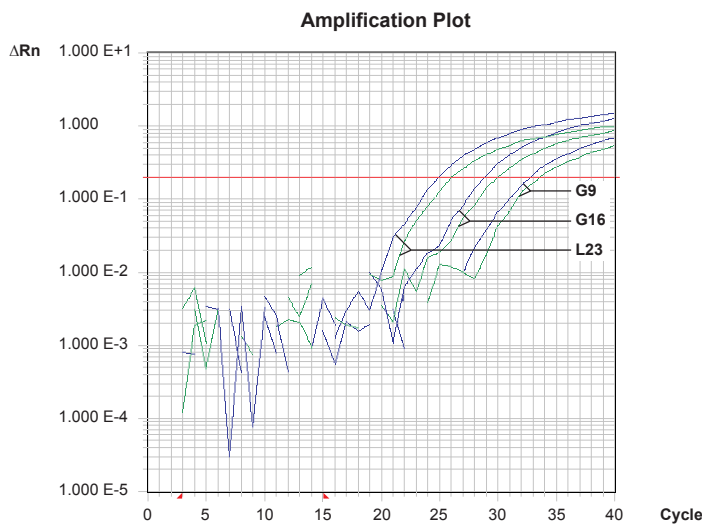


Figure 2.11 | Real-time amplification curves of Individuals #L23, #G9, #G16 for intronic SNP19 in ADAMTS14. Blue: Reporter dye FAM, Green: Reporter dye VIC

The ratios of described assays according to initial DNA content and amplification characteristics are reproduced in the scatter plot of the end-point analysis in Figure 2.8. Here, basically, the absolute quantification of emitting substances in each assay serves as the basis for data point distribution. Thus, the data points for sample #L23 ($Rn_{FAM;VIC} = 2.59;1.51$) was allocated at the top of the center cluster, #G16 ($Rn_{FAM;VIC} = 2.18;1.28$) was situated in the midsection and #G9 ($Rn_{FAM;VIC} = 1.39;1.38$) lied outside below the cluster. According to their positions in the scatter plot that described a specific sequence ($Rn_{L23} > Rn_{G16} > Rn_{G9}$), the amplification curves of these samples demonstrated the equivalent ratios, though shifted due to their time courses (cycle numbers). In conclusion, the similarity of the amplification kinetics from assay #G9 permitted the heterozygous A/G genotype assignment and use in further analysis.

The remaining outliers in the scatter plot were inspected for indicative characteristics

in their corresponding real-time data and to a great extent excluded. Based on the analysis, their DNA contents were re-measured and consequently adjusted or new assay solutions prepared and re-tested in a further PCR session.

2.11 Analytical tools for describing genomic structure and detecting disease association

The two-stage approach of the here described study included an overall test for association of genotypes for all 24 SNP markers tested on 383 individuals, and subsequently a more exhaustive scrutiny of 16 SNPs that were tested on 574 individuals.

Equipment

Statistical software packages:

Arlequin v.2.0	Anthropology and Ecology, Univ. of Geneva, Geneva, Swi
Haplovview	Whitehead Inst. for Biomedical Research, Cambridge, Ma, USA
SPSS 11.5	SPSS Inc, Chicago, IL, USA
PHASE 2.0.2	Dept. Statistics, Univ. of Washington, Seattle, Wa, USA

2.11.1 Descriptive analyses

Standard descriptive statistics for case and control populations, including allele and genotype frequencies in each group, were generated using a number of commercially available and open-source statistical packages. Hardy-Weinberg proportions and pairwise linkage disequilibrium between SNPs were tested as for the marker loci and haplotype data. A variety of techniques to investigate SNP-disease associations was applied. These included both single SNP associations and extended analyses of reassembled haplotypes and individually assigned haplotype pairs.

2.11.1.1 Establishing Hardy-Weinberg equilibrium (HWE) in population samples

When studying population genetics, the χ^2 -goodness-of-fit test for Hardy-Weinberg equilibrium (HWE; equation $p^2 + 2pq + q^2$)¹⁵⁹ was required to be verified. It estimates the expected allele frequencies in a given population and delivers potential deviation of investigated marker loci on tested samples. The calculation of HWE also served as a coarse quality check on the data as experience suggests that gross deviations from

HWE could indicate genotyping errors.¹⁶⁰ HWE was tested for significant departure at each SNP locus on a contingency table of observed versus predicted genotype frequencies using Arlequin v2.0.

2.11.1.2 Linkage Disequilibrium (LD) determination by software Haplovie

Linkage Disequilibrium (LD) is defined as the appropriate measure for non-random association of alleles in a chromosomal segment, which is eroded by gene conversion and recombinatorial activity in the genome.¹⁰¹ The amount of LD depends furthermore on the age of the mutations and the demographic history of a population.¹⁰¹ The standardized coefficient of LD, D',¹⁰² measures linkage between pairs of loci and was calculated applying the Haplovie software,¹⁶¹ which is based on a four gamete rule of block definitions, a variant on the algorithm described in Wang *et al.*¹⁶²

2.11.2 Case-control association analyses

Allelic frequency comparisons were based on contingency tables and if required, the Fisher's exact test was employed (SPSS). The global case-control analysis of genotypes was based upon the use of 2x3 contingency tables generating overall χ^2 and corresponding p-values. This approach served as a primary indicator of potential differences between distributions in cases and controls and was applied in the screening stage of the study only. The following single genotype case-control analysis was realized by means of 2x2 contingency tables. Statistical significance was defined at the standard 5% level. In addition, summary statistics such as risk parameter odds ratio (OR) and the interrelated quality term 95% confidence interval (95% CI) were ascertained.

2.11.2.1 Single SNP-disease association analyses

χ^2 estimation of allele and genotype comparisons were performed and minor allele frequencies derived. These were cross-checked for agreement with publicly stated prevalence in Caucasians, stated by Applied Biosystems (Tab. 2.9). The single genotype comparisons were performed as follows: a genotype count was always contrasted to the sum of remaining two genotypes. For example, SNP#9 is an A/G variant and displayed following distributions in tested samples:

MS: AA = 68; AG = 128; GG = 91

HC: AA = 61; AG = 156; GG = 68

“AA” counts were compared with the sum of “AG” and “GG” and further genotype combinations with the respective sums of the contrasting composites.

Gentotype counts inserted in a 2x2 contingency table:

	AA	AG+GG	Total
MS	68	219	287
HC	61	224	285
Total	129	443	1144

p=0.512; OR=1.1; 95%CI=0.8-1.7

	AG	AA+GG	Total
MS	128	159	287
HC	156	129	285
Total	284	288	1144

p=0.015; OR=0.7; 95%CI=0.5-0.9

	GG	AA+AG	Total
MS	91	196	287
HC	68	217	285
Total	159	413	1144

p=0.036; OR=1.5; 95%CI=1.0-2.1

2.11.2.2 Haplotype-disease association analyses

A haplotype is the pattern of alleles on a single chromosome and has been described in more detail before (see Introduction 1.7). Having genotyped the study populations with the increased sample size (n=572) at derived candidate loci, observed genotypes for every individual entered the extended analysis.

Phase determination by PHASE

Haplotypes and assignment of haplotype-pairs to each individual were obtained by using the PHASE program.^{163,164} It implements a Bayesian statistical method to reconstruct haplotypes from unphased population genotype data. This approach is indispensable and represents a reasonable alternative to laborious time- and finance-consuming DNA sequencing efforts. First, global haplotype compositions and corresponding frequencies were assigned to each group (as indicated in Tab. 2.10) and subsequently analyzed. As a further approximation to the genuine situation of studied populations, the program estimates probabilities for the occurrence of specific composite genotypes that define

two specific haplotypes, hence the haplotype pair of an individual. Possible uncertainty in the reconstruction stage that could lead to spurious conclusions was compensated by excluding haplotype pairs that did not exceed the accuracy threshold set at 90%.

Table 2.10 | Example of PHASE software output. Outlined are the software generated possibilities of reassembled haplotype pairs for an individual and the respective probability values. If latter exceeded 0.9, the corresponding haplotype pair was included in further analysis.

INDIVIDUAL: #		
	1 st reconstructed haplotype, 2 nd reconstructed haplotype, probability	3 rd reconstructed haplotype, 4 th reconstructed haplotype, probability
	5 th reconstructed haplotype, 6 th reconstructed haplotype, probability	
IND: #9		
GCGCT , ACGCT , 1.000	→	included in analysis
IND: #10		
ACGCA , ACGCA , 1.000	→	included in analysis
IND: #11		
GGGCA , ACGCA , 0.986	→	included in analysis
GCGCA , AGGCA , 0.014	→	excluded from analysis
IND: #12		
GCGCT , GCGCT , 1.000	→	included in analysis
IND: #13		
GGGCT , GGGTT , 1.000	→	included in analysis
IND: #14		
GGATA , ACGCT , 0.123	→	excluded from analysis
GGATT , ACGCA , 0.848	→	excluded from analysis
GGGCA , ACATT , 0.016	→	excluded from analysis
IND: #15		
GGGCA , ACGCT , 0.033	→	excluded from analysis
GGGCT , ACGCA , 0.923	→	included in analysis
GCGCA , AGGCT , 0.013	→	excluded from analysis
GCGCT , AGGCA , 0.031	→	excluded from analysis
IND: #16		
GGACA , GGGTT , 0.032	→	excluded from analysis
GGACT , GGGTA , 0.013	→	excluded from analysis
GGATA , GGGCT , 0.441	→	excluded from analysis
GGATT , GGGCA , 0.513	→	excluded from analysis

χ^2 estimation of reconstructed haplotype frequency comparisons were performed based on designation to respective groups. Employing the program SPSS, haplotype numbers of specific categories (MS clinical forms and healthy controls) were entered into 2x2 contingency tables and corresponding p-values and summary statistics were ascertained. The same was completed with counts of haplotype pairs. As shown in Table 2.11, assembled and accuracy-controlled haplotype pairs for every individual were designated to respective groups and counted.

Table 2.11 | Example of reassembled haplotype pair counts. Clinical and haplotype features of tested individual #13 are outlined and categorized.

Individual #13; RRMS; 5 loci	
	100% accurately assembled haplotype pair
	GGGCT (Haplotype 1); GGGTT (Haplotype 3)
→	1 count in category “RRMS, haplotype 1”
→	1 count in category “RRMS, haplotype 3”
→	1 count in category “RRMS, Pair H1/H3”

2.12 Accounting for multiple testing

The computation of significance tests on several sets of loci of identical individuals produces a bias and increases the detection of significance due to chance alone,¹⁶⁵ generating type I errors (false positives). The Bonferroni correction¹⁶⁶ was applied to control for multiple testing.

3

RESULTS

3.1 Genotyping of DNA Pools with microsatellite markers	64
3.2 Application of sliding windows on DNA pool data	66
3.2.1 Descriptive part	66
3.2.2 Sieving MS candidate regions and genes	71
3.3 Genotyping of individual DNA by means of single nucleotide polymorphism marker	79
3.3.1 Yield of applied 5' Nuclease assay	79
3.3.2 Hardy-Weinberg equilibrium (HWE) in healthy control and multiple sclerosis population samples	81
3.3.3 Linkage Disequilibrium block formation at genomic regions of interest 3p25.3 and 10q22.1	81
3.3.4 Detection of statistical significance derived from allele and single genotype comparisons	84
3.3.5 Correction for multiple testing through Sequential Bonferroni	88
3.4 Single gene inspection: haplotype analysis	89
3.4.1 <i>VGLL4</i> - Transcription cofactor vestigial-like protein	90
3.4.2 <i>PRF1</i> – Perforin	91
3.4.3 <i>ADAMTS14</i> - a disintegrin-like and metalloproteinase domain with thrombospondin type 1 modules 14	92
3.4.4 <i>C10orf27</i> – Chromosome 10 open reading frame 27	96
3.5 Combined gene haplotypes based on ascertained data of <i>ADAMTS14</i> and <i>C10orf27</i>	99

3.1 Genotyping of DNA Pools with microsatellite markers

Two pools of DNA were created and genotyped on a specified marker set: one consisting of 200 MS patients and the other of 200 controls. In total, of 5543 tested microsatellites in the initial screen, 5131 experiments generated satisfactory results from both pools, suiting described statistical analysis for evidence of association (Section 2.5). 472 markers were selected for an additional genotyping run on the basis of being potentially associated with either group. Applying stringent exclusion criteria on the replicate data, 191 markers were classified significant due to consistent empirical p-values below 0.05 and an unchanging peak count ratio of Pool A versus Pool B (Tab. 3.1). Eight positively associated markers on chromosome 6 map to the MHC region 6p21 (D6S459, D6S2444, D6S1017, D6S1014, TNF α , SA99, HO16369, G511525) that had repeatedly been reported to be associated with MS in preceding linkage analyses.^{53,54,141,144-148} This can be regarded as a good validation of the study's completion. In addition, 33 indicated markers outside 6p21 represented regions of particular interest for MS susceptibility in various genome-wide linkage scans or independent association studies.¹⁶⁷⁻¹⁷⁴ The remaining 150 microsatellite markers indicate novel evidence of associations at loci not previously implicated in susceptibility to multiple sclerosis.

Table 3.1 | Results for 191 twice significantly (empirical p<0.05, degree of freedom=1) associated markers. The smaller of two p-values is displayed, ranked according to greatest evidence for association; Rn: rank position; Com: comment (see table footnote); MHC: Major Histocompatibility Complex.

Rn	Marker	Com	Locus	P, df=1	Rn	Marker	Com	Locus	P, df=1
1	SA-99	° MHC	6p21.3	2.8*10-8	97	D19S565		19p13.3	0.015
2	D9S303*		9q21.32	4.5*10-6	98	D4S398	°	4q13.1	0.016
3	D18S52*	°	18p11.31	0.00001	99	D20S196		20q13.13	0.016
4	D16S2613*	°	16p13.11	0.00002	100	D3S2457		3q13.31	0.016
5	D6S1955	MHC	6p24.3	0.00005	101	D17S900		17p11.2	0.016
6	HO16369		6p21.2	0.00014	102	D5S1721	°	5q21.3	0.017
7	D1S2852		1p13.1	0.00016	103	D12S1301		12q12	0.017
8	D13S1236		13q12.11	0.00019	104	D3S1270		3p26.3	0.017
9	D10S1795		10q25.1	0.00021	105	D16S3083		16q23.1	0.018
10	D1S533		1q31.3	0.00024	106	D12S2077		12q22	0.018
11	G511525	MHC	6p21.3	0.00038	107	D13S263		13q14.3	0.019
12	D19S921		19q13.42	0.00050	108	D19S552		19q13.2	0.019
13	D13S777*		13q21.32	0.00052	109	D6S1284		6q16.2	0.019
14	D1S398		1q23.2	0.00064	110	D13S1491		13q14.11	0.020
15	D5S1953		5p15.2	0.00070	111	D3S3050		3p26.2	0.020
16	D9S1868		9p21.1	0.00081	112	D12S1710		12q21.33	0.020
17	D22S692*		22q12.3	0.0010	113	D7S2847		7q31.31	0.020
18	D9S157		9p22.2	0.0010	114	D18S51		18q21.33	0.020
19	DXS981		Xq13.1	0.0015	115	D18S872		18q12.3	0.020
20	D6S1017	° MHC	6p21.1	0.0016	116	D20S846		20p12.3	0.020
21	D12S1344		12q24.12	0.0018	117	D2S2241		2q23.3	0.021
22	D21S1435		21q21.3	0.0019	118	D3S1754		3q26.32	0.022
23	D6S2444	MHC	6p21.32	0.0020	119	D3S2422		3q13.13	0.023

Rn	Marker	Com	Locus	P, df=1	Rn	Marker	Com	Locus	P, df=1
24	D7S1818		7p12.3	0.0020	120	D17S974		17p12	0.023
25	D1S532		1p31.1	0.0021	121	D6S1961	°	6q24.1	0.023
26	D4S2987		4q13.2	0.0025	122	D7S679		7p13	0.023
27	D5S2076	°	5q11.2	0.0026	123	D1S513		1p35.2	0.023
28	D20S112		20p12.1	0.0029	124	D6S1662		6p12.1	0.024
29	D6S1275		6q12	0.0031	125	D7S1808		7p15.1	0.024
30	D3S3695		3q13.13	0.0033	126	D20S471		20p11.23	0.024
31	D14S588		14q24.1	0.0033	127	D8S543		8q13.2	0.025
32	D17S1290	°	17q22	0.0033	128	D9S270		9p21.1	0.025
33	D11S4453		11q14.1	0.0035	129	DXS8037		Xq13.3	0.026
34	D17S1293		17q12	0.0036	130	D4S2426	°	4q33	0.027
35	D3S2387		3p26.3	0.0036	131	D5S2089	°	5q12.3	0.027
36	D3S3693		3p25.2	0.0037	132	D5S423		5q34	0.027
37	D5S804		5q23.2	0.0038	133	D1S2737		1p31.3	0.028
38	D6S459	° MHC	6p21.1	0.0041	134	D14S275		14q12	0.028
39	D20S186		20p12.2	0.0042	135	D7S1796	°	7q21.3	0.028
40	D17S1303		17p11.2	0.0043	136	D2S309		2q33.1	0.029
41	D15S817		15q11.2	0.0045	137	D12S1042		12p11.23	0.029
42	D5S494		5q23.1	0.0046	138	D4S1560		4q22.3	0.029
43	D2S1363		2q36.1	0.0046	139	D4S2640		4q21.21	0.030
44	D10S2327		10q22.3	0.0049	140	D18S973		18p11.31	0.030
45	D13S290		13q13.1	0.0054	141	D12S2074		12q21.2	0.030
46	D3S2388		3p12.1	0.0055	142	D2S290		2p14	0.030
47	D20S603		20p12.3	0.0056	143	D11S1983		11q12.1	0.030
48	D5S1722	°	5q14.3	0.0062	144	D1S478	°	1p36.12	0.031
49	D4S404		4p15.1	0.0063	145	D4S2431	°	4q34.1	0.031
50	D8S1122		8q23.1	0.0064	146	D15S118		15q14	0.031
51	D5S815	°	5q14.3	0.0065	147	D1S1606	°	1p36.12	0.032
52	D1S2138		1q31.1	0.0066	148	D6S1277	°	6q26	0.032
53	DXS993		Xp11.4	0.0068	149	D19S724	°	1p36.22	0.032
54	D2S428		2p11.2	0.0073	150	D8S1988		8q22.1	0.032
55	D22S1159	°	22q13.31	0.0074	151	D4S2936	°	4q35.1	0.033
56	D18S865		18q12.3	0.0075	152	D2S2392	°	2q32.1	0.033
57	DXS6807		Xp22.32	0.0076	153	D3S1613	°	3p21.2	0.033
58	D7S2537	°	7q21.11	0.0077	154	D7S2415		7q11.22	0.033
59	D9S907		9q33.1	0.0078	155	D9S1782	°	9p22.3	0.034
60	D12S392		12q24.33	0.0078	156	D16S539		16q24.1	0.034
61	TNF α	MHC	6p21.33	0.0079	157	D7S1834		7p14.3	0.035
62	D3S4534		3q13.11	0.0080	158	D16S515		16q23.1	0.035
63	D4S1625	°	4q31.1	0.0085	159	D3S3515		3q13.32	0.035
64	D15S120		15q26.3	0.0086	160	D6S1004		6q15	0.035
65	D14S605		14q32.2	0.0087	161	D3S1759		3p23	0.035
66	D2S394		2p11.2	0.0089	162	D6S290	°	6q25.2	0.036
67	D2S386		2p15	0.0090	163	D14S1280		14q12	0.037
68	D17S808	°	17q23.2	0.0098	164	D14S739		14q31.1	0.037
69	D12S1648		12p11.2	0.010	165	DXS1001		Xq24	0.037
70	D16S2621		16q24.2	0.010	166	D14S614		14q32.2	0.037
71	D20S469		20q13.2	0.010	167	D11S1353		11q24.1	0.038
72	D21S1809		21q22.2	0.011	168	D2S165	°	2p23.2	0.038
73	D19S888		19q13.42	0.011	169	D1S2720		1p31.1	0.039
74	D4S405		4p14	0.011	170	D17S810	°	17q22	0.039
75	D12S320	°	12p13.1	0.011	171	D5S1478		5q23.1	0.039
76	D18S976		18p11.31	0.011	172	D3S3611		3p25.3	0.039
77	D6S1014	° MHC	6p21.32	0.011	173	D12S311		12q21.33	0.039
78	D3S3022	°	3q24	0.012	174	D16S3096		16q23.1	0.042

Rn	Marker	Com	Locus	P, df=1	Rn	Marker	Com	Locus	P, df=1
79	D5S1486		5p15.2	0.012	175	D9S301		9q21.12	0.042
80	D17S1603		17q25.1	0.012	176	D12S1653*		12q12	0.042
81	D4S3245*		4q22.1	0.012	177	D6S1021		6q16.3	0.043
82	D11S1396		11q14.1	0.013	178	D12S395		12q24.23	0.044
83	D16S497	*	16p13.11	0.013	179	D15S127		15q26.1	0.044
84	D10S221		10q26.11	0.013	180	D3S3026		3p21.31	0.045
85	D16S753		16p11.2	0.013	181	D12S393	*	12q23.1	0.045
86	D14S597		14q12	0.013	182	D6S1034		6p24.1	0.046
87	D19S434		19p12	0.013	183	D3S3668		3q26.1	0.046
88	D10S1685		10q22.1	0.013	184	DXS1002		Xp21.2	0.046
89	D20S486		20p11.21	0.014	185	D2S437		2q14.1	0.046
90	D12S1045		12q24.33	0.014	186	D7S663		7q11.21	0.047
91	D3S3052		3q26.1	0.014	187	D1S2636		1q32.1	0.047
92	D3S3509		3q25.2	0.014	188	D22S539		22q11.22	0.047
93	D6S1957		6q16.1	0.014	189	D17S917	*	17q23.2	0.048
94	D2S122		2q22.3	0.014	190	D7S527	*	7q21.3	0.048
95	D19S429		19p13.12	0.014	191	D8S1128		8q24.21	0.048
96	D3S2427		3q26.31	0.015					

* Selected microsatellite marker for individual genotyping on MS patients and healthy controls

° Previously associated with MS

3.2 Application of sliding windows on DNA pool data

3.2.1 Descriptive part

280 results of the initially 5131 markers had to be excluded from the analysis as corresponding genomic positions were not available from deCODE nor public databases; hence, they were labeled non-informative. Therefore, the sliding windows method was applied on empirical p-values of 4851 informative markers derived from the whole genome scan GAMES, exclusively of the first genotyping run.

Table 3.2 | Summary of sliding windows methodology applied to data derived from 4851 microsatellite marker, tested with pooled DNA of Spanish MS patients and healthy controls, respectively. cM: centi Morgan; sig: significant ($p<0.05$); Norm: normalized; wdw: window; CDP: cluster density position; smn: significant marker number; swn: significant window number.

Chr	Marker (n)	Marker density (m/cM)*	Total sig marker (n)	Norm sig marker (n)*	Window ($p<0.05$) (n) wdw sizes (cM)							Region of interest (total)	CDP (smn / swn)*
					0.5	1.0	1.5	2.0	2.5	3.0	sum		
1	534	1.9 ⁽¹⁾	39	20 ⁽⁵⁾	10	9	11	10	15	12	67	3 (7)	0.6 ⁽⁶⁾
2	371	1.4 ⁽⁶⁾	23	16 ⁽⁹⁾	3	7	9	9	12	10	53	2 (5)	0.4 ⁽³⁾
3	305	1.4 ⁽⁹⁾	35	26 ⁽¹⁾	8	10	7	6	5	4	40	3 (7)	0.9 ⁽¹²⁾
4	224	1.1 ⁽¹⁷⁾	22	21 ⁽⁴⁾	6	4	4	8	9	12	43	1 (3)	0.5 ⁽⁵⁾
5	241	1.2 ⁽¹⁴⁾	23	20 ⁽⁵⁾	3	6	9	10	14	15	57	2 (3)	0.4 ⁽¹⁾
6	298	1.5 ⁽³⁾	35	23 ⁽³⁾	9	12	13	14	16	17	81	2 (4)	0.4 ⁽²⁾
7	250	1.3 ⁽¹⁰⁾	25	19 ⁽⁷⁾	4	3	3	7	6	7	30	1 (4)	0.8 ⁽¹¹⁾
8	175	1.0 ⁽¹⁹⁾	15	14 ⁽¹⁴⁾	1	1	1	2	2	6	13	0 (3)	1.2 ⁽¹⁴⁾
9	192	1.2 ⁽¹³⁾	16	14 ⁽¹⁴⁾	2	2	1	1	1	0	7	0 (2)	2.3 ⁽¹⁸⁾
10	208	1.1 ⁽¹⁵⁾	17	15 ⁽¹³⁾	1	3	5	4	5	5	23	1 (3)	0.7 ⁽⁸⁾

11	294	1.9 (2)	30	16 (9)	2	2	3	5	2	2	16	0(5)	1.9 (17)
12	262	1.5 (5)	36	24 (2)	3	2	0	1	1	3	10	0(6)	3.6 (21)
13	120	0.9 (21)	11	12 (16)	0	0	1	2	4	2	9	0(2)	1.2 (15)
14	173	1.4 (8)	17	12 (16)	1	2	3	4	3	5	18	1(4)	0.9 (13)
15	171	1.2 (11)	9	7 (22)	0	0	0	0	0	1	1	0(1)	9.0 (22)
16	140	1.0 (20)	13	12 (16)	2	4	3	4	4	5	22	1(3)	0.6 (7)
17	192	1.4 (7)	14	10 (20)	0	2	4	4	5	2	17	0(2)	0.8 (10)
18	79	0.6 (22)	10	16 (9)	0	0	0	1	2	1	4	0(1)	2.5 (19)
19	173	1.5 (4)	24	16 (9)	2	0	0	0	2	4	8	0(4)	3.0 (20)
20	118	1.2 (12)	12	10 (20)	2	3	3	2	3	2	15	1(2)	0.8 (9)
21	50	0.6 (23)	7	11 (19)	0	1	0	1	1	1	4	0(1)	1.8 (16)
22	76	1.1 (16)	8	7 (22)	0	0	0	0	0	0	0	0	- (23)
X	205	1.1 (18)	19	18 (8)	2	7	8	9	7	7	40	1(3)	0.5 (4)
Σ	4851		460		61	80	88	104	119	123	578	19 (75)	

* Ranking order 1 to 23 when aligned for position, each column independently. The exponents in columns 3, 5 and 14 represent ranking order values; CDP (smn/swn): Cluster Density Position, ranking based on function significant marker number / significant window number.

460 informative markers revealed an empirical p-value below threshold set at 0.05 and 578 significant windows generated a total of 75 areas of interest (Tab. 3.2, column 13). These require further investigation in order to determine potential candidate regions harbouring candidate genes for MS susceptibility or resistance.

Table 3.2 provides with information confined to each chromosome and respective markers, the amount of significant markers and the degree of clustering of selfsames. The table should be examined in combination with the software output illustrations in Appendix C, which again can be cross-checked for agreement in the marker list (Appendix B). The first 3 columns indicate the analyzed chromosome, the total number of informative markers employed and the corresponding marker density per chromosome, ranked according to relative marker number per cM. Columns 4 and 5 display the total amount of significant markers per chromosome and the respective “normalized” marker amount. Latter was based on the total of significant markers divided by the marker density, incorporating thereby the recombinatorial landscape of each chromosome. The range of markers per cM extends from 0.6 to 1.9 and the distribution of significant markers appears non-random. Thus, ranking, a non-parametric tool for asymmetrical distribution of data, and normalization permitted the comparability between chromosomes.

The amount of significant windows that emerged, including those that overlap, were listed in accordance to window sizes and summarized (columns 6 to 12). Assessed regions of interest are specified in the penultimate column, expressing regions that appeared in all window sizes and in parenthesis the total of encountered regions per chromosome.

In order to describe the degree of clustering – how even or uneven significant markers are distributed over a chromosome – the last column displays ranking values resulting

from the interdependence of “normalized significant marker number per chromosome” (column 5) and “significant window number per chromosome” (column 12), labelled cluster density position (CPD). In spite of the normalization procedure, the relative numbers of assigned clusters varied considerably from chromosome to chromosome, indicating possibly regions of elevated association to MS.

When ranking positions of the distributions “marker density per chromosome” (column 3) and “amount of normalized significant markers per chromosome” (column 5) were compared, chromosomes 4, 18 and 17 deviated the most from expected order. Chromosomes 4 and 18 genotyping results disclosed proportionally more significant markers (Positions 17 -> 4 and 22 -> 9, respectively) whereas a reversed situation was seen in chromosome 17 (Position 7 -> 20). Chromosomes X and 5 (increased) and 14, 20, 15 (decreased) showed a similar pattern.

After ascertaining the over- or underrepresentation of significant markers on a chromosome as a whole, it is of interest of how these markers are organized on the respective strand. Comparing again ranking positions, chromosomes 17 (Position 20 -> 10), 16 (Position 16 -> 7), 20 (Position 20 -> 9) and 2 (Position 9 -> 3) showed the greatest “up”-relocations, hence a relatively increased degree of clustering. Conversely, chromosomes 12 (Position 2 -> 21), 18 (Position 9 -> 19) and 19 (Position 9 -> 20) contained proportionately few clustered significant markers. Nevertheless, determining the cluster density positions (columns 14) revealed most accumulation of significant markers on chromosomes 5 and 6.

Particular attention can be directed to Chromosome 6 which displayed the highest number of significant windows ($n=81$) and an elevated degree of clustering. As observed in the results table in Appendix C, one region, enclosing locus 6p21, contained windows with the highest number of accumulated significant markers ($n=7$). This is in good agreement with previous reports on MS susceptibility and the HLA region, validating the applied sliding windows method.

To assess the biological relevance of detected regions of interest, Table 3.3 provides a characterization displaying genome locations (cytogenetic band, genetic map information and nucleotide ranges), the corresponding publicly stated recombination rates (cM/Mb) and gene abbreviations that conform to HUGO gene symbols. Known genes were deduced from the November 2004 Genome Assembly (UCSC Genome Browser) and selected when located between or near – depending on the respective recombination rate, up to 20 kb – the outermost markers of a significant window. The table presents significant marker and window details, such as marker arrangement – if significant marker aligned contiguously or were interspersed by non-significant markers

– and significant marker number that constitute a significant window. The regions of interest on each chromosome appeared in order of the number of window sizes (0.5 to 3.0 cM; maximum 6) that were declared significant.

Table 3.3 | List of 75 loci of interest that contain 284 publicly known genes. Gene information was based on UCSC Genome browser (November 2004 Genome Assembly). Recombination rate assessed in centi Morgan per Megabase (cM/Mb).

Position	Region cM	Recomb. rate	in wdw size	Coverage (bp)	Nr. sig. marker	Marker positions	Known genes
1p21.1	126.6 - 128.4	1.1	6	1.316.503	3	not contiguous	no
1q23.2	157.4	1.9	6	0.020	2	contiguous	no
1q42.12	233.9 - 234.1	0.6	6	302.892	2	contiguous	H3F3A, ACBD3, MIXL1, TGS2
1q32.1	207.4 - 208.9	1.6	4	195.842	3	not contiguous	BTG2, FMOD, PRELP, OPTC, ATP2B4
1p31.3	87.2 - 87.3	0.4	3	222.768	2	not contiguous	no
1q32.1	199.0 - 200.7	0.7 - 2.0 - 2.6	3	1.845.702	2	not contiguous	TMEM9, CACNA1S
1q31.3	196.6 - 199.0	1.2 - 0.7	1	1.198.641	3	not contiguous	no
							$\Sigma = 11$
2p12-p11.2	109.6 - 110.5	0.6 - 0.1	6	1.965.191	3	not contiguous	SUCLG1
2q36.3	234.1	0.4	6	0.101	2	contiguous	no
2p25.1	29.2 - 30.3	2.6	4	497.784	2	not contiguous	ROCK2, E2F6
2q33.1	202.1 - 203.2	1.2 - 0.4 - 0.7	3	2.223.052	2	not contiguous	NDUFB3, CFLAR, CASP10, CASP8
2q22.1-q22.3	156.5 - 158.7	0.9 - 1.0 - 0.9	2	2.274.234	2	not contiguous	LRP1B, KYNU
							$\Sigma = 9$
3p25.3 - p25.2	29.4 - 32.0	1.3 - 1.5 - 0.6	6	2.270.619	4	not contiguous	ATP2B2, SLC6A11, SLC6A1, HRH1, APGL7, VGLL4, RPLR32
3p24.2	50.2 - 50.4	1.5 - 0.9	6	462.941	2	contiguous	no
3q26.32	187.4	1.7	6	0.072	2	contiguous	no
3q26.31	184.7 - 185.6	1.3 - 0.9	5	710.386	2	contiguous	no
3q24	154.1 - 154.7	1.5 - 1.2	2	374.176	2	contiguous	SLC9A9
3q26.1	171.2	0.3	2	145.396	2	contiguous	no
3p26.3	2.3 - 3.3	2.6	1	411.988	2	not contiguous	CNTN6
							$\Sigma = 9$
4q34.1	169.1 - 172.0	0.4 - 1.8	6	3.914.464	5	not contiguous	SCRG1, HAND2, MORF4
4q13.1	77.9 - 80.5	0.7 - 0.6 - 0.7	3	4.300.310	3	not contiguous	LPHN3, EPHA5
4q22.1	99.5 - 101.3	1.5 - 0.8	1	1.228.496	2	not contiguous	SNCA, MMRN1
							$\Sigma = 7$
5q14.3	107.6 - 108.0	0.8 - 0.2	6	1.229.913	4	contiguous	MASS1
5q23.1	127.1 - 130.1	0.1 - 0.4 - 0.6	6	3.423.378	3	not contiguous	DMXL1, HSD17B4
5p15.31	20.9 - 24.0	2.0 - 1.3 - 3.4	4	1.549.574	2	contiguous	ADCY2, MTRR, SEMA5A
							$\Sigma = 6$
6p24.3	21.6 - 22.0	1.3	6	324.925	3	contiguous	no
6p21.33-p21.32	53.7 - 54.7	0.2 - 0.8 - 0.9	6	1.850.249	7	not contiguous	82 genes; see table 3.3 for details
6q12	85.3 - 86.2	1.0 - 0.4	2	1.310.290	3	not contiguous	no
6q16.1-q16.2	104.8 - 107.1	0.2 - 0.8 - 0.6	2	3.265.014	3	not contiguous	FUT9, POU3F2, FXL4
							$\Sigma = 85$
7q31.2-31.31	126.0 - 126.8	0.5 - 0.2 - 1.2	6	3.594.012	3	contiguous	CFTR, LSM8, ANKRD7, KCND2, DLX5, NPTX2, TRRAP, SMURF1
7q21.3-q22.1	108.8 - 110.8	1.0	3	1.995.528	2	not contiguous	no
7p12.3-p12.1	72.3 - 74.8	1.4 - 1.2	1	1.746.124	2	not contiguous	GRB10, DDC
7q22.1	114.5 - 114.9	0.8	1	515.578	2	not contiguous	ZRF1, PSMC2, PRES, RELN
							$\Sigma = 16$
8q13.2-q13.3	81.9 - 85.9	2.0 - 1.4	4	2.536.537	3	contiguous	SULF1, SLC05A1, PRDM14, NCOA2, TRAM1, EYA1
8q23.1-q23.3	118.3 - 118.7	0.5 - 0.3	3	1.794.393	2	contiguous	EBAG9, KCNV1
8q12.1	70.2 - 72.7	0.5 - 0.9 - 1.1	1	2.908.205	2	not contiguous	LYN, CYP7A1, SDCBP, NSMAF
							$\Sigma = 12$

Position	Region cM	Recomb. rate	in wdw size	Coverage (bp)	Nr. sig. marker	Marker positions	Known genes
9p23	22.0 - 23.0	2.2	4	414.935	2	contiguous	no
9p21.1	54.5 - 54.8	0.9	2	375.907	2	contiguous	BA438B23.1
							$\Sigma = 1$
10q22.1	90.7 - 91.5	2.5 - 3.1	6	398.942	3	contiguous	GPR147, EIF4EBP2, NODAL, PRF1, ADAMTS14
10p14	21.8 - 23.7	2.0 - 2.7	3	1.016.276	2	not contiguous	ITIH2, KIN, ATP5C1, GATA3
10q25.1	127.7 - 128.5	0.9 - 1.0	2	534.770	2	not contiguous	SORCS1
							$\Sigma = 10$
11p13	48.0 - 50.1	0.3 - 0.5 - 2.6	4	2.496.203	3	not contiguous	DCD1, PAX6, RCN1, WT1, CD59,
11q21-q22.1	100.2 - 103.1	2.0 - 1.7 - 0.7	4	2.045.724	3	not contiguous	JRK1
11q24.1	131.8 - 133.0	3.4 - 1.0	3	322.297	3	not contiguous	SCN3B, ZNF202, OR6X1
11q14.1	90.2	0.7	1	28.536	2	contiguous	no
11q14.2	93.8 - 94.1	1.6 - 0.4	1	369.802	2	contiguous	no
							$\Sigma = 11$
12p13.2-p13.1	28.7 - 32.0	2.4 - 1.5	3	1.172.112	2	contiguous	LRP6, MANSC1, DUSP16, CREBL2, GPR19, CDKN1B, DDX47, GPCR5A, GPR5CD, HEBP1, EMP1
12q14.3-q15	83.2 - 86.1	1.5 - 2.1 - 0.6	2	1.404.002	3	not contiguous	DYRK2, IFNG, IL26, IL22, MDM1, RAP1B, NUP107
12q24.32	156.0 - 158.9	3.7 - 5.4	2	802.113	3	not contiguous	no
12p11.23-p11.22	51.8 - 52.7	1.4 - 1.0	1	1.353.097	2	contiguous	PPFIBP1, MRPS35, PTHLH
12q21.33-q22	103.9 - 104.0	1.6	1	115.362	2	contiguous	BTG1
12q23.2	115.3 - 116.0	1.4	1	399.849	2	contiguous	MYBPC1, ARL1
							$\Sigma = 24$
13q31.3	82.7 - 84.1	1.1 - 0.7	4	1.597.356	2	not contiguous	no
13q14.11	42.4 - 44.4	2.3 - 0.0	2	1.615.604	2	not contiguous	COG6, FOXO1A, MRPS31, SLC25A15, ELF1, WBP4, KBTBD6, KBTBD7, MTRF1
							$\Sigma = 9$
14q12	23.0 - 26.0	2.2 - 1.6 - 0.5	6	3.111.721	4	not contiguous	NOVA1, FOXG1B
14q32.2	110.2 - 112.1	1.8 - 3.6	3	956.963	2	contiguous	no
14q11.2	14.1 - 15.4	2.7	2	486.382	2	not contiguous	OR4E2
14q22.3	57.2 - 58.2	1.7 - 2.0	1	325.996	2	contiguous	PELI2
							$\Sigma = 4$
15q22.31-q23	70.0 - 72.9	2.0 - 1.6 - 2.4	1	2.165.938	2	not contiguous	MAP2K1, SNAPC5, RPL4, SMAD6, PIAS1, CLN6, ITA11
							$\Sigma = 7$
16p12.1	52.6 - 53.8	2.5	6	586.647	3	contiguous	no
16q23.1	94.7	1.3	2	31.641	2	contiguous	CNTNAP4
16p13.13	29.4 - 30.0	3.1 - 1.2	1	513.796	2	not contiguous	MHC2TA, SOCS1, TNP2, PRM2, PRM1, LITAF
							$\Sigma = 7$
17p13.1-p12	31.5 - 32.1	2.8	5	340.667	2	not contiguous	MYH3, SCO1
17q23.2-q23.3	93.1 - 94.2	1.3	3	948.761	2	not contiguous	BRIP1, THRAP, METL2, TLK2
							$\Sigma = 6$
18q12.3	62.7 - 64.6	0.8 - 0.6 - 0.7	3	2.923.030	2	contiguous	RIT2, SYT4
							$\Sigma = 2$
19p13.2-p13.13	34.0 - 36.0	0.8 - 2.1	2	1.128.162	3	not contiguous	ZNF490, MAN2B1, DHPS, TNPO2, ASNA1, NFIX, LYL1, TRM1, STX10, CACNA1A
19p13.11-p12	46.0 - 48.5	3.5 - 1.4 - 1.1	2	1.988.443	3	not contiguous	IFI30, KCNN1, IL12RB1, PIK3R2, RAB3A, PDE4C, JUND, ZNF14, ZNF253, ZNF90
19p13.11	43.0 - 46.0	3.5	1	679.187	3	not contiguous	MRPL34, BST2, PGLS, JAK3, RPL18A, SLC5A5
19q13.31-q13.32	73.9 - 74.1	1.8	1	65.397	2	contiguous	APOC2, RELB
							$\Sigma = 28$

Position	Region cM	Recomb. rate	in wdw size	Coverage (bp)	Nr. sig. marker	Marker positions	Known genes
20p12.3	21.9 - 22.0	2.7	6	63.783	2	not contiguous	BMP2
20p12.1	44.5 - 45.4	2.3	3	663.776	2	not contiguous	SNRPB2, PCSK2 $\Sigma = 3$
21q21.2-q21.3	26.1 - 27.9	1.7 - 0.7 - 1.8	4	1.371.856	3	not contiguous	JAM2, ATP5J, GABPA, APP, CYYR1 $\Sigma = 5$
Xq13.1	85.0 - 86.5	1.1 - 0.8	6	1.615.507	4	not contiguous	EFNB1, IGBP1, P2RY4, ARR3, KIF4A, DLG3, TEX11
Xp21.3-p21.2	45.8 - 46.8	1.4 - 2.0	5	895.100	2	not contiguous	IL1RAPL
Xp22.31-p22.2	15.6 - 18.3	1.4 - 1.7 - 1.8	1	1.632.426	2	not contiguous	VCX, PNPLA4, VCX2, TBL1X $\Sigma = 12$
$\Sigma_{\text{total}} = 284$							

In order to explore the descriptive data of Table 3.3, the ranking order of marker density from preceding Table 3.2 was considered for each chromosome. Chromosomes 5, 6 and 2 were found to show higher degrees of accumulated markers, whereas chromosomes 12, 18, and 19 occupied the lower end. Generally, data specifying the first group required at least twice the maximum number of varying significant window sizes ($n=6$) and were located in areas of lower recombinatorial activity.

One important goal of this study is to inspect the content and nature of genes in detected regions. Chromosome 6 represents the site with most genes ($n=85$), in particular the MHC II and III-harbouring area 6p21.3, followed by chromosomes 19 ($n=28$) and 12 ($n=24$), while chromosomes 20 ($n=3$), 18 ($n=2$), and 9 ($n=1$) showed the regions of interest with lowest gene number. There were no annotated genes present in 18 regions distributed over the genome (Chromosomes 1, 2, 3, 6, 9, 11, 12, 13, 14, 16). In conclusion, 284 annotated genes have been detected. These were analysed for basic functional data and specifications like tissue-restriction and cell types that preferentially express the gene of interest.

3.2.2 Sieving MS candidate regions and genes

In order to identify or further prioritize disease-related candidates, the gene set was subdivided on the basis of their attributes and their potential relevance in MS pathogenesis, displaying either typical immune system or brain and CNS linked features (Tab. 3.4), or characteristics that appeared to be less involved in studied disease (Appendix D). Table 3.4 lists a compilation of genes originating from the depicted genomic regions of interest that are known or assumed to be involved in the adaptive and innate immune response. The majority of these genes were implicated in pathways of transcriptional regulation (enhancer/activator or repressor), proliferation (cell cycle), signal transduction (cell-environment interaction), motility (cell trafficking), and apoptosis (cell death).

Table 3.4 | 142 candidate genes for MS pathogenesis, derived from sliding windows methodology applied on STR-genotyping data of pooled DNA samples from MS patients and healthy controls. CHR: chromosome.

CHR, n	Candidate genes	Gene symbol	tissue (predominantly)	cell type	function
1; 3	BTG family, member 2	BTG2	not CNS restricted		NGF-inducible anti-proliferative protein
	Transmembrane protein 9	TMEM9	Immune system		Involved in intracellular transport.
	Calcium channel, voltage-dependent, L type, α 1 subunit	CACNA1S	not CNS restricted		Involved in neurotransmitter release
2; 6	Rho-associated, coiled-coil containing protein kinase 2	ROCK2	not CNS restricted		Phosphorylation of important signaling proteins
	E2F transcription factor 6	E2F6	not CNS restricted		Transcription factor
	CASP8 and FADD-like apoptosis regulator	CFIAR	not CNS restricted		Apoptosis regulator; link between cell survival and cell death pathways
	Caspase 10 splice variant G	CASP10	not CNS restricted		Central role in execution-phase of cell apoptosis
	Caspase 8, apoptosis-related cysteine protease	CASP8	PBL		Participates in apoptotic pathways
	Kynureninase (L-kynurenone hydrolase)	KYNU	CNS / Brain		Involved in biosynthesis of NAD cofactors; Increased levels in several cerebral and systemic inflammatory conditions
3; 7	ATPase, Ca ⁺⁺ transporting, plasma membrane 2	ATP2B2	CNS / Brain		Intracellular calcium homeostasis
	Solute carrier family 6 (GABA), member 11	SLC6A11	CNS / Brain		Sodium:neurotransmitter symporter (SNF) family
	Solute carrier family 6 (GABA), member 1	SLC6A1	CNS / Brain		Sodium:neurotransmitter symporter (SNF) family
	Histamine receptor H1	HRH1	CNS / PNS		G-protein coupled receptor involved in signal transduction
	Transcription cofactor vestigial-like protein 4	VGLL4			Transcription cofactor
	Solute carrier family 9, isoform 9	SLC9A9	not CNS restricted		Sodium/hydrogen exchanger
	Contactin 6	CNTN6	CNS / Brain	Oligodendrocyte	Participates in oligodendrocyte generation by acting as ligand of NOTCH1
	Synuclein, α (non A4 component of amyloid precursor)	SNCA	CNS / Brain		Involved in neurodegenerative diseases (Parkinson's + Alzheimer's disease)
4; 1	Adenylyl cyclase 2	ADCY2	CNS / Brain		Enzyme that catalyzes second messenger (cAMP) formation
5; 2	Semaphorin 5A	SEMA5A	CNS / Brain		Positive axonal guidance cues
6; 56	RD RNA binding protein	RDBP	not CNS restricted		Causes transcriptional pausing
	Lymphotoxin α (TNF superfamily, member 1)	LTA	CNS / PNS	Lymphocytes	Cytokine; inflammatory, immunostimulatory, and antiviral immune responses
	Tumor necrosis factor α (TNF superfamily, member 2)	TNF α	CNS / PNS	Macrophages	Multifunctional proinflammatory cytokine, implicated in autoimmune diseases
	Lymphotoxin β (TNF superfamily, member 3)	LTB	Spleen and thymus		Specific role in immune response inducing inflammatory system
	Leukocyte specific transcript 1 protein (B144 protein)	LST1			Modulating immune responses
	Natural cytotoxicity triggering receptor 3	NCR1	resting + activated NK cell	Cytotoxicity activating receptor	
	Allograft inflammatory factor 1	AIF1	not CNS restricted	Macrophages	Anti-inflammatory response
	BAT2 protein	BAT2			Candidate gene for development of rheumatoid arthritis
	HLA-B associated transcript-3, isoform b	BAT3			Implicated in control of apoptosis and regulating heat shock protein
	HLA-B associated transcript 4	BAT4			Involved in some aspects of immunity

HLA-B associated transcript 5	BAT5	Lymphocytes	Involved in some aspects of immunity
Lymphocyte antigen 6 complex, locus G6C	LY6G6C	Lymphocytes	Secreted lymphocyte antigen
MutS homolog 5	MSH5	testis and thymus	Involved in meiotic recombination
V-Acyl-tRNA synthetase 2	VARS2	spermatids	Aminoacetylation of tRNA
Heat shock 70kDa protein 1-like	HSPA1L		Chaperone that stabilizes preexistent proteins
Heat shock 70kDa protein 1B	HSPA1B		Chaperone that stabilizes preexistent proteins
Heat shock 70kDa protein 1A	HSPA1A		Chaperone that stabilizes preexistent proteins
BAT8 protein (Fragment)	BAT8	not CNS restricted	Specific tag for epigenetic transcriptional repression
Zinc finger and BTB domain containing 12	ZBTB12		Involved in transcriptional regulation
C2 protein	C2	B cells	Part of classical pathway of complement system
B-factor, properdin	BF		Part of alternative pathway of complement activation
Superkiller viralicidic activity 2-like	SKIV2L		Putative RNA helicase
Serine/threonine kinase 19	STK19	PBL	Involved in transcriptional regulation
Complement component 4B proprotein	C4B	Circulates in blood	Mediator of local inflammation
Complement component 4A	C4A	Circulates in blood	Mediator of local inflammation
Cytochrome P450, family 21, subfamily A, polypeptide 2	CYP21A2		Drug metabolism and synthesis of cholesterol, steroids and other lipids
Tenascin XB	TNXB		Interaction between cells and ECM; inhibition of cell migration
cAMP responsive element binding protein-like 1	CREBL1		Cyclic-AMP-dependent transcriptional factor
FK506 binding protein like	FKBP1		Immunoregulation and basic cellular processes involving protein folding and trafficking; involvement in control of cell cycle
Notch homolog 4	NOTCH4		Intercellular signaling pathway regulating interactions between adjacent cells
Major histocompatibility complex, class II, DR α	HLA-DRA	APCs	Presentation of peptides derived from extracellular proteins
HLA-DRB5	HLA-DRB5	APCs	Presentation of peptides derived from extracellular proteins
HLA-DRB1 protein precursor	HLA-DRB1	APCs	Presentation of peptides derived from extracellular proteins
HLA class II histocompatibility antigen, DRB1-1 β chain precursor	HLA-DQA1	APCs	Presentation of peptides derived from extracellular proteins
HLA class II histocompatibility antigen, DQ(5) α chain precursor	HLA-DQB1	APCs	Presentation of peptides derived from extracellular proteins
HLA class II histocompatibility antigen, DQB1*0602 β chain precursor	HLA-DQA2	APCs	Presentation of peptides derived from extracellular proteins
Major histocompatibility complex, class II, DQ	HLA-DOB	APCs	Presentation of peptides derived from extracellular proteins
Major histocompatibility complex, class II, DO β	TAP2		Involved in MHC I / Antigen peptide association; Transporter associated with antigen processing by MHC class I molecule
Transporter 2, ATP-binding cassette, sub-family B	PSMB8		Immunoproteasome exerting processing of class I MHC peptides
Proteasome subunit, beta type, 8			Involved in peptide loading by MHC class I molecules; Transporter associated with antigen processing by MHC class I molecule
Transporter 1, ATP-binding cassette, sub-family B	TAP1		

Proteasome subunit, β type, 9	PSMB9	Immunoproteasome exerting processing of class I MHC peptides
Major histocompatibility complex, class II, DM β	HLA-DMB	Involved in peptide loading of MHC class II molecules
Major histocompatibility complex, class II, DM α	HLA-DMA	Involved in peptide loading of MHC class II molecules
Major histocompatibility complex, class II, DO α	HLA-DOA	Modulator in HLA class II restricted antigen presentation pathway
Major histocompatibility complex, class II, DP α 1	HLA-DPA1	Presentation of peptides derived from extracellular proteins
Major histocompatibility complex, class II, DP β 1	HLA-DPB1	Presentation of peptides derived from extracellular proteins
Retinoid X receptor β	RXR β	Nuclear hormone receptor
Solute carrier family 39 (zinc transporter), member 7	SLC39A7	Zinc transporter
Ring finger protein 1	RING1	Transcriptional factor maintaining transcriptionally repressive state of genes
Brain myo37 protein	B3GALT4	β -1,3-galactosyltransferase
HLA class II region expressed gene KE2	HKE2	Transfer of target proteins
TAPBP protein	TAPBP	Mediates interaction between newly assembled MHC class I molecules and the transporter associated with antigen processing
Zinc finger protein 297	ZNF297	Transcription factor
Death-associated protein 6	DAXX	Transcription repressor activity
BCL-2-antagonist/killer 1	BAK1	Pro-apoptotic activity
POU domain, class 3, transcription factor 2	POU3F2	CNS / Brain
7; 7 Cystic fibrosis transmembrane conductance regulator	CFTR	CNS / Brain
Potassium voltage-gated channel, member 2	KCND2	Neurons
Transmembrane 4 superfamily member 12	TM4SF12	Regulating neurotransmitter release and neuronal excitability
Hypothetical protein FLJ20089 (P47)	ING3	Regulation of cell development, activation, growth and motility
Transformation/transcription domain-associated protein	TRRAP	Activates p53 trans-activated promoters, inhibits cell growth and induces apoptosis
Proteasome 26S subunit, ATPase, 2	PSMC2	Specific tag for epigenetic transcription activation
Reelin	RELN	CNS / Brain
8; 5 Estrogen receptor binding site associated, antigen, 9	EBAG9	variety of tissues
Potassium channel, subfamily V, member 1	KCNV1	CNS / Brain
Cytochrome P450, family 7, subfamily A, polypeptide 1	CYP7A1	Neurons
Syndecan binding protein (syntenin)	SDCBP	variety of tissues
Neutral sphingomyelinase activation associated factor	NSMAF	variety of tissues
10; 5 Eukaryotic translation initiation factor 4E binding protein 2	EIF4EBP2	Regulation of protein translation by hormones, growth factors and other stimuli that signal through MAP kinase pathway
Perforin 1 (pore forming protein)	PRF1	Key effector molecule for T cell- and natural killer cell-mediated cytolysis

		A disintegrin-like and metalloprotease with thrombospondin type 1 motif, 14 GATA binding protein 3	ADAMTS14 GATA3	retina and brain CNS / Brain	T cells + endothelial cells	Secreted metalloproteinase associated with extracellular matrix Trans-acting T cell specific transcription factor
11; 4	Paired box gene 6 CD59 antigen p18-20	VPS10 domain-containing receptor SorCS1 precursor	SORCS1	CNS / Brain		Vacuolar protein sorting 10 (VPS10) domain-containing receptor
12; 11	Paired box gene 6 CAMP responsive element binding protein-like 2 G protein-coupled receptor 19 Cyclin-dependent kinase inhibitor 1B (p27, Kip1) DEAD-box protein 47 Interferon- γ Interleukin 26 Interleukin 22 Liprin-beta 1 Parathyroid hormone-like hormone B-cell translocation gene 1 protein	Paired box gene 6 CD59 Sodium channel, voltage-gated, type III, beta Zinc finger protein 202 Dual specificity phosphatase 16 CAMP responsive element binding protein-like 2 GPR19 Cdkn1B DDX47 IFNG IL26 IL22 PPFIBP1 PTHLH BTG1 E74-like factor 1 Neuro-oncological ventral antigen 1 Forkhead box G1B	PAX6 CD59 SCN3B ZNF202 DUSP16 CREBL2 GPR19 CDKN1B DDX47 IFNG IL26 IL22 PPFIBP1 PTHLH BTG1 ELF1 NOVA1 FOXP1B	Nervous system Brain Brain variety of tissues activated T cells T cells T cells Ubiquitous PTHLH BTG1 T cells Brain Brain	T cells + endothelial cells Regulation of gene transcription Inhibition of complement membrane attack complex (MAC) action and involvement in signal transduction for T cell activation Modulation of channel gating kinetics; subunit of sodium channels of nodes of Ranvier of developing axons and in mature myelinated axons. Transcriptional repressor of genes that participate in lipid metabolism. Involved in inactivation of MAP kinases Protein with DNA binding capabilities Orphan receptor Controls cell cycle progression at G1 Putative RNA helicase Cytokine displaying several important immunoregulatory functions Member of IL10 family of cytokines; expressed in herpesvirus saimiri-transformed T cells Member of IL10 family of cytokines; contributes to inflammatory response Involved in axon guidance and mammary gland development Neuroendocrine peptide which is a critical regulator of cellular and organ growth, development, migration, differentiation and survival Anti-proliferative protein associated with early G1 phase of cell cycle Transcription factor required for T cell receptor-mediated trans-activation Regulation RNA splicing or metabolism in specific set of developing neurons Transcription factor involved in development of brain and telencephalon	
13; 1	E74-like factor 1					
14; 2	Neuro-oncological ventral antigen 1					
15; 3	Mitogen-activated protein kinase kinase 1 Small nuclear RNA activating complex, polypeptide 5, 19kDa Protein inhibitor of activated STAT, 1	MAP2K1 SNAPC5 PIAS1				Stimulation of enzymatic activity of MAP kinases upon extra- and intracellular signals Complex required for transcription of both RNA polymerase II and III small-nuclear RNA genes. Transcriptional coregulation in various cellular pathways, including STAT pathway, p53 pathway and steroid/hormone signalling pathway
16; 4	Contactin associated protein-like 4 precursor MHC class II transactivator CIITA Suppressor of cytokine signaling 1 Lipoplysaccharide-induced TNF factor	CNTNAP4 MHC2TA SOCS1 LITAF				Vertebrate nervous system cell adhesion molecule and receptor Non-DNA binding transactivator that functions both in constitutive and inducible MHC Class II expression Involved in negative regulation of cytokines that signal through the JAK/STAT3 pathway Role in regulation of TNF- α gene transcription
17; 1	SCO cytochrome oxidase deficient homolog 1	SCO1	Brain, Heart, Muscle	Neurons		Involved in mitochondrial cytochrome c oxidase assembly
18; 2	GTP-binding protein R12	RT2	Brain	Neurons		Ras-like protein expressed in neurons

	Synaptotagmin IV	SYT4	Brain				
19; 14	Zinc finger protein 490	ZNF490					
	Lymphoblastic leukemia derived sequence 1	LYL1					
	Calcium channel, voltage-dependent, alpha 1A subunit	CACNA1A	Brain	T cells	DNA binding protein		
	Interferon- γ inducible protein 30	IFI30		Neurons	Mediates Ca ⁺⁺ entry into neuron; gives rise to P/Q-type calcium currents		
	Potassium intermediate/small conductance calcium-activated channel, subfamily N, member 1	KCNN1	Brain	APCs	Involved in MHC class II-restricted antigen processing		
	Interleukin 12 receptor, beta 1	IL12RB1		Neurons	Regulates neuronal excitability by contributing to slow component of synaptic afterhyperpolarization		
	Ras-related protein Rab-3A	RAB3A	Brain	Neurons	Receptor for interleukin-1 β and involved in IL12 transduction		
	Jun D proto-oncogene	JUND			Role in neurotransmitter release by regulating membrane flow in nerve terminal		
	Zinc finger protein 14 (KOX 6)	ZNF14			Protects cells from p53-dependent senescence and apoptosis		
	Zinc finger protein 253	ZNF253			Involved in transcriptional regulation		
	Zinc finger protein 90 (HTF9)	ZNF90			Involved in transcriptional repression activity		
	Bone marrow stromal cell antigen 2	BST2	variety of tissues		Involved in transcriptional regulation		
	JAK3 protein	JAK3		Immune cells	Participates in B-cell activation in rheumatoid arthritis		
	V-rel reticuloendotheliosis viral oncogene homolog B	RELB			Involved in signal transduction and interacts with members of the STAT family		
	V-rel reticuloendotheliosis viral oncogene homolog B”	SNRPB2			Transcription factor that stimulates promoter activity		
20; 1	Small nuclear ribonucleoprotein polypeptide B”				Role in pre-mRNA splicing		
21; 2	Junctional adhesion molecule 2	JAM2	high endothelial venules		Role in processes of lymphocyte homing to secondary lymphoid organs		
	Amyloid β (A4) precursor protein	APP	Brain		Cell surface receptor, physiological functions relevant to neurite growth, neuronal adhesion and axogenesis; involved in oxidative stress and neurotoxicity as enhancer of neuronal apoptosis; cell mobility and		
					Astrocytes, T cells transcription regulation through protein-protein interactions.		
X; 5	Ephrin-B1	EFNB1	variety of tissues		Involved in constraining the orientation of longitudinally projecting axons; induced by TNF α .		
	Immunoglobulin (CD79A) binding protein 1	IGBP1	variety of tissues		Associated to surface IgM-receptor; involved in B-cell antigen receptor (BCR) signal transduction		
	Discs, large homolog 3	DLG3			Interacts with cytoplasmic tail of the NMDA receptor subunit NR2B		
	Interleukin 1 receptor accessory protein-like 1	IL1RAPL	Brain		Specialized role in physiological processes underlying memory and learning abilities		
	Transducin (beta)-like 1X-linked	TBL1X			Recruitment of the ubiquitin/19S proteasome complex to nuclear receptor-regulated transcription units		
					STAT = signal transduction and activators of transcription		
					APCs (Antigen Presenting Cells) = B cells, dendritic cells, macrophages		

A fine candidate for MS pathology is the neuronal gene Contactin 6 (*CNTN6*) at 3p26.3, a member of the gene family that encode for Notch binding proteins which mediate cell surface interactions during nervous system development, participate in oligodendrocyte generation and possibly plays a role in neuroregeneration.^{175,176} Other brain and CNS specific genes that are predominantly expressed in neurons are involved in neurotransmitter release (*RAB3A*, 19p13.11), neuronal membrane excitability (*KCND2*, 7q31.31; *KCNV1*, 8q23.2; *SCN3B*, 11q24.1; *KCNN1*, 19p13.11; *CACNA1A*, 19p13.13) and neuronal migration (*RELN*, 7q22.1). Further brain-confined genes showing DNA- (*POU3F2*, 6q16.2) or RNA- (*NOVA1*, 14q12) binding properties seem of importance in light of disease regulation.

Special attention should be drawn to the well-characterised amyloid β precursor protein (*APP*) gene at 21q21.3, which is expressed in neurons, nonneuronal cells, astrocytes and T lymphocytes. It is reported to exert a multitude of functions acting as a cell surface receptor performing physiological functions on neurons relevant to neurite growth, neuronal adhesion and axonogenesis. Furthermore it is associated with oxidative stress response and neurotoxicity as an enhancer of neuronal apoptosis,^{177,178} with cell mobility and transcription regulation through protein-protein interactions. In some families, defects in *APP* are a cause of autosomal dominant Alzheimer's disease 1 (AD1).¹⁷⁹

More well-known genes that show elevated expression in brain were the mitochondrial cytochrome c oxidase (*SCO1*, 17p13.1), genes encoding integral membrane proteins (*SYT4*, *IL1RAPL*, *ATP2B2*, *SLC6A11*, *SLC6A1*, *ADCY2*, *SEMA5A*, *SORCS1*) of various functions, the cerebral inflammation associated kynureinase gene (*KYNU*; 2q22.2), and the soluble monomer Synuclein α (*SNCA*; 4q22.1). The latter can be found in presynaptic nerve terminals and has been described to form filamentous aggregates that are the major non amyloid component of intracellular inclusions in several neurodegenerative diseases (synucleinopathies).¹⁸⁰

In the context of MS as an autoimmune disorder it was of interest to determine candidate genes related to immune cells and inherent "partner molecules". In this respect, of relevance were variations in antigen presenting cell (APC) genes, such as B lymphocytes, dendritic cells and macrophages. Several genes of the MHC class II region should be acknowledged (*HLA-DR*, -*DQ*, -*DO*, -*DP*, and immunoproteasome subunits) that are involved in antigen processing, and MHC class I related peptide transporters (*TAP1*, *TAP2*), all located at 6p21.33–32. Deviations in T and B cell line genes as well as Natural Killer (NK) cells (*NCR1*), Neutrophils (*TAPBP*) and endothelial cells (*GATA3*, *JAM2*) completed the outlined field.

Genes encoding anti- or proinflammatory response-associated molecules like the interleukin and cytokine family members IL26, IL22, LTA, LTB, TNF α , AIF, BAT2, SOCS1 and members or modulators of the classic and alternative complement cascades (C2, C4a, C4b, CD59, BF, PRF) were detected, representing valuable candidates.

Cell-to-cell or cell-to-ECM interactions realized by type I membrane proteins that mediate cell adhesion represent another basic element in studied disease. Adhesion and signalling functions of aforementioned CNTN6, APP, and RELN in a brain-restricted manner have been also described for genes encoding implicated proteins of the broad immune system, namely JAM2 (lymphocyte homing), EFNB1 (axon projection), ROCK2 (cytoskeleton assembly), TNXB (cell-ECM interaction), TM4SF12 (signal transduction), BAK1 (pro-apoptotic), SDCBP (cytoskeleton assembly), PPFIBP1 (axon guidance), CNTNAP4 (cell adhesion), ADAMTS14 (ECM associated), and NOTCH4 (cell-cell interaction).

32 genes account for transcription factors and epigenetic regulators that influence cell processes. Their functions have been abundantly investigated and qualify as candidates in an autoimmune disease: *ELF1* and *GATA3*, *JAK3*, *BAT8*, *BTG2*, *CREBL1*, *DAXX*, *EBAG9*, *E2F6*, *FOXP1B*, *ING3*, *JUND*, *LITAF*, *NSMAF*, *PAX6*, *PIAS1*, *POU3F2*, *PSMC2*, *RDBP*, *RELB*, *RING1*, *RXRB*, *STK19*, *TRRAP*, *VGLL4*, *ZBTB12*, *ZNF14*, *ZNF90*, *ZNF202*, *ZNF253*, *ZNF297*, and *ZNF490*.

With respect to MS therapies and potential interference due to gene impairment, Cystic fibrosis transmembrane conductance regulator (*CFTR*) at 7q31.2 called forth special interest as it is implied in multidrug resistance.¹⁸¹⁻¹⁸³ The same applies to encountered monooxygenases *CYP7A1* (8q12.1) and *CYP21A2* (6p21.32), microsomal cytochrome P450 enzymes that catalyze many reactions involved in drug metabolism¹⁸⁴ and synthesis of cholesterol, steroids and other lipids. Eventually, it should be emphasized that the cell surface receptor mediator Janus kinase 3 (*JAK3*; 19p13.11) represents a part of the primary effectors and immune reponse mechanism to the immunomodulator recombinant Interferon- β (rIFN- β),^{185,186} which is regularly applied to RRMS patients.¹⁸⁷⁻¹⁸⁹ In conjunction with the variability of the drug effect as MS-treatment (poor versus good responder), a negative regulator of the JAK-STAT pathway, the suppressor of cytokine signaling 1 (*SOCS1*; 16p13.13),¹⁹⁰ was considered promising. Another prominent candidate is protein kinase *MAP2K1* (15q22.31), a member of the dual specificity protein kinase family, that acts as a mitogen-activated protein (MAP) kinase kinase and functions as an integration point for multiple biochemical signals.¹⁹¹ The protein kinase

operates upstream of MAP kinases and stimulates respective enzymatic activity directed at a wide variety of extra- and intracellular signals.

In order to further validate presented results, two regions of interest that displayed candidate genes of varying disease-related plausibility were selected. Adjacent microsatellites D3S3714 and D3S3680 warranted the selection of genes encoding for *APG7L* and *VGLL4* that map to chromosome band 3p25.3. The second site that underwent such analysis was at 10q22.1, harbouring the genes *PRF1*, *ADAMTS14* and the open reading frame 27 (*C10orf27*), which are located between and in the vicinity of D10S537 and D10S1685.

3.3 Genotyping of individual DNA by means of single nucleotide polymorphism marker

3.3.1 Yield of applied 5' Nuclease assay

A total of 24 SNP assays were applied to 574 DNA samples. Corresponding to the initial screening phase, each SNP was tested with 383 DNA samples (192 RR plus 191 HC) and succeeding the statistical analysis (Section 2.11) additional genotypes for SNPs #1, #6, #8, #9, #10, #12, #13, #16, #17, #18, #19, #20, #21, #22, #23, and #24 were determined in DNA from 191 individuals (96 PP plus 95 HC). In summary, of 12,216 completed PCRs, 360 assays failed to score unambiguous genotypes which represented a completion rate of 97.1%.

The data sets of two DNA samples from the initially distributed 574 DNA samples were not included in further analysis due to following reasons: 1) the clinical assignment of patient #1431 (Tab. 2.5, plate PP, position "A5"; Tab. 2.6, plate P2, position "A9, 10") was re-evaluated and defined a different clinical form of MS (from PPMS to PRMS=Primary Relapsing MS). This disease form was not subject of present study and therefore the sample excluded; 2) DNA dilutions from individual #C269 were accidentally distributed in two different panels (Tab. 2.5, positions "E9" in plate HC2 and "B3" in plate HC3; Tab. 2.6, positions "J18" in plate P1 and "D5, 6" in plate P2). The genotype-calls of #C269, now tested in duplicate (48 results), were 100% identical and could be considered a useful confirmation of employed technique. Consequently, only 24 genotypes (one result per SNP) were introduced into succeeding statistical analysis.

Failure to mark genotypes was primarily attributable to unsuccessful PCRs due to

insufficient product amplification. Data points in the scatter plot could not receive genotype-calls as they failed to cluster tightly with assembled dots. Real-time data analysis of these visual outliers did not allow for unambiguous classification in most cases. The main cause for described PCR inconsistencies appeared to be incomplete dispensation of either reaction solution or DNA dilutions through the respective robots when final assays were prepared. Genotyping newly constructed DNA plus probe assays attained a completion rate of 91.7% as 30 DNA samples consistently replicated their outlier position. Therefore, the overall degree of valuable assay completion was 99.8%, providing for subsequent statistical analyses 12,186 genotypes of 572 individuals (Tab. 3.5).

Table 3.5 | Summary of 5' Nuclease PCR assay realizations indicating actual counts (N) and degree of performance in %.

	Summary of processed genotyping assays					
	Valid		Missing		Total	
	N	Percent	N	Percent	N	Percent
Patients vs Controls *.snp3	383	100.0%	0	0.0%	383	100%
Patients vs Controls *.snp5	383	100.0%	0	0.0%	383	100%
Patients vs Controls *.snp7	383	100.0%	0	0.0%	383	100%
Patients vs Controls *.snp24	569	99.5%	3	0.5%	572	100%
Patients vs Controls *.snp9	572	100.0%	0	0.0%	572	100%
Patients vs Controls *.snp20	572	100.0%	0	0.0%	572	100%
Patients vs Controls *.snp11	383	100.0%	0	0.0%	383	100%
Patients vs Controls *.snp14	383	100.0%	0	0.0%	383	100%
Patients vs Controls *.snp15	383	100.0%	0	0.0%	383	100%
Patients vs Controls *.snp2	383	100.0%	0	0.0%	383	100%
Patients vs Controls *.snp4	383	100.0%	0	0.0%	383	100%
Patients vs Controls *.snp16	570	99.7%	2	0.3%	572	100%
Patients vs Controls *.snp1	571	99.8%	1	0.2%	572	100%
Patients vs Controls *.snp6	571	99.8%	1	0.2%	572	100%
Patients vs Controls *.snp19	563	98.4%	9	1.6%	572	100%
Patients vs Controls *.snp8	572	100.0%	0	0.0%	572	100%
Patients vs Controls *.snp23	569	99.5%	3	0.5%	572	100%
Patients vs Controls *.snp10	572	100.0%	0	0.0%	572	100%
Patients vs Controls *.snp21	570	99.7%	2	0.3%	572	100%
Patients vs Controls *.snp12	567	99.1%	5	0.9%	572	100%
Patients vs Controls *.snp22	570	99.7%	2	0.3%	572	100%
Patients vs Controls *.snp13	571	99.8%	1	0.2%	572	100%
Patients vs Controls *.snp17	571	99.8%	1	0.2%	572	100%
Patients vs Controls *.snp18	572	100.0%	0	0.0%	572	100%
	12,186	99.8%	30	0.2%	12,216	
	Total	Mean	Total	Mean	Total	

3.3.2 Hardy-Weinberg equilibrium (HWE) in healthy control and multiple sclerosis population samples

The HWE supplies information about genetic variation of alleles in diploid eukaryotic populations assuming an “ideal” population;¹⁹² that is, no genetic drift or other evolutionary forces are acting on the population. For SNP #19 and #8, respective HWE violations occurred in both population samples (controls and cases) to a comparable degree, whereas SNP #17 distribution deviates exclusively in MS patients (Tab. 3.6).

Table 3.6 | Hardy Weinberg equilibrium (HWE) data indicate strong deviation for SNP#19 and marginal HWE violation for downstream SNP#8 in controls and cases. SNP#17 deviates from expected frequencies only in the MS patients' population.

SNP #	Controls		MS cases	
	Chi	p-value	Chi	p-value
24	0.36	0.547	0.43	0.513
9	2.59	0.107	3.00	0.083
20	2.31	0.129	0.30	0.584
16	0.88	0.348	1.55	0.213
1	0.63	0.426	0.01	0.931
6	0.00	0.960	0.13	0.717
19	29.32	6.1x10⁻⁸	36.06	1.9x10⁻⁹
8	4.35	0.037	6.12	0.013
23	0.06	0.810	0.01	0.922
10	0.07	0.791	0.41	0.521
21	0.27	0.601	0.16	0.691
12	0.25	0.615	1.78	0.183
22	1.49	0.223	2.19	0.139
13	0.40	0.527	0.26	0.610
17	0.23	0.628	5.03	0.025
18	0.38	0.536	0.55	0.460

3.3.3 Linkage Disequilibrium block formation at genomic regions of interest 3p25.3 and 10q22.1

Linkage disequilibrium inferred from D' ($-1 < D' < 1$) was the basis of applied tests for identification of “block-like” structures between genotyped loci. It is supposed to be less sensitive to allele frequency than an alternative statistical LD measure,¹⁹³ r^2 , which renders D' less susceptible to Hardy-Weinberg deviations.

D' values for each pair of sites in examined regions of interest at 3p25.3 and 10q22.1, respectively, are shown in the graphical displays Figure 3.1 and 3.2. Here, the relative positions of genes and the interval of tested SNP markers in kilobases (kb) are indicated in corresponding regions. At 3p25.3, 188.7 kb were covered with 10 SNPs, and at 10q22.1, 13 SNPs encompassed 177.4 kb. The patterns of LD-measures (D' values) corresponding to each marker pair were specified in colored cases that form a triangle, in which areas of “block”-like structure were outlined in bold lines. Two-digit numbers specified the D' values (e.g. “74” denoted $D' = 0.74$) and empty boxes expressed perfect linkage ($D' = 1$, completely correlated) between markers. A value of 0.0 implies independence, whereas 1.0 means that all copies of the rarer allele occur exclusively with one of the two possible alleles at the other marker. Table 3.7 provides details on the color schemes.

Table 3.7 | Standard color scheme of output of Haplovew software. D' : linkage disequilibrium measure; LOD: Base₁₀ logarithm of likelihood of odds ratio for linkage.

Standard color scheme		
	$D' < 1$	$D' = 1$
LOD < 2	White	Blue
LOD ≥ 2	Shades of red	Bright red

In Figure 3.1, one could identify 3 different sized haplotype blocks (6.78 kb, 16.97 kb and 13.12 kb) expressing reduced local recombination rates between adjacent markers within these regions. 8 of 10 tested markers constituted together three sites of block-like structures, adding up to 36.87 kb of the 188.70 kb genomic sequence. According to the UCSC genome browser, the overall recombination rate in this region is designated 1.5 cM/Mb.

Region 10q22.1 in Figure 3.2 is stated to be recombinatorial more active (UCSC), evident by an elevated rate of 2.5 cM/Mb. Consistently, the examined DNA stretch of 177.36 kb enclosed only two block-like structures of together 15.63 kb, established by 5 from 13 tested SNP markers. In comparison with Figure 3.1, there exist more independent sites in this relatively equal-sized region of interest, reflecting the recombination rate heterogeneity described throughout the genome.¹⁹⁴

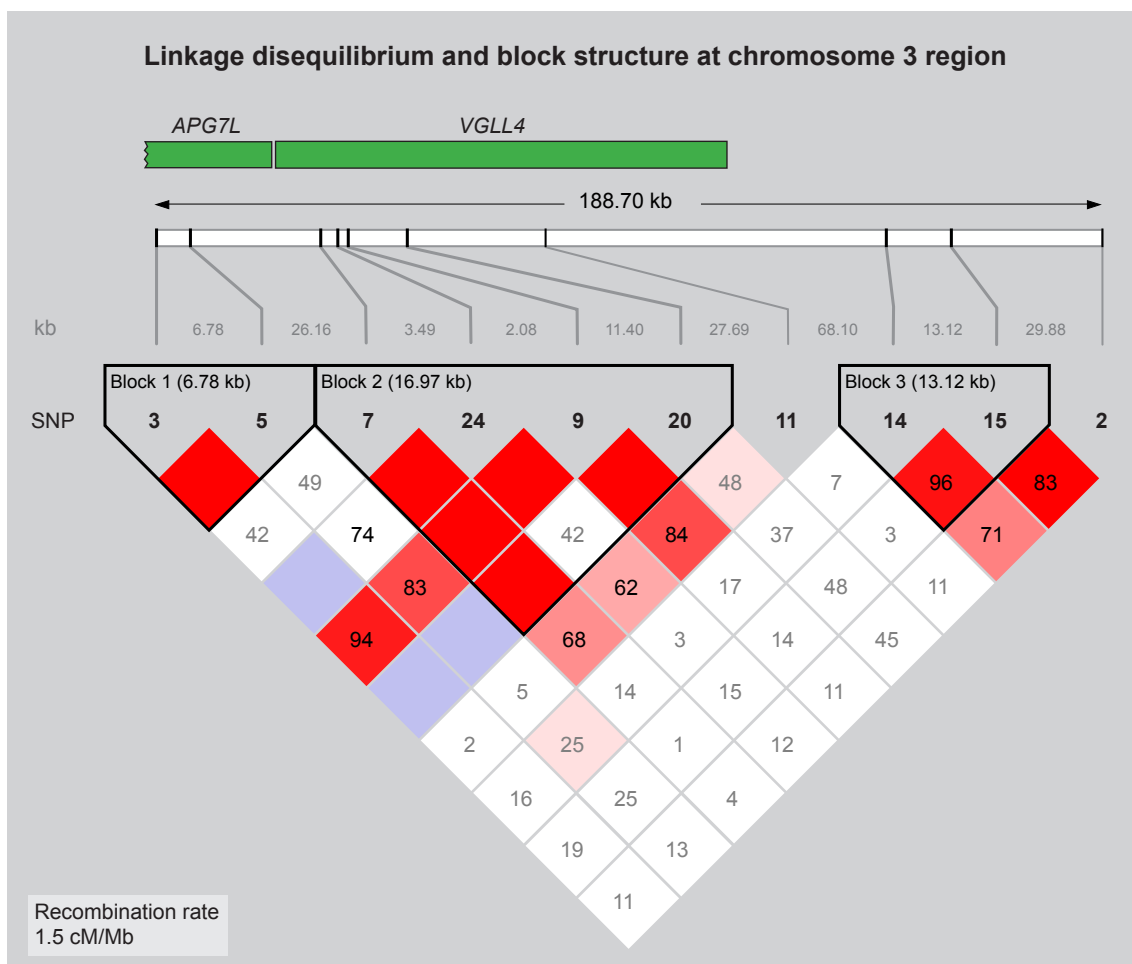


Figure 3.1 | Diagram of Haplovview generated block-like structures at chromosomal location 3p25.3, based on the 4 gamete rule defined by Barrett *et al.*¹⁶¹ Upper part: Gene segment of *APG7L* and complete gene *VGLL4*. Investigated DNA stretch length and intervals of 10 distributed SNP markers are indicated in kilobases (kb); lower part: Genomic sequence of tested SNPs and linkage disequilibrium (LD) plot of computed pairwise LD statistics for all markers. Three revealed “block”-like sites are identified in outlined triangles due to high LD established between consecutive markers. $D' = 1.0$, complete linkage between marker pair (empty box). $D' = 0$, no linkage between independent markers. D' values are specified in numbers: 74 denotes $D' = 0.74$. Pairwise LD measures were calculated from genotype data of $N=383$ individuals.

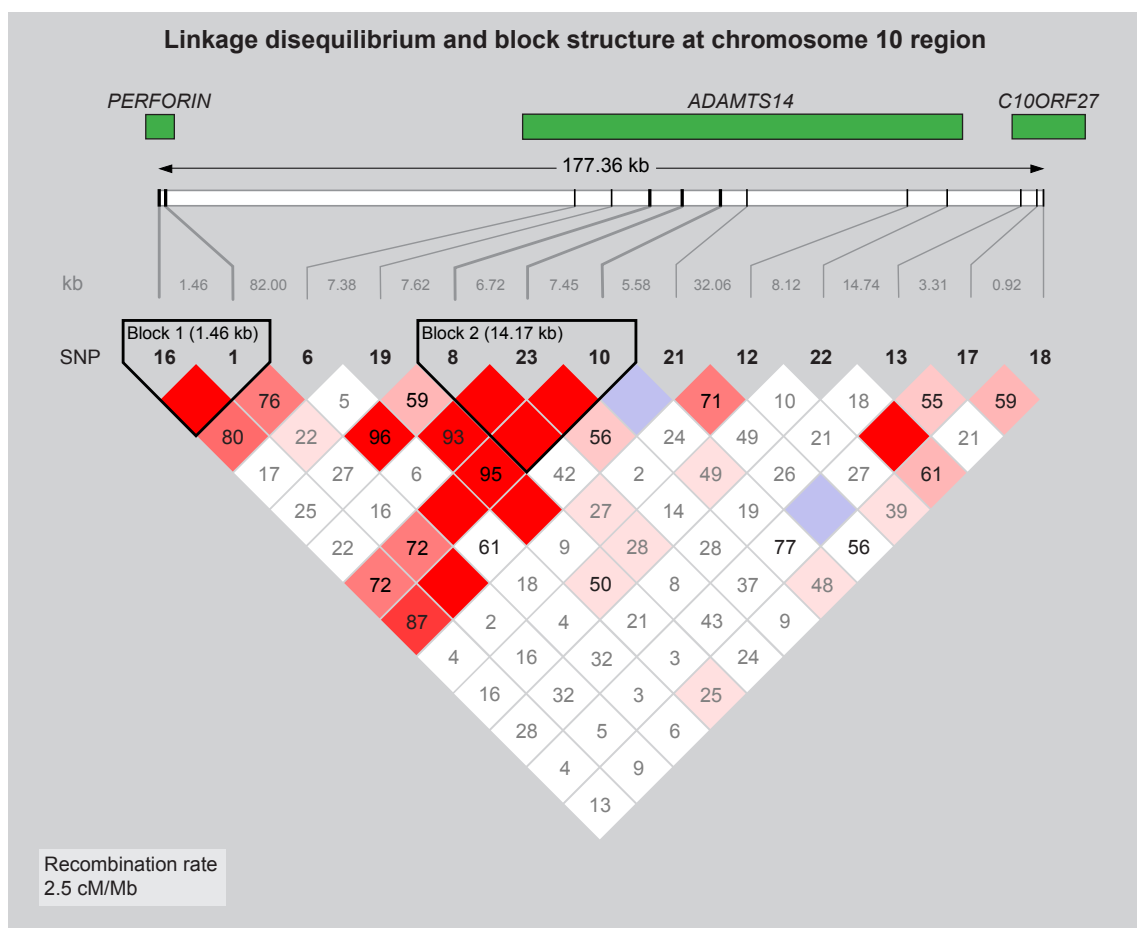


Figure 3.2 | Diagram of Haploview generated block-like structures at chromosomal location 10q22.1, based on the 4 gamete rule defined by Barrett *et al.*¹⁶¹ Upper part: Genes *Perforin*, *ADAMTS14* and *C10ORF27*. Investigated DNA stretch length and intervals of 13 distributed intragenic SNP markers are indicated in kilobases (kb); lower part: Genomic sequence of tested SNPs and linkage disequilibrium (LD) plot of computed pairwise LD statistics for all markers. Two revealed “block”-like sites are identified in outlined triangles due to high LD established between consecutive markers. $D' = 1.0$, complete linkage between marker pair (empty box). $D' = 0$, no linkage between independent markers. D' values specified in numbers: 76 denotes $D' = 0.76$. Pairwise LD measures were calculated from genotype data of $N=383$ individuals.

3.3.4 Detection of statistical significance derived from allele and single genotype comparisons

As previously described (Fig. 2.6a and 2.7a), the initial screen on genomic regions of interest was carried out with SNPs #1 to #15 on DNA of 383 RRMS patients and healthy controls. In this phase, it was of interest to detect overall differences that would confirm revealed findings of microsatellites tested on pooled DNA samples. This referred in particular to SNPs #11 16.713 kb upstream of D3S3714, #14 and #15 enclosing D3S3680 (5.958 kb and 6.824 kb, respectively), #1 and #6 closer to D10S537

(35.290 kb and 46.327 kb, respectively) and #10 and #12 adjacent to D10S1685 (7.684 kb and 29.588 kb, respectively). As shown in Table 3.8, only SNPs #1 and #6 disclosed supportive evidence after ascertaining the additional single genotype statistics. Comparison of genotype frequencies at SNP #1 showed a significantly different distribution of the homozygous state (GG) ($P=0.009$). The adjacent SNP #6 calculations showed promising trends for homozygous combinations CC and TT ($P=0.081$; $P=0.053$). Other previously mentioned SNPs located in vicinity of STR-markers suggesting evidence of association for MS were inconclusive in the sense that they seemed independent of the microsatellites. Nevertheless, promising details were revealed for SNPs #9 ($P=0.022$), #8 ($P=0.066$), and in particular for #13 ($P=0.004$, $P=0.019$) in the open reading frame on chromosome 10.

Table 3.8 | Statistical overview (stage one: screening phase) of two MS candidate regions on chromosome 3 (3p.25) and 10 (10q22.1). Chi square comparisons (genotype and allele) derived from genotyping results of 383 DNA samples at 15 SNPs. MAF: minor allele frequency in Caucasians stated by Celera; ho: homozygous genotype; he: heterozygous genotype. P^* = overall p-value generated by global group comparison (RRMS versus HC); P= single genotype frequency comparison (one genotype versus sum of other two); p-values < 0.10 were considered to show a trend (in bold print), p-values < 0.05 were statistically significant (colored green).

RRMS; n=192

HC; n=191			SNP(x/y)	MAF	RRMS vs. HC	ho (xx)	he (xy)	ho (yy)
SNP#	Chr	Gene			P*	P	P	P
3	3	APG7L	C/G	.11	0.308	0.910	0.417	0.172
5	3	APG7L	G/T	.20	0.781	0.527	0.871	0.645
7	3	VGLL-4	C/G	.38	0.979	0.858	0.883	0.959
9	3	VGLL-4	A/G	.48	0.067	0.125	0.022	0.267
11*	3	VGLL-4	C/G	.38	0.709	0.881	0.572	0.470
14*	3		C/T	.34	0.302	0.132	0.332	0.417
15*	3		A/C	.40	0.678	0.378	0.645	0.757
2	3		C/T	.35	0.335	0.161	0.575	0.359
4	10		G/T	.33	0.901	0.883	0.718	0.647
1*	10	PRF1	A/G	.28	0.026	0.120	0.107	0.009
6*	10	ADAMTS14	C/T	.19	0.073	0.081	0.255	0.053
8	10	ADAMTS14	C/G	.29	0.112	0.066	0.111	0.723
10*	10	ADAMTS14	A/G	.26	0.886	0.820	0.635	0.719
12*	10	ADAMTS14	A/G	.50	0.615	0.394	0.881	0.467
13	10	C10orf27	A/G	.35	0.013	0.004	0.019	0.218

* SNP-marker that were located next to significant STR-marker in preceding DNA pool approach.

These data were considered adequate to justify the realization of the second resolution increasing step, by enlarging the sample size (additional 95 PPMS cases and 94

healthy controls) and including 9 more SNP markers in a further genotyping session. This improved the marker density and augmented the statistical power, which would ideally consolidate detected significances and convert statistical trends into actual significancies.

Table 3.9 depicts the results of SNP genotyping with 16 markers on 572 DNA samples. At 3p25.3, two additional SNPs (#24 and #20) enclosing SNP #9 were selected and genotyped with the complete DNA sample set, whereas #9 was tested with the additional PPMS and HC samples. Aside from these three markers, the remaining in this chromosomal region did not pinpoint to other promising sites and hence were not further scrutinized. At 10q22.1, only SNP #4 was excluded from supplementary genotyping while seven new intragene markers were implemented, located in *PRF1* (#16), *ADAMTS14* (#19, #23, #21, #22) and *C10orf27* (#17, #18).

The inclusion of the clinical disease form PPMS at this stage of the study opened the possibility to substratify the MS group and possibly to better disentangle genetic factors that contribute to specific disease phenotypes. Therefore, following comparisons were performed: MS versus HC; RRMS versus HC; PPMS versus HC; PPMS versus RRMS.

Table 3.9 | Statistical overview (stage two: focusing phase) of two MS candidate regions on chromosome 3 (3p.25) and 10 (10q22.1). Chi square comparisons (genotype and allele) derived from genotyping results of 572 DNA samples at 16 SNPs. MAF: minor allele frequency in Caucasians stated by Celera; ho: homozygous genotype; he: heterozygous genotype. P*= overall p-value generated by global group comparison; P= single genotype frequency comparison (one genotype versus sum of other two); p-values < 0.10 were considered to show a trend (in bold print), p-values < 0.05 were statistically significant (colored green).

RRMS; n=192			PPMS; n=95			HC; n=285			MS / HC			RR / HC			PP / HC			PP / RR					
SNP#	Chr	Gene	x/y	P*	P	xx	xy	yy	P*	P	xx	xy	yy	P*	P	xx	xy	yy	P*	P	xx	xy	yy
3	3	APG7L	C/G																				
5	3	APG7L	G/T																				
7	3	VGLL-4	C/G																				
24	3	VGLL-4	A/G	0.945	1	0.937	0.939		0.645	1	0.612	0.616		0.392	1	0.341	0.348		0.247	1	0.200	0.206	
9	3	VGLL-4	A/G	0.347	0.512	0.015	0.036		0.919	0.152	0.010	0.123		0.065	0.338	0.285	0.038		0.095	0.055	0.360	0.438	
20	3	VGLL-4	A/C	0.377	0.239	0.151	0.449		0.519	0.342	0.217	0.653		0.379	0.301	0.249	1		0.737	0.800	0.883	0.553	
11*	3	VGLL-4	C/G																				
14*	3		C/T																				
15*	3		A/C																				
2	3		C/T																				
4	10		G/T																				
16	10	PRF1	A/G	0.092	0.190	0.866	0.163		0.072	0.127	0.673	0.179		0.470	0.725	0.749	0.385		0.519	0.421	0.539	0.858	
1*	10	PRF1	A/G	0.038	0.260	0.189	0.039		0.042	0.228	0.252	0.052		0.227	0.617	0.328	0.197		0.712	0.677	0.942	0.825	
6*	10	ADAMTS14	C/T	0.091	0.375	0.206	0.098		0.108	0.194	0.464	0.180		0.287	0.795	0.122	0.161		0.847	0.319	0.364	0.745	
19	10	ADAMTS14	A/G	0.482	0.477	0.833	0.705		0.475	0.738	0.636	0.488		0.009	0.046	0.765	0.055		0.003	0.034	0.525	0.020	
8	10	ADAMTS14	C/G	0.482	0.007	0.006	0.356		0.332	0.020	0.050	0.748		0.966	0.060	0.005	0.145		0.444	1	0.239	0.252	
23	10	ADAMTS14	A/G	0.048	0.241	0.135	0.066		0.075	0.376	0.148	0.088		0.190	0.334	0.395	0.248		0.947	1	0.787	0.866	
10	10	ADAMTS14	A/G	0.390	0.739	0.446	0.367		0.190	0.833	0.147	0.129		0.787	0.703	0.482	0.613		0.225	0.797	0.084	0.109	
21*	10	ADAMTS14	C/T	0.008	0.011	0.023	0.250		0.006	0.008	0.017	0.237		0.253	0.267	0.322	0.632		0.299	0.326	0.460	1	
12*	10	ADAMTS14	A/G	0.590	0.431	0.530	0.935		0.362	0.276	0.530	0.687		0.748	0.949	0.736	0.623		0.329	0.380	0.886	0.449	
22	10	ADAMTS14	A/T	0.362	0.557	0.036	0.083		0.723	0.339	0.066	0.233		0.169	0.809	0.122	0.077		0.304	0.335	0.933	0.425	
13	10	C10orf27	A/G	0.0004	0.0004	0.007	0.085		0.0004	0.0005	0.010	0.068		0.068	0.047	0.109	0.490		0.366	0.461	0.699	0.452	
17	10	C10orf27	C/T	0.460	0.109	0.982	0.678		0.530	0.152	0.166	0.303		0.005	0.576	0.014	0.007		0.002	-	0.001	0.001	
18	10	C10orf27	A/C	0.583	0.763	0.269	0.360		0.796	0.731	0.442	0.580		0.447	0.924	0.256	0.285		0.601	0.868	0.619	0.548	

* SNP-marker that were located next to significant STR-marker in DNA pooling experiment and MS.

Table 3.9 serves as an explorative tool to examine and compare where and how noticeable events of the screen results displayed in Table 3.8 maintained or vanished. Naturally, this made primarily sense when RRMS was compared with HC (Tab. 3.9, second main column). Here, of five sites of interest ($p < 0.10$ at SNPs #9, #1, #6, #8, and #13) derived from the genotyping of 383 individuals, four markers (#9, #1, #8, #13) revealed clearer or maintained significance and one (#6) basically dropped out. More detailed information about allele and genotype frequencies, correlation (odds ratio) and statistic robustness (confidence interval) of all Table 3.9-derived findings are presented in synoptical tables of Appendix E. There, minor allele frequencies of tested SNPs can be traced in allele frequency population data and compared to publicly available information (Tab. 2.9).

Intriguing was the finding that of the additional markers, SNP #21, positioned 2.107 kb upstream of D10S1685, showed a significant association with MS for allele C ($OR=1.7$; 95% CI=1.2 to 2.6; $p=0.008$) and the homozygous genotype CC ($OR=1.8$; 95% CI=1.1 to 2.7; $p=0.011$) (Appendix E9). This was even more evident when the stratified group RRMS was compared with HC (allele C: $OR=1.9$; 95% CI=1.2 to 3.1; $p=0.006$; genotype CC: $OR=2.0$; 95% CI=1.2 to 3.3; $p=0.008$), as shown in Appendix E10. It should be noted, that the MS DNA-pool for the GAMES experiment was created from DNA of MS patients diagnosed RR and SP, which are classified as belonging to the same clinical subgroup.²⁷ Tested with D10S1685, the same ratio – quantitatively more PCR fragments in MS patients than in controls – was observed, indicating the reasonable probability that indeed SNP #21 and the adjacent microsatellite D10S1685 are linked on the same DNA stretch, rendering it specific for the “relapsing” form of MS. Certainly the concordance rate (93%) of used samples in both experiments contributed to this congruent result; nevertheless, it supports the presented line of investigation.

After genotyping 572 samples, the mentioned three markers (#9, #8, #13) revealed a statistically increased significance when comparisons RRMS versus HC were computed (Tab. 3.9; Appendix E, Tab. 2, 10, 14). This was mainly due to an increased statistical power inherent with a larger sample size.

As anticipated, the inclusion of clinically distinct PPMS individuals had various effects on comparisons between categories, displaying both same and contrary frequencies in relation to the RRMS group. At SNP #9, the heterozygous state AG was negatively associated with MSRR and MS, respectively (Appendix E, Tab. 2, 1), rendering RRMS cases the separating group. The homozygosity GG association in the MS group, on the other hand, confined contribution of susceptibility to PPMS individuals (Appendix E,

Tab. 3). More information based on the stratification effect, though sometimes not in the range of statistical significance, can be obtained by comparing the odds ratio between analysed groups. Tables 2 and 3 of Appendix E showed a contrary distribution of genotype AA for RRMS and PPMS in comparison with healthy controls, which, when directly compared, was reflected in a PPMS-associated ratio (Tab. 4; OR=0.55; p= 0.055). Therefore, SNP #9 distinguished RRMS samples from healthy controls and in addition discriminated moderately between RRMS and PPMS.

At SNP #8, both MS subgroups uniformly deviated from the healthy control population (Appendix E, Tab. 9-11), and the PPMS individuals separated considerably well (Tab. 11: CG, OR: 2.0; p= 0.005). The same principle applied to SNP #13, where allele and genotype distributions were equally different, A and AA being over-represented in MS individuals, and more genotypes AG and GG counted in healthy controls (Appendix E, Tab. 13-15).

Furthermore, of the newly implemented markers, SNP #19 and #17 attained special relevance as both could be considered clear discriminators in PPMS vs. HC and PPMS vs. RRMS comparisons. While the overall comparisons between MS and HC did not reveal any distribution tendencies (Appendix E, Tab. 9 and 10; 13 and 14), the stratification process disclosed strong deviations for the PPMS group from healthy controls (Tab. 11, 15) and to a greater extent from the RRMS group (Tab. 12, 16). These findings rendered the two markers promising indicators for different genetic contributions in the clinical subforms of MS.

3.3.5 Correction for multiple testing through Bonferroni

After the MS group was stratified into RRMS and PPMS, and statistical comparisons performed on all groups, a correction of derived statistics had to be imposed in order to address the issue of multiple testing. The Bonferroni formula established a threshold for significance at a p-value of 0.0021, due to the number of tested SNPs (n=24) in accordance to the common degree of significance 0.05.

Table 3.9 revealed that 7 results at SNPs #13 and #17 stated a p-value below 0.0021 serving the Bonferroni correction. These comparisons could be considered sufficiently significant in order to overcome any bias inherent to repeated measurements. This outcome should not altogether undermine the precedently discussed relations of alleles and genotypes at remaining “non-significant” markers (e.g. SNP #21; comparison RRMS vs. HC). The correction process is an important tool to address the issue of multiple testing

of the same subjects. It aims to reduce the rate of false positive results by diminishing the effect of independency inherent with each test. Still, these thresholds are relative and their significancies depend to a certain degree on the investigator's point of view: he or she can choose the most strict criterion and state a solid conclusion independently, or, be less stringent and hence suggest fields open for replication in follow-on studies with identical and/or additional methodologies, describing thereby facets of the problem with different approaches.

3.4 Single gene inspection: haplotype analysis

4 genes that have been pre-analyzed in a screening stage - *VGLL*, *Prf*, *ADAMTS14*, *C10orf27* - were genotyped with altogether 16 SNPs on 572 individual DNA samples. As described in preceding chapter, allele and genotype frequencies were established and compared (Appendix E). When a significant association was revealed at one or more SNPs in a gene, a more comprehensive analysis including adjacent markers on the respective gene was performed (Appendix F). By means of the haplotype reconstructing software package PHASE haplotype pairs of each individual were designated and all assigned pairs not exceeding the accuracy threshold set at 90% were excluded from further analysis, thus leaving for analyses in each gene different numbers of unambiguous haplotypes. As a rule of thumb, the larger the amount of combined loci, the higher the probability that haplotype pairs remained inconclusive, expressed through an accuracy value below 0.9.

3.4.1 *VGLL4* - Transcription cofactor vestigial-like protein 4

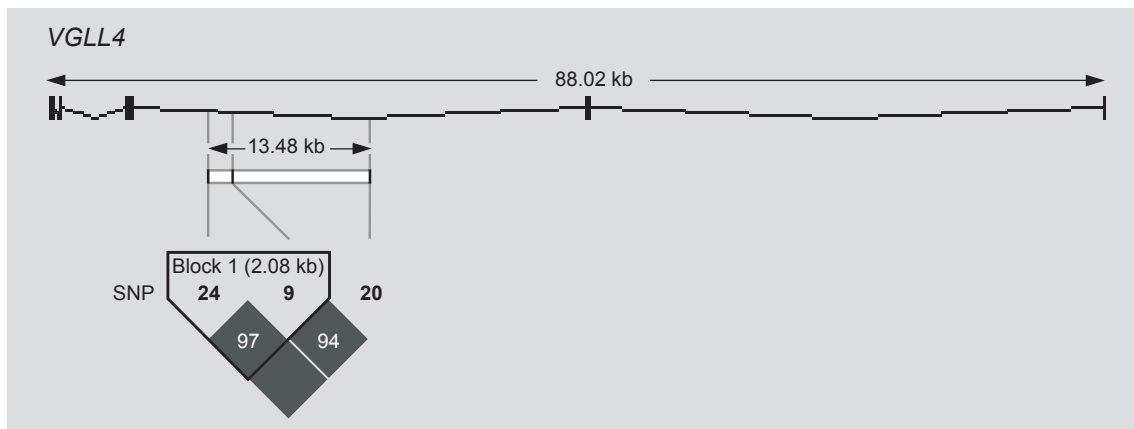


Figure 3.3 | **Diagram of block like structure of *VGLL4* at chromosomal location 3p25.3.** Upper part: Complete gene length and distinction exon (vertical bars) / intron (horizontal lines), distribution and relative positions of SNP markers spanning 13.48 kb; lower part: Linkage disequilibrium (LD) plot of computed pairwise statistics for all markers. Haplotype block identification due to complete LD ($D' = 1.0$ complete linkage between marker pair, $D' = 0$ no linkage, independent marker). Pairwise LD measures were calculated from genotype data of $N=572$ individuals.

In single allele and genotype comparisons of three intronic polymorphisms, significance was assessed for SNP #9 (Appendix E, Tab. 1-3). In order to extend the analysis and comply with the block-like structure in *VGLL4*, haplotypes were re-assembled with adjacent markers #24 and #20.

The PHASE software unequivocally assigned 568 control and 570 MS haplotypes, the latter comprising of 382 RRMS and 188 PPMS haplotypes (Appendix F1). Frequency comparisons did not generate additional relevance, neither did 2-SNP combinations and haplotype pair frequency comparisons (data not shown).

3.4.2 *PRF1* – Perforin

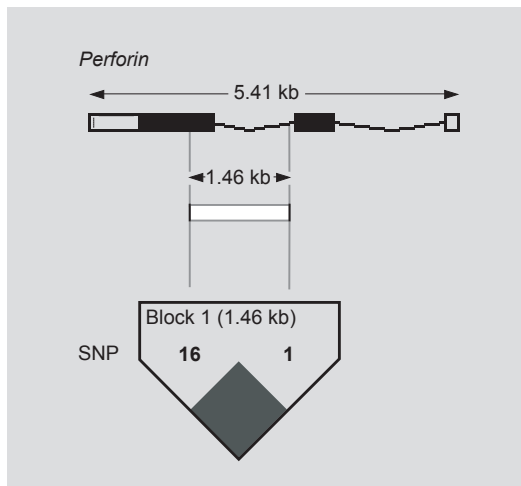


Figure 3.4 | Diagram of block like structure of *PRF1* at chromosomal location 10q22.1. Upper part: Complete gene length and distinction exon (vertical bars) / intron (horizontal lines), distribution and relative positions of SNP markers spanning 1.46 kb; lower part: Linkage disequilibrium (LD) plot of computed pairwise statistics for both markers. Haplotype block identification due to complete LD ($D' = 1.0$ complete linkage between marker pair, $D' = 0$ no linkage, independent marker). Pairwise LD measures were calculated from genotype data of $N=572$ individuals.

In single allele and genotype comparisons of the exonic and intronic polymorphisms, significance was assessed for SNP #1 (Appendix E, Tab. 5, 6).

The PHASE software assigned 570 control and 570 MS unambiguous haplotypes, the latter comprising of 384 RRMS and 186 PPMS haplotypes; extended haplotype frequency comparisons generated relevance for the haplotype GA (Tab. 3.10, H2: $p=0.029$; OR: 1.3). Subsequent haplotype pair frequency comparisons did not disclose further significance (Appendix F2).

Table 3.11 | Reconstructed haplotypes from two variable sites (SNPs #16, 1) within *PRF1*, their relative frequencies and corresponding statistics.

Frequencies, n (%)						
H	16 1	MS patients	Controls	P	OR (95% CI)	
1	A G	320 (56.1)	347 (60.9)	0.105		
2	G A	213 (37.4)	178 (31.2)	0.029	1.3 (1.0 – 1.7)	
3	G G	37 (6.5)	44 (7.7)	0.420		
4	A A	–	1 (0.2)	1.000		

*After stratifying the MS group, comparisons between RRMS patients at H2 with controls revealed statistical significance (H2: OR=1.3, $p=0.037$). H: haplotype number; Numbers 16 and 1 represent respective SNP position; OR: odds ratio; 95% CI: 95% confidence interval.

3.4.3 ADAMTS14 - a disintegrin-like and metalloproteinase domain with thrombospondin type 1 modules 14

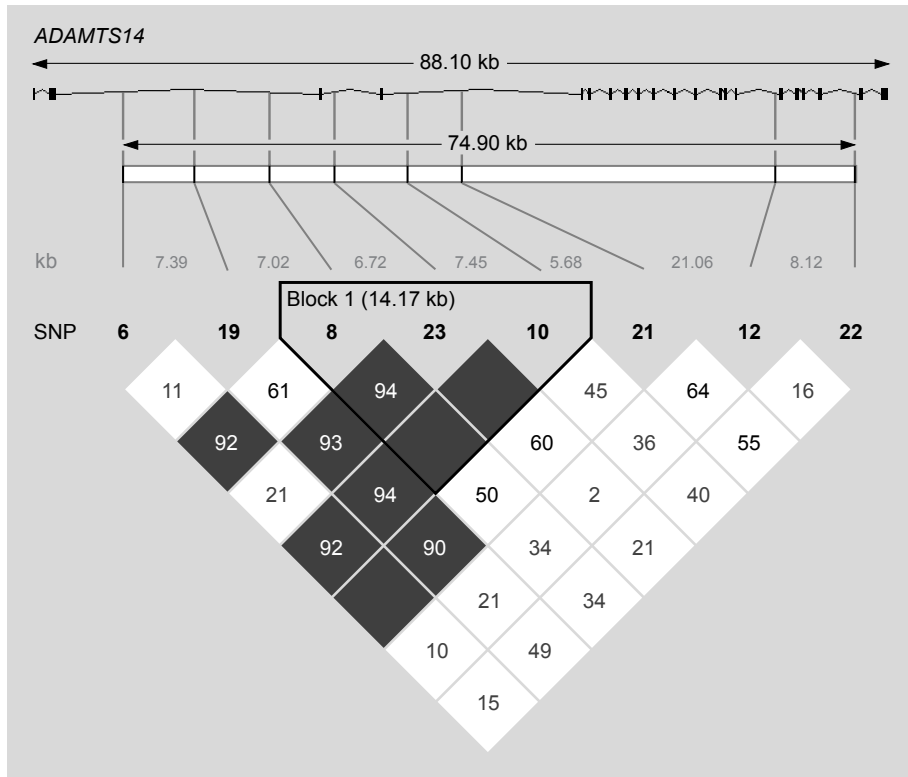


Figure 3.5 | Diagram of block like structure of *ADAMTS14* at chromosomal location 10q22.1. Upper part: Complete gene length and distinction exon (vertical bars) / intron (horizontal lines), distribution and relative positions of SNP markers spanning 74.90 kb; lower part: Linkage disequilibrium (LD) plot of computed pairwise statistics for all markers. Haplotype block identification due to complete LD constituted by consecutive markers 8, 23 and 10 ($D' = 1.0$ complete linkage between marker pair, $D' = 0$ no linkage, independent marker). Pairwise measures of LD were calculated from genotype data of $N=572$ individuals.

In single allele and genotype comparisons of eight intronic polymorphisms, significance was assessed for SNPs #19, 8, 23, 21, and 22 (Appendix E, Tab. 9-11). For this reason, haplotypes were reconstructed selecting these preliminary sites of interest. Haplotype reconstruction resulted unambiguously in 496 control and 492 MS haplotypes, the latter comprising of 332 RRMS and 160 PPMS haplotypes. Of 32 (2^5) possible haplotype combinations, 15 categories were detected in examined populations (Appendix F3a) and subsequently included in frequency and distribution examinations.

Frequency comparisons generated statistical significance for two haplotypes distinguishing MS patients from controls (Tab. 3.12, H8: $p=0.022$, OR= 0.5; H11: $p=0.039$, OR=2.9) and after clinical group stratification, these two haplotypes (H8, $p=0.029$; H11, $p=0.029$) plus an additional four (H1: $p=0.032$; H4: $p=0.049$, 0.025; H6: $p=0.012$; H7: $p=0.026$) revealed p-values below 0.05 (Appendix F3a).

Table 3.12 | Reconstructed haplotypes from five variable sites (SNPs #19, 8, 23, 21, 22) within *ADAMTS14*, their relative frequencies and corresponding statistics.

H	19 8 23 21 22	Frequencies, n (%)		P	OR (95% CI)
		MS patients	Controls		
1	GGGCT*	145 (29.5)	144 (29.0)	0.879	
2	ACGCA	118 (24.0)	121 (24.4)	0.880	
3	GGGCA	52 (10.6)	45 (9.1)	0.429	
4	GCGCT*	29 (5.9)	33 (6.7)	0.623	
5	GGACT	28 (5.7)	32 (6.5)	0.617	
6	ACGCT*	30 (6.1)	30 (6.0)	0.974	
7	AGGCT*	40 (8.1)	26 (5.2)	0.069	1.6 (1.0–2.7)
8	GGATT*	12 (2.4)	26 (5.2)	0.022	0.5 (0.2–0.9)
9	GCGTT	8 (1.6)	15 (3.0)	0.205	
10	GGATA	2 (0.4)	6 (1.2)	0.287	
11	AGGCA*	14 (2.8)	5 (1.0)	0.039	2.9 (1.0–8.1)
12	GGACA	6 (1.2)	5 (1.0)	0.772	
13	GCGCA	1 (0.2)	4 (0.8)	0.374	
14	GGGTT	6 (1.2)	4 (0.8)	0.545	
15	ACATT	1 (0.2)	0 (-)	0.498	

*After stratifying the MS group, comparisons between RRMS patients and controls (H8), and between PPMS patients and controls (H11) were statistically significant ($p=0.029$ each). Further five p-values below 0.05 were determined in comparisons between clinical subforms and controls at haplotypes H1, H4, H6, and H7. H: haplotype number; Numbers 19 through 22 represent SNP position; OR = odds ratio; 95% CI = 95% confidence interval.

Succeeding estimations of haplotype pair frequency distributions in MS patients and controls and the respective clinical subforms disclosed significance for assemblies 1/4 (RRMS vs HC, $p=0.036$), 2/2 (PPMS vs HC, $p=0.026$), 2/7 (MS vs HC, $p=0.031$), and 2/11 (PPMS vs HC, $p=0.028$) (Appendix F3a).

The haplotype analysis of SNP composites that revealed significance in single variation examinations (Appendix E, Tab. 9-12) generated a relatively wide range of haplotype structures ($n=15$), also caused by minor allele frequencies of the constituting variants. The software PHASE reassembled 156 haplotypes (78 haplotype pairs) that did not exceed the requested accuracy threshold (90%), which in turn reduced the statistical power and finally contributed to moderate p-values. In order to reduce the number of haplotype species, thereby increasing the number of employable haplotypes for statistical tests, and to comply with the suggested concept of linked SNPs that comprise a haplotype

block (Figure 3.5), the less frequent SNP #10 (MAF: 0.25) was substituted for SNP #22 (MAF: 0.39). This procedure diminished the general diversity of established haplotypes, expressed by an increased number of unequivocal haplotypes and a more limited variety of different haplotype states (n=11). Haplotype reconstruction with accuracy threshold set at 90% filtered only 66 ambiguous haplotypes and generated 534 control and 544 MS haplotypes, the latter comprising of 368 RRMS and 176 PPMS haplotypes (Appendix F3b).

Frequency comparisons generated relevance for two haplotypes distinguishing MS patients from controls (Tab. 3.13, H6: p=0.002, OR= 0.4; H7: p=0.004, OR=2.0) and after clinical group stratification, these two haplotypes revealed statistically significant p-values (Appendix F3b; H6: p=0.003, OR=0.4; H7: p=0.0004, OR=2.7).

Table 3.13 | Reconstructed haplotypes from five variable sites (SNPs #19, 8, 23, 10, 21) within *ADAMTS14*, their relative frequencies and corresponding statistics.

H	19 8 23 10 21	Frequencies, n (%)		P	OR (95% CI)
		MS patients	Controls		
1	ACGGC	147 (27.5)	152 (28.6)	0.553	
2	GGGAC	146 (27.3)	127 (23.7)	0.249	
3	GGGGC	78 (14.6)	79 (14.8)	0.832	
4	GGAGC	45 (8.4)	45 (8.4)	0.927	
5	GCGGC	41 (7.7)	42 (7.9)	0.840	
6	GGAGT*	17 (3.2)	39 (7.3)	0.002	0.4 (0.2–0.7)
7	AGGGC*	55 (10.3)	29 (5.4)	0.004	2.0 (1.2–3.1)
8	GCGGT	8 (1.5)	12 (2.2)	0.375	
9	GGGGT	7 (1.3)	3 (0.6)	0.342	
10	AGGAC	1 (0.2)	4 (0.7)	0.214	
11	AGGGT	1 (0.2)	2 (0.4)	0.621	

*After stratifying the MS group, comparisons between RRMS patients and controls (H6), and between PPMS patients and controls (H7) were statistically significant (p=0.0026 and p=0.0004, respectively). H: haplotype number; Numbers 19 through 21 represent SNP position; OR = odds ratio; 95% CI = 95% confidence interval.

Successive estimations of haplotype pair frequency distributions in MS patients and controls and the respective clinical subforms disclosed significance for assemblies 1/1 (MS vs. HC, p=0.026; RRMS vs HC, p=0.033), 1/7 (MS vs. HC, p=0.010; PPMS vs. HC, p=0.0009; PPMS vs. RRMS, p=0.022), and 3/6 (MS vs. HC, p=0.003; RRMS vs. HC, p=0.004) (Appendix F3b). Figure 3.6 represents the distribution of haplotypes assembled as pairs and outlines the associated groups.

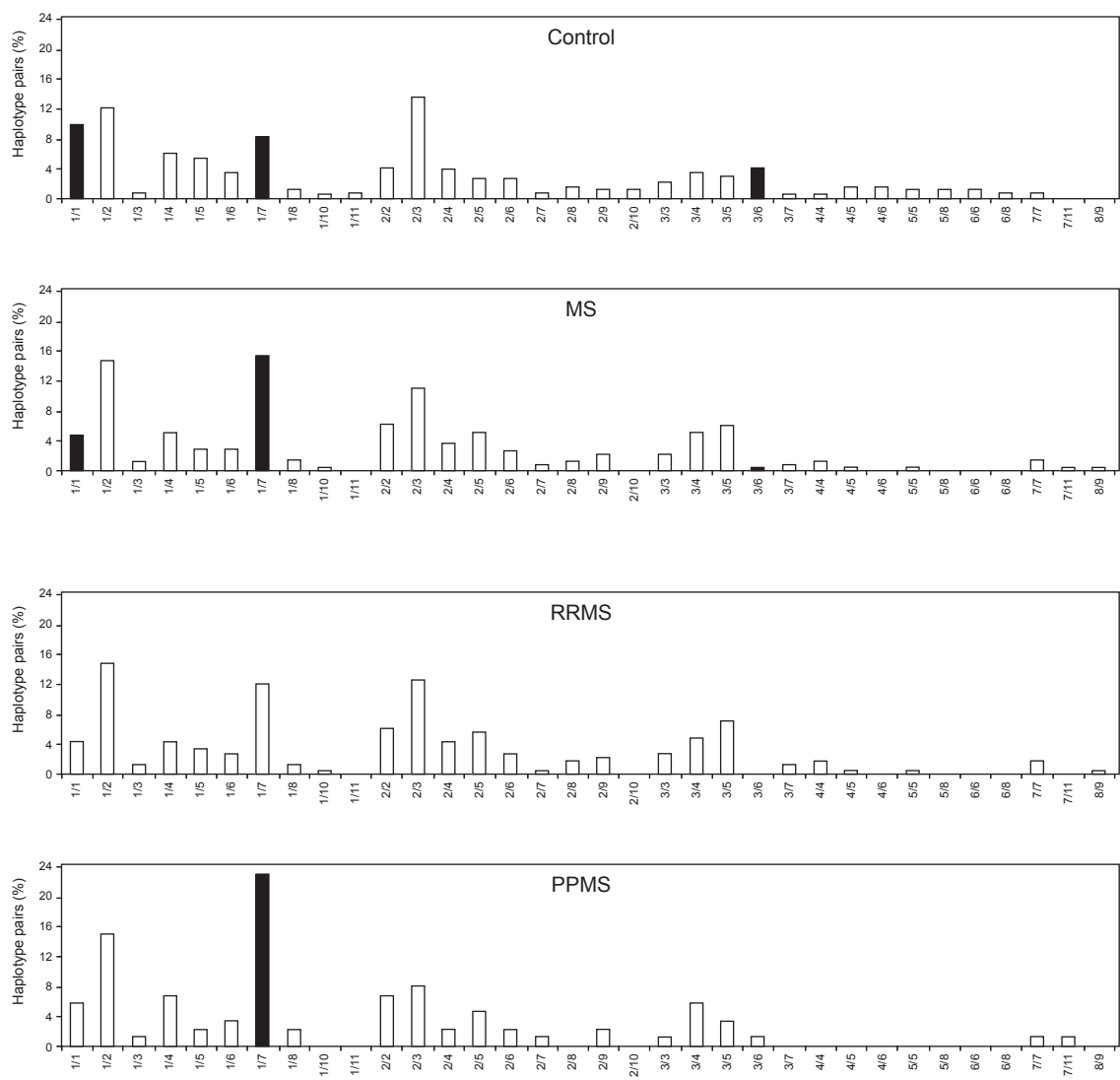


Figure 3.6 | Distribution of *ADAMTS14* haplotype pairs in control and MS group and respective MS subgroups. Haplotypes were reconstructed and assembled as pairs using software PHASE. The abscissa depicts haplotype combinations and the ordinate represents frequencies of corresponding haplotype pairs. Solid bars indicate the haplotype pair associated populations and statistically significant differences when compared between groups: MS vs controls (for 1/1, $p=0.026$; 1/7, $p=0.01$; and 3/6, $p=0.026$); RRMS vs. controls (3/6, $p=0.004$); PPMS vs. controls (1/7, $p=0.0009$).

3.4.4 C10orf27 – Chromosome 10 open reading frame 27

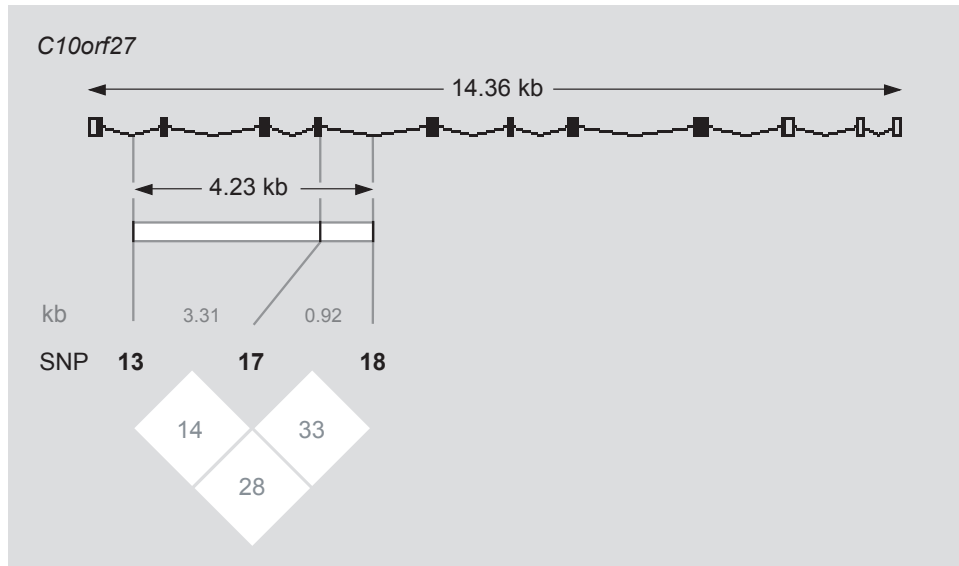


Figure 3.7 | **Diagram of block like structure of C10orf27 at chromosomal location 10q22.1.** Upper part: Complete gene length and distinction exon (vertical bars) / intron (horizontal lines), distribution and relative positions of SNP markers spanning 4.23 kb; lower part: Linkage disequilibrium (LD) plot of computed pairwise statistics for all markers. No haplotype block identification due to incomplete LD constituted by consecutive markers ($D' = 1.0$ complete linkage between marker pair, $D' = 0$ no linkage, independent marker). Pairwise measures of LD were calculated from genotype data of $N=572$ individuals.

In single allele and genotype comparisons of three intronic polymorphisms, significance was assessed for SNPs #13 and #17 (Appendix E, Tab. 13-16). In order to extract all available gene based data the non-significant SNP #18 was incorporated into the haplotype reconstruction process. Haplotype reconstruction resulted unambiguously in 518 control and 520 MS haplotypes, the latter comprising of 340 RRMS and 180 PPMS haplotypes. 8 haplotype categories were detected in examined populations and subsequently included in frequency and distribution examinations (Appendix F4). Frequency comparisons generated relevance for two haplotypes distinguishing MS patients from controls (Tab. 3.14, H3: $p=0.006$, OR= 0.7; H4: $p=0.004$, OR=0.4) and after clinical group stratification, these two haplotypes (H3, $p=0.0009$; H4, $p=0.003$) plus one additional (H5, $p=0.024$) revealed p-values below 0.05 (Appendix F4).

Table 3.14 | Reconstructed haplotypes from three variable sites (SNPs #13, 17, 18) within *C10orf27*, their relative frequencies and corresponding statistics.

H	13 17 18	Frequencies, n (%)		P value	OR (95% CI)
		MS patients	Controls		
1	ATC	215 (41.3)	200 (38.6)	0.368	
2	ATA	164 (31.5)	136 (26.3)	0.060	1.3 (1.0 – 1.7)
3	GTC*	94 (18.1)	130 (25.1)	0.006	0.7 (0.5 – 0.9)
4	GCA*	10 (1.9)	27 (5.2)	0.004	0.4 (0.2 – 0.8)
5	ACC*	32 (6.2)	21 (4.1)	0.124	
6	GTA	4 (0.8)	2 (0.4)	0.687	
7	GCC	0 (0)	2 (0.4)	0.249	
8	ACA	1 (0.2)	0 (0)	1.000	

*After stratifying the MS group, comparisons between both RRMS patients at H3 and PPMS patients at H4 with controls revealed statistical significance (H3: OR=0.6, p=0.0009 and H4: OR=0.1, p=0.003, respectively). H: haplotype number; Numbers 13 through 18 represent SNP position; OR: odds ratio; 95% CI: 95% confidence interval.

Successive estimations of haplotype pair frequency distributions in MS patients and controls and the respective clinical subforms disclosed significance for assemblies 2/4 (MS vs. HC, p=0.033), 2/5 (RRMS vs. HC, p=0.040; PPMS vs. RRMS, p=0.022), and 3/3 (RRMS vs. HC, p=0.034) (Appendix F4). Figure 3.8 represents the distribution of haplotypes assembled as pairs and outlines the associated groups.

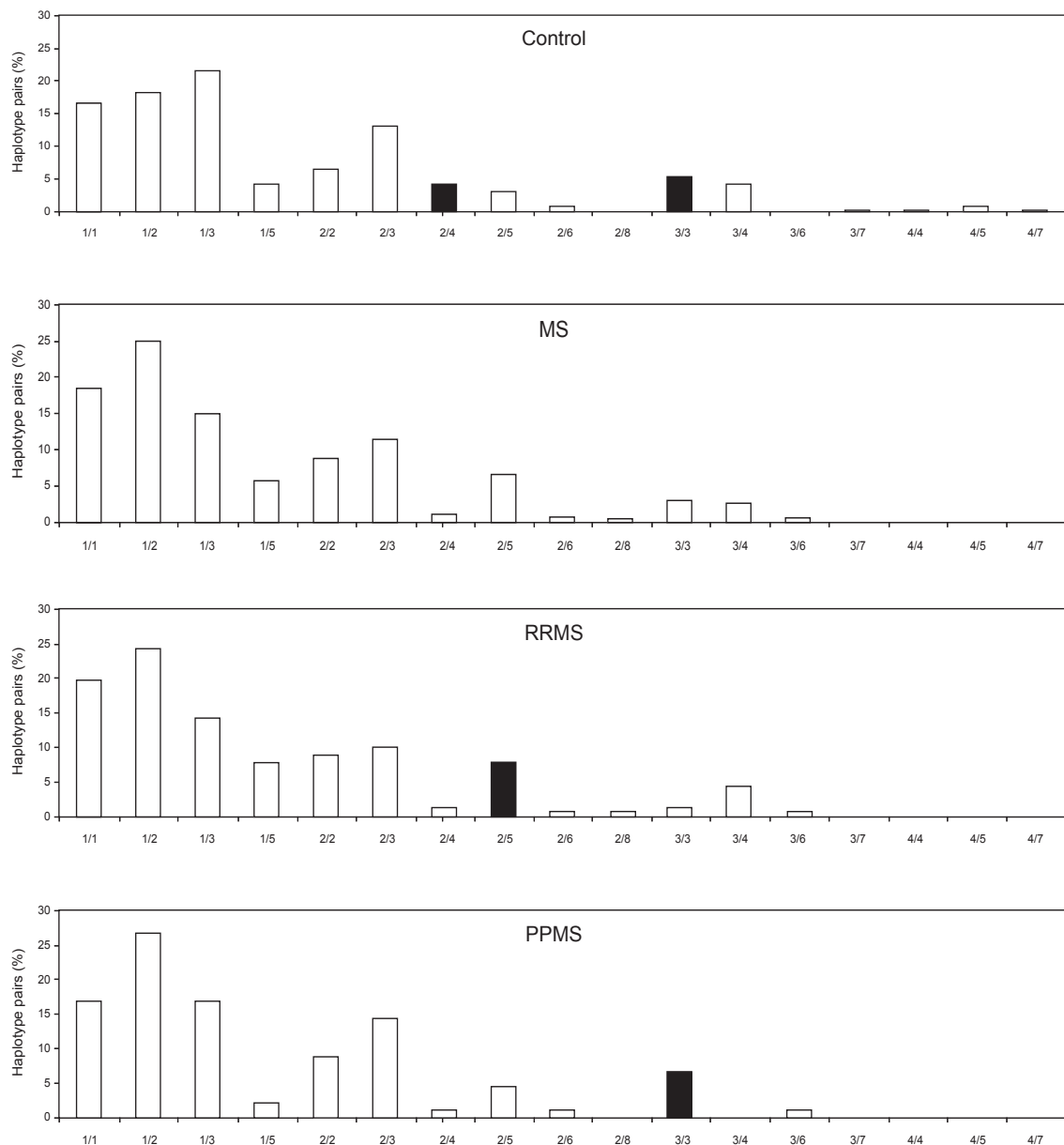


Figure 3.8 | Distribution of *C10orf27* haplotype pairs in control and MS group and respective MS subgroups of *C10orf27*. Haplotypes were reconstructed and assembled as pairs using software PHASE. The abscissa depicts haplotype combinations and the ordinate represents frequencies of corresponding haplotype pairs. Solid bars indicate the haplotype pair associated population and statistically significant differences when compared between groups: MS vs. controls (2/4, $p=0.033$); RRMS vs. controls (2/5, $p=0.040$; 3/3, $p=0.034$); RRMS vs. PPMS (3/3, $p=0.022$).

3.5 Combined gene haplotypes based on ascertained data of *ADAMTS14* and *C10orf27*

In order to determine association among SNPs located in adjacent genes, 8 markers from *ADAMTS14* and 3 markers from *C10orf27* were permuted as 2-SNP composites, rendering 24 possible pair combinations. Respective arrangements were introduced to the PHASE software and resulting frequencies of haplotype pairs were compared between respective groups.

Several composites revealed strong statistical significance, naturally of the most evident were combinations of SNPs that had already displayed association with MS. Both SNP #19 and #17 were found to be associated with MS and PPMS (Tab. 3.15). SNP #21 and #13 followed the same concept, except they were associated with MS and RRMS (Tab. 3.16).

Table 3.15a | Reconstructed haplotypes from SNPs #19 and #17 in genes *ADAMTS14* and *C10orf27*, their relative frequencies and statistics; MS versus controls.

H	19 17	Frequencies, n (%)		P value	OR (95% CI)
		MS patients	Controls		
1	GT	306 (58.4)	306 (57.1)	0.666	
2	AT	170 (32.4)	168 (31.3)	0.701	
3	GC	33 (6.3)	49 (9.1)	0.083	0.7 (0.4 – 1.1)
4	AC	15 (2.9)	13 (2.4)	0.657	

Table 3.15b | Reconstructed haplotypes from SNPs #19 and #17 in genes *ADAMTS14* and *C10orf27*, their relative frequencies and statistics; MS clinical subforms.

H	19 17	Frequencies, n (%)		P value	OR (95% CI)
		PPMS	RRMS		
1	GT	93 (52.2)	213 (61.6)	0.041	0.7 (0.5 – 1.0)
2	AT	77 (43.3)	93 (26.9)	0.00015	2.1 (1.4 – 3.0)
3	GC	6 (3.4)	27 (7.8)	0.057	0.4 (0.2 – 1.0)
4	AC	2 (1.1)	13 (3.8)	0.102	

Successive estimations of haplotype pair frequency distributions in MS patients and controls and the respective clinical subforms disclosed significance for assemblies 1/3 (PPMS vs. HC, $p=0.046$; PPMS vs. RRMS, $p=0.049$) and 2/2 (PPMS vs. HC, $p=0.017$; PPMS vs. RRMS, $p=0.0026$) (Appendix F5a). Figure 3.9 depicts the distribution of haplotypes assembled as pairs of PPMS and RRMS.

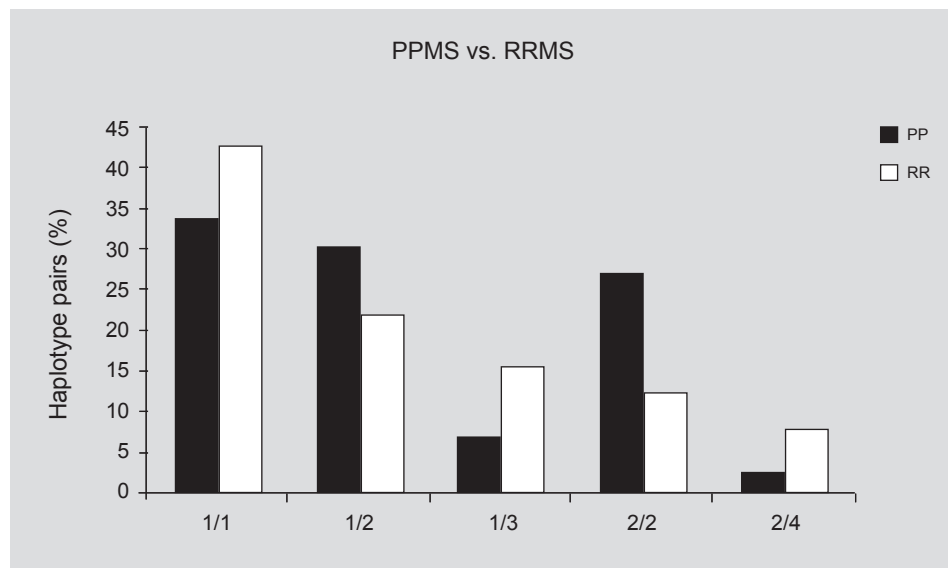


Figure 3.9 | Distribution of haplotype pairs derived from *ADAMTS14* and *C10orf27* SNP composites in PPMS and RRMS groups (SNPs #19–17). 2-variant haplotypes were computationally reconstructed and assembled as pairs using software PHASE. The abscissa depicts haplotype combinations and the ordinate represents frequencies of corresponding haplotype pairs. The haplotype pair 2/2 generated a p -value of 0.0026 ($OR=2.7$, 95% CI=1.4–5.1) that supplied evidence for a PPMS-discerning condition. Significance is indicated with an asterisk.

Furthermore, the combination of SNP #21 and #13 rendered haplotype association with the RRMS form.

Table 3.16a | Reconstructed haplotypes from SNPs #21 and #13 in genes *ADAMTS14* and *C10orf27*, their relative frequencies and statistics; MS versus controls.

H	21 13	Frequencies, n (%)		P value	OR (95% CI)
		MS patients	Controls		
1	CA	400 (73.3)	328 (63.8)	0.0009	1.6 (1.2 – 2.0)
2	CG	117 (21.4)	145 (28.2)	0.011	0.7 (0.5 – 0.9)
3	TA	25 (4.6)	27 (5.3)	0.612	
4	TG	4 (0.7)	14 (2.7)	0.016	0.3 (0.1 – 0.8)

Table 3.16b | Reconstructed haplotypes from SNPs#21 and #13 in genes *ADAMTS14* and *C10orf27*, their relative frequencies and statistics; MS clinical subforms.

H	21 13	Frequencies, n (%)		P value	OR (95% CI)
		RRMS	Controls		
1	CA	273 (74.2)	328 (63.8)	0.001	1.6 (1.2 – 2.2)
2	CG	77 (20.9)	145 (28.2)	0.014	0.7 (0.5 – 0.9)
3	TA	17 (4.6)	27 (5.3)	0.182	
4	TG	1 (0.3)	14 (2.7)	0.006	0.1 (0.0 – 0.7)

Successive estimations of haplotype pair frequency distributions in MS patients and controls and the respective clinical subforms disclosed significance for assembly 1/1 (MS vs. HC, p=0.002; RRMS vs. HC, p=0.003) (Appendix F5b). Figure 3.10 depicts the distribution of haplotypes assembled as pairs of MS and controls.

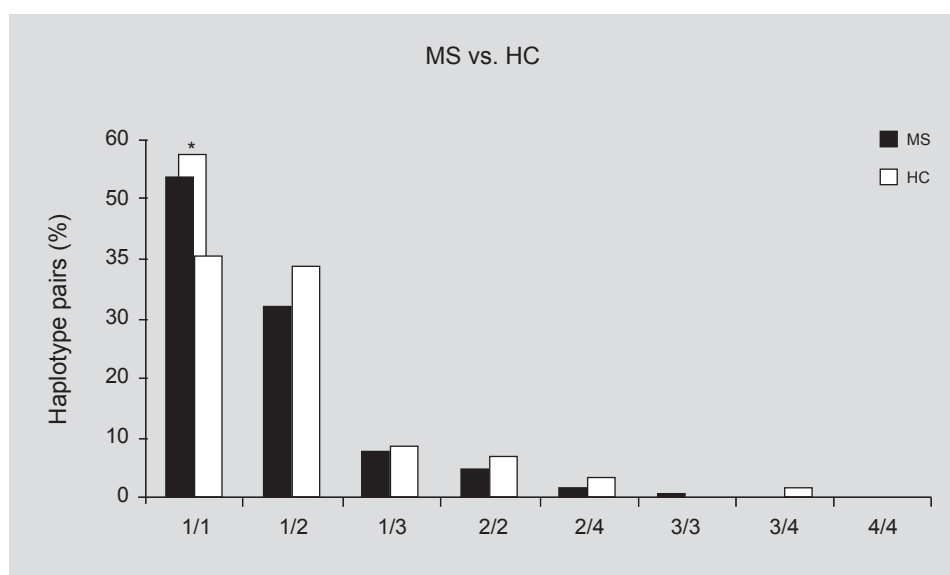


Figure 3.10 | Distribution of haplotype pairs derived from *ADAMTS14* and *C10orf27* SNP composites in MS and HC groups (SNPs #21–13). 2-variant haplotypes were computationally reconstructed and assembled as pairs using software PHASE. The abscissa depicts haplotype combinations and the ordinate represents frequencies of corresponding haplotype pairs. The haplotype pair 1/1 generated a p-value of 0.002 (OR=1.7, 95% CI=1.2–2.4) that supplied evidence for a PPMS-discerning condition. Significance is indicated with an asterisk.

4

DISCUSSION

4.1 A whole genome screen employing microsatellite markers and pooled DNA	104
4.2 284 candidate genes detected by “Sliding windows”	107
4.3 3p25.2: Apg7l and Vgll4	110
4.4 10q22.1: Perforin, ADAMTS14 and C10orf27	111
4.4.1 10q22.1: Intergenic haplotypes ADAMTS14 and C10orf27	115
4.5 Pros and Cons on association study design	116
4.5.1 Pros association study	116
4.5.2 Cons of association study	117
4.6 Multiple testing and epistasis	119
4.7 Conclusion and outlook	120

Genome scans are basically discovery-driven and automatically compel a major statistical issue of how to assign significance to a huge data set, also termed multiple testing problem. Therefore, one recommended strategy is to switch after such screen to a candidate region approach; it has the advantage of selecting candidates based on biological plausibility and the subsequent statistical analysis is somewhat simpler requiring fewer corrections than in a random search. Hence, the chosen strategy was to devise a candidate gene list that was appropriate to MS, establish the haplotype structure in the populations under study, define the haplotype frequency for the common variants in MS cases and healthy controls and identify the polymorphisms that best capture that diversity (tagging).

An initial genome wide screen on Spanish MS patients disclosed 460 microsatellite markers displaying evidence of association with the disease (Appendix B). In the following, by means of a newly devised analytical method termed “Sliding windows” that detects clusters of significant markers¹⁵¹ (Section 2.6; Appendix C), a list of 75 genomic regions of interest containing 284 genes was generated (Tab. 3.2), two of which – 3p25.2 and 10q22.1 – were further refined. Individual SNP genotyping was performed on 192 MS patients and 191 healthy controls, and showed significant association of the genes *VGLL4*, *Perforin*, *ADAMTS14* and *C10orf27* with MS. Further analysis with an increased sample size of 287 MS patients and 285 controls resulted in a statistically more robust confirmation of the previous findings and pointed *ADAMTS14*¹⁵² and *C10orf27* as most promising candidate genes for MS susceptibility.

4.1 A whole genome screen employing microsatellite markers and pooled DNA

A whole genome screen for evidence of linkage disequilibrium (LD) with MS was performed employing a panel of 5543 microsatellite markers and pooled DNA from Spanish patients and controls.¹⁵⁰ Results were estimated by means of an empirical p-value, a non-formal significance test that functioned satisfactorily in order to rank genomic regions of interest. The purpose of DNA pooling studies is not to deliver formal tests of association, but to provide a preliminary filter in order to prioritize loci for future study designs.

Furthermore, the pooling method introduces non-sampling errors into the data, which

were partly corrected by adapting factors for length dependent amplification and weighting factors.¹⁵⁶ Nevertheless, it appears noticeably difficult to completely estimate the random errors (secondary PCR products) or laboratory artefacts, hence the error variance.

191 candidate regions were identified through repeated testing of microsatellite markers (Section 3.2), delivering increasing support for areas that have previously been implicated in genetic susceptibility to MS and furthermore may direct new candidate gene studies. The confirmation of 8 HLA-restricted markers validated the pooled DNA approach for MS association studies; however, it must be noted that the screening was enriched with markers mapping to the gene-full MHC region.

Meta-analysis including data from all centers that participated in GAMES (n=18) was highly anticipated, but so far expectations have not been achieved. Several reasons might account for this unsatisfying situation. DNA pool formation was not part of standard GAMES design as some groups used HLA DR2-stratified samples exclusively^{195,196} or even incorporated additional PPMS individuals in their patients cohort.¹⁹⁶ Other teams determined DNA sample concentrations by photometric instead of proposed fluorescence-based techniques, therefore incorporating a considerable variance in pool accuracies. Furthermore, different genotyping centers like deCODE in Reykjavik and the laboratory in Cambridge, UK, applied different principles in their analyses. The single peak approach (SPA)^{150,154} has been outlined in section 2.5 of presented dissertation and the respective marker-based analysis is explained in Setakis *et al.*¹⁹⁷ Finally, different ethnical backgrounds seem to bear stronger limits than expected. Besides the overall MS-associated HLA-region, the concept of domestic, “nation”-specific sets of genes must be considered.

Individual genotyping of 7 Spanish candidate microsatellites

Subsequently, 7 of the 183 non-MHC markers were selected for genotyping on 372 individual DNA samples. It was attempted to replicate the DNA pool findings and therefore evaluate the merit of a genuine candidate region status. Methodology and results are outlined in Appendix A. The relative comparison of peak height distributions (allele image profile, AIP) of the DNA pool study to allele frequency distributions obtained from genotyping individual DNA samples provided a measure for the type I error rate (false positive result) of 28.6% for employed pooling methodology.

For described situation, the extent of this effect could not be methodically correctly estimated; an empirical p-value assigned to a peak of a marker from a pooled DNA analysis can not be compared straightforward with a formally computed p-value derived from a comparison of real allele counts of individually tested DNA samples. However, taking into account orientational aspects of a possible predisposing allele, a one-sided p-value <0.05 detected in individual genotyping was considered to consolidate preceding evidence of association.

Of the 7 microsatellites that displayed potential association with MS, 5 markers (D4S3245, D9S303, D12S1653, D13S777, D22S692) sustained statistical significance in individual genotyping. In addition, association with identical alleles and unchanged allele distribution ratios strengthened these findings (Appendix A; Table). Two regions of interest (D16S2613, D18S52), including D16S2613 that had been linked with MS independently in the past, could not be reproduced in presented data set. The dinucleotide marker D18S52 performed remarkably well in the majority of the GAMES population screens, but consistently failed to meet expectations after individual genotyping was performed with corresponding DNA samples (*oral communication*, DAS Compston), rendering it a problematic genetic marker.

Clearly, pooling DNA added new categories of variance and it appears rather difficult to derive basic rules on how to interpret results from genotyped microsatellites and DNA pools consisting of as many individuals as the present 200 per group. In addition to pool construction, the different kinetics of distinct marker types (di-, tri-, and tetranucleotide)¹⁵⁵ and inter-individual variations produce a multitude of inherent factors for variance which are difficult to control or correct for. For non-confirmatory markers it is legitimate to state: in spite of the obvious discordant distribution of allele percentages between AIP and single DNA genotyping results, the shorter allele repeats were generally over-represented whereas the longer fragments showed lower counts.

Of note, empirical p-values defining strong associations of single alleles declined more than expected in comparison to moderate ones, describing a relatively stable significance range of $0.05 > p > 0.01$. This would conform to the accepted principle of MS as a polygenic disease.

Based on presented data it can be stated that the allele profiles provided by DNA pools captured the majority of real alleles, missing only minor ones such as D13S777 “3” with a 1.9% allelic frequency (Appendix A, Fig. A4).

A relatively high type I error rate of 28.6% of realized pooling technology was suggested, though the limited number of 7 experiments should encourage scrutinizing this value by means of a 10 to 20 fold increase of genotyping tests (more markers with larger sample size).

These results illustrate that in an ideal situation for a tested microsatellite marker and its corresponding allele spectrum there should always exist a single correction factor (or template) for each allele. As many confounding factors remain, it would probably be necessary to determine these factors for data refinement empirically, which would require a great effort in material, time and costs. On the other hand, once completed and publicly available, pooling DNA and screening systematically their genomes with the appropriate analytical tools could generate important findings.

4.2 284 candidate genes detected by “Sliding windows”

Suggestive-linkage regions can contain common disease alleles with modestly relative risk, so there is some enthusiasm for association analysis of candidate regions of the genome identified as suggestive linkages. The sliding window method is a tool that extracts information from the genome scan by relating evidence of association of a marker with its genomic position and the distribution of neighbouring significant markers. This type of analysis is considered superior to a mere ranking of empirical pool p-values, as it extends from a sole degree of significance, which has been shown to bear a certain risk of inconsistency (Appendix A). In conclusion and according to epistatis theory, moderately significant marker regions seem more appealing to study.

As expected from displayed marker list in Appendix B, the MHC-region 6p21 contained windows with the highest number of accumulated significant markers ($n=7$). This is in good agreement with previous reports on MS susceptibility and the HLA region,^{xxx} and validates the applied sliding windows method. In sum, 75 detected regions of interest contained 284 annotated genes, 202 of them distributed over 56 non-MHC cluster.

STS-markers displaying evidence of MS association that do not appear in the significant windows (Tab. 3.1; Appendix B) could either be considered technical artefacts, hence false positives, or they are located within a recombinatorial highly active region of the genome, so called “hotspots”, that had not been saturated densely enough with the provided marker set. Therefore they might indicate a haplotype block in linkage disequilibrium with MS represented here by only one microsatellite marker.

The identification of susceptibility genes is an elusive task as the nature of relevant genes in MS pathogenesis or autoimmune diseases remains above all hypothesis-driven; this is why immune system-related genes are regarded as more appealing candidates and have been carefully described (Tab. 3.4). Attainable information on tissue restrictions and cell types served as explorative tools for the evaluation of pathogenesis-related functions of 142 genes.

No annotated genes were present in 18 regions of interest. However, it should be kept in mind that regulatory, gene predicted or other yet unknown genomic sequences of interest might remain undiscovered in vicinity of indicated areas of “no known genes” (Tab. 3.2); this may prove promising in the future when the genome exploration has advanced sufficiently. For example, some genes display a specially built structure that is not annotated by standard gene prediction methods, such as sequences encoding for T cell receptors (TCR), Immunoglobulins or Natural Killer cell receptors.¹⁹⁸⁻²⁰⁰ Principally, these regions ought to be treated as important as gene-containing regions, especially when regarding the regulatory properties of the genome, like the project ENCODE does.²⁰¹ Furthermore, recent comparative genomic studies have demonstrated that the level of evolutionary conserved non-coding sequence (NCS) is comparable to the amount of the evolutionary conserved exonic sequence.^{202,203} It seems quite plausible that disease-associated variants with modest effect will be distributed proportionally between noncoding and coding sequences. However, the ability to identify functional variation in conserved NCSs is still in its infancy stage.^{204,205} An in-depth analysis of these areas would be beyond the scope of this work and should be considered for ongoing or future studies.

Inasmuch as the listed 142 genes in Appendix D represent genes of interest they could be regarded as “to-date-hypothesis-free” candidates, which may be reconciled with autoimmune stages in the future. For example, the affiliated molecules hydroxysteroid (17-beta) dehydrogenase 4 (HSD17B4; 5q23.1) – it participates in beta-oxidation pathway for fatty acids – and family member hydroxysteroid (17-beta) dehydrogenase 8 (HSD17B8; 6p21.32) – it inactivates estradiol, testosterone, and dihydrotestosterone – could under impaired conditions contribute negatively to organism homeostasis. Still, a direct link to MS would be difficult to establish, rendering them, for now, speculative candidates. Describing in detail Appendix D candidates’ biological functions, if known, and potential relatedness to MS pathogenesis would go beyond this work’s scale and

it is recommended for encouraged readers to enquire public databases (e.g. OMIM, Genecard, GEO) and related literature.

Analyses of complete genomes, together with the availability of abundant gene-expression data, have converged to the opinion that eukaryotic gene order is not random.²⁰⁶ This at hand and knowledge about cis and/or trans inter-regulation of functionally related genes makes it conceivable to expect an increased biological understanding of suggestive genes and disease association.

Possibly, regions in a window are not in linkage disequilibrium on one entire stretch, but in functionally close proximity due to cis activity of related genes of a gene family or of functionally related genes comprising shared biological pathways. As a matter of fact, gene expression studies in MS have revealed supporting evidence for various candidate genes outlined in Table 3.4. Iglesias *et al.*²⁰⁷ detected differentially expressed transcripts for Notch homolog 4 (NOTCH4), Lymphotoxin β (LTB), Death-associated protein 6 (DAXX), E2F pathway members and a cytochrome P450 gene (CYP2A13) in peripheral blood derived from MS patients. Mandel *et al.*²⁰⁸ revealed apoptosis-related cysteine protease Caspase 8 (CASP8) and mitogen activated protein kinases (MAPK3, MAPK6), Koike *et al.*²⁰⁹ a cationic amino acid transporter (SLC7A1) and the MHC class I related peptide transporter 1 (TAP1). Satoh *et al.*²¹⁰ characterized expression profiles in T cells of MS cases and detected, amongst others, further members of the cytochrome P450 gene family (CYP1A2) and mitogen activated protein kinases (MAPK1), heat shock proteins (HSPA1A, HSPA1L), the cyclic AMP responsive element-binding protein 1 (CREB1), a CMP-sialic acid transporter (SLC35A1), and also DAXX. Interestingly, the beta subunit of GA-binding protein transcription factor (GABPB1) was downregulated and the corresponding alpha subunit (GABPA; Appendix D) was detected in this study. The latter is a fine example for a gene that initially did not seem functionally related to MS pathogenesis, but in conjunction with evidence derived from another experimental model (gene transcription), it ascends in the priority list of candidates that should be subjected to closer inspection. It remains to be learned if proposed candidate genes carry disease causing variations in their DNA sequences encoding for protein structure, for regulatory elements, e.g. promotor or transcription factor binding sites, or for so far unknown functions, e.g. intronic sequences. Obviously, this clustering detection method has mainly guidance value. Strict statistical interpretation is not recommended, since, first, multiple testing problems appear when testing for as many windows as markers

available in the genome and, secondly, because certain spurious associations linked to haplotype blocks could produce clustering patterns as well. Following steps in order to fine-map candidate regions involve testing promising regions derived from presented lists by means of individual DNA samples and SNP marker.

Two regions, loci 3p25.2 and 10q22.1, covering 5 genes were selected based on several features: twice evidence of associative status in GAMES, contiguous significant markers constituting significant windows, maximum score (6) of significant window sizes (0.5 to 3.0 cM), plus functional nature of genes in accordance to their potential implication in MS pathogenesis. The genes located on 10q22.1, *Perforin* and the metalloproteinase *ADAMTS14*, were considered likely to be functionally relevant, whereas *Apg7l* and *VgII4* at 3p25.2 might not bear apparent autoimmune disease features. In light of disclosed not too compelling potential of a candidate gene (*GABPA*) that received supportive evidence from another MS study,²¹⁰ it was regarded worthwhile to include this candidate region.

4.3 Locus 3p25.2: *Apg7l* and *VgII4*

The region 3p25.2 was specified by microsatellites D3S3714 and D3S3680, first positioned in *VgII4* (Fig. 2.6). In order to evenly distribute markers over the region of interest the upstream located *Apg7l* was included in the study.

Apg7l encodes a protein that shows homology to the ATP-binding and catalytic sites of the E1 ubiquitin activating enzymes. It was genotyped with two SNP markers (#3 and #5) on 383 individuals and rendered no indication of MS association, hence no further samples or markers were applied.

VgII4 (Transcription cofactor vestigial-like protein 4) may function as a specific coactivator for the transcriptional regulator thyrotrophic embryonic factor (TEF).²¹¹ This candidate was initially genotyped with 3 SNP markers (#7, #9 and #11) and after determination of significance (#9; p=0.022; Tab. 3.8), additional 2 SNPs (#20 and #24) were analyzed on final 572 DNA samples. SNP marker #9 maintained its degree of significance (p=0.010; Tab. 3.9; Appendix E2) and the inclusion of adjacent non-significant markers limited the potential intronic area of association to 13.5 kb (Fig. 2.6b, 3.3). Further scrutinizing of this area might reveal a moderate disease related haplotype block (Appendix F1).

4.4 Locus 10q22.1: *Perforin*, *ADAMTS14* and *C10orf27*

The region 10q22.1 was specified through microsatellites D10S537 and D10S1685, latter positioned within *ADAMTS14* (Fig. 2.7). In order to evenly distribute markers over the region of interest the downstream located *Chromosome 10 open reading frame 27* was included in the study.

One of the main pathways of lymphocyte-mediated cytotoxicity entails the polarized secretion of granule-stored perforin (OMIM *170280) onto target membranes leading to target-cell lysis. Perforin is a major cytoytic pore-forming protein with a mechanism of transmembrane channel formation. It is contained in cytoytic effector lymphocytes of T-cell or NK-cell type.²¹²

As outlined in the model of pathogenetic mechanisms of MS (Fig. 1.2), CD8⁺ cytolytic effector T-cells represent a crucial component of axonal dissection and degeneration. Several *in vitro* studies examined perforin-mediated cell injury and discovered myelinating oligodendrocytes as vulnerable targets by T-cell perforin.^{213,214} Also, inflammatory active phases of MS have been correlated with elevated perforin mRNA expression in PBMCs and CSF.²¹⁵⁻²¹⁷ So far, perforin gene defects in MS individuals were not reported, but are responsible for 10q21-22-linked familial hemophagocytic lymphohistiocytosis (FHL). It was stated that perforin-based effector systems are involved not only in the lysis of abnormal cells but also in the down-regulation of the cellular immune activation.²¹⁸

The intronic SNP #1 displayed a moderate association of MS individuals with the A allele ($p=0.038$) and the controls prone GG homozygosity ($p=0.039$), but no association for exonic marker #16 (Appendix E5). Nevertheless, subsequent analysis of reconstructed marker combinations (Appendix F2) revealed a modest significance for the GA (#16 – #1) haplotype ($p=0.029$), but no statistical relevance when examined as re-assembled pairs for each individual. An extended study on perforin is in progress (*oral communication* M Comabella), as individuals displaying specific MS disposing haplotype combinations donate blood in order to realize *in vitro* experiments and mRNA expression profiling.

Cell-cell and cell-extracellular matrix (ECM) interactions provide cells with information essential for controlling morphogenesis, cell fate specification, gain or loss of tissue-specific functions, cell migration, tissue repair, and cell death.²¹⁹ A presumably complementary role in controlling brain matrix structure and organization has been ascribed to the novel protease family A Disintegrin And Metalloproteinase Domain with

Thrombospondin Motifs (ADAMTS).²²⁰⁻²²² ADAMTS-14 (OMIM *607506)²²³⁻²²⁶ is a member of a structurally and functionally distinct subfamily of ADAMTS proteases (ADAMTS-2 and -3) and has been shown to be synthesized as a latent enzyme that requires cell type-regulated activation to display aminoprocollagen peptidase activity.²²⁵ Procollagen N-proteinases process the propeptides of fibrillar collagens in order to generate collagen molecules which assemble into fibrils. Evidence for a potential role of these proteases in the biology and pathology of the CNS bases on their decomposing activity on several proteoglycans enriched in the nervous system, and is derived from the expression of various members of this family (ADAMTS13, ADAMTS14, ADAMTS16 and ADAMTS18) in human brain.²²⁶

Genes encoding metalloproteinases are attractive candidates for MS research due to their role in brain ECM cleavage and regulation of inflammation and acquired immunity.^{227,228} Normal ECM is in a state of dynamic equilibrium, accounting for a stability between synthesis and degradation. For the degradative process there is a balance between disintegrating proteinases and the corresponding inhibitors. It is believed that in MS a disruption of this balance in favor of proteolysis leads to pathologic brain ECM destruction and MRI lesions.²²⁹ Even so, metalloproteinase tasks such as regulating axon elongation or facilitating dendrite outgrowth and remyelination suggest that metalloproteinase activity may also contribute beneficially to the disease.²³⁰⁻²³² To date, metalloproteinases (MMP-2 and 9), their inhibitors (TIMPs), and members of the A Disintegrin And Metalloproteinase family (ADAM-10 and 17) have been reported to be implied in MS pathogenesis.²³³⁻²³⁸ Nevertheless, association studies between metalloproteinase gene polymorphisms and MS are scanty and nearly confined to MMP-9 with discordant results.²³⁹⁻²⁴²

In the present work, 3 out of 8 SNPs distributed over the gene showed significant association in their genotype and allele frequencies with MS (SNPs #19, #8, and #21; Appendix E9–12). Though none of these markers are located in protein-coding sequences, nucleotide variation in introns has been demonstrated in various studies to display important regulatory features with phenotypic effect, such as an alteration in a binding site for a transcription factor in autoimmune diseases.²⁴³⁻²⁴⁵ In addition, alteration at intron-exon border consensus sequences can lead to incorrect processing of a gene, but the corresponding sequence examination did not generate such information for associated SNPs.

By means of haplotype inference comprising 5 variants, it was feasible to ascertain the overall haplotype distribution that disclosed differences between MS patients and controls (Appendix F3b). Two of the 11 haplotypes analysed (H6, H7) were particularly different in their frequencies and undermined the contribution of markers #19, #8 and #21 to the association between the over- and under-transmitted haplotypes and MS. Of note, H7 was a risk haplotype for MS in PPMS patients, and H6 was associated with reduced risk in RRMS patients. When haplotypes were assembled as pairs, combination of H7 and H1 (pair 1/7 = ACGGC/AGGGC) was strongly associated with PPMS, whereas combinations of H1 and H1 (pair 1/1 = ACGGC/ACGGC) or H6 and H3 were either counted less in MS or completely unseen in RRMS (Fig. 3.6).

The presence of different haplotypes conferring risk or resistance for MS in patients with PPMS and RRMS, respectively, may contribute to the heterogeneity found between these two groups. There exists general agreement that patients with PPMS differ significantly according to epidemiology, CNS histopathology, neuroimaging findings, and response to treatment in comparison with RRMS patients.²⁸ It is yet to be explored whether these haplotypes are related to different levels of gene expression or functional changes in the encoded protein.

In summary, the presented observations and biological plausibility support the hypothesis that individual polymorphisms within *ADAMTS14* may influence genetic predisposition for MS. Further studies in other MS cohorts will be required to confirm the association of *ADAMTS14* haplotypes for MS. Finally, functional *in vitro* and *in vivo* studies are needed to investigate differential gene expression patterns related to risk or protective haplotypes in PPMS and RRMS patients, as well as the immunohistochemical localization in MS brain specimen.

C10orf27 is expressed in several human tissues, and highest expression values have been reported for tested complementary DNA (cDNA) sources constructed from thymus (AK124147) and testis (AK057382). Bioinformatic analyses revealed a nucleic acid similarity degree of 79.3% of the *C10orf27* sequence with a syntenic mouse gene that translates into a stromal protein associated with thymii and lymph nodes (AK038284, NP_075551), showing a 51% (n=167) amino acid compatibility. A further homologue gene with 75.8% base pair agreement is the Spatial- δ gene in mouse²⁴⁶ and rat (XM_228291) which is an alternatively spliced variant and highly expressed in testis. Again, isoforms of this gene were found to be expressed excessively in thymus tissue and

lymph nodes,²⁴⁷ suggesting an active role of these related genes in the dynamics of the immune system.

Two out of 3 SNPs showed associations in their genotype and allele frequencies with MS (SNPs #13 and #17; Appendix E13-16). By means of haplotype inference it was feasible to ascertain haplotype pairs that conferred disease risk (pair 2/5 = ATA/ACC) or resistance (pair 2/4 = ATA/GCA; pair 3/3 = GTC/GTC), respectively and a characteristic haplotype assembly (pair 3/3) that distinguishes between PPMS and RRMS patients (Appendix F4).

As aforementioned, patients with PPMS are highly heterogeneous in comparison with RRMS patients. In this respect, it is interesting to comment on the genotyping data of SNP #17 (rs2254174). While comparing the under-representations of allele C and genotype CT in PPMS population with RRMS, and also with controls, a negative association with the PPMS group was determined (Appendix E15/16). But when examining haplotypes constituted of all three SNPs, frequency and pair analyses revealed an inverse contribution of the T allele at haplotype H3 = GTC. The 3-SNP-composite was less frequent in MS than in controls, although (numerically) more present as allele or genotype, respectively (Appendix F4). This allows various distinctions between PPMS and RRMS or controls on three levels (allele, genotype and haplotype). It represents a suitable example and fine justification for extended statistical analysis combining several polymorphisms to reconstruct haplotype pairs, when phase sequence information is not available. Allele T introduces a non-synonymous variant on codon position 2 and causes an amino acid change from arginine to glutamine at position 237 (Arg237Gln; NM_152710). Interestingly, MS patients carrying the homozygote TT genotype suffered from a more severe disease course as compared to CT carriers (*oral communication* M Comabella). These differences in the rate of disease progression may be explained by a functional alteration of the C10orf27 encoded protein related to the substitution of the basic Arg residue with the polar amino acid Gln. For now, functional implications of the amino acid change and its role in MS pathogenesis are speculative, inasmuch as functions of the C10orf27 protein remain largely unknown.

The role of C10orf27 as a candidate gene for MS is further supported by the finding of higher gene expression in brain tissue from MS patients as compared to control brain samples (*oral communication* S Baranzini). A subgroup of MS specimens showed an increase in C10orf27 expression of more than 2.5 fold compared with control specimens,

which may reflect pathological heterogeneity related to different stages of the disease. Further studies to ascertain the brain cellular source of *C10orf27* mRNA or protein are in progress. This shall enlarge understandings of structure, regulation, interaction and function of the *C10orf27* encoded protein, which is required to further implicate the gene as a predictive or prognostic factor for MS susceptibility and progression.

4.4.1 Locus 10q22.1: Intergenic haplotypes ADAMTS14 and C10orf27

In light of assumed moderate epigenetic contributions from several genes of investigated polygenic disease, the analysis of a two-SNP composite haplotype employing one marker each from adjacent genes *C10orf27* and *ADAMTS14* elicited particular interest (Section 3.5; Appendix F5).

The extended haplotype analysis allowed description of a pattern of genetic variation in the genome. Coalescence of genotyped SNP #19 and #17 disclosed a very strong association with the PPMS group vs. RRMS ($p=0.0002$), and less evident when compared with controls ($p=0.004$). The genomic distance of 85.6 kb between both markers does not necessarily support the concept of a common haplotype block structure stretched over such a distance,^{95,96,98,106} but rather argues for the scenario of two independent tag SNPs each indicating the PPMS status. Both could represent PP-prone genomic blocks which, in the ascertained combination, increase disease risk or, in other words, form a susceptibility “load”. The same outlined principle holds true for an additional SNP-composite consisting of SNP #21 and #13. Clear significance values propose association with MS ($p=0.0009$) and explicitly RRMS ($p=0.001$). When assembled as haplotype pairs, respective composites conveyed strongest evidence in their homozygous states (#19–17, H 2/2; #21–13, H1/1).

It can be concluded that in both situations did the combination analysis of respective two loci more accurately describe the genetic features of PPMS and RRMS, than did single locus analysis.

4.5 Pros and Cons on association study design

4.5.1 Pros of association studies

The first key advance and a prerequisite for a promising association study design was the completion of the human genome sequencing effort,^{85,87} which provides a direct way to connect a chromosomal region with its DNA sequence and gene content. The genetic variations responsible for complex traits are not exclusively mutations coding for aberrant gene products; they can also be polymorphisms of which function we are to date ignorant. They act independently or through epistasis, and each polymorphism can exert a small contributory effect on some as yet undefined structure or physiological function.¹³ Linkage analysis is more powerful than association analysis for identifying rare high-risk disease alleles, but latter is expected to be more powerful for the detection of common disease alleles that confer modest disease risks.^{69,94}

Association study designs will be greatly enhanced by an international effort, such as the International HapMap project which has been established to map the common patterns of genetic variation across the entire human genome. Upon completion of the first phase of the project in October 2005,²⁴⁸ it should be now possible to design genome-wide haplotype mapping programmes much in the way the progress in microsatellite markers enabled widespread use of genome mapping in Mendelian disease. Knowledge of the haplotype structure allows an optimal subset of SNPs to be selected that efficiently extracts 90–95% of information. Such can be applied to the design and execution of powerful genome-wide association studies.^{249,250} Therefore, the definition of the patterns of linkage disequilibrium at two presented loci was the prerequisite to ascertain MS tag-SNP candidates.

Although recombination events in a single meiosis are relatively rare over small regions, the large total number of meiosis that occurs each generation in a population has a substantial cumulative effect on patterns of LD, and so molecular data from population samples contain valuable information on fine-scale variations in recombination rate.^{101,102} LD is a test of non-random association of alleles at different loci and basically an approach to relate genetic variation in a population sample to the underlying recombination rate. It is important to clarify that the LD term D' can reach a value of 1.0 though the involved allele frequencies vary widely, as it reflects the correlation only since the most recent mutation occurred.²⁵¹ This kind of information could have important implications for the design and analysis of future LD mapping and association studies in MS. For example,

it would help in predicting patterns of variation at sites that have not been genotyped densely (perhaps sites influencing susceptibility to MS), and it would provide some indication of whether block structures observed in one sample are likely to be replicated in other samples – a crucial requirement for being able to select representative tag-SNPs¹⁰⁷ based on LD patterns observed in reference samples. Presented SNP markers #9, #1, #8, #19, #21, #13 and #17 located in respective block-ranges could be tag SNPs, which would represent certain-sized stretches of DNA. Ideally, disease-influencing variants are located within these blocks.

Haplotype studies are becoming essential to association analysis of candidate genes. In order to perform haplotype analysis in a population-based case-control study, haplotypes must be determined by estimation in the absence of family information or laboratory methods for establishing phase. A computer-based algorithm implementing a Bayesian approach to infer phase information was used; this approach is not based on HW equilibrium.^{164,165} When haplotype pairs of each individual were designated by the PHASE software, all assigned pairs not exceeding the accuracy threshold set at 90% were excluded from further analysis, leaving for analyses in each gene different numbers of unambiguous haplotypes. As a rule of thumb, the larger the amount of combined loci, the higher the probability that haplotype pairs remained inconclusive, expressed through an accuracy value below 0.9. Similarly, the Haplovew software generated different D' values when input files delivered genotype data from a varying number of individuals. The overall description of recombinational landscape of 3p25 and 10q22 in Figures 3.1 and 3.2, presenting 10 and 13 SNPs, respectively, were derived from 383 individuals. The more specific gene based LD patterns were created introducing genotype data from all 572 individuals (Fig. 3.3–3.5, 3.7). Eventually, individual SNPs may be investigated as candidates for causative variations in disease-related genes, but association tests with gene-based haplotypes provide greater statistical power and are more promising as they reveal further comprehensive genetic information of a gene.⁶⁹

4.5.2 Cons of association studies

Association studies are a powerful tool to delineate the genetic component of complex disease. Nevertheless it is evident from the literature that they also lead to confusion owing to conflicting results upon replication. This could be due to a number of reasons. First, to date, few association studies have determined the linkage disequilibrium

patterns around their candidate genes. Therefore, any reports of putative associations could be considered as candidate polymorphism rather than candidate gene studies. As these studies do not take into account the underlying haplotypic diversity, they do not provide the full range of diversity within the gene. Secondly, it is worth noting that conflicting results have also been obtained due to the replication of associations using different SNPs in the same gene, exposing differential association to the causative variation. Thirdly, population stratification may underlie the conflicting results in some studies, creating false signals. A degree of population subdivision can be influenced by migration, non-random mating, other forms of selection, small population size, mutation, or genotype misclassification. All scenarios are conceivable and could contribute independently to the overall result. This implies that the observed allele and haplotype frequency differences between cases and controls could in fact be due to covert population structure and not a representation of causality, leading to erroneous associations.^{252,253} The importance of population stratification is still under debate; however, reports in the literature suggest that the effects of stratification have been overstated^{254,255} and approaches are being developed to account for its effect.^{256,257} The Hardy Weinberg equilibrium (HWE) (Sections 2.11; 3.3.2) deals with such problems, though it entails several requirements that are not congruent with an outbred population. It describes a state in which the proportions of genotypes present depend only on the frequencies of alleles in the genotypes. Therefore, HWE deviations in an outbred population are not uncommon.

A possibility of population deviation between employed MS patients and healthy controls (SNPs #8 and #19; Tab. 3.6) might be due to enrolling control DNA from the University hospital blood bank, that mostly recruits individuals from nearby whereas several MS patients originate from much farther areas in Spain. If the population allele frequencies do not comply with HWE, this could also express genotyping errors, which have deleterious effects on association and linkage disequilibrium analysis¹⁶⁰ and therefore would affect the here described analysis. The easiest approach to the error problem is stated to be increased quality control in the laboratory, but a genotyping misclassification as a source can be mainly discarded, as error frequencies in the analysis model (allelic discrimination) have been shown to be minimal. The applied methodology was extraordinarily robust; in addition, the unarranged SNP ID numbers and corresponding independent assay realizations – of 572 distributed DNA samples, 381 were on one and 191 on a further plate – indicate a more profound population-specific cause. Therefore,

the likeliness of a Spanish population-specific substructure on these two contiguous loci, separated by 7.6 kb, can be assumed. Finally, many SNPs may violate HW equilibrium for noncausal reasons.

4.6 Multiple testing and epistasis

Evidence for an association is provided when a significant frequency difference is ascertained, here between cases and controls, as DNA pools or individually. This work demonstrated many so-called suggestive linkages with MS microsatellite-, allele-, genotype- and haplotype-wise, providing thereby also unrecognized candidates for disease pathogenesis. Suggestive linkage describes genomic regions with an observed trend toward excess sharing in affected individuals or controls that is not significant after correcting for multiple tests (Bonferroni correction) across the genome.^{122,123} A large number of suggestive linkages, derived from MS association and linkage studies, exist for which the underlying genetic defect has not been identified so far. These studies raise an important issue: even if it is difficult to establish significance within a single study, initial scans will at least help to focus subsequent efforts on interesting regions of the genome. Hence, significant results based on the empirical p-value reflecting DNA pool differences were not subjected to any correction.

Furthermore, Bonferroni correction conservatively assumes independent markers, but many markers, especially in presented SNP maps, are significantly associated with one another in block-like structures. Thus, it is difficult to theoretically establish a threshold for significance in whole-genome association analysis, and significance will be easier to address empirically by permutation analysis of the observed data.²⁵⁸

Nevertheless, the outcome of the Bonferroni correction (Tab. 3.9) should not altogether undermine the precedently discussed relations of alleles and genotypes at remaining “non-significant” markers (e.g. SNP #21; RRMS vs. HC, $p=0.006$). The correction process is an important tool to address the issue of multiple testing of the same subjects. It aims to reduce the rate of false positive results by diminishing the effect of independency inherent with each test. Still, these thresholds are relative and their significancies depend to a certain degree on the investigator’s point of view. If multiple testing is a major challenge at the level of single SNPs, the problem rapidly becomes intractable when one allows for gene–gene or gene–environment interactions. That is, for 600,000 tag SNPs

and ten environmental variables, there are more than 10^{11} possible pairwise gene–gene interactions, and six million possible gene–environment interactions. The question arises if the search space for gene–gene and gene–environment interactions can be logically limited.

One of the possible reasons why linkage analysis has only identified some high-frequency, modest-risk alleles is the mentioned statistical interaction (or epistasis) between multiple loci. Overall disease risk can be modelled as the product of risks at many independent risk loci. With such a model, high-risk combinations of genotype will exist, but the ability to detect any single locus is a function of the relative risk of that locus alone, therefore a single-locus analysis might miss the association. This entails a closer definition of the term interaction. Statistical interaction between loci requires a dependent effect, wherein the risk associated with a genotype at a locus is dependent on a genotype at another locus. There are several possible epistatic models as outlined in the Introduction.

However, one of the most striking results of this work, the PPMS prone 2-SNP-composite haplotype of *ADAMTS14* and *C10orf27* (#19+#17; Table 3.15b; $p=0.00015$), would withstand subjection to conservative Bonferroni correction. Here, it is believed that the high degree of permutation on identical markers, in addition to group stratifications request a more rigid adjustment for repeated measurements. Therefore, the significance threshold for this analysis results from multiplying 24 combinations with 4 possible haplotypes in a p -value of $0.05/96 = 0.00052$.

4.7 Conclusion and outlook

Recently, an informative convergence of genetic data from animal models of MS – e.g. experimental autoimmune encephalomyelitis (EAE) – and from studies of MS patient populations have been reported.²⁶⁰ The patient populations permit the identification of relatively large chromosomal regions that constitute disease susceptibility loci. Murine studies have more easily permitted the identification of particular genes from within those loci that lead to autoimmunity, which in turn can then be directly examined for critical disease-associated polymorphisms within patient populations. This approach has great potential for facilitating the identification of disease-associated genes.

Although still providing an incomplete picture, the genetic discoveries in MS are beginning to help build a model of this autoimmune disease. MS is best represented as a continuum

of phenotypes, from severe to mild, and the ultimate goal is to construct a specific model for each clinical disease subform whereby the effect of individual risk factors (genetic and non-genetic), their interactions, and their impact on disease susceptibility, disease progression and clinical management, are understood. Referring to Figure 1.3 it is needed to ascertain the individual-specific set of genes and environmental factors and their response profile to disease therapy(ies).

Genome-wide haplotype-based association studies are not yet a reality, but such efforts will undoubtedly be launched now that the HapMap is completed. Even with the known limitations of the HapMap,²⁴⁸ such efforts, if well designed, will be an important first step in evaluating the role in MS disease susceptibility of most of the common variation in the human genome.²⁶¹ This area offers tremendous opportunities to further understand the molecular pathogenesis of studied complex trait. Moreover, initial findings will justify genetic analysis in clinical practice which shall be able to determine clinically and biologically meaningful differences.

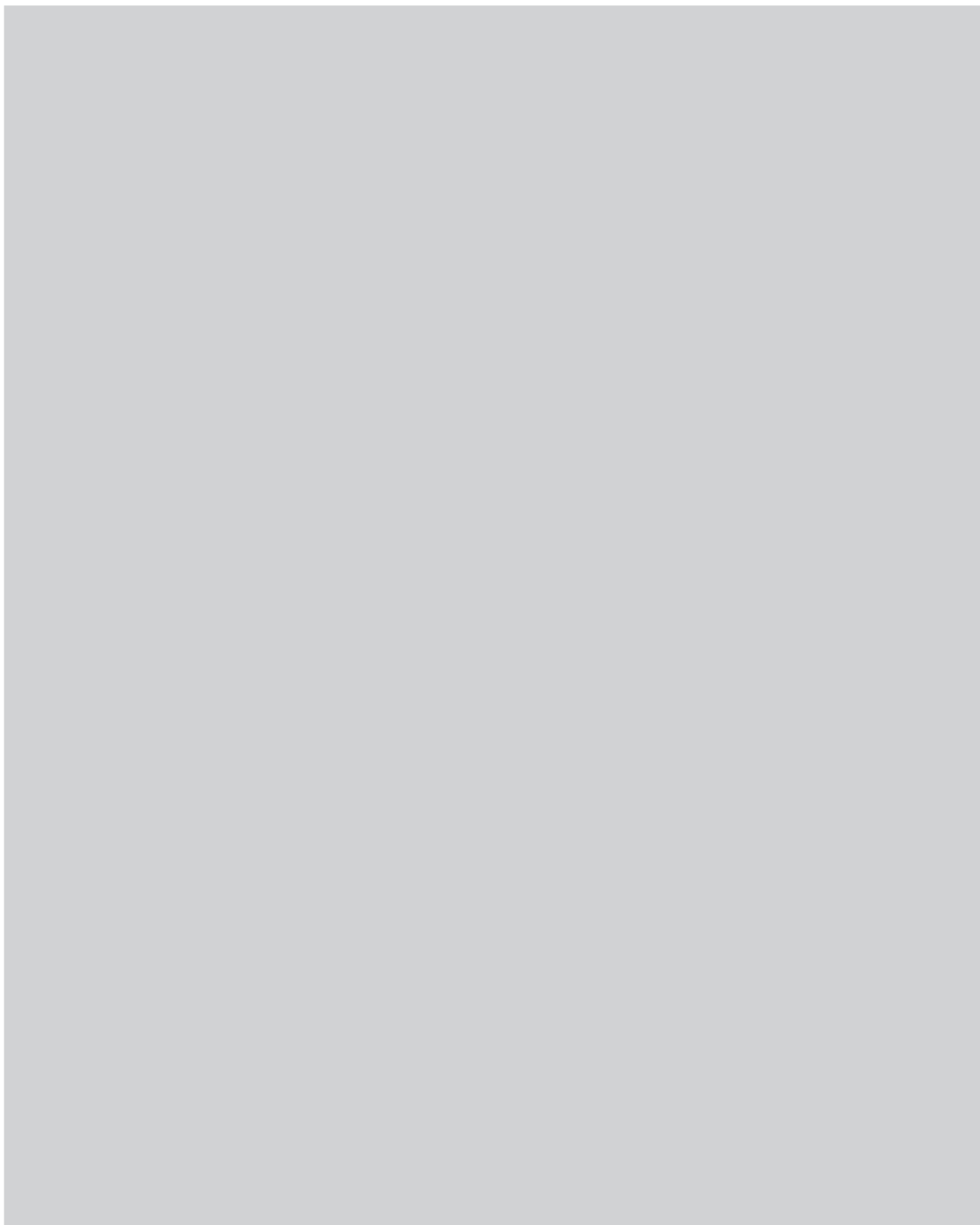
Finally, it is likely that clinical neuroscience will adopt many of these approaches in the area of pharmacogenetics and -genomics, attempting to identify common genetic variants which determine response to drugs and adverse side effect risks. One linking strategy in the field of functional genomics is to collect biological material, e.g. peripheral blood, from a cohort of patients that respond well to a certain medication and from a second group that does not respond. Whole genome mRNA expression profiling might generate distinct signatures and hence provide candidate genes which would undergo haplotype determination. The challenge then is having identified the “block” that is associated with a responder (or non responder) phenotype to identify where within the block the causal variant lies.²⁶²

As described, it is of importance of taking findings beyond the genotyping stage and integrating them with the rest of the discovery pipeline. The ‘list of genes’ resulting from presented analysis should not be viewed as an end in itself; its real value increases only as that list moves through biological validation, ranging from the replication in additional MS cohorts to ascertaining the meaning of the results, such as finding common promoter regions or biological relationships between the genes. However, even if tools that link these genes back to known biological pathways, as well as discovering new ones, are still in their early stages, providing the scientific MS community with the necessary “real input data” – amongst others the candidate genes of presented work – will accelerate

the development and correct refining of bioinformatic algorithms that reconstruct the true biological mechanisms in the autoimmune disease MS.

5

SUMMARY



After a genome-wide screen for association with the autoimmune disease multiple sclerosis (MS) applying 5131 microsatellite markers , 191 displayed evidence twice for a genetic predisposition to afflict the disease. Seven of these 191 markers were genotyped on individual DNA samples and in part consolidated screen-derived findings.

The application of a heuristic sliding windows approach disclosed 75 regions of interest that contain 284 known genes.

Two biologically plausible candidate regions on 3p25.3 and 10q22.1 were tested with 24 single nucleotide polymorphism (SNP) markers. Fine-scale mapping included the description of linkage disequilibrium (LD) between contiguous SNPs which provided information about structure (LD pattern revealed five block like regions) and dependency in respective genomic regions.

Finally, the computational reconstruction of gene-based haplotypes allowed for statistical inferences of certain haplotypes in association with stratified clinical subcategories of MS (RRMS and PPMS, respectively) and the indication of potential tag SNPs.

The main results of completed study are the identification of the candidate genes metalloproteinase *ADAMTS14*¹⁵² and *C10orf27* at 10q22.1. Both demonstrated clear genetic association with MS, independently and in conjunction, and therefore imply genuine contributions to MS pathogenesis.

6

REFERENCE LIST

- 1 Burnet FM 1959 Clonal selection theory of acquired immunity. Cambridge: Cambridge University Press, Nashville: Vanderbilt University Press.
- 2 de Boer RJ, Hogeweg P. Immunological discrimination between self and non-self by precursor depletion and memory accumulation. *J Theor Biol.* 1987 Feb 7;124(3):343-69.
- 3 Burnet FM. Auto-immune disease: some general principles. *Postgrad Med.* 1961 Aug;30: 91-5.
- 4 Steinman L. Autoimmune disease. *Sci Am.* 1993 Sep;269(3):106-14.
- 5 Vyse TJ, Todd JA. Genetic analysis of autoimmune disease. *Cell.* 1996 May 3;85(3):311-8.
- 6 Jacobson DL, Gange SJ, Rose NR, Graham NM. Epidemiology and estimated population burden of selected autoimmune diseases in the United States. *Clin Immunol Immunopathol.* 1997 Sep;84(3):223-43.
- 7 Marrack P, Kappler J, Kotzin BL. Autoimmune disease: why and where it occurs. *Nat Med.* 2001 Aug;7(8):899-905.
- 8 Salaman MR. A two-step hypothesis for the appearance of autoimmune disease. *Autoimmunity.* 2003 Mar;36(2):57-61.
- 9 Becker KG. The common genetic hypothesis of autoimmune/inflammatory disease. *Curr Opin Allergy Clin Immunol.* 2001 Oct;1(5):399-405.
- 10 Steinman L. Multiple sclerosis: a two-stage disease. *Nat Immunol.* 2001 Sep;2(9):762-4.
- 11 Hafler DA. Multiple sclerosis. *J Clin Invest.* 2004 Mar;113(6):788-94.
- 12 Noseworthy JH, Lucchinetti C, Rodriguez M, Weinshenker BG. Multiple sclerosis. *N Engl J Med.* 2000 Sep 28;343(13):938-52.
- 13 Compston A, Coles A. Multiple sclerosis. *Lancet.* 2002 Apr 6;359(9313):1221-31.
- 14 Rosati G. The prevalence of multiple sclerosis in the world: an update. *Neurol Sci.* 2001 Apr;22(2):117-39.

- 15 Pugliatti M, Sotgiu S, Rosati G. The worldwide prevalence of multiple sclerosis. *Clin Neurol Neurosurg.* 2002 Jul;104(3):182-91.
- 16 Karpuz MV, Steinman L, Oksenberg JR. Multiple sclerosis: a polygenic disease involving epistatic interactions, germline rearrangements and environmental effects. *Neurogenetics.* 1997 May;1(1):21-8.
- 17 Liblau R, Gautam AM. HLA, molecular mimicry and multiple sclerosis. *Rev Immunogenet.* 2000;2(1):95-104.
- 18 Barcellos LF, Oksenberg JR, Green AJ, Bucher P, Rimmier JB, Schmidt S, Garcia ME, Lincoln RR, Pericak-Vance MA, Haines JL, Hauser SL; Multiple Sclerosis Genetics Group. Genetic basis for clinical expression in multiple sclerosis. *Brain.* 2002 Jan;125(Pt 1):150-8.
- 19 Sotgiu S, Pugliatti M, Fois ML, Arru G, Sanna A, Sotgiu MA, Rosati G. Genes, environment, and susceptibility to multiple sclerosis. *Neurobiol Dis.* 2004 Nov;17(2):131-43.
- 20 McAlpine's Multiple Sclerosis, 4th edition, Compston A; Churchill Livingstone, 2005 (Lassmann H, Wekerle H The pathology of multiple sclerosis. In: Ed. DAS Compston. McAlpine's Multiple Sclerosis. 2006. pp 557-599.)
- 21 Hauser SL, Goodkin DE, 1998. Multiple sclerosis and other demyelinating diseases. In: Fauci A et al. (Eds.), Harrison's Principle of Internal Medicine, 14th ed. McGraw Hill, New York, pp. 2409-2418.
- 22 Genain CP, Cannella B, Hauser SL, Raine CS. Identification of autoantibodies associated with myelin damage in multiple sclerosis. *Nat Med.* 1999 Feb;5(2):170-5.
- 23 Raine CS, Cannella B, Hauser SL, Genain CP. Demyelination in primate autoimmune encephalomyelitis and acute multiple sclerosis lesions: a case for antigen-specific antibody mediation. *Ann Neurol.* 1999 Aug;46(2):144-60.
- 24 Lucchinetti CF, Bruck W, Rodriguez M, Lassmann H. Distinct patterns of multiple sclerosis pathology indicates heterogeneity on pathogenesis. *Brain Pathol.* 1996 Jul;6(3):259-74.
- 25 McDonald WI, Compston A, Edan G, Goodkin D, Hartung HP, Lublin FD, McFarland HF, Paty DW, Polman CH, Reingold SC, Sandberg-Wollheim M, Sibley W, Thompson A, van den Noort S, Weinshenker BY, Wolinsky JS. Recommended diagnostic criteria for multiple sclerosis: guidelines from the International Panel on the diagnosis of multiple sclerosis. *Ann Neurol.* 2001 Jul;50(1):121-7.
- 26 Miller D, Barkhof F, Montalban X, Thompson A, Filippi M. Clinically isolated syndromes suggestive of multiple sclerosis, part 2: non-conventional MRI, recovery processes, and management. *Lancet Neurol.* 2005 Jun;4(6):341-8.
- 27 Lublin FD, Reingold SC. Defining the clinical course of multiple sclerosis: results of an international survey. National Multiple Sclerosis Society (USA) Advisory Committee on Clinical Trials of New Agents in Multiple Sclerosis. *Neurology.* 1996 Apr;46(4):907-11.

- 28 Thompson AJ, Polman CH, Miller DH, McDonald WI, Brochet B, Filippi M Montalban X, De Sa J. Primary progressive multiple sclerosis. *Brain*. 1997 Jun;120 (Pt 6):1085-96.
- 29 Stevenson VL, Miller DH, Rovaris M, Barkhof F, Brochet B, Dousset V, Dousset V, Filippi M, Montalban X, Polman CH, Rovira A, de Sa J, Thompson AJ. Primary and transitional progressive MS: a clinical and MRI cross-sectional study. *Neurology*. 1999 Mar 10;52(4):839-45.
- 30 Weinshenker BG. The natural history of multiple sclerosis. *Neurol Clin*. 1995 Feb;13(1): 119-46.
- 31 Revesz T, Kidd D, Thompson AJ, Barnard RO, McDonald WI. A comparison of the pathology of primary and secondary progressive multiple sclerosis. *Brain*. 1994 Aug;117 (Pt 4):759-65.
- 32 Dale RC, de Sousa C, Chong WK, Cox TC, Harding B, Neville BG. Acute disseminated encephalomyelitis, multiphasic disseminated encephalomyelitis and multiple sclerosis in children. *Brain*. 2000 Dec;123 Pt 12:2407-22.
- 33 Hartung HP, Grossman RI. ADEM: distinct disease or part of the MS spectrum? *Neurology*. 2001 May 22;56(10):1257-60.
- 34 Baló J. Leukoencephalitis periaxialis concentrica. *Ról Magy Orv Arch*, 1927, 28: 108-24. Translation in: *Archives of Neurology and Psychiatry*, Chicago, 1928, 19: 242-64.
- 35 Schilder PF. Zur Kenntnis der sogenannten diffusen Sklerose (über Encephalitis periaxialis diffusa). *Zeitschrift für die gesamte Neurologie und Psychiatrie*, 1912; 10: 1-60.
- 36 Devic E. Myélite subaiguë compliquée de névrite optique. *Bull Méd (Lyon)* 1894; 8: 1093-4.
- 37 Marburg O. Die sogenannte "akute multiple sklerose" (encephalomyelitis periaxialis scleroticans). *Jahrb Psychiat* 1906; 27: 213- 312.
- 38 Kidd D, Thompson AJ, Kendall BE, Miller DH, McDonald WI. Benign form of multiple sclerosis: MRI evidence for less frequent and less inflammatory disease activity. *J Neurol Neurosurg Psychiatry*. 1994 Sep;57(9):1070-2.
- 39 Lucchinetti C, Bruck W, Parisi J, Scheithauer B, Rodriguez M, Lassmann H. Heterogeneity of multiple sclerosis lesions: implications for the pathogenesis of demyelination. *Ann Neurol*. 2000 Jun;47(6):707-17.
- 40 Trapp BD, Peterson J, Ransohoff RM, Rudick R, Mork S, Bo L. Axonal transection in the lesions of multiple sclerosis. *N Engl J Med*. 1998 Jan 29;338(5):278-85.
- 41 Traugott U, Reinherz EL, Raine CS. Multiple sclerosis: distribution of T cell subsets within active chronic lesions. *Science*. 1983 Jan 21;219(4582):308-10.
- 42 Hauser SL, Bhan AK, Gilles F, Kemp M, Kerr C, Weiner HL. Immunohistochemical analysis of the cellular infiltrate in multiple sclerosis lesions. *Ann Neurol*. 1986 Jun;19(6):578-87.

- 43 Wucherpfennig KW, Newcombe J, Li H, Keddy C, Cuzner ML, Hafler DA. Gamma delta T-cell receptor repertoire in acute multiple sclerosis lesions. *Proc Natl Acad Sci U S A.* 1992 May 15;89(10):4588-92.
- 44 Prineas JW, Wright RG. Macrophages, lymphocytes, and plasma cells in the perivascular compartment in chronic multiple sclerosis. *Lab Invest.* 1978 Apr;38(4):409-21.
- 45 Lassmann H, Bruck W, Lucchinetti C. Heterogeneity of multiple sclerosis pathogenesis: implications for diagnosis and therapy. *Trends Mol Med.* 2001 Mar;7(3):115-21.
- 46 Kornek B, Lassmann H. Neuropathology of multiple sclerosis-new concepts. *Brain Res Bull.* 2003 Aug 15;61(3):321-6.
- 47 Hohlfeld R. Biotechnological agents for the immunotherapy of multiple sclerosis. Principles, problems and perspectives. *Brain.* 1997 May;120 (Pt 5):865-916.
- 48 Steinman L, Martin R, Bernard C, Conlon P, Oksenberg JR. Multiple sclerosis: deeper understanding of its pathogenesis reveals new targets for therapy. *Annu Rev Neurosci.* 2002;25: 491-505.
- 49 Hemmer B, Archelos JJ, Hartung HP. New concepts in the immunopathogenesis of multiple sclerosis. *Nat Rev Neurosci.* 2002 Apr;3(4):291-301.
- 50 Davidson A, Diamond B. Autoimmune diseases. *N Engl J Med.* 2001 Aug 2;345(5):340-50.
- 51 Sospedra M, Martin R. Immunology of multiple sclerosis. *Annu Rev Immunol.* 2005;23: 683-747.
- 52 Oksenberg JR, Baranzini SE, Barcellos LF, Hauser SL. Multiple sclerosis: genomic rewards. *J Neuroimmunol.* 2001 Feb 15;113(2):171-84.
- 53 Barcellos LF, Oksenberg JR, Begovich AB, Martin ER, Schmidt S, Vittinghoff E, Goodin DS, Pelletier D, Lincoln RR, Bucher P, Swerdlow A, Pericak-Vance MA, Haines JL, Hauser SL; Multiple Sclerosis Genetics Group. HLA-DR2 dose effect on susceptibility to multiple sclerosis and influence on disease course. *Am J Hum Genet.* 2003 Mar;72(3):710-6.
- 54 Villoslada P, Barcellos LF, Rio J, Begovich AB, Tintore M, Sastre-Garriga J, Baranzini SE, Casquero P, Hauser SL, Montalban X, Oksenberg JR. The HLA locus and multiple sclerosis in Spain. Role in disease susceptibility, clinical course and response to interferon-beta. *J Neuroimmunol.* 2002 Sep;130(1-2):194-201.
- 55 Dyment DA, Ebers GC, Sadovnick AD. Genetics of multiple sclerosis. *Lancet Neurol.* 2004 Feb;3(2):104-10.
- 56 Benoist C, Mathis D. Autoimmunity provoked by infection: how good is the case for T cell epitope mimicry? *Nat Immunol.* 2001 Sep;2(9):797-801.

- 57 Lang HL, Jacobsen H, Ikemizu S, Andersson C, Harlos K, Madsen L, Hjorth P, Sondergaard L, Svejgaard A, Wucherpfennig K, Stuart DI, Bell JI, Jones EY, Fugger L. A functional and structural basis for TCR cross-reactivity in multiple sclerosis. *Nat Immunol.* 2002 Oct;3(10):940-3.
- 58 Viglietta V, Baecher-Allan C, Weiner HL, Hafler DA. Loss of functional suppression by CD4+CD25+ regulatory T cells in patients with multiple sclerosis. *J Exp Med.* 2004 Apr 5;199(7):971-9.
- 59 Jacobsen M, Cepok S, Quak E, Happel M, Gaber R, Ziegler A, Schock S, Oertel WH, Sommer N, Hemmer B. Oligoclonal expansion of memory CD8+ T cells in cerebrospinal fluid from multiple sclerosis patients. *Brain.* 2002 Mar;125(Pt 3):538-50.
- 60 Bjartmar C, Wujek JR, Trapp BD. Axonal loss in the pathology of MS: consequences for understanding the progressive phase of the disease. *J Neurol Sci.* 2003 Feb 15;206(2):165-71.
- 61 Rioux JD, Abbas AK. Paths to understanding the genetic basis of autoimmune disease. *Nature.* 2005 Jun 2;435(7042):584-9.
- 62 Reich DE, Lander ES. On the allelic spectrum of human disease. *Trends Genet.* 2001 Sep;17(9):502-10.
- 63 Pritchard JK. Are rare variants responsible for susceptibility to complex diseases? *Am J Hum Genet.* 2001 Jul;69(1):124-37.
- 64 Pritchard JK, Cox NJ. The allelic architecture of human disease genes: common disease-common variant...or not? *Hum Mol Genet.* 2002 Oct 1;11(20):2417-23.
- 65 Becker KG. The common variants/multiple disease hypothesis of common complex genetic disorders. *Med Hypotheses.* 2004;62(2):309-17.
- 66 Larsen CE, Alper CA. The genetics of HLA-associated disease. *Curr Opin Immunol.* 2004 Oct;16(5):660-7.
- 67 Morahan G, Morel L. Genetics of autoimmune diseases in humans and in animal models. *Curr Opin Immunol.* 2002 Dec;14(6):803-11.
- 68 Slager SL, Huang J, Vieland VJ. Effect of allelic heterogeneity on the power of the transmission disequilibrium test. *Genet Epidemiol.* 2000 Feb;18(2):143-56.
- 69 Botstein D, Risch N. Discovering genotypes underlying human phenotypes: past successes for mendelian disease, future approaches for complex disease. *Nat Genet.* 2003 Mar;33 Suppl:228-37.
- 70 Zondervan KT, Cardon LR. The complex interplay among factors that influence allelic association. *Nat Rev Genet.* 2004 Feb;5(2):89-100.

- 71 Becker KG, Simon RM, Bailey-Wilson JE, Freidlin B, Biddison WE, McFarland HF, Trent JM. Clustering of non-major histocompatibility complex susceptibility candidate loci in human autoimmune diseases. *Proc Natl Acad Sci U S A.* 1998 Aug 18;95(17):9979-84.
- 72 Risch N. Linkage strategies for genetically complex traits. I. Multilocus models. *Am J Hum Genet.* 1990 Feb;46(2):222-8.
- 73 Nagel RL. Epistasis and the genetics of human diseases. *C R Biol.* 2005 Jul;328(7):606-15.
- 74 Nadeau JH. Modifier genes and protective alleles in humans and mice. *Curr Opin Genet Dev.* 2003 Jun;13(3):290-5.
- 75 Wandstrat A, Wakeland E. The genetics of complex autoimmune diseases: non-MHC susceptibility genes. *Nat Immunol.* 2001 Sep;2(9):802-9.
- 76 Subramanian S, Wakeland EK. The importance of epistatic interactions in the development of autoimmunity. *Novartis Found Symp.* 2005;267:76-88
- 77 Wright, S. An analysis of variability in number of digits in an inbred strain of guinea pigs. *Genetics* 19, 506–536 (1933).
- 78 Risch N, Ghosh S, Todd JA. Statistical evaluation of multiple-locus linkage data in experimental species and its relevance to human studies: application to nonobese diabetic (NOD) mouse and human insulin-dependent diabetes mellitus (IDDM). *Am J Hum Genet.* 1993 Sep;53(3):702-14.
- 79 Sundvall M, Jirholt J, Yang HT, Jansson L, Engstrom A, Pettersson U, Holmdahl R. Identification of murine loci associated with susceptibility to chronic experimental autoimmune encephalomyelitis. *Nat Genet.* 1995 Jul;10(3):313-7.
- 80 McAleer MA, Reifsnyder P, Palmer SM, Prochazka M, Love JM, Copeman JB, Powell EE, Rodrigues NR, Prins JB, Serreze DV, et al. Crosses of NOD mice with the related NON strain. A polygenic model for IDDM. *Diabetes.* 1995 Oct;44(10):1186-95.
- 81 Drake CG, Rozzo SJ, Hirschfeld HF, Smarnworawong NP, Palmer E, Kotzin BL. Analysis of the New Zealand Black contribution to lupus-like renal disease. Multiple genes that operate in a threshold manner. *J Immunol.* 1995 Mar 1;154(5):2441-7.
- 82 Vyse TJ, Todd JA, Kotzin BL, in *The Autoimmune Diseases* (eds Rose, N. R. & Mackay, I. R.) 85–118 (Academic Press, London, 1998).
- 83 Collins FS, Guyer MS, Charkravarti A. Variations on a theme: cataloging human DNA sequence variation. *Science.* 1997 November 28;278(5343):1580-1581.
- 84 Collins A, Lonjou C, Morton NE. Genetic epidemiology of single-nucleotide polymorphisms. *Proc Natl Acad Sci U S A.* 1999 Dec 21;96(26):15173-7.

- 85 Lander ES, Linton LM, Birren B, Nusbaum C, Zody MC, et al. Initial sequencing and analysis of the human genome. *Nature*. 2001 Feb 15;409(6822):860-921.
- 86 Kruglyak L, Nickerson DA. Variation is the spice of life. *Nat Genet*. 2001 Mar;27(3):234-6.
- 87 International Human Genome Sequencing Consortium. Finishing the euchromatic sequence of the human genome. *Nature*. 2004 Oct 21;431(7011):931-45.
- 88 Singer MF. Highly repeated sequences in mammalian genomes. *Int Rev Cytol*. 1982;76:67-112.
- 89 Weber JL, May PE. Abundant class of human DNA polymorphisms which can be typed using the polymerase chain reaction. *Am J Hum Genet*. 1989 Mar;44(3):388-96.
- 90 Zhao Z, Fu YX, Hewett-Emmett D, Boerwinkle E. Investigating single nucleotide polymorphism (SNP) density in the human genome and its implications for molecular evolution. *Gene*. 2003 Jul 17;312:207-13.
- 91 Wang DG, Fan JB, Siao CJ, Berno A, Young P, Sapolsky R, Ghandour G, Perkins N, Winchester E, Spencer J, Kruglyak L, Stein L, Hsie L, Topaloglou T, Hubbell E, Robinson E, Mittmann M, Morris MS, Shen N, Kilburn D, Rioux J, Nusbaum C, Rozen S, Hudson TJ, Lipshutz R, Chee M, Lander ES. Large-scale identification, mapping, and genotyping of single-nucleotide polymorphisms in the human genome. *Science*. 1998 May 15;280(5366):1077-82.
- 92 Sachidanandam R, Weissman D, Schmidt SC, Kakol JM, Stein LD, Marth G, Sherry S, Mullikin JC, Mortimore BJ, Willey DL, Hunt SE, Cole CG, Coggill PC, Rice CM, Ning Z, Rogers J, Bentley DR, Kwok PY, Mardis ER, Yeh RT, Schultz B, Cook L, Davenport R, Dante M, Fulton L, Hillier L, Waterston RH, McPherson JD, Gilman B, Schaffner S, Van Etten WJ, Reich D, Higgins J, Daly MJ, Blumenstiel B, Baldwin J, Stange-Thomann N, Zody MC, Linton L, Lander ES, Altshuler D; International SNP Map Working Group. A map of human genome sequence variation containing 1.42 million single nucleotide polymorphisms. *Nature*. 2001 Feb 15;409(6822):928-33.
- 93 Reich DE, Gabriel SB, Altshuler D. Quality and completeness of SNP databases. *Nat Genet*. 2003 Apr;33(4):457-8.
- 94 Risch N, Merikangas K. The future of genetic studies of complex human diseases. *Science*. 1996 Sep 13;273(5281):1516-7.
- 95 Patil N, Berno AJ, Hinds DA, Barrett WA, Doshi JM, Hacker CR, Kautzer CR, Lee DH, Marjoribanks C, McDonough DP, Nguyen BT, Norris MC, Sheehan JB, Shen N, Stern D, Stokowski RP, Thomas DJ, Trulson MO, Vyas KR, Frazer KA, Fodor SP, Cox DR. Blocks of limited haplotype diversity revealed by high-resolution scanning of human chromosome 21. *Science*. 2001 Nov 23;294(5547):1719-23.

- 96 Daly MJ, Rioux JD, Schaffner SF, Hudson TJ, Lander ES. High-resolution haplotype structure in the human genome. *Nat Genet.* 2001 Oct;29(2):229-32.
- 97 Jeffreys AJ, Kauppi L, Neumann R. Intensely punctate meiotic recombination in the class II region of the major histocompatibility complex. *Nat Genet.* 2001 Oct;29(2):217-22.
- 98 Gabriel SB, Schaffner SF, Nguyen H, Moore JM, Roy J, Blumenstiel B, Higgins J, DeFelice M, Lochner A, Faggart M, Liu-Cordero SN, Rotimi C, Adeyemo A, Cooper R, Ward R, Lander ES, Daly MJ, Altshuler D. The structure of haplotype blocks in the human genome. *Science.* 2002 Jun 21;296(5576):2225-9.
- 99 Reich DE, Schaffner SF, Daly MJ, McVean G, Mullikin JC, Higgins JM, Richter DJ, Lander ES, Altshuler D. Human genome sequence variation and the influence of gene history, mutation and recombination. *Nat Genet.* 2002 Sep;32(1):135-42.
- 100 McVean GA, Myers SR, Hunt S, Deloukas P, Bentley DR, Donnelly P. The fine-scale structure of recombination rate variation in the human genome. *Science.* 2004 Apr 23;304(5670):581-4.
- 101 Lewontin RC, Kojima K. The evolutionary dynamics of complex polymorphisms. *Evolution.* 1960 14:450-472.
- 102 Lewontin, RC. The interaction of selection and linkage. I. General considerations; heterotic models. *Genetics.* 1964 49:49-67.
- 103 The International HapMap Consortium. The International HapMap Project. *Nature.* 2003 Dec 18;426(6968):789-96.
- 104 Judson R, Stephens JC, Windemuth A. The predictive power of haplotypes in clinical response. *Pharmacogenomics.* 2000 Feb;1(1):15-26.
- 105 Goldstein DB. Islands of linkage disequilibrium. *Nat Genet.* 2001 Oct;29(2):109-11.
- 106 Reich DE, Cargill M, Bolk S, Ireland J, Sabeti PC, Richter DJ, Lavery T, Kouyoumjian R, Farhadian SF, Ward R, Lander ES. Linkage disequilibrium in the human genome. *Nature.* 2001 May 10;411(6834):199-204.
- 107 Johnson GC, Esposito L, Barratt BJ, Smith AN, Heward J, Di Genova G, Ueda H, Cordell HJ, Eaves IA, Dudbridge F, Twells RC, Payne F, Hughes W, Nutland S, Stevens H, Carr P, Tuomilehto-Wolf E, Tuomilehto J, Gough SC, Clayton DG, Todd JA. Haplotype tagging for the identification of common disease genes. *Nat Genet.* 2001 Oct;29(2):233-7.
- 108 Goldstein DB, Weale ME. Population genomics: linkage disequilibrium holds the key. *Curr Biol.* 2001 Jul 24;11(14):R576-9.
- 109 Gusella JF, Wexler NS, Conneally PM, Naylor SL, Anderson MA, Tanzi RE, Watkins PC, Ottina K, Wallace MR, Sakaguchi AY, et al. A polymorphic DNA marker genetically linked to Huntington's disease. *Nature.* 1983 Nov 17-23;306(5940):234-8.

- 110 Spielman RS, McGinnis RE, Ewens WJ. Transmission test for linkage disequilibrium: the insulin gene region and insulin-dependent diabetes mellitus (IDDM). *Am J Hum Genet.* 1993 Mar;52(3):506-16.
- 111 Nickerson DA, Taylor SL, Fullerton SM, Weiss KM, Clark AG, Stengard JH, Salomaa V, Boerwinkle E, Sing CF. Sequence diversity and large-scale typing of SNPs in the human apolipoprotein E gene. *Genome Res.* 2000 Oct;10(10):1532-45.
- 112 Bader JS. The relative power of SNPs and haplotype as genetic markers for association tests. *Pharmacogenomics.* 2001 Feb;2(1):11-24.
- 113 Kruglyak L. Prospects for whole-genome linkage disequilibrium mapping of common disease genes. *Nat Genet.* 1999 Jun;22(2):139-44.
- 114 Carlson CS, Eberle MA, Rieder MJ, Yi Q, Kruglyak L, Nickerson DA. Selecting a maximally informative set of single-nucleotide polymorphisms for association analyses using linkage disequilibrium. *Am J Hum Genet.* 2004 Jan;74(1):106-20.
- 115 Sawcer S, Jones HB, Feakes R, Gray J, Smaldon N, Chataway J, Robertson N, Clayton D, Goodfellow PN, Compston A. A genome screen in multiple sclerosis reveals susceptibility loci on chromosome 6p21 and 17q22. *Nat Genet.* 1996 Aug;13(4):464-8.
- 116 Haines JL, Ter-Minassian M, Bazyk A, Gusella JF, Kim DJ, Terwedow H, Pericak-Vance MA, Rimmier JB, Haynes CS, Roses AD, Lee A, Shaner B, Menold M, Seboun E, Fitoussi RP, Gartioux C, Reyes C, Ribierre F, Gyapay G, Weissenbach J, Hauser SL, Goodkin DE, Lincoln R, Usuku K, Oksenberg JR, et al. A complete genomic screen for multiple sclerosis underscores a role for the major histocompatibility complex. The Multiple Sclerosis Genetics Group. *Nat Genet.* 1996 Aug;13(4):469-71.
- 117 Ebers GC, Kukay K, Bulman DE, Sadovnick AD, Rice G, Anderson C, Armstrong H, Cousin K, Bell RB, Hader W, Paty DW, Hashimoto S, Oger J, Duquette P, Warren S, Gray T, O'Connor P, Nath A, Auty A, Metz L, Francis G, Paulseth JE, Murray TJ, Pryse-Phillips W, Nelson R, Freedman M, Brunet D, Bouchard JP, Hinds D, Risch N. A full genome search in multiple sclerosis. *Nat Genet.* 1996 Aug;13(4):472-6.
- 118 Kuokkanen S, Gschwend M, Rioux JD, Daly MJ, Terwilliger JD, Tienari PJ, Wikstrom J, Palo J, Stein LD, Hudson TJ, Lander ES, Peltonen L. Genomewide scan of multiple sclerosis in Finnish multiplex families. *Am J Hum Genet.* 1997 Dec;61(6):1379-87.
- 119 Coraddu F, Sawcer S, D'Alfonso S, Lai M, Hensiek A, Solla E, Broadley S, Mancosu C, Pugliatti M, Marrosu MG, Compston A. A genome screen for multiple sclerosis in Sardinian multiplex families. *Eur J Hum Genet.* 2001 Aug;9(8):621-6.
- 120 Sawcer S, Compston A. The genetic analysis of multiple sclerosis in Europeans: concepts and design. *J Neuroimmunol.* 2003 Oct;143(1-2):13-6.

- 121 Sawcer S, Maranian M, Setakis E, Curwen V, Akesson E, Hensiek A, Coraddu F, Roxburgh R, Sawcer D, Gray J, Deans J, Goodfellow PN, Walker N, Clayton D, Compston A. A whole genome screen for linkage disequilibrium in multiple sclerosis confirms disease associations with regions previously linked to susceptibility. *Brain*. 2002 Jun;125(Pt 6):1337-47.
- 122 Lander E, Kruglyak L. Genetic dissection of complex traits: guidelines for interpreting and reporting linkage results. *Nat Genet*. 1995 Nov;11(3):241-7.
- 123 Sawcer S, Jones HB, Judge D, Visser F, Compston A, Goodfellow PN, Clayton D. Empirical genomewide significance levels established by whole genome simulations. *Genet Epidemiol*. 1997;14(3):223-9.
- 124 Haines JL, Terwedow HA, Burgess K, Pericak-Vance MA, Rimmier JB, Martin ER, Oksenberg JR, Lincoln R, Zhang DY, Banatao DR, Gatto N, Goodkin DE, Hauser SL. Linkage of the MHC to familial multiple sclerosis suggests genetic heterogeneity. The Multiple Sclerosis Genetics Group. *Hum Mol Genet*. 1998 Aug;7(8):1229-34.
- 125 Compston A. The genetics of multiple sclerosis. *Clin Chem Lab Med*. 2000 Feb;38(2):133-5.
- 126 Haines JL, Bradford Y, Garcia ME, Reed AD, Neumeister E, Pericak-Vance MA, Rimmier JB, Menold MM, Martin ER, Oksenberg JR, Barcellos LF, Lincoln R, Hauser SL; Multiple Sclerosis Genetics Group. Multiple susceptibility loci for multiple sclerosis. *Hum Mol Genet*. 2002 Sep 15;11(19):2251-6.
- 127 Kobelt G, Pugliatti M. Cost of multiple sclerosis in Europe. *Eur J Neurol*. 2005 Jun;12 Suppl 1:63-7.
- 128 Kurtzke JF. Epidemiologic contributions to multiple sclerosis: an overview. *Neurology*. 1980 Jul;30(7 Pt 2):61-79.
- 129 Kurtzke JF. Epidemiologic evidence for multiple sclerosis as an infection. *Clin Microbiol Rev*. 1993 Oct;6(4):382-427.
- 130 Ebers GC, Sadovnick, AD. Epidemiology. In: Paty DW, Ebers GC Eds, *Multiple Sclerosis*. Philadelphia, FA Davis Company 1998; 5-28.
- 131 Yu YL, Woo E, Hawkins BR, Ho HC, Huang CY. Multiple sclerosis amongst Chinese in Hong Kong. *Brain*. 1989 Dec;112 (Pt 6):1445-67.
- 132 Cook SD, MacDonald J, Tapp W, Poskanzer D, Dowling PC. Multiple sclerosis in the Shetland Islands: an update. *Acta Neurol Scand*. 1988 Feb;77(2):148-51.
- 133 Detels R, Visscher BR, Malmgren RM, Coulson AH, Lucia MV, Dudley JP. Evidence for lower susceptibility to multiple sclerosis in Japanese-Americans. *Am J Epidemiol*. 1977 Apr;105(4):303-10.

- 134 Kurtzke, J.F., 1983. Epidemiology of MS. In: Hallpike, J.F., Adams, C.W.M., Tourtelotte, W.W. (Eds.), *Multiple Sclerosis*. Williams and Wilkins, Baltimore, MD, pp. 49–95.
- 135 Martyn CN, Gale CR. The epidemiology of multiple sclerosis. *Acta Neurol Scand Suppl*. 1997;169:3-7.
- 136 Risch NJ, Devlin B. On the probability of matching DNA fingerprints. *Science*. 1992 Feb 7;255(5045):717-20.
- 137 Ebers GC, Sadovnick AD. The role of genetic factors in multiple sclerosis susceptibility. *J Neuroimmunol*. 1994 Oct;54(1-2):1-17.
- 138 Oksenberg JR, Seboun E, Hauser SL. Genetics of demyelinating diseases. *Brain Pathol*. 1996 Jul;6(3):289-302.
- 139 Sadovnick AD, Ebers GC. Genetics of multiple sclerosis. *Neurol Clin*. 1995 Feb;13(1):99-118.
- 140 Ebers GC, Sadovnick AD, Risch NJ. A genetic basis for familial aggregation in multiple sclerosis. Canadian Collaborative Study Group. *Nature*. 1995 Sep 14;377(6545):150-1.
- 141 Sadovnick AD, Armstrong H, Rice GP, Bulman D, Hashimoto L, Paty DW, Hashimoto SA, Warren S, Hader W, Murray TJ, et al. A population-based study of multiple sclerosis in twins: update. *Ann Neurol*. 1993 Mar;33(3):281-5.
- 142 Mumford CJ, Wood NW, Kellar-Wood H, Thorpe JW, Miller DH, Compston DA. The British Isles survey of multiple sclerosis in twins. *Neurology*. 1994 Jan;44(1):11-5.
- 143 Willer CJ, Dyment DA, Risch NJ, Sadovnick AD, Ebers GC; Canadian Collaborative Study Group. Twin concordance and sibling recurrence rates in multiple sclerosis. *Proc Natl Acad Sci U S A*. 2003 Oct 28;100(22):12877-82.
- 144 Allen M, Sandberg-Wollheim M, Sjogren K, Erlich HA, Petterson U, Gyllensten U. Association of susceptibility to multiple sclerosis in Sweden with HLA class II DRB1 and DQB1 alleles. *Hum Immunol*. 1994 Jan;39(1):41-8.
- 145 Weinshenker BG, Santrach P, Bissonet AS, McDonnell SK, Schaid D, Moore SB, Rodriguez M. Major histocompatibility complex class II alleles and the course and outcome of MS: a population-based study. *Neurology*. 1998 Sep;51(3):742-7.
- 146 Saruhan-Direskeneli G, Esin S, Baykan-Kurt B, Ornek I, Vaughan R, Eraksoy M. HLA-DR and -DQ associations with multiple sclerosis in Turkey. *Hum Immunol*. 1997 Jun;55(1):59-65.
- 147 Coraddu F, Reyes-Yanez MP, Parra A, Gray J, Smith SI, Taylor CJ, Compston DA. HLA associations with multiple sclerosis in the Canary Islands. *J Neuroimmunol*. 1998 Jul 1;87(1-2):130-5.

- 148 Marrosu MG, Murru R, Murru MR, Costa G, Zavattari P, Whalen M, Cocco E, Mancosu C, Schirru L, Solla E, Fadda E, Melis C, Porru I, Rolesu M, Cucca F. Dissection of the HLA association with multiple sclerosis in the founder isolated population of Sardinia. *Hum Mol Genet.* 2001 Dec 1;10(25):2907-16.
- 149 Haines JL, Terwedow HA, Burgess K, Pericak-Vance MA, Rimmier JB, Martin ER, Oksenberg JR, Lincoln R, Zhang DY, Banatao DR, Gatto N, Goodkin DE, Hauser SL. Linkage of the MHC to familial multiple sclerosis suggests genetic heterogeneity. The Multiple Sclerosis Genetics Group. *Hum Mol Genet.* 1998 Aug;7(8):1229-34.
- 150 Goertsches R, Villoslada P, Comabella M, Montalban X, Navarro A, de la Concha EG, Arroyo R, Lopez de Munain A, Otaegui D, Palacios R, Perez-Tur J, Jonasdottir A, Benediktsson K, Fossdal R, Sawcer S, Setakis E, Compston A; Spanish MS Genetics Group. A genomic screen of Spanish multiple sclerosis patients reveals multiple loci associated with the disease. *J Neuroimmunol.* 2003 Oct;143(1-2):124-8.
- 151 Marques-Bonet T, Lao O, Goertsches R, Comabella M, Montalban X, Navarro A. Abstract Association Cluster Detector: a tool for heuristic detection of significance clusters in whole-genome scans. *Bioinformatics.* 2005 Sep 1;21 Suppl 2:ii180-ii181.
- 152 Goertsches R, Comabella M, Navarro A, Perkal H, Montalban X. Genetic association between polymorphisms in the ADAMTS14 gene and multiple sclerosis. *J Neuroimmunol.* 2005 Jul;164(1-2):140-7.
- 153 Miller SA, Dykes DD, Polesky HF. A simple salting out procedure for extracting DNA from human nucleated cells. *Nucleic Acids Res.* 1988 Feb 11;16(3):1215.
- 154 Jonasdottir A, Thorlacius T, Fossdal R, Jonasdottir A, Benediktsson K, Benedikz J, Jonsson HH, Sainz J, Einarsdottir H, Sigurdardottir S, Kristjansdottir G, Sawcer S, Compston A, Stefansson K, Gulcher J. A whole genome association study in Icelandic multiple sclerosis patients with 4804 markers. *J Neuroimmunol.* 2003 Oct;143(1-2):88-92.
- 155 Barcellos LF, Klitz W, Field LL, Tobias R, Bowcock AM, Wilson R, Nelson MP, Nagatomi J, Thomson G. Association mapping of disease loci, by use of a pooled DNA genomic screen. *Am J Hum Genet.* 1997 Sep;61(3):734-47.
- 156 Yeo TW, Roxburgh R, Maranian M, Singlehurst S, Gray J, Hensiek A, Setakis E, Compston A, Sawcer S. Refining the analysis of a whole genome linkage disequilibrium association map: the United Kingdom results. *J Neuroimmunol.* 2003 Oct;143(1-2):53-9.
- 157 Förster T. Zwischenmolekulare Energiewanderung und Fluoreszenz. *Ann. Physik* 2. 1948 55-75.
- 158 Poser CM, Paty DW, Scheinberg L, McDonald WI, Davis FA, Ebers GC, Johnson KP, Sibley WA, Silberberg DH, Tourtellotte WW. New diagnostic criteria for multiple sclerosis: guidelines for research protocols. *Ann Neurol.* 1983 Mar;13(3):227-31.

- 159 Hardy GH. A Course of Pure Mathematics. 1908. Cambridge: The University Press 1908.
- 160 Akey JM, Zhang K, Xiong M, Doris P, Jin L. The effect that genotyping errors have on the robustness of common linkage-disequilibrium measures. *Am J Hum Genet.* 2001 Jun;68(6):1447-56.
- 161 Barrett JC, Fry B, Maller J, Daly MJ. Haplovview: analysis and visualization of LD and haplotype maps. *Bioinformatics.* 2005 Jan 15;21(2):263-5.
- 162 Wang N, Akey JM, Zhang K, Chakraborty R, Jin L. Distribution of recombination crossovers and the origin of haplotype blocks: the interplay of population history, recombination, and mutation. *Am J Hum Genet.* 2002 Nov;71(5):1227-34.
- 163 Stephens M, Smith NJ, Donnelly P. A new statistical method for haplotype reconstruction from population data. *Am J Hum Genet.* 2001 Apr;68(4):978-89.
- 164 Stephens M, Donnelly P. A comparison of bayesian methods for haplotype reconstruction from population genotype data. *Am J Hum Genet.* 2003 Nov;73(5):1162-9.
- 165 Swinscow TDV, Campbell MJ. Statistics at Square One. 10th Edition. London: BMJ Books, 2002
- 166 Rice WR. Analyzing tables of statistical tests. *Evolution.* 1989 43, 223–225.
- 167 Epplen C, Jackel S, Santos EJ, D'Souza M, Poehlau D, Dotzauer B, Sindern E, Haups M, Rude KP, Weber F, Stover J, Poser S, Gehler W, Malin JP, Przuntek H, Epplen JT. Genetic predisposition to multiple sclerosis as revealed by immunoprinting. *Ann Neurol.* 1997 Mar;41(3):341-52.
- 168 He B, Xu C, Yang B, Landtblom AM, Fredrikson S, Hillert J. Linkage and association analysis of genes encoding cytokines and myelin proteins in multiple sclerosis. *J Neuroimmunol.* 1998 Jun 1;86(1):13-9.
- 169 Xu C, Dai Y, Fredrikson S, Hillert J. Association and linkage analysis of candidate chromosomal regions in multiple sclerosis: indication of disease genes in 12q23 and 7ptr-15. *Eur J Hum Genet.* 1999 Feb-Mar;7(2):110-6.
- 170 D'Alfonso S, Nistico L, Zavattari P, Marrosu MG, Murru R, Lai M, Massacesi L, Ballerini C, Gestri D, Salvetti M, Ristori G, Bomprezzi R, Trojano M, Liguori M, Gambi D, Quattrone A, Fruci D, Cucca F, Richiardi PM, Tosi R. Linkage analysis of multiple sclerosis with candidate region markers in Sardinian and Continental Italian families. *Eur J Hum Genet.* 1999 Apr;7(3):377-85.
- 171 Oturai A, Larsen F, Ryder LP, Madsen HO, Hillert J, Fredrikson S, Sandberg-Wollheim M, Laaksonen M, Koch-Henriksen N, Sawcer S, Fugger L, Sorensen PS, Svejgaard A. Linkage and association analysis of susceptibility regions on chromosomes 5 and 6 in 106 Scandinavian sibling pair families with multiple sclerosis. *Ann Neurol.* 1999 Oct;46(4):612-6.

- 172 Dyment DA, Willer CJ, Scott B, Armstrong H, Ligers A, Hillert J, Paty DW, Hashimoto S, Devonshire V, Hooge J, Kastrukoff L, Oger J, Metz L, Warren S, Hader W, Power C, Auty A, Nath A, Nelson R, Freedman M, Brunet D, Paulseth JE, Rice G, O'Connor P, Duquette P, Lapierre Y, Francis G, Bouchard JP, Murray TJ, Bhan V, Maxner C, Pryse-Phillips W, Stefanelli M, Sadovnick AD, Risch N, Ebers GC. Genetic susceptibility to MS: a second stage analysis in Canadian MS families. *Neurogenetics*. 2001 Jul;3(3):145-51.
- 173 Akesson E, Oturai A, Berg J, Fredrikson S, Andersen O, Harbo HF, Laaksonen M, Myhr KM, Nyland HI, Ryder LP, Sandberg-Wollheim M, Sorensen PS, Spurkland A, Svejagaard A, Holmans P, Compston A, Hillert J, Sawcer S. A genome-wide screen for linkage in Nordic sib-pairs with multiple sclerosis. *Genes Immun*. 2002 Aug;3(5):279-85.
- 174 Giedraitis V, Modin H, Callander M, Landtblom AM, Fossdal R, Stefansson K, Hillert J, Gulcher J. Genome-wide TDT analysis in a localized population with a high prevalence of multiple sclerosis indicates the importance of a region on chromosome 14q. *Genes Immun*. 2003 Dec;4(8):559-63.
- 175 Cui XY, Hu QD, Tekaya M, Shimoda Y, Ang BT, Nie DY, Sun L, Hu WP, Karsak M, Duka T, Takeda Y, Ou LY, Dawe GS, Yu FG, Ahmed S, Jin LH, Schachner M, Watanabe K, Arsenijevic Y, Xiao ZC. NB-3/Notch1 pathway via Deltex1 promotes neural progenitor cell differentiation into oligodendrocytes. *J Biol Chem*. 2004 Jun 11;279(24):25858-65.
- 176 Hu QD, Cui XY, Ng YK, Xiao ZC. Axoglial interaction via the notch receptor in oligodendrocyte differentiation. *Ann Acad Med Singapore*. 2004 Sep;33(5):581-8.
- 177 Mattson MP. Oxidative stress, perturbed calcium homeostasis, and immune dysfunction in Alzheimer's disease. *J Neurovirol*. 2002 Dec;8(6):539-50.
- 178 Matsumoto K, Akao Y, Yi H, Shamoto-Nagai M, Maruyama W, Naoi M. Overexpression of amyloid precursor protein induces susceptibility to oxidative stress in human neuroblastoma SH-SY5Y cells. *J Neural Transm*. 2005 Jun 15
- 179 Mullan M, Crawford F, Axelman K, Houlden H, Lilius L, Winblad B, Lannfelt L. A pathogenic mutation for probable Alzheimer's disease in the APP gene at the N-terminus of beta-amyloid. *Nat Genet*. 1992 Aug;1(5):345-7.
- 180 Heintz N, Zoghbi H. alpha-Synuclein--a link between Parkinson and Alzheimer diseases? *Nat Genet*. 1997 Aug;16(4):325-7.
- 181 Bear C, Ling V. Multidrug resistance and cystic fibrosis genes: complementarity of function? *Trends Genet*. 1993 Mar;9(3):67-8.
- 182 Senior AE, Gadsby DC. ATP hydrolysis cycles and mechanism in P-glycoprotein and CFTR. *Semin Cancer Biol*. 1997 Jun;8(3):143-50.

- 183 Klein I, Sarkadi B, Varadi A. An inventory of the human ABC proteins. *Biochim Biophys Acta*. 1999 Dec 6;1461(2):237-62.
- 184 Eloranta JJ, Kullak-Ublick GA. Coordinate transcriptional regulation of bile acid homeostasis and drug metabolism. *Arch Biochem Biophys*. 2005 Jan 15;433(2):397-412.
- 185 O'Shea JJ, Notarangelo LD, Johnston JA, Candotti F. Advances in the understanding of cytokine signal transduction: the role of Jak s and STATs in immunoregulation and the pathogenesis of immunodeficiency. *J Clin Immunol*. 1997 Nov;17(6):431-47.
- 186 Leonard WJ. Role of Jak kinases and STATs in cytokine signal transduction. *Int J Hematol*. 2001 Apr;73(3):271-7.
- 187 Paty DW, Li DK. Interferon beta-1b is effective in relapsing-remitting multiple sclerosis. II. MRI analysis results of a multicenter, randomized, double-blind, placebo-controlled trial. UBC MS/MRI Study Group and the IFNB Multiple Sclerosis Study Group. *Neurology*. 1993 Apr;43(4):662-7.
- 188 Jacobs LD, Cookfair DL, Rudick RA, Herndon RM, Richert JR, Salazar AM, Fischer JS, Goodkin DE, Granger CV, Simon JH, Alam JJ, Bartoszak DM, Bourdette DN, Braiman J, Brownschedle CM, Coats ME, Cohan SL, Dougherty DS, Kinkel RP, Mass MK, Munschauer FE 3rd, Priore RL, Pullicino PM, Scherokman BJ, Whitham RH, et al. Intramuscular interferon beta-1a for disease progression in relapsing multiple sclerosis. The Multiple Sclerosis Collaborative Research Group (MSCRG) *Ann Neurol*. 1996 Mar;39(3):285-94.
- 189 No authors listed. Randomised double-blind placebo-controlled study of interferon beta-1a in relapsing/remitting multiple sclerosis. PRISMS (Prevention of Relapses and Disability by Interferon beta-1a Subcutaneously in Multiple Sclerosis) Study Group. *Lancet*. 1998 Nov 7;352(9139):1498-504.
- 190 Rakesh K, Agrawal DK. Controlling cytokine signaling by constitutive inhibitors. *Biochem Pharmacol*. 2005 Sep 1;70(5):649-57.
- 191 Schaeffer HJ, Weber MJ. Mitogen-activated protein kinases: specific messages from ubiquitous messengers. *Mol Cell Biol*. 1999 Apr;19(4):2435-44.
- 192 Hartl DL, Clark AG. 1997 Principles of Population Genetics. 3 ed. Sinauer Associates, Sunderland, Massachusetts. 542 pp.
- 193 Pritchard JK, Przeworski M. Linkage disequilibrium in humans: models and data. *Am J Hum Genet*. 2001 Jul;69(1):1-14.
- 194 Ardlie KG, Kruglyak L, Seielstad M. Patterns of linkage disequilibrium in the human genome. *Nat Rev Genet*. 2002 Apr;3(4):299-309.

- 195 Goedde R, Sawcer S, Boehringer S, Mitterski B, Sindern E, Haupts M, Schimrigk S, Compston A, Epplen JT. A genome screen for linkage disequilibrium in HLA-DRB1*15-positive Germans with multiple sclerosis based on 4666 microsatellite markers. *Hum Genet.* 2002 Sep;111(3):270-7.
- 196 Ban M, Sawcer SJ, Heard RN, Bennetts BH, Adams S, Booth D, Perich V, Setakis E, Compston A, Stewart GJ. A genome-wide screen for linkage disequilibrium in Australian HLA-DRB1*1501 positive multiple sclerosis patients. *J Neuroimmunol.* 2003 Oct;143(1-2):60-4.
- 197 Setakis E. Statistical analysis of the GAMES studies. *J Neuroimmunol.* 2003 Oct;143(1-2):47-52.
- 198 Lefranc MP, Lefranc G. The T Cell Receptor Facts Book. London, Academic Press, 2001.
- 199 Lefranc MP, Lefranc G. The Immunoglobulin Facts Book. London, Academic Press, 2001.
- 200 Bradshaw D, Schammel CM, Posch P, Steiner NK, Hurley CK. Development of informatics tools for complex gene systems: killer-cell immunoglobulin-like receptor genes. *Tissue Antigens.* 2003 Feb;61(2):118-35.
- 201 ENCODE Project Consortium. The ENCODE (ENCyclopedia Of DNA Elements) Project. *Science.* 2004 Oct 22;306(5696):636-40.
- 202 Mayor C, Brudno M, Schwartz JR, Poliakov A, Rubin EM, Frazer KA, Pachter LS, Dubchak I. VISTA : visualizing global DNA sequence alignments of arbitrary length. *Bioinformatics.* 2000 Nov;16(11):1046-7.
- 203 Schwartz S, Elnitski L, Li M, Weirauch M, Riemer C, Smit A, Green ED, Hardison RC, Miller W; NISC Comparative Sequencing Program. MultiPipMaker and supporting tools: Alignments and analysis of multiple genomic DNA sequences. *Nucleic Acids Res.* 2003 Jul 1;31(13):3518-24.
- 204 Boffelli D, McAuliffe J, Ovcharenko D, Lewis KD, Ovcharenko I, Pachter L, Rubin EM. Phylogenetic shadowing of primate sequences to find functional regions of the human genome. *Science.* 2003 Feb 28;299(5611):1391-4.
- 205 Thomas JW, Touchman JW, Blakesley RW, Bouffard GG, Beckstrom-Sternberg SM, Margulies EH, Blanchette M, Siepel AC, Thomas PJ, McDowell JC, Maskeri B, Hansen NF, Schwartz MS, Weber RJ, Kent WJ, Karolchik D, Bruen TC, Bevan R, Cutler DJ, Schwartz S, Elnitski L, Idol JR, Prasad AB, Lee-Lin SQ, Maduro VV, Summers TJ, Portnoy ME, Dietrich NL, Akhter N, Ayele K, Benjamin B, Cariaga K, Brinkley CP, Brooks SY, Granite S, Guan X, Gupta J, Haghghi P, Ho SL, Huang MC, Karlins E, Laric PL, Legaspi R, Lim MJ, Maduro QL, Masiello CA, Mastrian SD, McCloskey JC, Pearson R, Stantripop S, Tiongson EE, Tran JT, Tsurgeon C, Vogt JL, Walker MA, Wetherby KD, Wiggins LS, Young AC, Zhang LH, Osoegawa K, Zhu B, Zhao B, Shu CL, De Jong PJ, Lawrence CE, Smit AF, Chakravarti A, Haussler D, Green P, Miller W, Green ED. Comparative analyses of multi-species sequences from targeted genomic regions. *Nature.* 2003 Aug 14;424(6950):788-93.

- 206 Hurst LD, Pal C, Lercher MJ. The evolutionary dynamics of eukaryotic gene order. *Nat Rev Genet.* 2004 Apr;5(4):299-310.
- 207 Iglesias AH, Camelo S, Hwang D, Villanueva R, Stephanopoulos G, Dangond F. Microarray detection of E2F pathway activation and other targets in multiple sclerosis peripheral blood mononuclear cells. *J Neuroimmunol.* 2004 May;150(1-2):163-77.
- 208 Mandel M, Gurevich M, Pauzner R, Kaminski N, Achiron A. Autoimmunity gene expression portrait: specific signature that intersects or differentiates between multiple sclerosis and systemic lupus erythematosus. *Clin Exp Immunol.* 2004 Oct;138(1):164-70.
- 209 Koike F, Satoh J, Miyake S, Yamamoto T, Kawai M, Kikuchi S, Nomura K, Yokoyama K, Ota K, Kanda T, Fukazawa T, Yamamura T. Microarray analysis identifies interferon beta-regulated genes in multiple sclerosis. *J Neuroimmunol.* 2003 Jun;139(1-2):109-18.
- 210 Satoh J, Nakanishi M, Koike F, Miyake S, Yamamoto T, Kawai M, Kikuchi S, Nomura K, Yokoyama K, Ota K, Kanda T, Fukazawa T, Yamamura T. Microarray analysis identifies an aberrant expression of apoptosis and DNA damage-regulatory genes in multiple sclerosis. *Neurobiol Dis.* 2005 Apr;18(3):537-50.
- 211 Hunger SP, Li S, Fall MZ, Naumovski L, Cleary ML. The proto-oncogene HLF and the related basic leucine zipper protein TEF display highly similar DNA-binding and transcriptional regulatory properties. *Blood.* 1996 Jun 1;87(11):4607-17.
- 212 Stanley K, Luzio P. Perforin. A family of killer proteins. *Nature.* 1988 Aug 11;334(6182):475-6.
- 213 Scolding NJ, Jones J, Compston DA, Morgan BP. Oligodendrocyte susceptibility to injury by T-cell perforin. *Immunology.* 1990 May;70(1):6-10.
- 214 Zeine R, Cammer W, Barbarese E, Liu CC, Raine CS. Structural dynamics of oligodendrocyte lysis by perforin in culture: relevance to multiple sclerosis. *J Neurosci Res.* 2001 May 15;64(4):380-91.
- 215 Rubesa G, Podack ER, Sepcic J, Rukavina D. Increased perforin expression in multiple sclerosis patients during exacerbation of disease in peripheral blood lymphocytes. *J Neuroimmunol.* 1997 Apr;74(1-2):198-204.
- 216 Matusevicius D, Kivisakk P, Navikas V, Soderstrom M, Fredrikson S, Link H. Interleukin-12 and perforin mRNA expression is augmented in blood mononuclear cells in multiple sclerosis. *Scand J Immunol.* 1998 Jun;47(6):582-90.
- 217 Kivisakk P, Stawiarz L, Matusevicius D, Fredrikson S, Soderstrom M, Hindmarsh T, Link H. High numbers of perforin mRNA expressing CSF cells in multiple sclerosis patients with gadolinium-enhancing brain MRI lesions. *Acta Neurol Scand.* 1999 Jul;100(1):18-24.

- 218 Stepp SE, Dufourcq-Lagelouse R, Le Deist F, Bhawan S, Certain S, Mathew PA, Henter JI, Bennett M, Fischer A, de Saint Basile G, Kumar V. Perforin gene defects in familial hemophagocytic lymphohistiocytosis. *Science*. 1999 Dec 3;286(5446):1957-9.
- 219 Werb Z. ECM and cell surface proteolysis: regulating cellular ecology. *Cell*. 1997 Nov 14;91(4):439-42.
- 220 Kuno K, Kanada N, Nakashima E, Fujiki F, Ichimura F, Matsushima K. Molecular cloning of a gene encoding a new type of metalloproteinase-disintegrin family protein with thrombospondin motifs as an inflammation associated gene. *J Biol Chem*. 1997 Jan 3;272(1):556-62.
- 221 Kuno K, Matsushima K. ADAMTS-1 protein anchors at the extracellular matrix through the thrombospondin type I motifs and its spacing region. *J Biol Chem*. 1998 May 29;273(22):13912-7.
- 222 Kuno K, Terashima Y, Matsushima K. ADAMTS-1 is an active metalloproteinase associated with the extracellular matrix. *J Biol Chem*. 1999 Jun 25;274(26):18821-6.
- 223 Tang BL. ADAMTS: a novel family of extracellular matrix proteases. *Int J Biochem Cell Biol*. 2001 Jan;33(1):33-44.
- 224 Bolz H, Ramirez A, von Brederlow B, Kubisch C. Characterization of ADAMTS14, a novel member of the ADAMTS metalloproteinase family. *Biochim Biophys Acta*. 2001 Dec 30;1522(3):221-5.
- 225 Colige A, Vandenberghe I, Thiry M, Lambert CA, Van Beeumen J, Li SW, Prockop DJ, Lapierre CM, Nusgens BV. Cloning and characterization of ADAMTS-14, a novel ADAMTS displaying high homology with ADAMTS-2 and ADAMTS-3. *J Biol Chem*. 2002 Feb 22;277(8):5756-66.
- 226 Cal S, Obaya AJ, Llamazares M, Garabaya C, Quesada V, Lopez-Otin C. Cloning, expression analysis, and structural characterization of seven novel human ADAMTSs, a family of metalloproteinases with disintegrin and thrombospondin-1 domains. *Gene*. 2002 Jan 23;283(1-2):49-62.
- 227 Romanic AM, Madri JA. Extracellular matrix-degrading proteinases in the nervous system. *Brain Pathol*. 1994 Apr;4(2):145-56.
- 228 Parks WC, Wilson CL, Lopez-Boado YS. Matrix metalloproteinases as modulators of inflammation and innate immunity. *Nat Rev Immunol*. 2004 Aug;4(8):617-29.
- 229 Waubant E, Goodkin DE, Gee L, Bacchetti P, Sloan R, Stewart T, Andersson PB, Stabler G, Miller K. Serum MMP-9 and TIMP-1 levels are related to MRI activity in relapsing multiple sclerosis. *Neurology*. 1999 Oct 22;53(7):1397-401.

- 230 Larsen PH, Wells JE, Stallcup WB, Opdenakker G, Yong VW. Matrix metalloproteinase-9 facilitates remyelination in part by processing the inhibitory NG2 proteoglycan. *J Neurosci*. 2003 Dec 3;23(35):11127-35.
- 231 Hayashita-Kinoh H, Kinoh H, Okada A, Komori K, Itoh Y, Chiba T, Kajita M, Yana I, Seiki M. Membrane-type 5 matrix metalloproteinase is expressed in differentiated neurons and regulates axonal growth. *Cell Growth Differ*. 2001 Nov;12(11):573-80.
- 232 Uhm JH, Dooley NP, Oh LY, Yong VW. Oligodendrocytes utilize a matrix metalloproteinase, MMP-9, to extend processes along an astrocyte extracellular matrix. *Glia*. 1998 Jan;22(1): 53-63.
- 233 Leppert D, Ford J, Stabler G, Grygar C, Lienert C, Huber S, Miller KM, Hauser SL, Kappos L. Matrix metalloproteinase-9 (gelatinase B) is selectively elevated in CSF during relapses and stable phases of multiple sclerosis. *Brain*. 1998 Dec;121 (Pt 12):2327-34.
- 234 Kouwenhoven M, Ozenci V, Gomes A, Yarilin D, Giedraitis V, Press R, Link H. Multiple sclerosis: elevated expression of matrix metalloproteinases in blood monocytes. *J Autoimmun*. 2001 Jun;16(4):463-70.
- 235 Galboiz Y, Shapiro S, Lahat N, Rawashdeh H, Miller A. Matrix metalloproteinases and their tissue inhibitors as markers of disease subtype and response to interferon-beta therapy in relapsing and secondary-progressive multiple sclerosis patients. *Ann Neurol*. 2001 Oct;50(4): 443-51.
- 236 Avolio C, Ruggieri M, Giuliani F, Liuzzi GM, Leante R, Riccio P, Livrea P, Trojano M. Serum MMP-2 and MMP-9 are elevated in different multiple sclerosis subtypes. *J Neuroimmunol*. 2003 Mar;136(1-2):46-53.
- 237 Seifert T, Kieseier BC, Ropele S, Strasser-Fuchs S, Quehenberger F, Fazekas F, Hartung HP. TACE mRNA expression in peripheral mononuclear cells precedes new lesions on MRI in multiple sclerosis. *Mult Scler*. 2002 Dec;8(6):447-51.
- 238 Kieseier BC, Pischel H, Neuen-Jacob E, Tourtellotte WW, Hartung HP. ADAM-10 and ADAM-17 in the inflamed human CNS. *Glia*. 2003 Jun;42(4):398-405.
- 239 Chataway J, Sawcer S, Feakes R, Coraddu F, Broadley S, Jones HB, Clayton D, Gray J, Goodfellow PN, Compston A. A screen of candidates from peaks of linkage: evidence for the involvement of myeloperoxidase in multiple sclerosis. *J Neuroimmunol*. 1999 Aug 3;98(2): 208-13.
- 240 Nelissen I, Vandenbroeck K, Fitton P, Hillert J, Olsson T, Marrosu MG, Opdenakker G. Polymorphism analysis suggests that the gelatinase B gene is not a susceptibility factor for multiple sclerosis. *J Neuroimmunol*. 2000 Jun 1;105(1):58-63.

- 241 Nelissen I, Fiten P, Vandenbroeck K, Hillert J, Olsson T, Marrosu MG, Opdenakker G. PECAM1, MPO and PRKAR1A at chromosome 17q21-q24 and susceptibility for multiple sclerosis in Sweden and Sardinia. *J Neuroimmunol.* 2000 Aug 1;108(1-2):153-9.
- 242 Fiotti N, Zivadinov R, Altamura N, Nasuelli D, Bratina A, Tommasi MA, Bosco A, Locatelli L, Grop A, Cazzato G, Guarnieri G, Giansante C, Zorzon M. MMP-9 microsatellite polymorphism and multiple sclerosis. *J Neuroimmunol.* 2004 Jul;152(1-2):147-53.
- 243 Prokunina L, Castillejo-Lopez C, Oberg F, Gunnarsson I, Berg L, Magnusson V, Brookes AJ, Tentler D, Kristjansdottir H, Grondal G, Bolstad AI, Svenungsson E, Lundberg I, Sturfelt G, Jonsson A, Truedsson L, Lima G, Alcocer-Varela J, Jonsson R, Gyllensten UB, Harley JB, Alarcon-Segovia D, Steinsson K, Alarcon-Riquelme ME. A regulatory polymorphism in PDCD1 is associated with susceptibility to systemic lupus erythematosus in humans. *Nat Genet.* 2002 Dec;32(4):666-9.
- 244 Tokuhiro S, Yamada R, Chang X, Suzuki A, Kochi Y, Sawada T, Suzuki M, Nagasaki M, Ohtsuki M, Ono M, Furukawa H, Nagashima M, Yoshino S, Mabuchi A, Sekine A, Saito S, Takahashi A, Tsunoda T, Nakamura Y, Yamamoto K. An intronic SNP in a RUNX1 binding site of SLC22A4, encoding an organic cation transporter, is associated with rheumatoid arthritis. *Nat Genet.* 2003 Dec;35(4):341-8.
- 245 Helms C, Cao L, Krueger JG, Wijsman EM, Chamian F, Gordon D, Heffernan M, Daw JA, Robarge J, Ott J, Kwok PY, Menter A, Bowcock AM. A putative RUNX1 binding site variant between SLC9A3R1 and NAT9 is associated with susceptibility to psoriasis. *Nat Genet.* 2003 Dec;35(4):349-56.
- 246 Irla M, Puthier D, Granjeaud S, Saade M, Victorero G, Mattei MG, Nguyen C. Genomic organization and the tissue distribution of alternatively spliced isoforms of the mouse Spatial gene. *BMC Genomics.* 2004 Jul 5;5(1):41.
- 247 Flomerfelt FA, Kim MG, Schwartz RH. Spatial, a gene expressed in thymic stromal cells, depends on three-dimensional thymus organization for its expression. *Genes Immun.* 2000 Aug;1(6):391-401.
- 248 Altshuler D, Brooks LD, Chakravarti A, Collins FS, Daly MJ, Donnelly P; International HapMap Consortium. A haplotype map of the human genome. *Nature.* 2005 Oct 27;437(7063):1299-320.
- 249 Hirschhorn JN, Daly MJ. Genome-wide association studies for common diseases and complex traits. *Nat Rev Genet.* 2005 Feb;6(2):95-108.
- 250 Wang WY, Barratt BJ, Clayton DG, Todd JA. Genome-wide association studies: theoretical and practical concerns. *Nat Rev Genet.* 2005 Feb;6(2):109-18.

- 251 Weiss KM, Clark AG. Linkage disequilibrium and the mapping of complex human traits. *Trends Genet.* 2002 Jan;18(1):19-24.
- 252 Wright AF, Carothers AD, Pirastu M. Population choice in mapping genes for complex diseases. *Nat Genet.* 1999 Dec;23(4):397-404.
- 253 Pritchard JK, Stephens M, Rosenberg NA, Donnelly P. Association mapping in structured populations. *Am J Hum Genet.* 2000 Jul;67(1):170-81.
- 254 Ardlie KG, Lunetta KL, Seielstad M. Testing for population subdivision and association in four case-control studies. *Am J Hum Genet.* 2002 Aug;71(2):304-11.
- 255 Freedman ML, Reich D, Penney KL, McDonald GJ, Mignault AA, Patterson N, Gabriel SB, Topol EJ, Smoller JW, Pato CN, Pato MT, Petryshen TL, Kolonel LN, Lander ES, Sklar P, Henderson B, Hirschhorn JN, Altshuler D. Assessing the impact of population stratification on genetic association studies. *Nat Genet.* 2004 Apr;36(4):388-93.
- 256 Reich DE, Goldstein DB. Detecting association in a case-control study while correcting for population stratification. *Genet Epidemiol.* 2001 Jan;20(1):4-16.
- 257 Siddiqui A, Kerb R, Weale ME, Brinkmann U, Smith A, Goldstein DB, Wood NW, Sisodiya SM. Association of multidrug resistance in epilepsy with a polymorphism in the drug-transporter gene ABCB1. *N Engl J Med.* 2003 Apr 10;348(15):1442-8.
- 258 Storey JD, Tibshirani R. Statistical significance for genomewide studies. *Proc Natl Acad Sci U S A.* 2003 Aug 5;100(16):9440-5.
- 259 Benjamini Y, Hochberg Y. Controlling the false discovery rate: a practical and powerful approach to multiple testing. *J Roy Statist Soc Ser.* 1995 B 57:289-300.
- 260 Fernald GH, Yeh RF, Hauser SL, Okkenberg JR, Baranzini SE. Mapping gene activity in complex disorders: Integration of expression and genomic scans for multiple sclerosis. *J Neuroimmunol.* 2005 Oct;167(1-2):157-69.
- 261 Goldstein DB, Ahmadi KR, Weale ME, Wood NW. Genome scans and candidate gene approaches in the study of common diseases and variable drug responses. *Trends Genet.* 2003 Nov;19(11):615-22.
- 262 Weiss KM, Terwilliger JD. How many diseases does it take to map a gene with SNPs? *Nat Genet.* 2000 Oct;26(2):151-7.

7

APPENDIX

Appendix A	
STR-Genotyping of individual DNA samples	148
Appendix B	
STR genotyping data from DNA pools	167
Appendix C	
Sliding window plots and synoptical tables	197
Appendix D	
Genes of interest derived from sliding windows	245
Appendix E	
Allele and genotype frequency distributions and corresponding statistics	249
Appendix F	
Haplotype and haplotype pair frequency distributions and corresponding statistics	259

APPENDIX A – STR-Genotyping of individual DNA samples

Genotyping 7 microsatellites of interest on individual DNA samples: refining DNA pool results.

In order to evaluate several target regions located in the genome apart from the HLA region, 5 microsatellites (D9S303, D13S777, D16S2613, D18S52, D22S6902) that ranged in the upper extreme end (top 10%), one marker (D4S3245) from the interquartile range (rank 81) and one marker from the lower extreme end (D12S1653; rank 176) (Tab. 3.1) were randomly selected for testing on 372 individual DNA samples that mainly constituted genotyped DNA pools. The comparison of peak height distributions (allele image profile, AIP) observed in the DNA pool study to allele frequency distributions obtained from genotyping individual DNA samples provides a measure for the type I error (false positive result) rate of employed pooling methodology.

Reagents and consumables

PCR reagents, conditions and microsatellite markers were equal to those applied for DNA pools (Section 2.4).

Material

DNA samples of 186 selected cases (140 RRMS and 46 SPMS patients) and 186 controls constituted mainly the sample sets used in previous DNA pool study (concordance rate: 89 and 96%).

Analysis of individually genotyped DNA samples

Equipment

Software GENESCAN vers. 3.5	Applied Biosystems
Software GENOTYPER vers. 3.6	Applied Biosystems
SPSS package for MS-windows vers. 11.5	SPSS Inc.

GENESCAN and GENOTYPER performed size-calling alleles and defined corresponding peak heights, respectively. Allele lengths could not be specified formally according to GENESCAN realized size-calls, because no genotype-known reference sample providing base sequence information was analysed in parallel. In order to determine alleles of tested microsatellites, numerations were realized by default, based on the patients pool (replicates A1 and 2). The peak of an AIP that received the highest mean relative count (Section 2.5.2) was selected as the reference peak and correspondingly designated “allele 0”. In accordance to the marker type (di-, tri- or tetranucleotide), adjacent peaks in up- and downstream directions were indicated in descending and ascending order, respectively. Figure A2a depicts the dinucleotide microsatellite D18S52 and corresponding AIPs. Peak number 5 at base length 117.2 proved to be the highest relative peak (Fig. A2b; value 170.1), hence peaks 6, 7, 8, 9 were designated alleles “2”, “4”, “6”, “8”, and peaks 4, 3, 2, 1 received “-2”, “-4”, “-6”, “-8”, respectively.

Due to *a priori* knowledge of relative peak count ratios between MS cases and controls in pooled DNA, a one-tailed Chi-square test (degree of freedom = 1) was performed comparing groups at each allele category detected in the individually typed DNA samples, and if an expected value was <5 the Fisher’s exact test was applied. Statistical computations were carried out with the SPSS software.

Allele frequency percentages of AIPs (mean values) were positioned between replicates A1/2 and B1/2 in profile images (Fig. A1a) and indicated in bar charts (ordinate) of allele frequencies established by individual genotyping (Fig. A1c). Thereby, a rather qualitative inspection of successful or failing pool result replication was feasible, as applied statistical terms, the one-sided and the empirical p-value, operate distinctly and could not be used for formal comparisons. Still, the significance threshold <0.05 was applied in both situations and served as a tool to express a degree of confirmation.

Individual DNA genotyping of a microsatellite marker generated in contrast to pooled DNA genotyping a preciser overview of genuine alleles and, correspondingly, their

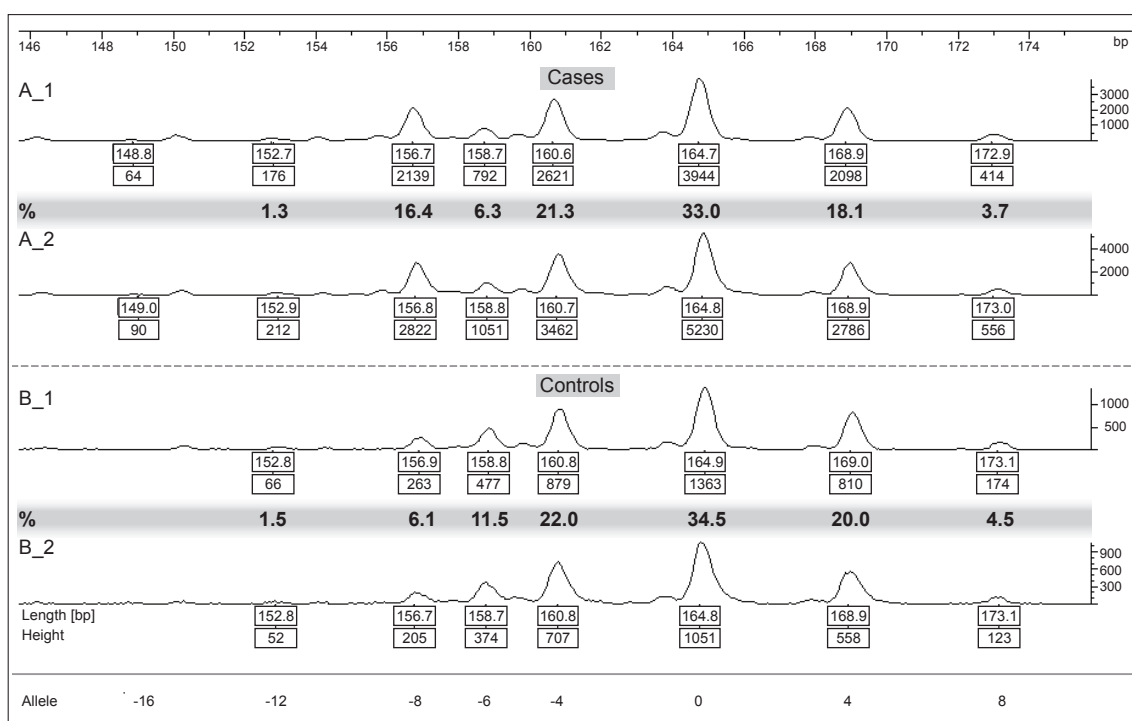
frequency distributions. Therefore, in some cases alleles were revealed in genotyping results which remained undetected in allele image profiles of typed DNA pools (Fig. A2, A3, A4, A7). The genotyping of individual DNA samples hence represents a further step towards the detection of genuine differences in allele frequencies between MS patients and healthy controls. The evidence for association decreased considerably in two (D18S52, D16S2613) of the 7 tested markers.

D9S303 – ranking position 2**Figure A1**

The tetranucleotide marker generated a range of 7 alleles (allele -16 to 8) plus a PCR- or marker related intermediate allele “-6”, that was present in both experiments. Allele -8 was over-represented in the estimated patient DNA pool (Fig. A1a+b: Pool A=16.4% vs. Pool B=6.1%, hypothetical $p=4.5 \times 10^{-6}$) and results confirmed a nearly equal degree of association in individual DNA samples of patients (Fig. A1c; Cases=11.9% vs. Controls=1.7%, one sided $p=1 \times 10^{-5}$). The frequency percentages were lower after individual typing, but the ratio A>B was consistent. In addition, allele frequency proportions of patients versus controls from remaining alleles displayed high concordance.

Figure A1 | d9s303

a) Allele Image Profile (AIP)



b) AIP analysis

PEAK ORDER	1	2	3	4	5	6	7	8
A1	0	176	2139	792	2621	3944	2098	414
A2	0	212	2822	1051	3462	5230	2786	556
B1	0	66	263	477	879	1363	810	174
B2	0	52	205	374	707	1051	558	123
Allele	-16	-12	-8	-6	-4	0	4	8
	0.971	0.943	0.916	0.889	0.863	0.838	0.814	0.790

COR. PEAKS	1	2	3	4	5	6	7	8
A1	0	187	2336	891	3037	4706	2578	524
A2	0	225	3083	1182	4011	6240	3423	704
B1	0	70	287	537	1018	1626	995	220
B2	0	55	224	421	819	1254	686	156

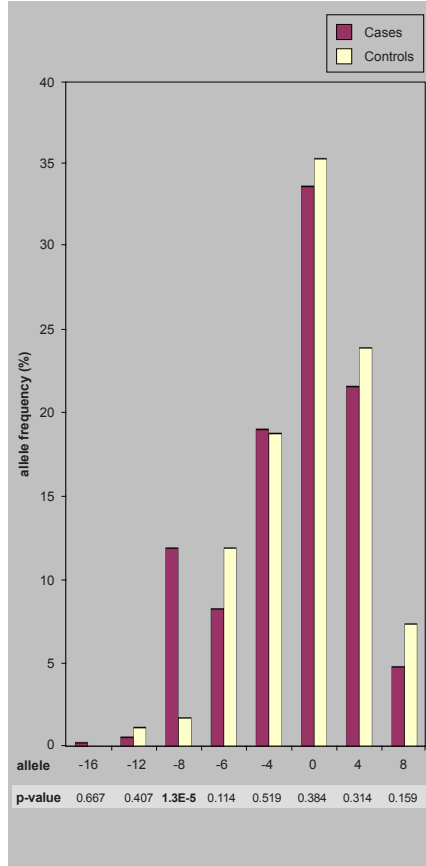
REL. PEAK HEIGHTS:	1	2	3	4	5	6	7	8
A1	0	5.2	65.5	25.0	85.2	132.0	72.3	14.7
A2	0	4.8	65.4	25.1	85.0	132.3	72.6	14.9
B1	0	5.9	24.2	45.2	85.7	136.8	83.7	18.5
B2	0	6.1	24.8	46.6	90.7	138.8	75.9	17.2
CV A1/A2	0.07	0.00	0.00	0.00	0.00	0.00	0.00	0.01
CV B1/B2	0.03	0.02	0.02	0.04	0.01	0.07	0.05	
Arith. mean A	5.0	65.4	25.0	85.1	132.2	72.5	14.8	
Arith. mean B	6.0	24.5	45.9	88.2	137.8	79.8	17.9	

(A+B)/2	1	2	3	4	5	6	7	8
	5.5	45.0	35.4	86.6	135.0	76.1	16.3	
	395.0	334.6	375.0	314.9	267.8	327.6	385.2	
chi 1	394.5	355.0	364.6	313.4	265.0	323.9	383.7	
chi 2	0.045	9.334	3.059	0.027	0.059	0.178	0.144	
	0.001	1.182	0.297	0.007	0.030	0.042	0.006	

Chi - value	1	2	3	4	5	6	7	8
p-value	0.09	21.03	6.71	0.07	0.18	0.44	0.30	
Allele	0.763	4.5E-6	0.001	0.793	0.672	0.507	0.584	
LDA:	-16	-12	-8	-6	-4	0	4	8
	0.029							

Weight:	1	400

c) Individual Genotyping

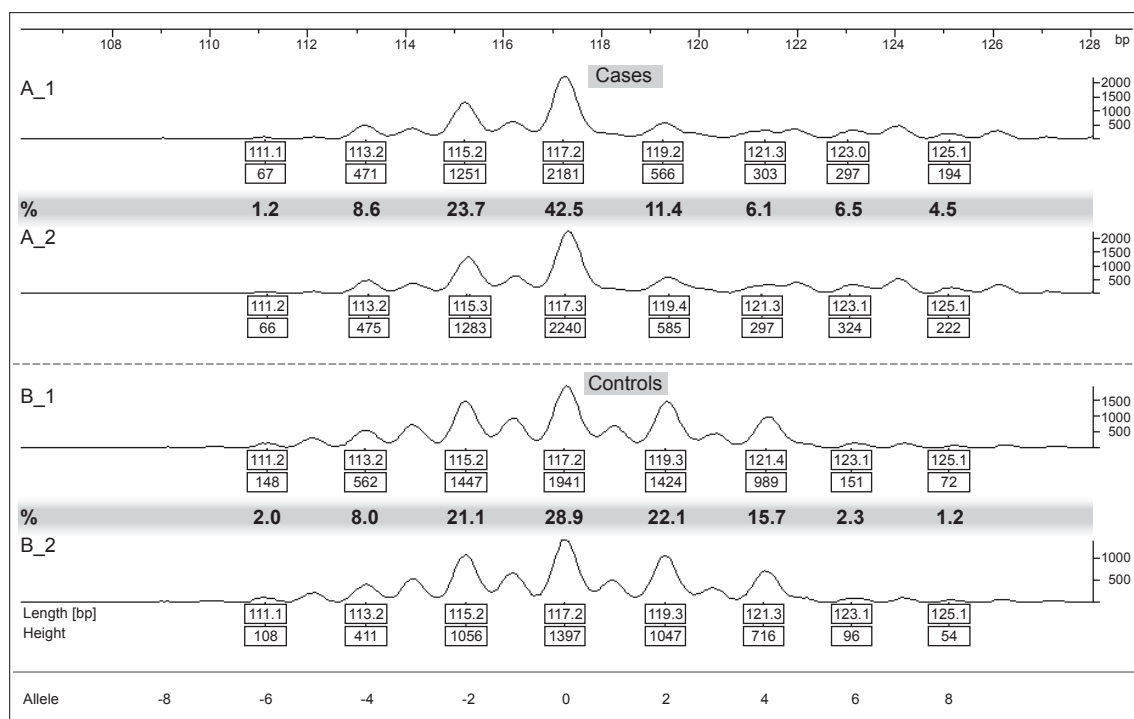


D18S52 – ranking position 3**Figure A2**

The dinucleotide marker produced 9 alleles ranging from -8 to 8 and served as an example of unsuccessful pool result replication. DNA pool B AIP displayed a higher rate of stutter bands or monoalleles than pool A (Fig. A2a). Strikingly, the marker genotyped on pools revealed 5 alleles (0, 2, 4, 6, 8) with prominent evidence of association - all displayed a p-value < 0.01 - and different peak count ratios (alleles 0, 6, 8: A > B; alleles 2, 4: A < B), which conferred it an interesting marker considering potential allele combinations and disease types. Nevertheless, individual DNA sample genotyping did not replicate these findings in either respect, statistic nor ratio-wise, rendering D18S52 a highly ambiguous and problematic genetic marker. An extreme discrepancy was detected for allele 0: in the pooled DNA comparison it displayed a frequency difference over 13% (Fig. A2a+b: Pool A=42.5% vs. Pool B=28.9%, empirical p=0.0001); this was not sustained in the individual genotyping step (Fig. A2c: Cases=31.2% vs. Controls=29.4%), expressed by the one-sided p=0.339, since the allele over-representation in MS patients disappeared.

The situation at allele 2 showed a reduced deviation between cases and controls (Fig. A2b+c: empirical p=0.0001, one sided p=0.121) after individual genotyping, but more striking were the strong increases in the allele frequencies of both populations (Fig. A2a+c: Pool A=11.4% vs. Pool B=22.1%; Cases=26.4% vs. Controls=30.9%) counted in individually typed DNA samples.

Finally, allele 4 (Fig. A2a+b: Pool A=6.1% vs. Pool B=15.7%, empirical p=0.00001) displayed the greatest inconsistency after determining individual frequencies (Fig. A2c: Cases=17.2% vs. Controls=16.5%, one sided p=0.443) as, furthermore, a reversed frequency ratio was revealed. Alleles 6 and 8 follow the frequency patterns of the pooled controls in both individually tested populations (Fig. A2a+c: Pool B=2.3% and 1.2%, respectively; Cases=1.9% and 0.3%; Controls=2.1% and 0%) and were of no further relevance.

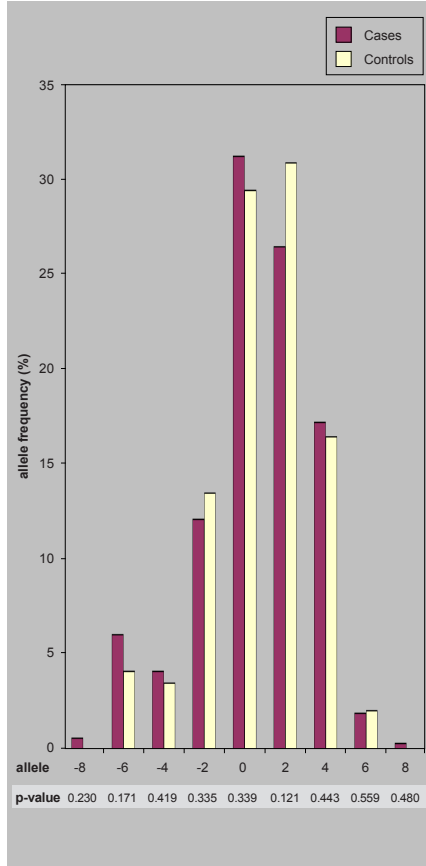
Figure A2 | d18s52AIP**a) Allele Image Profile (AIP)****b) AIP analysis**

PEAK ORDER	1	2	3	4	5	6	7	8	9
A1	0	67	471	1251	2181	566	303	297	194
A2	0	66	475	1283	2240	585	297	324	222
B1	0	148	562	1447	1941	1424	989	151	72
B2	0	108	411	1056	1397	1047	716	96	54
Allele	-8	-6	-4	-2	0	2	4	6	8
	0.971	0.943	0.916	0.889	0.863	0.838	0.814	0.790	0.767

COR. PEAKS	1	2	3	4	5	6	7	8	9
A1	0	71	515	1407	2527	675	372	376	253
A2	0	70	519	1443	2595	698	365	410	289
B1	0	157	614	1628	2249	1699	1215	191	94
B2	0	115	449	1188	1619	1249	880	122	70

REL. PEAK HEIGHTS:	1	2	3	4	5	6	7	8	9
A1	0	4.8	34.6	94.7	170.1	45.5	25.1	25.3	17.0
A2	0	4.6	34.0	94.6	170.2	45.8	23.9	26.9	19.0
B1	0	8.1	31.7	84.0	116.0	87.7	62.7	9.9	4.8
B2	0	8.2	32.0	84.5	115.2	88.9	62.6	8.6	5.0
CV A1/A2	0.03	0.01	0.00	0.00	0.01	0.03	0.04	0.08	
CV B1/B2	0.01	0.01	0.01	0.01	0.01	0.00	0.09	0.02	
Arith. mean A	4.7	34.3	94.7	170.1	45.6	24.5	26.1	18.0	
Arith. mean B	8.1	31.8	84.3	115.6	88.3	62.7	9.3	4.9	

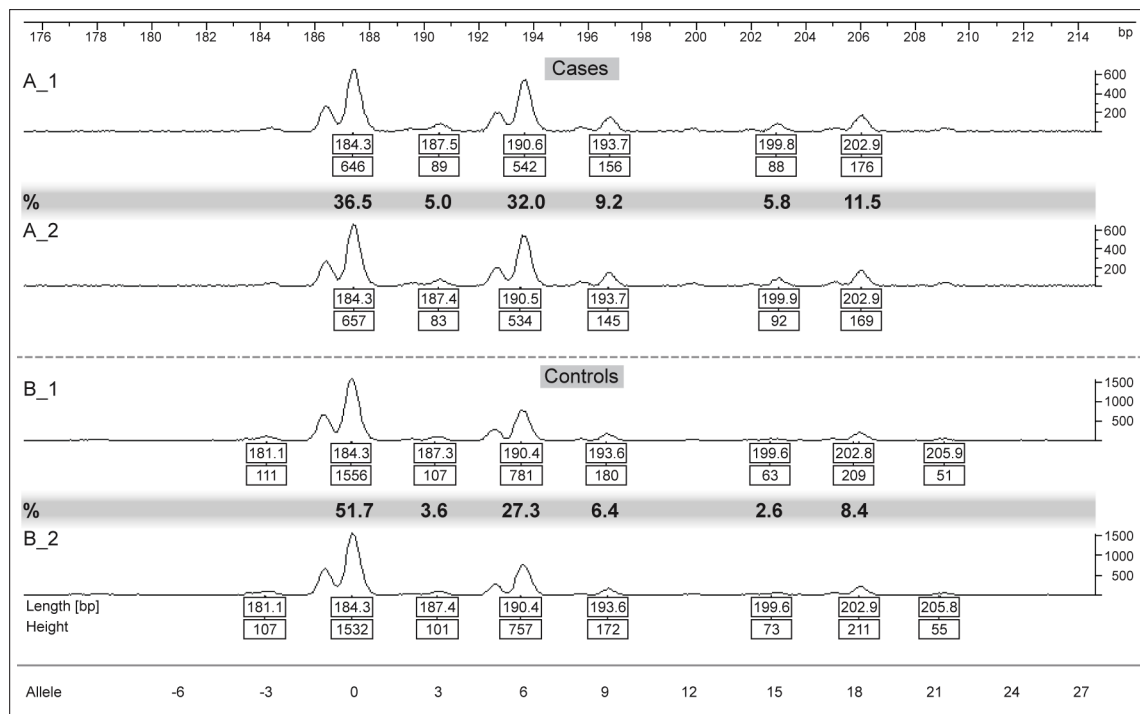
(A+B)/2	1	2	3	4	5	6	7	8	9
	6.4	33.1	89.5	142.9	66.9	43.6	17.7	11.5	
	395.3	365.7	305.3	229.9	354.4	375.5	373.9	382.0	
	393.6	366.9	310.5	257.1	333.1	356.4	382.3	388.5	
chi 1	0.462	0.048	0.303	5.200	6.800	8.356	4.011	3.726	
chi 2	0.008	0.004	0.087	2.889	1.367	1.022	0.185	0.110	
Chi - value	0.94	0.10	0.78	16.18	16.33	18.75	8.39	7.67	
p-value	0.333	0.747	0.377	0.00006	0.00005	0.00002	0.004	0.006	
Allele	-8	-6	-4	-2	0	2	4	6	8
LDA:	0.029								
Weight:	1		400						

c) Individual Genotyping

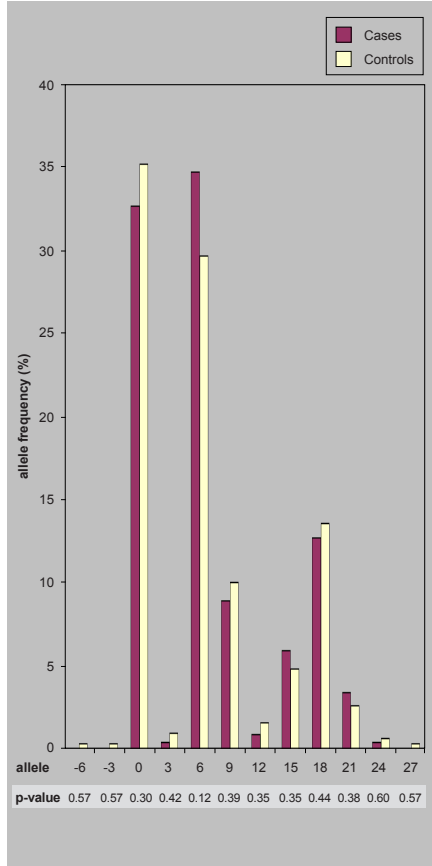
D16S2613 – ranking position 4**Figure A3**

The highly polymorphic trinucleotide microsatellite created 12 alleles when genotyped with single samples, whereas the allele image profiles displayed only 6 in both DNA pools (Fig. A3c and a). Again, the highly significant result of allele 0 (peak 3) (Fig. A3a+b: Pool A=36.5% vs. Pool B=51.7%, empirical $p=0.00002$) did not maintain the group distinguishing character, expressed by a non-significant p-value comparing the individually tested population samples (Fig. A3c: Cases=32.6% vs. Controls=35.2%; $p=0.299$). Here, the pooled control samples appeared to have incorporated a deviation bias that could not be confirmed in individual samples.

The second site, allele 15, that generated a moderate association with MS patients (empirical $p=0.025$) in DNA pool comparsion could not be verified either and produced a p-value distinctly exceeding the significance threshold ($p=0.353$). Once more, Pool B allele estimation (2.6%) caused the discordance (lack of agreement between pooled and individual samples) after genotyping the marker (4.8%) on healthy control individuals. Interestingly, this marker is located at 16p13, a non-MHC loci associated with MS, and received recognition in an American genome-wide linkage screen.¹¹⁶

Figure A3 | d16s2613AIP**a) Allele Image Profile (AIP)****b) AIP analysis**

PEAK ORDER	1	2	3	4	5	6	7	8	9	10	11	12
A1	0	0	646	89	542	156	0	88	176	0	0	0
A2	0	0	657	83	534	145	0	92	169	0	0	0
B1	0	0	1556	107	781	180	0	63	209	0	0	0
B2	0	0	1532	101	757	172	0	73	211	0	0	0
Allele	-6	-3	0	3	6	9	12	15	18	21	24	27
	0.971	0.943	0.916	0.889	0.863	0.838	0.814	0.790	0.767	0.745	0.723	0.702
COR. PEAKS:												
A1	0	0	706	100	628	186	0	111	229	0	0	0
A2	0	0	718	93	619	173	0	116	220	0	0	0
B1	0	0	1700	120	905	215	0	80	272	0	0	0
B2	0	0	1673	114	877	205	0	92	275	0	0	0
REL. PEAK HEIGHTS:												
A1	0	0	144.0	20.4	128.1	38.0	0	22.7	46.8	0	0	0
A2	0	0	148.0	19.3	127.6	35.7	0	24.0	45.4	0	0	0
B1	0	0	206.5	14.6	110.0	26.1	0	9.7	33.1	0	0	0
B2	0	0	206.8	14.0	108.4	25.4	0	11.4	34.0	0	0	0
CV A1/A2	0.02	0.04	0.00	0.04			0.04	0.02				
CV B1/B2	0.00	0.03	0.01	0.02			0.12	0.02				
Arith. mean A	146.0	19.8	127.9	36.8			23.4	46.1				
Arith. mean B	206.7	14.3	109.2	25.7			10.6	33.5				
(A+B)/2			176.3	17.1	118.5	31.3		17.0	39.8			
			254.0	380.2	272.1	363.2		376.6	353.9			
chi 1			223.7	382.9	281.5	368.7		383.0	360.2			
chi 2			5.220	0.444	0.737	0.985		2.421	0.992			
Chi - value			4.116	0.020	0.310	0.084		0.107	0.110			
p-value			18.67	0.93	2.09	2.14		5.06	2.20			
Allele	-6	-3	0	3	6	9	12	15	18	21	24	27
LDA:	0.029											
Weight:	1	400										

c) Individual Genotyping

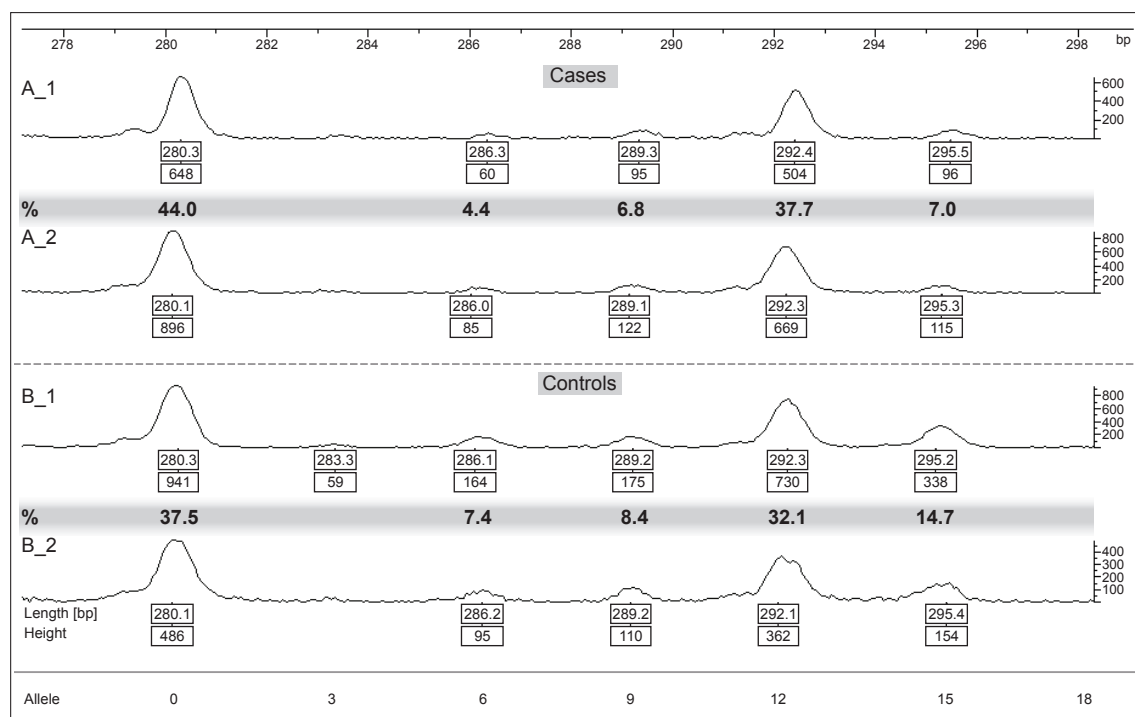
D13S777 – ranking position 13**Figure A4**

Genotyping this trinucleotide provided an allele spectra consisting of 7 alleles of which 4 (alleles 0, 9, 12, and 15) exceeded the 5% frequency limit in both DNA pools (Fig. A4a). Counts of allele 15 exhibited a disproportionated distribution between pooled genotypes (Fig. A4a+b: Pool A=7.0% vs. Pool B=14.7%, empirical $p=0.0005$) providing a strong association with controls, but revealed less relevance after individual genotyping (Fig. A4c: Cases=7.3% vs. Controls=12.9%, $p=0.019$).

Conversely, allele 0 received a nearly significant value after pool comparsion (Fig. A4a+b: Pool A=44.0% vs. Pool B=37.5%, empirical $p=0.056$) and was found to be significantly associated with patients when individually tested (Fig. A4c: Cases=50.8% vs. Controls=41.5%, $p=0.018$). In spite of minor allele count discrepancies at alleles 0, 9 and 12, the individual genotyping outcome proved to be concordant with indications from the genotyped pools.

Figure A4 | d13s777AIP

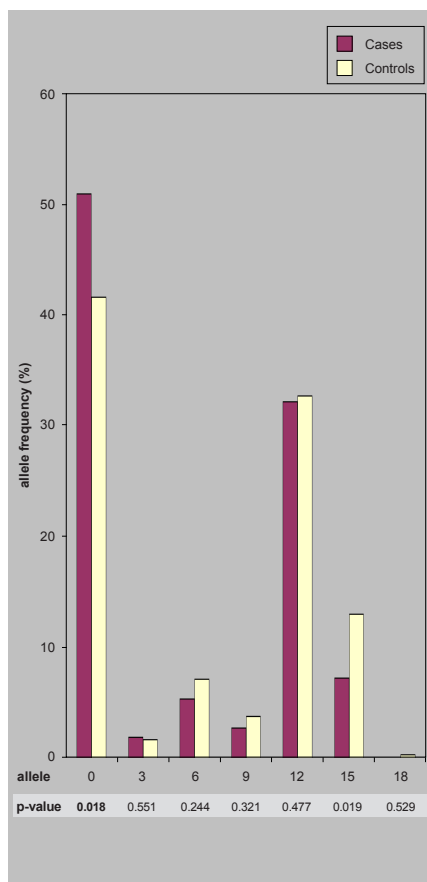
a) Allele Image Profile (AIP)



b) AIP analysis

PEAK ORDER	1	2	3	4	5	6	7
A1	648	0	60	95	504	96	0
A2	896	0	85	122	669	115	0
B1	941	0	164	175	730	338	0
B2	486	0	95	110	362	154	0
Allele	0	3	6	9	12	15	18
COR. PEAKS	0.971	0.943	0.916	0.889	0.863	0.838	0.814
REL. PEAK HEIGHTS:							
A1	173.5	0	17.0	27.8	151.8	29.8	0
A2	178.7	0	18.0	26.6	150.1	26.6	0
B1	149.4	0	27.6	30.4	130.4	62.2	0
B2	150.4	0	31.2	37.2	126.0	55.2	0
CV A1/A2	0.02		0.04	0.03	0.01	0.08	
CV B1/B2	0.01		0.09	0.14	0.02	0.08	
Arith. mean A	176.1		17.5	27.2	151.0	28.2	
Arith. mean B	149.9		29.4	33.8	128.2	58.7	
(A+B)/2	163.0		23.5	30.5	139.6	43.4	
chi 1	223.9		382.5	372.8	249.0	371.8	
chi 2	237.0		376.5	369.5	260.4	356.6	
Chi - value	3.56		3.20	0.77	2.85	12.03	
p-value	0.059		0.074	0.380	0.091	0.0005	
Allele	0	3	6	9	12	15	18
LDA:	0.029						
Weight:	1		400				

c) Individual Genotyping

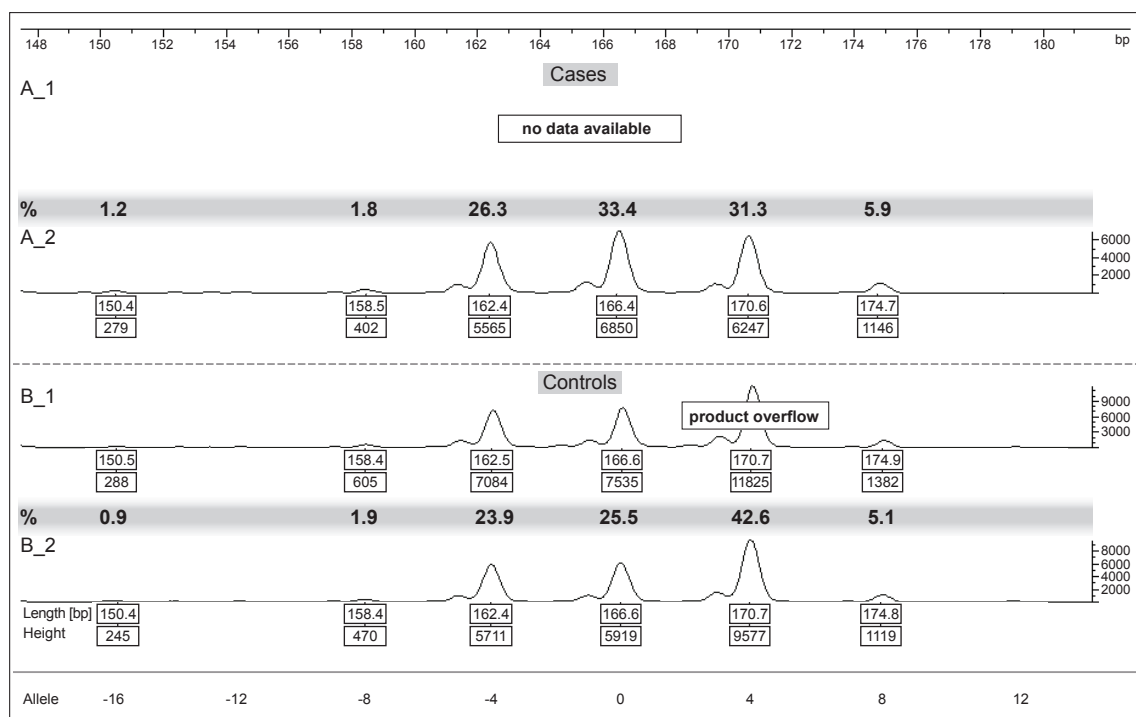


D22S692 – ranking position 17**Figure A5**

The allele distribution established by the 8 possible tetranucleotide repeats was mainly represented by alleles -4 to 8 in both DNA pools (Fig. A5a). The AIP analysis was completed as described in 2.5.2, excluding profile B_1 data due to an unreliable fluorescent signal at allele 4 (signal intensity > 10,000) which would otherwise distort an acceptable empirical p-value calculation;¹²¹ therefore, incorporating AIP peak values from replicates A_2 and B_2 had to suffice. Similar to the results for marker D13S777, the pool-associated alleles 0 (Fig. A5a+b: Pool A=33.4% vs. Pool B=25.5%, empirical p=0.015) and 4 (Fig. A5a+b: Pool A=31.3% vs. Pool B=42.6%, empirical p=0.001) displayed after individual genotyping a relatively consistent significance for the moderate susceptibility allele 0 (Fig. A5c: Cases=32.4% vs. Controls=24.1%, p=0.017) and a proportionately stronger reduction of relevance for the protective allele 4 (Fig. A5c: Cases=38.0% vs. Controls=44.0%, p=0.083).

Figure A5 | d22s692AIP

a) Allele Image Profile (AIP)



b) AIP analysis

PEAK ORDER	1	2	3	4	5	6	7	8
A1	279	0	402	5565	6850	6247	1146	0
A2	279	0	402	5565	6850	6247	1146	0
B1	245	0	470	5711	5919	9577	1119	0
B2	245	0	470	5711	5919	9577	1119	0
Allele	-16	-12	-8	-4	0	4	8	12
	0.971	0.943	0.916	0.889	0.863	0.838	0.814	0.790

COR. PEAKS	287	0	439	6260	7936	7453	1408	0
A1	287	0	439	6260	7936	7453	1408	0
A2	287	0	439	6260	7936	7453	1408	0
B1	252	0	513	6424	6857	11427	1375	0
B2	252	0	513	6424	6857	11427	1375	0

REL. PEAK HEIGHTS:	4.8	0	7.4	105.3	133.5	125.4	23.7	0
A1	4.8	0	7.4	105.3	133.5	125.4	23.7	0
A2	4.8	0	7.4	105.3	133.5	125.4	23.7	0
B1	3.8	0	7.6	95.7	102.2	170.2	20.5	0
B2	3.8	0	7.6	95.7	102.2	170.2	20.5	0

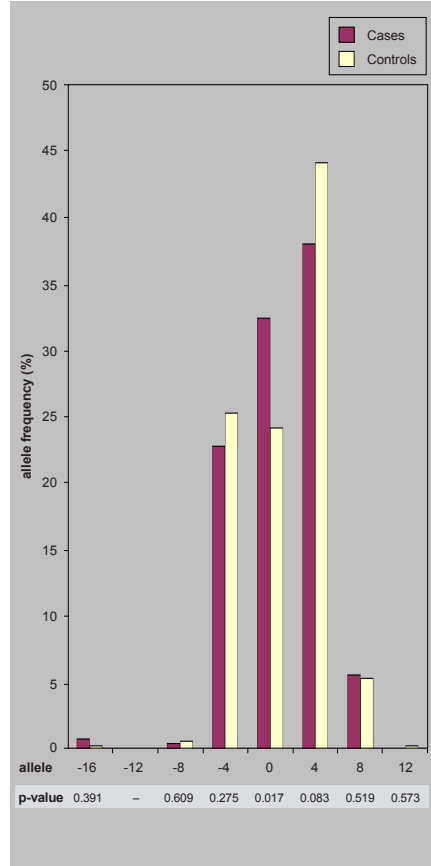
CV A1/A2	-	-	-	-	-	-	-
CV B1/B2	-	-	-	-	-	-	-
Arith. mean A	4.8	7.4	105.3	133.5	125.4	23.7	
Arith. mean B	3.8	7.6	95.7	102.2	170.2	20.5	

(A+B)/2	4.3		7.5	100.5	117.8	147.8	22.1	
	395.2		392.6	294.7	266.5	274.6	376.3	
	395.7		392.5	299.5	282.2	252.2	377.9	
chi 1	0.067		0.002	0.228	2.079	3.408	0.116	
chi 2	0.001		0.000	0.076	0.868	1.997	0.007	

Chi - value	0.14	0.01	0.61	5.90	10.81	0.25	
p-value	0.713		0.945	0.435	0.015	0.001	0.621
Allele	-16	-12	-8	-4	0	4	8
LDA:	0.029						

Weight:	1		400	
---------	---	--	-----	--

c) Individual Genotyping

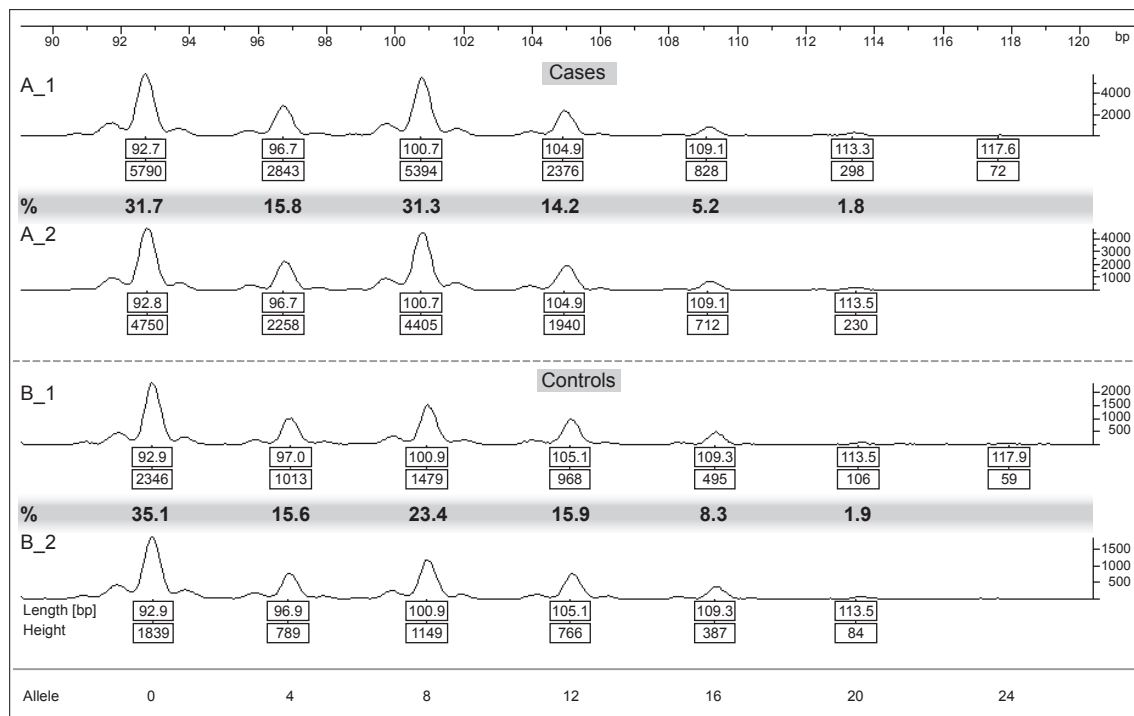


D4S3245 – ranking position 81**Figure A6**

Testing this tetranucleotide revealed seven alleles in pooled and individual DNA samples (Fig. A6a). The verification of different allele distribution ratios was present for significant allele 8 (Pool A=31.3% vs. Pool B=23.4%, empirical $p=0.012$; Cases=32.1% vs. Controls=24.6%, one-sided $p=0.026$) and the trend of allele 16 (Pool A=5.2% vs. Pool B=8.3%, empirical $p=0.082$; Cases=6.7% vs. Controls=10.1%, one-sided $p=0.072$). Interestingly, allele 0 distribution was in accordance with its general ratio ($A < B$), but resulted highly significant (Cases=26.2% vs. Controls=35.9%, $p=0.008$) in comparison with the preceding AIP outcome (Pool A=31.7% vs. Pool B=35.1%, empirical $p=0.314$). An inversed relationship between cases and controls after individual genotyping was observed for allele 12 (Pool A=14.2%, Pool B=15.9% vs. Cases=17.9%, Controls=13.1%), which displayed a statistical trend (one-sided $p=0.066$).

Figure A6 | d4s3245AIP

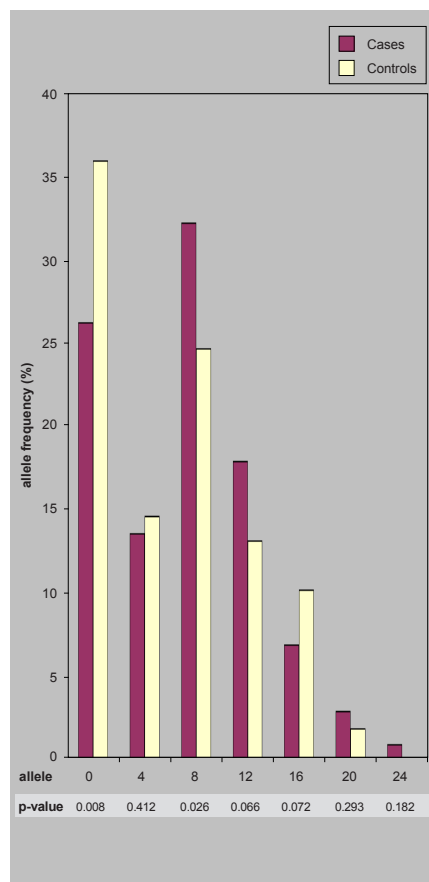
a) Allele Image Profile (AIP)



b) AIP analysis

	1	2	3	4	5	6	7
A1	5790	2843	5394	2376	828	298	0
A2	4750	2258	4405	1940	712	230	0
B1	2346	1013	1479	968	495	106	0
B2	1839	789	1149	766	387	84	0
Allele	0	4	8	12	16	20	24
	0.971	0.943	0.916	0.889	0.863	0.838	0.814
COR. PEAKS							
A1	5963	3015	5892	2673	959	356	0
A2	4892	2395	4812	2182	825	274	0
B1	2416	1074	1616	1089	574	127	0
B2	1894	837	1255	862	448	100	0
REL. PEAK HEIGHTS:							
A1	126.5	64.0	125.0	56.7	20.3	7.5	0
A2	127.2	62.3	125.1	56.8	21.5	7.1	0
B1	140.2	62.3	93.7	63.2	33.3	7.3	0
B2	140.4	62.0	93.0	63.9	33.2	7.4	0
CV A1/A2	0.00	0.02	0.00	0.00	0.04	0.04	
CV B1/B2	0.00	0.00	0.01	0.01	0.00	0.01	
Arith. mean A	126.9	63.1	125.1	56.7	20.9	7.3	
Arith. mean B	140.3	62.2	93.4	63.5	33.3	7.4	
(A+B)/2	133.6	62.7	109.2	60.1	27.1	7.4	
chi 1							
chi 1	273.1	336.9	274.9	343.3	379.1	392.7	
chi 2	266.4	337.3	290.8	339.9	372.9	392.6	
chi 1	0.337	0.004	2.297	0.192	1.409	0.0001	
chi 2	0.169	0.001	0.863	0.034	0.102	0	
Chi - value	1.01	0.01	6.32	0.45	3.02	0.00	
p-value	0.314	0.927	0.012	0.501	0.082	0.991	
Allele	0	4	8	12	16	20	24
LDA:	0.029						
Weight:	1		400				

c) Individual Genotyping

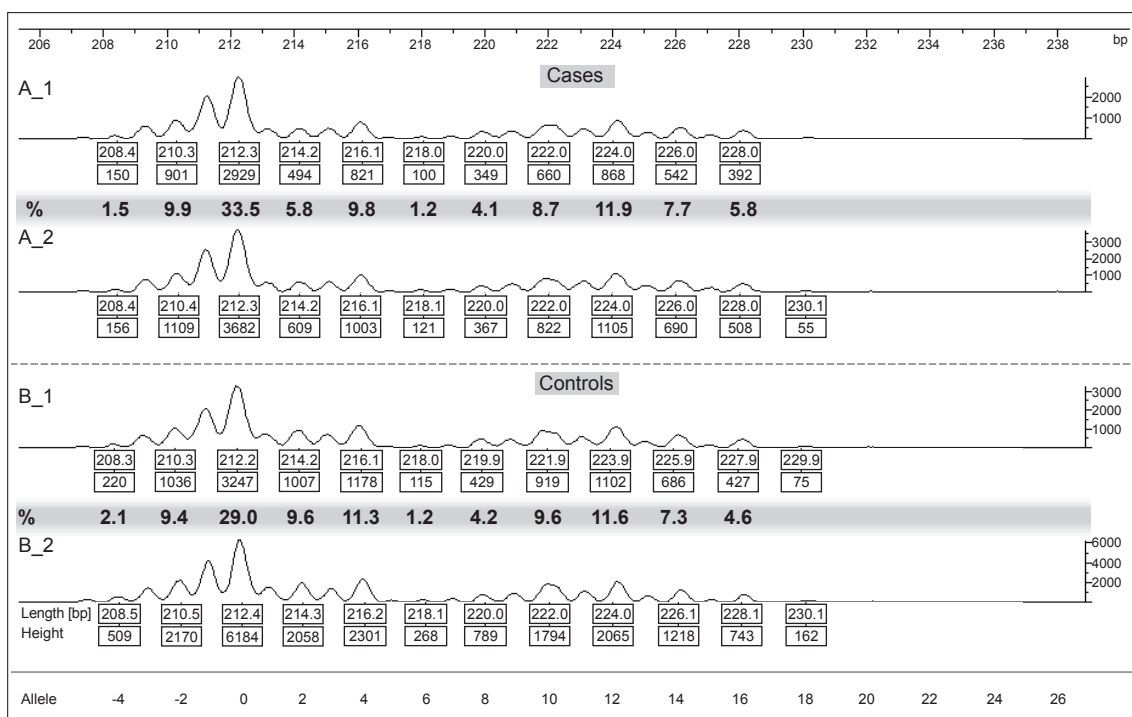


D12S1653 – ranking position 176**Figure A7**

The dinucleotide marker detected 12 alleles (-4 to 18) in the pooled DNA samples and 16 alleles (-4 to 26) in individual DNA tests (Fig. A7a+c). The initially moderate association of allele 2 (Pool A=5.8% vs. Pool B=9.6%, empirical $p=0.042$) remained and established a similar difference between cases (2.1%) and controls (5.0%) (one-sided $p=0.029$), though based on less allele counts. The ratio of each allele comparison between cases and controls was mainly in agreement with suggested combinations in the AIPs.

Figure A7 | d12s1653AIP

a) Allele Image Profile (AIP)



b) AIP analysis

PEAK ORDER	1	2	3	4	5	6	7	8	9	10	11	12	13
A1	150	901	2929	494	821	100	349	660	868	542	392	0	0
A2	156	1109	3682	609	1003	121	367	822	1105	690	508	0	0
B1	220	1036	3247	1007	1178	115	429	919	1102	686	427	0	0
B2	509	2170	6184	2058	2301	268	789	1794	2065	1218	743	0	0
Allele	-4	-2	0	2	4	6	8	10	12	14	16	18	20
	0.971	0.943	0.916	0.889	0.863	0.838	0.814	0.790	0.767	0.745	0.723	0.702	0.682

COR. PEAKS

A1	154	956	3199	556	951	119	429	835	1131	727	542	0	0
A2	161	1176	4022	685	1162	144	451	1040	1440	926	702	0	0
B1	227	1099	3547	1133	1365	137	527	1163	1436	921	590	0	0
B2	524	2302	6755	2315	2666	320	969	2270	2691	1635	1027	0	0

REL. PEAK HEIGHTS:

A1	6.4	39.8	133.3	23.2	39.6	5.0	17.9	34.8	47.1	30.3	22.6	0	0
A2	5.4	39.5	135.1	23.0	39.0	4.8	15.1	34.9	48.4	31.1	23.6	0	0
B1	7.5	36.5	117.7	37.4	45.3	4.6	17.5	38.6	47.7	30.6	19.6	0	0
B2	9.0	39.5	116.0	39.4	45.8	5.5	16.7	39.0	46.2	28.1	17.6	0	0
CV A1/A2	0.12	0.01	0.01	0.01	0.01	0.02	0.12	0.00	0.02	0.02	0.03		
CV B1/B2	0.13	0.06	0.01	0.04	0.01	0.13	0.03	0.01	0.02	0.06	0.07		
Arith. mean A	5.9	39.7	134.2	23.1	39.3	4.9	16.5	34.9	47.8	30.7	23.1		
Arith. mean B	8.2	37.7	116.0	38.4	45.2	5.0	16.9	38.5	46.6	29.1	18.5		

(A+B)/2

394.1	360.3	265.8	376.9	360.7	395.1	383.5	365.1	352.3	369.3	376.9		
392.9	361.3	274.9	369.3	357.7	395.1	383.3	363.3	352.8	370.1	379.2		
0.186	0.025	0.664	1.904	0.203	0.000	0.003	0.090	0.007	0.022	0.255		

chi 1

chi 2

Chi - value

p-value

Allele

LDA:

Weight:

c) Individual Genotyping

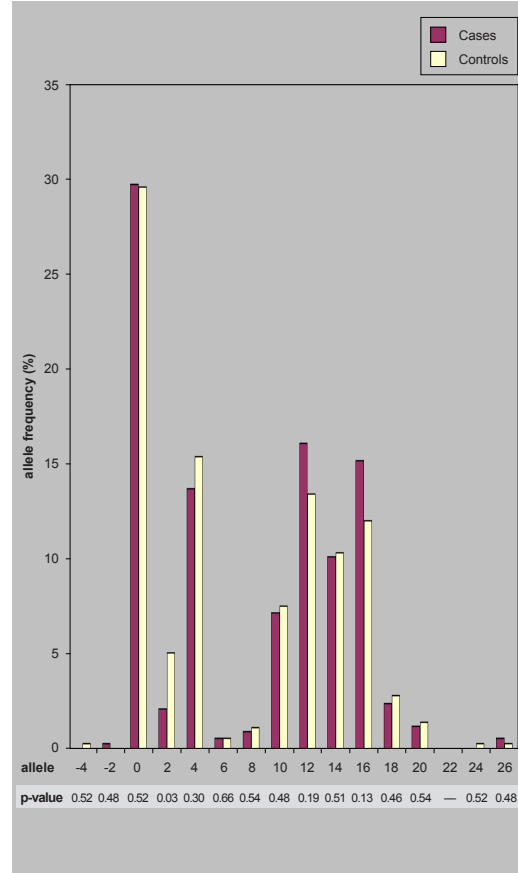


Table A lists the alleles that were considered significant after testing for association, either expressed by the empirical p-value estimated for genotyped DNA pools or by the one-sided Chi² test applied for individual allele counts. Establishing 0.05 as the significance threshold, five from seven markers corresponding to 71.4% confirmed the estimated evidence of association derived from testing genotyped DNA pools.

Allele -8 of tetranucleotide marker D9S303 displayed the strongest association with MS patients, although the “extra” allele -6 complicates its interpretation. Microsatellite D13S777 rendered prominent, containing two significantly associated alleles with opposing ratios and possibly delivering genetic contributions to disease susceptibility and protection in either DNA sequence. The same applied to D4S3245. Markers D22S692 and D12S1653 sustained their associations with MS patients and controls, respectively, while the supposedly most promising candidate markers D18S52 and D16S2613 failed to be replicated at together seven alleles.

The distorting effect of PCR generated length dependent amplification was observable in illustrated allele frequency comparisons of mainly four markers (Fig. A2c, A3c, A6c, A7c). Despite applied correction factors, shorter PCR fragments were over- and longer pieces underestimated in corresponding AIPs.

Table A | Allele-by-allele comparison of degree of evidence for MS association derived from DNA pooling (200 cases vs. controls) and single DNA (186 cases vs. 186 controls) experiments.

Chr.	Marker	Marker Type	Allele	Rank	Ratio	empirical p-value (pool)	Ratio	one-sided p-value (ind.)
9	D9S303	tetra	-8	2	MS > HC	4.5E-6	MS > HC	0.00001
			-6		MS < HC	0.001	MS < HC	0.114
18	D18S52	di	4	3	MS < HC	0.00002	MS = HC	0.443
			2		MS < HC	0.00005	MS < HC	0.121
16	D16S2613	tri	0		MS > HC	0.00006	MS > HC	0.339
			6		MS > HC	0.004	MS = HC	0.559
			8		MS > HC	0.006	MS = HC	0.480
			0	4	MS < HC	0.00002	MS < HC	0.299
			15		MS > HC	0.025	MS > HC	0.353
13	D13S777	tri	15	13	MS < HC	0.0005	MS < HC	0.019
			0		MS > HC	0.056	MS > HC	0.018
22	D22S692	tetra	4	17	MS < HC	0.001	MS < HC	0.083
			0		MS > HC	0.015	MS > HC	0.017
4	D4S3245	tetra	8	81	MS > HC	0.012	MS > HC	0.026
			0		MS < HC	0.314	MS < HC	0.008
12	D12S1653	di	2	176	MS < HC	0.042	MS < HC	0.029

Discussion

The detection of genuinely associated markers with non-MHC loci relating to MS susceptibility would provide further insights into the etiology of the disease.

For this purpose, 7 microsatellites that displayed eventual association with MS in DNA pools were selected and tested for confirmation by individual genotyping.

Of particular importance, an empirical p-value assigned to a peak of a marker in pooled DNA analysis can not be compared straightforward with a formally computed p-value derived from a comparison of real allele counts of individually tested DNA samples. However, taking into account orientational aspects of a possible predisposing allele's performance, a one-sided p-value <0.05 detected in individual genotyping was considered to verify preceding evidence of association.

Of the 7 microsatellites that displayed potential association with MS, 5 markers (D4S3245, D9S303, D12S1653, D13S777, D22S692) sustained statistical significance in individual genotyping. In addition, association with identical alleles and maintained allele distribution ratios strengthened these findings (Tab. A). Two regions of interest (D16S2613, D18S52), including D16S2613 that had been linked with MS independently in the past, could not be reproduced in presented data set. The dinucleotide marker D18S52 performed remarkably well in the majority of the GAMES population screens, but consistently failed to meet expectations after individual genotyping was performed with corresponding DNA samples (*oral communication*, DAS Compston), rendering it a problematic genetic marker.

Based on presented data it can be stated that the allele profiles provided by DNA pools captured the majority of real alleles, missing only minor ones such as D13S777 "3" with a 1.9% allelic frequency. A type I error rate of 28.6% of realized pooling technology was suggested, though the limited number of experiments should encourage scrutinizing this value by means of a 10 to 20 fold increase of genotyping tests (more markers with larger samples size). Of note, p-values describing strong associations of single alleles dropped more than expected in comparison to moderate ones, describing a relatively stable range between $0.05 > p > 0.01$.

Correction factors introduced by Yeo *et al.* aimed to average out artefactual effects that result from errors in pool construction; PCR and electrophoresis seemed little effective in some situations (4 markers) when allele frequency variance between AIPs and individual allele counts were high, yet in remaining comparisons the AIPs fitted considerably well

with genuine allele numbers. Some markers do not even need this factor.

It appears extremely difficult to derive basic rules of how to interpret results from genotyped microsatellites and DNA pools consisting of as much individuals as the present 200 per group. The different kinetics of distinct marker types (di-, tri-, and tetranucleotide) and inter-individual variations produce a multitude of inherent factors for variance which are difficult to control or correct for. For non-confirmatory markers it is legitimate to state: in spite of the obvious discordant distribution of allele percentages between AIP and single DNA genotyping results, the shorter allele repeats were generally over-represented whereas the longer fragments showed lower counts. The employed approach suggests for future studies of creating several pools of the same population comprising less individuals; this would not inflate typing costs in relation to the reduced degree of variance.

Appendix B – STR genotyping data from DNA pools

Presented data display marker name, empirical p-values derived from initial genome scan on pooled DNA ($p<0.05$ printed in bold) and corresponding locations on genetic and physical map (SA6 genome assembly; deCODE genetics, Reykjavik, Iceland).

Marker name	pvalue	Chr	cM	Mb	Marker name	pvalue	Chr	cM	Mb
Chromosome 1									
D1S243	0.338	C01	1.679	2.008.687	D1S247	0.088	C01	50.560	30.378.051
D1S468	0.380	C01	4.160	3.367.940	D1S2781	0.089	C01	50.908	30.456.153
D1S2845	0.177	C01	6.653	4.128.599	D1S513	0.024	C01	52.591	30.834.201
D1S2893	0.061	C01	6.654	4.261.844	D1S233	0.249	C01	52.948	30.986.445
D1S2660	0.252	C01	7.319	4.474.821	D1S2765	0.551	C01	53.020	31.569.943
D1S1608	0.057	C01	7.910	4.673.923	D1S2832	0.307	C01	53.347	31.804.049
D1S2795	0.272	C01	9.294	5.270.659	D1S2676	0.128	C01	54.185	32.988.097
D1S2145	0.288	C01	9.677	5.450.018	D1S2677	0.394	C01	54.186	32.988.098
D1S2633	0.392	C01	10.396	5.786.925	D1S164	0.618	C01	54.463	33.381.959
D1S2870	0.898	C01	11.675	5.999.149	D1S201	0.123	C01	54.565	33.525.567
D1S253	0.399	C01	11.783	6.068.980	D1S2830	0.072	C01	55.022	33.675.691
D1S2731	0.617	C01	12.311	6.410.876	D1S2783	0.157	C01	55.577	33.857.790
D1S2642	0.254	C01	12.312	6.559.934	D1S2614	0.025	C01	56.792	34.163.642
D1S214	0.264	C01	12.366	6.671.624	D1S2613	0.527	C01	56.793	34.163.642
D1S1646	0.426	C01	12.452	6.851.954	D1S195	0.270	C01	57.137	34.621.868
D1S2663	0.113	C01	13.158	6.967.140	D1S496	0.149	C01	57.345	34.835.135
D1S2694	0.651	C01	13.228	7.051.311	D1S441	0.117	C01	57.421	35.105.097
D1S548	0.329	C01	13.400	7.152.385	D1S2657	0.237	C01	57.583	35.622.014
D1S2666	0.192	C01	13.401	7.164.334	D1S2656	0.386	C01	57.584	35.622.014
D1S508	0.321	C01	13.895	7.316.929	D1S2729	0.557	C01	59.252	36.498.567
D1S1612	0.082	C01	14.153	7.827.384	D1S472	0.524	C01	59.255	36.861.396
D1S1615	0.055	C01	14.758	8.278.858	ATA4E01	0.244	C01	59.374	36.901.981
D1S160	0.674	C01	15.416	8.770.320	D1S2637	0.377	C01	59.375	36.934.722
D1S503	0.526	C01	15.882	9.118.369	D1S2723	0.197	C01	59.376	36.935.014
D1S2736	0.083	C01	17.176	10.325.170	D1S255	0.325	C01	59.975	37.077.375
D1S2667	0.342	C01	20.363	11.196.506	D1S380	0.204	C01	61.886	37.907.740
D1S2740	0.307	C01	21.566	11.630.546	GGAA24E02	0.206	C01	62.765	38.365.435
D1S489	0.393	C01	21.801	11.757.597	D1S1157	0.137	C01	63.232	38.608.486
D1S434	0.422	C01	21.802	12.041.739	D1S432	0.087	C01	63.581	38.790.364
D1S1193	0.080	C01	22.196	12.258.616	D1S1591	0.245	C01	63.906	38.959.312
D1S2718	0.206	C01	22.290	12.310.247	D1S2892	0.053	C01	64.741	39.604.213
D1S1597	0.078	C01	23.810	13.146.884	D1S168	0.615	C01	64.757	39.402.827
D1S228	0.366	C01	24.571	13.349.107	D1S2131	0.250	C01	66.022	40.061.471
D1S407	0.253	C01	26.407	14.216.826	D1S2743	0.719	C01	66.151	40.128.163
D1S507	0.196	C01	26.828	14.391.467	D1S2632	0.426	C01	66.584	40.353.907
D1S2728	0.251	C01	27.396	14.522.928	D1S2706	0.023	C01	66.837	40.485.561
D1S2672	0.248	C01	27.817	14.641.352	D1S2722	0.097	C01	67.304	40.966.764
D1S436	0.267	C01	28.916	15.233.212	D1S2130	0.081	C01	67.406	41.230.805
D1S170	0.290	C01	31.599	16.678.622	D1S2645	0.639	C01	67.770	41.669.872
D1S1592	0.221	C01	33.028	17.448.618	D1S463	0.382	C01	67.982	41.926.026
D1S2644	0.121	C01	36.516	18.459.547	D1S1586	0.155	C01	67.983	42.190.584
D1S483	0.124	C01	37.894	18.701.543	D1S193	0.549	C01	68.179	42.432.569
D1S552	0.124	C01	38.275	18.736.441	D1S2861	0.492	C01	68.180	42.520.145
D1S2647	0.109	C01	38.456	19.297.590	D1S443	0.601	C01	68.607	43.001.762
D1S199	0.123	C01	38.457	19.426.493	D1S2733	0.040	C01	69.413	43.910.010
D1S2843	0.168	C01	39.747	19.980.037	D1S2713	0.068	C01	69.428	43.926.770
D1S2732	0.611	C01	40.040	20.105.781	D1S421	0.424	C01	70.482	44.669.937
ATA47D07	0.145	C01	40.318	20.381.403	D1S2802	0.165	C01	70.483	45.009.250
D1S478	0.015	C01	41.010	21.069.202	D1S451	0.348	C01	70.484	45.170.619
D1S2828	0.259	C01	41.653	21.411.895	D1S2797	0.158	C01	70.485	46.303.509
GGAA30B06	0.125	C01	41.674	21.449.412	D1S2720	0.039	C01	72.222	47.277.704
D1S2725	0.371	C01	41.760	21.599.295	D1S2879	0.075	C01	72.234	47.284.222
D1S2864	0.125	C01	42.192	22.342.503	D1S2824	0.263	C01	73.234	48.132.582
D1S2698	0.153	C01	43.821	22.738.306	D1S2724	0.540	C01	73.364	48.605.063
D1S458	0.523	C01	43.822	22.906.470	D1S2748	0.135	C01	73.674	49.731.907
D1S2734	0.410	C01	43.934	23.309.395	D1S197	0.110	C01	73.675	50.120.415
D1S482	0.163	C01	43.935	23.322.748	D1S162	0.061	C01	73.783	50.266.420
D1S2838	0.545	C01	43.936	23.330.613	D1S427	0.492	C01	74.041	50.615.474
D1S2620	0.541	C01	43.937	23.332.986	D1S1661	0.050	C01	74.042	50.800.627
D1S2674	0.121	C01	45.150	24.201.109	D1S232	0.417	C01	74.043	51.088.089
D1S234	0.278	C01	45.571	24.502.568	D1S231	0.680	C01	74.180	51.573.117
D1S2885	0.346	C01	45.968	25.743.578	D1S161	0.176	C01	74.181	51.824.623
GGAA2D04	0.103	C01	46.780	26.584.330	D1S509	0.436	C01	75.479	53.178.063
D1S455	0.466	C01	47.404	26.894.054	D1S2662	0.147	C01	76.663	53.704.531
D1S2749	0.300	C01	47.417	26.900.416	D1S2661	0.711	C01	76.664	53.704.531
D1S2787	0.228	C01	47.848	27.731.522	D1S417	0.300	C01	78.869	54.683.711
D1S2884	0.230	C01	48.886	28.898.934	D1S2652	0.142	C01	78.870	54.836.748
D1S2854	0.094	C01	48.899	28.965.267	D1S475	0.134	C01	79.173	55.254.362
D1S470	0.258	C01	49.492	29.661.139	D1S200	0.344	C01	79.264	55.380.038
D1S493	0.648	C01	49.989	29.935.136	D1S2742	0.107	C01	79.759	56.063.346
D1S449	0.260	C01	50.436	30.222.228	D1S2690	0.437	C01	81.381	56.525.457
D1S450	0.487	C01	50.437	30.222.229	D1S519	0.062	C01	81.823	56.776.947
					D1S2665	0.191	C01	82.660	57.063.051
					D1S2890	0.121	C01	82.661	57.243.317

Marker name	pvalue	Chr	cM	Mb
D1S1150	1.6E-11	C01	83.059	57.530.792
D1S476	0.282	C01	83.244	57.608.832
D1S2650	0.636	C01	83.950	57.906.831
D1S2869	0.187	C01	84.152	58.130.396
D1S2648	0.363	C01	84.339	58.269.086
D1S2752	0.089	C01	84.834	58.484.052
D1S2700	0.145	C01	84.841	58.486.962
D1S2831	0.696	C01	85.678	58.948.862
D1S2741	0.321	C01	86.097	59.095.738
D1S1596	0.210	C01	86.137	59.100.150
D1S2801	0.384	C01	86.333	59.271.292
D1S2770	0.407	C01	86.810	59.328.484
D1S2873	0.051	C01	86.841	59.823.723
D1S1643	0.030	C01	87.173	60.473.164
D1S203	0.321	C01	87.264	60.651.809
D1S2737	0.024	C01	87.265	60.695.932
D1S2822	0.054	C01	87.588	60.902.605
D1S2846	0.274	C01	87.952	60.969.599
D1S2788	0.220	C01	89.078	61.226.752
D1S473	0.410	C01	89.079	61.276.740
D1S209	0.473	C01	89.336	61.342.115
D1S230	0.334	C01	89.955	61.972.201
D1S2835	0.212	C01	90.552	62.697.075
D1S2836	0.343	C01	90.553	62.697.075
D1S2638	0.406	C01	91.140	62.922.886
D1S438	0.627	C01	91.461	63.186.575
D1S1613	0.041	C01	91.987	63.604.144
D1S3467	0.069	C01	92.203	63.775.826
D1S2617	0.237	C01	92.287	63.842.903
D1S2684	0.056	C01	92.530	63.943.612
D1S2710	0.650	C01	93.080	64.033.399
ATA52G05	0.001	C01	93.330	64.511.499
D1S2754	0.575	C01	93.468	64.599.474
D1S2825	0.367	C01	93.499	64.696.182
D1S2886	0.846	C01	93.556	64.877.905
D1S2866	0.480	C01	93.660	65.207.713
D1S520	0.039	C01	94.391	65.892.027
D1S198	0.370	C01	94.913	66.381.078
D1S2806	0.443	C01	96.431	67.238.068
D1S2829	0.204	C01	96.912	67.622.420
D1S3473	0.115	C01	97.349	67.852.576
D1S2803	0.085	C01	98.175	68.288.099
D1S448	0.247	C01	98.472	68.541.216
D1S1631	0.022	C01	98.790	68.812.638
D1S1630	0.700	C01	98.791	68.812.638
D1S219	0.380	C01	98.974	69.210.916
D1S411	0.293	C01	99.165	69.424.608
D1S1603	0.282	C01	99.209	69.478.328
D1S1590	0.239	C01	99.301	69.588.862
D1S159	0.715	C01	99.302	69.588.862
D1S2798	0.583	C01	99.669	70.034.740
D1S462	0.234	C01	99.670	70.040.224
D1S501	0.250	C01	99.671	70.274.413
D1S192	0.959	C01	100.455	70.856.104
D1S2895	0.318	C01	100.646	70.997.879
D1S224	0.321	C01	101.254	71.510.102
D1S1648	0.432	C01	101.590	72.783.457
D1S1665	0.116	C01	101.591	73.599.296
D1S2761	0.143	C01	102.088	74.486.388
D1S464	0.117	C01	102.428	75.154.538
D1S481	0.240	C01	102.520	75.302.373
D1S2855	0.093	C01	102.823	75.503.592
D1S532	0.019	C01	104.951	76.915.030
D1S216	0.121	C01	105.038	77.077.916
D1S499	0.208	C01	105.110	77.212.378
D1S1611	0.065	C01	105.269	77.508.665
D1S2876	0.192	C01	105.464	78.406.687
D1S2841	0.136	C01	105.857	78.909.887
D1S2618	0.806	C01	106.337	79.097.082
D1S500	0.218	C01	106.401	79.392.104
D1S1607	0.399	C01	107.126	80.491.806
D1S465	0.585	C01	107.195	80.597.064
D1S430	0.353	C01	107.366	80.700.134
D1S1672	0.110	C01	108.927	81.421.139
D1S2862	0.083	C01	109.073	81.635.858
D1S2856	0.361	C01	109.232	81.780.146
D1S207	0.200	C01	109.233	81.966.032
D1S454	0.268	C01	109.234	82.190.693
D1S551	0.232	C01	109.373	82.317.889
D1S2807	0.124	C01	109.725	82.690.619
D1S488	0.101	C01	110.001	82.708.254
D1S2774	0.333	C01	110.002	82.882.673
D1S2889	0.433	C01	110.429	84.258.387
D1S3471	0.150	C01	112.105	85.391.755
D1S2766	0.288	C01	112.106	85.494.878
D1S167	0.196	C01	114.779	88.207.747

Marker name	pvalue	Chr	cM	Mb
D1S2627	0.028	C01	115.044	88.377.404
D1S213	0.506	C01	116.235	89.578.232
D1S435	0.132	C01	117.670	91.025.498
D1S1588	0.189	C01	118.393	91.686.052
D1S188	7.9E-10	C01	118.467	91.967.766
D1S424	0.158	C01	118.567	92.351.964
D1S2804	0.321	C01	118.568	92.353.470
D1S2776	0.232	C01	118.569	92.681.840
D1S2849	0.281	C01	119.036	92.991.613
D1S236	0.173	C01	120.095	94.282.229
D1S2775	0.483	C01	120.452	94.717.057
D1S2813	0.122	C01	120.467	94.735.320
D1S2819	0.205	C01	120.682	94.997.378
D1S2664	0.555	C01	121.065	95.417.683
D1S2719	0.317	C01	121.449	96.289.881
D1S2793	0.362	C01	121.609	96.565.490
D1S415	0.676	C01	122.251	97.941.020
D1S420	0.471	C01	122.274	97.960.028
D1S2753	0.263	C01	122.299	97.981.534
D1S1587	0.322	C01	122.318	97.992.490
D1S2739	0.395	C01	122.867	98.294.528
D1S2808	0.166	C01	123.048	98.720.167
D1S1629	0.562	C01	123.234	99.129.912
D1S540	0.375	C01	123.257	99.179.750
D1S2767	0.203	C01	123.998	99.430.647
D8S536	0.237	C01	124.548	100.181.621
D1S2671	0.514	C01	124.949	100.729.331
D1S223	0.163	C01	124.950	101.060.328
D1S206	0.281	C01	124.951	101.148.260
D1S2896	0.087	C01	125.078	101.435.556
D1S486	0.702	C01	125.300	101.610.716
D1S495	0.070	C01	126.349	102.024.259
D1S2626	0.233	C01	126.418	102.458.556
D1S1657	0.009	C01	126.621	103.731.039
D1S535	0.038	C01	126.622	103.731.134
D1S2699	0.784	C01	126.926	104.134.973
D1S2888	0.217	C01	127.495	104.444.354
D1S429	0.032	C01	128.403	105.047.542
D1S2759	0.422	C01	128.479	105.199.466
D1S239	0.125	C01	129.083	106.194.079
D1S2688	0.278	C01	129.084	106.293.687
D1S1627	0.380	C01	129.085	106.318.339
D1S1623	0.504	C01	129.086	106.430.371
D1S248	0.489	C01	129.087	106.509.593
D1S2778	0.508	C01	130.954	108.394.456
D1S2695	0.202	C01	133.385	109.994.765
D1S457	0.134	C01	133.386	110.177.476
D1S2708	0.747	C01	134.081	110.360.971
D1S2726	0.167	C01	134.610	110.482.992
D1S2809	0.201	C01	134.611	110.713.066
D1S2789	0.138	C01	134.833	111.298.612
D1S2837	0.529	C01	135.556	111.573.824
D1S418	0.727	C01	136.510	112.267.264
D1S2746	0.285	C01	136.511	112.324.312
D1S487	0.343	C01	136.629	112.458.993
D1S2756	0.485	C01	136.714	112.554.253
D1S1691	0.385	C01	137.783	113.761.156
D1S2881	0.062	C01	138.008	114.014.057
D1S1675	0.139	C01	138.030	114.038.880
D1S250	0.298	C01	139.119	114.509.783
D1S2852	0.003	C01	139.120	114.652.758
D1S467	0.571	C01	139.121	115.295.998
D1S2687	0.398	C01	139.942	115.548.332
D1S189	0.320	C01	140.460	116.040.225
D1S2744	0.070	C01	141.520	116.618.254
D1S252	0.514	C01	141.757	116.903.151
D1S2820	0.327	C01	142.208	117.188.064
D1S2784	0.063	C01	142.209	117.188.421
D1S453	0.061	C01	142.505	117.511.124
D1S2669	0.114	C01	142.506	117.849.071
D1S2875	0.547	C01	142.507	118.110.413
D1S2863	0.191	C01	142.777	118.423.754
D1S534	0.062	C01	143.297	119.024.645
D1S514	0.528	C01	143.635	119.615.134
D1S1156	0.201	C01	144.650	143.691.841
D1S442	0.682	C01	144.724	143.379.192
D1S2344	0.226	C01	144.725	143.280.633
D1S2612	0.127	C01	144.726	145.483.612
D1S2222	0.208	C01	147.242	147.103.989
D1S498	0.391	C01	147.704	148.518.146
D1S2347	0.210	C01	147.721	148.538.362
D1S2345	0.355	C01	147.896	148.749.848
D1S2343	0.269	C01	147.897	148.750.456
D1S2346	0.202	C01	149.255	150.386.114
D1S2858	0.302	C01	149.982	151.261.178
D1S305	0.227	C01	150.132	151.498.712

Marker name	pvalue	Chr	cM	Mb	Marker name	pvalue	Chr	cM	Mb
D1S2715	0.282	C01	151.056	152.332.310	D1S492	0.746	C01	192.607	186.848.435
D1S2714	0.612	C01	151.057	152.332.310	D1S2823	0.212	C01	193.073	187.783.789
D1S2777	0.341	C01	151.438	152.677.151	D1S422	0.181	C01	193.873	188.667.065
D1S303	0.050	C01	151.625	152.854.463	D1S3468	0.104	C01	193.874	188.829.096
D1S2140	0.067	C01	151.678	152.905.182	D1S2625	0.222	C01	193.875	189.556.883
D1S2624	0.338	C01	153.288	153.848.083	D1S533	0.002	C01	196.564	191.346.191
D1S1179	0.352	C01	153.466	154.041.652	D1S412	0.138	C01	196.565	191.354.201
D1S2125	0.625	C01	153.705	154.526.664	D1S1614	0.119	C01	196.590	191.400.549
D1S394	0.007	C01	153.922	154.536.203	D1S2757	0.213	C01	196.940	192.025.985
D1S1600	0.274	C01	154.353	155.003.318	D1S2794	0.006	C01	197.250	192.544.832
D1S176	0.253	C01	154.366	155.013.820	D1S2816	0.222	C01	197.442	193.938.791
D1S178	0.152	C01	154.367	155.013.820	D1S3469	0.261	C01	198.368	195.318.048
D1S1653	0.607	C01	154.538	155.149.566	D1S2840	0.529	C01	198.521	195.546.370
D1S2635	0.308	C01	157.177	156.387.025	D1S1660	0.143	C01	198.522	195.899.604
D1S1655	0.021	C01	157.404	156.855.681	D1S413	0.129	C01	198.523	195.908.655
D1S398	0.001	C01	157.405	156.855.701	D1S1726	0.049	C01	198.954	196.563.713
D1S2707	0.170	C01	159.033	157.289.243	D1S2817	0.425	C01	199.480	197.365.369
D1S2771	0.125	C01	159.407	157.812.209	D1S2716	0.043	C01	200.685	198.409.415
D1S484	0.144	C01	160.450	157.984.102	D1S2738	0.241	C01	200.715	198.435.121
D1S2675	0.706	C01	162.025	159.397.370	D1S477	0.186	C01	201.680	198.542.450
D1S1679	0.092	C01	162.361	159.549.140	D1S1723	0.068	C01	202.255	198.679.075
D1S2768	0.484	C01	162.695	159.699.938	D1S306	0.076	C01	202.314	198.693.209
D1S2844	0.197	C01	163.409	160.136.150	D1S321	0.099	C01	202.315	198.693.209
D1S104	0.362	C01	164.923	160.824.212	D1S2764	0.301	C01	202.316	198.874.563
D1S2628	0.067	C01	168.681	162.336.016	D1S2615	0.545	C01	203.669	199.206.213
D1S426	0.315	C01	168.807	162.494.418	D1S1606	0.032	C01	203.842	199.288.063
D1S194	0.268	C01	169.042	162.624.618	D1S1727	0.140	C01	204.233	199.472.335
D1S1625	0.154	C01	169.372	163.036.069	D1S1647	0.141	C01	205.024	199.846.053
ATA38A05	0.079	C01	169.373	163.036.121	D1S2655	0.566	C01	205.040	199.853.527
D1S2681	0.142	C01	169.536	163.240.722	D1S1724	0.094	C01	205.041	199.875.444
D1S2673	0.171	C01	170.245	163.768.330	D1S2686	0.074	C01	205.121	199.924.799
D1S2762	0.362	C01	170.443	164.143.514	D1S2683	0.388	C01	206.634	200.359.959
D1S2630	0.695	C01	171.031	164.403.461	D1S2760	0.027	C01	207.388	200.576.898
D1S196	0.064	C01	172.571	164.791.504	D1S510	0.010	C01	208.069	200.772.740
D1S2750	0.085	C01	172.728	164.917.325	D1S511	0.150	C01	208.070	200.772.740
D1S431	0.060	C01	172.857	165.007.251	D1S1725	0.197	C01	208.112	201.146.545
D1S445	0.274	C01	172.858	165.141.777	D1S2717	0.230	C01	208.146	201.238.025
D1S2799	0.091	C01	172.859	165.280.057	D1S2668	0.061	C01	208.176	201.258.913
D1S2658	0.494	C01	173.074	165.441.855	D1S1620	0.029	C01	208.870	201.741.685
D1S433	0.545	C01	173.225	165.555.554	D1S504	0.269	C01	208.987	201.822.683
D1S3464	0.408	C01	174.256	166.236.009	D1S2872	0.242	C01	209.299	200.002.858
D1S2851	0.160	C01	176.134	167.504.232	D1S2773	0.102	C01	213.175	204.175.577
D1S452	0.035	C01	176.386	167.710.987	D1S2727	0.252	C01	213.435	204.320.874
D1S210	0.334	C01	177.328	168.048.127	D1S3465	0.131	C01	213.482	204.443.083
D1S2815	0.132	C01	178.050	168.954.294	D1S2796	0.406	C01	213.635	204.843.120
D1S2790	0.258	C01	178.241	170.263.484	D1S2782	0.237	C01	213.636	204.880.421
D1S2814	0.274	C01	179.517	171.211.800	D1S2685	0.477	C01	213.637	205.073.540
D1S1589	0.328	C01	179.518	171.500.478	D1S2692	0.282	C01	213.711	205.122.575
D1S242	0.210	C01	179.519	171.611.630	D1S2891	0.251	C01	214.355	205.536.126
D1S218	0.173	C01	179.561	171.742.468	D1S245	0.264	C01	216.774	206.685.807
D1S2691	0.123	C01	179.644	172.238.041	D1S471	0.420	C01	216.775	206.796.631
D1S416	0.363	C01	180.170	172.433.495	D1S491	0.406	C01	216.994	206.822.392
D1S2643	0.374	C01	180.501	172.762.235	D1S205	0.307	C01	217.215	207.190.218
D1S2887	0.220	C01	181.340	173.580.068	D1S2812	0.163	C01	218.316	208.007.502
D1S2769	0.056	C01	181.544	173.868.671	D1S414	0.456	C01	218.317	208.122.125
D1S2659	0.127	C01	181.747	173.911.214	D1S2810	0.385	C01	218.542	208.484.126
D1S2786	0.199	C01	181.748	174.527.558	D1S2780	0.154	C01	218.942	209.123.829
D1S480	0.110	C01	181.957	174.586.423	D1S425	0.381	C01	218.952	209.139.688
D1S2791	0.289	C01	182.551	175.090.982	D1S505	0.513	C01	219.758	209.674.267
D1S212	0.369	C01	182.666	175.321.944	D1S1667	0.152	C01	219.759	209.827.132
D1S215	0.511	C01	183.438	176.867.915	D1S217	0.271	C01	219.890	210.104.732
D1S2751	0.351	C01	183.657	177.250.540	D1S2703	0.355	C01	219.954	210.145.963
D1S2883	0.538	C01	183.802	177.344.501	D1S2705	0.096	C01	219.955	210.145.963
D1S2640	0.133	C01	183.803	177.966.555	D1S2646	0.224	C01	221.880	211.114.719
D1S2619	0.149	C01	186.733	179.515.441	D1S419	0.065	C01	222.178	211.594.563
D1S466	0.196	C01	186.912	179.542.980	D1S237	0.200	C01	222.179	211.785.805
D1S2818	0.393	C01	187.029	179.578.341	D1S2857	0.309	C01	223.173	211.809.392
D1S2623	0.433	C01	187.587	180.112.875	D1S2141	0.107	C01	223.174	212.251.798
D1S158	0.475	C01	188.954	181.380.402	D1S2144	0.588	C01	223.175	212.251.798
D1S2701	0.236	C01	189.473	181.862.005	D1S2629	0.144	C01	223.238	212.502.169
D1S2127	0.218	C01	189.730	181.977.841	D1S474	0.189	C01	223.297	212.733.657
D1S2711	0.118	C01	189.920	182.757.162	D1S2827	0.301	C01	223.634	213.195.551
D1S444	0.198	C01	190.187	182.995.628	D1S227	0.110	C01	227.006	214.350.936
D1S254	0.483	C01	190.194	183.018.968	D1S2621	0.492	C01	228.158	215.404.744
D1S191	0.685	C01	190.195	183.060.979	D1S1605	0.109	C01	228.244	215.486.237
D1S2848	0.484	C01	190.196	183.074.002	D1S2616	0.537	C01	229.062	216.257.091
D1S2138	0.031	C01	190.499	183.604.818	D1S2758	0.065	C01	229.277	217.012.984
D1S202	0.183	C01	190.984	184.204.352	D1S2880	0.278	C01	229.760	217.593.531
D1S1642	0.489	C01	191.062	184.470.206	D1S2641	0.366	C01	230.379	218.190.674
D1S518	0.120	C01	191.465	184.789.171	D1S1626	0.157	C01	230.449	218.345.163
D1S1604	0.231	C01	191.466	184.874.119	D1S2689	0.110	C01	230.681	218.687.303
D1S238	0.178	C01	191.997	185.385.169					
D1S3470	0.035	C01	192.603	186.281.820					
D1S2877	0.213	C01	192.604	186.632.839					
D1S461	0.430	C01	192.605	186.706.680					
D1S428	0.540	C01	192.606	186.753.498					

Marker name	pvalue	Chr	cM	Mb
D1S2894	0.527	C01	230.682	218.855.311
D1S469	0.167	C01	231.586	219.997.942
D1S2763	0.208	C01	232.663	221.436.304
D1S439	0.114	C01	233.679	222.752.222
D1S479	0.031	C01	233.918	223.184.310
D1S1644	0.035	C01	234.086	223.487.202
D1S1601	0.451	C01	235.790	225.203.252
D1S1617	0.114	C01	237.242	226.665.352
D1S2847	0.243	C01	237.402	226.826.569
D1S2631	0.300	C01	237.403	227.231.711
D1S1671	0.209	C01	238.219	227.721.995
D1S2805	0.384	C01	238.229	227.728.090
D1S2833	0.313	C01	238.230	227.783.016
D1S103	0.371	C01	238.440	227.871.740
D1S1656	0.176	C01	238.955	227.940.310
D1S225	0.124	C01	238.956	228.195.222
D1S251	0.517	C01	239.498	228.749.269
D1S3462	0.588	C01	239.639	228.985.521
D1S2709	0.611	C01	239.640	229.065.354
D1S437	0.049	C01	241.594	229.510.822
D1S459	0.432	C01	241.595	229.578.925
D1S2800	0.230	C01	245.265	231.542.623
D1S446	0.281	C01	245.667	231.764.745
D1S447	0.155	C01	245.668	231.764.745
D1S2712	0.217	C01	246.266	231.980.761
D1S2649	0.151	C01	248.747	232.419.897
D1S2680	0.418	C01	251.416	233.670.796
D1S2850	0.053	C01	251.419	233.671.771
D1S2678	0.305	C01	251.420	233.682.773
D1S2670	0.293	C01	258.609	236.590.326
D1S1594	0.235	C01	261.768	237.821.137
D1S2785	0.266	C01	262.682	237.917.831
D1S304	0.172	C01	263.283	238.329.629
D1S180	0.065	C01	263.717	238.406.371
D1S204	0.148	C01	264.396	238.647.360
D1S547	0.044	C01	264.397	238.797.086
D1S2842	0.340	C01	267.136	239.819.442
D1S2679	0.444	C01	268.006	239.937.224
D1S2811	0.196	C01	268.628	240.637.850
D1S1609	0.125	C01	268.982	241.012.601
D1S102	0.436	C01	269.061	241.113.174
D1S2693	0.072	C01	269.166	241.247.061
D1S423	0.112	C01	274.932	242.492.380
D1S2682	0.418	C01	279.989	245.027.798

Chromosome 2

D2S2268	0.346	C02	1.989	205.168
D2S2393	0.206	C02	4.016	1.943.458
D2S323	0.215	C02	4.612	2.555.761
D2S319	0.192	C02	7.814	5.036.485
D2S304	0.297	C02	10.990	4.238.195
D2S205	0.213	C02	10.991	4.293.774
D2S2166	0.099	C02	11.306	4.446.232
D2S330	0.154	C02	15.744	6.802.850
D2S2211	0.242	C02	18.385	7.493.116
D2S1329	0.492	C02	19.817	7.867.326
D2S2952	0.002	C02	20.355	8.099.777
D2S359	0.359	C02	20.713	8.209.638
D2S2164	0.135	C02	20.714	8.248.777
D2S2326	0.311	C02	23.523	8.784.702
D2S162	0.085	C02	23.524	8.882.034
D2S2243	0.334	C02	24.109	9.300.251
D2S287	0.379	C02	24.110	9.618.718
D2S2207	0.085	C02	24.283	9.649.402
D2S423	0.142	C02	26.280	9.962.316
D2S398	0.181	C02	27.796	10.565.293
D2S297	0.031	C02	29.218	11.130.894
D2S2278	0.193	C02	29.505	11.245.080
D2S168	0.067	C02	29.949	11.467.214
D2S1400	0.029	C02	30.272	11.628.678
D2S2377	0.092	C02	30.698	11.818.157
D2S131	0.306	C02	35.059	13.389.277
D2S2267	0.296	C02	35.627	13.757.405
D2S149	0.234	C02	35.628	14.414.734
D2S312	0.422	C02	36.277	15.249.001
D2S2346	0.038	C02	40.616	16.833.127
D2S332	0.423	C02	41.229	17.414.463
D2S1360	0.169	C02	41.230	17.476.470
D2S2155	0.516	C02	41.231	17.610.807
D2S320	0.699	C02	41.232	18.231.331
D2S2375	0.487	C02	42.303	18.633.946
D2S387	0.214	C02	42.767	19.326.949
D2S305	0.162	C02	42.818	19.402.889
D2S310	0.587	C02	42.909	19.538.502
D2S2233	0.193	C02	43.073	19.783.649

Marker name	pvalue	Chr	cM	Mb
D2S175	0.108	C02	43.232	19.926.453
D2S2150	0.512	C02	45.095	20.516.447
D2S2201	0.294	C02	46.422	21.550.414
D2S2221	0.416	C02	47.916	23.198.438
D2S1324	0.862	C02	48.462	23.321.121
D2S2337	0.088	C02	49.147	23.734.793
D2S2168	0.067	C02	49.373	25.062.733
D2S171	0.132	C02	49.374	25.392.907
D2S144	0.182	C02	49.375	25.475.368
D2S2303	0.241	C02	49.376	25.585.983
D2S2223	0.172	C02	50.882	26.533.651
D2S2350	0.259	C02	50.883	26.702.783
D2S174	0.318	C02	51.086	26.814.370
D2S165	0.039	C02	52.343	28.577.816
D2S365	0.075	C02	52.344	28.580.713
D2S1322	0.301	C02	52.368	28.925.674
D2S170	0.125	C02	52.369	29.188.277
D2S405	0.485	C02	52.879	29.451.166
D2S146	0.317	C02	53.103	29.566.656
D2S390	0.617	C02	53.917	29.986.379
D2S375	0.397	C02	55.724	30.935.333
D2S400	0.389	C02	56.040	31.117.711
D2S2255	0.102	C02	56.150	31.197.769
D2S367	0.109	C02	59.437	34.415.683
D2S368	0.112	C02	59.438	34.415.683
D2S1325	0.238	C02	61.307	35.991.231
D2S1788	0.075	C02	61.416	36.234.802
D2S2230	0.212	C02	61.586	36.613.245
D2S2186	0.365	C02	62.975	37.047.473
D2S2163	0.062	C02	63.657	37.910.179
D2S177	0.231	C02	64.187	38.001.426
D2S1348	0.423	C02	64.725	38.241.530
D2S1346	0.194	C02	64.726	38.241.668
D2S2238	0.243	C02	66.382	40.152.847
D2S2328	0.183	C02	66.767	40.653.348
D2S2272	0.633	C02	66.965	40.870.746
D2S2305	0.471	C02	67.406	27.399.104
D2S2306	0.134	C02	68.519	42.579.194
D2S2259	0.164	C02	68.734	42.971.176
D2S1356	0.095	C02	69.480	43.348.056
D2S2294	0.447	C02	70.262	43.850.178
D2S119	0.050	C02	70.263	44.048.517
D2S2298	0.390	C02	70.550	44.116.813
D2S2378	0.260	C02	73.718	46.233.166
D2S2182	0.098	C02	73.719	46.240.155
D2S391	0.061	C02	74.107	46.385.901
D2S288	0.132	C02	74.431	46.519.594
D2S2227	0.500	C02	75.044	47.244.220
D2S1352	0.121	C02	78.058	50.808.166
D2S123	0.295	C02	78.418	51.262.971
D2S2292	0.534	C02	80.346	53.513.135
D2S2251	0.299	C02	80.347	54.184.363
D2S2153	0.125	C02	80.348	54.682.999
D2S1364	0.650	C02	82.827	57.556.847
D2S2734	0.122	C02	83.753	58.808.912
D2S1337	0.167	C02	84.386	59.343.630
D2S2736	0.074	C02	84.627	59.961.691
D2S444	0.525	C02	84.880	60.373.640
D2S386	0.009	C02	85.620	60.844.127
D2S2332	0.482	C02	86.044	61.266.837
D2S337	0.155	C02	86.045	61.644.399
D2S2206	0.345	C02	86.415	62.492.163
D2S2225	0.311	C02	86.746	62.790.110
D2S2320	0.366	C02	86.747	63.031.690
D2S147	0.340	C02	86.748	64.139.669
D2S2235	0.397	C02	89.987	65.970.599
D2S136	0.258	C02	89.992	66.072.343
D2S296	0.422	C02	90.109	66.181.385
D2S134	0.091	C02	90.335	66.641.597
D2S290	0.030	C02	90.343	66.657.631
D2S166	0.088	C02	91.269	66.782.709
D2S379	0.476	C02	91.390	66.994.127
D2S1772	0.162	C02	91.391	67.025.636
D2S2368	0.322	C02	91.392	67.188.144
D2S285	0.332	C02	92.069	67.620.941
D2S2171	0.150	C02	92.499	67.810.580
D2S1779	0.206	C02	93.415	68.213.550
D2S358	0.102	C02	93.951	68.872.088
D2S2152	0.222	C02	94.616	69.689.794
D2S327	0.335	C02	95.066	70.234.889
D2S2113	0.197	C02	95.067	70.492.646
D2S292	0.124	C02	95.207	70.676.541
D2S443	0.243	C02	95.454	70.762.608
D2S291	0.111	C02	98.752	71.909.481
D2S2110	0.533	C02	99.577	73.046.803
D2S2111	0.083	C02	99.578	73.291.516

Marker name	pvalue	Chr	cM	Mb	Marker name	pvalue	Chr	cM	Mb
D2S145	0.262	C02	99.579	73.389.979	D2S2313	0.457	C02	160.676	145.920.708
D2S2109	0.255	C02	100.036	73.552.269	D2S2301	0.685	C02	160.678	147.207.467
HRC	0.205	C02	102.117	75.087.339	D2S151	0.565	C02	160.987	147.997.291
HK2	0.346	C02	102.118	75.087.339	D2S1399	0.269	C02	161.510	148.420.878
D2S286	0.291	C02	102.428	75.316.666	D2S2365	0.149	C02	162.094	149.309.140
D2S2114	0.072	C02	102.829	75.804.891	D2S2184	0.302	C02	162.168	149.380.535
D2S1774	0.084	C02	103.960	77.181.269	D2S2324	0.284	C02	163.620	150.955.315
D2S1775	0.501	C02	103.961	77.181.269	D2S356	0.523	C02	164.856	151.963.533
D2S169	0.867	C02	105.040	78.621.688	D2S2236	0.485	C02	165.640	153.016.284
D2S329	0.180	C02	105.897	79.355.751	D2S2241	0.021	C02	166.874	154.715.354
D2S139	0.108	C02	106.420	79.738.071	D2S1388	0.177	C02	168.828	156.146.880
D2S2180	0.353	C02	107.937	80.480.665	D2S142	0.495	C02	168.829	156.485.775
D2S1770	0.481	C02	108.995	81.861.630	D2S141	0.481	C02	169.300	157.037.046
D2S289	0.384	C02	109.628	82.688.812	D2S2360	0.463	C02	170.122	158.000.627
D2S1396	0.280	C02	109.629	82.922.076	D2S284	0.580	C02	170.851	158.854.276
D2S428	0.005	C02	109.630	82.956.302	D2S1353	0.247	C02	171.625	159.761.475
D2S1332	0.527	C02	109.953	83.246.808	D2S2370	0.106	C02	171.626	160.278.984
D2S2162	0.115	C02	110.093	83.372.728	D2S2190	0.174	C02	171.627	160.324.231
D2S435	0.027	C02	110.346	83.713.816	D2S156	0.093	C02	171.779	160.851.323
D2S440	0.365	C02	110.472	84.893.922	GCG	0.431	C02	173.028	163.205.511
D2S394	0.009	C02	110.475	84.921.493	D2S354	0.517	C02	174.004	164.121.297
D2S2161	0.170	C02	110.778	85.261.526	D2S382	0.303	C02	174.742	166.170.313
D2S2333	0.689	C02	111.423	85.462.713	D2S124	0.557	C02	174.743	166.347.606
D2S2232	0.525	C02	112.750	85.965.385	D2S111	0.209	C02	174.744	166.462.774
D2S388	0.365	C02	112.751	86.051.472	D2S2330	0.248	C02	174.846	166.899.956
D2S1331	0.052	C02	112.953	86.557.551	D2S1395	0.484	C02	175.389	168.074.442
D2S2216	0.327	C02	114.147	88.311.814	D2S399	0.092	C02	175.534	168.191.363
D2S2181	0.092	C02	114.679	88.578.831	D2S2345	0.281	C02	176.406	168.922.963
D2S2154	0.212	C02	115.303	95.033.225	D2S294	0.092	C02	178.940	170.579.218
D2S2159	0.137	C02	115.351	95.534.530	D2S376	0.160	C02	180.466	171.576.800
D2S2187	0.685	C02	116.177	98.726.606	D2S2284	0.860	C02	181.248	171.695.949
D2S2209	0.634	C02	117.537	100.863.578	D2S333	0.168	C02	181.955	172.591.906
D2S2264	0.150	C02	118.855	102.041.021	D2S335	0.060	C02	181.956	172.769.039
D2S373	0.119	C02	118.856	102.762.369	D2S2381	0.373	C02	182.091	172.860.907
D2S2356	0.557	C02	119.443	103.127.836	D2S2188	0.181	C02	186.247	175.807.113
D2S299	0.250	C02	119.813	103.576.619	D2S2257	0.306	C02	186.384	176.372.689
D2S1321	0.159	C02	121.005	105.008.327	D2S2314	0.065	C02	187.064	177.064.950
D2S1343	0.640	C02	121.006	105.100.882	D2S138	0.144	C02	187.875	177.947.314
D2S135	0.318	C02	121.007	105.132.843	D2S148	0.464	C02	188.322	178.433.967
D2S2229	0.155	C02	121.807	105.949.730	D2S2173	0.236	C02	188.519	178.648.080
D2S176	0.155	C02	121.994	106.140.763	D2S385	0.210	C02	189.604	179.827.920
D2S1897	0.234	C02	122.020	106.167.822	D2S324	0.557	C02	189.605	179.858.768
D2S436	0.174	C02	122.524	106.864.532	D2S2261	0.307	C02	190.549	181.699.697
D2S293	0.400	C02	122.551	106.895.157	D2S384	0.090	C02	190.552	181.705.278
D2S2386	0.688	C02	122.969	107.135.334	D2S364	0.031	C02	192.000	183.237.075
D2S1784	0.235	C02	123.786	107.969.476	D2S350	0.970	C02	192.684	184.051.486
D2S1890	0.176	C02	123.787	108.040.569	D2S2366	0.234	C02	193.373	184.694.525
D2S340	0.758	C02	124.858	108.530.148	D2S1391	0.374	C02	193.498	185.194.972
D2S160	0.041	C02	127.909	113.093.637	D2S1330	0.359	C02	193.744	186.278.960
D2S1895	0.279	C02	128.261	114.150.500	D2S152	0.521	C02	194.110	188.434.138
D2S121	0.469	C02	128.812	114.636.951	D2S426	0.715	C02	194.733	190.556.057
D2S2953	0.057	C02	129.460	115.272.716	D2S118	0.448	C02	195.342	191.809.011
D2S308	0.382	C02	129.807	115.307.851	D2S2246	0.769	C02	197.178	192.585.391
D2S410	0.226	C02	130.254	116.336.074	D2S318	0.469	C02	197.179	192.778.305
D2S1771	0.270	C02	130.949	117.436.377	D2S161	0.373	C02	197.180	192.931.607
D2S363	0.120	C02	130.950	117.490.697	D2S280	0.188	C02	198.566	193.057.644
D2S437	0.036	C02	130.951	117.686.609	D2S315	0.735	C02	198.567	193.565.985
D2S100	0.061	C02	132.168	119.329.548	D2S2167	0.260	C02	198.817	193.586.182
D2S2254	0.327	C02	132.186	120.083.999	D2S2735	0.223	C02	198.843	193.779.053
D2S283	0.369	C02	135.037	121.738.627	D2S425	0.205	C02	199.066	195.463.462
D2S2265	0.153	C02	135.622	121.798.558	D2S1350	0.287	C02	199.067	195.465.703
D2S343	0.332	C02	136.948	122.508.098	D2S117	0.132	C02	199.069	195.821.245
D2S2353	0.395	C02	137.114	122.602.695	D2S342	0.432	C02	199.347	196.086.676
D2S110	0.201	C02	137.400	122.766.357	D2S2336	0.184	C02	200.488	197.176.510
D2S2737	0.064	C02	137.953	123.221.801	D2S311	0.169	C02	200.705	197.769.387
D2S347	0.188	C02	138.309	124.344.954	D2S316	0.215	C02	200.977	197.999.668
D2S1340	0.251	C02	138.873	124.724.277	D2S2318	0.191	C02	200.978	198.917.131
D2S1328	0.060	C02	140.676	126.281.874	D2S115	0.311	C02	200.979	199.172.775
D2S2339	0.163	C02	141.240	126.672.028	D2S348	0.442	C02	200.980	199.414.456
D2S2271	0.350	C02	143.620	128.193.171	D2S2392	0.001	C02	202.055	199.913.729
D2S2215	0.494	C02	145.454	130.084.418	D2S2396	0.310	C02	202.190	200.234.566
D2S112	0.463	C02	149.030	133.419.468	D2S116	0.561	C02	202.939	201.870.845
D2S2219	0.192	C02	149.163	133.588.021	D2S309	0.032	C02	203.149	202.136.781
D2S114	0.587	C02	150.180	134.535.824	D2S2309	0.156	C02	203.691	202.825.933
D2S1334	0.249	C02	152.541	136.667.217	D2S2214	0.257	C02	203.775	202.933.228
D2S2196	0.174	C02	152.910	137.099.423	D2S346	0.555	C02	204.271	203.165.974
D2S2367	0.417	C02	153.756	138.325.241	D2S2289	0.303	C02	204.980	203.864.218
D2S1326	0.381	C02	155.357	140.133.774	D2S307	0.331	C02	205.300	204.857.108
D2S397	0.650	C02	155.358	140.324.348	D2S1384	0.218	C02	205.848	205.429.671
D2S150	0.261	C02	155.359	140.774.176	D2S2237	0.056	C02	206.532	205.831.732
D2S127	0.086	C02	156.507	141.897.923	D2S155	0.057	C02	208.465	207.151.386
D2S129	0.029	C02	156.508	142.108.005	D2S1782	0.186	C02	208.561	207.217.232
D2S1769	0.479	C02	156.912	142.691.034	D2S369	0.362	C02	208.799	207.593.225
D2S2266	0.481	C02	157.048	142.818.858	D2S2358	0.086	C02	208.816	207.733.855
D2S122	0.007	C02	158.719	144.382.239	D2S355	0.055	C02	209.441	208.311.672
D2S381	0.466	C02	160.675	145.774.833	D2S2192	0.303	C02	209.448	208.317.934

Marker name	pvalue	Chr	cM	Mb
D2S325	0.188	C02	209.449	208.473.178
D2S2321	0.126	C02	209.450	208.476.361
D2S2208	0.254	C02	209.591	208.927.376
D2S2178	0.728	C02	210.896	210.056.392
D2S322	0.324	C02	211.113	211.005.869
D2S371	0.183	C02	212.193	212.515.638
D2S317	0.051	C02	213.808	213.704.096
D2S334	0.460	C02	214.986	214.834.695
D2S143	0.109	C02	215.153	215.175.649
D2S1327	0.068	C02	215.195	215.262.380
D2S128	0.589	C02	215.350	215.294.846
D2S1345	0.048	C02	215.351	215.368.224
D2S2361	0.416	C02	216.936	216.680.968
D2S137	0.542	C02	218.238	217.021.568
D2S2382	0.147	C02	218.524	217.251.106
D2S2383	0.122	C02	218.525	217.251.106
D2S301	0.461	C02	219.617	218.089.614
D2S2248	0.456	C02	219.618	218.141.491
D2S164	0.489	C02	220.292	218.162.391
D2S1371	0.677	C02	220.648	218.449.404
D2S295	0.397	C02	220.740	218.524.220
D2S2210	0.536	C02	220.741	218.534.704
D2S434	0.173	C02	220.742	218.779.033
D2S173	0.355	C02	221.676	218.976.657
D2S433	0.296	C02	223.200	219.968.224
D2S163	0.108	C02	226.246	220.994.810
D2S2359	0.407	C02	226.416	221.148.295
D2S424	0.071	C02	226.569	221.550.909
D2S377	0.352	C02	227.779	222.026.314
D2S126	0.178	C02	228.270	222.219.452
D2S2372	0.574	C02	228.670	222.229.132
D2S2148	0.039	C02	228.671	222.315.730
D2S1323	0.506	C02	229.806	222.892.393
D2S313	0.407	C02	230.281	223.471.101
D2S2300	0.094	C02	230.282	223.502.159
D2S360	0.225	C02	231.001	223.898.066
D2S130	0.261	C02	231.043	223.932.985
D2S408	0.101	C02	231.167	224.036.711
D2S133	0.412	C02	232.122	224.837.492
D2S351	0.621	C02	233.078	225.922.160
D2S1333	0.014	C02	234.125	227.232.025
D2S1363	0.012	C02	234.126	227.232.126
D2S2308	0.155	C02	234.425	227.495.596
D2S2354	0.217	C02	234.488	227.551.844
D2S2389	0.712	C02	234.825	227.848.990
D2S1349	0.108	C02	235.412	228.012.349
D2S159	0.532	C02	235.461	228.025.927
D2S2158	0.347	C02	235.568	228.262.770
D2S401	0.455	C02	235.658	228.460.669
D2S439	0.256	C02	237.756	229.382.630
D2S1370	0.133	C02	238.516	229.739.016
D2S362	0.444	C02	238.908	229.940.180
D2S2213	0.594	C02	239.237	230.304.171
D2S2297	0.373	C02	239.771	230.572.344
D2S341	0.485	C02	240.322	230.778.097
D2S396	0.187	C02	240.434	230.886.132
D2S2317	0.100	C02	240.668	231.111.683
D2S1392	0.376	C02	242.632	232.408.739
D2S427	0.232	C02	242.633	232.408.801
D2S2193	0.174	C02	242.681	232.439.912
D2S2344	0.353	C02	244.510	233.647.233
D2S206	0.245	C02	245.227	233.910.313
D2S2176	0.321	C02	245.263	233.950.171
D2S331	0.161	C02	245.350	234.046.450
D2S2348	0.161	C02	246.011	234.434.843
D2S407	0.362	C02	250.543	236.306.245
D2S2202	0.445	C02	253.231	236.916.705
D2S1397	0.067	C02	253.232	237.080.234
D2S338	0.289	C02	253.840	237.522.143
D2S345	0.371	C02	254.551	238.088.761
D2S2338	0.639	C02	257.353	239.136.741
D2S2285	0.207	C02	262.897	241.222.240
D2S125	0.251	C02	264.008	241.488.777
D2S140	0.338	C02	265.280	242.060.200

Chromosome 3

D3S2387	0.007	C03	2.332	1.011.272
D3S1307	0.383	C03	2.606	1.324.917
D3S1270	0.012	C03	3.277	1.423.260
D3S2426	0.401	C03	3.630	1.501.610
D3S1297	0.375	C03	5.052	2.013.402
D3S3525	0.108	C03	5.968	2.343.095
D3S3630	0.177	C03	6.223	2.675.495
D3S3050	0.020	C03	10.680	3.271.461
D3S1620	0.659	C03	10.894	3.474.216

Marker name	pvalue	Chr	cM	Mb
D3S1304	0.075	C03	20.484	6.894.241
D3S3728	0.484	C03	21.922	7.427.144
D3S3591	0.596	C03	23.902	8.160.756
D3S1597	0.515	C03	27.725	9.340.445
D3S3611	0.030	C03	29.370	10.529.106
D3S3601	0.170	C03	29.371	10.643.476
D3S1263	0.234	C03	30.710	11.492.252
D3S3714	0.019	C03	30.891	11.643.608
D3S3680	0.001	C03	30.959	11.701.147
D3S1259	0.064	C03	31.404	12.073.680
D3S3701	0.493	C03	32.022	12.592.516
D3S3693	0.003	C03	32.023	12.799.725
D3S3610	0.105	C03	32.024	12.980.655
D3S2403	0.538	C03	32.389	13.147.396
D3S3608	0.487	C03	33.553	13.679.235
D3S2385	0.823	C03	33.554	13.853.968
D3S3602	0.626	C03	33.555	13.901.067
D3S3595	0.230	C03	34.837	14.617.369
D3S3613	0.196	C03	36.134	15.337.002
D3S3614	0.476	C03	36.135	15.337.002
D3S1286	0.131	C03	36.959	15.794.136
D3S3509	0.010	C03	37.910	16.497.251
D3S2338	0.342	C03	38.726	16.824.410
D3S3510	0.144	C03	40.856	19.073.529
D3S1293	0.398	C03	44.627	21.902.013
D3S1599	0.143	C03	45.043	22.496.261
D3S3659	0.312	C03	45.377	22.913.782
D3S2336	0.279	C03	48.337	24.899.637
D3S1583	0.569	C03	49.944	25.530.072
D3S2466	0.034	C03	50.162	25.961.604
D3S2335	0.025	C03	50.396	26.424.545
D3S1266	0.232	C03	52.218	27.932.335
D3S1283	0.623	C03	53.629	28.701.591
D3S1609	0.480	C03	55.856	29.915.040
D3S3547	0.616	C03	56.447	30.131.191
D3S3727	0.234	C03	57.291	30.652.496
D3S3567	0.109	C03	57.405	30.713.677
D3S1759	0.035	C03	59.303	32.007.592
D3S2432	0.081	C03	59.493	32.136.945
D3S1619	0.285	C03	61.790	34.087.750
D3S1612	0.430	C03	62.045	34.561.277
D3S3512	0.259	C03	62.046	34.565.909
D3S1768	0.514	C03	62.047	34.596.173
D3S1277	0.440	C03	62.071	34.627.632
D3S1278	0.115	C03	62.072	34.627.632
D3S3718	0.390	C03	63.238	36.130.137
D3S2411	0.486	C03	63.436	36.319.249
D3S2412	0.111	C03	63.437	36.319.249
D3S1561	0.317	C03	63.937	36.444.720
D3S1611	0.434	C03	64.733	37.029.105
D3S2417	0.574	C03	64.754	37.394.956
D3S3623	0.166	C03	64.755	37.404.156
D3S1298	0.064	C03	65.086	38.009.388
D3S3639	0.481	C03	65.278	38.360.322
D3S1260	0.299	C03	65.285	38.372.333
D3S3521	0.122	C03	66.393	38.830.243
D3S3572	0.313	C03	66.394	38.989.222
D3S3573	0.282	C03	66.395	38.989.222
D3S3574	0.224	C03	66.396	38.989.222
D3S3527	0.157	C03	66.507	39.305.916
D3S3522	0.409	C03	67.507	40.749.589
D3S3658	0.359	C03	67.586	40.863.646
D3S2407	0.429	C03	67.929	41.355.384
D3S3564	0.137	C03	68.706	42.379.457
D3S3685	0.069	C03	68.857	42.429.724
D3S3559	0.025	C03	69.310	42.649.217
D3S3647	0.279	C03	69.820	43.539.661
D3S3597	0.197	C03	70.479	43.924.153
D3S3624	0.300	C03	70.869	44.574.409
D3S1767	0.425	C03	72.126	46.917.001
D3S3640	0.634	C03	72.682	47.957.478
D3S3729	0.173	C03	72.683	47.998.706
D3S2420	0.231	C03	72.684	48.027.962
D3S3560	0.596	C03	72.685	48.154.865
D3S2409	0.127	C03	72.911	49.377.096
D3S3629	0.436	C03	72.941	49.542.187
D3S3604	0.233	C03	73.018	49.952.172
D3S3667	0.204	C03	73.019	49.991.028
D3S1568	0.122	C03	73.021	50.464.756
D3S1621	0.221	C03	73.021	50.552.942
D3S1573	0.526	C03	73.022	51.063.793
D3S3026	0.049	C03	73.101	51.866.300
D3S3688	0.172	C03	73.102	51.818.406
D3S1578	0.454	C03	74.498	53.664.071
D3S1588	0.283	C03	74.833	54.055.277

Marker name	pvalue	Chr	cM	Mb	Marker name	pvalue	Chr	cM	Mb
D3S3666	0.430	C03	76.490	54.609.585	D3S2457	0.016	C03	128.825	118.511.901
D3S1613	0.018	C03	77.359	54.917.749	D3S1558	0.639	C03	128.934	118.571.662
D3S2408	0.174	C03	79.024	55.667.713	D3S3649	0.486	C03	129.210	118.965.737
D3S3588	0.101	C03	79.468	56.043.086	D3S3650	0.961	C03	129.211	118.965.737
D3S3721	0.414	C03	79.469	55.842.181	D3S1303	0.101	C03	129.212	119.479.174
D3S3048	0.118	C03	79.583	56.094.908	D3S3515	0.029	C03	129.730	119.853.702
D3S3621	0.333	C03	79.677	56.276.098	D3S3620	0.376	C03	130.121	120.836.900
D3S2400	0.004	C03	79.707	56.780.115	D3S3576	0.310	C03	131.968	123.566.341
D3S3532	0.471	C03	80.932	57.431.940	D3S1267	0.168	C03	133.534	124.364.103
D3S2402	0.134	C03	81.129	58.174.193	D3S4011	0.055	C03	134.097	124.651.038
D3S1592	0.091	C03	81.158	58.396.271	D3S3552	0.203	C03	134.125	124.693.669
D3S2452	0.275	C03	81.216	58.655.898	D3S3519	0.383	C03	134.300	124.955.942
D3S1766	0.046	C03	81.413	58.939.010	D3S3558	0.125	C03	134.351	125.032.732
D3S1313	0.276	C03	81.513	59.082.097	D3S1551	0.077	C03	135.537	126.178.356
D3S3722	0.352	C03	82.322	59.520.853	D3S1552	0.161	C03	135.538	126.178.356
D3S3577	0.602	C03	82.323	59.576.535	D3S1589	0.306	C03	136.430	127.264.797
D3S1300	0.320	C03	84.480	60.467.241	D3S3584	0.046	C03	137.540	128.497.641
D3S3631	0.343	C03	85.843	60.854.089	D3S3607	0.313	C03	138.387	128.593.876
D3S3566	0.520	C03	87.360	62.499.927	D3S1587	0.672	C03	141.407	132.119.726
D3S3698	0.478	C03	88.690	63.077.123	D3S3548	0.364	C03	141.789	132.509.089
D3S1600	0.373	C03	89.040	63.277.176	D3S3514	0.086	C03	142.174	132.900.954
D3S1287	0.238	C03	90.594	64.164.217	D3S1292	0.278	C03	142.175	132.951.217
DXS1056	0.320	C03	90.595	64.164.217	D3S1596	0.092	C03	142.552	133.388.729
D3S3571	0.177	C03	90.692	64.340.225	D3S1290	0.199	C03	143.563	134.311.826
D3S1285	0.324	C03	92.060	64.896.447	D3S3713	0.119	C03	145.231	134.570.096
D3S3697	0.162	C03	93.787	66.307.379	D3S3657	0.060	C03	145.440	134.746.872
D3S3524	0.459	C03	95.393	67.626.136	D3S3637	0.168	C03	146.456	135.632.086
D3S1296	0.368	C03	96.511	69.696.536	D3S1590	0.454	C03	147.165	136.276.905
D3S1566	0.355	C03	97.190	70.232.460	D3S3528	0.338	C03	147.472	137.444.455
D3S1562	0.367	C03	98.495	71.144.661	D3S2453	0.099	C03	147.522	137.598.750
D3S3568	0.383	C03	98.896	71.466.276	D3S1549	0.064	C03	147.553	137.696.259
D3S3516	0.216	C03	99.114	71.619.462	D3S3586	0.122	C03	148.764	140.314.150
D3S2406	0.129	C03	103.265	73.179.282	D3S1764	0.082	C03	148.966	140.509.196
D3S3039	0.196	C03	104.857	73.763.143	D3S3554	0.300	C03	149.266	140.926.894
D3S3581	0.976	C03	105.494	73.996.568	D3S1309	0.695	C03	150.071	142.047.222
D3S2389	0.061	C03	105.971	74.834.078	D3S3694	0.305	C03	152.297	143.511.567
D3S3653	0.488	C03	106.925	76.507.997	D3S1569	0.156	C03	154.110	144.692.337
D3S1274	0.423	C03	109.347	78.792.110	D3S3599	0.037	C03	154.111	144.695.407
D3S3049	0.174	C03	109.387	78.830.141	DS2378	0.020	C03	154.733	145.069.583
D3S1604	0.967	C03	110.090	79.493.188	D3S3704	0.474	C03	155.544	145.900.324
D3S1577	0.140	C03	110.344	80.196.454	D3S1557	0.403	C03	155.855	146.490.816
D3S2446	0.406	C03	110.979	81.889.383	D3S1593	0.326	C03	155.856	146.648.905
D3S2388	0.032	C03	111.309	83.085.058	D3S2394	0.474	C03	156.177	146.869.300
D3S1276	0.260	C03	111.553	85.177.041	D3S1608	0.454	C03	156.400	147.022.125
D3S2451	0.286	C03	111.634	85.773.403	D3S3627	0.056	C03	156.708	147.666.876
D3S1595	0.275	C03	111.848	86.091.642	D3S1744	0.208	C03	156.909	148.413.430
D3S3679	0.367	C03	112.068	86.419.384	D3S1306	0.315	C03	157.750	149.121.789
D3S2386	0.157	C03	112.346	87.839.351	D3S1555	0.051	C03	160.187	150.127.379
D3S3636	0.091	C03	113.297	95.363.955	D3S1308	0.298	C03	160.668	150.355.028
D3S2462	0.101	C03	113.379	97.439.585	D3S3705	0.263	C03	161.133	150.367.822
D3S1752	0.065	C03	114.351	99.066.246	D3S3022	0.012	C03	161.356	150.609.236
D3S1603	0.100	C03	114.777	99.780.706	D3S1315	0.421	C03	163.645	152.110.520
D3S3716	0.068	C03	114.778	100.056.888	D3S1594	0.109	C03	163.769	152.332.196
D3S2419	0.099	C03	114.779	100.997.843	D3S1279	0.517	C03	163.840	152.346.156
D3S1271	0.136	C03	115.243	102.055.630	D3S1584	0.327	C03	164.108	152.636.498
D12S318	0.157	C03	115.512	102.388.192	D3S1746	0.061	C03	164.360	153.050.650
D3S3655	0.136	C03	116.026	103.025.328	D3S3689	0.123	C03	164.440	153.181.442
D3S3656	0.564	C03	116.027	103.025.328	D2S157	0.024	C03	164.570	153.304.877
D3S1753	0.017	C03	116.028	103.173.600	D3S1280	0.382	C03	164.700	153.429.118
D3S3652	0.174	C03	116.348	103.324.522	D3S3710	0.121	C03	166.469	155.427.398
D3S2459	0.105	C03	116.349	103.496.185	D3S1570	0.120	C03	167.568	156.763.256
D3S4534	0.025	C03	117.361	105.226.659	D3S3587	0.455	C03	167.753	156.970.897
D3S1559	0.498	C03	117.706	105.817.707	D3S1275	0.078	C03	167.754	157.467.103
D3S1291	0.695	C03	117.813	106.111.239	D3S1607	0.470	C03	168.315	158.285.032
D3S3654	0.514	C03	118.918	107.406.455	D3S1605	0.136	C03	168.413	158.567.051
D3S1563	0.689	C03	118.919	107.412.873	D3S1553	0.403	C03	169.122	160.621.387
D3S3638	0.424	C03	118.970	107.524.289	D3S3579	0.437	C03	170.160	161.901.190
D3S3045	0.350	C03	120.290	108.310.819	D3S3708	0.076	C03	170.563	163.442.395
D3S1616	0.397	C03	120.650	108.925.161	D3S3702	0.296	C03	170.957	164.722.260
D3S2495	0.134	C03	121.627	109.457.325	D3S1268	0.334	C03	171.082	165.240.947
D3S1302	0.278	C03	121.628	109.873.443	D3S3052	0.025	C03	171.150	165.522.576
D3S3695	0.039	C03	122.135	110.442.617	D3S3668	0.026	C03	171.185	165.667.972
D3S3044	0.178	C03	123.014	112.283.480	D3S3712	0.219	C03	172.250	168.290.512
D3S2422	0.023	C03	123.015	112.394.775	D3S1264	0.080	C03	172.251	168.526.690
D3S1572	0.320	C03	123.016	112.586.477	D3S1763	0.332	C03	172.252	168.560.593
D3S4018	0.060	C03	123.134	112.975.114	D3S3622	0.197	C03	173.202	169.184.873
D3S3675	0.531	C03	123.942	114.166.882	D3S1614	0.291	C03	173.730	169.531.038
D3S1610	0.482	C03	123.943	114.393.139	D3S3523	0.486	C03	174.775	170.858.716
D3S3683	0.423	C03	124.142	114.582.493	D3S1564	0.089	C03	175.207	171.509.727
D3S3585	0.620	C03	124.633	114.995.025	D3S3723	0.701	C03	175.208	171.572.325
D3S3665	0.180	C03	125.264	115.524.384	D3S3724	0.277	C03	175.209	171.572.325
D3S3526	0.349	C03	125.599	115.806.139	D3S1574	0.413	C03	177.857	173.000.015
D3S1310	0.066	C03	125.600	116.103.337	D3S3725	0.435	C03	178.272	173.130.553
D3S1586	0.193	C03	125.601	116.270.724	D3S3726	0.203	C03	178.273	173.130.553
D3S3670	0.421	C03	125.839	116.482.364	D3S3520	0.181	C03	179.772	173.492.027
D3S1575	0.103	C03	126.997	117.510.134	D3S1556	0.565	C03	181.198	173.835.498

Marker name	pvalue	Chr	cM	Mb
D3S1565	0.344	C03	181.867	174.803.580
D3S2425	0.108	C03	182.192	174.884.284
D3S2421	0.021	C03	184.680	176.395.222
D3S2427	0.009	C03	185.545	177.105.608
D3S3041	0.362	C03	186.392	177.800.996
D3S3511	0.702	C03	187.347	178.716.472
D3S3715	0.266	C03	187.360	178.733.316
D3S3037	0.012	C03	187.380	178.762.465
D3S1754	0.018	C03	187.381	178.762.537
D3S3730	0.259	C03	188.194	179.867.513
D3S3565	0.646	C03	188.975	180.802.808
D3S3603	0.428	C03	188.976	181.235.788
D3S1618	0.395	C03	193.372	184.672.760
D3S1571	0.288	C03	193.605	184.860.825
D3S2399	0.164	C03	194.133	185.287.035
D3S3592	0.328	C03	195.053	185.731.334
D3S1617	0.293	C03	196.833	187.205.280
D3S1602	0.141	C03	197.908	187.352.605
D3S1262	0.550	C03	198.552	187.544.392
D3S3686	0.306	C03	202.474	188.738.369
D3S3651	0.269	C03	202.981	188.962.055
D3S1580	0.202	C03	206.428	189.863.705
D3S3550	0.601	C03	207.466	190.270.532
D3S3530	0.002	C03	207.594	190.476.551
D3S2398	0.196	C03	207.759	190.741.940
D3S1294	0.104	C03	208.184	190.983.021
D3S1289	0.408	C03	209.142	191.566.354
D3S2747	0.554	C03	209.188	191.601.281
D3S2455	0.062	C03	211.279	192.201.010
D3S1601	0.216	C03	212.642	192.998.188
D3S3557	0.442	C03	213.146	193.199.940
D3S3663	0.375	C03	213.152	193.202.499
D3S2418	0.395	C03	213.956	193.637.781
D3S3669	0.515	C03	214.298	193.822.877
D3S3642	0.304	C03	214.959	194.123.001
D3S2748	0.263	C03	216.723	195.052.813
D3S1265	0.458	C03	222.338	196.852.567
D3S1272	0.133	C03	225.045	198.342.644
D3S1311	0.258	C03	225.046	198.344.496

Chromosome 4

D4S2936	0.018	C04	0.904	682.247
D4S43	0.597	C04	3.108	2.313.276
D4S1614	0.416	C04	3.618	2.678.158
D4S127	0.484	C04	4.135	3.048.313
D4S412	0.450	C04	4.567	3.412.068
D4S3023	0.188	C04	7.377	4.365.876
D4S2375	0.225	C04	8.058	5.037.205
D4S2366	0.204	C04	12.909	6.549.327
D4S2935	0.322	C04	13.305	6.625.619
D4S394	0.171	C04	15.279	7.024.409
D4S2983	0.220	C04	19.304	7.809.982
D4S2928	0.212	C04	23.836	10.363.119
D4S1582	0.394	C04	24.120	10.452.468
D4S1599	0.059	C04	24.242	10.646.666
D4S3036	0.124	C04	26.772	11.969.827
D4S2944	0.277	C04	27.657	13.282.514
D4S403	0.224	C04	27.833	13.501.787
D4S2942	0.623	C04	27.852	13.521.888
D4S2362	0.323	C04	30.669	15.208.820
D4S1601	0.093	C04	31.560	15.777.317
D4S1567	0.249	C04	32.246	16.206.310
GGAT18G02	0.380	C04	32.247	16.270.278
D4S2946	0.089	C04	35.696	17.504.296
D4S2633	0.192	C04	36.333	18.596.095
D4S419	0.172	C04	36.334	18.599.642
GATA87B03	0.132	C04	36.335	18.985.014
D4S2399	0.930	C04	36.500	19.815.126
D4S2994	0.202	C04	38.579	21.254.033
D4S2933	0.283	C04	39.507	22.813.008
D4S425	0.577	C04	40.329	23.406.971
D4S3013	0.289	C04	40.727	23.648.309
D4S404	0.020	C04	40.998	23.986.049
D4S1551	0.265	C04	41.606	24.501.925
D4S2948	0.615	C04	43.045	24.760.021
D4S3044	0.305	C04	43.892	25.330.686
D4S3022	0.083	C04	43.893	25.365.412
D4S2397	0.350	C04	48.353	27.008.750
D4S1609	0.423	C04	48.719	27.224.513
D4S391	0.181	C04	48.955	27.363.115
D4S3244	0.359	C04	50.551	28.797.459
D4S418	0.069	C04	51.243	29.116.091
D4S1643	0.374	C04	52.116	30.180.804
D4S2912	0.104	C04	54.037	31.865.229
D4S1587	0.353	C04	55.944	35.366.700

Marker name	pvalue	Chr	cM	Mb
D4S2995	0.060	C04	55.945	35.961.408
D4S2629	0.274	C04	56.863	36.438.782
D4S1581	0.193	C04	58.796	38.034.563
D4S2382	0.262	C04	61.698	39.947.943
D4S405	0.014	C04	62.104	40.268.086
D4S174	0.075	C04	63.086	40.749.467
D4S2974	0.342	C04	64.813	41.566.052
D4S2369	0.098	C04	65.418	42.289.946
D4S3025	0.290	C04	66.239	43.376.348
D4S1627	0.214	C04	66.522	44.094.355
D4S1547	0.455	C04	66.531	44.105.473
D4S3251	0.097	C04	67.003	44.464.838
D4S396	0.690	C04	67.630	46.233.237
D4S3242	0.132	C04	67.732	46.843.193
D4S3255	0.050	C04	68.725	52.715.282
D4S2971	0.168	C04	68.763	53.642.254
D4S2996	0.250	C04	70.861	55.202.648
D4S3254	0.059	C04	70.934	55.352.561
D4S428	0.228	C04	71.030	55.549.947
D4S3019	0.649	C04	74.888	57.552.723
D4S1592	0.582	C04	74.889	57.597.359
D4S2638	0.417	C04	75.738	58.503.436
D4S1569	0.236	C04	76.732	59.564.491
D4S1645	0.173	C04	77.766	61.986.356
D4S398	0.016	C04	77.905	62.250.292
D4S3004	0.174	C04	80.140	65.662.895
D4S2987	0.026	C04	80.312	66.105.226
D4S1574	0.495	C04	80.397	66.244.641
D4S1541	0.042	C04	80.505	66.550.602
D4S416	0.122	C04	80.958	66.628.487
D4S3253	0.155	C04	81.187	67.472.939
D4S2367	0.172	C04	81.583	68.286.181
D4S392	0.298	C04	82.669	70.838.881
D4S2931	0.580	C04	84.181	72.629.445
D4S1558	0.526	C04	87.551	76.250.009
D4S2958	0.484	C04	87.765	77.272.960
D4S3042	0.207	C04	87.766	77.364.258
D4S2640	0.030	C04	90.015	79.433.270
D4S2630	0.132	C04	90.095	79.567.700
D4S2947	0.509	C04	90.451	80.165.794
D4S2963	0.502	C04	90.596	80.408.844
D4S2964	0.222	C04	91.087	81.233.733
D4S3243	0.403	C04	91.180	81.390.769
D4S2922	0.533	C04	92.080	82.902.075
D4S1553	0.223	C04	92.447	83.163.959
D4S400	0.673	C04	92.448	83.433.225
D4S2932	0.701	C04	92.449	83.961.717
D4S395	0.061	C04	93.446	84.704.596
D4S1538	0.143	C04	94.298	85.242.117
D4S1534	0.356	C04	95.643	86.766.686
D4S2409	0.331	C04	96.694	87.376.750
D4S2462	0.325	C04	97.226	87.950.590
D4S1542	0.321	C04	97.227	88.131.324
D4S1563	0.130	C04	99.463	89.991.607
D4S2460	0.036	C04	99.464	90.292.042
D4S2371	0.086	C04	100.455	90.591.168
D4S2461	0.599	C04	100.786	90.690.984
D4S3245	0.012	C04	101.270	91.520.538
D4S410	0.773	C04	101.466	91.855.502
D4S3006	0.150	C04	102.428	92.636.918
D4S414	0.390	C04	102.696	92.897.169
D4S423	0.108	C04	102.697	92.931.147
D4S3037	0.587	C04	102.778	93.692.458
D4S2364	0.898	C04	102.794	93.975.734
D4S1557	0.192	C04	104.022	95.422.443
D4S2433	0.252	C04	104.288	95.790.573
D4S2909	0.230	C04	104.699	96.358.197
D4S2973	0.227	C04	105.313	97.199.238
D4S1559	0.037	C04	105.501	97.456.448
D4S1578	0.334	C04	105.502	97.537.060
D4S2407	0.182	C04	105.561	97.706.047
D4S1560	0.022	C04	105.693	98.075.023
D4S1628	0.132	C04	105.933	98.744.772
D4S1647	0.185	C04	106.343	99.893.367
D4S2986	0.264	C04	106.890	100.116.057
D4S2626	0.692	C04	107.336	100.536.224
D4S2634	0.151	C04	107.337	100.536.239
D4S421	0.302	C04	108.837	101.730.311
D4S2966	0.241	C04	109.006	102.014.105
D4S1591	0.441	C04	109.399	102.671.593
D4S3043	0.186	C04	110.138	104.032.634
D4S1572	0.427	C04	110.139	104.228.523
D4S2907	0.128	C04	111.788	105.600.806
D4S411	0.294	C04	111.789	105.972.23

Marker name	pvalue	Chr	cM	Mb
D4S3256	0.012	C04	113.519	108.344.788
D4S2917	0.109	C04	114.137	109.191.937
D4S1571	0.192	C04	115.567	110.567.028
D4S2945	0.176	C04	116.940	111.727.179
D4S406	0.108	C04	117.484	112.177.195
D4S1651	0.697	C04	118.429	112.591.223
D4S407	0.167	C04	118.708	113.035.536
D4S2989	0.415	C04	118.918	113.257.945
D4S1611	0.077	C04	121.130	114.906.201
D4S1550	0.172	C04	121.931	116.653.045
D4S1573	0.579	C04	123.475	117.602.472
D4S2392	0.237	C04	123.683	118.179.465
D4S3024	0.636	C04	124.632	119.968.282
D4S402	0.064	C04	124.951	120.607.000
D4S427	0.287	C04	125.559	121.885.657
D4S1612	0.116	C04	126.310	122.783.366
D4S2628	0.238	C04	126.735	123.595.743
D4S3250	0.368	C04	127.119	124.376.341
D4S2395	0.296	C04	127.536	124.848.200
D4S1615	0.418	C04	129.752	128.668.469
D4S2625	0.057	C04	130.922	130.592.948
D4S2394	0.450	C04	131.022	130.756.654
D4S429	0.160	C04	133.202	133.570.829
D4S2423	0.269	C04	134.197	134.707.715
D4S1575	0.737	C04	134.670	135.249.176
D4S422	0.086	C04	136.039	137.731.613
D4S1576	0.109	C04	137.791	139.790.032
D4S1579	0.146	C04	139.994	141.308.504
D4S1644	0.217	C04	141.058	142.329.080
D4S424	0.309	C04	142.051	142.775.272
D4S1625	0.008	C04	143.281	144.078.582
D4S1561	0.353	C04	143.282	144.234.597
D4S2981	0.100	C04	143.283	144.871.777
D4S2998	0.588	C04	143.474	146.143.819
D4S2376	0.047	C04	143.736	146.479.168
D4S1586	0.282	C04	144.419	147.356.873
D4S2962	0.383	C04	148.056	150.941.622
D4S2428	0.298	C04	149.001	153.317.810
D4S1588	0.306	C04	149.878	154.407.632
D4S3049	0.497	C04	152.638	155.352.160
D4S3021	0.389	C04	153.058	155.513.457
GATA72A08	0.022	C04	153.507	156.541.479
D4S3016	0.384	C04	154.047	157.181.422
D4S1629	0.125	C04	155.649	158.914.437
D4S413	0.074	C04	155.662	158.930.781
D4S1626	0.180	C04	159.118	163.250.935
D4S1653	0.196	C04	159.119	163.265.511
D4S3046	0.286	C04	159.326	163.968.418
D4S2952	0.148	C04	164.316	167.033.202
D4S417	0.086	C04	165.503	168.815.985
D4S1596	0.635	C04	166.086	169.642.288
D4S2414	0.004	C04	167.029	170.242.462
D4S1597	0.684	C04	167.278	170.539.004
D4S243	0.145	C04	169.018	171.539.374
D4S2426	0.003	C04	169.127	171.602.093
D4S2373	0.690	C04	169.470	172.238.561
D4S2910	0.431	C04	169.551	172.388.405
D4S1545	0.113	C04	169.956	172.998.657
D4S1617	0.390	C04	169.974	173.012.299
D4S1646	0.041	C04	170.133	173.135.224
D4S2383	0.202	C04	171.766	174.737.686
D4S1595	0.453	C04	171.767	175.013.618
D4S2992	0.028	C04	171.768	175.016.354
D4S2991	0.023	C04	171.769	175.209.438
D4S2431	0.024	C04	171.969	175.516.557
D4S2637	0.329	C04	173.748	176.367.964
D4S1539	0.383	C04	173.749	176.384.029
D4S3028	0.232	C04	174.107	177.285.565
D4S3030	0.349	C04	174.553	177.455.089
D4S415	0.231	C04	177.034	179.407.081
D4S1537	0.365	C04	182.879	182.354.372
D4S1607	0.500	C04	184.143	182.627.444
D4S3005	0.293	C04	184.977	183.377.947
D4S1584	0.250	C04	185.027	183.415.109
D4S2951	0.451	C04	186.756	183.855.996
D4S3015	0.615	C04	187.268	183.988.209
D4S3041	0.095	C04	189.524	184.470.139
D4S2921	0.089	C04	190.057	185.026.592
D4S2920	0.358	C04	190.058	185.026.592
D4S1554	0.207	C04	191.561	185.384.474
D4S2957	0.222	C04	193.088	185.748.786
D4S2954	0.393	C04	193.089	185.748.786
D4S408	0.293	C04	193.499	185.846.914
D4S1535	0.302	C04	193.500	185.931.798
D4S3047	0.293	C04	194.386	186.106.100
D4S3032	0.585	C04	196.926	186.713.818

Marker name	pvalue	Chr	cM	Mb
D4S171	0.370	C04	196.927	186.878.087
D4S1540	0.095	C04	197.042	186.952.248
D4S2924	0.215	C04	197.349	187.147.894
D4S3051	0.512	C04	204.693	188.720.823
D4S426	0.109	C04	207.471	189.803.619
D4S2390	0.071	C04	208.978	190.448.883
D4S1652	0.319	C04	209.268	190.780.219
D4S2930	0.520	C04	209.269	190.792.739

Chromosome 5

D5S2488	0.161	C05	0.001	180.169
D5S392	0.011	C05	0.302	354.902
D5S1981	0.262	C05	1.212	1.207.151
D5S678	0.564	C05	2.087	1.418.486
D5S417	0.103	C05	9.355	3.173.940
D5S1980	0.114	C05	9.984	3.449.302
D5S2849	0.387	C05	10.048	3.477.202
D5S1492	0.529	C05	10.706	3.765.429
D5S405	0.315	C05	10.707	3.994.614
D5S2088	0.223	C05	11.871	4.349.171
D5S406	0.335	C05	13.117	5.046.780
D5S2054	0.297	C05	16.644	5.944.719
D5S635	0.352	C05	18.108	6.365.317
D5S676	0.260	C05	20.701	7.492.225
D5S1953	1.7E-4	C05	20.939	7.711.070
D5S1957	0.006	C05	22.949	8.549.660
D5S807	0.014	C05	24.020	9.260.644
D5S630	0.166	C05	24.872	9.613.700
D5S1486	0.061	C05	27.247	10.192.425
D5S1997	0.256	C05	39.287	17.035.107
D5S486	0.050	C05	39.348	17.224.383
D5S2096	0.529	C05	39.436	17.500.114
D5S2031	0.221	C05	42.230	21.148.887
D5S2074	0.242	C05	42.231	21.198.923
D5S411	0.055	C05	42.572	21.797.061
D5S1473	0.165	C05	43.781	23.040.760
D5S813	0.106	C05	44.360	23.636.743
D5S502	0.538	C05	46.909	25.729.873
D5S814	0.327	C05	46.910	25.930.915
D5S1502	0.080	C05	47.541	26.606.108
D5S419	0.130	C05	47.665	26.704.042
D5S627	0.417	C05	47.666	26.794.302
D5S2113	0.043	C05	47.814	26.821.969
D5S2493	0.086	C05	49.431	29.032.622
D5S819	0.473	C05	51.716	30.919.211
D5S1993	0.405	C05	53.233	31.750.653
D5S1986	0.086	C05	53.234	31.775.925
D5S477	0.067	C05	54.613	31.941.878
D5S1996	0.143	C05	55.307	32.161.481
D5S1470	0.101	C05	55.533	32.537.791
D5S651	0.238	C05	56.415	33.427.560
D5S674	0.079	C05	56.711	33.636.454
D5S2062	0.302	C05	57.537	33.806.278
D5S631	0.232	C05	58.117	34.684.061
D5S426	0.450	C05	58.504	34.808.296
D5S493	0.265	C05	58.626	34.997.660
D5S395	0.157	C05	59.460	35.842.754
D5S2021	0.285	C05	61.330	37.863.179
D5S1460	0.682	C05	64.110	38.681.838
D5S2489	0.221	C05	66.570	39.757.422
D5S418	0.207	C05	66.571	40.061.267
D5S2494	0.401	C05	66.676	40.263.793
D5S1457	0.205	C05	67.098	41.079.360
D5S1969	0.375	C05	70.937	53.258.732
D5S628	0.613	C05	71.142	53.403.723
D5S260	0.248	C05	71.143	53.467.356
D5S2076	0.002	C05	72.099	54.222.748
D5S664	0.346	C05	72.765	54.989.592
D5S407	0.307	C05	73.999	56.010.643
D5S491	0.574	C05	74.875	56.416.939
D5S2102	0.626	C05	75.011	56.825.247
D5S2507	0.242	C05	75.070	56.853.482
D5S1715	0.461	C05	76.226	57.403.928
D5S2107	0.453	C05	76.898	58.165.689
D5S2500	0.117	C05	77.307	58.712.925
D5S1474	0.141	C05	78.714	61.325.678
D5S427	0.237	C05	79.196	62.918.977
D5S1956	0.284	C05	79.237	63.135.147
D5S668	0.421	C05	79.517	63.634.104
D5S2089	0.028	C05	80.819	65.959.674
D5S2072	0.629	C05	80.820	66.058.756
D5S2121	0.122	C05	81.439	66.629.450
D5S2046	0.131	C05</td		

Marker name	pvalue	Chr	cM	Mb
D5S650	0.418	C05	86.166	71.995.579
D5S112	0.425	C05	87.474	73.163.225
D5S1982	0.241	C05	87.769	73.370.672
D5S1988	0.105	C05	87.987	73.539.507
D5S2042	0.286	C05	88.262	73.753.321
D5S2003	0.418	C05	90.541	74.611.746
D5S424	0.552	C05	93.230	76.241.791
D5S1977	0.436	C05	93.898	76.398.575
D5S2041	0.075	C05	94.241	76.757.808
D5S1501	0.369	C05	96.527	78.552.498
D5S672	0.079	C05	97.323	78.971.483
D5S1464	0.092	C05	99.807	80.872.969
D5S2029	0.270	C05	100.921	81.541.343
D5S626	0.696	C05	100.922	81.706.876
D5S620	0.099	C05	100.923	81.757.103
D5S2067	0.420	C05	101.164	81.894.545
D5S641	0.096	C05	101.540	82.087.010
D5S2094	0.146	C05	102.720	82.472.755
D5S1959	0.611	C05	102.721	82.671.642
D5S1948	0.277	C05	102.868	82.996.671
D5S1716	0.213	C05	103.799	83.629.120
D5S107	0.280	C05	103.800	83.683.640
D5S1459	0.222	C05	104.446	85.254.845
D5S428	0.351	C05	104.447	85.494.696
D5S617	0.474	C05	104.729	86.166.534
D5S2495	0.358	C05	105.382	87.158.000
D5S1722	0.006	C05	105.718	88.484.230
D5S401	0.418	C05	105.719	88.651.978
D5S2103	0.439	C05	106.031	88.812.866
D5S1725	0.290	C05	106.879	89.250.675
D5S488	0.129	C05	107.141	89.385.709
D5S618	0.184	C05	107.142	89.850.389
D5S2044	0.319	C05	107.383	89.894.508
D5S1463	0.004	C05	107.622	90.290.331
D5S815	0.011	C05	108.004	91.074.519
D5S2499	0.014	C05	108.005	91.520.244
D5S652	0.254	C05	111.248	95.881.262
D5S644	0.158	C05	111.252	95.886.766
D5S484	0.163	C05	111.829	96.656.668
D5S1467	0.237	C05	112.878	98.056.931
D5S1503	0.028	C05	113.021	98.247.876
D5S495	0.175	C05	114.118	99.706.082
D5S456	0.509	C05	114.824	102.665.056
D5S409	0.340	C05	114.892	102.806.070
D5S505	0.444	C05	114.893	103.277.485
D5S433	0.041	C05	115.442	104.038.838
D5S669	0.524	C05	115.446	104.051.362
D5S1721	0.017	C05	115.609	104.496.766
D5S1461	0.183	C05	115.672	104.658.453
D5S460	0.383	C05	115.819	105.035.091
D5S2084	0.312	C05	116.407	106.676.828
D5S475	0.448	C05	117.584	107.029.043
D5S1453	0.821	C05	117.831	107.814.207
D5S1466	0.391	C05	118.234	109.095.769
D5S2496	0.375	C05	118.322	109.171.574
D5S2501	0.077	C05	119.416	110.112.531
D5S492	0.628	C05	119.595	110.328.042
D5S2027	0.555	C05	120.952	111.221.634
D5S1965	0.159	C05	120.953	111.885.714
D5S346	0.134	C05	121.259	112.289.840
D5S656	0.117	C05	121.609	112.751.103
D5S2001	0.265	C05	121.610	112.870.998
D5S421	0.362	C05	121.611	112.930.358
D5S489	0.091	C05	122.271	113.579.976
D5S2065	0.428	C05	122.491	113.797.372
D5S659	0.210	C05	122.492	114.193.690
D5S1720	0.191	C05	122.574	114.294.903
D5S1484	0.167	C05	122.714	114.468.995
D5S2055	0.351	C05	123.592	115.373.017
D5S404	0.100	C05	127.059	116.923.415
D5S494	0.019	C05	127.060	117.063.732
ATA24E05	0.150	C05	128.044	118.166.530
D5S1478	0.003	C05	128.045	118.987.001
D5S471	0.218	C05	128.046	119.125.159
D5S1505	0.436	C05	128.059	119.177.862
D5S657	0.044	C05	128.418	120.487.110
D5S467	0.462	C05	129.402	121.483.007
D5S1975	0.824	C05	130.375	122.201.083
D5S622	0.238	C05	130.376	122.608.674
D5S1714	0.071	C05	130.377	122.613.187
D5S818	0.386	C05	130.378	123.187.401
D5S2039	0.328	C05	130.782	123.450.385
D5S2098	0.235	C05	131.354	123.821.905
D5S804	0.004	C05	133.108	125.161.282
D5S1495	0.127	C05	133.370	125.426.209
D5S490	0.213	C05	134.522	126.918.914

Marker name	pvalue	Chr	cM	Mb
D5S2078	0.045	C05	135.559	128.239.786
D5S642	0.332	C05	135.563	128.267.679
D5S666	0.257	C05	136.610	130.603.841
D5S2110	0.498	C05	136.694	130.933.629
D5S2057	0.223	C05	136.700	130.945.021
D5S1984	0.313	C05	137.108	131.670.938
D5S2497	0.173	C05	138.213	133.027.948
D5S458	0.222	C05	139.386	134.093.283
D5S2056	0.212	C05	139.431	134.373.781
D5S396	0.299	C05	139.647	134.471.424
D5S2115	0.429	C05	139.988	134.795.463
D5S816	0.636	C05	141.297	135.377.605
D5S393	0.204	C05	141.507	135.777.544
D5S399	0.173	C05	141.644	136.039.751
D5S479	0.173	C05	142.084	136.381.823
D5S1983	0.469	C05	142.229	137.074.111
D5S414	0.195	C05	142.230	137.654.512
D5S500	0.034	C05	142.231	137.923.067
D5S476	0.420	C05	142.648	138.021.297
D5S2009	0.234	C05	142.649	139.124.412
D5S2116	0.254	C05	143.182	139.905.914
D5S658	0.308	C05	143.824	140.401.387
D5S2508	0.183	C05	143.920	140.475.601
D5S2119	8.4E-6	C05	143.921	140.837.059
D5S1979	0.611	C05	143.922	141.153.225
D5S2011	0.438	C05	143.923	141.250.586
D5S2017	0.136	C05	145.351	141.761.627
D5S643	0.355	C05	150.303	145.003.174
D5S436	0.400	C05	150.780	145.232.427
D5S2099	0.135	C05	150.975	145.361.123
D5S2033	0.348	C05	151.927	145.988.591
D5S638	0.168	C05	152.494	146.362.768
D5S2490	0.154	C05	153.719	147.012.816
D5S463	0.189	C05	153.720	147.158.587
D5S2090	0.479	C05	153.721	147.258.402
D5S434	0.459	C05	153.722	147.343.703
D5S413	0.225	C05	155.334	148.395.839
D5S1469	0.360	C05	157.002	149.484.330
CSF1R	0.374	C05	157.029	149.491.378
D5S2015	0.327	C05	157.476	149.606.847
D5S2013	0.375	C05	157.495	149.611.847
D5S636	0.096	C05	158.707	149.925.026
D5S2014	0.198	C05	159.098	149.992.426
D5S2077	0.234	C05	162.081	151.363.736
D5S673	0.062	C05	162.294	151.634.593
D5S410	0.496	C05	162.446	152.803.484
D5S2026	0.315	C05	163.604	153.895.975
D5S487	0.331	C05	164.816	155.649.131
D5S2016	0.710	C05	164.973	155.727.862
D5S2049	0.580	C05	165.956	157.699.927
D5S412	0.382	C05	166.003	158.183.578
D5S403	0.413	C05	168.808	159.866.570
D5S1476	0.369	C05	169.065	160.399.162
D5S1955	0.339	C05	169.178	160.719.698
D5S2118	0.268	C05	169.179	160.734.901
D5S1465	0.366	C05	169.667	161.394.749
D5S2093	0.163	C05	171.446	162.814.741
D5S2066	0.233	C05	171.447	163.333.571
D5S423	0.027	C05	173.705	164.945.487
D5S2032	0.108	C05	173.706	164.958.596
D5S2040	0.164	C05	173.900	165.049.871
D5S415	0.208	C05	174.158	165.171.161
D5S2050	0.313	C05	176.971	166.494.686
D5S1458	0.429	C05	179.478	167.556.631
D5S2045	0.572	C05	181.037	168.305.447
D5S400	0.263	C05	181.337	168.423.764
D5S353	0.151	C05	182.942	168.981.015
D5S1456	0.191	C05	182.996	169.013.415
D5S1713	0.200	C05	183.835	169.380.196
D5S397	0.093	C05	184.164	169.588.322
D5S625	0.064	C05	187.275	170.150.908
D5S462	0.349	C05	188.438	171.179.649
D5S429	0.311	C05	188.774	171.321.480
D5S1960	0.270	C05	189.288	171.494.913
D5S677	0.277	C05	194.836	173.127.248
D5S2108	0.083	C05	196.327	173.552.890
D5S498	0.153	C05	197.374	173.794.600
D5S2008	0.201	C05	204.661	177.679.014
D5S2073	0.056	C05	209.105	179.289.714
D5S408	0.267	C05	210.411	180.097.901

Chromosome 6

D6S1600	0.453	C06	0.459	145.000
D6S344</td				

Marker name	pvalue	Chr	cM	Mb	Marker name	pvalue	Chr	cM	Mb
D6S1713	0.111	C06	12.179	4.285.213	D6S1549	0.128	C06	63.989	41.432.221
D6S1685	0.297	C06	16.205	5.755.814	D6S1017	0.006	C06	65.654	41.724.051
D6S1574	0.291	C06	16.206	5.957.131	D6S1552	0.158	C06	66.136	42.001.964
D6S1591	0.329	C06	16.207	5.965.442	D6S1582	0.266	C06	68.119	43.145.568
D6S1677	0.393	C06	17.425	6.429.281	D6S282	0.121	C06	68.355	43.281.429
D6S1668	0.327	C06	18.030	6.592.882	D6S271	0.224	C06	68.706	43.547.748
D6S1598	0.683	C06	19.309	6.939.085	D6S459	0.007	C06	72.595	45.846.096
D6S1674	0.464	C06	21.285	7.992.244	D6S1638	0.093	C06	74.580	46.517.401
D6S309	0.039	C06	21.603	8.169.920	D6S452	0.363	C06	74.581	46.962.879
D6S277	0.030	C06	21.963	8.449.645	D6S1566	0.393	C06	75.566	47.674.766
D6S263	0.047	C06	22.012	8.494.845	D6S438	0.375	C06	75.838	48.700.476
D6S410	0.332	C06	22.496	8.940.333	D6S1280	0.041	C06	75.881	48.896.676
D6S470	0.128	C06	24.914	10.133.771	D6S269	0.223	C06	75.882	49.223.682
D6S1955	0.013	C06	25.362	10.311.763	D6S2410	0.319	C06	76.414	50.690.363
D6S1279	0.170	C06	30.350	12.292.149	D6S272	0.525	C06	76.515	50.893.184
D6S1034	0.046	C06	30.410	12.315.897	D6S1963	0.059	C06	76.516	50.911.335
D6S1721	0.772	C06	31.851	12.888.277	D6S436	0.381	C06	76.517	50.958.001
D6S1006	0.382	C06	31.852	12.968.137	D6S427	0.165	C06	76.565	51.035.435
D6S1263	0.555	C06	31.972	13.005.891	D6S1960	0.074	C06	80.398	53.551.335
D6S1593	0.556	C06	32.645	13.589.729	D6S1662	0.017	C06	80.508	53.655.585
D6S429	0.091	C06	33.079	14.182.419	D6S1573	0.154	C06	80.509	53.762.653
D6S1653	0.149	C06	34.008	14.557.209	D6S295	0.281	C06	80.764	54.326.016
D6S259	0.271	C06	34.974	14.843.926	D6S1952	0.468	C06	80.970	55.027.060
D6S1578	0.290	C06	34.975	15.129.264	D6S1661	0.546	C06	81.675	55.685.010
D6S1559	0.429	C06	36.339	15.262.356	D6S257	0.311	C06	82.215	55.965.272
D6S289	0.215	C06	36.340	15.389.917	D6S414	0.268	C06	82.776	56.310.923
D6S260	0.235	C06	36.407	15.512.453	D6S1710	0.537	C06	83.262	62.754.790
D6S1630	0.424	C06	36.711	16.070.524	D6S402	0.231	C06	83.263	62.962.235
D6S1676	0.530	C06	36.982	16.182.972	D6S1046	0.432	C06	83.485	63.478.465
D6S1605	0.088	C06	37.432	16.416.483	D6S1048	0.684	C06	83.486	63.478.585
D6S274	0.103	C06	38.951	16.854.120	D6S1628	0.250	C06	83.487	64.091.064
D6S1667	0.061	C06	39.730	17.056.003	D6S1658	0.284	C06	83.762	64.348.222
D6S1567	0.275	C06	40.175	17.552.968	D6S1026	0.494	C06	83.888	65.213.994
D6S1688	0.625	C06	41.809	18.393.054	D6S1551	0.283	C06	84.616	66.551.551
D6S285	0.170	C06	42.257	18.679.007	D6S430	0.242	C06	84.617	67.000.291
D6S1266	0.295	C06	42.609	19.066.659	D6S1275	0.003	C06	85.252	67.237.557
D6S1959	0.263	C06	43.476	20.020.078	D6S1262	0.832	C06	85.633	67.890.892
D6S1700	0.239	C06	43.565	20.117.735	D6S405	0.224	C06	85.806	68.187.643
D6S1678	0.830	C06	43.641	20.142.445	D6S1962	0.027	C06	86.210	68.608.316
D6S422	0.426	C06	44.681	20.478.015	D6S1282	0.006	C06	86.211	68.608.490
D6S1643	0.176	C06	44.690	20.495.058	D6S1619	0.206	C06	86.528	69.716.371
D6S1665	0.308	C06	44.990	21.096.284	D6S467	0.119	C06	86.562	69.920.925
D6S1597	0.624	C06	45.791	21.834.287	D6S313	0.087	C06	86.698	70.925.426
D6S1588	0.126	C06	46.737	22.153.394	D6S455	0.224	C06	88.000	71.514.176
D6S1686	0.382	C06	47.007	22.178.710	D6S1673	0.191	C06	88.115	71.752.119
D6S1029	0.102	C06	47.085	22.185.990	D6S1681	0.472	C06	88.611	72.212.605
D6S1663	0.061	C06	47.949	22.710.740	D6S493	0.155	C06	90.016	73.405.402
D6S1660	0.281	C06	48.373	23.421.755	D6S280	0.328	C06	90.411	73.741.259
D6S461	0.319	C06	48.954	23.689.545	D6S406	0.579	C06	90.567	74.466.307
D6S1691	0.393	C06	49.215	24.032.524	D6S1625	0.077	C06	91.972	77.827.531
D6S276	0.039	C06	49.839	24.293.837	D6S1589	0.110	C06	92.923	78.451.865
D6S1554	0.399	C06	50.779	24.951.730	D6S284	0.253	C06	92.924	79.340.817
D6S1571	0.200	C06	51.181	25.072.257	D6S286	0.198	C06	92.925	79.437.108
D6S1545	0.159	C06	51.421	25.091.182	D6S460	0.451	C06	93.396	80.346.439
D6S1281	0.181	C06	51.597	25.405.006	ATA41H06	0.167	C06	93.533	80.743.134
D6S1558	0.093	C06	52.254	27.140.259	D6S1707	0.607	C06	93.715	81.267.986
D6S1271	0.573	C06	52.425	27.622.406	D6S1052	0.075	C06	93.818	81.481.459
D6S464	0.108	C06	52.502	27.839.683	D6S1646	0.110	C06	94.054	82.190.537
D6S306	0.467	C06	52.829	28.034.074	D6S445	0.548	C06	94.387	82.450.368
D6S1022	0.146	C06	52.830	28.752.616	D6S1020	0.130	C06	95.413	83.974.000
D6S265	0.486	C06	52.990	30.125.635	D6S1634	0.357	C06	95.529	84.624.991
TNFα	0.001	C06	53.691	31.647.141	D6S1627	0.521	C06	95.770	85.402.892
D6S273	0.105	C06	53.751	31.787.969	D6S1270	0.311	C06	96.087	85.578.961
D6S1615	0.027	C06	53.762	31.813.334	D6S1601	0.122	C06	96.088	85.580.118
D6S1014	0.028	C06	53.953	32.263.046	D6S1652	0.110	C06	96.113	85.949.975
SA-99508	2.8E-8	C06	53.991	32.352.019	D6S1004	0.035	C06	96.263	88.153.155
D6S2447	0.002	C06	54.128	32.672.793	D6S1595	0.566	C06	96.287	88.507.535
D6S2444	0.009	C06	54.167	32.764.096	D6S1644	0.169	C06	97.333	89.723.458
D6S497	0.018	C06	54.706	33.497.390	D6S1613	0.215	C06	99.822	90.591.179
D6S1560	0.381	C06	54.707	33.601.540	D6S462	0.625	C06	100.777	90.924.184
D6S1583	0.269	C06	54.708	33.765.987	D6S1570	0.164	C06	101.538	91.189.528
D6S1629	0.504	C06	54.709	33.834.658	D6S450	0.425	C06	102.306	92.017.038
D6S1542	0.118	C06	55.832	34.084.243	D6S1631	0.589	C06	102.307	92.035.935
D6S1618	0.144	C06	55.833	34.151.083	D6S1043	0.066	C06	102.708	92.445.511
D6S439	0.381	C06	57.023	35.198.935	D6S458	0.362	C06	102.773	92.564.745
D6S1645	0.212	C06	57.212	35.629.661	D6S444	0.638	C06	102.774	92.645.844
D6S291	0.253	C06	57.511	36.312.368	D6S417	0.058	C06	102.839	92.649.651
D6S1576	0.389	C06	57.941	36.588.420	D6S275	0.252	C06	102.858	93.060.551
D6S1051	0.118	C06	58.083	36.679.853	D6S1274	0.074	C06	103.081	93.402.093
D6S1602	0.906	C06	58.810	37.479.399	D6S1056	0.184	C06	103.566	94.093.106
D6S1548	0.017	C06	58.911	37.591.002	D6S300	0.360	C06	103.764	94.759.931
D6S1610	0.192	C06	60.495	39.306.459	D6S1720	0.230	C06	103.993	95.080.180
D6S1562	0.120	C06	62.104	40.322.032	D6S1054	0.353	C06	103.994	95.237.521
D6S1607	0.267	C06	62.558	40.571.157	D6S1586	0.120	C06	104.119	95.286.690
D6S1616	0.110	C06	62.692	40.644.574	D6S492	0.219	C06	104.427	95.407.503
D6S1575	0.160	C06	63.694	41.194.460	D6S424	0.449	C06	104.549	95.514.543

Marker name	pvalue	Chr	cM	Mb
D6S1957	0.006	C06	104.749	96.453.593
D6S1041	0.415	C06	104.835	96.855.923
D6S501	0.079	C06	105.792	97.877.215
D6S1060	0.074	C06	105.855	97.962.588
D6S1284	0.004	C06	106.448	98.760.774
D6S1716	0.144	C06	106.469	98.789.625
D6S1717	0.026	C06	107.053	99.718.607
D6S475	0.215	C06	107.458	100.649.646
D6S468	0.209	C06	108.168	101.675.928
D6S1543	0.355	C06	108.545	102.012.704
D6S1642	0.225	C06	109.169	102.315.598
D6S1709	0.548	C06	109.245	102.404.198
D6S283	0.307	C06	109.246	102.405.337
D6S434	0.262	C06	109.319	102.481.509
D6S1580	0.152	C06	109.638	103.515.756
D6S301	0.460	C06	109.756	103.740.526
D6S1015	0.082	C06	110.161	104.512.706
D6S1021	0.043	C06	110.269	104.719.491
D6S447	0.236	C06	111.363	106.079.535
D6S1592	0.419	C06	112.062	106.408.350
D6S278	0.393	C06	115.477	108.373.654
D6S1594	0.174	C06	115.727	108.555.211
ATA56D06	0.102	C06	116.277	108.953.599
D6S1698	0.083	C06	118.753	111.361.272
D6S404	0.142	C06	119.438	111.986.028
D6S302	0.206	C06	119.439	112.044.846
D6S416	0.073	C06	119.653	112.496.846
D6S432	0.498	C06	120.386	112.981.801
D6S423	0.368	C06	120.878	113.571.965
D6S266	0.447	C06	120.963	113.728.211
D6S261	0.350	C06	121.129	114.201.954
D6S401	0.052	C06	121.130	114.412.684
D6S454	0.346	C06	121.154	115.422.972
D6S1706	0.404	C06	122.456	118.248.492
D6S304	0.314	C06	122.973	119.409.831
D6S287	0.180	C06	122.974	119.534.174
D6S1696	0.071	C06	122.984	119.552.149
D6S1278	0.023	C06	123.088	119.732.168
D6S412	0.544	C06	123.255	120.491.373
D6S1657	0.105	C06	123.256	120.650.271
D6S1608	0.181	C06	123.257	120.891.961
D6S1037	0.084	C06	123.352	121.289.596
D6S1712	0.315	C06	123.794	122.115.258
D6S1639	0.079	C06	129.238	125.061.180
D6S408	0.752	C06	129.272	125.079.524
D6S1702	0.214	C06	129.273	125.373.102
D6S1958	0.354	C06	130.893	126.549.104
D6S1030	0.153	C06	131.552	128.676.752
D6S407	0.320	C06	131.678	128.795.246
D6S1690	0.475	C06	131.886	128.815.959
D6S1620	0.679	C06	132.911	129.928.299
D6S1705	0.141	C06	133.732	130.298.343
D6S1040	0.576	C06	134.208	130.966.323
D6S1572	0.365	C06	134.459	131.318.136
D6S435	0.163	C06	134.511	131.543.240
D6S262	0.472	C06	134.549	131.711.201
D6S457	0.321	C06	134.751	131.835.740
D6S1656	0.364	C06	134.761	132.119.382
D6S472	0.136	C06	135.073	132.522.735
D6S413	0.094	C06	135.153	132.626.573
D6S975	0.157	C06	135.969	133.526.852
D6S1038	0.153	C06	136.079	134.037.113
D6S1722	0.250	C06	136.448	134.043.359
D6S1265	0.063	C06	136.719	134.139.067
D6S976	0.382	C06	137.413	134.383.836
D6S270	0.055	C06	138.783	134.635.402
D6S1009	0.042	C06	142.713	137.282.654
D6S1587	0.359	C06	145.180	138.402.176
D6S1569	0.620	C06	146.769	139.034.320
D6S403	0.331	C06	147.750	139.693.776
D6S471	0.232	C06	148.205	139.819.893
D6S1961	0.023	C06	148.815	140.142.314
D6S1684	0.059	C06	148.816	140.164.910
D6S308	0.208	C06	148.928	141.237.134
D6S453	0.589	C06	148.929	141.361.763
D6S1648	0.045	C06	149.252	142.057.453
D6S310	0.632	C06	149.253	142.082.902
D6S1055	0.186	C06	150.079	143.058.441
D6S409	0.464	C06	150.351	143.497.819
D6S1704	0.333	C06	150.576	143.862.551
D6S1003	0.068	C06	150.934	144.574.867
D6S1010	0.746	C06	151.383	145.470.532
D6S1703	0.561	C06	151.648	145.998.361
D6S1042	0.036	C06	151.748	146.515.224
D6S978	0.583	C06	151.998	146.833.467
D6S1637	0.431	C06	154.786	148.812.841

Marker name	pvalue	Chr	cM	Mb
D6S1564	0.152	C06	156.324	149.168.946
D6S1553	0.380	C06	156.739	149.751.514
D6S1687	0.503	C06	158.293	151.054.632
D6S495	0.265	C06	161.064	151.986.724
D6S440	0.240	C06	162.127	152.364.087
D6S290	0.004	C06	163.576	153.115.243
D6S441	0.124	C06	165.048	153.845.292
D6S425	0.200	C06	165.960	154.674.447
D6S473	0.499	C06	167.209	155.276.657
D6S1556	0.243	C06	167.423	155.327.189
D6S1577	0.074	C06	168.000	155.463.361
D6S442	0.050	C06	168.619	155.783.422
D6S1708	0.047	C06	169.009	156.208.589
D6S1633	0.084	C06	170.243	157.005.741
D6S419	0.224	C06	170.827	157.688.322
D6S1612	0.080	C06	171.170	158.040.707
D6S1655	0.203	C06	171.263	158.289.894
D6S437	0.231	C06	171.530	158.673.182
D6S1614	0.094	C06	172.488	159.104.965
D6S1035	0.052	C06	174.334	159.936.423
D6S1581	0.206	C06	174.456	160.186.055
D6S1550	0.157	C06	176.392	161.827.828
D6S411	0.208	C06	176.590	161.940.725
D6S305	0.384	C06	176.923	162.104.464
D6S1599	0.319	C06	179.130	162.748.882
D6S1008	0.067	C06	180.024	163.527.058
D6S1277	0.032	C06	180.806	164.207.029
D6S1273	0.493	C06	181.448	164.654.939
D6S1719	0.210	C06	183.345	165.978.988
D6S264	0.372	C06	185.783	166.618.477
D6S297	0.290	C06	187.646	167.145.972
D6S1697	0.196	C06	189.019	167.753.456
D6S503	0.344	C06	190.173	167.947.283
D6S1027	0.296	C06	192.125	168.965.750
D6S281	0.115	C06	193.435	169.754.316
D6S446	0.309	C06	194.224	170.408.810
D6S1590	0.243	C06	194.670	170.616.374

Chromosome 7

D7S2477	0.132	C07	2.391	257.304
D7S2474	0.160	C07	3.710	723.942
D7S2484	0.061	C07	7.069	2.729.505
D7S2521	0.175	C07	7.516	2.842.315
D7S531	0.633	C07	7.702	2.966.602
D7S2424	0.220	C07	8.620	3.581.378
D7S3056	0.102	C07	8.903	4.237.329
D7S517	0.212	C07	8.904	4.242.252
D7S2445	0.095	C07	9.232	4.359.655
D7S511	0.244	C07	9.471	4.445.035
D7S1492	0.156	C07	10.905	4.958.255
D7S2201	0.084	C07	12.205	5.374.993
D7S481	0.384	C07	12.699	5.875.519
D7S2514	0.518	C07	15.278	7.562.158
D7S641	0.449	C07	17.854	8.458.093
D7S1790	0.364	C07	19.234	8.970.035
D7S2547	0.515	C07	20.891	9.584.772
D7S2464	0.208	C07	20.953	9.819.590
D7S513	0.150	C07	23.238	11.395.687
D7S664	0.677	C07	26.724	13.434.443
D7S2557	0.364	C07	29.624	15.016.673
D7S2508	0.404	C07	32.312	17.326.592
D7S507	0.157	C07	32.456	17.341.382
D7S488	0.473	C07	33.290	18.133.177
D7S638	0.095	C07	33.704	18.512.264
D7S2532	0.195	C07	33.753	18.557.241
D7S2495	0.263	C07	34.178	18.946.424
D7S2559	0.241	C07	34.472	19.119.867
D7S503	0.052	C07	34.473	19.208.228
D7S654	0.382	C07	35.276	19.726.976
D7S2535	0.567	C07	36.405	20.588.814
D7S2562	0.127	C07	37.520	21.229.775
D7S493	0.234	C07	37.926	21.549.405
D7S1795	0.180	C07	38.947	21.818.848
D7S2458	0.503	C07	39.009	21.835.344
D7S1810	0.167	C07	39.937	22.450.100
D7S629	0.223	C07	40.057	22.556.172
D7S682	0.492	C07	40.381	22.826.695
D7S2463	0.369	C07	40.505	23.387.190
D7S673	0.235	C07	40.809	23.590.670
D7S2493	0.246	C07	41.910	24.636.321
D7S1821	0.202	C07	42.153	24.866.968
D7S529	0.744	C07	42.400	25.128.129
D7S2534	0.294	C07	43.058	25.331.543
D7S814	0.409	C07	44.752	27.487.203

Marker name	pvalue	Chr	cM	Mb	Marker name	pvalue	Chr	cM	Mb
D7S516	0.422	C07	45.356	27.939.967	D7S524	0.462	C07	100.345	84.291.310
D7S2515	0.199	C07	46.042	28.453.891	D7S2537	0.008	C07	100.459	84.536.193
D7S435	0.150	C07	48.395	29.134.192	D7S2555	0.176	C07	100.769	85.202.324
D7S2848	0.029	C07	48.643	29.243.608	D7S644	0.289	C07	101.092	85.897.031
D7S1806	0.562	C07	48.653	29.248.064	D7S2481	0.161	C07	101.215	86.187.348
D7S2492	0.398	C07	49.317	29.856.026	D7S630	0.033	C07	102.009	88.055.713
D7S2551	0.378	C11	49.965	33.790.554	D7S492	0.071	C07	103.064	89.178.667
D7S632	0.137	C07	51.196	30.566.829	D7S2410	0.222	C07	103.208	89.991.387
D7S1834	0.035	C07	53.249	31.568.702	D7S2409	0.458	C07	104.927	90.908.190
D7S2252	0.366	C07	53.388	31.815.852	D7S1789	0.212	C07	104.928	91.343.759
D7S817	0.279	C07	53.389	31.878.591	D7S646	0.190	C07	105.215	92.216.215
D7S795	0.045	C07	53.501	31.907.959	D7S689	0.546	C07	105.584	92.335.452
D7S690	0.153	C07	54.241	32.102.277	D7S657	0.339	C07	105.585	92.418.214
D7S656	0.277	C07	55.336	33.939.506	D7S652	0.420	C07	105.586	92.481.394
D7S497	0.239	C07	55.683	34.506.812	D7S2430	0.143	C07	106.052	92.824.706
D7S484	0.464	C07	55.898	35.027.092	D7S1820	0.132	C07	106.243	92.965.700
D7S2250	0.037	C07	55.899	35.120.636	D7S2431	0.196	C07	108.202	94.754.606
D7S2843	0.346	C07	59.299	36.806.505	D7S527	0.049	C07	108.439	95.227.141
D7S2209	0.348	C07	60.296	37.300.670	D7S1812	0.472	C07	108.440	95.369.915
D7S528	0.328	C07	60.519	37.768.947	D7S821	0.066	C07	108.441	95.669.545
D7S2846	0.007	C07	60.570	37.875.639	D7S479	0.164	C07	108.687	95.944.875
D7S2497	0.244	C07	61.049	38.002.272	D7S2539	0.151	C07	108.734	95.997.460
D7S2507	0.358	C07	61.288	38.640.903	D7S476	0.150	C07	108.801	96.071.479
D7S510	0.275	C07	61.944	38.930.562	D7S1796	0.028	C07	108.833	96.164.459
D7S668	0.506	C07	62.474	39.408.673	D7S554	0.096	C07	109.670	96.936.585
D7S485	0.300	C07	62.538	39.478.195	D7S651	0.026	C07	110.764	98.159.987
D7S2524	0.316	C07	63.026	40.004.685	D7S2480	0.383	C07	111.983	99.667.100
D7S521	0.338	C07	63.710	40.742.798	D7S477	0.262	C07	112.712	100.336.839
D7S2469	0.147	C07	63.823	40.864.287	D7S662	0.150	C07	113.058	100.724.072
D7S2454	0.068	C07	64.145	41.165.664	D7S2536	0.509	C07	113.313	101.009.381
D7S691	0.315	C07	64.932	41.770.388	D7S515	0.177	C07	113.541	101.263.969
D7S678	0.214	C07	66.413	43.021.886	D7S666	0.308	C07	113.667	101.308.607
D7S2528	0.768	C07	67.736	44.210.828	D7S518	0.260	C07	113.668	101.422.398
D7S2488	0.494	C07	67.870	44.290.307	D7S2509	0.008	C07	114.476	102.547.756
D7S2436	0.194	C07	68.157	44.460.755	D7S2504	0.246	C07	114.874	103.025.570
D7S2427	0.122	C07	68.159	44.705.473	D7S796	0.022	C07	114.905	103.063.334
D7S519	0.080	C07	70.244	45.856.774	D7S658	0.606	C07	115.091	103.286.763
D7S2558	0.129	C07	70.648	46.378.605	D7S2446	0.102	C07	115.339	103.561.622
D7S679	0.020	C07	71.034	46.876.656	D7S2494	0.111	C07	115.340	103.610.092
D7S670	0.454	C07	71.059	46.909.750	D7S2453	0.179	C07	117.920	105.218.420
D7S2561	0.145	C07	71.060	47.134.207	D7S501	0.086	C07	118.779	106.000.896
D7S665	0.304	C07	71.061	47.156.956	D7S2420	0.195	C07	119.151	106.450.348
D7S2506	0.308	C07	71.695	47.421.234	D7S496	0.122	C07	119.370	106.715.216
D7S1818	0.002	C07	72.323	49.133.676	D7S2459	0.770	C07	120.049	106.892.032
D7S674	0.205	C07	72.890	49.284.034	D7S2456	0.714	C07	120.734	107.243.749
D7S2422	0.049	C07	74.843	50.879.800	D7S692	0.602	C07	120.735	107.900.052
D7S1830	0.050	C07	75.781	51.496.591	D7S2425	0.546	C07	120.736	107.907.529
D7S2467	0.516	C07	75.923	51.611.601	D7S3052	0.102	C07	121.276	108.942.042
D7S506	0.130	C07	76.915	52.626.436	D7S525	0.312	C07	121.355	109.203.739
D7S2475	0.528	C07	77.337	53.352.387	D7S2418	0.211	C07	122.151	109.539.255
D7S2552	0.274	C07	77.773	54.490.367	D7S2554	0.350	C07	124.134	114.002.389
D7S2542	0.198	C07	77.774	54.496.260	D7S687	0.562	C07	124.302	114.140.606
D7S2550	0.301	C07	78.065	54.870.929	D7S2502	0.320	C07	124.816	115.012.666
D7S659	0.110	C07	79.120	55.394.423	D7S2543	0.361	C07	124.817	115.357.523
D7S494	0.622	C07	80.224	57.259.707	D7S486	0.130	C07	124.818	115.449.265
D7S2429	0.113	C07	80.225	61.946.164	D7S522	0.054	C07	124.819	115.627.114
D7S2530	0.188	C07	80.407	63.051.065	D7S2460	0.743	C07	125.576	115.962.467
D7S520	0.307	C07	80.586	64.131.672	D7S633	0.625	C07	125.987	116.565.258
D7S2512	0.336	C07	80.620	64.339.470	D7S677	0.028	C07	125.988	116.693.917
D7S663	0.056	C07	80.698	66.128.018	D7S2847	0.020	C07	126.371	118.374.015
D7S502	0.492	C07	80.864	66.469.152	D7S643	0.022	C07	126.808	120.287.929
D7S482	0.274	C07	80.968	66.681.545	D7S480	0.146	C07	126.982	120.519.555
D7S2503	0.325	C07	81.908	67.417.119	D7S685	0.143	C07	127.867	120.846.854
D7S2489	0.256	C07	82.099	67.608.019	D7S2486	0.429	C07	128.467	121.722.100
D7S2483	0.061	C07	82.706	67.851.935	D7S1809	0.292	C07	128.771	122.165.476
D7S2435	0.283	C07	83.670	68.477.386	D7S2520	0.377	C07	129.445	123.191.875
D7S645	0.068	C07	83.671	68.763.635	D7S648	0.424	C07	129.446	123.412.073
D7S2516	0.076	C07	85.323	70.526.536	D7S2527	0.136	C07	130.119	124.264.685
D7S2415	0.033	C07	86.423	71.145.843	D7S1835	0.586	C07	130.556	124.818.417
D7S653	0.137	C07	86.424	71.254.462	D7S1873	0.144	C07	131.069	125.647.582
D7S672	0.123	C07	86.425	71.274.619	D7S1801	0.031	C07	131.070	125.841.798
D7S2476	0.202	C07	87.243	72.427.508	D7S1874	0.228	C07	131.071	125.933.888
D7S2472	0.654	C07	88.415	73.295.042	D7S514	0.203	C07	131.548	126.582.348
D7S1870	0.434	C07	88.745	73.538.871	D7S635	0.032	C07	131.549	126.828.140
D7S2470	0.289	C07	90.062	75.650.669	D7S2501	0.203	C07	131.550	127.067.013
D7S2455	0.292	C07	90.893	76.983.459	D7S1875	0.216	C07	131.782	127.304.971
D7S2421	0.062	C07	91.245	77.286.030	D7S461	0.067	C07	132.369	127.905.563
D7S669	0.402	C07	91.309	77.484.486	D7S530	0.160	C07	133.201	128.755.458
D7S2499	0.467	C07	92.875	78.053.764	D7S2519	0.532	C07	133.669	129.516.700
D7S634	0.016	C07	94.466	79.460.284	D7S649	0.209	C07	136.400	130.273.891
D7S2443	0.317	C07	94.467	79.499.670	D7S640	0.533	C07	141.630	132.055.891
D7S1797	0.237	C07	95.088	80.180.596	D7S2452	0.581	C07	141.631	132.840.133
D7S660	0.036	C07	95.116	80.210.879	D7S2437	0.188	C07	141.632	132.954.051
D7S2540	0.405	C07	98.490	82.729.036	D7S681	0.415	C07	141.633	132.976.971
D7S2845	0.149	C07	100.343	83.667.476	D7S2438	0.227	C07	141.676	133.327.026
D7S2485	0.262	C07	100.344	83.771.550	D7S631	0.091	C07	141.739	134.356.052

Marker name	pvalue	Chr	cM	Mb
D7S2533	0.489	C07	141.740	133.845.240
D7S500	0.273	C07	142.658	134.524.817
D7S1837	0.099	C07	144.765	136.124.426
D7S509	0.534	C07	145.559	136.726.928
D7S495	0.442	C07	148.415	137.422.254
D7S2560	0.340	C07	148.974	137.607.994
D7S2450	0.327	C07	149.344	137.731.150
D7S684	0.141	C07	149.790	137.958.086
D7S2468	0.413	C07	150.773	138.401.862
D7S2202	0.879	C07	151.860	139.188.647
D7S1824	0.026	C07	152.076	139.419.842
D7S2513	0.174	C07	153.382	140.814.695
MBP	0.079	C07	154.606	141.685.208
D7S2473	0.554	C07	154.517	141.414.279
D7S661	0.399	C07	155.037	142.993.729
D7S794	0.209	C07	155.107	143.115.424
D7S676	0.502	C07	155.315	143.474.406
D7S1798	0.092	C07	156.874	144.768.572
D7S2442	0.634	C07	163.014	147.740.105
D7S2419	0.066	C07	163.234	147.813.772
D7S2426	0.246	C07	165.033	148.864.301
D7S1826	0.548	C07	165.639	150.015.810
D7S642	0.099	C07	166.326	150.348.201
D7S483	0.192	C07	170.597	151.589.916
D7S798	0.092	C07	173.809	152.203.512
D7S2462	0.151	C07	175.859	152.953.365
D7S1807	0.556	C07	176.133	153.053.568
D7S2546	0.483	C07	177.626	153.599.468
D7S637	0.239	C07	178.161	153.795.200
D7S2447	0.211	C07	179.624	153.852.948
D7S550	0.307	C07	183.851	154.934.452
D7S2423	0.642	C07	192.273	157.014.642

Chromosome 8

D8S504	0.095	C08	0.001	1.004.849
D8S264	0.090	C08	3.538	2.117.740
D8S1824	0.193	C08	6.889	3.539.860
D8S262	0.179	C08	6.891	3.664.439
D8S518	0.110	C08	9.788	4.475.009
D8S1099	0.071	C08	15.092	6.163.341
D8S1742	0.158	C08	15.212	6.201.415
D8S277	0.119	C08	15.933	6.504.083
D8S561	0.171	C08	16.667	6.609.423
D8S1819	0.317	C08	16.906	6.737.377
D8S1706	0.453	C08	18.942	6.928.203
D8S1825	0.253	C08	19.634	8.962.119
D8S1469	0.008	C08	20.151	9.127.046
D8S516	0.517	C08	20.795	9.447.350
D8S1721	0.194	C08	20.796	10.177.957
D8S542	0.053	C08	21.483	10.194.817
D8S520	0.104	C08	21.592	10.593.769
D8S1755	0.690	C08	21.615	11.027.533
D8S265	0.288	C08	22.502	11.317.148
D8S1695	0.070	C08	22.615	11.387.131
D8S1759	0.216	C08	22.866	11.515.049
D8S1130	0.064	C08	23.487	11.871.344
D8S552	0.370	C08	24.400	12.752.520
D8S1109	0.152	C08	24.401	12.846.190
D8S1754	0.137	C08	26.086	13.000.035
D8S1790	0.183	C08	26.087	13.076.500
D8S511	0.260	C08	27.057	14.689.791
D8S1827	0.131	C08	27.058	14.828.722
D8S261	0.233	C08	31.254	17.836.462
D8S258	0.290	C08	36.656	20.377.467
D8S280	0.643	C08	36.769	20.437.062
D8S282	0.057	C08	38.639	21.425.082
D8S1116	0.391	C08	38.668	21.440.672
D8S560	0.107	C08	39.006	21.612.119
D8S298	0.331	C08	39.570	21.783.784
D8S1733	0.451	C08	40.797	22.542.514
D8S1752	0.223	C08	42.098	22.690.067
D8S1734	0.417	C08	42.099	22.817.139
D8S1989	0.318	C08	44.594	24.663.049
D8S1771	0.299	C08	45.211	25.463.023
D8S1839	0.106	C08	47.960	27.404.471
D8S1820	0.503	C08	49.166	28.019.515
D8S1809	0.281	C08	49.376	28.213.286
D8S540	0.180	C08	53.849	30.576.154
D8S1769	0.206	C08	54.336	31.203.002
D8S513	0.360	C08	55.975	33.726.888
D8S505	0.397	C08	55.976	34.508.605
D8S1750	0.475	C08	56.663	35.470.956
D8S1722	0.272	C08	58.337	37.718.760
D8S1791	0.427	C08	58.619	38.171.429
D8S2317	0.275	C08	58.940	38.657.741

Marker name	pvalue	Chr	cM	Mb
D8S255	0.345	C08	59.771	39.902.485
D8S532	0.372	C08	61.589	40.805.739
D8S1118	0.366	C08	61.725	41.062.063
D8S531	0.395	C08	63.930	49.073.816
D8S519	0.099	C08	63.937	49.135.436
D8S589	0.255	C08	64.757	50.975.963
D8S1133	0.434	C08	64.758	51.384.557
D8S1815	0.207	C08	66.625	53.048.381
D8S1110	0.182	C08	67.375	53.230.905
D8S509	0.247	C08	69.412	55.643.867
D8S566	0.525	C08	69.582	55.770.038
D8S593	0.118	C08	69.589	55.774.961
D8S1828	0.012	C08	70.222	56.849.959
D8S285	0.491	C08	70.259	57.117.017
D8S1816	0.266	C08	70.573	57.411.067
D8S1102	0.271	C08	70.574	57.460.188
D8S1113	0.004	C08	72.726	59.758.164
D8S1812	0.143	C08	74.169	60.734.658
D8S1986	0.080	C08	75.503	61.785.848
D8S260	0.420	C08	75.632	61.871.769
D8S1718	0.128	C08	76.024	62.085.005
D8S510	0.255	C08	76.603	62.301.392
D8S1843	0.112	C08	76.772	62.307.967
D8S1696	0.148	C08	77.160	63.895.476
D8S512	0.290	C08	78.059	65.443.526
D8S1141	0.207	C08	78.060	65.779.446
D8S1473	0.297	C08	78.061	65.779.662
D8S1748	0.358	C08	78.200	66.001.625
D8S1841	0.248	C08	78.413	66.102.998
D8S553	0.147	C08	78.963	66.982.615
D8S1797	0.261	C08	79.063	67.298.482
D8S1767	0.338	C08	80.232	68.753.317
D8S1775	0.148	C08	80.359	68.876.188
D8S1117	0.139	C08	81.394	69.900.129
D8S543	0.031	C08	81.877	70.062.811
D8S1795	0.015	C08	83.322	70.815.706
D8S1807	0.036	C08	85.891	72.599.348
D8S530	0.190	C08	85.892	72.626.672
D8S279	0.390	C08	86.515	73.037.973
D8S1776	0.193	C08	88.449	73.554.580
D8S1123	0.456	C08	88.860	73.924.349
GATA14E09	0.136	C08	89.282	74.304.290
D8S286	0.264	C08	90.201	75.131.546
D8S594	0.267	C08	91.790	78.425.801
D8S501	0.034	C08	92.177	80.025.846
D8S1705	0.158	C08	92.178	80.295.851
D8S1475	0.190	C08	92.179	80.799.537
D8S1730	0.231	C08	92.709	81.242.257
D8S275	0.079	C08	95.267	82.451.349
D8S525	0.078	C08	95.268	82.609.997
D8S1697	0.233	C08	95.579	83.318.960
D8S1119	0.112	C08	97.166	87.128.399
D8S1707	0.410	C08	97.461	87.844.835
D8S1800	0.836	C08	98.311	89.651.363
D8S1811	0.331	C08	99.053	91.189.228
D8S270	0.449	C08	99.732	92.976.952
D8S1988	0.032	C08	100.064	93.447.012
D8S1794	0.573	C08	102.510	95.538.194
D8S1699	0.110	C08	102.988	95.966.053
D8S1822	0.281	C08	103.905	96.683.446
D8S1127	0.215	C08	103.955	96.751.853
D8S1789	0.494	C08	107.604	100.626.124
D8S559	0.158	C08	107.877	101.365.835
D8S546	0.226	C08	107.971	101.393.316
D8S1762	0.614	C08	108.054	101.417.619
D8S1714	0.154	C08	110.271	102.065.966
D8S521	0.501	C08	110.624	102.262.580
D8S545	0.375	C08	112.948	103.401.961
D8S1834	0.049	C08	113.420	103.669.592
D8S1844	0.127	C08	115.094	105.827.386
D8S1784	0.625	C08	115.270	106.059.755
D8S1703	0.652	C08	115.463	106.305.444
D8S1830	0.853	C08	116.035	107.373.916
D8S1122	0.006	C08	118.251	110.383.726
D8S1470	0.019	C08	118.703	112.178.119
D8S539	0.345	C08	119.407	113.834.400
D8S1139	0.049	C08	119.417	114.208.192
D8S555	0.425	C08	119.424	114.344.261
D8S1142	0.104	C08	119.557	114.713.791
D8S565	0.363	C08	120.145	116.353.875
D8S547	0.132	C08	120.146	116.418.699
D8S1694	0.694	C08	121.454	118.300.887
D8S592	0.124	C08	121.532	118.412.739
D8S527	0.266	C08	122.026	119.122.766
D8S522	0.180	C08	122.341	119.517.035
D8S1823	0.357	C08	123.300	120.458.713

Marker name	pvalue	Chr	cM	Mb
D8S269	0.509	C08	123.301	120.530.482
D8S586	0.067	C08	123.995	121.142.315
D8S1112	0.013	C08	124.637	121.707.183
D8S1101	0.562	C08	125.653	122.601.539
D8S1726	0.477	C08	127.600	123.690.782
D8S514	0.151	C08	127.609	123.698.690
D8S1826	0.170	C08	128.731	123.812.750
D8S1804	0.166	C08	130.541	124.821.163
D8S1832	0.389	C08	131.565	125.404.436
D8S1799	0.288	C08	131.797	125.533.359
D8S1179	0.078	C08	132.064	125.852.693
D8S1461	0.550	C08	132.391	126.243.788
D8S266	0.299	C08	133.027	126.652.020
D8S568	0.093	C08	133.086	126.690.172
D8S1793	0.402	C08	135.126	127.262.050
D8S1813	0.253	C08	136.239	127.638.661
D8S1128	0.041	C08	138.939	128.551.737
D8S1720	0.548	C08	140.458	128.906.338
D8S263	0.340	C08	141.475	129.257.364
D8S1780	0.810	C08	142.703	130.632.548
D8S1732	0.239	C08	143.015	130.695.777
D8S1701	0.559	C08	143.056	130.846.435
D8S284	0.215	C08	143.224	131.468.211
D8S1712	0.112	C08	143.591	131.608.673
D8S1985	0.252	C08	144.774	132.198.393
D8S557	0.185	C08	145.650	133.046.805
D8S256	0.372	C08	148.757	134.400.852
D8S1990	0.305	C08	149.415	134.531.412
D8S1710	0.223	C08	150.194	135.607.365
D8S537	0.219	C08	150.928	135.800.522
D8S1753	0.103	C08	151.960	136.697.036
D8S1111	0.039	C08	152.022	136.785.917
D8S1100	0.495	C08	152.211	137.057.639
D8S272	0.282	C08	153.678	137.706.378
D8S1837	0.092	C08	157.789	139.598.979
D8S1743	0.560	C08	160.009	140.621.011
D8S1717	0.362	C08	162.608	141.533.775
D8S1836	0.184	C08	167.477	143.813.354

Chromosome 9

D9S917	0.387	C09	0.001	434.256
D9S1779	0.012	C09	0.002	506.799
D9S1858	0.283	C09	0.260	687.007
D9S939	0.819	C09	7.846	3.345.943
D9S1871	0.187	C09	8.581	3.849.166
D9S288	0.099	C09	8.716	3.941.638
D9S1873	0.220	C09	8.717	4.027.483
D9S178	0.189	C09	8.718	4.111.245
D9S1813	0.044	C09	9.595	4.123.677
D9S1792	0.690	C09	9.910	4.256.413
D9S1686	0.107	C09	11.931	4.634.417
D9S1810	0.138	C09	12.758	4.817.621
D9S935	0.179	C09	13.227	5.190.385
GATA62F03	0.330	C09	13.227	5.190.389
D9S1681	0.162	C09	13.335	5.276.035
D9S1852	0.153	C09	14.337	6.225.983
D9S324	0.317	C09	14.706	6.575.674
D9S281	0.306	C09	14.991	6.846.364
D9S1849	0.202	C09	16.605	7.291.403
D9S286	0.082	C09	18.529	8.043.377
D9S1676	0.250	C09	19.248	8.360.124
D9S144	0.046	C09	22.042	9.591.059
D9S775	0.033	C09	22.984	10.005.994
D9S921	0.085	C09	24.104	10.499.434
D9S168	0.556	C09	24.283	10.578.255
D9S256	0.120	C09	24.939	10.996.450
D9S267	0.269	C09	27.586	12.903.284
D9S1687	0.361	C09	27.659	12.965.100
D9S268	0.310	C09	27.993	13.046.166
D9S1808	0.367	C09	28.239	13.412.991
D9S274	0.232	C09	31.457	14.344.485
D9S285	0.373	C09	34.860	16.067.944
D9S1782	0.059	C09	34.861	16.131.305
D9S156	0.322	C09	35.346	16.234.090
D9S1839	0.470	C09	36.171	16.408.748
D9S157	3.4E-4	C09	37.621	17.618.218
D9S925	0.071	C09	38.109	18.279.027
D9S1684	0.204	C09	41.709	19.605.770
D9S162	0.578	C09	41.710	19.669.802
D9S1778	0.140	C09	42.948	20.347.763
D9S1846	0.681	C09	43.849	21.626.545
D9S1814	0.646	C09	44.971	22.078.175
D9S1870	0.299	C09	44.972	22.092.920
D9S932	0.177	C09	47.075	24.426.324
D9S171	0.174	C09	47.163	24.524.208

Marker name	pvalue	Chr	cM	Mb
D9S1679	0.463	C09	47.849	24.770.113
D9S1833	0.273	C09	48.184	24.960.457
D9S1121	0.372	C09	48.298	25.393.090
D9S265	0.087	C09	48.313	25.448.537
D9S259	0.100	C09	49.852	26.009.818
D9S169	0.468	C09	51.287	27.228.648
D9S161	0.105	C09	53.202	27.622.317
D9S263	0.321	C09	53.571	27.827.351
D9S746	0.091	C09	53.842	27.993.248
D9S1678	0.527	C09	54.417	28.345.115
D9S270	0.001	C09	54.498	28.394.862
D9S1868	0.018	C09	54.748	28.770.769
D9S52	0.076	C09	54.855	29.302.299
D9S1853	0.078	C09	55.170	29.849.713
D9S248	0.058	C09	55.218	29.911.590
D9S43	0.293	C09	55.782	30.870.553
D9S147E	0.634	C09	55.851	31.034.743
D9S304	0.227	C09	56.439	32.313.898
D9S1788	0.242	C09	56.885	33.125.842
D9S1845	0.452	C09	56.896	33.146.800
D9S165	0.516	C09	56.905	33.163.287
D9S1878	0.361	C09	57.151	33.611.299
D9S1817	0.298	C09	58.233	33.849.625
D9S1805	0.375	C09	58.507	34.186.859
D9S163	0.167	C09	58.959	35.116.935
D9S1794	0.064	C09	59.488	36.206.217
D9S1874	0.508	C09	61.257	37.212.264
D9S226	0.202	C09	66.059	42.449.847
D9S1844	0.390	C09	66.132	42.528.253
D9S1787	0.088	C09	67.670	66.952.474
D9S273	0.604	C09	68.860	67.996.513
D9S166	0.703	C09	69.020	68.645.984
D9S301	0.028	C09	69.105	69.259.776
D9S237	0.196	C09	69.478	69.907.699
D9S1822	0.741	C09	70.095	70.387.423
D9S1876	0.056	C09	70.422	70.689.812
D9S927	0.274	C09	71.053	72.280.180
D9S175	0.256	C09	72.803	73.404.673
D9S284	0.065	C09	72.939	73.543.059
D9S1807	0.128	C09	74.411	74.339.896
D9S1860	0.641	C09	76.413	74.937.640
D9S1674	0.222	C09	76.609	75.378.359
D9S1123	0.165	C09	78.109	75.881.992
D9S153	0.607	C09	79.008	77.038.449
D9S1780	0.370	C09	79.231	77.326.002
D9S1867	0.158	C09	79.706	77.907.287
D9S1843	0.219	C09	79.874	77.996.261
D9S922	0.351	C09	80.084	78.425.401
D9S303	9.3E-5	C09	82.725	80.348.012
D9S1785	0.356	C09	83.036	80.750.839
D9S264	0.105	C09	83.379	80.909.717
D9S167	0.205	C09	83.380	81.241.126
D9S152	0.454	C09	83.729	81.562.770
D9S1877	0.908	C09	84.244	81.897.662
D9S1790	0.034	C09	86.507	83.369.281
D9S776	0.381	C09	86.508	83.825.764
D9S1812	0.440	C09	88.464	84.780.736
D9S1680	0.173	C09	89.230	85.078.711
D9S257	0.108	C09	90.809	85.747.861
D9S278	0.277	C09	94.750	87.309.429
D9S906	0.093	C09	95.240	87.626.140
D9S318	0.214	C09	96.872	88.283.121
D9S1836	0.099	C09	97.381	89.027.688
D9S1796	0.292	C09	97.493	89.191.608
D9S1842	0.810	C09	97.494	89.242.592
D9S1781	0.294	C09	98.124	89.765.778
D9S1841	0.052	C09	98.125	89.770.565
D9S1803	0.189	C09	99.398	91.415.243
D9S197	0.306	C09	99.399	91.606.105
D9S196	0.439	C09	99.400	91.815.415
D9S280	0.062	C09	100.681	92.476.821
D9S1816	0.198	C09	101.399	93.618.205
D9S287	0.343	C09	101.542	93.845.927
D9S1809	0.285	C09	101.543	93.938.395
D9S1851	0.413	C09	102.533	94.950.558
D9S1786	0.496	C09	102.739	94.419.849
D9S180	0.342	C09	103.254	96.029.311
D9S910	0.049	C09	104.520	97.003.578
D9S272	0.200	C09	104.828	97.130.987
D9S176	0.157	C09	105.570	97.437.999
D9S1783	0.178	C09	105.571	97.612.364
D9S173	0.623	C09	105.572	98.522.188
D9S1857	0.264	C09	105.573	98.617.627
D9S1690	0.026	C09	106.996	99.480.009
D9S271	0.226	C09	108.498	101.095.232
D9S277	0.236	C09	108.562	101.148.033

Marker name	pvalue	Chr	cM	Mb
D9S1866	0.061	C09	110.672	103.238.471
D9S299	0.369	C09	111.572	104.070.276
D9S1677	0.202	C09	115.917	107.317.363
D9S1835	0.858	C09	116.231	107.432.806
D9S160	0.309	C09	116.232	107.758.834
D9S2026	0.152	C09	116.664	108.011.711
D9S1675	0.333	C09	117.445	108.468.845
D9S1854	0.302	C09	117.465	108.489.819
D9S1828	0.069	C09	117.673	108.712.553
D9S2128	0.079	C09	117.958	108.906.526
D9S1683	0.399	C09	118.453	109.243.032
D9S1880	0.170	C09	118.454	109.425.558
D9S1688	0.045	C09	118.984	109.761.087
D9S1856	0.201	C09	119.874	110.323.134
D9S174	0.546	C09	120.704	111.201.223
D9S779	0.801	C09	120.800	111.268.539
D9S262	0.179	C09	120.984	111.398.750
D9S289	0.424	C09	122.791	111.791.612
D9S1824	0.180	C09	123.555	112.268.150
D9S1855	0.516	C09	124.282	112.886.960
D9S155	0.624	C09	124.821	113.274.491
D9S1776	0.351	C09	124.822	113.335.479
D9S926	0.463	C09	124.823	113.337.855
D9S907	0.008	C09	124.903	113.804.899
D9S241	0.058	C09	126.005	114.277.281
D9S170	0.101	C09	126.418	114.443.355
D9S322	0.447	C09	126.419	114.518.429
D9S154	0.434	C09	126.422	114.716.722
D9S1802	0.218	C09	126.757	114.999.339
D9S934	0.021	C09	127.719	116.471.799
D9S275	0.285	C09	128.606	116.962.390
D9S1848	0.520	C09	128.607	117.112.910
D9S1872	0.324	C09	128.719	117.165.546
D9S195	0.077	C09	129.444	117.505.460
D9S258	0.211	C09	131.142	118.302.371
D9S1850	0.421	C09	131.492	118.826.137
D9S1823	0.145	C09	131.571	119.076.282
D9S1685	0.299	C09	131.807	119.817.606
D9S1682	0.544	C09	132.086	120.369.230
D9S282	0.191	C09	134.614	122.184.754
D9S242	0.066	C09	134.698	122.245.196
D9S1840	0.141	C09	135.910	122.663.324
D9S1825	0.177	C09	136.348	123.264.177
D9S266	0.112	C09	136.500	124.108.336
D9S1798	0.559	C09	137.044	124.548.441
D9S1821	0.072	C09	137.485	124.705.570
D9S1819	0.086	C09	138.508	125.577.320
D9S904	0.450	C09	138.597	125.613.315
D9S290	0.202	C09	139.866	126.903.497
D9S260	0.210	C09	139.943	127.094.465
D9S1795	0.313	C09	142.116	127.682.537
D9S1861	0.137	C09	143.702	128.646.791
D9S1863	0.032	C09	143.914	128.775.890
D9S179	0.333	C09	146.844	130.367.635
D9S1847	0.135	C09	149.199	130.712.977
D9S1830	0.332	C09	149.357	130.991.806
D9S164	0.307	C09	150.640	131.531.975
D9S1818	0.623	C09	154.264	132.578.283
D9S1826	0.562	C09	162.103	133.887.592
D9S158	0.468	C09	162.764	134.538.389
D9S1838	0.156	C09	164.102	135.855.330

Chromosome 10

D10S249	0.172	C10	1.190	234.790
D10S594	0.232	C10	2.772	1.577.986
D10S1435	0.185	C10	5.709	2.197.272
D10S1745	0.093	C10	5.990	2.513.371
D10S533	0.704	C10	6.930	2.683.408
D10S1706	0.082	C10	8.716	2.840.249
D10S1218	0.154	C10	11.297	3.066.976
D10S591	0.181	C10	14.952	4.363.185
D10S552	0.324	C10	15.994	4.731.038
D10S1729	0.415	C10	16.001	4.798.170
D10S1713	0.507	C10	17.147	5.282.570
D10S189	0.142	C10	20.561	6.725.879
D10S1751	0.021	C10	21.776	7.199.611
D10S1691	0.611	C10	21.994	7.315.613
D10S1779	0.014	C10	23.688	8.215.887
D10S226	0.075	C10	25.805	8.922.794
D10S1649	0.404	C10	26.554	9.424.072
D10S547	0.191	C10	28.717	10.554.415
D10S1216	0.107	C10	29.731	11.700.179
D10S1705	0.418	C10	31.776	12.593.551
D10S1430	0.117	C10	32.113	12.740.995
D10S2325	0.110	C10	32.114	12.796.951

Marker name	pvalue	Chr	cM	Mb
D10S1721	0.125	C10	32.449	12.924.114
D10S570	0.175	C10	32.732	12.929.170
D10S223	0.360	C10	35.110	13.835.273
D10S1664	0.474	C10	36.818	14.307.868
D10S191	0.227	C10	37.420	14.563.668
D10S1653	0.320	C10	38.925	15.681.867
D10S674	0.130	C10	41.189	16.523.137
D10S1477	0.135	C10	41.261	16.586.033
D10S1661	0.441	C10	41.399	16.707.223
D10S1476	0.109	C10	41.453	16.728.357
D10S548	0.762	C10	44.682	18.725.141
D10S1714	0.278	C10	45.146	18.843.971
D10S1423	0.022	C10	45.549	19.441.699
D10S563	0.484	C10	47.757	23.419.915
D10S550	0.466	C10	48.603	24.157.107
D10S1673	0.199	C10	48.923	24.475.255
D10S582	0.303	C10	49.045	24.486.629
D10S586	0.354	C10	50.048	24.699.968
D10S572	0.735	C10	50.767	25.641.090
D10S197	0.438	C10	51.416	26.530.886
D10S111	0.729	C10	52.138	26.774.660
D10S1641	0.482	C10	52.701	27.182.999
D10S1733	0.449	C10	53.057	27.535.922
D10S1215	0.069	C10	53.162	27.640.059
D10S611	0.101	C10	53.174	27.651.533
D10S588	0.514	C10	53.626	28.492.610
D10S600	0.174	C10	54.324	28.664.110
D10S1732	0.461	C10	55.870	29.284.985
D10S213	0.336	C10	56.479	29.477.074
D10S224	0.300	C10	57.362	29.622.562
D10S204	0.440	C10	57.363	29.732.706
D10S1684	0.384	C10	57.364	30.006.070
D10S1426	0.171	C10	59.126	30.499.790
D10S193	0.691	C10	59.127	30.577.300
D10S1674	0.064	C10	59.944	30.820.805
D10S208	0.591	C10	61.445	31.684.089
D10S1781	0.327	C10	61.446	31.820.202
D10S1243	0.028	C10	61.581	32.261.198
D10S199	0.448	C10	61.611	32.357.145
D10S1654	0.305	C10	61.971	33.531.698
D10S1666	0.645	C10	62.127	33.696.501
D10S675	0.218	C10	62.690	34.292.054
D10S1208	0.367	C10	63.608	35.261.637
D10S1247	0.280	C10	63.892	35.562.013
D10S1780	0.236	C10	63.893	35.893.689
D10S1217	0.217	C10	63.894	36.164.922
D10S1768	0.512	C10	63.895	36.193.482
D10S578	0.515	C10	64.717	37.046.091
D10S1791	0.473	C10	64.774	37.105.618
D10S1746	0.563	C10	65.421	42.302.761
D10S1669	0.176	C10	66.257	43.409.944
D10S1783	0.264	C10	66.495	43.724.452
D10S604	0.416	C10	66.792	44.120.734
ZNF22	0.082	C10	67.282	44.776.222
D10S225	0.480	C10	71.446	51.325.898
D10S196	0.152	C10	71.950	51.486.884
D10S538	0.049	C10	71.951	51.553.909
D10S1220	0.090	C10	71.952	52.023.167
D10S567	0.204	C10	74.779	54.363.856
D10S539	0.067	C10	74.880	54.405.007
D10S1790	0.278	C10	74.881	54.550.044
D10S1762	0.426	C10	74.888	54.570.866
D10S1643	0.071	C10	74.904	54.616.075
D10S1227	0.527	C10	76.923	56.874.471
D10S596	0.568	C10	76.924	57.031.208
D10S1659	0.197	C10	77.251	58.406.845
D10S207	0.556	C10	78.261	60.421.455
D10S589	0.103	C10	79.972	60.810.894
D10S1794	0.132	C10	80.860	61.653.450
D10S609	0.037	C10	82.334	63.105.061
D10S1652	0.079	C10	82.680	63.752.097
D10S581	0.326	C10	83.705	65.193.908
D10S557	0.164	C10	84.233	66.044.149
D10S1241	0.504	C10	84.376	66.754.575
D10S1743	0.210	C10	84.380	66.771.732
D10S599	0.267	C10	84.381	66.878.638
D10S1646	0.651	C10	85.621	67.967.441
D10S210	0.022	C10	86.715	69.393.795
D10S1418	0.193	C10	87.071	69.857.173
D10S1647	0.316	C10	87.205	70.288.917
D10S560	0.430	C10	89.288	70.898.473
D10S529	0.709	C10	90.052	71.183.865
D10S676	0.046	C10	90.696	71.424.551
D10S537	0.035	C10	91.456	71.739.930
D10S1685	0.020	C10	91.533	7

Marker name	pvalue	Chr	cM	Mb
D10S584	0.495	C10	93.911	72.619.589
D10S1432	0.371	C10	96.367	74.003.999
D10S188	0.262	C10	96.368	74.750.346
D10S195	0.171	C10	97.120	76.963.859
D10S580	0.330	C10	97.935	77.403.299
D10S1752	0.275	C10	98.201	77.676.016
D10S109	0.096	C10	99.042	78.108.546
D10S1730	0.084	C10	99.249	78.275.636
D10S206	0.171	C10	99.887	78.791.010
D10S569	0.513	C10	99.888	78.794.330
D10S607	0.295	C10	100.269	79.309.268
D10S1645	0.235	C10	100.497	79.325.741
D10S1677	0.168	C10	100.715	79.551.628
D10S2327	0.014	C10	101.297	80.056.652
D10S1667	0.417	C10	101.704	80.209.218
D10S1777	0.326	C10	102.064	80.493.839
D10S1786	0.143	C10	105.814	83.597.897
D10S551	0.141	C10	106.801	85.059.693
D10S1686	0.394	C10	107.614	85.230.877
D10S1689	0.089	C10	107.947	85.337.951
D10S1717	0.787	C10	108.324	85.530.059
D10S573	0.258	C10	108.625	85.966.492
D10S1769	0.477	C10	109.758	87.511.585
D10S1698	0.789	C10	109.801	87.569.849
D10S1744	0.294	C10	109.885	87.997.738
D10S1687	0.269	C10	109.957	88.363.867
D10S579	0.049	C10	110.536	89.094.702
D10S215	0.679	C10	110.537	89.130.369
D10S1765	0.499	C10	110.538	89.266.112
D10S541	0.178	C10	110.539	89.656.154
D10S1735	0.099	C10	111.636	90.316.504
D10S1739	0.437	C10	111.637	90.476.680
D10S1753	0.036	C10	113.418	92.077.550
D10S564	0.272	C10	113.419	92.264.249
D10S536	0.597	C10	114.189	92.547.883
D10S583	0.324	C10	114.903	94.033.504
D10S185	0.311	C10	116.043	94.852.709
D10S200	0.558	C10	116.218	94.978.266
D10S677	0.686	C10	117.837	95.628.896
D10S571	0.462	C10	118.143	96.803.027
D10S574	0.332	C10	119.350	98.027.958
D10S1758	0.084	C10	120.396	98.608.140
D10S577	0.421	C10	120.479	98.736.348
D10S1709	0.507	C10	120.748	99.149.952
D10S1726	0.073	C10	122.520	100.376.483
D10S198	0.476	C10	122.901	100.744.925
D10S603	0.077	C10	122.902	101.721.899
D10S1266	0.475	C10	123.468	101.992.625
D10S192	0.087	C10	123.571	102.100.786
D10S1692	0.192	C10	125.147	104.253.452
D10S205	0.067	C10	125.253	104.763.986
D10S540	0.166	C10	125.895	105.823.383
D10S1264	0.150	C10	126.365	106.450.142
D10S1671	0.133	C10	126.366	106.516.775
D10S530	0.801	C10	126.367	107.185.260
D10S566	0.275	C10	127.079	107.652.808
D10S1663	0.026	C10	127.676	108.410.704
D10S1741	0.253	C10	128.195	108.792.877
D10S1795	2.0E-4	C10	128.524	108.945.474
D10S1750	0.330	C10	129.056	109.779.161
D10S1246	0.117	C10	129.439	110.615.849
D10S597	0.862	C10	129.567	110.895.371
D10S543	0.531	C10	130.310	111.503.597
D10S1682	0.063	C10	131.524	112.985.415
D10S1269	0.374	C10	132.299	114.185.994
D10S554	0.285	C10	135.438	115.695.920
D10S1776	0.370	C10	137.871	116.140.680
D10S562	0.635	C10	137.872	116.304.948
D10S1731	0.629	C10	138.002	117.001.647
D10S1773	0.082	C10	139.224	117.708.612
D10S544	0.333	C10	140.013	118.164.613
D10S531	0.093	C10	140.179	118.260.686
D10S1657	0.443	C10	140.457	118.287.426
D10S545	0.469	C10	140.458	118.299.603
D10S187	0.365	C10	140.459	118.317.620
D10S221	0.013	C10	140.886	118.766.354
D10S1425	0.420	C10	141.114	119.004.742
D10S1693	0.298	C10	141.504	119.109.493
D10S190	0.279	C10	143.198	119.510.348
D10S542	0.240	C10	144.639	120.417.003
D10S1792	0.314	C10	145.417	121.042.188
D10S1757	0.212	C10	147.327	121.989.256
D10S209	0.083	C10	147.334	121.995.142
D10S1230	0.208	C10	147.861	122.407.279
D10S1483	0.121	C10	149.635	122.948.181
D10S587	0.264	C10	152.266	124.728.783

Marker name	pvalue	Chr	cM	Mb
D10S1708	0.572	C10	154.369	125.439.499
D10S1656	0.410	C10	154.802	125.676.174
D10S2322	0.125	C10	154.971	125.733.597
D10S75	0.516	C10	160.194	127.506.309
D10S1782	0.007	C10	162.722	128.561.334
D10S1222	0.458	C10	163.397	128.735.149
D10S1727	0.342	C10	163.446	128.800.998
D10S217	0.312	C10	163.607	129.014.639
D10S1676	0.325	C10	164.599	129.480.530
D10S1655	0.376	C10	170.209	130.430.309
D10S1675	0.378	C10	179.397	133.012.693
D10S590	0.609	C10	179.655	133.081.922
D10S212	0.380	C10	181.655	133.883.978
D10S1700	0.308	C10	183.595	134.649.974

Chromosome 11

D11S4177	0.105	C11	0.951	1.454.483
D11S4046	0.038	C11	1.293	1.927.951
D11S1318	0.268	C11	2.485	2.291.499
D11S4088	0.851	C11	3.390	2.719.260
D11S4146	0.229	C11	5.479	3.706.452
D11S1758	0.029	C11	7.234	4.700.189
D11S4181	0.117	C11	7.450	4.732.150
D11S2362	0.138	C11	7.451	4.876.478
D11S1760	0.325	C11	8.786	5.348.645
D11S4124	0.247	C11	8.787	5.523.330
D11S1338	0.368	C11	9.993	5.952.285
D11S1323	0.335	C11	9.994	6.240.913
D11S1331	0.296	C11	12.380	7.256.319
D11S1996	0.053	C11	13.098	7.672.742
D11S932	0.614	C11	14.546	8.355.072
D11S909	0.003	C11	15.362	8.739.788
D11S4188	0.155	C11	16.206	9.031.414
D11S4149	0.208	C11	16.388	9.094.218
D11S4465	0.367	C11	17.280	10.542.515
D11S1329	0.402	C11	17.373	10.681.159
D11S1999	0.150	C11	17.473	10.684.256
D11S1346	0.306	C11	17.950	10.923.683
D11S1349	0.060	C11	20.322	11.716.810
D11S1315	0.639	C11	22.263	12.768.885
D11S4116	0.391	C11	22.553	12.914.982
D11S1794	0.506	C11	22.779	13.300.065
D11S926	0.532	C11	23.075	13.416.774
D11S1348	0.498	C11	23.126	13.833.000
D11S1307	0.020	C11	23.402	14.215.621
D11S4170	0.552	C11	23.403	14.399.823
D11S4193	0.109	C11	23.404	14.801.534
D11S4121	0.433	C11	24.113	15.267.136
D11S1791	0.113	C11	24.114	15.502.161
D11S1397	0.294	C11	25.127	16.161.875
D11S4099	0.040	C11	25.970	16.878.172
D11S4160	0.002	C11	26.125	17.010.026
D11S1981	0.785	C11	26.126	17.050.513
D11S921	0.350	C11	26.127	17.248.732
D11S902	0.612	C11	26.226	17.452.815
D11S4138	0.413	C11	27.544	17.720.060
D11S4130	0.350	C11	27.571	17.725.513
D11S1888	0.185	C11	27.762	17.742.216
D11S1310	0.357	C11	27.930	17.904.237
D11S4096	0.350	C11	28.596	18.545.640
D11S2368	0.036	C11	29.323	19.245.375
D11S899	0.503	C11	29.942	19.383.223
D11S1308	0.188	C11	30.489	19.615.226
D11S4106	0.412	C11	33.406	19.942.108
D11S1755	0.229	C11	35.148	20.217.841
D11S4114	0.335	C11	35.823	20.594.629
D11S1759	0.105	C11	37.747	21.906.811
D11S1359	0.513	C11	38.503	22.404.248
D11S915	0.371	C11	40.130	23.566.877
D11S4164	0.611	C11	41.321	24.390.071
D11S4084	0.100	C11	41.786	24.619.715
D11S4163	0.646	C11	42.670	25.056.552
D11S4080	0.314	C11	43.286	25.665.728
D11S929	0.225	C11	43.467	25.816.248
D11S2361	0.105	C11	43.569	25.901.257
D11S4204	0.054	C11	43.990	26.177.096
D11S930	0.099	C11	44.068	26.259.470
D11S2364	0.035	C11	44.250	26.451.080
D11S904	0.203	C11	44.517	26.644.911
D11S1750	0.296	C11	44.518	26.822.754
D11S1977	0.251	C11	44.909	27.227.260
D11S4152	0.140			

Marker name	pvalue	Chr	cM	Mb
D11S4156	0.556	C11	47.055	29.905.751
D11S4154	0.546	C11	47.631	30.639.833
D11S1312	0.304	C11	48.003	30.964.502
D11S2369	0.037	C11	48.004	31.327.123
D11S914	0.291	C11	48.005	31.327.585
D11S1322	0.049	C11	48.059	31.519.985
D11S4101	0.186	C11	49.145	33.328.829
D11S1776	0.159	C11	49.461	33.506.505
D11S1301	0.031	C11	50.062	33.823.326
D11S2014	0.485	C11	50.260	33.888.541
D11S2010	0.648	C11	51.051	33.932.943
D11S1392	0.201	C11	51.618	34.604.313
D11S907	0.169	C11	51.978	34.631.734
D11S4200	0.265	C11	52.127	34.816.817
D11S4203	0.086	C11	53.645	35.777.766
D11S935	0.522	C11	53.963	35.987.488
D11S4185	0.189	C11	53.964	36.016.248
D11S4083	0.201	C11	54.832	36.457.721
D11S4102	0.315	C11	55.391	36.741.675
D11S1980	0.518	C11	57.083	37.702.634
D11S4148	0.160	C11	57.339	39.143.966
D11S4173	0.028	C11	58.179	40.273.075
D11S1330	0.198	C11	58.180	40.362.429
D11S4455	0.221	C11	58.200	40.369.744
D11S4949	0.396	C11	58.479	40.616.055
D11S905	0.329	C11	58.480	40.938.581
D11S1785	0.525	C11	59.334	42.347.645
D11S1763	0.803	C11	59.833	42.825.724
D11S1355	0.572	C11	59.834	42.886.245
D11S1993	0.272	C11	60.314	43.574.406
D11S903	0.205	C11	60.942	44.110.218
D11S986	0.147	C11	62.768	44.686.491
D11S4133	0.554	C11	62.896	44.727.179
D11S4103	0.336	C11	63.090	44.788.300
D11S1361	0.162	C11	64.013	44.909.839
D11S4174	0.718	C11	64.161	45.222.325
D11S4137	0.125	C11	64.372	45.565.528
D11S1385	0.163	C11	64.640	46.001.731
D11S1344	0.043	C11	64.720	46.131.168
D11S4109	0.307	C11	65.016	47.565.714
D11S4117	0.434	C11	65.028	47.897.801
D11S1784	0.111	C11	65.032	47.987.015
D11S1350	0.304	C11	65.038	48.144.941
D11S4183	0.063	C11	65.041	48.225.425
D11S1326	0.133	C11	65.080	49.288.766
D11S4165	0.465	C11	65.126	50.176.397
D11S1395	0.206	C11	65.175	51.390.911
D11S1920	0.168	C11	65.176	54.964.769
D11S2005	0.332	C11	65.177	55.981.120
D11S1313	0.333	C11	65.178	56.009.418
D11S4459	0.181	C11	65.179	56.289.808
D11S1357	0.188	C11	65.180	56.398.610
D11S1777	0.702	C11	65.419	57.240.863
D11S4202	0.208	C11	65.420	58.141.456
D11S1983	0.048	C11	65.421	58.220.409
D11S2019	0.218	C11	65.450	58.271.602
D11S4075	0.315	C11	66.016	59.288.305
D11S1335	0.433	C11	66.031	59.315.511
D11S2006	0.218	C11	66.143	59.497.248
D11S1368	0.300	C11	66.144	59.497.430
D11S4191	0.431	C11	66.180	59.775.077
D11S1765	0.286	C11	67.160	60.553.899
D11S1286	0.605	C11	67.857	61.002.073
D11S4076	0.519	C11	68.069	61.138.495
D11S4205	0.159	C11	70.273	62.958.211
D11S913	0.198	C11	72.907	65.711.520
D11S1889	0.394	C11	73.566	67.088.503
D11S987	0.451	C11	73.567	67.668.620
D11S1296	0.573	C11	73.712	67.793.140
D11S4087	0.609	C11	73.806	67.874.402
D11S4178	0.284	C11	73.808	67.964.468
D11S4113	0.163	C11	75.015	68.540.986
D11S4095	0.151	C11	76.062	69.041.089
D11S4136	0.248	C11	77.220	69.388.641
D11S4196	0.354	C11	78.805	70.233.883
D11S4162	0.644	C11	79.309	70.702.054
D11S1314	0.539	C11	80.354	72.049.451
D11S4184	0.114	C11	80.499	72.397.151
D11S916	0.591	C11	82.021	72.838.423
D11S4207	0.273	C11	82.239	73.402.063
D11S4119	0.555	C11	82.411	73.845.185
D11S4128	0.416	C11	82.781	74.799.929
D11S4081	0.221	C11	82.827	74.922.615
D11S1902	0.053	C11	82.828	74.949.615
D11S1321	0.253	C11	82.829	75.388.492
D11S4179	0.117	C11	84.131	76.122.568

Marker name	pvalue	Chr	cM	Mb
D11S4186	0.300	C11	84.932	76.694.826
D11S1789	0.127	C11	85.025	76.761.986
D11S4079	0.359	C11	85.026	76.845.729
D11S906	0.461	C11	85.232	77.058.501
D11S911	0.110	C11	85.273	77.174.889
D11S937	0.353	C11	85.418	77.580.628
D11S4166	0.213	C11	85.528	78.173.777
D11S918	0.085	C11	85.529	78.452.601
D11S1352	0.267	C11	86.320	78.550.675
D11S4172	0.311	C11	86.736	78.602.272
D11S1761	0.068	C11	87.281	78.918.230
D11S1362	0.173	C11	88.329	79.526.566
D11S2002	0.159	C11	89.007	79.691.711
D11S4959	0.288	C11	89.550	80.426.282
D11S1396	0.009	C11	90.217	81.300.663
D11S4453	0.003	C11	90.239	81.329.199
D11S901	0.412	C11	90.240	81.570.856
D11S1365	0.291	C11	90.966	82.319.974
D11S4187	0.165	C11	91.227	83.287.332
D11S4147	0.012	C11	91.911	84.256.374
D11S1354	0.146	C11	91.934	84.398.842
D11S2015	0.648	C11	91.999	84.794.040
D11S1979	0.251	C11	92.090	85.345.666
D11S4197	0.242	C11	92.139	85.646.827
D11S1887	0.525	C11	92.140	86.117.328
D11S4082	0.013	C11	93.754	87.006.673
D11S1780	0.046	C11	94.116	87.376.475
D11S1367	0.326	C11	94.159	88.395.672
D11S1367	0.090	C11	94.160	88.395.672
D11S931	0.376	C11	94.849	89.964.066
D11S1358	0.284	C11	94.889	90.054.131
D11S1974	0.056	C11	95.105	90.056.913
D11S1332	0.377	C11	95.898	91.794.878
D11S1995	0.924	C11	96.230	92.029.882
D11S4182	0.207	C11	97.140	93.021.275
D11S1311	0.115	C11	97.141	93.036.155
D11S4118	0.364	C11	97.142	93.047.093
D11S4176	0.156	C11	97.318	93.760.314
D11S1757	0.153	C11	97.944	94.387.483
D11S1788	0.107	C11	97.945	94.516.167
D11S1333	0.120	C11	98.035	94.571.727
D11S919	0.036	C11	100.205	95.717.110
D11S1366	0.023	C11	101.948	96.387.197
D11S917	0.118	C11	102.674	96.666.191
D11S4120	0.027	C11	103.099	97.762.834
D11S1891	0.509	C11	104.175	98.466.175
D11S1317	0.139	C11	105.154	99.988.851
D11S923	0.055	C11	105.155	100.090.053
D11S4100	0.045	C11	105.156	100.122.625
D11S900	0.091	C11	105.157	100.266.509
D11S898	0.294	C11	105.634	100.594.192
D11S940	0.170	C11	106.001	101.010.958
D11S1762	0.163	C11	106.118	101.553.210
D11S1339	0.094	C11	106.127	101.595.222
D11S4159	0.098	C11	107.414	103.666.682
D11S4161	0.340	C11	107.474	103.764.016
D11S1394	0.159	C11	107.537	103.871.027
D11S4951	0.080	C11	107.709	104.162.277
D11S1886	0.564	C11	107.710	104.352.758
D11S2000	0.077	C11	108.423	105.096.395
D11S1325	0.347	C11	108.535	105.212.717
D11S1781	0.638	C11	109.222	106.622.978
D11S1343	0.652	C11	109.425	106.623.503
D11S2017	0.219	C11	109.426	107.055.341
D11S4206	0.404	C11	110.805	109.112.715
D11S1391	0.144	C11	111.774	110.232.767
D11S1793	0.133	C11	111.974	110.413.483
D11S1986	0.054	C11	112.127	110.761.120
D11S4192	0.452	C11	112.387	111.350.110
D11S1347	0.130	C11	113.488	111.669.730
D11S4078	0.427	C11	113.489	111.787.704
D11S1987	0.522	C11	114.689	112.218.349
D11S3178	0.752	C11	114.769	112.360.860
D11S4090	0.113	C11	114.849	112.618.898
D11S3179	0.461	C11	114.850	112.652.962
D11S4122	0.100	C11	115.139	112.982.340
D11S1786	0.420	C11	115.861	113.384.718
D11S938	0.271	C11	116.114	113.442.307
D11S1792	0.903	C11	116.873	113.615.713
D11S1327	0.281	C11	116.874	113.686.813
D11S1885	0.096	C11	117.787	114.526.627
D11S908	0.198	C11	118.662	114.824.952
D11S1992	0.424	C11	118.663	115.188.353
D11S4111	0.248	C11	118.664	115.384.123
D11S4145	0.382	C11	118.665	115.624.579

Marker name	pvalue	Chr	cM	Mb
D11S1340	0.391	C11	119.789	116.124.489
D11S29	0.218	C11	121.818	117.026.011
D11S4092	0.181	C11	121.888	117.057.286
D11S4127	0.680	C11	122.231	117.181.769
D11S1998	0.173	C11	122.378	117.235.382
D11S939	0.101	C11	122.644	117.343.954
D11S1356	0.160	C11	122.725	117.453.600
D11S4195	0.022	C11	122.818	117.534.184
D11S1341	0.501	C11	122.919	117.659.194
D11S1364	0.641	C11	122.992	118.032.178
D11S4104	0.781	C11	122.993	118.173.071
D11S4171	0.151	C11	123.971	118.917.244
D11S4129	0.445	C11	123.991	118.932.198
D11S924	0.188	C11	124.097	118.975.442
D11S4132	0.101	C11	124.673	119.486.027
D11S4460	0.146	C11	126.086	120.129.310
D11S1774	0.522	C11	126.303	120.228.271
D11S925	0.255	C11	126.546	120.365.862
D11S4089	0.008	C11	126.830	120.527.274
D11S4107	0.357	C11	126.911	120.586.657
D11S4167	0.142	C11	128.405	121.687.972
D11S4157	0.155	C11	128.522	121.774.058
D11S1345	0.028	C11	128.605	121.835.436
D11S1336	0.054	C11	129.530	122.176.671
D11S4094	0.407	C11	131.312	122.827.885
D11S936	0.094	C11	131.623	122.831.515
D11S1353	0.038	C11	131.748	122.841.982
D11S4144	0.091	C11	132.379	122.969.002
D11S1316	0.012	C11	132.581	123.009.756
D11S4464	0.033	C11	132.998	123.164.279
D11S4958	0.506	C11	132.999	123.403.555
D11S1328	0.458	C11	133.000	123.565.358
D11S1752	0.457	C11	133.197	123.826.195
D11S933	0.376	C11	133.955	124.209.631
D11S4158	0.149	C11	134.087	124.461.841
D11S1896	0.397	C11	135.303	125.490.912
D11S934	0.210	C11	135.659	125.617.963
D11S4151	0.322	C11	135.733	125.829.622
D11S4110	0.475	C11	138.601	126.509.324
D11S912	0.290	C11	140.628	128.161.744
D11S4123	0.594	C11	140.629	128.197.455
D11S4150	0.065	C11	140.921	128.298.886
D11S4126	0.760	C11	149.138	131.143.342
D11S910	0.275	C11	149.458	131.258.889
D11S1320	0.735	C11	150.173	131.460.047
D11S4198	0.479	C11	150.455	131.520.211
D11S1895	0.636	C11	150.616	131.594.549
D11S4085	0.159	C11	151.626	132.059.798
D11S1309	0.516	C11	153.956	132.748.108
D11S969	0.489	C11	154.041	132.772.414
D11S968	0.107	C11	155.836	133.356.027
D11S4098	0.151	C11	155.838	133.472.332
D11S4125	0.021	C11	155.839	133.592.308

Chromosome 12

D12S352	0.201	C12	0.001	531.651
D12S341	0.270	C12	0.691	719.466
D12S94	0.342	C12	0.917	780.661
D12S91	0.488	C12	1.052	817.436
D12S389	0.067	C12	1.723	984.102
D12S1587	0.077	C12	1.724	1.204.821
D12S1608	0.145	C12	3.761	1.629.392
D12S1656	0.183	C12	4.232	1.677.486
D12S100	0.108	C12	4.879	2.046.822
D12S1689	0.251	C12	4.880	2.205.511
D12S1694	0.399	C12	4.881	2.256.632
D12S1615	0.672	C12	5.771	2.640.633
D12S1626	0.190	C12	7.244	3.165.834
D12S372	0.132	C12	8.635	3.457.623
D12S1050	0.025	C12	8.788	3.538.244
D12S1685	0.071	C12	10.912	3.861.986
D12S1725	0.625	C12	13.608	4.315.826
D12S1624	0.341	C12	14.030	4.581.209
D12S314	0.331	C12	14.439	4.838.576
D12S1594	0.214	C12	15.055	5.014.976
D12S93	0.131	C12	15.490	5.201.115
D12S328	0.293	C12	15.491	5.221.280
D12S99	0.301	C12	15.688	5.434.814
D12S1673	0.254	C12	16.223	5.614.752
D12S356	0.052	C12	16.481	5.718.970
D12S1623	0.036	C12	19.381	6.791.990
D12S1625	0.363	C12	19.877	6.975.688
D12S397	0.253	C12	23.324	8.048.772
D12S1695	0.198	C12	24.646	9.046.709
D12S336	0.189	C12	24.756	9.385.421

Marker name	pvalue	Chr	cM	Mb
D12S1674	0.249	C12	25.048	10.087.237
D12S1690	0.035	C12	25.336	10.171.988
D12S77	0.347	C12	25.571	10.252.834
D12S1697	0.028	C12	26.932	11.685.562
D12S89	0.294	C12	27.103	11.793.256
D12S98	0.373	C12	28.255	11.990.693
D12S391	0.024	C12	28.661	12.341.197
D12S1581	0.044	C12	30.628	12.975.624
D12S320	0.008	C12	31.965	13.513.309
D12S364	0.173	C12	31.966	13.724.569
D12S308	0.126	C12	32.463	14.164.651
D12S1303	0.175	C12	34.062	15.524.891
D12S1728	0.569	C12	34.880	16.227.490
D12S1715	0.549	C12	35.801	16.588.250
D12S1630	0.565	C12	36.095	16.775.403
D12S373	0.275	C12	36.163	16.906.194
D12S1595	0.062	C12	36.475	17.992.461
D12S310	0.340	C12	37.085	18.864.801
D12S1669	0.132	C12	37.444	19.429.660
D12S1650	0.195	C12	38.927	20.161.981
D12S1654	0.152	C12	40.453	21.460.313
D12S1688	0.634	C12	42.904	22.242.686
D12S1606	0.180	C12	43.821	23.275.636
D12S1591	0.165	C12	44.813	23.984.840
D12S1057	0.236	C12	46.484	24.568.411
D12S1617	0.279	C12	46.943	24.991.278
D12S1596	0.566	C12	48.825	25.789.077
D12S1640	0.164	C12	50.652	27.477.571
D12S1042	0.023	C12	51.799	27.538.639
D12S1292	0.046	C12	52.706	28.891.736
D12S1704	0.118	C12	52.931	29.112.094
D12S1053	0.077	C12	52.932	29.224.750
D12S1643	0.279	C12	52.933	29.238.668
D12S1631	0.066	C12	53.363	29.520.879
D12S333	0.005	C12	53.780	29.794.146
D12S87	0.544	C12	54.520	30.279.205
D12S1681	0.653	C12	54.629	30.358.956
D12S1648	0.006	C12	55.253	31.075.728
D12S1584	0.489	C12	55.933	31.610.487
D12S1621	0.243	C12	56.061	31.754.699
D12S345	0.220	C12	56.470	32.216.079
D12S1692	0.161	C12	56.668	32.878.989
D12S2080	0.039	C12	56.796	33.305.760
D12S331	0.048	C12	57.469	37.547.313
D12S2194	0.408	C12	57.658	38.738.007
D12S1048	0.277	C12	57.749	39.312.730
D12S1668	0.316	C12	58.146	39.489.691
D12S1065	0.442	C12	58.276	39.744.812
D12S1589	0.108	C12	58.734	40.641.088
D12S1592	0.194	C12	58.791	40.731.727
D12S1653	0.114	C12	59.019	41.093.479
D12S1301	0.002	C12	59.731	42.348.911
D12S1663	0.411	C12	59.879	42.557.887
D12S85	0.543	C12	61.768	45.622.953
D12S1661	0.303	C12	64.054	46.892.566
D12S1590	0.128	C12	64.566	47.817.076
D12S1635	0.444	C12	65.344	49.323.388
D12S361	0.268	C12	65.912	49.771.435
D12S1633	0.587	C12	65.913	50.179.594
D12S1629	0.391	C12	65.914	50.198.874
D12S347	0.467	C12	66.515	50.298.254
D12S1677	0.264	C12	66.882	50.599.193
D12S1712	0.326	C12	67.314	50.732.163
D12S368	0.375	C12	67.917	50.917.731
D12S390	0.207	C12	68.220	51.157.078
D12S96	0.425	C12	68.532	51.403.180
D12S398	0.019	C12	68.795	51.483.354
D12S1604	0.051	C12	69.992	52.014.232
D12S359	0.241	C12	70.200	52.028.717
D12S1618	0.420	C12	70.242	52.178.882
D12S1586	0.063	C12	70.314	52.433.038
D12S325	0.400	C12	70.315	52.480.591
D12S1622	0.521	C12	71.127	53.053.034
D12S1724	0.225	C12	71.274	53.156.547
D12S1707	0.159	C12	71.478	53.320.311
D12S1632	0.312	C12	73.128	54.701.682
D12S1644	0.107	C12	74.205	55.791.242
D12S90	0.307	C12	74.206	56.710.412
D12S305	0.041	C12	74.453	57.126.464
D12S355	0.072	C12	74.591	57.624.607
D12S1700	0.132	C12	75.367	58.303.040

Marker name	pvalue	Chr	cM	Mb
D12S1726	0.583	C12	76.593	60.746.018
D12S1293	0.197	C12	77.059	61.109.601
D12S329	0.377	C12	77.467	61.428.342
D12S1022	0.355	C12	78.134	61.940.695
D12S1610	0.348	C12	79.851	63.260.582
D12S1585	0.262	C12	79.955	63.339.939
D12S1649	0.001	C12	80.649	63.873.706
D12S1686	0.085	C12	80.750	63.951.347
GGAT1D12	0.706	C12	80.890	64.059.137
D12S1601	0.049	C12	83.191	65.827.019
D12S1291	0.033	C12	83.686	66.220.450
D12S335	0.377	C12	84.111	66.415.787
D12S1676	0.197	C12	84.378	66.499.297
D12S313	0.130	C12	85.041	66.787.095
D12S375	0.035	C12	86.063	67.231.021
D12S1703	0.418	C12	86.227	68.165.095
D12S1680	0.193	C12	86.234	68.202.211
D12S1693	0.721	C12	86.768	68.512.977
D12S1043	0.182	C12	87.056	69.244.866
D12S1722	0.298	C12	87.077	69.298.949
D12S1025	0.052	C12	87.078	69.409.252
D12S80	0.432	C12	88.049	70.309.508
D12S1039	0.133	C12	88.239	71.109.361
D12S1040	0.180	C12	88.266	71.223.694
D12S344	0.096	C12	88.918	72.379.818
D12S92	0.422	C12	88.919	72.420.148
D12S376	0.217	C12	89.204	73.499.976
D12S1052	0.485	C12	89.462	73.895.610
D12S337	0.583	C12	90.049	74.605.590
D12S1660	0.314	C12	90.970	74.748.572
D12S1709	0.086	C12	91.536	75.670.382
D12S1684	0.178	C12	91.595	75.765.705
D12S350	0.322	C12	91.701	75.850.264
D12S326	0.099	C12	92.970	76.476.308
D12S2074	0.034	C12	96.317	78.933.769
D12S1038	0.287	C12	96.683	79.202.978
D12S1708	0.263	C12	97.672	80.907.719
D12S2068	0.181	C12	98.206	81.487.620
D12S1670	0.252	C12	98.623	81.941.677
D12S379	0.059	C12	100.022	83.461.396
D12S81	0.376	C12	100.078	84.010.109
D12S365	0.427	C12	100.079	84.854.125
D12S88	0.400	C12	100.080	84.873.851
D12S1719	0.211	C12	100.081	85.667.821
D12S1593	0.332	C12	100.200	86.157.371
D12S1710	0.021	C12	101.522	88.184.756
D12S1024	0.413	C12	101.654	88.669.174
D12S1678	0.296	C12	101.661	88.696.949
D12S316	0.191	C12	101.797	89.197.329
D12S1717	0.314	C12	101.812	89.251.231
D12S351	0.481	C12	103.104	90.407.809
D12S1699	0.553	C12	103.381	90.648.997
D12S322	0.253	C12	103.457	90.715.695
D12S2077	0.018	C12	103.892	91.094.097
D12S311	0.020	C12	104.024	91.209.459
D12S95	0.192	C12	104.424	91.439.521
D12S1044	0.382	C12	106.026	92.679.329
D12S1346	0.532	C12	106.027	92.686.998
D12S327	0.331	C12	107.127	93.272.754
D12S362	0.462	C12	108.895	94.214.749
D12S309	0.257	C12	110.308	94.967.566
D12S348	0.362	C12	110.309	95.053.063
D12S1716	0.634	C12	110.588	95.447.539
D12S1051	0.302	C12	110.589	96.072.235
D12S1657	0.167	C12	110.590	96.161.901
D12S393	0.038	C12	112.159	97.003.411
D12S1063	0.070	C12	112.160	97.201.954
D12S1706	0.119	C12	112.340	97.371.231
D12S346	0.338	C12	113.367	98.030.790
D12S1641	0.289	C12	114.264	99.087.112
D12S1588	0.609	C12	114.309	99.096.637
D12S332	0.118	C12	114.355	99.450.327
D12S1041	0.467	C12	114.725	99.960.829
D12S1727	0.151	C12	115.045	100.203.407
D12S1070	0.041	C12	115.310	100.361.300
D12S1607	0.026	C12	115.981	100.761.149
D12S1074	0.332	C12	116.518	101.311.345
D12S1030	0.529	C12	116.631	101.427.274
D12S360	0.497	C12	118.289	102.581.591
D12S78	0.118	C12	118.522	102.767.016
D12S338	0.185	C12	118.870	103.043.825
D12S1647	0.252	C12	119.746	103.591.523
D12S317	0.030	C12	119.747	104.099.018
D12S1597	0.216	C12	120.027	104.253.991
D12S1636	0.411	C12	120.165	104.326.613
D12S1683	0.306	C12	120.853	104.687.945

Marker name	pvalue	Chr	cM	Mb
D12S2072	0.099	C12	123.853	105.635.105
D12S330	0.345	C12	123.873	105.682.006
D12S1613	0.389	C12	124.076	106.141.008
D12S353	0.410	C12	124.507	106.534.007
D12S1605	0.311	C12	125.342	107.206.306
D12S84	0.345	C12	125.792	107.524.532
D12S105	0.369	C12	126.510	107.777.605
D12S1583	0.156	C12	127.220	108.287.449
D12S1645	0.200	C12	127.361	108.501.385
D12S1339	0.380	C12	127.381	108.530.473
D12S1344	0.002	C12	128.840	110.737.452
D12S1616	0.201	C12	130.276	111.706.120
D12S1340	0.294	C12	130.315	111.727.116
D12S1646	0.077	C12	133.074	113.222.537
D12S1341	0.368	C12	133.591	113.502.827
D12S354	0.551	C12	133.659	113.539.542
D12S1023	0.763	C12	133.660	113.883.271
D12S369	0.141	C12	134.333	114.023.296
D12S1602	0.515	C12	134.468	114.245.118
D12S79	0.327	C12	134.642	114.472.408
D12S1665	0.133	C12	134.878	114.484.625
D12S2079	0.037	C12	136.543	115.655.910
D12S1718	0.449	C12	137.124	116.064.371
D12S2082	0.784	C12	137.754	116.245.662
D12S1720	0.450	C12	138.872	116.567.129
D12S366	0.271	C12	140.324	116.984.558
D12S86	0.339	C12	141.036	117.582.275
D12S1619	0.486	C12	141.037	117.590.060
D12S1282	0.276	C12	142.043	118.382.006
D12S321	0.456	C12	142.326	118.559.331
D12S395	0.032	C12	142.391	118.600.412
D12S1666	0.485	C12	142.543	118.695.566
D12S1721	0.374	C12	143.185	119.098.086
D12S2073	0.228	C12	144.137	119.695.231
D12S1349	0.290	C12	144.438	120.719.302
GGAT1E2	0.205	C12	144.995	122.711.792
D12S378	0.260	C12	145.072	123.016.088
D12S304	0.381	C12	148.977	124.226.435
D12S1614	0.173	C12	148.984	124.228.549
D12S342	0.366	C12	148.985	124.236.938
D12S340	0.217	C12	150.018	124.494.835
D12S1639	0.132	C12	150.964	124.731.267
D12S324	0.591	C12	151.953	124.978.184
D12S1634	0.235	C12	153.119	125.517.346
D12S307	0.215	C12	153.120	125.569.409
D12S1658	0.140	C12	154.651	125.927.627
D12S2075	0.023	C12	155.986	126.314.140
D12S2078	0.031	C12	155.987	126.314.239
D12S1675	0.131	C12	156.822	126.496.035
D12S1679	0.048	C12	158.885	127.116.253
D12S1659	0.097	C12	163.126	127.769.507
D12S1714	0.052	C12	165.267	128.174.905
D12S1045	0.014	C12	167.939	128.750.569
D12S97	0.277	C12	167.941	128.754.355
D12S343	0.347	C12	169.835	129.157.707
D12S1599	0.178	C12	170.357	129.317.802
D12S392	0.028	C12	171.378	129.580.363
D12S1723	0.493	C12	173.293	130.315.822
D12S1628	0.875	C12	173.736	130.615.875
D12S357	0.150	C12	174.886	131.393.757

Chromosome 13

D13S175	0.564	C13	0.350	18.646.379
D13S1236	6.7E-5	C13	6.410	20.494.180
D13S292	0.294	C13	9.243	21.983.058
D13S1243	0.490	C13	11.572	22.605.962
D13S283	0.281	C13	13.951	23.398.789
D13S1294	0.054	C13	16.580	24.274.909
D13S221	0.061	C13	16.880	24.374.760
D13S1304	0.514	C13	17.865	25.168.018
D13S1244	0.460	C13	19.374	26.044.977
D13S1250	0.405	C13	22.240	26.721.494
D13S1242	0.078	C13	22.651	26.943.011
D13S217	0.298	C13	22.887	27.169.790
D13S1299	0.122	C13	25.022	28.392.417
D13S1246	0.073	C13	27.399	28.903.436
D13S289	0.362	C13	28.145	29.063.702
D13S290	0.023	C13	28.688	29.227.173
D13S893	0.290	C1		

Marker name	pvalue	Chr	cM	Mb
D13S894	0.381	C13	39.629	36.536.509
D13S1808	0.192	C13	39.630	36.536.560
D13S218	0.384	C13	40.440	36.830.230
D13S1253	0.134	C13	42.094	37.944.297
D13S765	0.074	C13	42.373	38.263.372
D13S765	0.032	C13	42.374	38.263.372
D13S1248	0.148	C13	42.632	38.558.005
D13S263	0.022	C13	44.406	39.878.976
D13S1247	0.478	C13	45.336	40.759.681
D13S325	0.132	C13	45.559	40.971.249
D13S1297	0.347	C13	45.560	40.992.311
D13S1227	0.056	C13	45.857	41.340.982
D13S291	0.274	C13	48.833	42.617.141
D13S326	0.113	C13	49.152	42.754.047
D13S1272	0.277	C13	49.534	42.883.627
D13S887	0.257	C13	49.787	43.119.870
D13S161	0.271	C13	52.418	45.581.922
D13S153	0.082	C13	53.084	46.688.734
D13S1269	0.373	C13	54.718	49.005.194
D13S788	0.129	C13	56.345	49.690.623
D13S1325	0.173	C13	56.459	50.276.041
D13S1492	0.046	C13	57.815	53.503.743
D13S321	0.056	C13	57.907	54.381.124
D13S163	0.488	C13	57.987	55.155.708
D13S1319	0.480	C13	57.988	55.457.793
D13S1303	0.013	C13	57.989	56.022.077
D13S146	0.088	C13	58.337	57.082.271
D13S801	0.581	C13	60.558	60.359.585
D13S1320	0.135	C13	60.687	61.601.601
D13S172	0.569	C13	60.688	61.621.119
D13S799	0.077	C13	60.690	62.428.733
D13S1289	0.434	C13	60.693	62.433.106
D13S1317	0.402	C13	62.815	64.863.262
D13S776	0.366	C13	63.027	65.225.302
D13S777	2.0E-4	C13	63.336	66.412.047
D13S276	0.314	C13	64.009	66.807.806
D13S275	0.056	C13	64.043	67.536.664
D13S318	0.461	C13	64.393	68.373.586
D13S279	0.156	C13	65.825	69.393.129
D13S798	0.060	C13	65.997	69.696.956
D13S1257	0.165	C13	69.019	71.230.051
D13S152	0.378	C13	69.020	71.232.387
D13S800	0.191	C13	69.437	71.672.693
D13S1326	0.431	C13	69.621	71.952.924
D13S156	0.554	C13	71.452	72.455.425
D13S891	0.252	C13	71.562	72.617.097
D13S792	0.220	C13	71.839	72.950.367
D13S162	0.072	C13	73.301	73.774.632
D13S1306	0.230	C13	75.055	75.443.319
D13S1281	0.446	C13	75.056	76.260.789
D13S160	0.763	C13	76.427	76.976.601
D13S1263	0.734	C13	77.650	78.620.609
D13S170	0.309	C13	78.012	78.907.129
D13S317	0.084	C13	79.319	80.520.033
D13S231	0.425	C13	79.635	81.087.954
D13S790	0.142	C13	79.942	82.233.228
D13S1235	0.054	C13	80.245	83.142.573
D13S282	0.291	C13	80.656	84.017.632
D13S764	0.186	C13	80.930	84.695.449
D13S1283	0.280	C13	81.265	85.728.453
D13S1239	0.269	C13	82.251	87.574.605
D13S794	0.401	C13	82.387	87.816.866
D13S265	0.021	C13	82.701	88.070.920
D13S1234	0.453	C13	83.585	88.785.696
D13S886	0.008	C13	84.120	89.668.276
D13S795	0.055	C13	84.910	90.388.360
D13S762	0.150	C13	86.535	92.133.575
D13S281	0.103	C13	86.609	92.261.572
D13S775	0.275	C13	86.929	92.461.694
D13S154	0.172	C13	90.766	93.960.282
D13S1280	0.126	C13	90.767	94.445.961
D13S1241	0.560	C13	91.339	95.248.300
D13S1494	0.254	C13	91.340	95.554.017
D13S159	0.122	C13	94.001	96.751.595
D13S770	0.285	C13	94.981	97.329.337
D13S1284	0.056	C13	95.517	97.587.256
D13S1240	0.060	C13	97.561	98.866.808
D13S779	0.665	C13	97.860	99.201.956
D13S147	0.168	C13	98.714	99.750.874
D13S174	0.605	C13	100.117	100.652.077
D13S280	0.200	C13	100.656	101.246.004
D13S158	0.148	C13	101.150	101.674.397
D13S781	0.049	C13	102.388	101.982.020
D13S274	0.517	C13	102.389	102.259.152
D13S1322	0.730	C13	106.711	103.453.158
D13S1809	0.171	C13	107.618	103.830.755

Marker name	pvalue	Chr	cM	Mb
D13S797	0.217	C13	107.619	103.830.779
D13S763	0.230	C13	110.183	104.601.262
D13S173	0.194	C13	111.852	105.504.948
D13S796	0.123	C13	112.167	105.586.966
D13S778	0.343	C13	115.544	106.174.243
D13S1265	0.258	C13	117.119	107.026.457
D13S895	0.191	C13	117.599	107.286.266
D13S1315	0.402	C13	118.998	108.043.245
D13S261	0.436	C13	125.023	109.721.658
D13S285	0.202	C13	126.858	110.743.433
D13S293	0.354	C13	131.920	112.232.432

Chromosome 14

D14S261	0.283	C14	4.517	18.830.515
D14S72	0.040	C14	9.826	19.361.115
D14S1023	0.575	C14	9.827	19.432.028
D14S1003	0.086	C14	14.057	20.106.472
D14S585	0.036	C14	14.058	20.191.160
D14S582	0.052	C14	14.059	20.191.251
D14S283	0.041	C14	15.375	20.677.542
D14S990	0.404	C14	16.121	21.576.515
D14S581	0.168	C14	19.329	22.288.637
D14S64	0.263	C14	19.754	22.550.218
D14S264	0.074	C14	20.405	23.270.071
D14S1041	0.150	C14	20.566	23.472.767
D14S1032	0.454	C14	21.686	24.201.345
D14S1280	0.037	C14	23.036	24.645.919
D14S275	0.028	C14	23.037	24.686.900
D14S615	0.089	C14	25.271	26.506.802
D14S608	0.121	C14	25.342	26.839.483
D14S597	0.039	C14	25.421	27.212.069
D14S1042	0.275	C14	25.456	27.250.521
D14S262	0.527	C14	25.731	27.550.641
D14S740	0.025	C14	25.956	27.757.640
D14S1021	0.474	C14	27.787	29.262.155
D14S257	0.085	C14	29.186	29.719.734
D14S1071	0.263	C14	29.187	29.818.465
D14S1040	0.538	C14	29.807	30.201.451
D14S297	0.319	C14	30.666	30.524.412
D14S741	0.315	C14	34.998	31.743.911
D14S70	0.167	C14	37.632	32.449.232
D14S735	0.053	C14	37.810	32.643.836
D14S551	0.163	C14	37.824	32.659.487
D14S1049	0.420	C14	38.498	32.767.631
D14S988	0.586	C14	39.408	33.502.088
D14S1014	0.288	C14	39.409	33.610.741
D14S253	0.011	C14	39.410	34.204.571
D14S69	0.618	C14	40.774	35.049.317
D14S75	0.375	C14	41.356	35.417.816
D14S306	0.180	C14	42.778	36.318.121
D14S1048	0.305	C14	43.752	37.412.626
D14S278	0.392	C14	43.967	37.968.634
D14S1039	0.394	C14	44.085	38.274.509
D14S579	0.062	C14	44.363	38.915.535
D14S1053	0.587	C14	44.576	39.406.434
D14S79	0.426	C14	44.717	39.841.234
D14S552	0.500	C14	44.875	40.585.663
D14S301	0.070	C14	44.876	40.924.626
D14S266	0.452	C14	45.366	42.084.928
D14S288	0.094	C14	45.367	42.091.881
D14S583	0.075	C14	45.391	42.208.512
D14S259	0.305	C14	46.366	44.087.876
D14S1068	0.335	C14	46.367	45.123.344
D14S1009	0.424	C14	46.798	45.535.671
D14S1277	0.239	C14	46.799	45.711.109
D14S748	0.264	C14	46.800	46.071.316
D14S976	0.296	C14	46.804	46.078.273
D14S1055	0.372	C14	46.896	46.220.957
D14S255	0.093	C14	47.447	47.509.771
D14S984	0.496	C14	47.792	48.087.278
D14S1031	0.548	C14	47.988	48.301.210
D14S978	0.095	C14	50.460	49.903.158
D14S1018	0.506	C14	51.357	50.484.260
D14S589	0.671	C14	51.526	51.370.384
D14S989	0.187	C14	52.341	51.695.069
D15S658	0.317	C14	52.379	51.961.318
D14S587	0.051	C14	53.073	52.356.863
D14S747	0.255	C14	53.425	52.557.684
D14S281	0.485	C14	54.831	53.096.483
D14S991	0.565	C14	55.138	53.213.996
D14S1057	0.214	C14	55.665	53.357.512
D14S276	0.553	C14	56.023	53.673.056
D14S1064	0.619	C14	56.954	54.493.613
D14S1056	0.021	C14	57.206	54.638.430
D14S285	0.004	C14		

Marker name	pvalue	Chr	cM	Mb
D14S66	0.101	C14	58.149	55.040.689
D14S980	0.194	C14	58.402	55.142.608
D14S750	0.130	C14	58.794	55.282.878
D14S274	0.478	C14	59.819	55.649.564
D14S1038	0.303	C14	61.771	57.613.368
D14S586	0.012	C14	62.009	58.792.916
D14S592	0.407	C14	62.216	59.386.897
D14S997	0.631	C14	63.518	60.690.421
D14S290	0.260	C14	64.350	61.522.894
D14S1059	0.255	C14	64.365	61.537.925
D14S1012	0.424	C14	64.794	61.812.419
D14S1001	0.428	C14	64.955	62.083.849
D14S63	0.040	C14	65.284	62.641.061
D14S1026	0.065	C14	65.631	62.710.286
D14S271	0.244	C14	65.633	63.123.322
D14S1046	0.412	C14	65.647	63.173.154
D14S981	0.173	C14	66.827	63.804.444
D14S298	0.963	C14	68.174	65.013.948
D14S1069	0.452	C14	68.320	66.378.231
D14S1011	0.087	C14	69.675	67.555.954
D14S588	0.007	C14	70.011	68.210.327
D14S580	0.135	C14	70.224	68.421.991
D14S1029	0.416	C14	70.283	68.480.441
D14S603	0.245	C14	70.317	68.513.994
D14S258	0.151	C14	70.399	68.572.892
D14S251	0.327	C14	71.136	69.115.621
D14S1002	0.302	C14	71.137	69.291.050
D14S289	0.402	C14	71.410	69.555.244
D14S277	0.339	C14	72.923	71.017.499
D14S268	0.341	C14	73.757	71.261.760
D14S1028	0.098	C14	73.917	71.372.353
D14S986	0.510	C14	74.333	72.499.384
D14S71	0.190	C14	74.334	72.570.883
D14S1025	0.206	C14	74.384	72.229.504
D14S1047	0.100	C14	74.860	72.888.685
D14S999	0.068	C14	74.941	73.315.418
D14S273	0.255	C14	75.467	73.767.915
D14S76	0.170	C14	75.482	73.772.314
D14S1036	0.146	C14	75.696	73.787.009
D14S61	0.119	C14	76.663	74.325.349
D14S270	0.394	C14	77.202	74.640.267
D14S263	0.146	C14	78.785	75.319.515
D14S279	0.223	C14	79.134	75.428.588
D14S983	0.574	C14	79.397	75.510.561
D14S254	0.483	C14	79.852	76.368.769
D14S1020	0.148	C14	79.934	76.482.106
D14S555	0.533	C14	79.978	76.513.423
D14S74	0.193	C14	80.165	76.648.434
D14S1008	0.395	C14	82.328	77.891.953
D14S1000	0.456	C14	83.504	80.095.960
D14S739	0.037	C14	83.774	80.256.560
D14S616	0.158	C14	85.448	83.183.943
D14S604	0.439	C14	85.710	83.707.389
D14S1022	0.582	C14	85.739	83.765.578
D14S1061	0.240	C14	86.019	84.324.214
D14S974	0.288	C14	86.384	84.619.943
D14S73	0.527	C14	87.517	85.072.553
D14S1063	0.424	C14	87.519	85.371.548
D14S1279	0.316	C14	88.601	85.967.707
D14S610	0.177	C14	88.656	86.195.780
D14S1033	0.531	C14	88.657	86.280.271
D14S68	0.313	C14	88.827	86.617.806
D14S1058	0.085	C14	88.837	86.638.159
D14S256	0.136	C14	89.122	87.201.499
D14S1005	0.613	C14	89.371	87.368.049
D14S1066	0.469	C14	91.506	87.792.310
D14S1044	0.418	C14	92.856	88.060.452
D14S280	0.071	C14	96.753	90.172.907
D14S617	0.182	C14	98.807	90.192.831
D14S1015	0.713	C14	97.362	90.726.167
D14S1016	0.467	C14	97.685	90.904.599
D14S1050	0.183	C14	97.687	90.905.564
D14S977	0.080	C14	98.146	91.159.350
D14S302	0.389	C14	98.496	91.352.498
D14S81	0.121	C14	99.251	91.769.846
D14S1062	0.498	C14	99.989	92.327.646
D14S744	0.129	C14	100.045	92.369.718
D14S749	0.360	C14	100.046	92.369.723
D14S1054	0.237	C14	102.520	93.286.637
D14S1030	0.270	C14	103.630	93.592.377
D14S265	0.129	C14	104.241	93.754.008
D14S996	0.515	C14	105.161	93.974.091
D14S62	0.351	C14	105.162	93.979.590
D14S605	0.009	C14	106.081	94.424.331
D14S987	0.393	C14	106.216	94.585.137
D14S611	0.329	C14	108.880	95.523.513

Marker name	pvalue	Chr	cM	Mb
D14S979	0.210	C14	108.968	95.559.240
D14S65	0.269	C14	109.097	95.611.512
D14S998	0.356	C14	109.250	95.734.559
D14S614	0.030	C14	110.207	96.257.276
D14S267	0.005	C14	112.140	97.214.239
D14S250	0.465	C14	117.641	98.448.295
D14S78	0.859	C14	117.655	98.461.781
D14S1426	0.073	C14	117.805	98.609.606
D14S985	0.584	C14	118.781	99.286.651
D14S1051	0.847	C14	121.715	100.220.282
D14S272	0.082	C14	125.008	101.267.965
D14S293	0.554	C14	125.030	101.444.066
D14S260	0.311	C14	125.834	102.380.779
D14S543	0.061	C14	126.126	102.578.886
D14S292	0.546	C14	126.138	102.586.744

Chromosome 15

Marker name	pvalue	Chr	cM	Mb
D15S817	0.004	C15	0.093	22.151.482
D15S646	0.312	C15	0.150	21.896.314
D15S1021	0.522	C15	5.079	22.563.166
D15S128	0.266	C15	6.060	22.678.161
D15S122	0.176	C15	7.598	23.227.357
D15S986	0.438	C15	8.556	23.569.546
D15S97	0.111	C15	11.147	24.378.883
GABRB3	0.336	C15	11.799	24.564.892
D15S822	0.046	C15	13.160	24.953.339
D15S975	0.276	C15	13.460	25.038.827
D15S1002	0.277	C15	15.336	25.452.092
D15S156	0.147	C15	15.596	25.509.363
D15S217	0.158	C15	16.120	25.676.534
D15S1019	0.129	C15	21.441	27.379.480
D15S1048	0.485	C15	21.928	27.585.472
D15S210	0.252	C15	21.991	27.631.615
D15S1043	0.099	C15	22.432	27.953.995
D15S165	0.333	C15	23.509	28.976.675
D15S1031	0.329	C15	25.540	29.804.246
D15S1010	0.259	C15	27.168	30.806.373
D15S231	0.339	C15	27.428	30.966.546
D15S144	0.575	C15	29.265	31.316.942
D15S995	0.243	C15	29.843	31.382.534
D15S1007	0.217	C15	29.844	31.453.817
D15S1040	0.623	C15	30.953	31.842.433
ACTC	0.299	C15	33.139	32.800.083
D15S971	0.109	C15	33.824	33.099.995
D15S118	0.019	C15	35.231	33.952.899
D15S102	0.451	C15	38.294	35.691.551
D15S221	0.381	C15	39.056	36.409.748
D15S1012	0.263	C15	39.389	36.723.582
D15S1044	0.447	C15	41.612	37.385.017
THBS1	0.174	C15	42.301	37.589.806
D15S146	0.645	C15	43.142	37.840.108
D15S129	0.416	C15	43.882	38.115.704
D15S214	0.389	C15	43.884	38.116.289
D15S514	0.123	C15	44.183	39.926.394
D15S784	0.051	C15	44.626	41.635.820
D15S222	0.295	C15	45.294	43.161.686
D15S659	0.266	C15	45.936	44.090.064
D15S132	0.107	C15	47.150	44.917.206
D15S1006	0.477	C15	47.658	45.263.019
D15S161	0.122	C15	47.722	45.375.853
D15S990	0.358	C15	47.778	45.477.435
D15S1039	0.169	C15	47.779	45.480.050
D15S143	0.286	C15	47.780	45.619.209
D15S123	0.140	C15	47.781	45.780.577
D15S196	0.640	C15	48.813	46.425.450
D15S992	0.328	C15	48.997	46.555.798
D15S978	0.413	C15	49.658	46.990.731
D15S101	0.331	C15	49.672	47.001.331
D15S126	0.109	C15	49.694	47.018.327
D15S103	0.382	C15	49.754	47.064.369
D15S119	0.639	C15	49.942	47.209.181
CYP19	0.149	C15	51.174	49.235.859
D15S982	0.207	C15	51.648	50.074.981
D15S1016	0.258	C15	52.712	51.248.885
D15S209	0.653	C15	53.048	51.488.620
D15S170	0.314	C15	53.137	51.583.210
D15S1003	0.502	C15	53.178	51.627.448
D15S1049	0.404	C15	54.908	53.471.392
D15S1029	0.551	C15	55.012	53.679.098
D15S121	0.258	C15	55.058	53.769.585
D15S962	0.238	C15	55.320	54.291.124
D15S1008	0.025	C15	55.641	54.928.662
D15S648	0.156	C15	55.724	55.094.365
D15S998	0.264	C15	56.277	55.609.472
D15S1022	0.449	C15	56.278	55.705.559

Marker name	pvalue	Chr	cM	Mb
D15S198	0.395	C15	58.088	56.187.570
D15S117	0.189	C15	58.089	56.195.602
D15S150	0.412	C15	58.173	56.367.795
D15S1033	0.550	C15	58.226	56.477.336
D15S148	0.384	C15	60.402	56.759.014
D15S643	0.089	C15	61.221	57.429.822
D15S98	0.460	C15	61.975	58.046.770
D15S195	0.123	C15	61.976	58.068.147
D15S155	0.745	C15	61.977	58.129.100
D15S970	0.505	C15	64.159	59.016.285
D15S1036	0.231	C15	65.913	60.267.438
D15S1011	0.030	C15	66.519	60.458.541
D15S974	0.233	C15	66.663	60.590.376
D15S987	0.248	C15	67.125	61.014.263
D15S159	0.164	C15	67.515	61.142.689
D15S993	0.244	C15	67.688	61.933.671
D15S644	0.204	C15	67.689	62.002.351
D15S1018	0.090	C15	67.690	62.008.167
D15S1009	0.271	C15	67.691	62.871.489
D15S108	0.170	C15	67.692	62.900.273
D15S1020	0.090	C15	68.282	63.714.398
D15S651	0.072	C15	68.343	64.019.838
D15S213	0.485	C15	69.151	64.168.708
D15S153	0.003	C15	69.958	64.275.680
D15S988	0.336	C15	70.386	65.042.401
D15S1015	0.786	C15	71.323	65.555.199
D15S983	0.039	C15	72.944	66.441.618
D15S1025	0.661	C15	75.085	67.119.241
D15S1000	0.121	C15	75.086	67.286.979
D15S814	0.084	C15	75.087	67.333.684
D15S216	0.113	C15	75.088	67.719.572
D15S650	0.075	C15	76.188	67.972.883
D15S145	0.064	C15	78.132	68.577.001
D15S981	0.381	C15	78.281	68.608.687
D15S131	0.218	C15	78.575	68.899.593
D15S1050	0.480	C15	79.379	69.696.706
D15S110	0.663	C15	79.629	69.944.012
D15S204	0.211	C15	79.702	70.016.576
D15S197	0.246	C15	79.787	70.100.975
D15S124	0.301	C15	80.500	70.808.085
D15S980	0.569	C15	80.501	70.829.190
D15S215	0.056	C15	80.502	71.349.168
D15S169	0.305	C15	81.072	71.867.682
D15S818	0.241	C15	81.168	71.946.384
D15S160	0.388	C15	81.638	72.147.943
D15S1001	0.148	C15	81.974	72.291.762
D15S991	0.129	C15	82.226	72.316.399
CYP11A	0.619	C15	82.234	72.375.742
D15S114	0.735	C15	82.513	74.581.014
D15S1023	0.252	C15	84.015	76.857.503
D15S989	0.734	C15	86.030	77.821.734
D15S1005	0.206	C15	86.488	78.040.715
D15S969	0.254	C15	86.610	78.099.164
D15S1047	0.456	C15	88.194	78.857.017
D15S1041	0.476	C15	88.750	79.380.979
D15S206	0.207	C15	89.386	79.920.061
D15S115	0.175	C15	89.627	80.124.649
D15S95	0.375	C15	89.925	80.377.895
D15S811	0.018	C15	90.875	81.183.847
D15S200	0.416	C15	91.175	81.438.878
D15S660	0.168	C15	91.505	81.878.211
D15S205	0.199	C15	91.558	81.950.435
D15S154	0.111	C15	91.559	82.407.375
D15S653	0.075	C15	91.679	83.111.360
D15S152	0.161	C15	91.763	83.612.665
D15S999	0.059	C15	91.764	83.975.129
D15S189	0.080	C15	91.794	84.039.891
D15S201	0.553	C15	91.909	84.288.143
D15S1030	0.724	C15	93.996	85.284.964
D15S151	0.196	C15	93.997	85.326.915
D15S199	0.233	C15	94.475	85.661.450
D15S655	0.152	C15	94.592	85.705.833
D15S1046	0.457	C15	94.836	85.888.118
D15S99	0.344	C15	95.207	86.165.031
D15S171	0.199	C15	95.403	86.312.097
D15S979	0.293	C15	95.738	86.562.127
D15S1045	0.257	C15	97.402	87.325.320
D15S202	0.381	C15	98.064	87.731.376
D15S116	0.554	C15	98.065	87.743.344
D15S996	0.350	C15	99.301	88.717.134
D15S127	0.066	C15	99.865	89.127.510
D15S158	0.186	C15	100.888	89.471.421
D15S963	0.163	C15	100.997	89.521.931
D15S652	0.058	C15	102.568	90.247.102
D15S647	0.339	C15	103.844	90.534.788
D15S649	0.415	C15	110.278	91.985.619

Marker name	pvalue	Chr	cM	Mb
D15S1004	0.057	C15	110.612	92.060.836
D15S130	0.107	C15	111.551	92.440.937
D15S1038	0.568	C15	114.360	92.703.288
D15S100	0.146	C15	114.752	93.292.754
D15S157	0.214	C15	116.137	93.565.385
D15S207	0.539	C15	118.577	93.940.546
D15S657	0.156	C15	120.029	94.434.616
D15S1034	0.453	C15	123.207	95.601.514
D15S1014	0.149	C15	123.830	95.732.234
D15S212	0.250	C15	124.465	95.865.429
D15S107	0.252	C15	125.213	96.022.405
D15S985	0.314	C15	127.258	96.451.624
D15S966	0.059	C15	127.947	96.684.022
D15S120	0.009	C15	130.403	97.327.430
D15S203	0.589	C15	131.301	97.364.129
D15S87	0.100	C15	134.979	98.829.254
D15S642	0.268	C15	138.094	100.070.035

Chromosome 16

D16S521	0.069	C16	8.189	34.295
D16S3024	0.430	C16	2.760	1.594.203
D16S3027	0.221	C16	11.270	4.051.157
D16S423	0.752	C16	14.968	6.043.433
D16S3392	0.289	C16	17.340	6.365.787
D16S3042	0.512	C16	18.475	6.726.264
D16S3135	0.170	C16	18.828	6.809.704
D16S3058	0.575	C16	18.904	6.914.682
D16S3128	0.477	C16	18.993	7.037.617
D16S3088	0.488	C16	19.337	7.215.483
D16S509	0.301	C16	19.790	7.366.518
D16S3092	0.405	C16	20.368	7.559.064
D16S418	0.455	C16	20.609	7.639.505
D16S3108	0.592	C16	20.977	7.713.209
D16S502	0.041	C16	21.866	7.919.965
D16S495	0.646	C16	22.876	8.155.047
D16S3052	0.454	C16	22.950	8.172.421
D16S513	0.254	C16	23.558	8.313.753
D16S768	0.272	C16	23.805	8.371.408
D16S406	0.409	C16	24.153	8.452.275
D16S3020	0.153	C16	24.736	8.833.082
D16S404	0.039	C16	26.041	9.685.410
D16S3126	0.264	C16	26.264	10.040.892
D16S3064	0.569	C16	26.269	10.049.321
D16S407	0.310	C16	26.392	10.244.617
D16S414	0.172	C16	29.429	11.019.077
D16S497	0.013	C16	29.444	11.046.949
D16S3122	0.082	C16	29.513	11.181.076
D16S519	0.086	C16	29.514	11.252.758
D16S2613	1.6E-5	C16	29.958	11.560.745
D16S748	0.250	C16	30.745	12.105.782
D16S3075	0.459	C16	30.746	12.175.632
D16S3102	0.242	C16	30.871	12.523.890
D16S3062	0.577	C16	32.066	12.985.712
D16S292	0.171	C16	32.806	13.260.660
D16S500	0.295	C16	33.908	13.670.143
D16S2619	0.041	C16	34.013	13.708.946
D16S3060	0.369	C16	37.589	15.826.544
D16S764	0.097	C16	38.522	16.613.165
D16S501	0.547	C16	40.451	18.047.232
D16S499	0.528	C16	40.641	18.113.566
D16S3056	0.425	C16	41.537	18.810.342
D16S410	0.096	C16	41.834	19.041.408
D16S3041	0.675	C16	43.425	19.355.309
D16S3036	0.421	C16	43.472	19.490.603
D16S749	0.167	C16	43.583	19.807.732
D16S3054	0.648	C16	43.736	20.219.582
D16S3046	0.255	C16	44.636	20.852.950
D16S3045	0.178	C16	44.843	21.001.504
D16S3076	0.171	C16	47.293	23.001.170
D16S403	0.435	C16	47.294	23.004.203
D16S412	0.161	C16	47.295	23.128.957
D16S417	0.211	C16	47.984	23.743.582
D16S420	0.321	C16	49.303	24.202.632
D16S3113	0.201	C16	50.127	24.564.552
D16S401	0.625	C16	50.238	24.652.541
D16S3133	0.424	C16	50.249	24.684.996
D16S3068	0.526	C16	51.268	25.527.151
D16S3116	0.220	C16	51.546	25.650.641
D16S3131	0.148	C16	52.270	25.971.706
D16S769	0.036	C16	52.579	26.125.312
D16S3100	0.022	C16	53.429	26.548.205
D16S3093	0.049	C16	53.837	26.711.959
D16S753	0.008	C16	58.769	31.309.564
D16S3105	0.339	C16	59.851	46.573.187
D16S3044	0.349	C16	59.866	47.218.

Marker name	pvalue	Chr	cM	Mb
D16S409	0.215	C16	60.351	48.553.814
D16S261	0.610	C16	60.925	49.016.127
D16S517	0.391	C16	61.088	49.431.975
D16S3080	0.431	C16	61.100	49.461.377
D16S411	0.368	C16	61.488	49.514.761
D16S541	0.213	C16	62.312	50.372.738
D16S3136	0.491	C16	62.362	50.484.265
D16S3117	0.736	C16	63.077	50.747.030
D16S757	0.155	C16	64.346	51.335.394
D16S416	0.359	C16	64.379	51.353.744
D16S2623	0.071	C16	65.346	51.888.316
D16S419	0.371	C16	67.446	52.731.963
D16S3034	0.131	C16	68.274	52.919.103
D16S415	0.142	C16	69.143	53.449.262
D16S3137	0.874	C16	69.162	53.461.095
D16S771	0.093	C16	70.516	54.287.606
D16S3032	0.286	C16	72.384	55.163.383
D16S3053	0.085	C16	72.898	55.327.359
D16S3110	0.133	C16	73.822	55.775.106
D16S3039	0.231	C16	73.823	55.775.429
D16S3140	0.613	C16	73.824	56.086.942
D16S408	0.437	C16	73.825	56.095.966
D16S494	0.403	C16	79.013	58.701.100
D16S3094	0.324	C16	79.436	59.399.443
D16S3089	0.306	C16	82.009	60.284.654
D16S514	0.192	C16	83.448	62.113.269
D16S3143	0.094	C16	83.634	62.350.317
D16S3129	0.827	C16	83.765	62.771.394
D16S508	0.367	C16	83.766	62.859.262
D16S400	0.334	C16	84.184	63.222.461
D16S265	0.192	C16	84.239	63.288.745
D16S503	0.241	C16	84.309	63.374.016
D16S3050	0.233	C16	85.650	64.842.185
D16S3021	0.270	C16	85.843	65.060.301
D16S3043	0.077	C16	86.028	65.268.450
D16S186	0.652	C16	86.107	65.358.088
D16S3019	0.287	C16	86.592	65.905.499
D16S496	0.473	C16	87.916	68.724.892
D16S3095	0.082	C16	88.715	69.722.415
D16S752	0.204	C16	89.464	71.111.196
D16S2624	0.060	C16	89.820	71.511.313
D16S3106	0.340	C16	89.821	71.963.894
D16S3066	0.134	C16	91.199	73.109.352
D16S3083	0.018	C16	94.692	76.264.913
D16S515	0.005	C16	94.693	76.296.554
D16S3142	0.144	C16	95.593	76.462.690
D16S3097	0.207	C16	95.966	77.168.584
D16S3138	0.199	C16	96.080	77.383.294
D16S518	0.090	C16	98.119	77.917.554
D16S3049	0.452	C16	98.850	78.700.820
D16S3096	0.042	C16	100.345	78.824.422
D16S516	0.407	C16	101.239	78.903.542
D16S504	0.128	C16	101.711	78.945.335
D16S3040	0.105	C16	103.249	79.431.146
D16S750	0.191	C16	103.250	79.437.732
D16S3119	0.471	C16	103.251	79.442.970
D16S3073	0.223	C16	103.252	79.732.050
D16S3055	0.332	C16	103.253	79.768.947
D16S507	0.302	C16	103.501	79.855.977
D16S3098	0.335	C16	107.425	81.227.927
D16S505	0.221	C16	108.071	81.453.842
D16S511	0.485	C16	108.168	81.480.825
D16S422	0.085	C16	112.536	82.691.031
D16S3091	0.343	C16	112.785	82.760.134
D16S402	0.402	C16	114.198	83.073.098
D16S3061	0.313	C16	121.293	84.714.234
D16S3037	0.294	C16	121.294	84.723.599
D16S539	2.9E-4	C16	126.472	86.167.512
D16S520	0.206	C16	126.833	86.297.624
D16S3074	0.170	C16	129.114	86.866.226
D16S3077	0.091	C16	129.515	86.999.955
D16S413	0.603	C16	131.252	87.675.469
D16S3026	0.819	C16	134.173	89.236.555
D16S3121	0.444	C16	134.181	89.242.138

Chromosome 17

D17S849	0.400	C17	0.067	417.288
D17S1308	0.047	C17	0.202	607.699
D17S926	0.235	C17	0.258	614.982
D17S1866	0.464	C17	0.957	120.513
D17S1529	0.170	C17	2.997	1.034.119
D17S831	0.272	C17	7.466	2.117.079
D17S1528	0.407	C17	7.493	2.231.367
D17S1798	0.257	C17	7.613	2.764.898
D17S1845	0.115	C17	7.646	2.911.458

Marker name	pvalue	Chr	cM	Mb
D17S1298	0.157	C17	10.671	3.873.140
D17S919	0.061	C17	10.672	3.895.328
D17S1828	0.201	C17	10.930	4.017.057
D17S1876	0.278	C17	11.896	4.551.610
D17S1810	0.507	C17	13.122	5.229.471
D17S1854	0.173	C17	14.272	5.865.906
D17S1832	0.423	C17	16.789	6.173.139
D17S938	0.263	C17	17.601	6.449.832
D17S796	0.285	C17	17.610	6.452.086
D17S1881	0.436	C17	17.927	6.728.256
D17S516	0.231	C17	18.787	6.854.151
D17S906	0.075	C17	19.079	6.896.898
D17S578	0.516	C17	19.952	7.024.572
D17S960	0.484	C17	21.088	7.458.093
TP53	0.129	C17	21.435	7.779.869
D17S1796	0.132	C17	21.673	7.987.728
D17S1805	0.240	C17	22.645	8.777.330
D17S1844	0.220	C17	22.823	8.817.987
D17S786	0.609	C17	23.992	9.012.346
D17S1858	0.429	C17	24.139	9.068.679
D17S952	0.236	C17	24.775	9.314.235
D17S1791	0.171	C17	25.051	9.356.990
D17S945	0.085	C17	28.765	10.023.803
D17S1879	0.066	C17	30.184	10.313.022
D17S520	0.323	C17	30.961	10.469.574
D17S1852	0.309	C17	31.499	10.716.066
D17S974	0.012	C17	31.506	10.719.277
D17S954	0.508	C17	31.975	10.992.304
D17S1303	0.001	C17	32.080	11.059.944
D17S1875	0.228	C17	33.718	11.585.181
D17S1803	0.270	C17	36.229	12.764.802
D17S1808	0.407	C17	37.842	13.335.948
D17S799	0.101	C17	37.942	13.371.521
D17S936	0.054	C17	39.210	13.633.749
D17S1856	0.227	C17	41.550	14.117.498
D17S922	0.377	C17	41.551	14.231.677
D17S900	0.014	C17	41.787	14.395.477
D17S918	0.058	C17	45.318	15.356.238
D17S122	0.544	C17	45.442	15.409.910
D17S261	0.049	C17	45.790	15.560.330
D17S1843	0.577	C17	47.422	16.264.940
D17S953	0.363	C17	47.445	16.303.063
D17S1857	0.622	C17	47.635	16.615.782
D17S740	0.581	C17	48.280	17.200.133
D17S751	0.927	C17	48.451	17.354.521
D17S1794	0.097	C17	48.785	17.712.050
D17S805	0.058	C17	50.204	19.537.470
D17S959	0.547	C17	50.808	20.794.382
D17S842	0.277	C17	50.894	20.829.303
D17S1871	0.204	C17	51.171	20.923.891
D17S783	0.213	C17	52.219	25.457.647
D17S1878	0.499	C17	53.031	26.256.562
D17S1824	0.198	C17	53.223	26.805.633
D17S935	0.336	C17	53.224	26.928.883
D17S925	0.148	C17	53.493	27.452.428
D17S1873	0.151	C17	53.625	27.602.907
D17S841	0.351	C17	53.700	27.688.015
D17S1157	0.248	C17	53.715	27.715.527
D17S1841	0.709	C17	53.875	28.007.323
D17S975	0.111	C17	54.102	28.245.550
D17S1863	0.042	C17	54.376	29.075.956
D17S1166	0.314	C17	54.377	29.794.578
NF1	0.297	C17	54.401	29.807.360
D17S1800	0.148	C17	54.939	30.082.332
D17S1880	0.147	C17	57.042	31.159.355
D17S798	0.130	C17	57.043	31.435.361
D17S1850	0.405	C17	59.794	32.283.280
D17S1293	0.001	C17	61.735	32.705.555
D17S1842	0.405	C17	63.203	33.072.936
D17S1846	0.103	C17	63.884	33.811.639
D17S1833	0.280	C17	64.756	34.269.600
D17S927	0.133	C17	66.001	35.201.893
D17S1867	0.589	C17	66.959	35.574.897
D17S946	0.569	C17	68.968	37.227.874
D17S838	0.437	C17	69.180	37.406.003
D17S250	0.130	C17	69.324	37.527.054
D17S1818	0.282	C17	69.325	37.538.070
D17S1814	0.242	C17	70.322	38.493.847
D17S1299	0.184	C17	71.133	39.367.471
D17S800	0.222	C17	71.191	39.429.422
D17S1787	0.229	C17	71.812	40.098.149
D17S1802	0.153	C17	72.725	40.726.629
D17S1793	0.432	C17	72.734	40.732.569
D17S1801	0.397	C17	72.813	40.788.894
D17S932	0.266	C17	73.342	41.577.894
D17S902	0.071	C17	73.707	42.122.369

Marker name	pvalue	Chr	cM	Mb
D17S965	0.312	C17	73.766	42.209.463
D17S951	0.397	C17	73.823	42.295.182
D17S1860	0.249	C17	74.438	42.845.420
D17S1861	0.273	C17	74.439	43.282.178
D17S1804	0.178	C17	74.451	43.490.302
D17S934	0.109	C17	74.524	43.532.670
D17S810	0.039	C17	75.263	43.964.400
D17S920	0.152	C17	75.314	45.289.661
D17S1834	0.784	C17	75.472	45.457.657
D17S931	0.367	C17	75.506	45.470.359
D17S1859	0.299	C17	75.743	46.299.133
D17S1785	0.143	C17	76.082	46.496.178
D17S958	0.350	C17	76.083	46.723.687
D17S1827	0.434	C17	76.084	47.113.122
D17S1868	0.243	C17	76.300	47.659.383
D17S797	0.239	C17	76.930	48.028.874
D17S943	0.067	C17	77.218	48.314.933
D17S1795	0.309	C17	77.303	48.399.632
D17S1815	0.245	C17	79.587	49.141.578
D17S1877	0.724	C17	80.630	49.955.604
D17S1820	0.090	C17	80.631	50.259.492
D17S941	0.270	C17	80.632	50.311.255
D17S788	0.410	C17	80.863	50.764.493
D17S790	0.319	C17	82.326	53.273.502
D17S787	0.164	C17	83.220	53.756.722
D17S1306	0.211	C17	83.227	53.760.493
GCT6E11	0.922	C17	83.283	53.790.940
D17S1799	0.362	C17	83.513	53.915.208
D17S957	0.178	C17	89.636	55.948.346
D17S1605	0.141	C17	89.637	56.015.671
D17S1853	0.481	C17	89.718	56.059.147
D17S1606	0.435	C17	89.753	56.078.269
D17S1160	0.521	C17	89.823	56.115.640
D17S1290	0.003	C17	90.359	56.806.087
MPO	0.109	C17	90.373	56.822.787
D17S792	0.698	C17	91.828	58.714.165
D17S923	0.189	C17	91.829	58.843.241
D17S1838	0.130	C17	92.299	59.926.919
D17S917	0.033	C17	93.058	60.196.708
D17S1855	0.386	C17	93.096	60.210.272
D17S808	0.012	C17	94.201	61.145.469
D17S794	0.305	C17	94.361	61.290.623
D17S924	0.601	C17	94.861	61.410.147
D17S948	0.495	C17	94.887	61.462.765
D17S944	0.344	C17	95.110	61.909.677
D17S1297	0.312	C17	95.586	62.687.588
D17S1809	0.360	C17	96.060	63.247.551
D17S1825	0.167	C17	96.340	63.578.048
D17S1792	0.192	C17	96.367	63.609.573
D17S113	0.107	C17	97.129	64.509.820
D17S1874	0.116	C17	97.330	64.747.024
D17S1816	0.091	C17	97.886	64.970.738
D17S942	0.229	C17	97.887	65.039.229
D17S807	0.204	C17	98.740	65.409.027
D17S1821	0.501	C17	99.724	65.835.569
D17S1813	0.312	C17	100.046	66.036.089
D17S1870	0.194	C17	100.197	66.130.069
D17S789	0.240	C17	101.989	67.225.637
D17S795	0.165	C17	101.990	67.275.327
D17S940	0.447	C17	102.596	67.675.484
D17S2182	0.453	C17	102.597	67.736.821
D17S1766	0.347	C17	103.277	68.091.713
D17S1295	0.425	C17	104.271	68.611.092
D17S949	0.122	C17	105.506	69.062.454
D17S2059	0.061	C17	105.507	69.098.093
D17S840	0.224	C17	105.839	69.205.246
D17S1304	0.074	C17	106.924	70.058.463
D17S1534	0.292	C17	107.600	70.494.646
D17S1797	0.744	C17	108.574	71.122.860
D17S1351	0.713	C17	108.829	71.269.275
D17S1848	0.112	C17	109.121	71.460.943
SSTR2	0.293	C17	110.268	71.758.521
D17S1862	0.079	C17	110.904	71.923.686
D17S1829	0.034	C17	112.504	72.364.335
D17S1352	0.364	C17	113.309	72.594.963
D17S1864	0.178	C17	114.321	72.630.582
D17S1602	0.366	C17	115.638	72.808.365
D17S929	0.101	C17	115.639	72.837.957
D17S1807	0.060	C17	115.843	72.957.660
D17S1536	0.125	C17	116.326	73.155.376
D17S968	0.333	C17	116.334	73.201.434
D17S1301	0.206	C17	116.335	73.278.058
D17S1839	0.088	C17	117.275	74.398.986
D17S1603	0.021	C17	117.820	74.663.930
D17S785	0.361	C17	118.095	75.028.496
D17S1817	0.361	C17	118.203	75.079.216

Marker name	pvalue	Chr	cM	Mb
D17S801	0.626	C17	118.318	75.103.769
D17S937	0.195	C17	120.904	75.944.381
D17S939	0.008	C17	121.472	76.059.230
D17S802	0.464	C17	123.715	76.831.733
D17S1847	0.261	C17	126.708	77.621.826
D17S836	0.376	C17	128.025	77.896.957
D17S1806	0.164	C17	129.107	78.042.794
D17S1822	0.180	C17	132.358	78.481.152
D17S1830	0.256	C17	132.628	78.496.149
D17S784	0.719	C17	132.738	78.502.239
D17S928	0.104	C17	139.293	80.931.693

Chromosome 18

D18S59	0.178	C18	1.403	636.459
D18S476	0.138	C18	5.826	2.167.865
D18S481	0.375	C18	9.133	3.056.132
D18S63	0.190	C18	9.837	3.428.519
D18S52	3.9E-4	C18	12.870	4.247.911
D18S1132	0.369	C18	14.444	4.609.789
D18S976	0.020	C18	16.548	5.238.944
D18S464	0.532	C18	33.370	9.951.257
D18S1153	0.736	C18	34.062	10.123.107
D18S1150	0.022	C18	34.519	10.236.590
D18S1158	0.795	C18	36.229	10.732.701
D18S53	0.415	C18	38.814	11.482.737
D18S482	0.764	C18	39.114	11.836.214
D18S71	0.250	C18	40.687	12.586.865
D18S453	0.245	C18	40.897	12.904.797
D18S1114	0.455	C18	40.898	12.914.044
D18S852	0.054	C18	41.239	13.640.193
D18S40	0.002	C18	41.316	13.743.792
D18S45	0.205	C18	43.788	17.072.490
D18S1149	0.304	C18	43.967	17.313.120
D18S1107	0.358	C18	47.287	20.379.976
D18S975	0.493	C18	47.890	20.695.529
D18S866	0.539	C18	49.660	21.622.579
D18S478	0.385	C18	52.453	23.399.290
D18S1151	0.251	C18	52.560	23.433.716
D18S877	0.311	C18	54.033	24.977.030
D18S965	0.287	C18	54.312	25.261.692
D18S847	0.101	C18	54.991	25.955.300
D18S463	0.678	C18	55.192	26.394.187
D18S36	0.612	C18	56.199	27.416.157
D18S47	0.133	C18	56.476	28.033.216
D18S457	0.257	C18	56.514	28.118.231
D18S536	0.186	C18	57.593	29.840.273
D18S1102	0.312	C18	59.894	33.175.078
D18S468	0.291	C18	62.591	36.481.434
D18S665	0.006	C18	62.717	36.590.138
D18S872	0.009	C18	64.616	39.513.168
D18S1145	0.240	C18	65.096	40.407.818
D18S970	0.077	C18	70.426	43.985.745
D18S450	0.637	C18	70.781	44.296.970
D18S472	0.064	C18	73.856	46.255.545
D18S474	0.540	C18	74.788	46.946.668
D18S851	0.112	C18	76.683	48.359.408
D18S1156	0.485	C18	76.838	49.020.881
D18S487	0.444	C18	77.608	49.989.449
D18S1119	0.432	C18	78.374	51.353.978
D18S1127	0.320	C18	78.456	51.520.179
D18S69	0.026	C18	79.026	51.991.385
D18S977	0.378	C18	80.652	53.465.185
D18S1103	0.130	C18	82.855	55.079.105
D18S1155	0.110	C18	83.323	55.212.629
D18S64	0.534	C18	84.270	55.574.999
D18S1109	0.307	C18	84.349	55.605.265
D18S38	0.560	C18	87.196	56.694.549
D18S1134	0.311	C18	87.197	56.870.530
D18S1148	0.111	C18	88.096	57.285.527
D18S1147	0.191	C18	88.505	57.560.672
D18S60	0.553	C18	88.991	58.011.389
D18S51	0.025	C18	90.162	59.097.813
D18S1270	0.129	C18	90.703	59.541.470
D18S68	0.213	C18	91.039	59.686.664
D18S537	0.187	C18	92.875	60.952.741
D18S465	0.082	C18	92.907	61.044.904
D18S857	0.277	C18	95.095	62.326.748
D18S979	0.146	C18	96.962	64.059.060
D18S61	0.392	C18	100.091	65.585.025
D18S848	0.530	C18	101.687	67.449.636
D18S541	0.383	C18	102.962	68.323.159
D18S1269	0.031	C18	103.233	68.361.132
D18S43	0.236	C18	105.714	68.949.169
D18S850	0.479	C18	106.	

Marker name	pvalue	Chr	cM	Mb
D18S844	0.156	C18	116.009	72.481.661
D18S462	0.515	C18	119.147	73.262.428
D18S871	0.199	C18	119.902	73.813.279
D18S1122	0.133	C18	120.884	74.184.635
D18S1141	0.091	C18	123.741	75.022.663
D18S1095	9.7E-8	C18	124.847	75.347.204
D18S70	0.184	C18	126.947	75.963.194

Chromosome 19

D19S886	0.215	C19	0.001	949.791
D19S883	0.342	C19	1.216	1.364.756
D19S565	0.012	C19	8.627	2.518.233
D19S591	0.105	C19	10.588	3.026.853
D19S247	0.029	C19	11.119	3.090.981
D19S424	0.152	C19	11.835	3.177.373
D19S209	0.277	C19	12.435	3.347.390
D19S894	0.177	C19	15.950	4.343.405
D19S216	0.448	C19	17.768	4.900.356
D19S549	0.134	C19	19.477	5.443.422
INSR	0.202	C19	24.733	7.117.137
D19S901	0.717	C19	25.363	7.387.395
D19S567	0.773	C19	25.364	7.445.409
D19S873	0.110	C19	25.365	7.482.724
D19S395	0.392	C19	25.383	7.489.310
D19S905	0.180	C19	25.635	7.575.875
D19S912	0.368	C19	26.223	7.777.648
D19S884	0.085	C19	27.040	8.056.011
D19S916	0.475	C19	29.724	8.978.848
D19S865	0.212	C19	29.900	9.039.373
D19S413	0.077	C19	29.903	9.040.254
D19S403	0.132	C19	30.839	9.591.484
D19S586	0.232	C19	30.965	9.665.792
D19S583	0.279	C19	31.469	9.919.272
EPOR	0.169	C19	33.414	11.355.832
D19S906	0.061	C19	33.781	11.787.025
D19S1165	0.261	C19	33.782	12.155.333
D19S221	0.035	C19	33.951	12.573.793
D19S914	0.195	C19	34.313	12.802.814
D19S558	0.031	C19	34.901	13.174.061
D19S564	0.090	C19	35.339	13.385.640
D19S840	0.030	C19	35.995	13.701.955
RFX1	0.421	C19	36.657	13.966.478
D19S226	0.155	C19	37.979	14.494.399
D19S179	0.166	C19	38.056	14.563.684
D19S415	0.828	C19	38.415	14.886.464
D19S929	0.150	C19	38.976	15.021.439
D19S923	0.194	C19	39.544	15.158.087
D19S432	0.227	C19	39.980	15.542.989
D19S714	0.055	C19	39.981	15.589.132
D19S411	0.176	C19	40.125	15.763.093
D19S885	0.234	C19	40.461	16.070.698
D19S199	0.254	C19	41.634	16.829.058
D19S930	0.288	C19	41.635	16.829.232
D19S899	0.075	C19	42.772	17.095.082
D19S593	0.083	C19	43.022	17.169.106
D19S410	0.037	C19	43.023	17.258.423
D19S429	0.008	C19	43.024	17.496.924
D19S710	0.070	C19	43.025	17.497.103
D19S915	0.364	C19	44.898	17.778.892
D19S1037	0.035	C19	45.953	17.937.610
D19S212	5.0E-8	C19	46.345	18.204.059
D19S898	0.066	C19	46.537	18.334.781
D19S566	0.183	C19	47.549	19.022.980
D19S407	0.045	C19	48.516	19.926.053
D19S911	0.383	C19	49.353	20.708.313
D19S925	0.001	C19	49.354	21.153.314
D19S215	0.464	C19	49.427	21.474.512
D19S401	0.200	C19	49.510	21.841.760
D19S568	0.470	C19	49.611	22.286.962
D19S434	0.013	C19	49.641	22.559.657
D19S1035	0.075	C19	49.694	23.044.301
D19S910	0.189	C19	49.734	23.414.508
D19S1036	0.052	C19	49.737	23.444.661
D19S931	0.006	C19	50.978	33.315.292
D19S222	0.665	C19	51.013	33.417.729
D19S920	0.558	C19	51.328	34.189.679
D19S409	0.419	C19	51.447	34.422.411
D19S932	0.190	C19	51.448	34.469.524
D19S875	0.392	C19	51.449	34.489.180
D19S561	0.138	C19	52.104	34.568.508
D19S919	1.2E-4	C19	52.258	34.602.835
D19S459	0.200	C19	52.259	34.777.347
D19S433	0.147	C19	52.756	35.108.867
D19S405	0.172	C19	53.234	35.417.435
D19S396	0.267	C19	53.314	35.447.109

Marker name	pvalue	Chr	cM	Mb
D19S882	0.438	C19	53.396	35.477.162
D19S250	0.009	C19	53.427	35.549.316
D19S249	0.183	C19	55.061	36.234.075
D19S114	0.596	C19	55.744	36.574.416
D19S414	0.729	C19	55.808	36.606.563
D19S75	0.572	C19	55.973	36.818.077
D19S251	0.131	C19	55.974	36.841.774
D19S431	0.104	C19	56.222	37.013.386
D19S225	0.131	C19	57.355	37.518.191
D19S555	0.078	C19	57.955	38.172.774
D19S719	0.490	C19	58.208	38.605.668
D19S416	0.130	C19	58.726	38.760.490
D19S874	0.148	C19	58.727	38.760.845
D19S248	0.019	C19	58.755	38.765.182
D19S245	0.444	C19	58.913	38.789.927
D19S213	0.193	C19	58.939	38.803.094
D19S587	0.025	C19	61.107	39.901.933
D19S425	0.272	C19	62.014	40.185.716
D19S893	0.259	C19	62.669	40.267.680
D19S208	0.398	C19	63.103	40.321.920
D19S191	0.403	C19	63.199	40.370.248
D19S876	0.494	C19	64.705	41.130.182
D19S224	0.368	C19	64.805	41.219.912
D19S896	0.136	C19	65.606	42.170.482
D19S570	0.263	C19	65.666	42.419.583
D19S713	0.070	C19	65.704	42.576.021
D19S220	0.346	C19	65.836	42.123.394
D19S228	0.552	C19	65.850	43.181.339
D19S897	0.084	C19	65.915	43.451.099
D19S421	0.718	C19	66.318	43.562.945
D19S422	0.101	C19	66.319	43.861.960
D19S881	0.192	C19	66.320	44.039.969
D19S417	0.159	C19	66.695	44.164.323
D19S190	2.4E-4	C19	67.546	44.640.448
D19S447	0.421	C19	68.200	45.006.027
D19S554	0.060	C19	68.587	45.301.489
D19S552	0.019	C19	68.641	45.343.153
D19S200	0.338	C19	68.694	45.383.593
D19S223	0.099	C19	68.913	46.086.644
D19S400	0.052	C19	69.157	46.219.373
D19S582	0.169	C19	70.548	46.821.030
D19S197	0.287	C19	70.555	46.824.241
D19S198	0.356	C19	70.603	46.844.863
CEA	0.112	C19	70.642	46.905.262
D19S423	0.342	C19	70.727	47.035.510
LIPE	0.260	C19	71.093	47.599.126
D19S872	0.164	C19	71.140	47.672.188
D19S211	0.163	C19	71.202	48.075.706
D19S420	0.016	C19	71.203	48.500.639
D19S537	0.731	C19	71.777	48.723.667
D19S408	0.063	C19	72.066	48.739.098
D19S900	0.056	C19	72.437	48.859.097
D19S913	0.293	C19	72.515	48.883.373
D19S217	0.137	C19	72.804	48.973.202
D19S178	0.087	C19	72.805	49.097.486
D19S903	0.193	C19	73.474	49.737.740
BCL3	0.733	C19	73.689	49.942.888
D19S559	0.180	C19	73.690	50.022.028
APOC2	0.003	C19	73.920	50.141.220
D19S918	0.009	C19	74.046	50.206.617
D19S908	0.510	C19	74.733	50.562.366
D19S219	0.276	C19	74.793	50.685.577
D19S112	0.269	C19	75.631	51.070.820
D19S412	0.121	C19	77.007	51.702.813
D19S606	0.607	C19	77.963	52.665.381
D19S902	0.549	C19	78.516	53.023.839
D19S596	0.190	C19	81.611	53.942.842
D19S879	0.769	C19	82.504	54.207.729
D19S550	0.171	C19	83.656	54.549.848
D19S867	0.713	C19	84.599	55.230.494
D19S585	0.033	C19	84.646	55.272.919
D19S866	0.059	C19	84.840	55.446.401
D19S904	0.234	C19	84.865	55.468.607
D19S246	0.284	C19	85.955	55.647.396
D19S907	0.380	C19	86.100	55.753.062
D19S402	0.353	C19	92.592	56.861.628
D19S397	0.825	C19	94.251	57.144.911
D19S206	0.296	C19	94.252	57.243.159
D19S601	0.208	C19	94.253	57.285.644
D19S571	0.182	C19	96.233	57.988.748
D19S888	0.001	C19	97.251	58.350.325
D19S180	0.265	C19	97.811	58.441.513
D19S921	0.077	C19	97.812	58.462.957
D19S589	0.089	C19	98.027	58.498.394
D19S572	0.175	C19	99.842	58.797.162
D19S924				

Marker name	pvalue	Chr	cM	Mb
D19S927	0.227	C19	101.769	58.990.106
D19S926	0.112	C19	107.436	60.180.648
D19S418	0.156	C19	107.708	60.237.788
D19S880	0.221	C19	107.852	60.374.288
D19S605	0.379	C19	108.448	60.443.648
D19S210	0.214	C19	112.616	61.711.332
D19S544	0.154	C19	113.181	61.883.100
D19S573	0.293	C19	113.227	61.897.021
D19S887	0.373	C19	113.797	62.325.668
D19S214	0.386	C19	113.798	62.473.811
D19S218	0.145	C19	113.799	62.893.502

Chromosome 20

D20S864	0.310	C20	0.286	193.257
D20S103	0.118	C20	2.611	554.245
D20S105	0.262	C20	2.983	647.862
D20S117	0.272	C20	2.992	650.091
D20S199	0.428	C20	6.067	1.089.062
D20S906	0.140	C20	6.068	1.500.566
D20S179	0.366	C20	7.342	1.972.335
D20S113	0.161	C20	7.685	2.030.487
D20S842	0.459	C20	9.708	2.681.203
D20S181	0.573	C20	10.954	3.167.513
D20S193	0.331	C20	10.955	3.308.327
D20S473	0.095	C20	11.198	3.460.441
D20S116	0.250	C20	12.583	4.048.190
D20S482	0.240	C20	13.649	4.501.247
D20S97	0.513	C20	13.650	4.519.215
D20S895	0.346	C20	15.769	5.081.622
D20S835	0.187	C20	16.782	5.309.896
D20S873	0.391	C20	18.119	5.591.746
D20S882	0.049	C20	18.301	5.630.097
D20S95	0.287	C20	18.939	5.711.249
D20S916	0.282	C20	20.316	5.857.106
D20S905	0.102	C20	20.471	5.858.609
D20S192	0.191	C20	21.933	6.692.019
D20S603	0.011	C20	21.940	6.696.149
D20S892	0.127	C20	22.028	6.745.073
D20S846	0.016	C20	22.029	6.759.932
D20S900	0.256	C20	25.064	7.356.582
D20S115	0.473	C20	25.351	7.654.866
D20S879	0.474	C20	28.289	8.559.923
D20S177	0.879	C20	28.290	8.790.195
D20S175	0.120	C20	28.693	9.190.083
D20S917	0.341	C20	28.917	9.283.084
D20S901	0.217	C20	31.188	10.036.532
D20S894	0.276	C20	33.115	10.694.879
D20S188	0.079	C20	33.398	11.036.672
D20S189	0.104	C20	34.885	11.168.806
D20S186	0.004	C20	35.475	11.518.794
D20S604	0.103	C20	36.684	12.579.288
D20S852	0.366	C20	40.502	15.422.570
D20S98	0.213	C20	41.713	15.647.874
D20S904	0.072	C20	42.544	15.720.305
D20S104	0.447	C20	43.174	16.182.064
D20S875	0.045	C20	44.450	16.647.263
D20S114	0.186	C20	45.360	17.251.930
D20S112	0.023	C20	45.361	17.311.039
D20S182	0.570	C20	46.140	17.834.283
D20S885	0.099	C20	46.432	17.958.678
D20S860	0.060	C20	47.155	18.329.130
D20S471	0.026	C20	49.661	19.826.374
D20S912	0.155	C20	52.186	20.855.811
D20S868	0.519	C20	52.622	21.672.249
D20S477	0.327	C20	53.146	22.407.084
D20S184	0.858	C20	54.278	23.119.343
D20S871	0.037	C20	54.614	23.330.568
D20S101	0.150	C20	54.923	23.634.167
D20S848	0.413	C20	55.358	24.328.754
D20S844	0.480	C20	55.469	24.443.297
D20S486	0.014	C20	55.651	24.630.134
D20S484	0.630	C20	56.571	30.812.928
D20S863	0.636	C20	56.623	31.322.816
D20S872	0.051	C20	56.635	31.325.770
D20S195	0.443	C20	57.663	32.541.340
D20S106	0.606	C20	58.460	34.222.948
D20S914	0.452	C20	58.522	35.369.642
D20S865	0.351	C20	58.560	35.446.333
D20S847	0.348	C20	58.713	35.568.856
D20S841	0.560	C20	59.685	36.735.928
D20S884	0.380	C20	59.754	36.756.033
D20S881	0.608	C20	61.809	37.740.952
D20S174	0.433	C20	62.280	38.410.540
D20S908	0.056	C20	62.313	38.499.382
D20S206	0.148	C20	62.488	38.976.402

Marker name	pvalue	Chr	cM	Mb
D20S607	0.342	C20	62.673	39.482.278
D20S107	0.154	C20	63.189	39.567.939
D20S850	0.174	C20	64.269	40.096.686
D20S99	0.430	C20	64.682	40.299.058
D20S855	0.267	C20	64.725	41.027.219
D20S170	0.253	C20	65.635	41.515.886
D20S108	0.164	C20	66.191	41.643.472
D20S858	0.567	C20	66.926	42.402.281
D20S96	0.045	C20	68.058	42.780.853
D20S169	0.085	C20	69.565	43.290.817
D20S861	0.191	C20	69.592	43.292.797
D20S119	0.074	C20	70.965	44.334.278
D20S838	0.190	C20	71.234	45.322.818
D20S856	0.916	C20	71.235	45.338.173
D20S836	0.087	C20	71.898	45.625.669
D20S888	0.302	C20	72.403	45.869.326
D20S886	0.516	C20	72.647	45.936.504
D20S891	0.257	C20	74.081	46.615.018
D20S197	0.274	C20	75.035	46.846.125
D20S178	0.317	C20	75.467	47.237.348
D20S176	0.436	C20	77.419	47.998.882
D20S866	0.272	C20	77.420	48.048.755
D20S887	0.069	C20	77.422	48.358.591
D20S196	0.039	C20	80.219	50.247.178
D20S857	0.396	C20	82.547	50.793.651
D20S185	0.399	C20	82.688	51.004.297
D20S845	0.515	C20	82.852	51.248.541
D20S1083	0.069	C20	83.326	51.319.996
D20S893	0.226	C20	83.467	51.444.271
D20S902	0.581	C20	84.892	52.436.689
D20S883	0.328	C20	85.282	52.588.790
D20S854	0.303	C20	85.826	52.682.079
D20S183	0.279	C20	85.904	52.695.403
D20S840	0.351	C20	86.207	52.832.755
D20S211	0.420	C20	86.208	52.853.960
D20S913	0.690	C20	87.273	53.186.348
D20S120	0.613	C20	88.573	53.690.882
D20S469	0.037	C20	89.423	54.324.261
D20S1082	0.206	C20	89.842	54.551.247
D20S853	0.692	C20	89.843	54.557.870
D20S832	0.453	C20	89.844	54.580.896
D20S100	0.287	C20	90.847	54.999.474
D20S102	0.164	C20	93.051	55.676.796
D20S171	0.168	C20	100.839	58.493.440
D20S173	0.272	C20	100.842	59.563.362

Chromosome 21

D21S408	0.333	C21	4.714	14.606.388
D21S1911	0.505	C21	6.374	15.062.607
D21S1904	0.727	C21	7.227	15.432.268
D21S415	0.272	C21	7.837	15.764.783
D21S1432	0.409	C21	8.754	16.265.317
D21S1886	0.309	C21	10.703	16.651.614
D21S1256	0.489	C21	13.278	18.244.636
D21S409	0.107	C21	14.128	18.461.368
D21S1899	0.203	C21	16.200	18.989.654
D21S366	0.770	C21	16.724	19.258.789
D21S1437	0.001	C21	18.925	20.568.710
D21S1902	0.296	C21	20.181	21.052.138
D21S1441	0.015	C21	20.479	21.166.842
D21S1922	0.477	C21	20.618	21.220.615
D21S1884	0.378	C21	21.471	21.548.909
D21S1257	0.184	C21	23.543	23.735.731
D21S1914	0.226	C21	25.068	24.544.272
D21S367	0.019	C21	26.069	25.398.855
D21S265	0.106	C21	26.175	25.841.347
D21S1443	0.014	C21	26.914	26.444.700
D21S1435	0.002	C21	27.884	26.770.711
D21S260	0.565	C21	27.986	26.893.301
D21S269	0.366	C21	27.987	26.922.995
D21S1442	0.131	C21	30.284	27.740.350
D21S1258	0.223	C21	30.410	27.741.551
D21S1916	0.196	C21	30.736	27.902.926
D21S1270	0.117	C21	32.657	30.627.208
D21S263	0.615	C21	33.345	31.142.361
D21S1909	0.582	C21	33.806	31.453.692
D21S2049	0.245	C21	34.097	31.655.150
D21S261	0.467	C21	34.907	32.216.729
D21S262	0.229	C21	36.563	32.736.671
D21S1920	0.176	C21	40.327	34.617.588
D21S1895	0.393	C21	42.150	35.271.380
D21S1894	0.062	C21	42.996	35.574.836
D21S1252	0.224	C21	44.036	36.747.254
D21S267	0.149	C21	45.974	37.387.7

Marker name	pvalue	Chr	cM	Mb
D21S1919	0.285	C21	46.049	37.485.125
D21S270	0.154	C21	46.248	37.750.917
D21S1439	0.873	C21	46.500	38.061.931
D21S1440	0.131	C21	46.501	38.062.023
D21S364	0.031	C21	47.947	38.265.827
D21S1255	0.233	C21	48.281	38.715.106
D21S1809	0.037	C21	48.530	38.810.457
D21S416	0.642	C21	51.107	39.867.733
D21S1235	0.448	C21	51.108	39.867.733
D21S1893	0.408	C21	53.267	40.276.734
D21S266	0.379	C21	57.332	41.604.960
D21S1224	0.080	C21	57.463	41.648.326
D21S1446	0.253	C21	80.455	46.893.787

Chromosome 22

D22S420	0.385	C22	3.048	16.233.834
D22S427	0.184	C22	6.002	16.965.930
D22S264	0.077	C22	11.790	19.097.785
D22S446	0.436	C22	15.172	20.343.712
D22S539	0.034	C22	15.820	20.582.333
D22S686	0.192	C22	16.617	21.393.069
D22S425	0.389	C22	16.618	21.407.028
D22S257	0.355	C22	17.977	21.892.982
D22S1174	0.217	C22	20.026	22.813.039
D22S156	0.635	C22	20.185	23.216.863
D22S536	0.279	C22	20.476	23.515.543
D22S925	0.271	C22	23.745	24.106.232
D22S926	0.353	C22	23.746	24.149.175
D22S419	0.106	C22	23.900	24.267.767
D22S258	0.060	C22	23.909	24.276.593
D22S315	0.450	C22	23.910	24.340.416
D22S1164	0.475	C22	23.911	24.447.299
D22S1148	0.121	C22	25.512	24.670.956
D22S1154	0.107	C22	25.726	24.942.080
D22S310	0.571	C22	25.727	24.952.776
D22S1144	0.171	C22	31.007	26.007.486
D22S1163	0.305	C22	32.148	26.243.204
D22S689	0.074	C22	34.606	27.181.014
D22S1150	0.173	C22	35.162	27.825.879
D22S531	0.314	C22	36.195	29.023.790
D22S1176	0.531	C22	36.523	30.551.156
D22S280	0.712	C22	38.780	31.533.925
D22S1172	0.082	C22	39.208	31.998.945
D22S1162	0.339	C22	40.312	32.635.498
D22S281	0.283	C22	40.313	32.661.261
D22S1158	0.041	C22	40.555	32.899.099
D22S691	0.046	C22	40.833	33.200.196
D22S1147	0.386	C22	40.834	33.335.911
D22S422	0.254	C22	40.835	33.461.081
D22S1152	0.163	C22	40.836	33.463.664
D22S304	0.314	C22	40.837	33.695.236
D22S1265	0.267	C22	40.838	33.714.476
D22S424	0.186	C22	41.632	34.023.566
D22S277	0.219	C22	42.516	34.543.312
D22S1142	0.397	C22	42.520	34.545.666
D22S278	0.244	C22	42.521	34.678.417
D22S683	0.023	C22	43.125	34.785.740
D22S1173	0.192	C22	43.815	34.908.372
D22S283	0.496	C22	43.881	35.022.517
D22S426	0.570	C22	44.022	35.266.252
D22S692	8.2E-6	C22	44.081	35.368.583
D22S1177	0.204	C22	45.348	35.506.142
D22S1045	0.251	C22	46.602	35.779.337
IL2RB	0.243	C22	46.603	35.788.758
D22S1156	0.154	C22	48.112	36.624.810
D22S272	0.377	C22	49.232	37.328.931
PDGFB	0.175	C22	50.019	37.888.787
D22S428	0.446	C22	50.454	38.197.990
D22S284	0.115	C22	50.938	38.559.934
D22S530	0.686	C22	50.939	38.618.508
D22S423	0.171	C22	51.075	38.625.224
D22S302	0.081	C22	51.079	38.668.036
D22S279	0.456	C22	51.128	39.265.852
D22S276	0.344	C22	51.211	40.255.328
D22S1267	0.027	C22	51.233	40.296.483
D22S417	0.073	C22	51.853	41.335.399
D22S418	0.318	C22	51.854	41.649.864
D22S1151	0.635	C22	51.855	41.771.830
D22S1179	0.187	C22	51.967	41.823.458
D22S282	0.049	C22	52.759	42.090.888
D22S927	0.297	C22	52.760	42.343.398
D22S1165	0.136	C22	52.761	42.481.794
D22S1159	0.007	C22	56.781	43.027.166
D22S1168	0.312	C22	58.269	43.426.543
D22S274	0.064	C22	58.574	43.545.681

Marker name	pvalue	Chr	cM	Mb
D22S928	0.241	C22	59.393	43.752.015
D22S1141	0.795	C22	60.724	43.995.391
D22S532	0.288	C22	62.661	44.399.727
D22S1149	0.629	C22	63.953	44.885.131
D22S1170	0.220	C22	68.417	46.562.965
D22S922	0.657	C22	70.626	47.393.307

Chromosome X

DXS8095	0.364	CX	4.153	3.928.518
DXS6807	0.002	CX	4.582	4.204.887
DXS7107	0.022	CX	9.838	4.640.890
DXS1060	0.250	CX	13.185	4.871.358
DXS8105	0.459	CX	13.186	5.211.402
DXS996	0.373	CX	13.187	5.320.656
DXS1283E	0.006	CX	15.566	7.278.308
DXS1223	0.384	CX	16.518	7.905.416
DXS8051	0.005	CX	18.292	8.910.734
DXS7103	0.406	CX	18.429	8.988.672
DXS7108	0.103	CX	19.628	9.603.742
DXS1043	0.275	CX	22.017	10.829.670
DXS7109	0.303	CX	22.712	11.382.766
DXS7104	0.278	CX	22.713	11.516.383
DXS1224	0.461	CX	26.381	12.596.935
DXS16	0.109	CX	27.259	12.914.310
DXS8022	0.243	CX	28.315	13.296.143
DXS8108	0.316	CX	29.053	13.322.363
DXS987	0.053	CX	29.054	14.070.727
DXS1053	0.437	CX	30.528	14.930.165
DXS43	0.471	CX	30.818	15.580.694
DXS8036	0.373	CX	31.187	16.409.816
DXS1195	0.252	CX	31.188	16.896.009
DXS8019	0.190	CX	31.189	17.103.247
DXS999	0.142	CX	32.828	18.196.450
DXS7161	0.657	CX	33.208	18.415.970
DXS1229	0.540	CX	35.804	19.915.408
DXS7101	0.190	CX	35.805	21.055.981
DXS1683	0.289	CX	38.089	21.628.670
DXS7105	0.215	CX	38.408	21.708.692
DXS7593	0.202	CX	38.512	21.754.779
DXS1052	0.125	CX	38.823	21.892.063
DXS1226	0.387	CX	39.766	22.308.847
DXS7110	0.315	CX	40.671	22.472.948
DXS989	0.178	CX	41.294	22.545.868
DXS8104	0.207	CX	41.931	22.757.020
DXS8099	0.426	CX	43.205	23.780.632
DXS8027	0.695	CX	43.351	23.898.171
DXS8058	0.434	CX	43.352	24.650.853
DXS1202	0.044	CX	43.651	25.832.770
DXS7102	0.491	CX	43.703	26.040.454
DXS1048	0.372	CX	43.714	26.081.930
DXS8065	0.603	CX	43.893	26.790.467
DXS1061	0.128	CX	43.909	26.803.511
DXS8047	0.287	CX	44.160	27.006.892
DXS8010	0.263	CX	44.469	27.271.722
DXS1218	0.034	CX	45.818	28.516.734
DXS1065	0.662	CX	46.722	29.351.323
DXS8049	0.025	CX	46.787	29.411.834
DXS1214	0.513	CX	47.363	30.622.209
DXS1036	0.074	CX	48.886	31.135.944
DXS1067	0.055	CX	48.955	31.159.057
DXS997	0.129	CX	49.169	31.241.448
DXS1237	0.143	CX	49.442	31.346.811
DXS538	0.218	CX	54.696	33.676.062
DXS1049	0.501	CX	56.628	34.538.471
DXS1069	0.188	CX	62.128	37.656.017
DXS8016	0.592	CX	62.130	38.005.539
DXS8113	0.392	CX	62.459	38.176.967
DXS8025	0.306	CX	63.021	38.552.286
DXS1058	0.374	CX	63.186	38.627.460
DXS8018	0.697	CX	63.570	38.802.811
DXS8015	0.207	CX	63.597	38.815.084
DXS8042	0.128	CX	63.598	38.876.318
DXS993	0.002	CX	66.171	40.178.574
DXS1201	0.154	CX	67.994	41.282.257
DXS8085	0.083	CX	67.995	41.356.492
DXS228	0.285	CX	68.649	41.761.599
DXS8379	0.065	CX	69.296	42.388.839
DXS7	0.189	CX	69.369	42.482.184
DXS8080	0.371	CX	69.999	43.289.305
DXS8054	0.221	CX	71.410	43.614.622
DXS8083	0.440	CX	71.544	44.287.420
DXS1055	0.368	CX	74.346	45.472.356
DXS337	0.214	CX	75.817	46.407.426
ARAF1	0.222</			

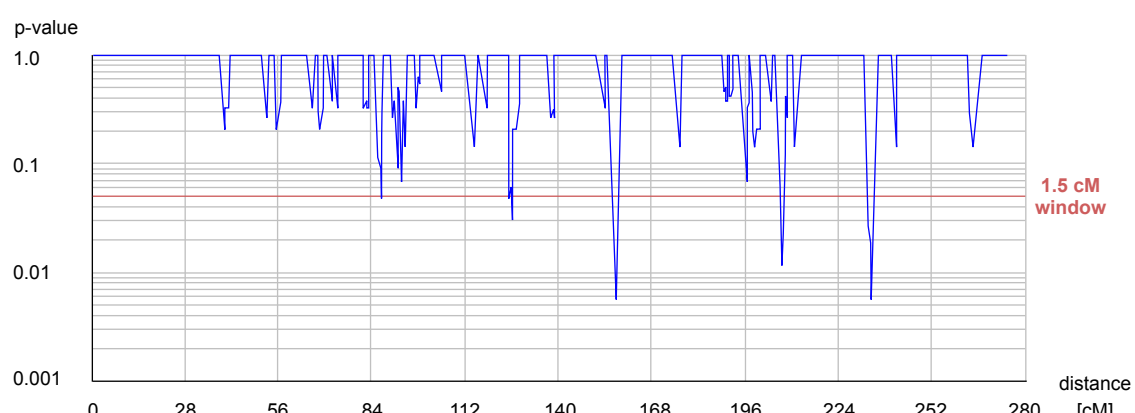
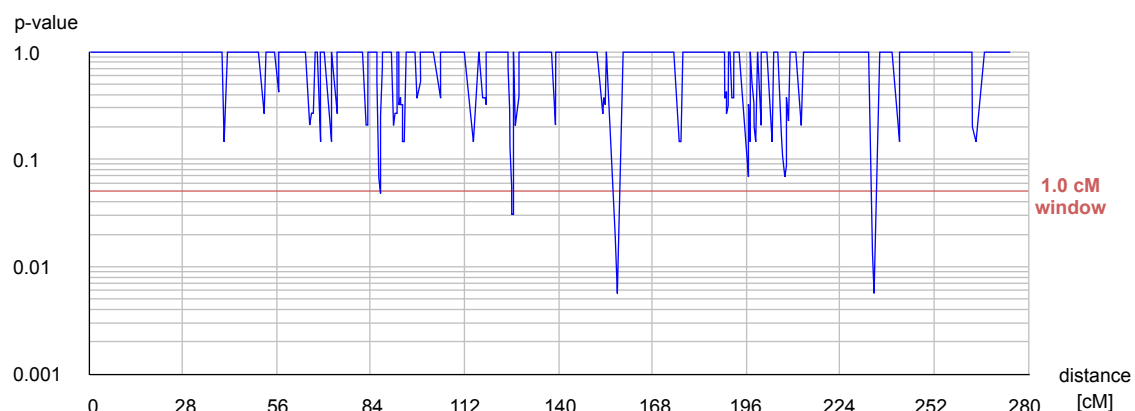
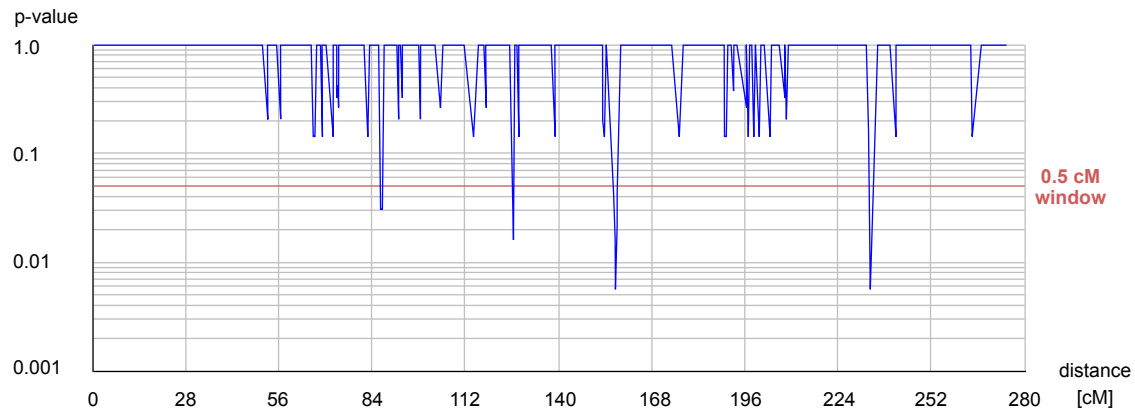
Marker name	pvalue	Chr	cM	Mb	Marker name	pvalue	Chr	cM	Mb
DXS1126	0.370	CX	77.309	47.739.118	DXS737	0.197	CX	134.663	126.163.948
DXS1039	0.362	CX	78.022	48.375.831	DXS1047	0.436	CX	135.280	127.780.943
DXS8024	0.092	CX	78.023	49.485.024	DXS8068	0.063	CX	135.678	128.825.585
DXS1000	0.953	CX	80.028	52.257.297	DXS1187	0.188	CX	138.375	129.738.690
DXS988	0.446	CX	80.088	52.319.825	DXS8071	0.089	CX	138.376	130.141.408
DXS1204	0.447	CX	80.780	53.076.388	DXS8041	0.348	CX	140.666	132.409.267
DXS8032	0.404	CX	81.464	53.794.461	DXS8074	0.234	CX	141.050	132.789.368
DXS991	0.466	CX	81.465	54.485.829	DXS8033	0.741	CX	141.958	132.793.440
DXS1190	0.683	CX	81.466	55.948.647	DXS691	0.145	CX	143.185	134.099.094
DXS7132	0.266	CX	82.281	63.522.127	CD40LG	0.394	CX	143.496	134.430.409
DXS8029	0.759	CX	82.282	63.808.778	DXS300	0.135	CX	143.964	134.928.410
DXS1213	0.408	CX	82.789	64.129.451	DXS8094	0.835	CX	143.977	134.942.361
DXS1194	0.335	CX	82.907	64.286.753	DXS1041	0.450	CX	144.146	135.241.506
DXS8380	0.098	CX	84.227	66.041.024	DXS8050	0.269	CX	144.399	135.691.561
DXS135	0.386	CX	84.912	66.952.653	DXS1062	0.591	CX	145.101	136.008.560
DXS981	0.001	CX	84.996	67.064.149	DXS1211	0.156	CX	145.992	137.010.944
DXS1216	0.479	CX	85.301	67.231.143	DXS1192	0.082	CX	145.993	137.073.700
DXS8111	0.508	CX	85.720	67.360.071	DXS102	0.264	CX	146.028	137.088.974
DXS1275	0.290	CX	85.732	67.381.282	DXS1232	0.293	CX	148.097	137.985.729
DXS339	0.013	CX	85.745	67.403.410	DXS8013	0.438	CX	148.572	138.191.727
DXS8031	0.012	CX	85.745	67.403.754	DXS984	0.268	CX	149.841	138.337.334
DXS106	0.489	CX	85.938	67.744.829	DXS1227	0.185	CX	154.527	139.496.017
DXS8052	0.008	CX	86.508	68.679.656	DXS8106	0.273	CX	158.660	140.877.724
DXS8030	0.235	CX	87.268	69.479.747	DXS8073	0.075	CX	164.419	142.429.481
DXS227	0.588	CX	88.001	71.265.296	DXS8028	0.096	CX	165.594	142.910.895
DXS8070	0.720	CX	88.106	71.522.768	DXS8045	0.131	CX	168.690	144.179.737
DXS8079	0.542	CX	88.107	71.988.032	DXS1200	0.191	CX	169.281	144.412.921
DXS8060	0.058	CX	88.108	72.330.800	DXS998	0.668	CX	170.423	145.275.585
DXS8092	0.495	CX	88.799	72.989.709	DXS731	0.259	CX	171.048	145.840.106
DXS8037	0.185	CX	88.800	72.990.251	DXS1215	0.399	CX	171.197	145.974.194
DXS441	0.049	CX	88.941	74.223.042	DXS8091	0.289	CX	171.910	146.308.352
DXS1225	0.083	CX	88.998	76.968.652	DXS1193	0.587	CX	174.056	147.085.762
DXS8082	0.618	CX	89.062	77.130.474	DXS1123	0.241	CX	174.423	147.191.796
DXS6800	0.357	CX	89.181	77.436.284	DXS1113	0.084	CX	174.809	147.302.946
DXS1197	0.775	CX	89.182	77.932.685	DXS8069	0.382	CX	178.186	148.277.525
DXS986	0.380	CX	89.183	78.136.903	DXS8103	0.585	CX	183.793	148.755.617
DXS738	0.352	CX	89.639	80.039.172	DXS1684	0.330	CX	183.829	148.766.165
DXS8076	0.672	CX	89.641	81.551.165	DXS8061	0.080	CX	190.270	150.639.232
DXS1002	0.046	CX	90.297	84.298.997	DXS15	0.291	CX	191.115	151.043.377
DXS8114	0.276	CX	90.367	84.385.848	DXS8087	1.3E-10	CX	191.781	151.362.229
DXS8109	0.222	CX	90.625	84.706.357	DXS1073	0.442	CX	193.734	152.296.459
DXS1066	0.488	CX	91.026	85.763.801	DXS1108	0.145	CX	195.818	153.293.680
DXS1222	0.169	CX	91.027	86.195.210					
DXS1217	0.601	CX	92.234	87.167.686					
DXS3	0.599	CX	97.431	91.354.746					
DXS1203	0.676	CX	97.661	91.539.913					
DXS990	0.057	CX	97.662	91.772.453					
DXS8077	0.009	CX	99.587	94.047.008					
DXS458	0.079	CX	100.465	94.900.406					
DXS8020	0.137	CX	104.167	98.340.582					
DXS8034	0.131	CX	104.168	98.398.640					
DXS178	0.461	CX	106.301	99.505.864					
DXS8089	0.191	CX	106.303	99.506.941					
DXS8100	0.529	CX	106.568	99.850.708					
DXS8063	0.352	CX	106.569	99.970.197					
DXS101	0.353	CX	106.570	100.166.990					
DXS1153	0.671	CX	106.571	101.031.681					
DXS1106	0.132	CX	106.572	101.503.788					
DXS8096	0.281	CX	106.573	101.553.899					
DXS1191	0.719	CX	107.080	102.065.536					
DXS8075	0.400	CX	107.081	102.642.722					
DXS8112	0.527	CX	107.082	103.681.141					
DXS8048	0.367	CX	107.578	104.708.372					
DXS1120	0.025	CX	107.579	105.390.287					
DXS6797	0.230	CX	107.580	106.252.922					
DXS571	0.375	CX	107.581	106.315.774					
DXS7133	0.817	CX	108.041	107.805.514					
DXS1188	0.100	CX	109.698	109.415.760					
DXS8110	0.086	CX	110.322	110.023.505					
DXS1059	0.130	CX	110.323	110.089.939					
DXS8021	0.252	CX	110.324	110.208.992					
DXS1072	0.285	CX	112.621	110.867.801					
DXS8088	0.219	CX	115.832	112.124.996					
DXS1220	0.204	CX	118.089	113.372.316					
DXS8055	0.353	CX	118.090	113.419.140					
DXS424	0.269	CX	118.787	115.066.707					
DXS8064	0.346	CX	119.677	116.026.996					
DXS8067	0.438	CX	123.004	118.114.494					
DXS1001	0.037	CX	123.763	118.590.627					
DXS8059	1.1E-5	CX	127.105	119.961.166					
DXS1212	0.322	CX	127.356	121.184.493					
DXS8098	0.569	CX	127.358	121.611.956					
DXS8057	0.362	CX	129.745	122.274.552					
DXS1206	0.170	CX	134.336	125.084.595					
DXS8078	0.708	CX	134.337	125.246.836					
DXS8044	0.537	CX	134.338	125.311.605					

Appendix C - Sliding window plots and synoptical tables

Sliding windows data displaying six window sizes of 0.5, 1.0, 1.5, 2.0, 2.5 and 3.0 cM, applied on 23 human chromosomes and STR-marker genotyped data derived from PCRs with pooled DNA (Appendix B). The red line in plots indicates the significance threshold set at 0.05.

In Section 3, Table 3.3 and 3.4 and in Appendix D genes that are located in significant windows are displayed.

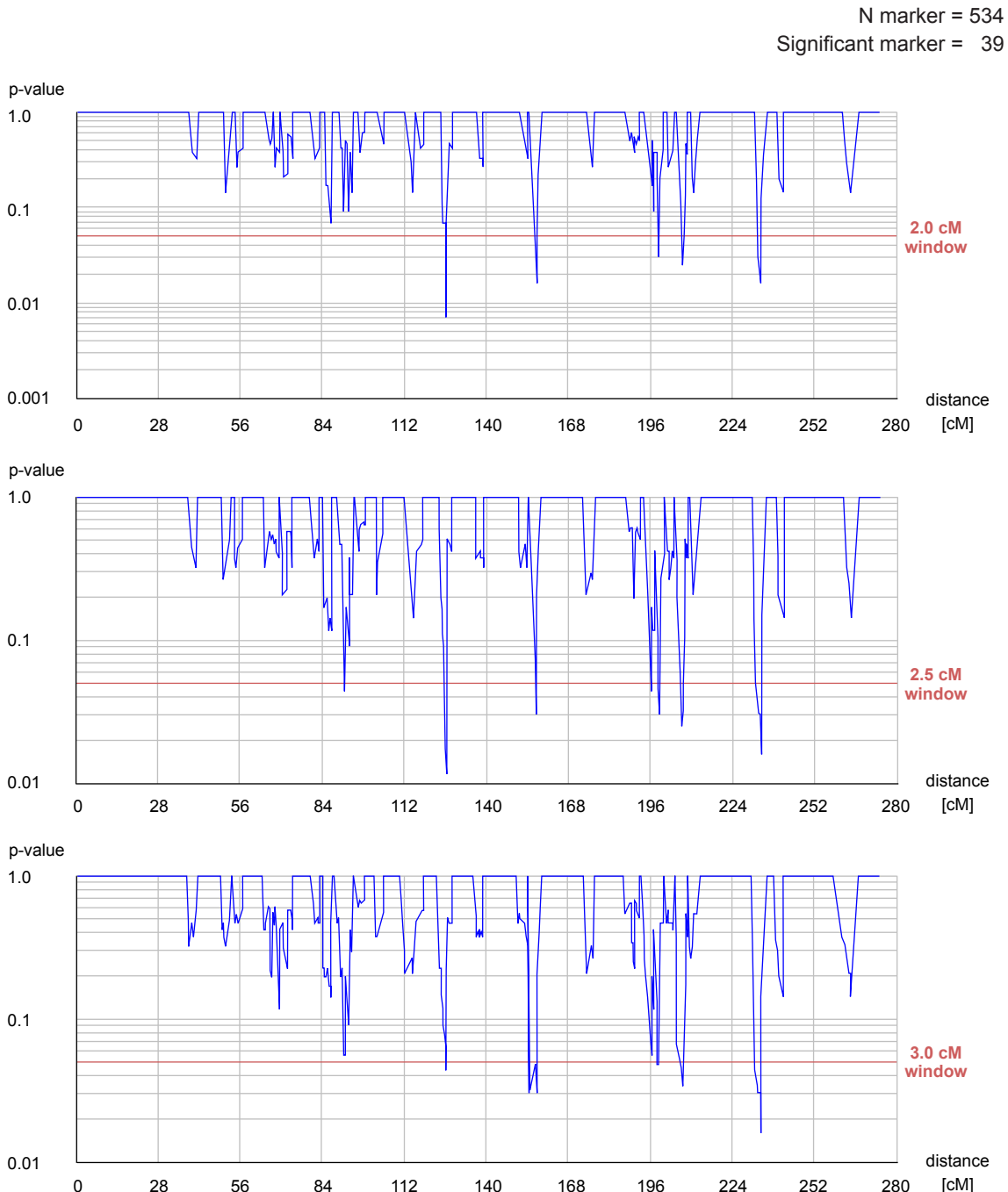
Chromosome 1



windows size → 0.5		
Selected Windows position (cM)	p-value	Significative Markers
86.810 - 87.310	0.0457	D1S1643 D1S2737
86.841 - 87.341	0.0290	D1S1643 D1S2737
87.173 - 87.673	0.0290	D1S1643 D1S2737
126.349 - 126.849	0.0290	D1S1657 D1S335
126.418 - 126.918	0.0161	D1S1657 D1S335
126.621 - 127.121	0.0161	D1S1657 D1S335
157.177 - 157.677	0.0161	D1S1655 D1S398
157.404 - 157.904	0.0056	D1S1655 D1S398
233.679 - 234.179	0.0161	D1S479 D1S1644
233.918 - 234.418	0.0056	D1S479 D1S1644

windows size → 1.0		
Selected Windows position (cM)	p-value	Significative Markers
86.841 - 87.841	0.0457	D1S1643 D1S2737
87.173 - 88.173	0.0457	D1S1643 D1S2737
126.349 - 127.349	0.0457	D1S1657 D1S535
126.418 - 127.418	0.0290	D1S1657 D1S535
126.621 - 127.621	0.0290	D1S1657 D1S535
157.177 - 158.177	0.0161	D1S1655 D1S398
157.404 - 158.404	0.0056	D1S1655 D1S398
233.679 - 234.679	0.0161	D1S479 D1S1644
233.918 - 234.918	0.0056	D1S479 D1S1644

windows size → 1.5		
Selected Windows position (cM)	p-value	Significative Markers
87.173 - 88.673	0.0457	D1S1643 D1S2737
125.300 - 126.800	0.0457	D1S1657 D1S535
126.418 - 127.918	0.0457	D1S1657 D1S535
126.621 - 128.121	0.0290	D1S1657 D1S535
157.177 - 158.677	0.0161	D1S1655 D1S398
157.404 - 158.904	0.0056	D1S1655 D1S398
206.634 - 208.134	0.0457	D1S2760 D1S510
207.388 - 208.888	0.0118	D1S2760 D1S510 D1S1620
232.663 - 234.163	0.0290	D1S479 D1S1644
233.679 - 235.179	0.0161	D1S479 D1S1644
233.918 - 235.418	0.0056	D1S479 D1S1644



windows size → 2.0
Selected Windows position (cM) p-value Significative Markers

126.418 - 128.418	0.0071	D1S1657 D1S535 D1S429
126.621 - 128.621	0.0071	D1S1657 D1S535 D1S429
126.622 - 128.622	0.0457	D1S535 D1S429
157.177 - 159.177	0.0290	D1S1655 D1S398
157.404 - 159.404	0.0161	D1S1655 D1S398
198.954 - 200.954	0.0290	D1S1726 D1S2716
207.388 - 209.388	0.0252	D1S2760 D1S510 D1S1620
232.663 - 234.663	0.0290	D1S479 D1S1644
233.679 - 235.679	0.0161	D1S479 D1S1644
233.918 - 235.918	0.0161	D1S479 D1S1644

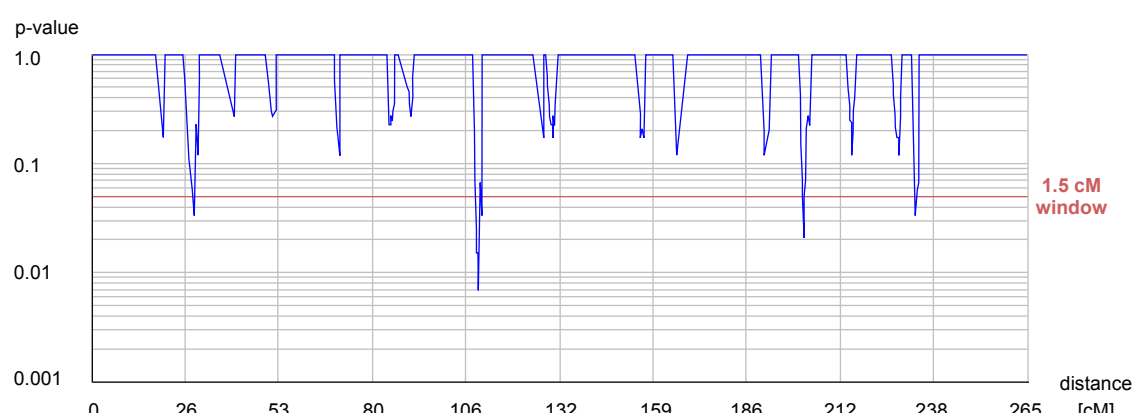
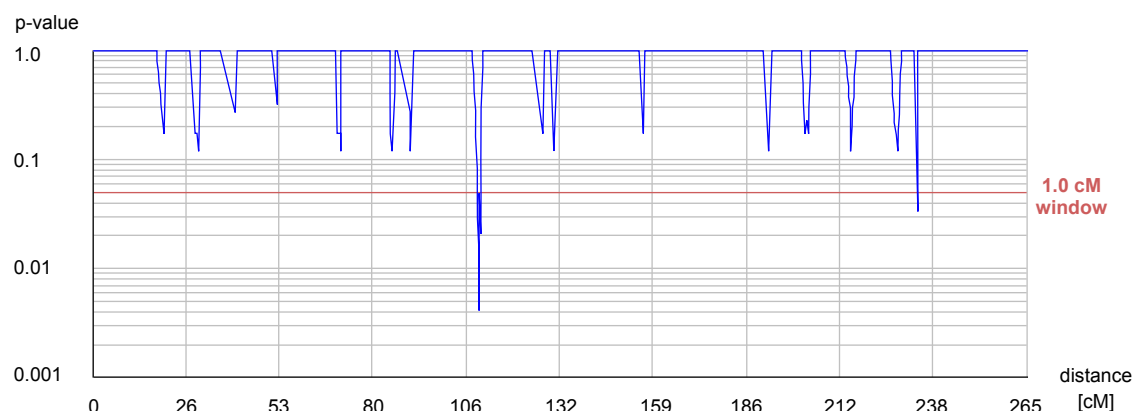
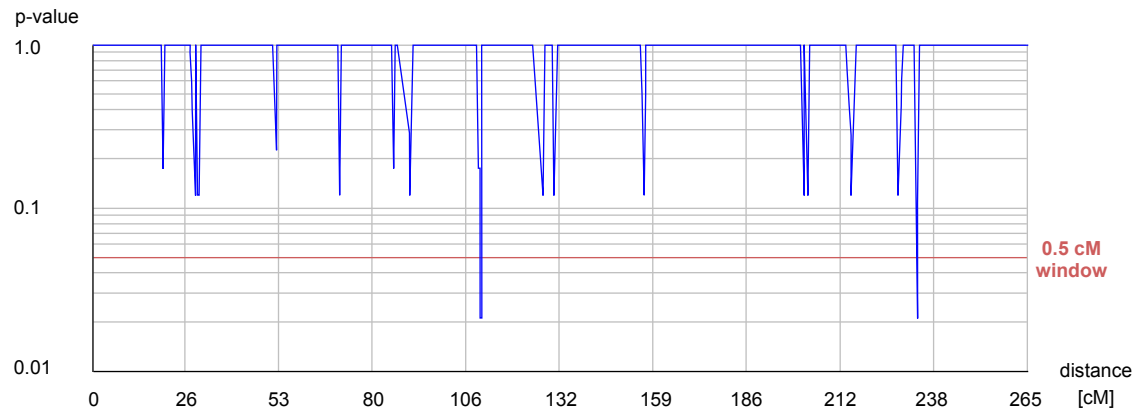
windows size → 2.5
Selected Windows position (cM) p-value Significative Markers

91.987 - 94.487	0.0442	D1S1613 ATA52G05 D1S520
126.349 - 128.849	0.0178	D1S1657 D1S535 D1S429
126.418 - 128.918	0.0118	D1S1657 D1S535 D1S429
126.621 - 129.121	0.0442	D1S1657 D1S535 D1S429
157.177 - 159.677	0.0457	D1S1655 D1S398
157.404 - 159.904	0.0290	D1S1655 D1S398
198.523 - 201.023	0.0457	D1S1726 D1S2716
198.954 - 201.454	0.0290	D1S1726 D1S2716
206.634 - 209.134	0.0252	D1S2760 D1S510 D1S1620
207.388 - 209.888	0.0340	D1S2760 D1S510 D1S1620
231.586 - 234.086	0.0457	D1S479 D1S1644
232.663 - 235.163	0.0290	D1S479 D1S1644
233.679 - 236.179	0.0290	D1S479 D1S1644
233.918 - 236.418	0.0161	D1S479 D1S1644

windows size → 3.0
Selected Windows position (cM) p-value Significative Markers

126.621 - 129.621	0.0442	D1S1657 D1S535 D1S429
154.538 - 157.538	0.0290	D1S1655 D1S398
157.177 - 160.177	0.0457	D1S1655 D1S398
157.404 - 160.404	0.0290	D1S1655 D1S398
198.523 - 201.523	0.0457	D1S1726 D1S2716
198.954 - 201.954	0.0457	D1S1726 D1S2716
206.634 - 209.634	0.0442	D1S2760 D1S510 D1S1620
207.388 - 210.388	0.0340	D1S2760 D1S510 D1S1620
231.586 - 234.586	0.0457	D1S479 D1S1644
232.663 - 235.663	0.0290	D1S479 D1S1644
233.679 - 236.679	0.0290	D1S479 D1S1644
233.918 - 236.918	0.0161	D1S479 D1S1644

Chromosome 2

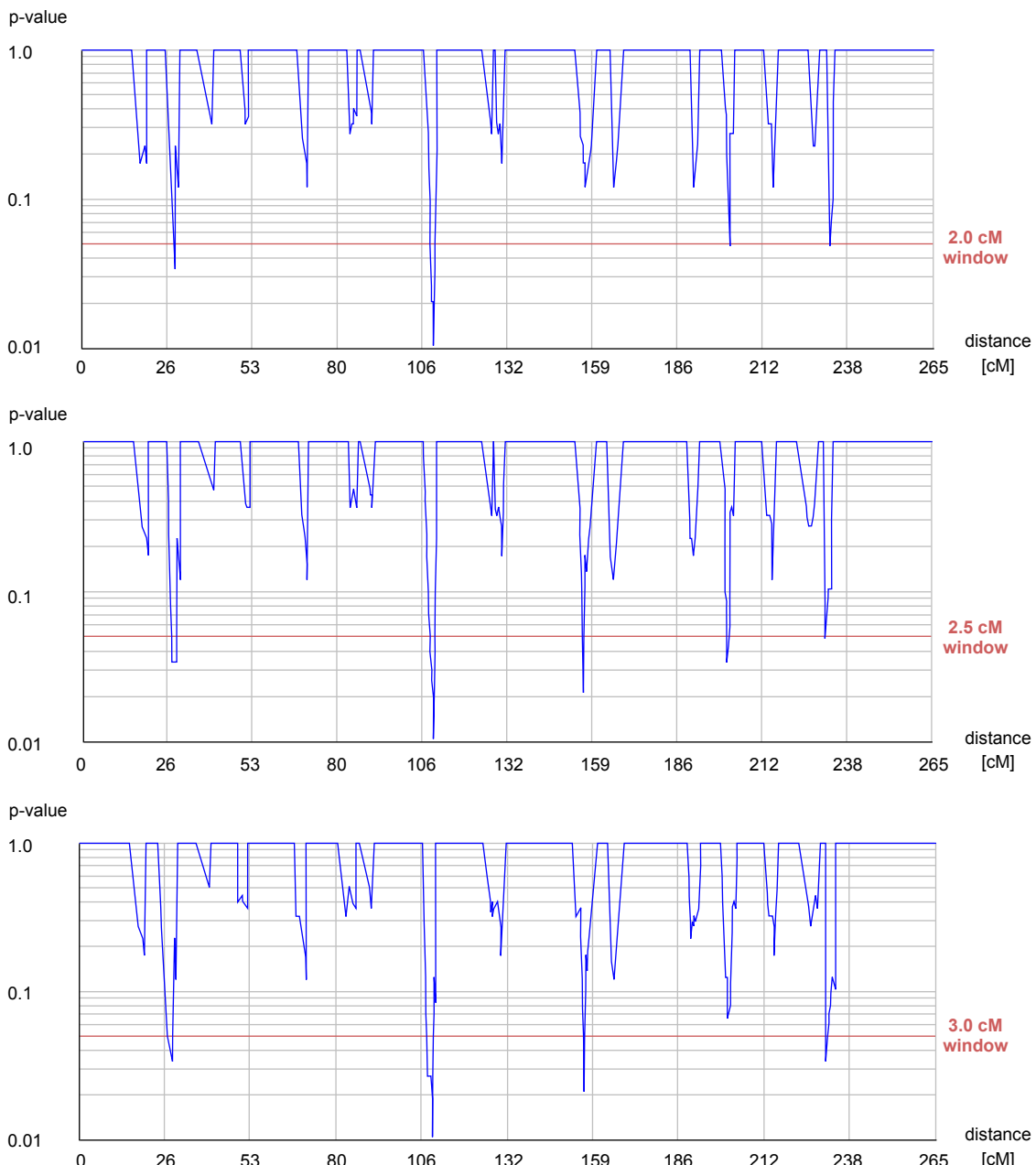


windows size → 0.5		
Selected Windows	p-value	Significative Markers
position (cM)		
110.093 - 110.593	0.0212	D2S435 D2S394
110.346 - 110.846	0.0212	D2S435 D2S394
234.125 - 234.625	0.0212	D2S1333 D2S1363

windows size → 1.0		
Selected Windows	p-value	Significative Markers
position (cM)		
109.628 - 110.628	0.0105	D2S428 D2S435 D2S394
109.629 - 110.629	0.0069	D2S428 D2S435 D2S394
109.630 - 110.630	0.0041	D2S428 D2S435 D2S394
109.953 - 110.953	0.0488	D2S435 D2S394
110.093 - 111.093	0.0339	D2S435 D2S394
110.346 - 111.346	0.0212	D2S435 D2S394
234.125 - 235.125	0.0339	D2S1333 D2S1363

windows size → 1.5		
Selected Windows	p-value	Significative Markers
position (cM)		
29.218 - 30.718	0.0339	D2S297 D2S1400
108.995 - 110.495	0.0151	D2S428 D2S435 D2S394
109.628 - 111.128	0.0151	D2S428 D2S435 D2S394
109.629 - 111.129	0.0105	D2S428 D2S435 D2S394
109.630 - 111.130	0.0069	D2S428 D2S435 D2S394
110.093 - 111.593	0.0488	D2S435 D2S394
110.346 - 111.846	0.0339	D2S435 D2S394
202.055 - 203.555	0.0212	D2S2392 D2S309
233.078 - 234.578	0.0339	D2S1333 D2S1363

N marker = 371
 Significant marker = 23

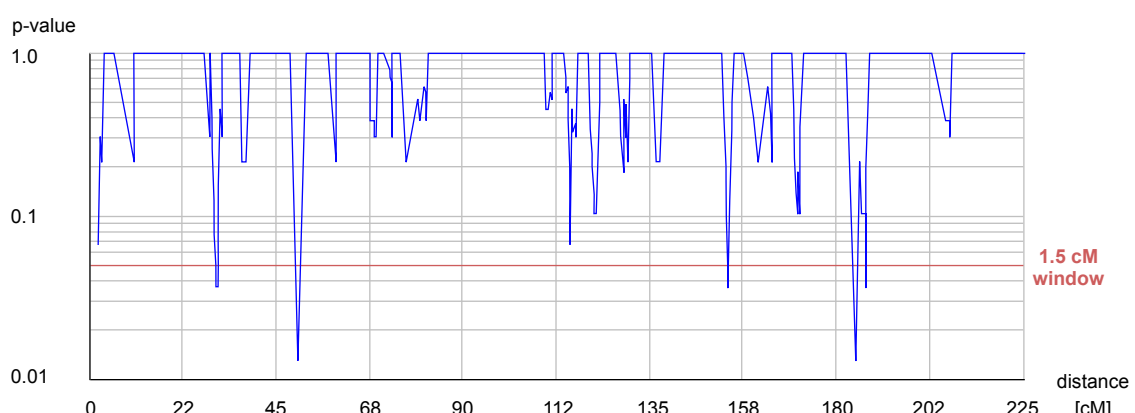
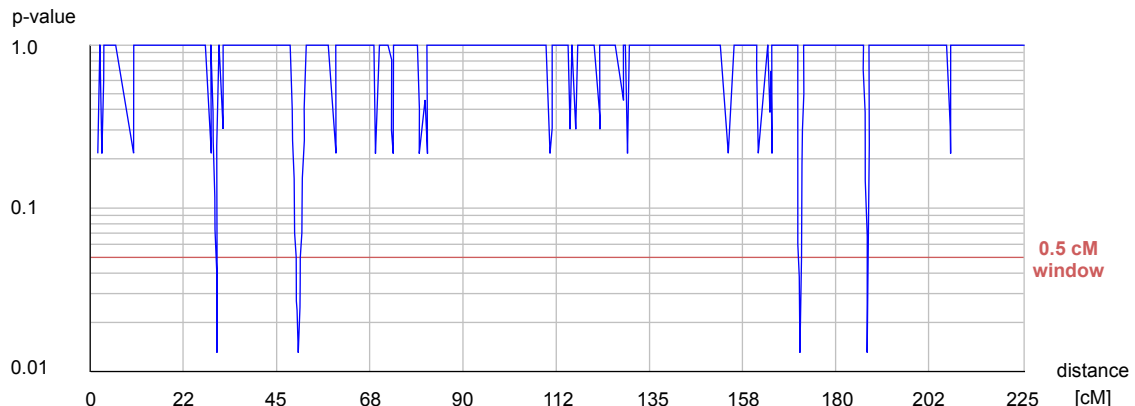


windows size → 2.0		
Selected Windows position (cM)	p-value	Significative Markers
29.218 - 31.218	0.0339	D2S297 D2S1400
108.995 - 110.995	0.0206	D2S428 D2S435 D2S394
109.628 - 111.628	0.0206	D2S428 D2S435 D2S394
109.629 - 111.629	0.0151	D2S428 D2S435 D2S394
109.630 - 111.630	0.0105	D2S428 D2S435 D2S394
110.093 - 112.093	0.0488	D2S435 D2S394
110.346 - 112.346	0.0339	D2S435 D2S394
202.055 - 204.055	0.0488	D2S2392 D2S309
233.078 - 235.078	0.0488	D2S1333 D2S1363

windows size → 2.5		
Selected Windows position (cM)	p-value	Significative Markers
27.796 - 30.296	0.0339	D2S297 D2S1400
29.218 - 31.718	0.0339	D2S297 D2S1400
108.995 - 111.495	0.0270	D2S428 D2S435 D2S394
109.628 - 112.128	0.0206	D2S428 D2S435 D2S394
109.629 - 112.129	0.0151	D2S428 D2S435 D2S394
109.630 - 112.130	0.0105	D2S428 D2S435 D2S394
110.093 - 112.593	0.0488	D2S435 D2S394
156.507 - 159.007	0.0339	D2S129 D2S122
156.508 - 159.008	0.0212	D2S129 D2S122
200.979 - 203.479	0.0488	D2S2392 D2S309
200.980 - 203.480	0.0339	D2S2392 D2S309
232.122 - 234.622	0.0488	D2S1333 D2S1363

windows size → 3.0		
Selected Windows position (cM)	p-value	Significative Markers
27.796 - 30.796	0.0488	D2S297 D2S1400
29.218 - 32.218	0.0339	D2S297 D2S1400
107.937 - 110.937	0.0270	D2S428 D2S435 D2S394
108.995 - 111.995	0.0270	D2S428 D2S435 D2S394
109.628 - 112.628	0.0206	D2S428 D2S435 D2S394
109.629 - 112.629	0.0151	D2S428 D2S435 D2S394
109.630 - 112.630	0.0105	D2S428 D2S435 D2S394
156.507 - 159.507	0.0339	D2S129 D2S122
156.508 - 159.508	0.0212	D2S129 D2S122
231.167 - 234.167	0.0339	D2S1333 D2S1363

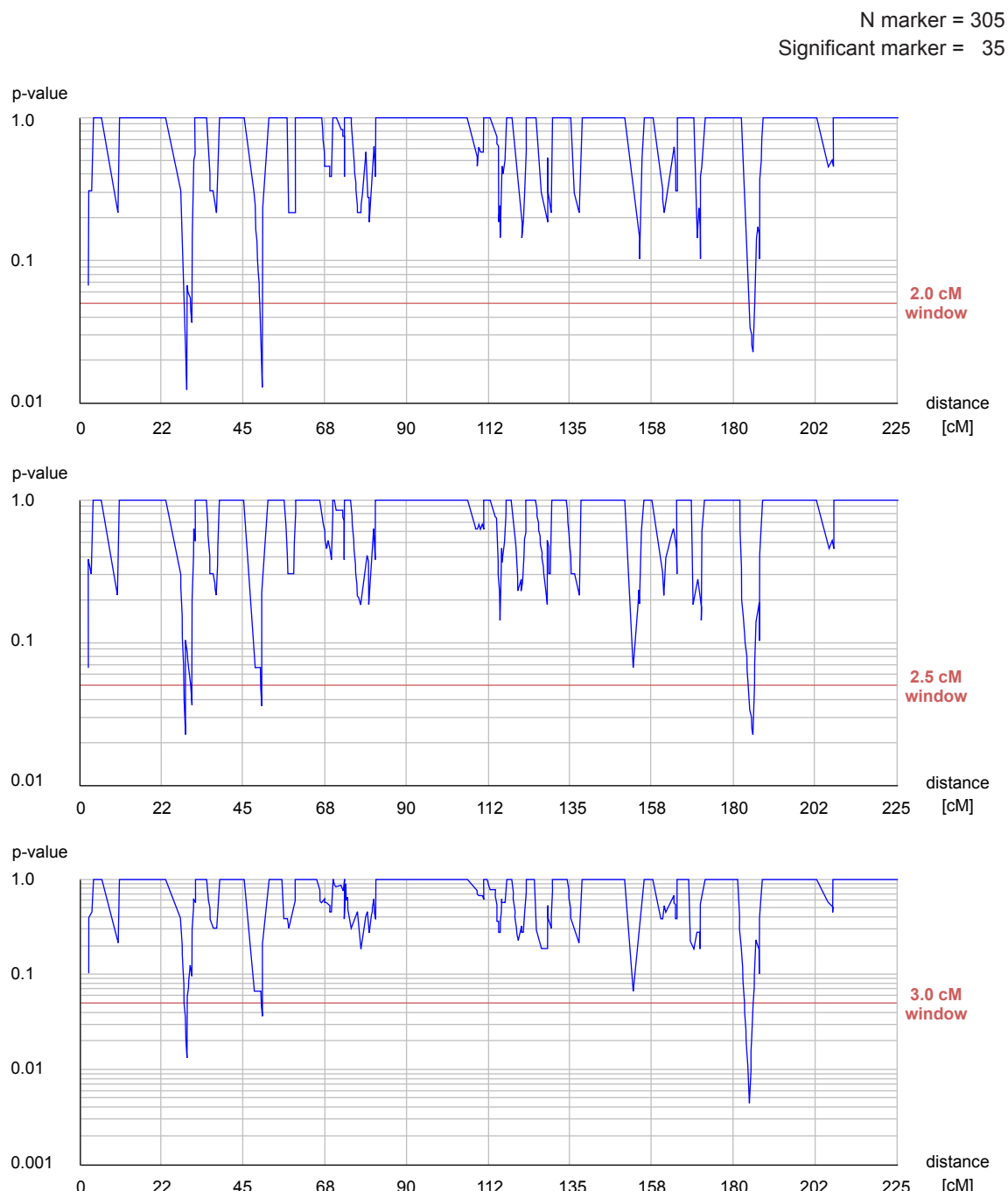
Chromosome 3



windows size → 0.5		
Selected Windows position (cM)	p-value	Significative Markers
30.710 - 31.210	0.0363	D3S3714 D3S3680
30.891 - 31.391	0.0131	D3S3714 D3S3680
49.944 - 50.444	0.0363	D3S2466 D3S2335
50.162 - 50.662	0.0131	D3S2466 D3S2335
171.082 - 171.582	0.0363	D3S3052 D3S3668
171.150 - 171.650	0.0131	D3S3052 D3S3668
187.360 - 187.860	0.0363	D3S3037 D3S1754
187.380 - 187.880	0.0131	D3S3037 D3S1754

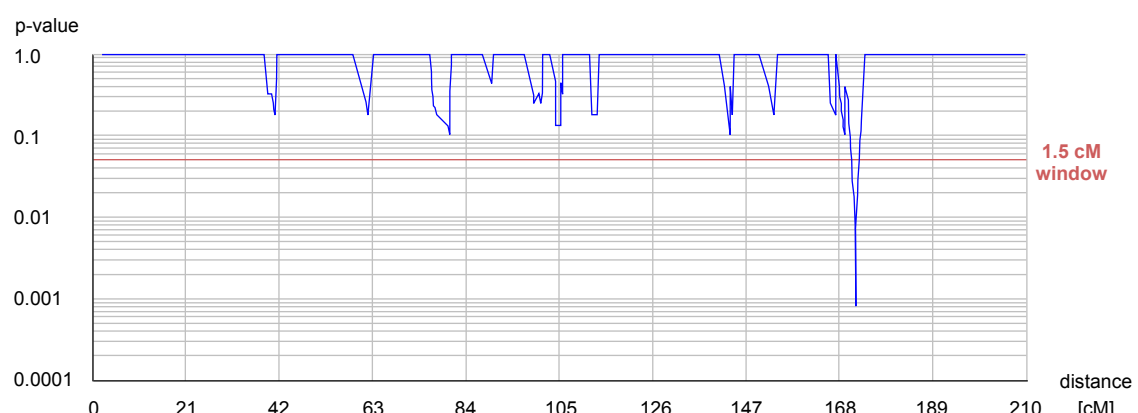
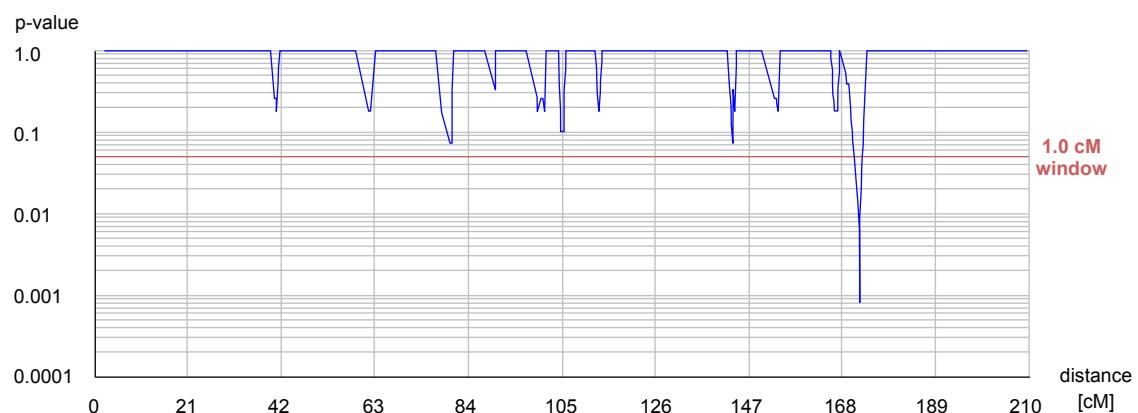
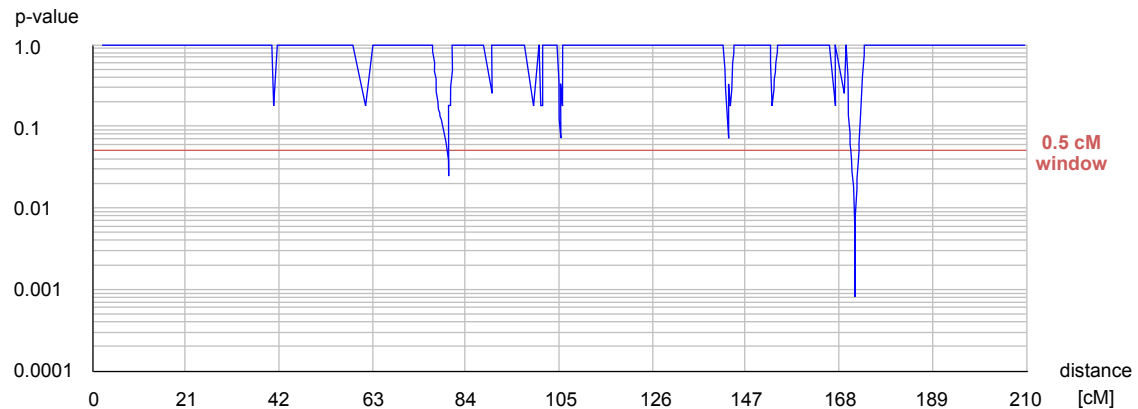
windows size → 1.0		
Selected Windows position (cM)	p-value	Significative Markers
2.332 - 3.332	0.0363	D3S2387 D3S1270
30.891 - 31.891	0.0363	D3S3714 D3S3680
49.944 - 50.944	0.0363	D3S2466 D3S2335
50.162 - 51.162	0.0131	D3S2466 D3S2335
154.110 - 155.110	0.0363	D3S3599 D4S2378
154.111 - 155.111	0.0131	D3S3599 D4S2378
171.082 - 172.082	0.0363	D3S3052 D3S3668
171.150 - 172.150	0.0131	D3S3052 D3S3668
184.680 - 185.680	0.0131	D3S2421 D3S2427
187.380 - 188.380	0.0363	D3S3037 D3S1754

windows size → 1.5		
Selected Windows position (cM)	p-value	Significative Markers
30.710 - 32.210	0.0367	D3S3714 D3S3680 D3S3693
30.891 - 32.391	0.0367	D3S3714 D3S3680 D3S3693
49.944 - 51.444	0.0363	D3S2466 D3S2335
50.162 - 51.662	0.0131	D3S2466 D3S2335
154.111 - 155.611	0.0363	D3S3599 D4S2378
184.680 - 186.180	0.0131	D3S2421 D3S2427
187.380 - 188.880	0.0363	D3S3037 D3S1754



windows size → 2.0			windows size → 2.5			windows size → 3.0		
Selected Windows	p-value	Significative Markers	Selected Windows	p-value	Significative Markers	Selected Windows	p-value	Significative Markers
position (cM)			position (cM)			position (cM)		
29.370 - 31.370	0.0125	D3S3611 D3S3714 D3S3680	29.370 - 31.870	0.0229	D3S3611 D3S3714 D3S3680	29.370 - 32.370	0.0134	D3S3611 D3S3714 D3S3680
30.891 - 32.891	0.0367	D3S3714 D3S3680 D3S3693	30.891 - 33.391	0.0367	D3S3714 D3S3680 D3S3693	30.891 - 32.891		D3S3693
49.944 - 51.944	0.0363	D3S2466 D3S2335	50.162 - 52.662	0.0363	D3S2466 D3S2335	50.162 - 53.162	0.0363	D3S2466 D3S2335
50.162 - 52.162	0.0131	D3S2466 D3S2335	184.680 - 187.180	0.0363	D3S2421 D3S2427	184.680 - 187.680	0.0045	D3S2421 D3S2427 D3S3037 D3S1754
184.680 - 186.680	0.0363	D3S2421 D3S2427	185.545 - 188.045	0.0229	D3S2427 D3S3037 D3S1754	185.545 - 188.545	0.0367	D3S2427 D3S3037 D3S1754
185.545 - 187.545	0.0229	D3S2427 D3S3037 D3S1754						

Chromosome 4

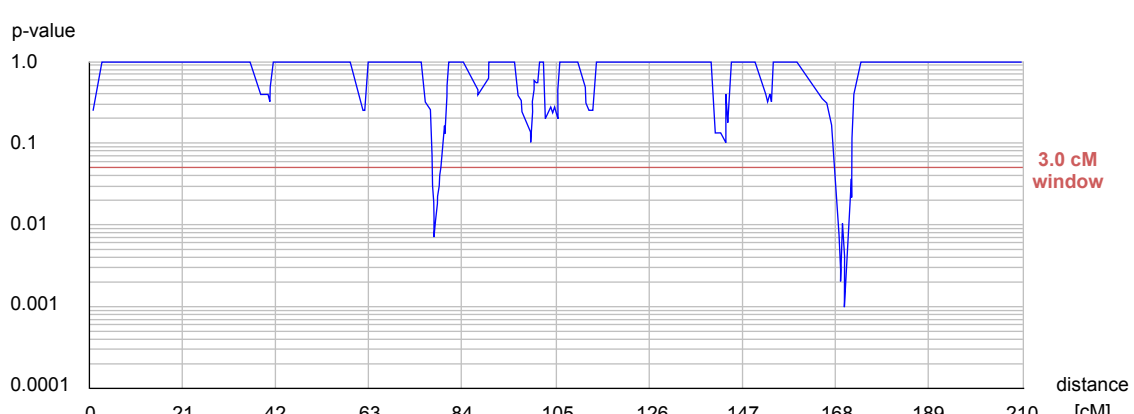
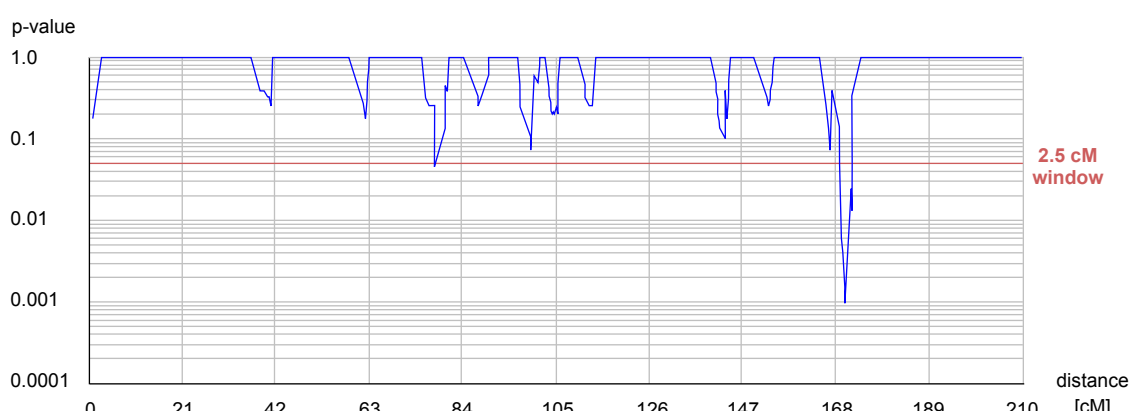
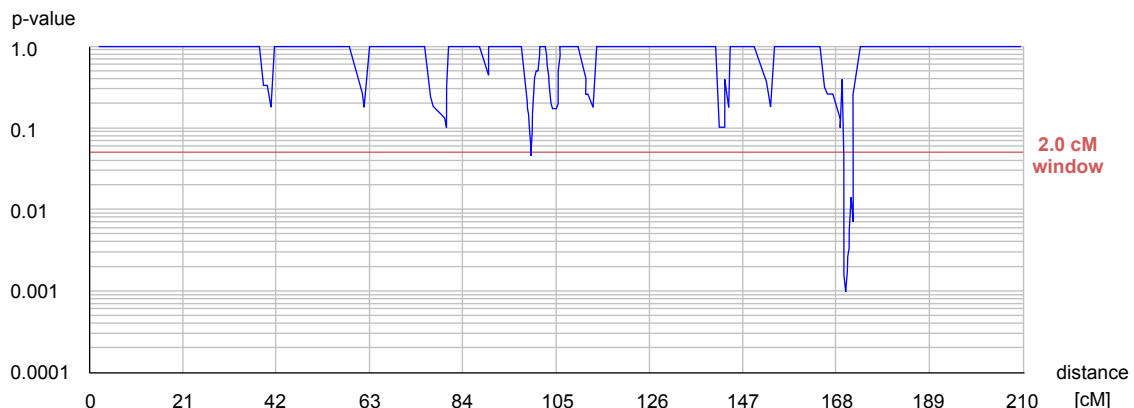


windows size → 0.5		
Selected Windows position (cM)	p-value	Significative Markers
80.140 - 80.640	0.0464	D4S2987 D4S1541
80.312 - 80.812	0.0247	D4S2987 D4S1541
171.766 - 172.266	0.0071	D4S2992 D4S2991 D4S2431
171.767 - 172.267	0.0031	D4S2992 D4S2991 D4S2431
171.768 - 172.268	8.0E-4	D4S2992 D4S2991 D4S2431
171.769 - 172.269	0.0088	D4S2991 D4S2431

windows size → 1.0		
Selected Windows position (cM)	p-value	Significative Markers
171.766 - 172.766	0.0071	D4S2992 D4S2991 D4S2431
171.767 - 172.767	0.0031	D4S2992 D4S2991 D4S2431
171.768 - 172.768	8.0E-4	D4S2992 D4S2991 D4S2431
171.769 - 172.769	0.0088	D4S2991 D4S2431

windows size → 1.5		
Selected Windows position (cM)	p-value	Significative Markers
171.766 - 173.266	0.0071	D4S2992 D4S2991 D4S2431
171.767 - 173.267	0.0031	D4S2992 D4S2991 D4S2431
171.768 - 173.268	8.0E-4	D4S2992 D4S2991 D4S2431
171.769 - 173.269	0.0088	D4S2991 D4S2431

N marker = 224
Significant marker = 22

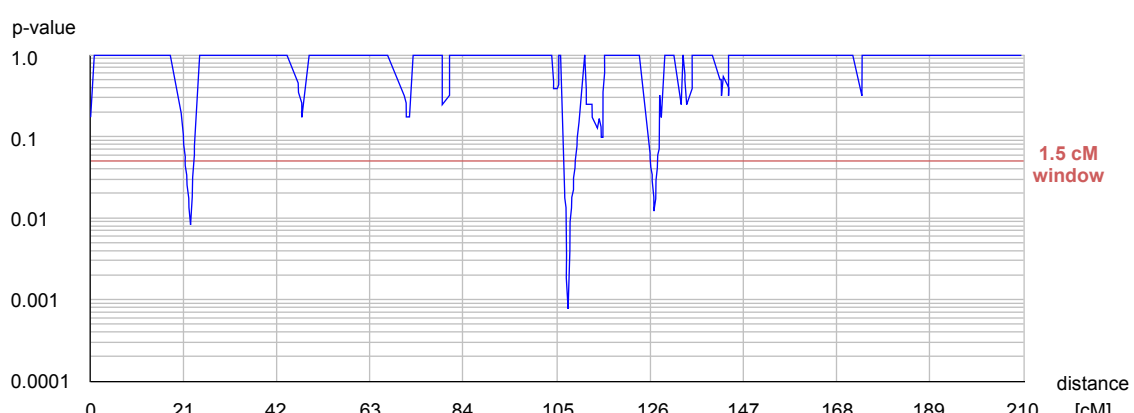
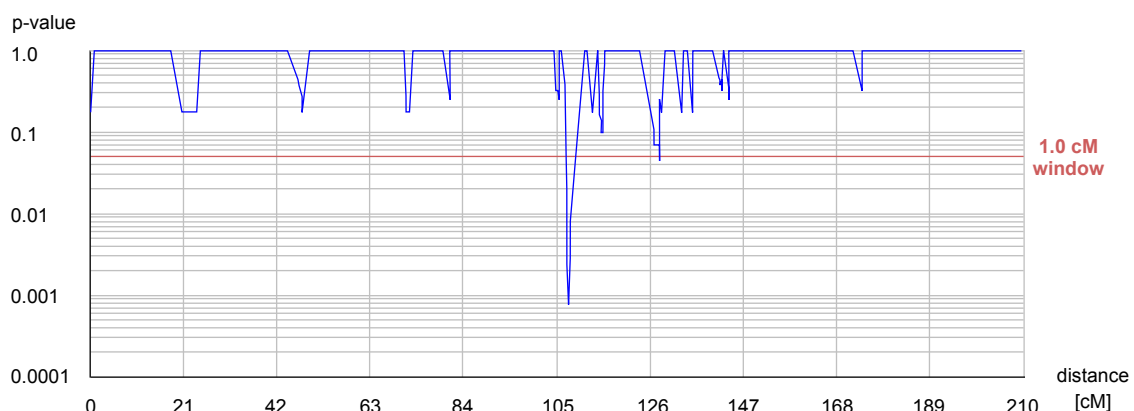
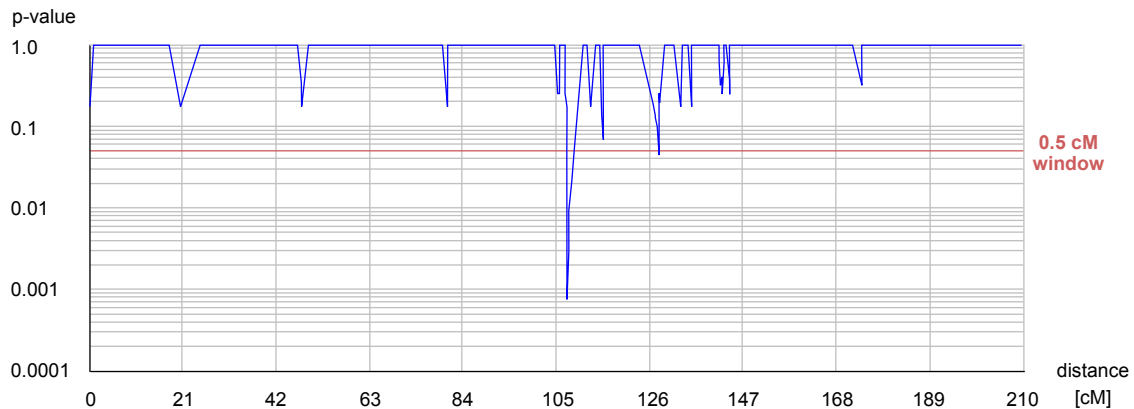


windows size → 2.0		
Selected Windows position (cM)	p-value	Significative Markers
99.464 - 101.464	0.0464	D4S2460 D4S3245
169.956 - 171.956	0.0216	D4S1646 D4S2992 D4S2991
169.974 - 171.974	0.0021	D4S1646 D4S2992 D4S2991
D4S2431		
170.133 - 172.133	0.0010	D4S1646 D4S2992 D4S2991
D4S2431		
171.766 - 173.766	0.0216	D4S2992 D4S2991 D4S2431
171.767 - 173.767	0.0133	D4S2992 D4S2991 D4S2431
171.768 - 173.768	0.0071	D4S2992 D4S2991 D4S2431
171.769 - 173.769	0.0464	D4S2991 D4S2431

windows size → 2.5		
Selected Windows position (cM)	p-value	Significative Markers
77.905 - 80.405	0.0464	D4S398 D4S2987
169.470 - 171.970	0.0102	D4S1646 D4S2992 D4S2991
D4S2431		
169.551 - 172.051	0.0066	D4S1646 D4S2992 D4S2991
D4S2431		
169.956 - 172.456	0.0040	D4S1646 D4S2992 D4S2991
D4S2431		
169.974 - 172.474	0.0021	D4S1646 D4S2992 D4S2991
D4S2431		
170.133 - 172.633	0.0010	D4S1646 D4S2992 D4S2991
D4S2431		
171.766 - 174.266	0.0322	D4S2992 D4S2991 D4S2431
171.767 - 174.267	0.0216	D4S2992 D4S2991 D4S2431
171.768 - 174.268	0.0133	D4S2992 D4S2991 D4S2431

windows size → 3.0		
Selected Windows position (cM)	p-value	Significative Markers
77.766 - 80.766	0.0133	D4S398 D4S2987 D4S1541
77.905 - 80.905	0.0071	D4S398 D4S2987 D4S1541
D4S2431		
169.018 - 172.018	0.0033	D4S2426 D4S1646 D4S2992
D4S2991 D4S2431		
169.127 - 172.127	0.0021	D4S2426 D4S1646 D4S2992
D4S2991 D4S2431		
169.470 - 172.470	0.0102	D4S1646 D4S2992 D4S2991
D4S2431		
169.551 - 172.551	0.0066	D4S1646 D4S2992 D4S2991
D4S2431		
169.956 - 172.956	0.0040	D4S1646 D4S2992 D4S2991
D4S2431		
169.974 - 172.974	0.0021	D4S1646 D4S2992 D4S2991
D4S2431		
170.133 - 173.133	0.0010	D4S1646 D4S2992 D4S2991
D4S2431		
171.766 - 174.766	0.045	D4S2992 D4S2991 D4S2431
171.767 - 174.767	0.0322	D4S2992 D4S2991 D4S2431
171.768 - 174.768	0.0216	D4S2992 D4S2991 D4S2431

Chromosome 5

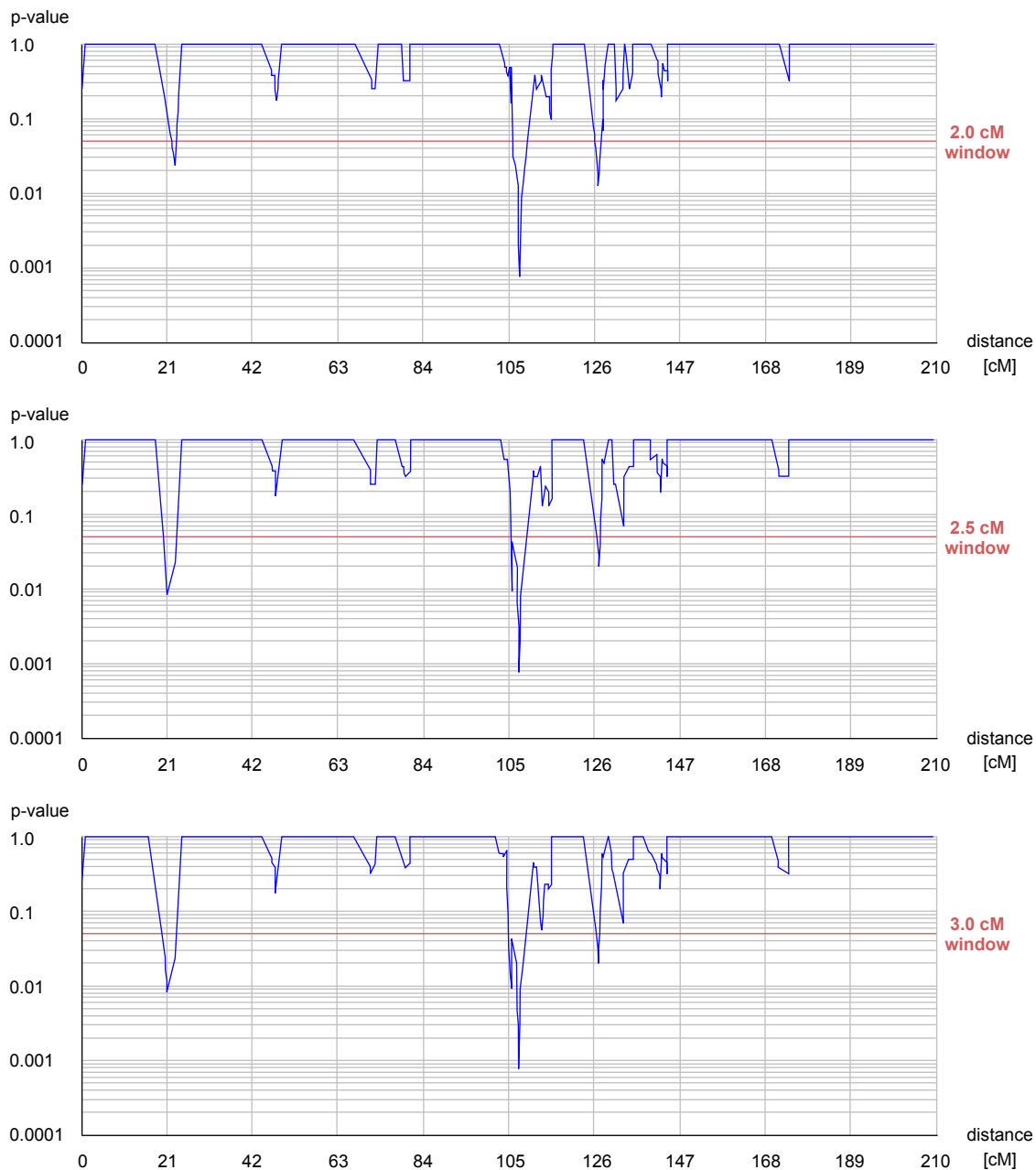


windows size → 0.5		
Selected Windows	p-value	Significative Markers
position (cM)		
107.622 - 108.122	8.0E-4	D5S1463 D5S815 D5S2499
108.004 - 108.504	0.0084	D5S815 D5S2499
128.045 - 128.545	0.0445	D5S1478 D5S657

windows size → 1.0		
Selected Windows	p-value	Significative Markers
position (cM)		
107.141 - 108.141	0.0125	D5S1463 D5S815 D5S2499
107.142 - 108.142	0.0067	D5S1463 D5S815 D5S2499
107.383 - 108.383	0.0029	D5S1463 D5S815 D5S2499
107.622 - 108.622	8.0E-4	D5S1463 D5S815 D5S2499
108.004 - 109.004	0.0084	D5S815 D5S2499
128.045 - 129.045	0.0445	D5S1478 D5S657

windows size → 1.5		
Selected Windows	p-value	Significative Markers
position (cM)		
22.949 - 24.449	0.0084	D5S1957 D5S807
106.879 - 108.379	0.0203	D5S1463 D5S815 D5S2499
107.141 - 108.641	0.0125	D5S1463 D5S815 D5S2499
107.142 - 108.642	0.0067	D5S1463 D5S815 D5S2499
107.383 - 108.883	0.0029	D5S1463 D5S815 D5S2499
107.622 - 109.122	8.0E-4	D5S1463 D5S815 D5S2499
108.004 - 109.504	0.0084	D5S815 D5S2499
127.059 - 128.559	0.0203	D5S494 D5S1478 D5S657
127.060 - 128.560	0.0125	D5S494 D5S1478 D5S657

N marker = 241
Significant marker = 23

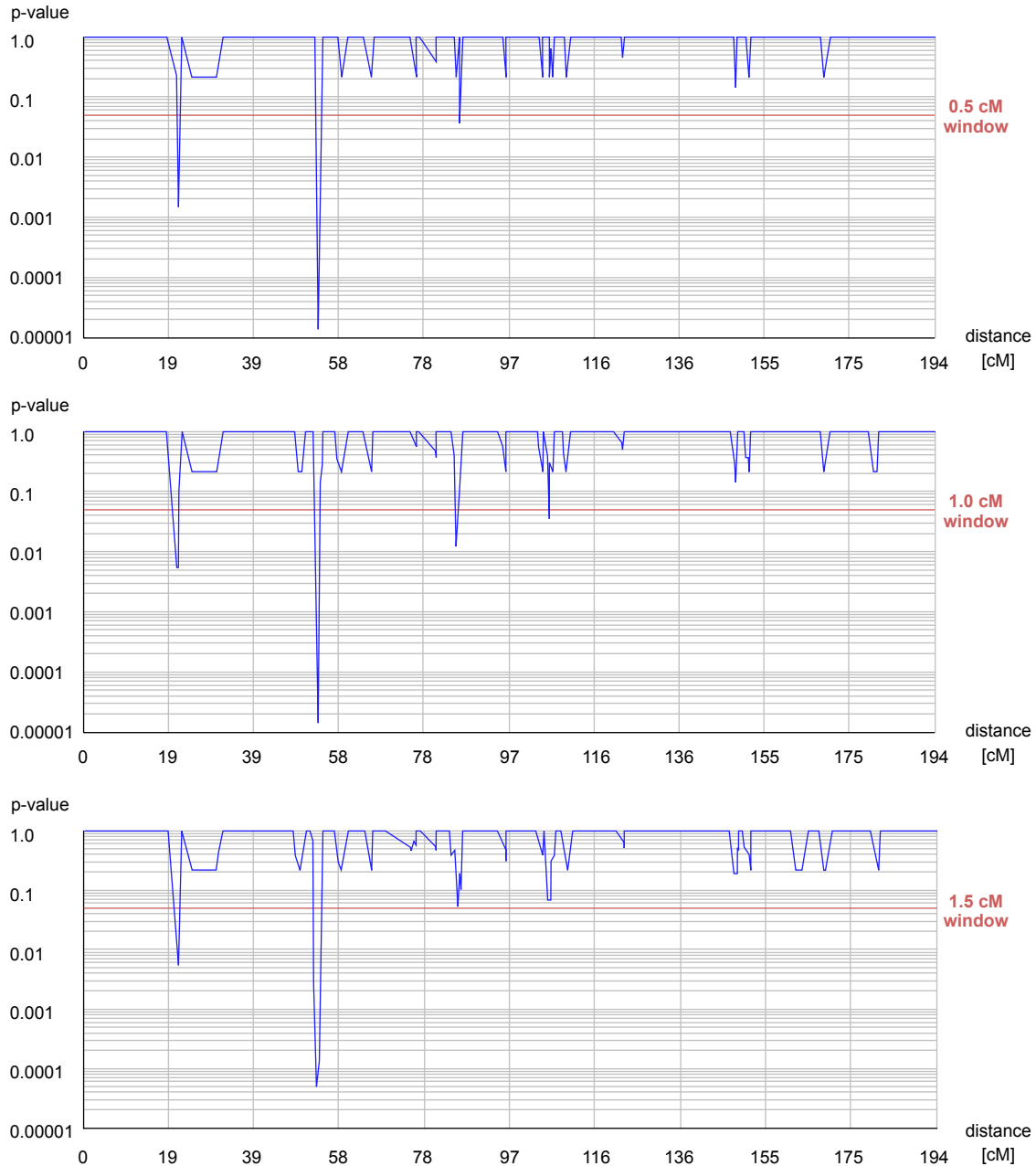


windows size → 2.0		
Selected Windows position (cM)	p-value	Significative Markers
22.949 - 24.949	0.0237	D5S1957 D5S807
106.031 - 108.031	0.0303	D5S1463 D5S815 D5S2499
106.879 - 108.879	0.0203	D5S1463 D5S815 D5S2499
107.141 - 109.141	0.0125	D5S1463 D5S815 D5S2499
107.142 - 109.142	0.0067	D5S1463 D5S815 D5S2499
107.383 - 109.383	0.0029	D5S1463 D5S815 D5S2499
107.622 - 109.622	8.0E-4	D5S1463 D5S815 D5S2499
108.004 - 110.004	0.0084	D5S815 D5S2499
127.059 - 129.059	0.0203	D5S494 D5S1478 D5S657
127.060 - 129.060	0.0125	D5S494 D5S1478 D5S657

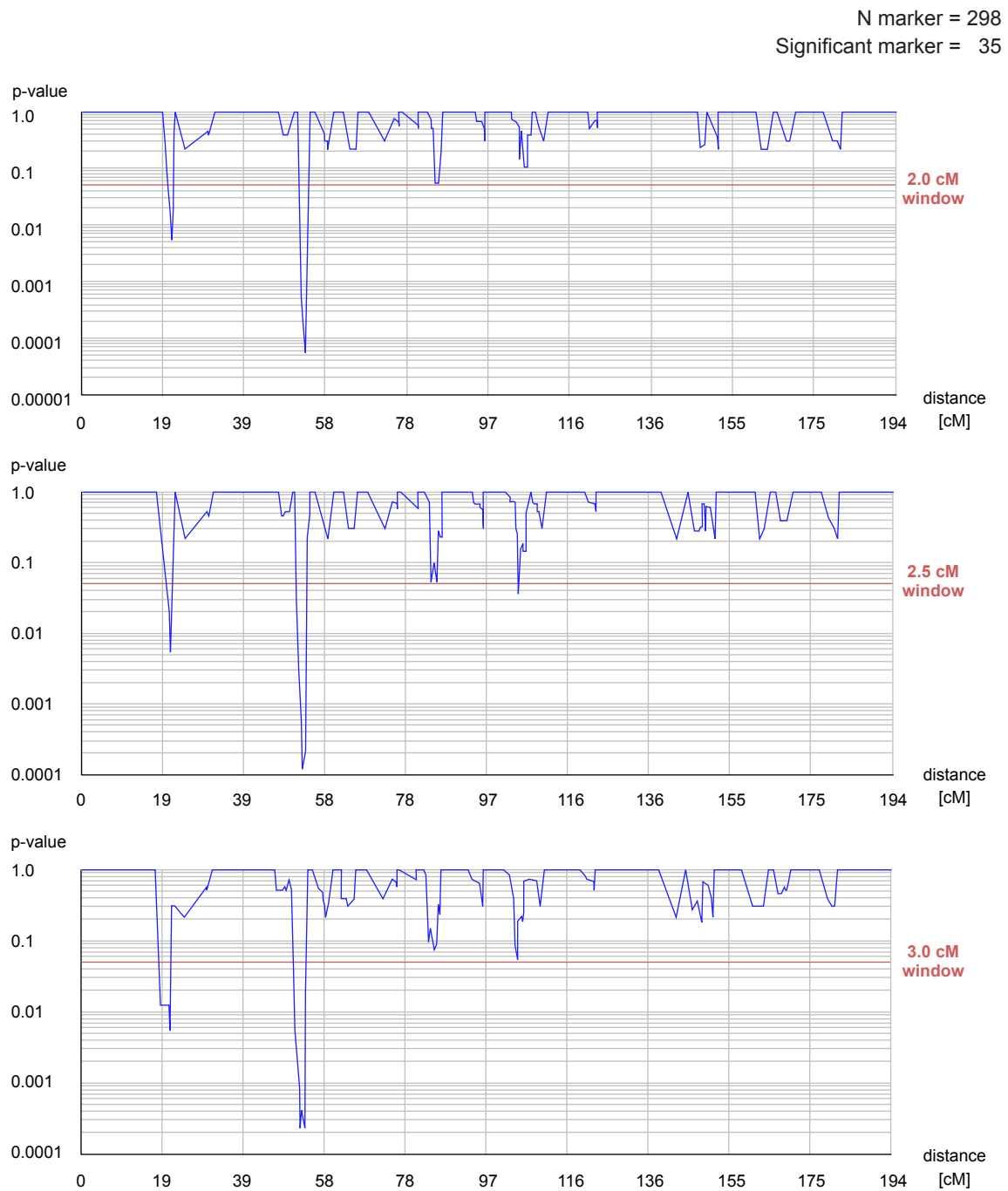
windows size → 2.5		
Selected Windows position (cM)	p-value	Significative Markers
20.701 - 23.201	0.0237	D5S1953 D5S1957
20.939 - 23.439	0.0084	D5S1953 D5S1957
22.949 - 25.449	0.0237	D5S1957 D5S807
105.718 - 108.218	0.0094	D5S1722 D5S1463 D5S815
105.719 - 108.219	0.0424	D5S1463 D5S815 D5S2499
106.031 - 108.531	0.0303	D5S1463 D5S815 D5S2499
106.879 - 109.379	0.0203	D5S1463 D5S815 D5S2499
107.141 - 109.641	0.0125	D5S1463 D5S815 D5S2499
107.383 - 109.883	0.0029	D5S1463 D5S815 D5S2499
107.622 - 110.122	8.0E-4	D5S1463 D5S815 D5S2499
108.004 - 110.504	0.0084	D5S815 D5S2499
127.059 - 129.559	0.0303	D5S494 D5S1478 D5S657
127.060 - 129.560	0.0203	D5S494 D5S1478 D5S657

windows size → 3.0		
Selected Windows position (cM)	p-value	Significative Markers
20.701 - 23.701	0.0237	D5S1953 D5S1957
20.939 - 23.939	0.0084	D5S1953 D5S1957
22.949 - 25.949	0.0237	D5S1957 D5S807
105.382 - 108.382	0.0137	D5S1722 D5S1463 D5S815
105.718 - 108.718	0.0094	D5S1722 D5S1463 D5S815
105.719 - 108.719	0.0424	D5S1463 D5S815 D5S2499
106.031 - 109.031	0.0303	D5S1463 D5S815 D5S2499
106.879 - 109.879	0.0203	D5S1463 D5S815 D5S2499
107.141 - 110.141	0.0125	D5S1463 D5S815 D5S2499
107.142 - 110.142	0.0067	D5S1463 D5S815 D5S2499
107.383 - 110.383	0.0029	D5S1463 D5S815 D5S2499
107.622 - 110.622	8.0E-4	D5S1463 D5S815 D5S2499
108.004 - 111.004	0.0084	D5S815 D5S2499
127.059 - 130.059	0.0303	D5S494 D5S1478 D5S657
127.060 - 130.060	0.0203	D5S494 D5S1478 D5S657

Chromosome 6

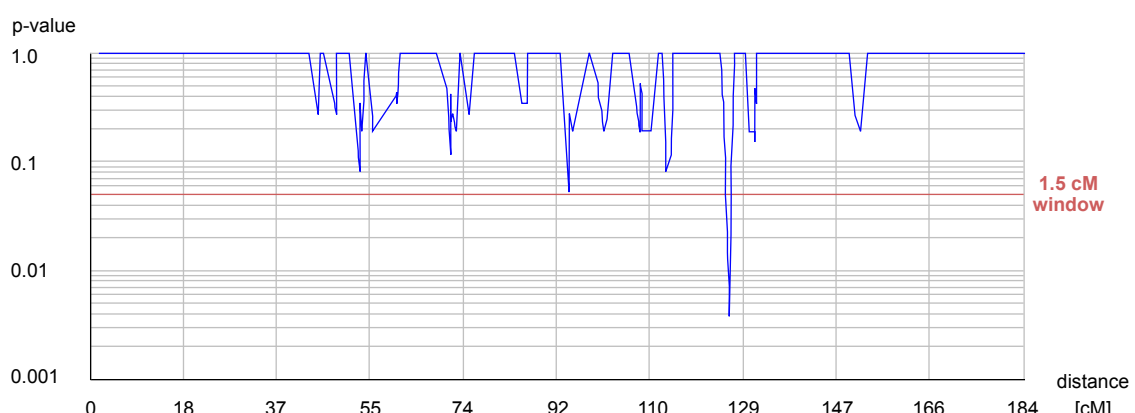
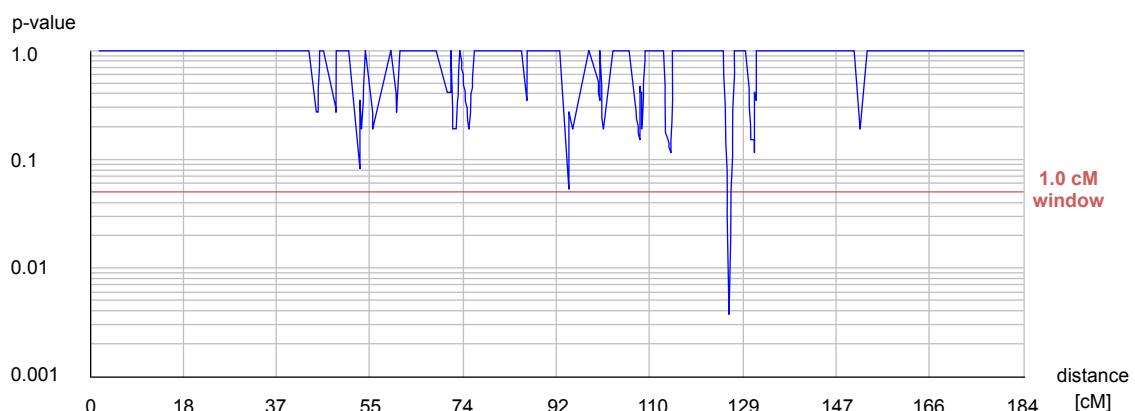
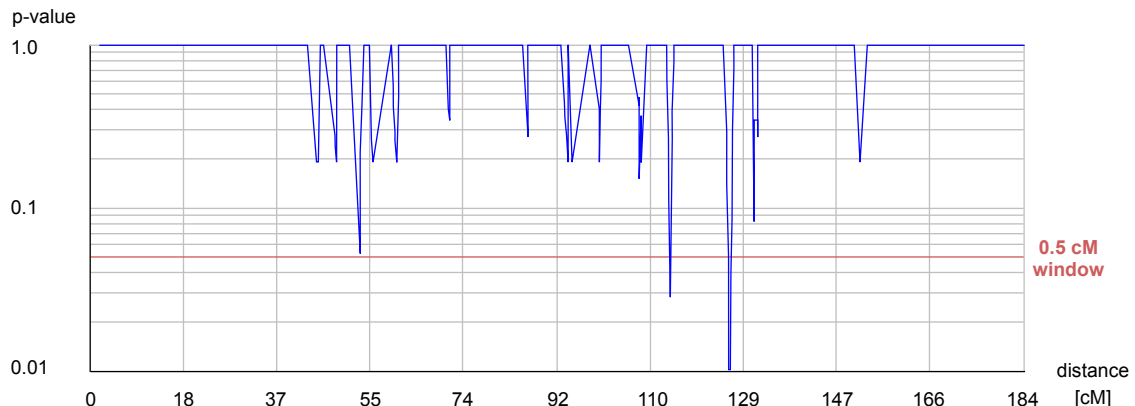


windows size → 0.5			windows size → 1.0			windows size → 1.5		
Selected Windows position (cM)	p-value	Significative Markers	Selected Windows position (cM)	p-value	Significative Markers	Selected Windows position (cM)	p-value	Significative Markers
21.603 - 22.103	0.002	D6S309 D6S277 D6S263	21.285 - 22.285	0.005	D6S309 D6S277 D6S263	21.285 - 22.785	0.012	D6S309 D6S277 D6S263
21.963 - 22.463	0.013	D6S277 D6S263	21.603 - 22.603	0.005	D6S309 D6S277 D6S263	21.603 - 23.103	0.005	D6S309 D6S277 D6S263
53.691 - 54.191	0.0	TNFa D6S1615 D6S1014 SA99 D6S2447 D6S2444	53.691 - 53.990	0.012	TNFa D6S1615 D6S1014	52.502 - 54.002	0.013	TNFa D6S1615 D6S1014 SA99
53.751 - 54.251	1.0E-4	D6S1615 D6S1014 SA99 D6S2447 D6S2444	53.691 - 54.691	0.0	TNFa D6S1615 D6S1014 SA99 D6S2447 D6S2444	52.829 - 54.329	3.0E-4	TNFa D6S1615 D6S1014 SA99 D6S2447 D6S2444
53.762 - 54.262	0.0	D6S1615 D6S1014 SA99 D6S2447 D6S2444	53.751 - 54.751	3.0E-4	D6S1615 D6S1014 SA99 D6S2447 D6S2444 D6S497	52.830 - 54.330	1.0E-4	TNFa D6S1615 D6S1014 SA99 D6S2447 D6S2444
53.953 - 54.453	2.0E-4	D6S1014 SA99 D6S2447 D6S2444	53.762 - 54.762	1.0E-4	D6S1615 D6S1014 SA99 D6S2447 D6S2444 D6S497	52.990 - 54.490	1.0E-4	TNFa D6S1615 D6S1014 SA99 D6S2447 D6S2444
53.991 - 54.491	0.002	SA99 D6S2447 D6S2444	53.953 - 54.953	8.0E-4	D6S1014 SA99 D6S2447 D6S2444 D6S497	53.691 - 55.191	1.0E-4	TNFa D6S1615 D6S1014 SA99 D6S2447 D6S2444
54.128 - 54.628	0.013	D6S2447 D6S2444	53.991 - 54.991	0.005	SA99 D6S2447 D6S2444 D6S497	54.128 - 55.128	0.023	D6S2447 D6S2444 D6S497
85.806 - 86.306	0.036	D6S1962 D6S1282	54.128 - 55.128	0.023	D6S2447 D6S2444 D6S497	53.751 - 55.251	3.0E-4	D6S1615 D6S1014 SA99 D6S2447 D6S2444 D6S497
			85.252 - 86.252	0.012	D6S1275 D6S1962 D6S1282	53.762 - 55.262	1.0E-4	D6S1615 D6S1014 SA99 D6S2447 D6S2444 D6S497
			106.448 - 107.448	0.036	D6S1284 D6S1717	53.953 - 55.453	8.0E-4	D6S1014 SA99 D6S2447 D6S2444 D6S497
						53.991 - 55.491	0.005	SA99 D6S2447 D6S2444 D6S497
						54.128 - 55.628	0.023	D6S2447 D6S2444 D6S497



windows size → 2.0			windows size → 2.5			windows size → 3.0		
Selected Windows position (cM)	p-value	Significative Markers	Selected Windows position (cM)	p-value	Significative Markers	Selected Windows position (cM)	p-value	Significative Markers
21.285 - 23.285	0.012	D6S309 D6S277 D6S263	21.285 - 23.785	0.012	D6S309 D6S277 D6S263	19.309 - 22.309	0.012	D6S309 D6S277 D6S263
21.603 - 23.603	0.005	D6S309 D6S277 D6S263	21.603 - 24.103	0.005	D6S309 D6S277 D6S263	21.285 - 24.285	0.012	D6S309 D6S277 D6S263
21.963 - 23.963	0.036	D6S277 D6S263	21.963 - 24.463	0.036	D6S277 D6S263	21.603 - 24.603	0.005	D6S309 D6S277 D6S263
52.254 - 54.254	0.002	TNF α D6S1615 D6S1014 SA99 D6S2447 D6S2444	51.597 - 54.097	0.040	TNF α D6S1615 D6S1014 SA99 D6S2447 D6S2444 D6S407	51.181 - 54.181	0.006	TNF α D6S1615 D6S1014 SA99 D6S2447 D6S2444
52.425 - 54.425	0.001	SA99 D6S2447 D6S1014	52.425 - 54.925	0.001	TNF α D6S1615 D6S1014 SA99 D6S2447 D6S2444 D6S497	51.421 - 54.421	0.004	TNF α D6S1615 D6S1014 SA99 D6S2447 D6S2444
52.502 - 54.502	6.0E-4	TNF α D6S1615 D6S1014	52.502 - 55.002	7.0E-4	TNF α D6S1615 D6S1014 SA99 D6S2447 D6S2444 D6S497	51.597 - 54.597	0.003	TNF α D6S1615 D6S1014 SA99 D6S2447 D6S2444 D6S497
52.829 - 54.829	4.0E-4	TNF α D6S1615 D6S1014 SA99 D6S2447 D6S2444 D6S497	52.829 - 55.329	4.0E-4	TNF α D6S1615 D6S1014 SA99 D6S2447 D6S2444 D6S497	52.254 - 55.254	0.002	TNF α D6S1615 D6S1014 SA99 D6S2447 D6S2444 D6S497
52.830 - 54.830	2.0E-4	TNF α D6S1615 D6S1014 SA99 D6S2447 D6S2444 D6S497	52.830 - 55.330	2.0E-4	TNF α D6S1615 D6S1014 SA99 D6S2447 D6S2444 D6S497	52.425 - 55.425	0.001	TNF α D6S1615 D6S1014 SA99 D6S2447 D6S2444 D6S497
52.990 - 54.990	1.0E-4	TNF α D6S1615 D6S1014 SA99 D6S2447 D6S2444 D6S497	52.990 - 55.490	1.0E-4	TNF α D6S1615 D6S1014 SA99 D6S2447 D6S2444 D6S497	52.502 - 55.502	7.0E-4	TNF α D6S1615 D6S1014 SA99 D6S2447 D6S2444 D6S497
53.691 - 55.691	1.0E-4	TNF α D6S1615 D6S1014 SA99 D6S2447 D6S2444 D6S497	53.691 - 56.191	2.0E-4	TNF α D6S1615 D6S1014 SA99 D6S2447 D6S2444 D6S497	52.829 - 55.829	4.0E-4	TNF α D6S1615 D6S1014 SA99 D6S2447 D6S2444 D6S497
53.751 - 55.751	3.0E-4	D6S1615 D6S1014 SA99 D6S2447 D6S2444 D6S497	53.751 - 56.251	0.001	D6S1615 D6S1014 SA99 D6S2447 D6S2444 D6S497	52.830 - 55.830	2.0E-4	TNF α D6S1615 D6S1014 SA99 D6S2447 D6S2444 D6S497
53.762 - 55.762	1.0E-4	D6S1615 D6S1014 SA99 D6S2447 D6S2444 D6S497	53.762 - 56.262	6.0E-4	D6S1615 D6S1014 SA99 D6S2447 D6S2444 D6S497	52.990 - 55.990	4.0E-4	TNF α D6S1615 D6S1014 SA99 D6S2447 D6S2444 D6S497
53.953 - 55.953	0.003	D6S1014 SA99 D6S2447 D6S2444 D6S497	53.953 - 56.453	0.003	D6S1014 SA99 D6S2447 D6S2444 D6S497	53.691 - 56.691	2.0E-4	D6S1615 D6S1014 SA99 D6S2447 D6S2444 D6S497
53.991 - 55.991	0.013	D6S1615 D6S1014 SA99 D6S2447 D6S2444 D6S497	53.991 - 56.491	0.013	D6S1957 D6S1284 D6S1717	53.751 - 56.751	0.001	D6S1615 D6S1014 SA99 D6S2447 D6S2444 D6S497
			104.749 - 107.249	0.037	D6S1957 D6S1284 D6S1717	53.762 - 56.762	6.0E-4	D6S1615 D6S1014 SA99 D6S2447 D6S2444 D6S497
						53.953 - 56.953	0.003	D6S1615 D6S1014 SA99 D6S2447 D6S2444 D6S497
						53.991 - 56.991	0.013	D6S1615 D6S1014 SA99 D6S2447 D6S2444 D6S497

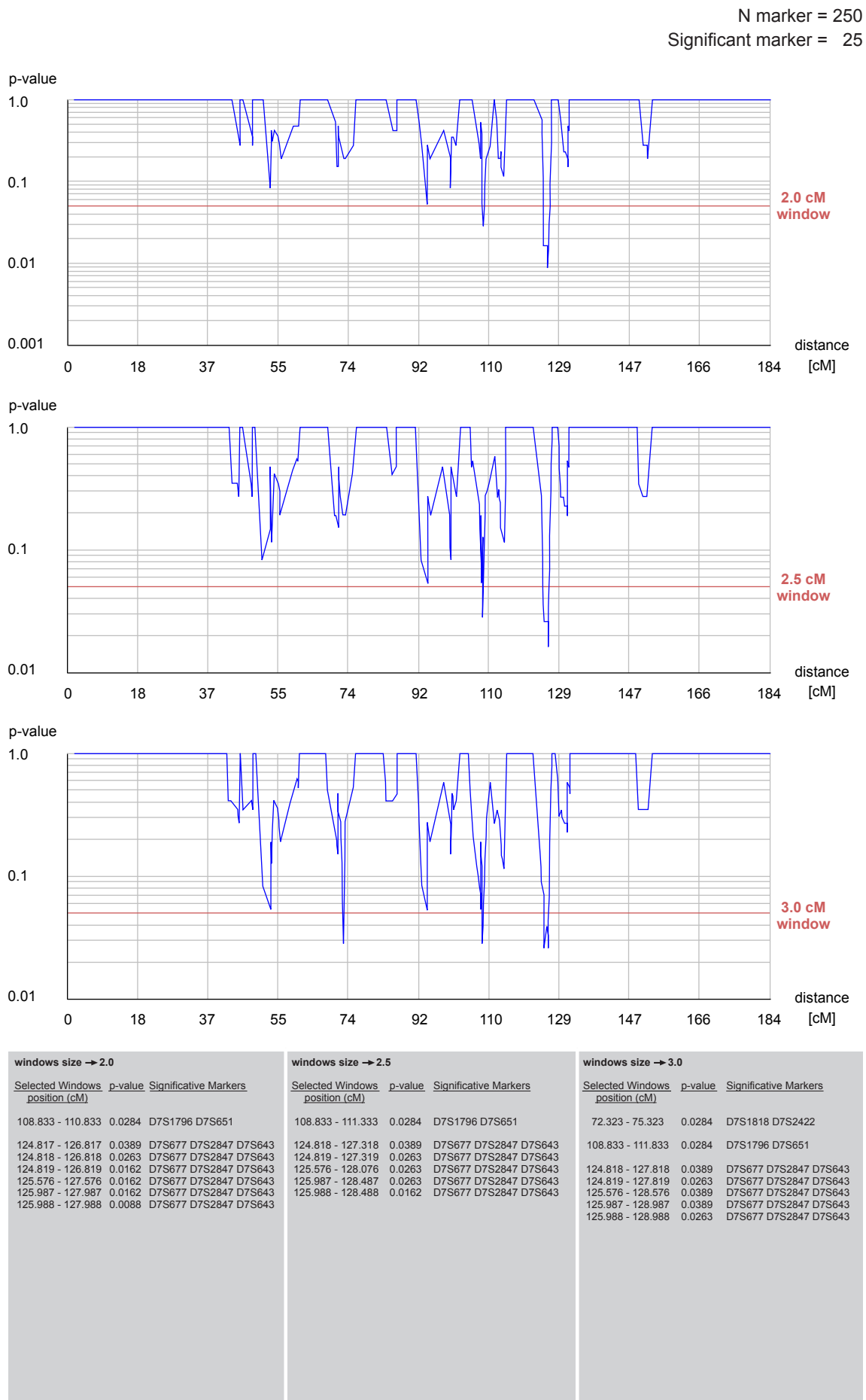
Chromosome 7



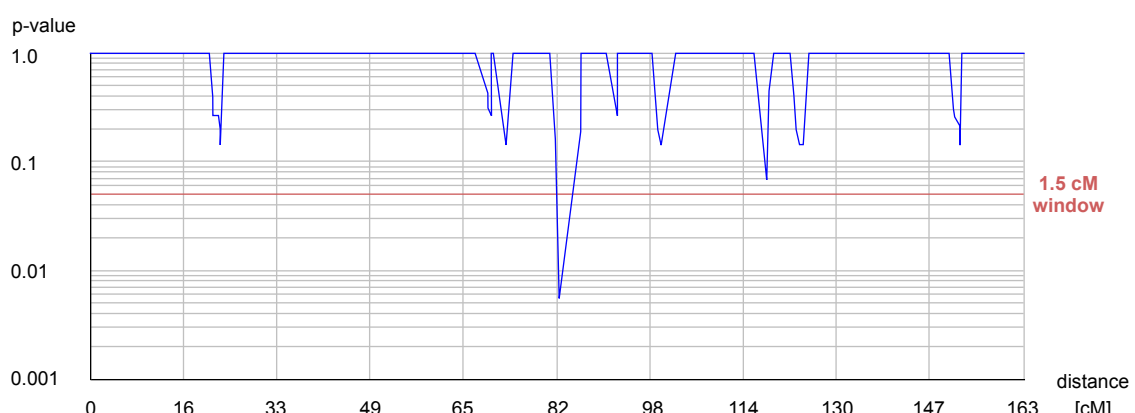
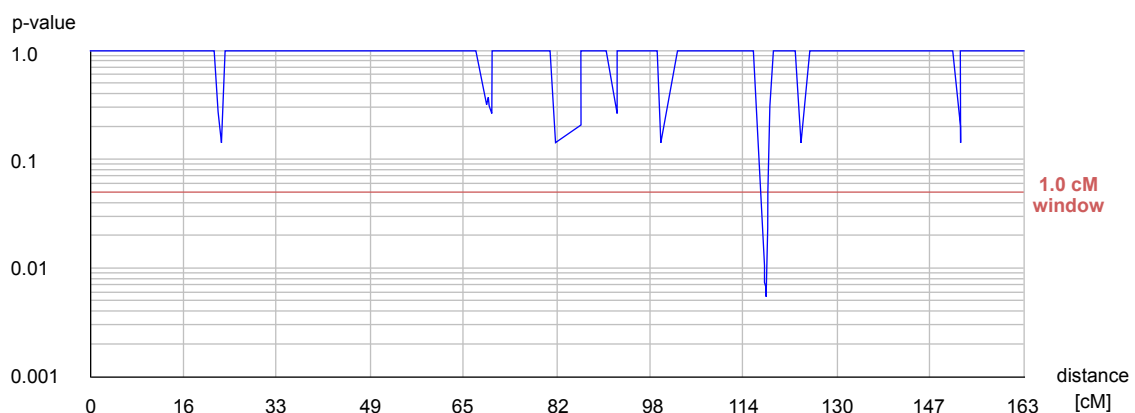
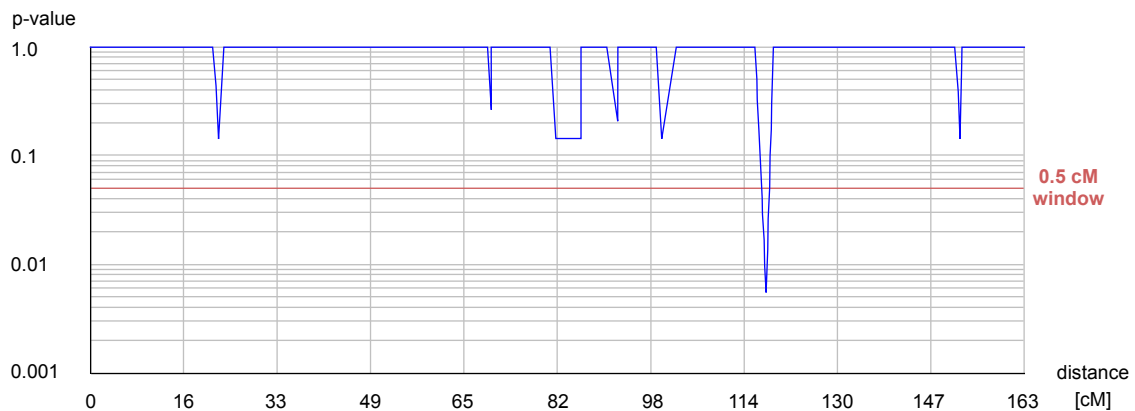
windows size → 0.5		
Selected Windows position (cM)	p-value	Significative Markers
114.476 - 114.976	0.0284	D7S2509 D7S796
125.987 - 126.487	0.0284	D7S677 D7S2847
125.988 - 126.488	0.0102	D7S677 D7S2847
126.371 - 126.871	0.0102	D7S2847 D7S643

windows size → 1.0		
Selected Windows position (cM)	p-value	Significative Markers
125.987 - 126.987	0.0088	D7S677 D7S2847 D7S643
125.988 - 126.988	0.0038	D7S677 D7S2847 D7S643
126.371 - 127.371	0.0284	D7S2847 D7S643

windows size → 1.5		
Selected Windows position (cM)	p-value	Significative Markers
125.576 - 127.076	0.0162	D7S677 D7S2847 D7S643
125.987 - 127.487	0.0088	D7S677 D7S2847 D7S643
125.988 - 127.488	0.0038	D7S677 D7S2847 D7S643



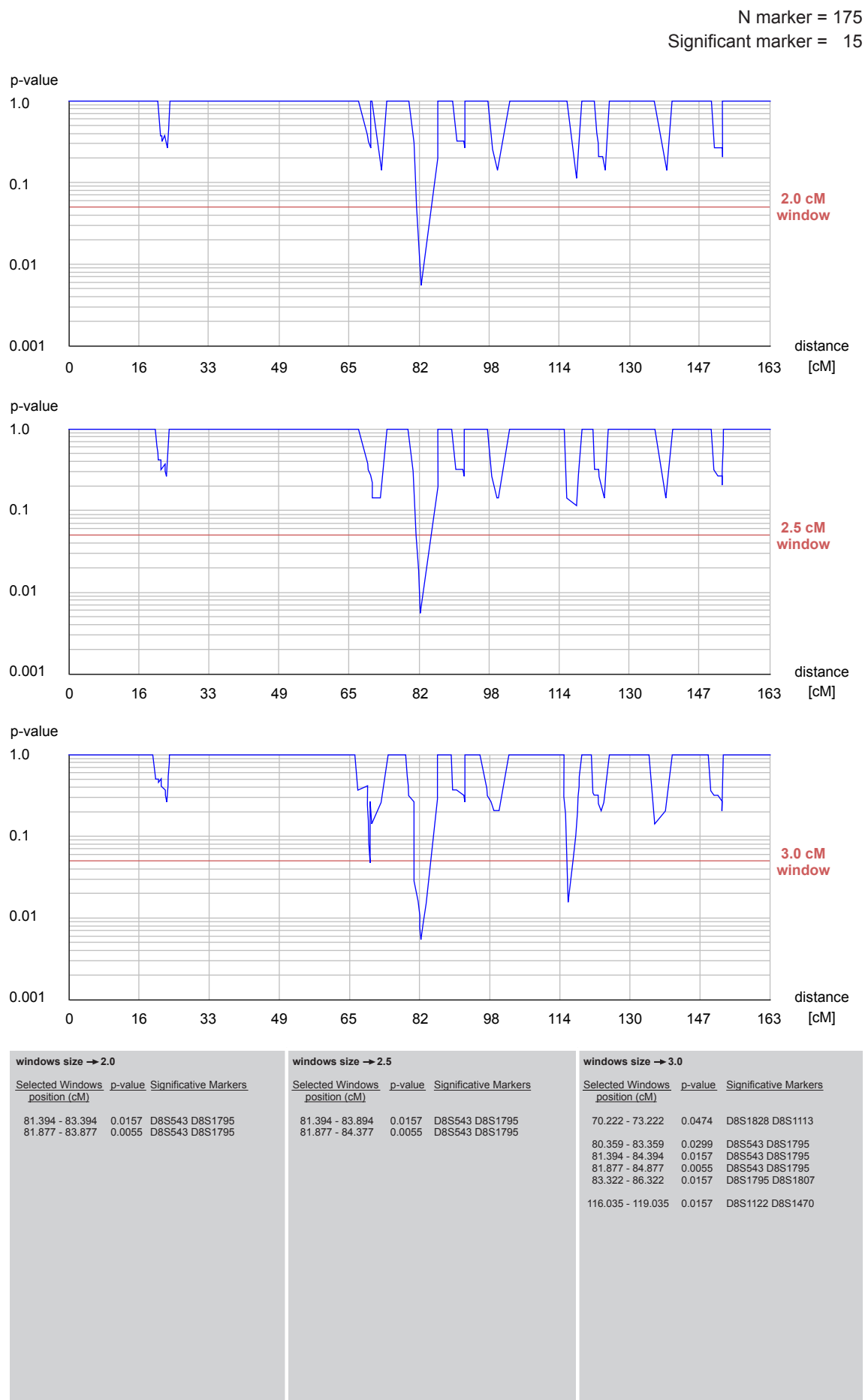
Chromosome 8



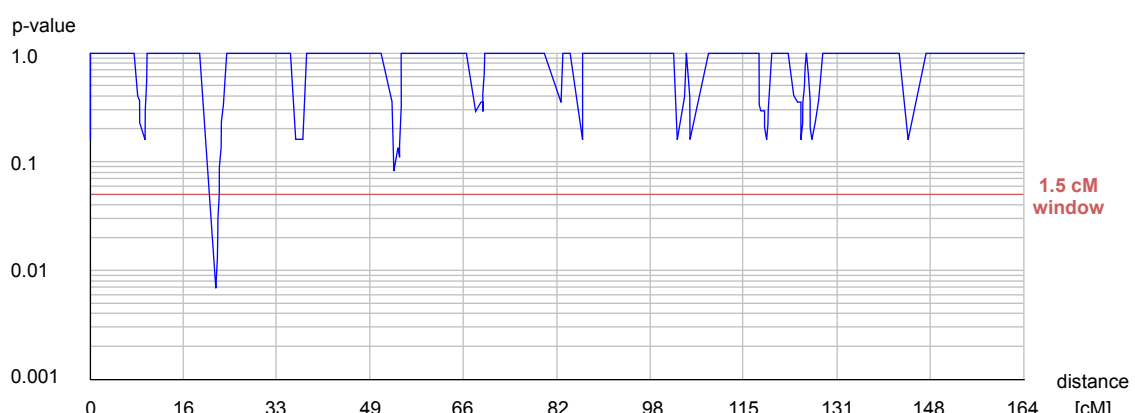
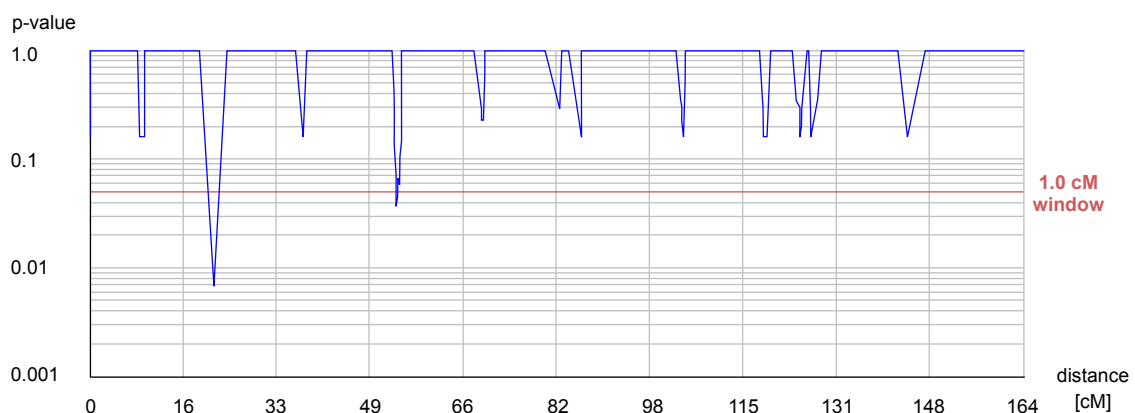
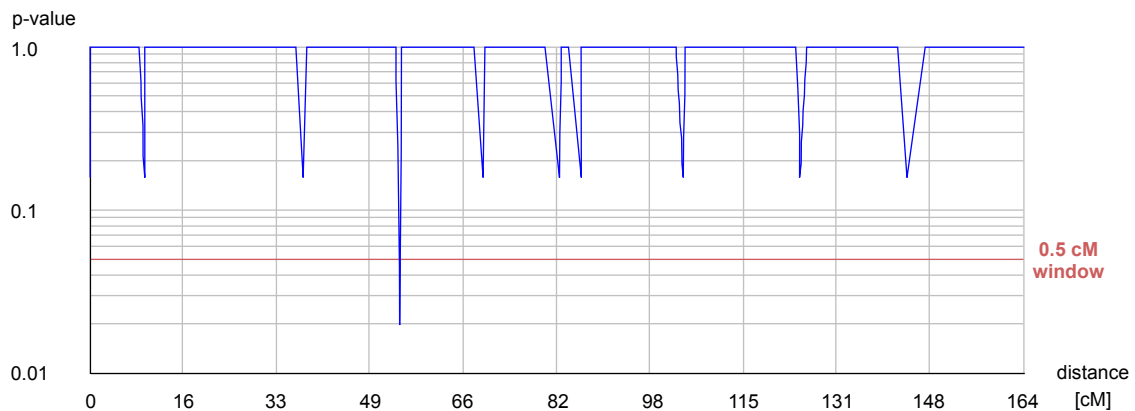
windows size → 0.5		
Selected Windows	p-value	Significative Markers
position (cM)		
118.251 - 118.751	0.0055	D8S1122 D8S1470

windows size → 1.0		
Selected Windows	p-value	Significative Markers
position (cM)		
118.251 - 119.251	0.0055	D8S1122 D8S1470

windows size → 1.5		
Selected Windows	p-value	Significative Markers
position (cM)		
81.877 - 83.377	0.0055	D8S543 D8S1795



Chromosome 9

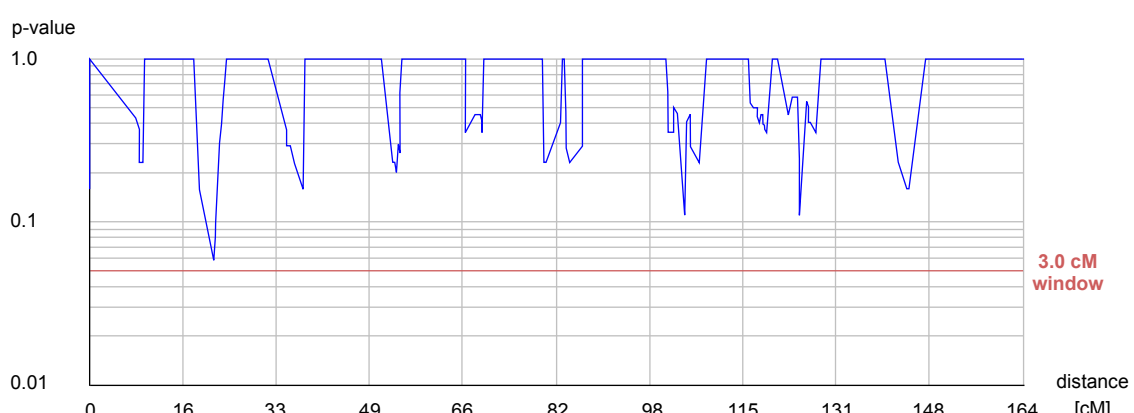
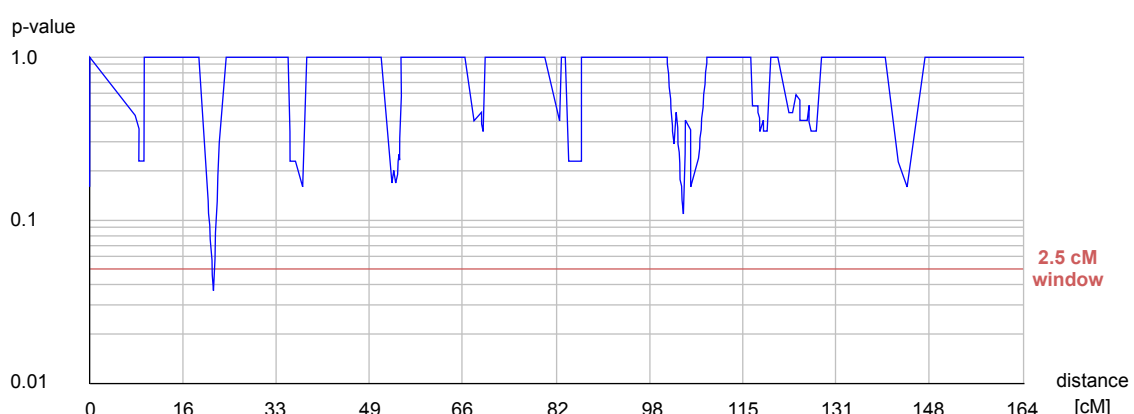
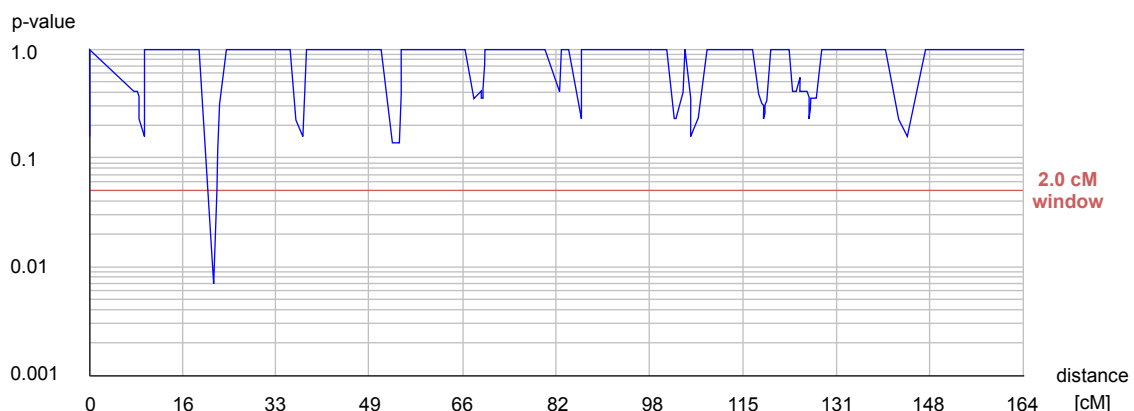


windows size → 0.5		
Selected Windows position (cM)	p-value	Significative Markers
54.417 - 54.917	0.0372	D9S270 D9S1868
54.498 - 54.998	0.0197	D9S270 D9S1868

windows size → 1.0		
Selected Windows position (cM)	p-value	Significative Markers
22.042 - 23.042	0.0069	D9S144 D9S775
53.842 - 54.842	0.0372	D9S270 D9S1868

windows size → 1.5		
Selected Windows position (cM)	p-value	Significative Markers
22.042 - 23.542	0.0069	D9S144 D9S775

N marker = 192
 Significant marker = 16

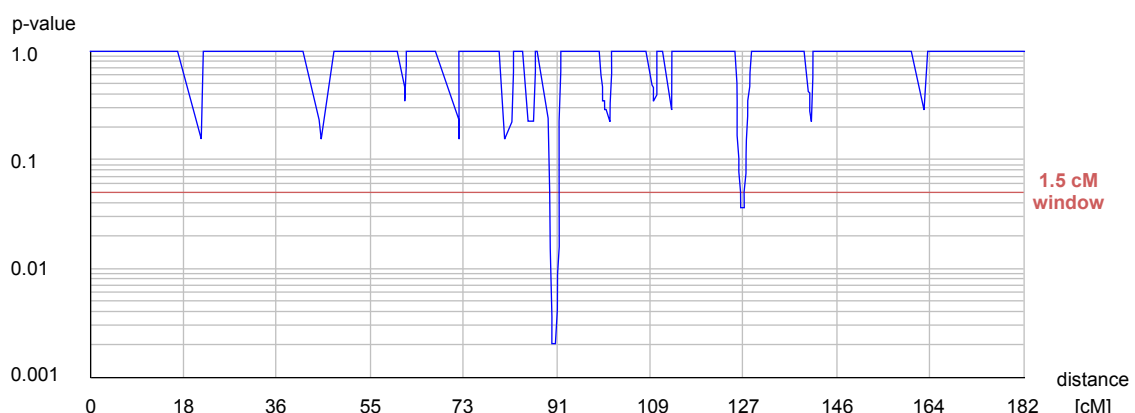
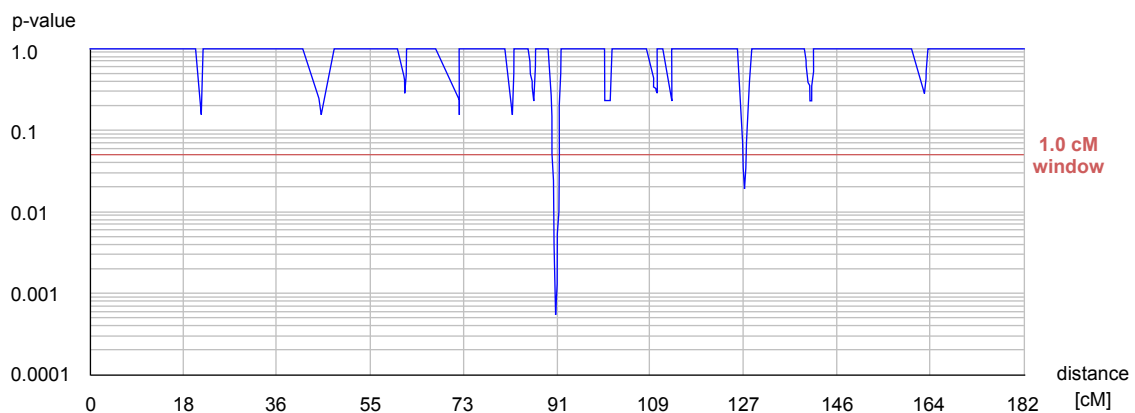
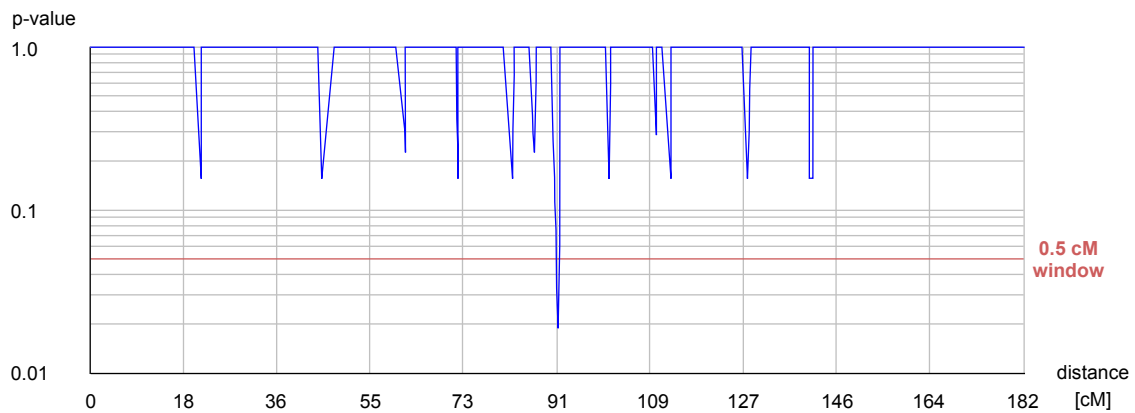


windows size → 2.0		
Selected Windows	p-value	Significative Markers
position (cM)		
22.042 - 24.042	0.0069	D9S144 D9S775

windows size → 2.5		
Selected Windows	p-value	Significative Markers
position (cM)		
22.042 - 24.542	0.0372	D9S144 D9S775

windows size → 3.0		
Selected Windows	p-value	Significative Markers
position (cM)		

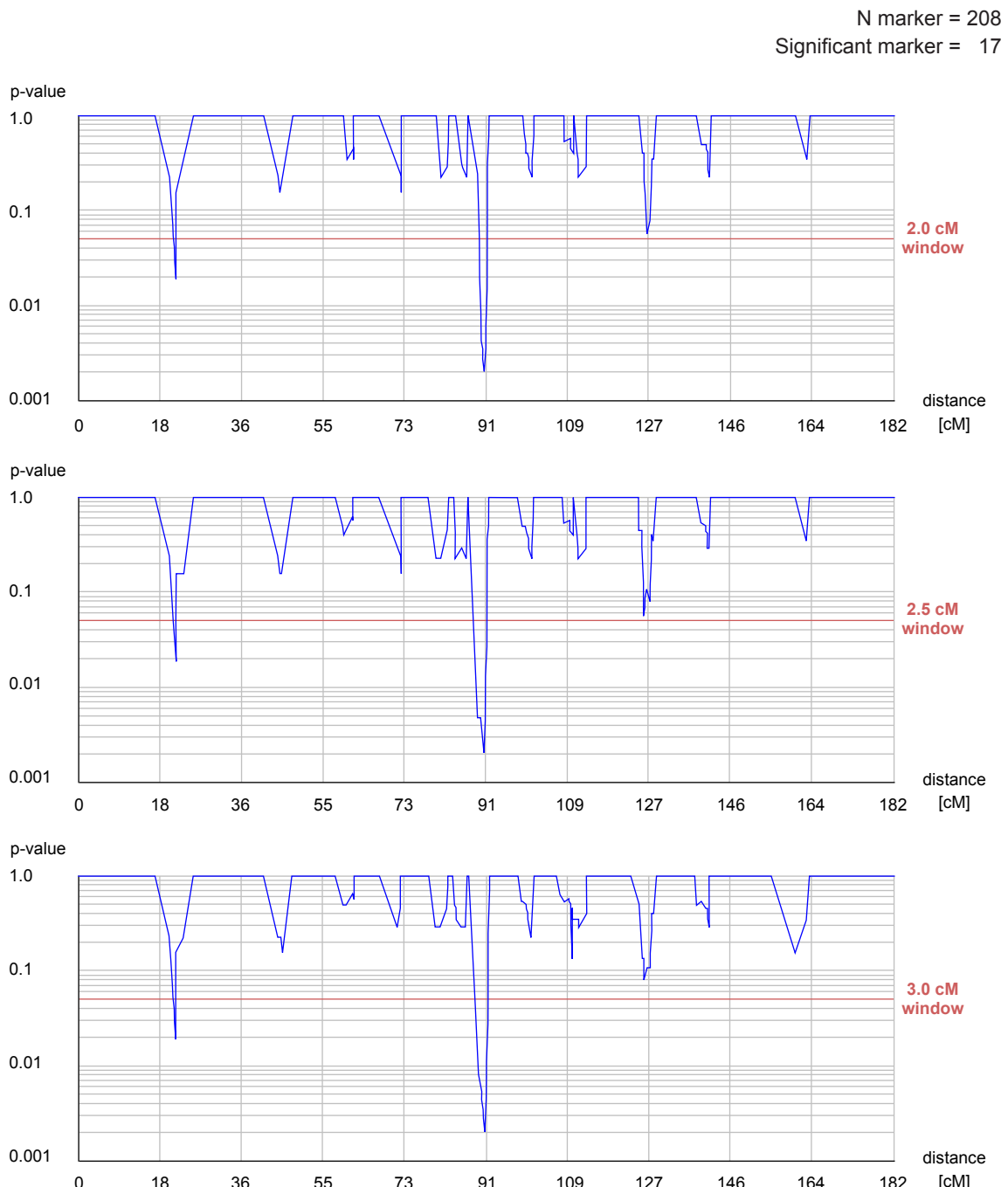
Chromosome 10



windows size → 0.5		
Selected Windows position (cM)	p-value	Significative Markers
91.456 - 91.956	0.0189	D10S537 D10S1685

windows size → 1.0		
Selected Windows position (cM)	p-value	Significative Markers
90.696 - 91.696	5.0E-4	D10S676 D10S537 D10S1685
91.456 - 92.456	0.0189	D10S537 D10S1685
127.676 - 128.676	0.0189	D10S1663 D10S1795

windows size → 1.5		
Selected Windows position (cM)	p-value	Significative Markers
90.052 - 91.552	0.0020	D10S676 D10S537 D10S1685
90.696 - 92.196	0.0020	D10S676 D10S537 D10S1685
91.456 - 92.956	0.0189	D10S537 D10S1685
127.079 - 128.579	0.0358	D10S1663 D10S1795
127.676 - 129.176	0.0358	D10S1663 D10S1795

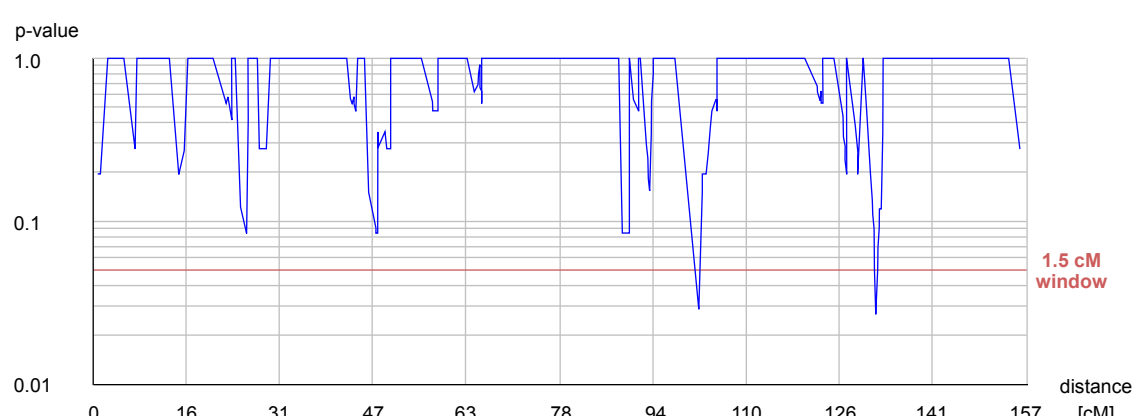
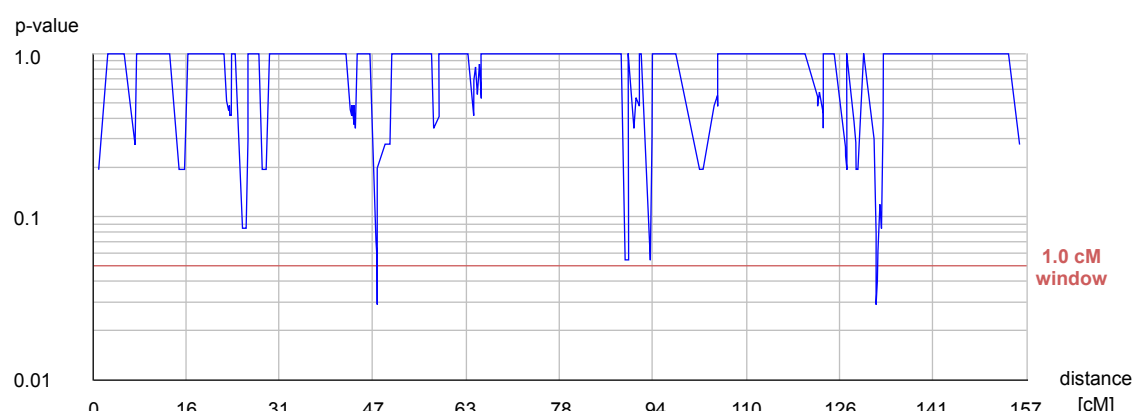
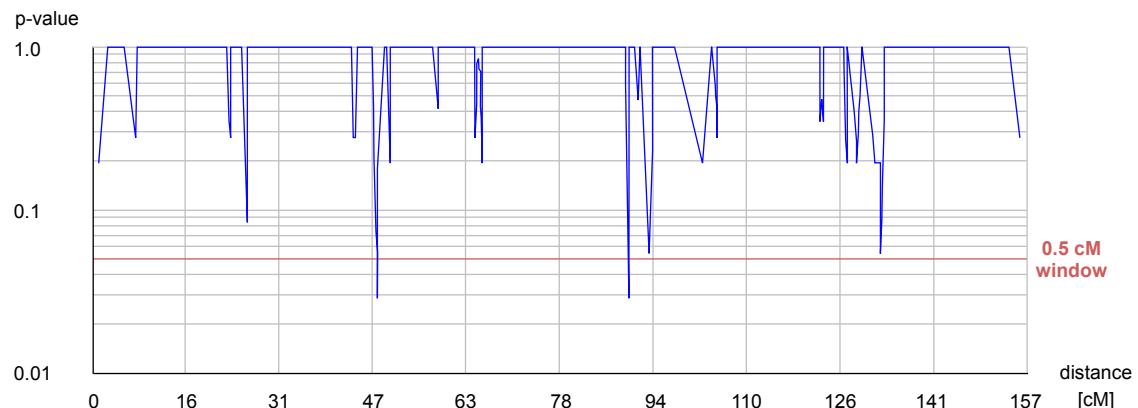


windows size → 2.0		
Selected Windows position (cM)	p-value	Significative Markers
21.776 - 23.776	0.0189	D10S1751 D10S1779
90.052 - 92.052	0.0048	D10S676 D10S537 D10S1685
90.696 - 92.696	0.0020	D10S676 D10S537 D10S1685
91.456 - 93.456	0.0189	D10S537 D10S1685

windows size → 2.5		
Selected Windows position (cM)	p-value	Significative Markers
21.776 - 24.276	0.0189	D10S1751 D10S1779
89.288 - 91.788	0.0048	D10S676 D10S537 D10S1685
90.052 - 92.552	0.0048	D10S676 D10S537 D10S1685
90.696 - 93.196	0.0020	D10S676 D10S537 D10S1685
91.456 - 93.956	0.0358	D10S537 D10S1685

windows size → 3.0		
Selected Windows position (cM)	p-value	Significative Markers
21.776 - 24.776	0.0189	D10S1751 D10S1779
89.288 - 92.288	0.0090	D10S676 D10S537 D10S1685
90.052 - 93.052	0.0048	D10S676 D10S537 D10S1685
90.696 - 93.696	0.0020	D10S676 D10S537 D10S1685
91.456 - 94.456	0.0358	D10S537 D10S1685

Chromosome 11

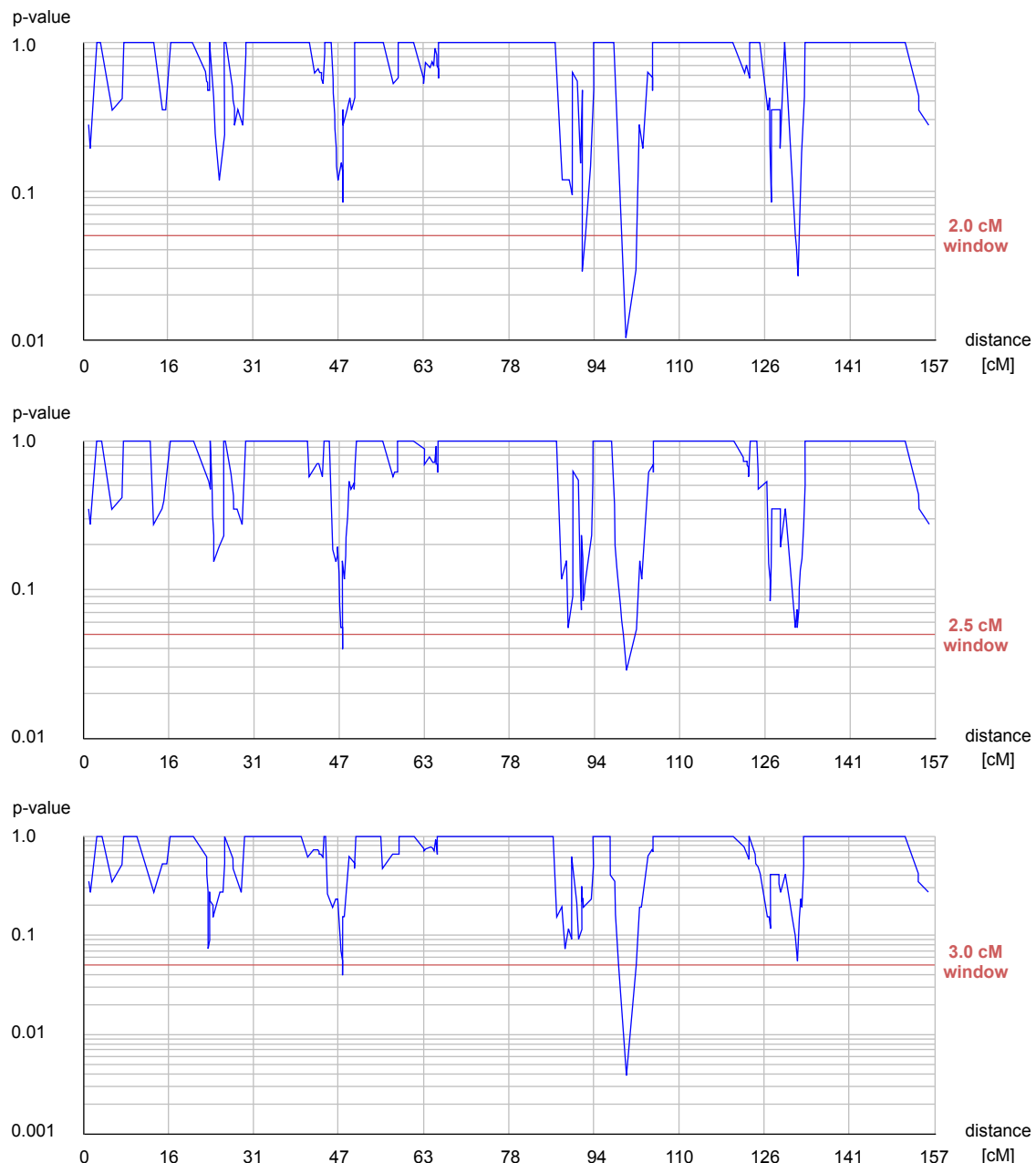


windows size → 0.5		
Selected Windows	p-value	Significative Markers position (cM)
48.004 - 48.504	0.0291	D11S2369 D11S1322
90.217 - 90.717	0.0291	D11S1396 D11S4453

windows size → 1.0		
Selected Windows	p-value	Significative Markers position (cM)
48.004 - 49.004	0.0291	D11S2369 D11S1322
131.748 - 132.748	0.0291	D11S1353 D11S1316

windows size → 1.5		
Selected Windows	p-value	Significative Markers position (cM)
101.948 - 103.448	0.0291	D11S1366 D11S4120
131.623 - 133.123	0.0271	D11S1353 D11S1316 D11S4464
131.748 - 133.248	0.0271	D11S1353 D11S1316 D11S4464

N marker = 294
Significant marker = 30

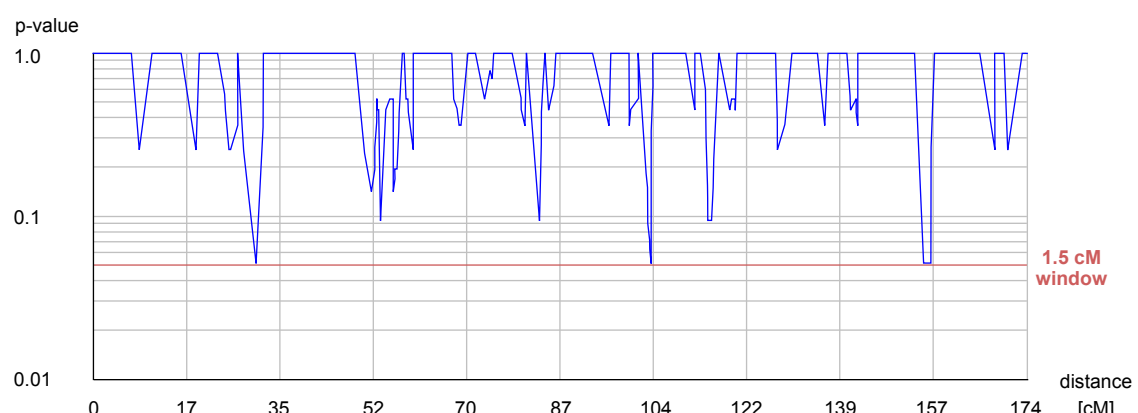
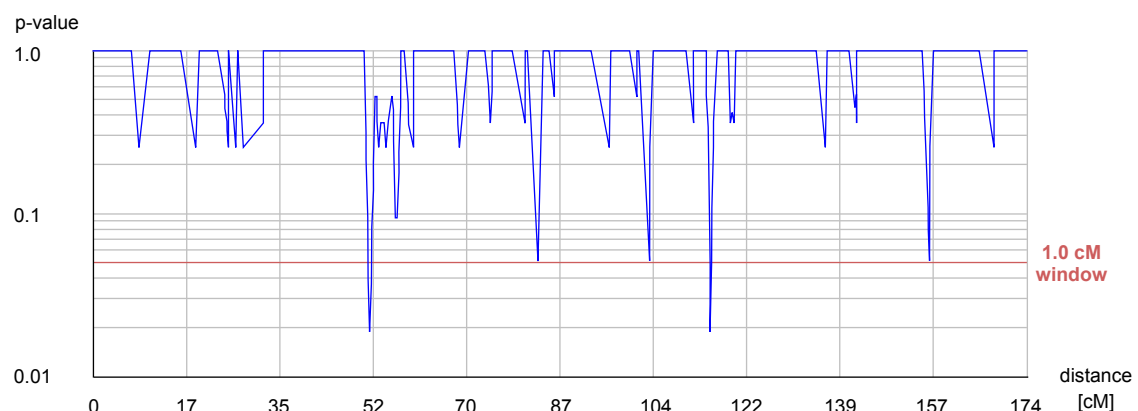
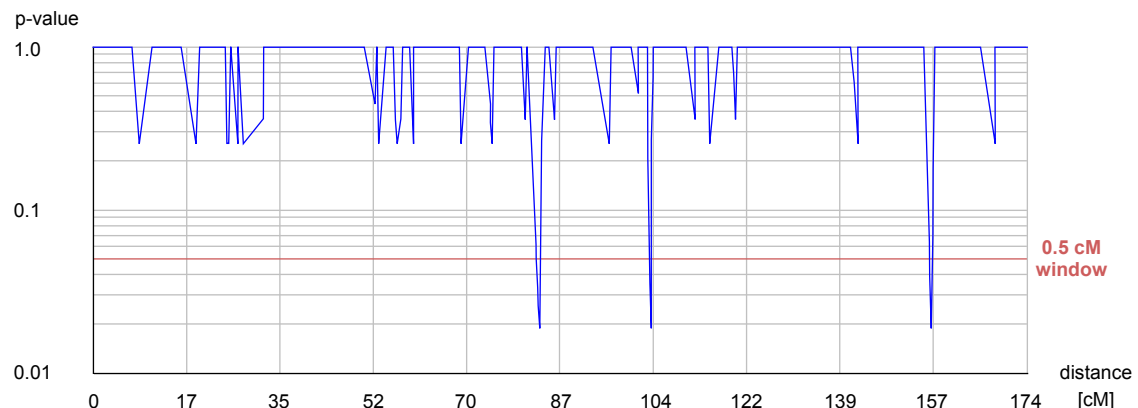


windows size → 2.0		
Selected Windows	p-value	Significative Markers
position (cM)		
92.14 - 94.14	0.0291	D11S4082 D11S1780
100.205 - 102.205	0.0104	D11S919 D11S1366
101.948 - 103.948	0.0291	D11S1366 D11S4120
131.623 - 133.623	0.0401	D11S1353 D11S1316
D11S4464		
131.748 - 133.748	0.0271	D11S1353 D11S1316
D11S4464		

windows size → 2.5		
Selected Windows	p-value	Significative Markers
position (cM)		
48.004 - 50.504	0.0398	D11S2369 D11S1322
D11S1301		
100.205 - 102.705	0.0289	D11S919 D11S1366

windows size → 3.0		
Selected Windows	p-value	Significative Markers
position (cM)		
48.004 - 51.004	0.0398	D11S2369 D11S1322
D11S1301		
100.205 - 103.205	0.0039	D11S919 D11S1366
D11S4120		

Chromosome 12

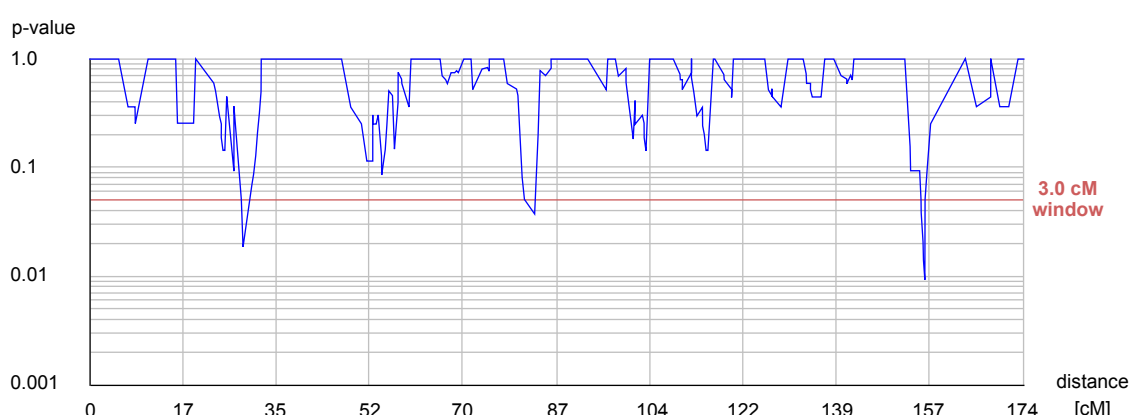
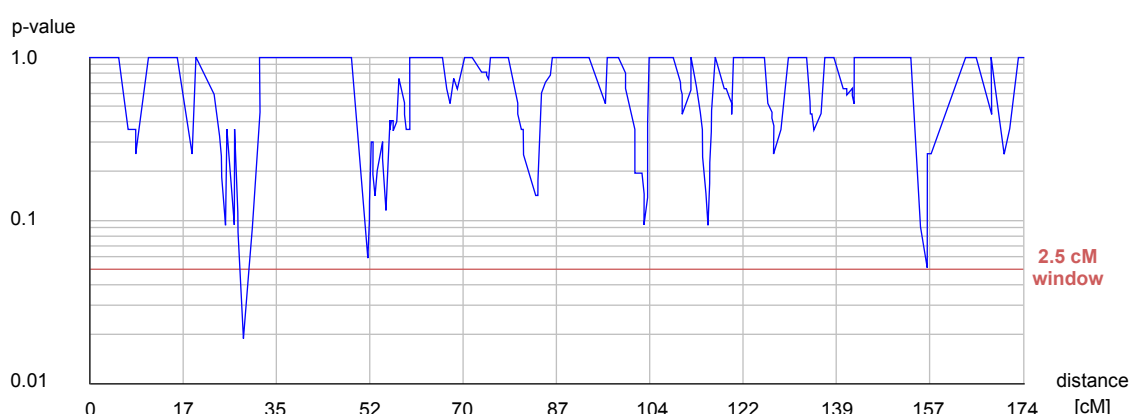


windows size → 0.5		
Selected Windows	p-value	Significative Markers
position (cM)		
83.191 - 83.691	0.0189	D12S1601 D12S1291
103.892 - 104.392	0.0189	D12S2077 D12S311
155.986 - 156.486	0.0189	D12S2075 D12S2078

windows size → 1.0		
Selected Windows	p-value	Significative Markers
position (cM)		
51.799 - 52.799	0.0189	D12S1042 D12S1292
115.310 - 116.310	0.0189	D12S1070 D12S1607

windows size → 1.5		
Selected Windows	p-value	Significative Markers
position (cM)		

N marker = 262
Significant marker = 36

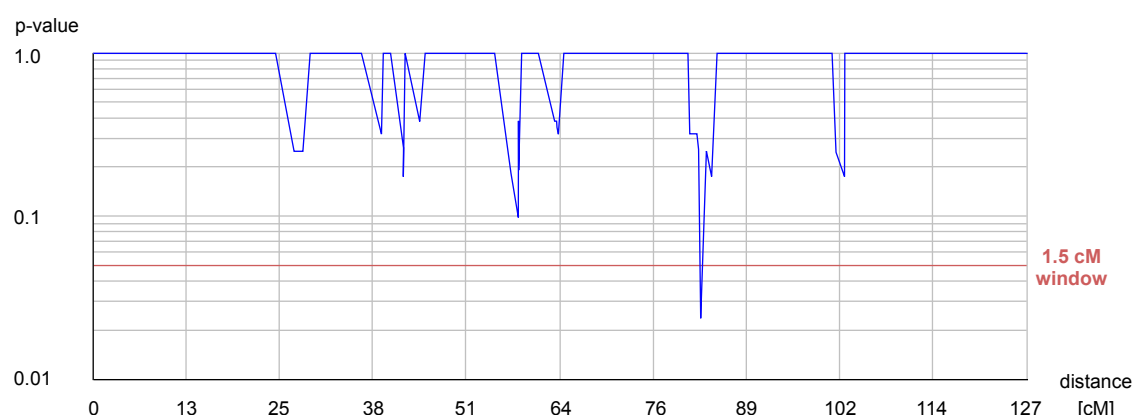
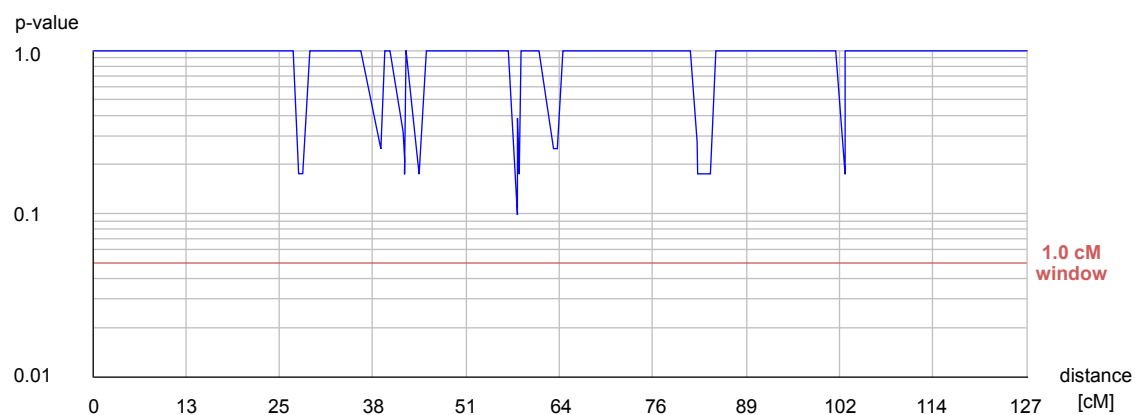
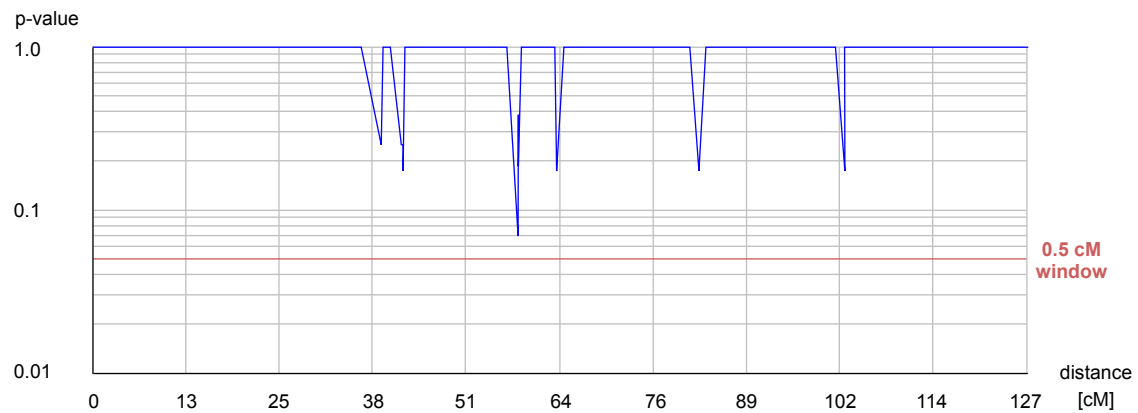


windows size → 2.0		
<u>Selected Windows</u>	<u>p-value</u>	<u>Significative Markers</u>
<u>position (cM)</u>		
28.661 - 30.661	0.0189	D12S391 D12S1581

windows size → 2.5		
<u>Selected Windows</u>	<u>p-value</u>	<u>Significative Markers</u>
<u>position (cM)</u>		
28.661 - 31.161	0.0189	D12S391 D12S1581

windows size → 3.0		
<u>Selected Windows</u>	<u>p-value</u>	<u>Significative Markers</u>
<u>position (cM)</u>		
28.661 - 31.661	0.0189	D12S391 D12S1581
83.191 - 86.191	0.0375	D12S1601 D12S1291 D12S375
155.986 - 158.986	0.0093	D12S2075 D12S2078 D12S1679

Chromosome 13

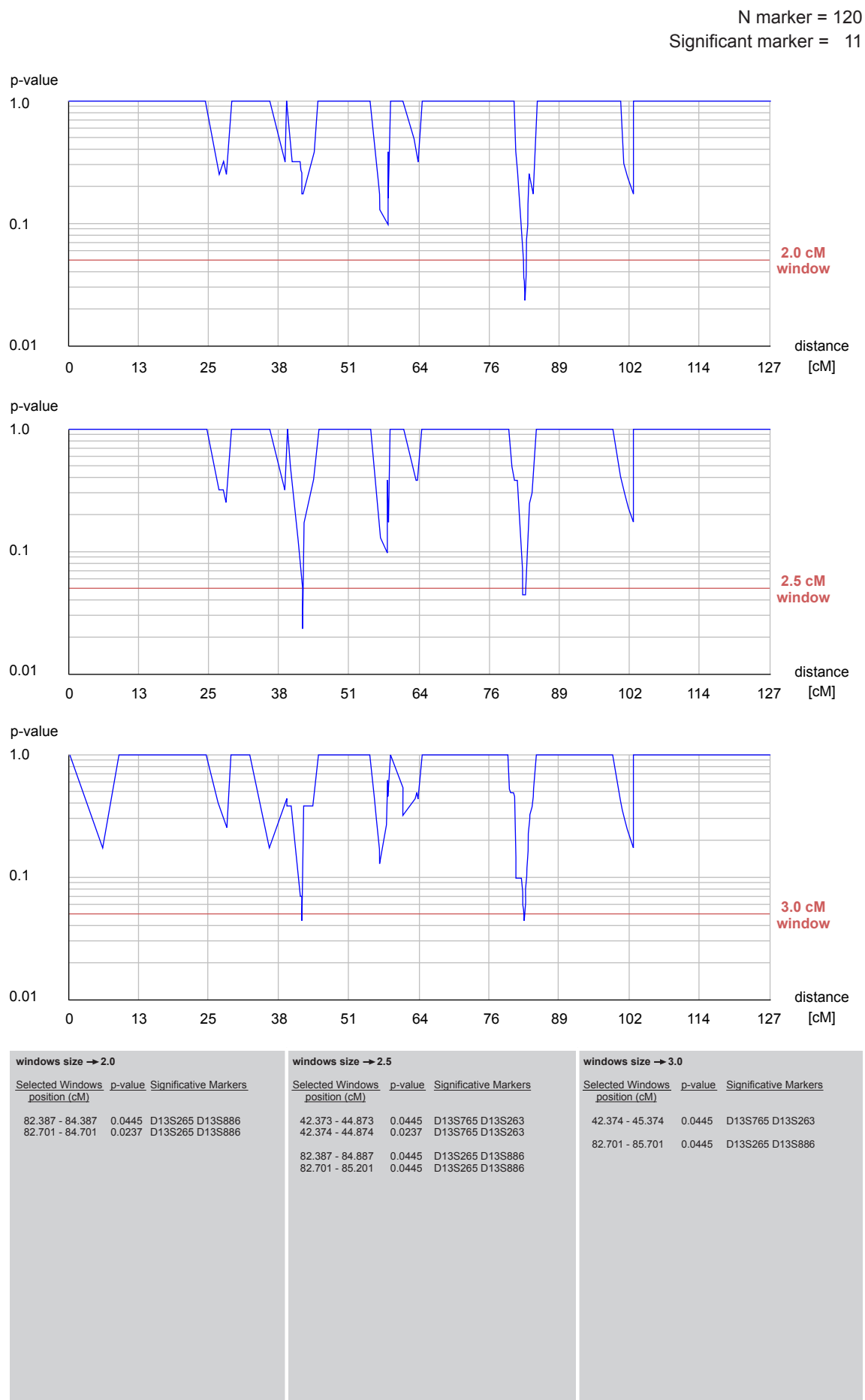


windows size → 0.5
Selected Windows p-value Significative Markers
position (cM)

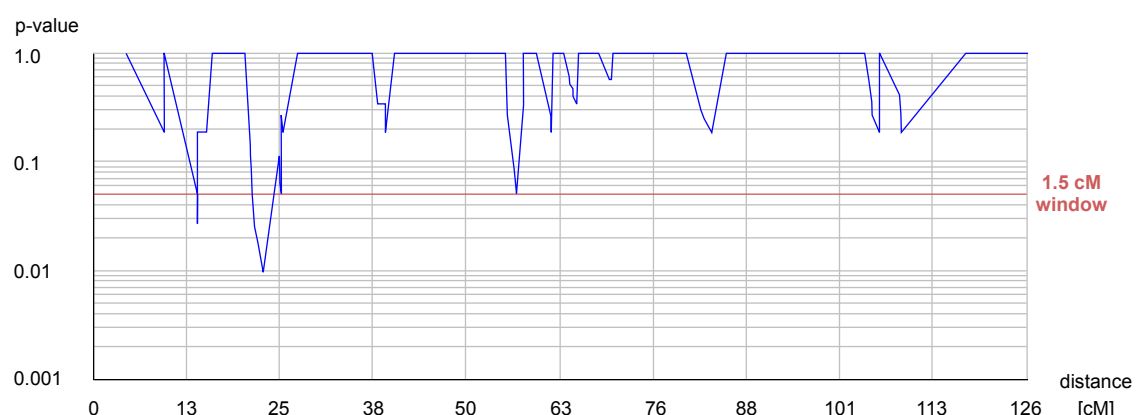
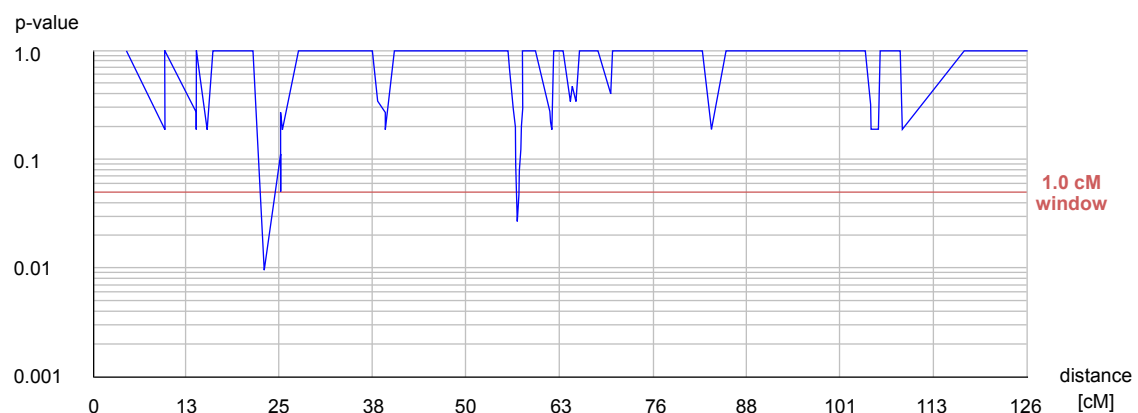
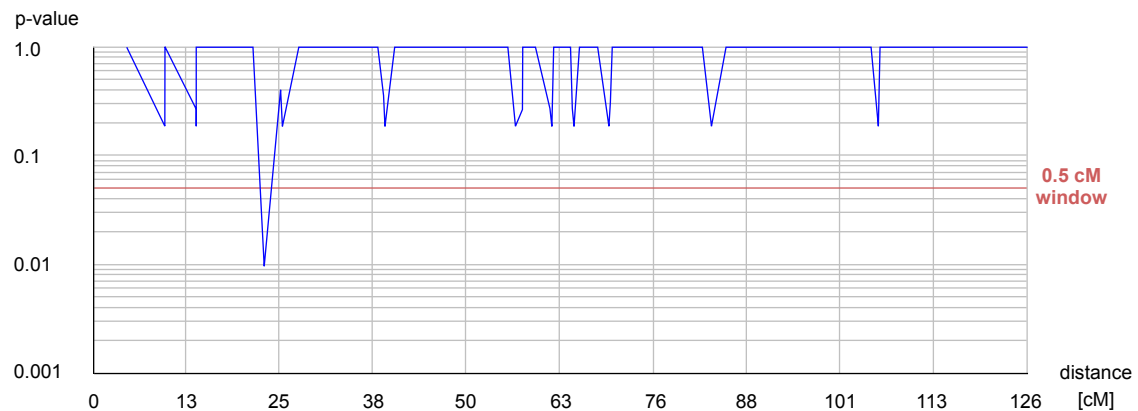
windows size → 1.0
Selected Windows p-value Significative Markers
position (cM)

windows size → 1.5
Selected Windows p-value Significative Markers
position (cM)

82.701 - 84.201	0.0237	D13S265 D13S886
-----------------	--------	-----------------



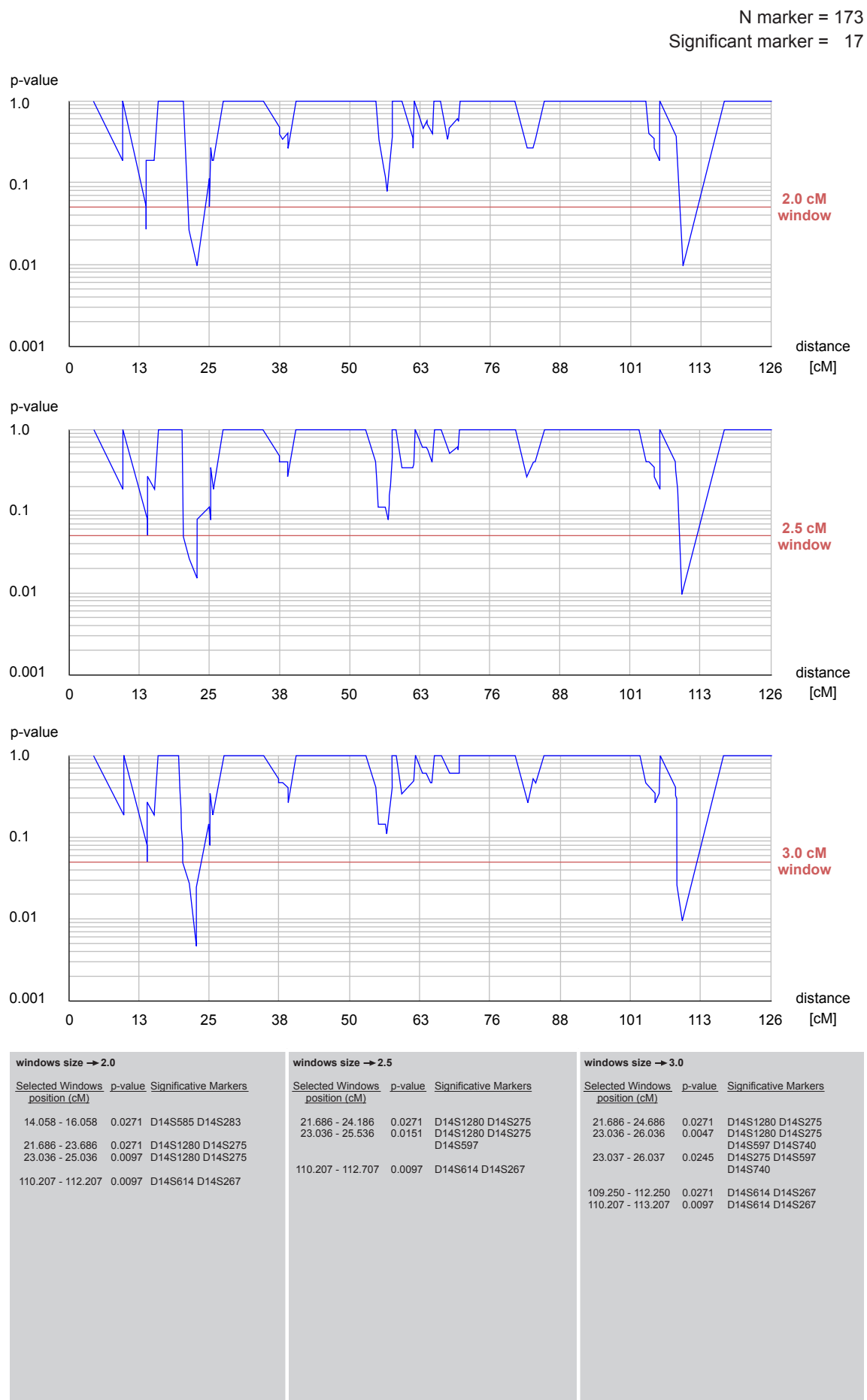
Chromosome 14



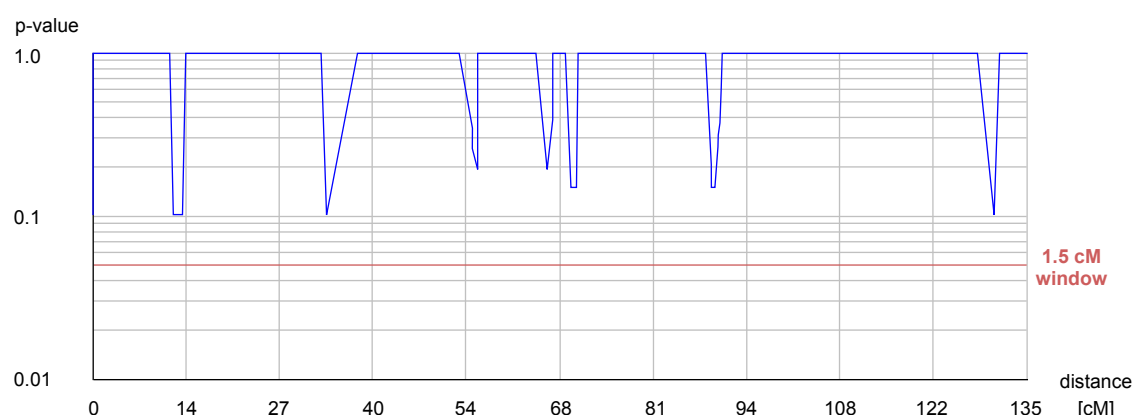
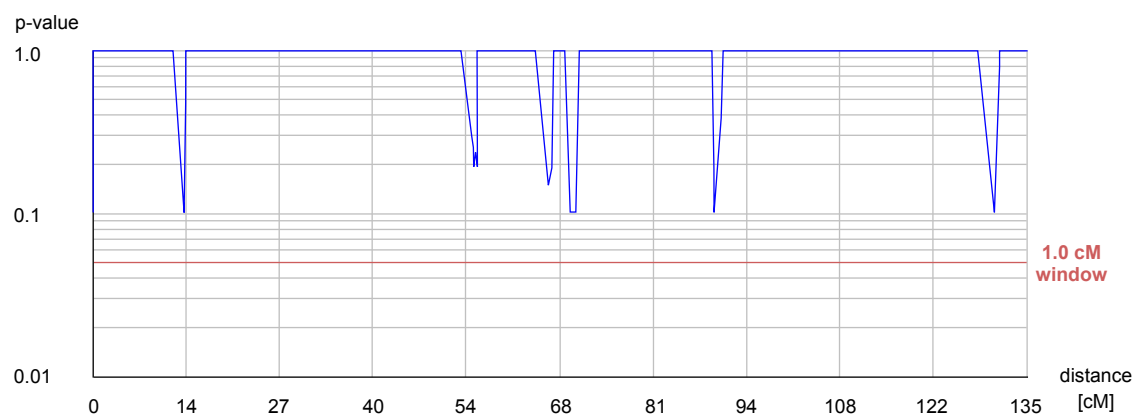
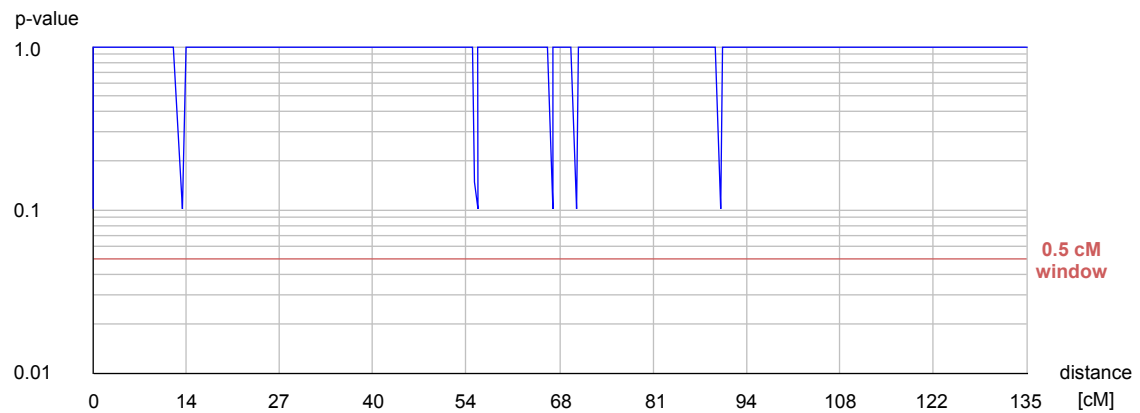
windows size → 0.5		
Selected Windows	p-value	Significative Markers
position (cM)		
23.036 - 23.536	0.0097	D14S1280 D14S275

windows size → 1.0		
Selected Windows	p-value	Significative Markers
position (cM)		
23.036 - 24.036	0.0097	D14S1280 D14S275
57.206 - 58.206	0.0271	D14S1056 D14S285

windows size → 1.5		
Selected Windows	p-value	Significative Markers
position (cM)		
14.058 - 15.558	0.0271	D14S585 D14S283
21.686 - 23.186	0.0271	D14S1280 D14S275
23.036 - 24.536	0.0097	D14S1280 D14S275



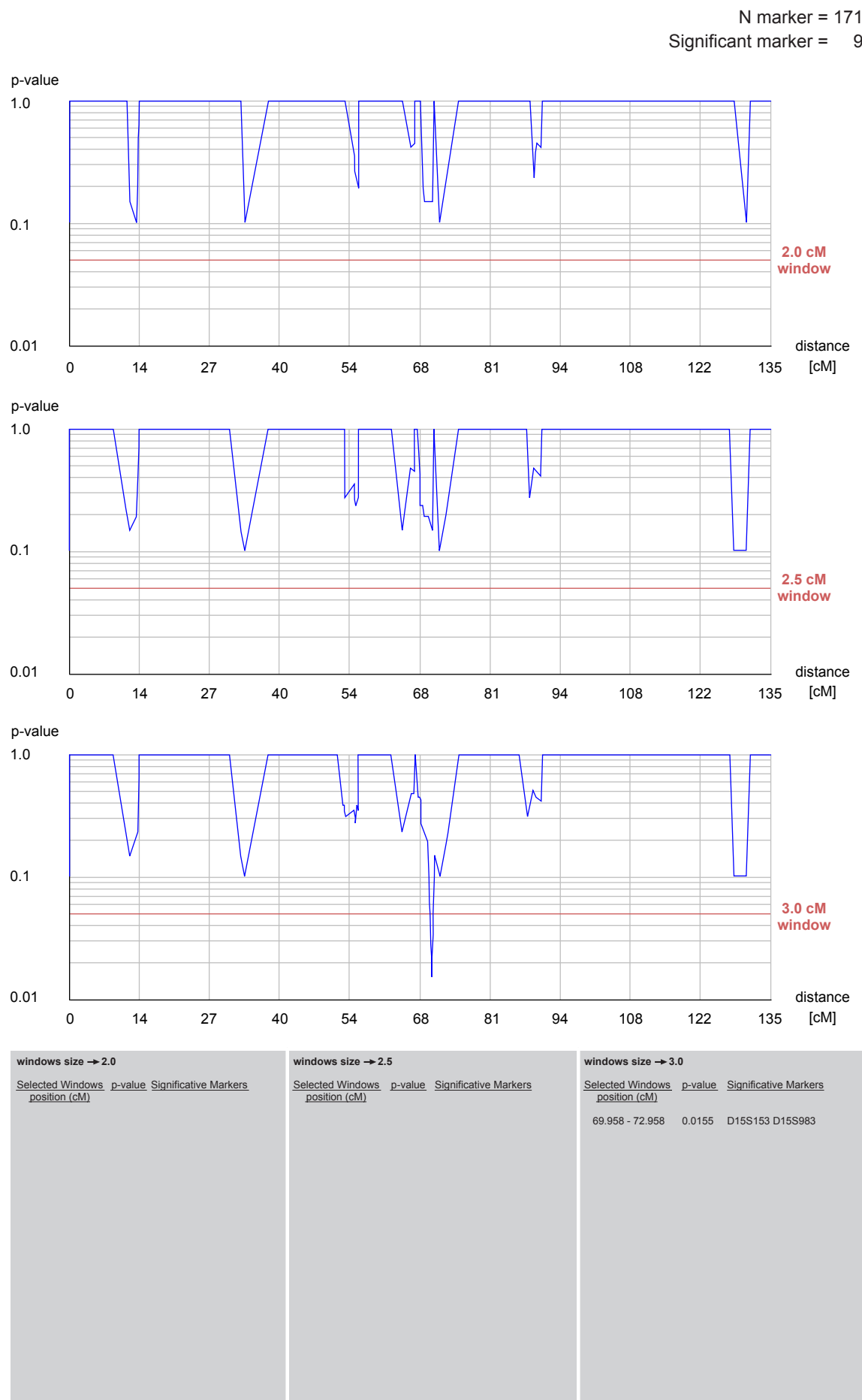
Chromosome 15



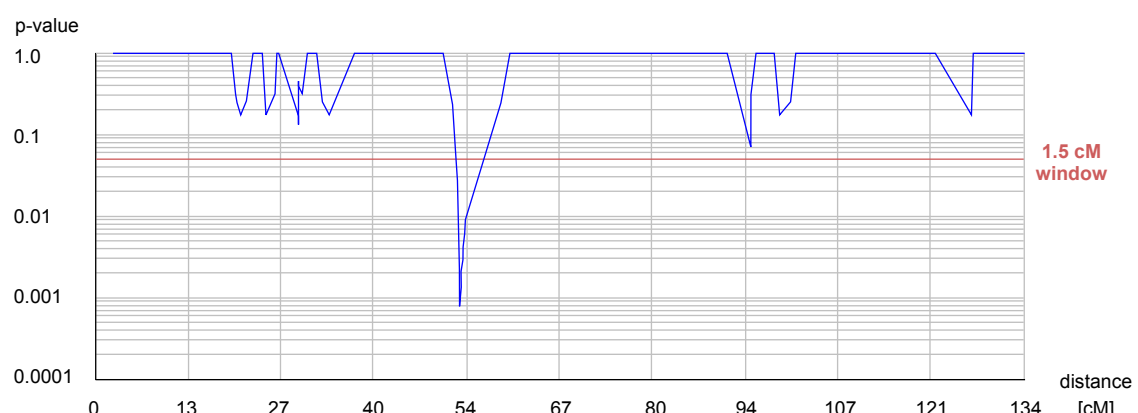
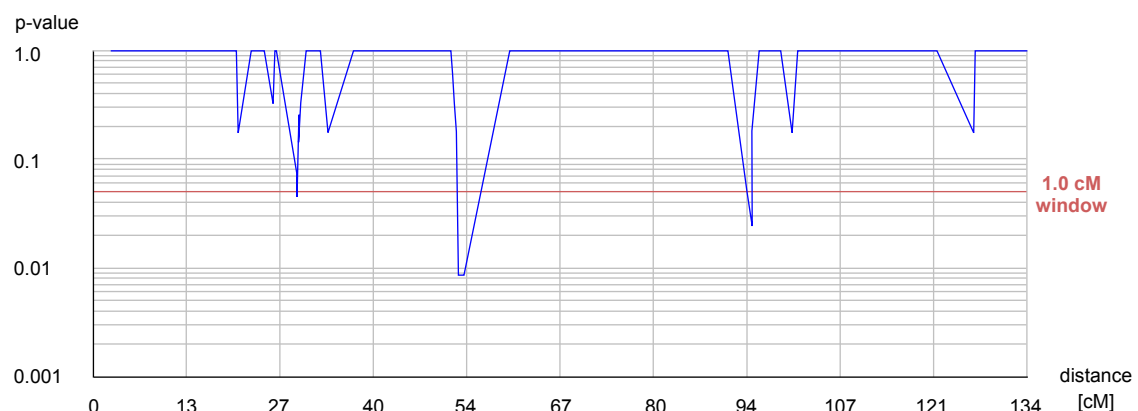
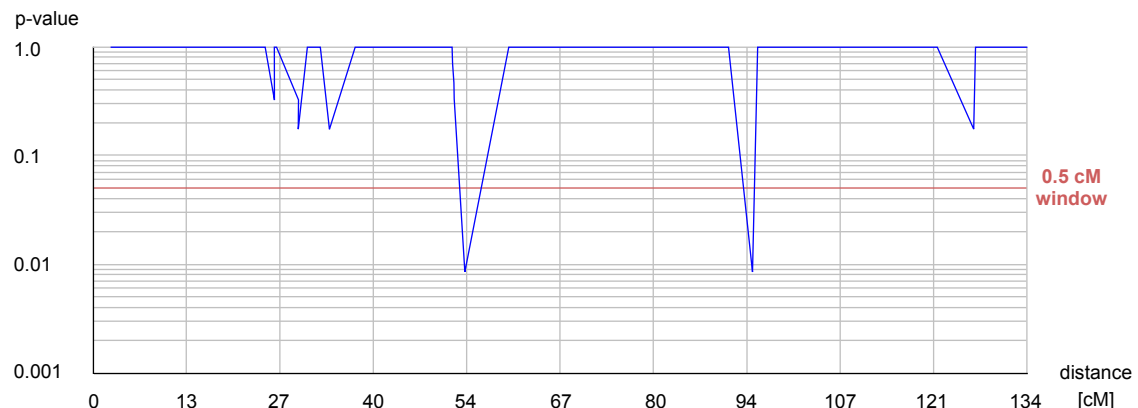
windows size → 0.5
Selected Windows p-value Significative Markers
position (cM)

windows size → 1.0
Selected Windows p-value Significative Markers
position (cM)

windows size → 1.5
Selected Windows p-value Significative Markers
position (cM)



Chromosome 16

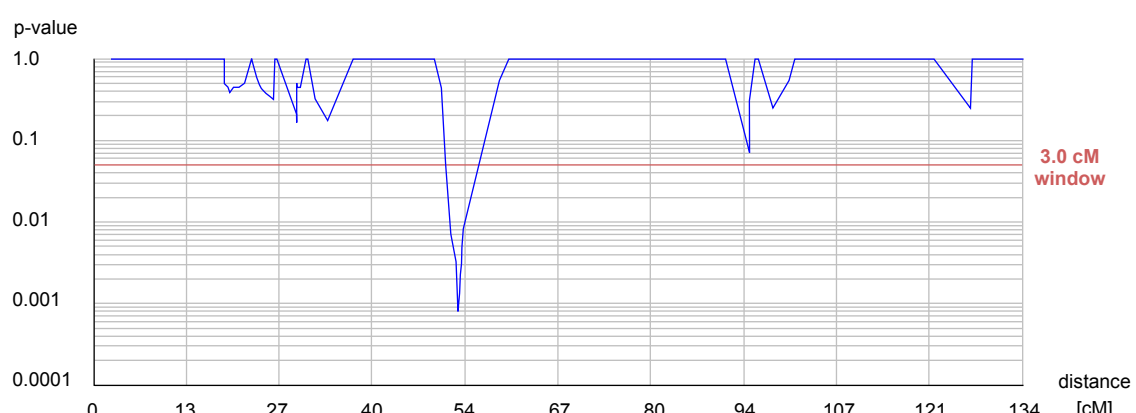
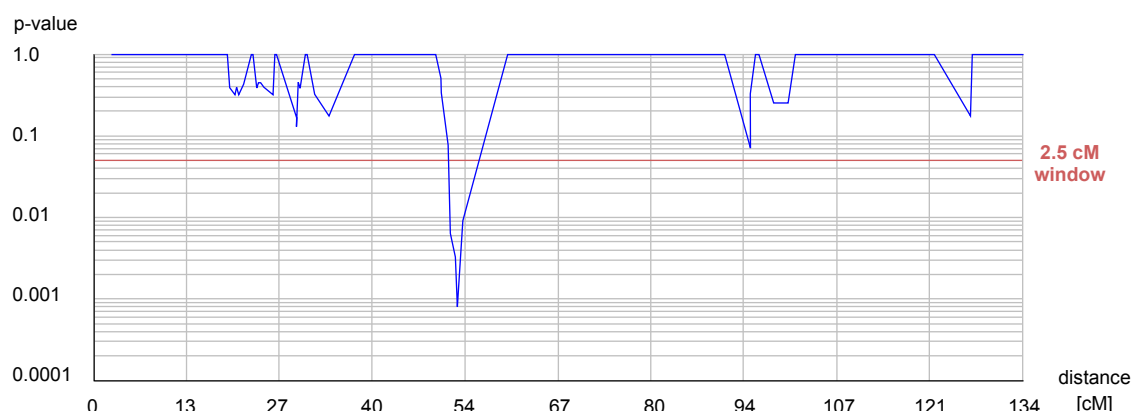
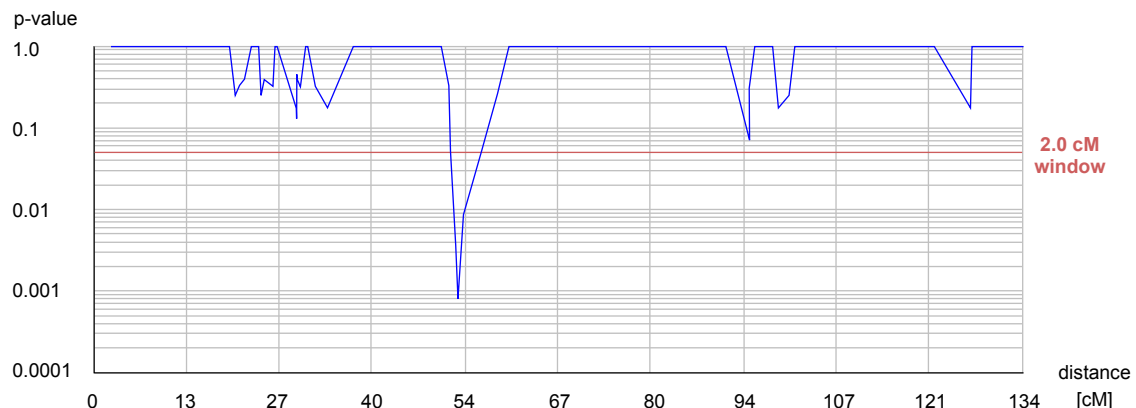


windows size → 0.5		
Selected Windows	p-value	Significative Markers
position (cM)		
53.429 - 53.929	0.0086	D16S3100 D16S3093
94.692 - 95.192	0.0086	D16S3083 D16S515

windows size → 1.0		
Selected Windows	p-value	Significative Markers
position (cM)		
29.444 - 30.444	0.0456	D16S497 D16S2613
52.579 - 53.579	0.0086	D16S769 D16S3100
53.429 - 54.429	0.0086	D16S3100 D16S3093
94.692 - 95.692	0.0243	D16S3083 D16S515

windows size → 1.5		
Selected Windows	p-value	Significative Markers
position (cM)		
52.270 - 53.770	0.0243	D16S769 D16S3100
52.579 - 54.079	8.0E-4	D16S769 D16S3100
53.429 - 54.929	0.0086	D16S3100 D16S3093

N marker = 140
Significant marker = 13

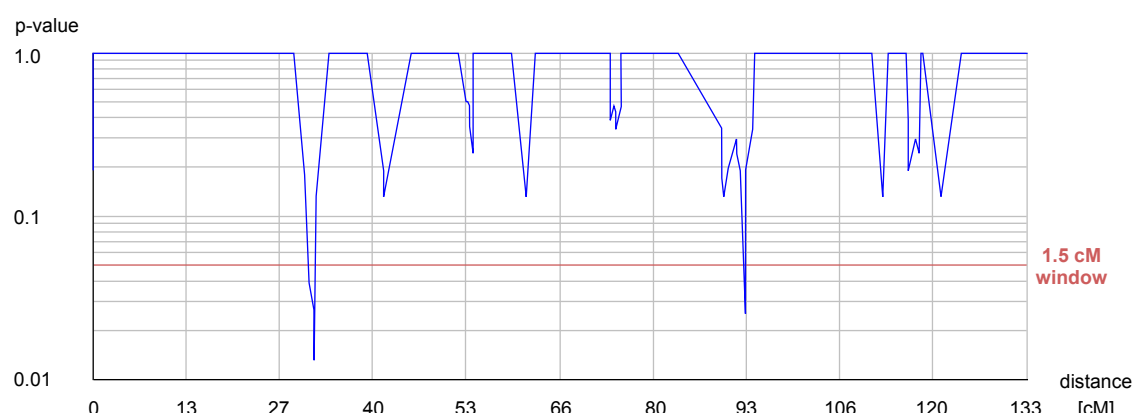
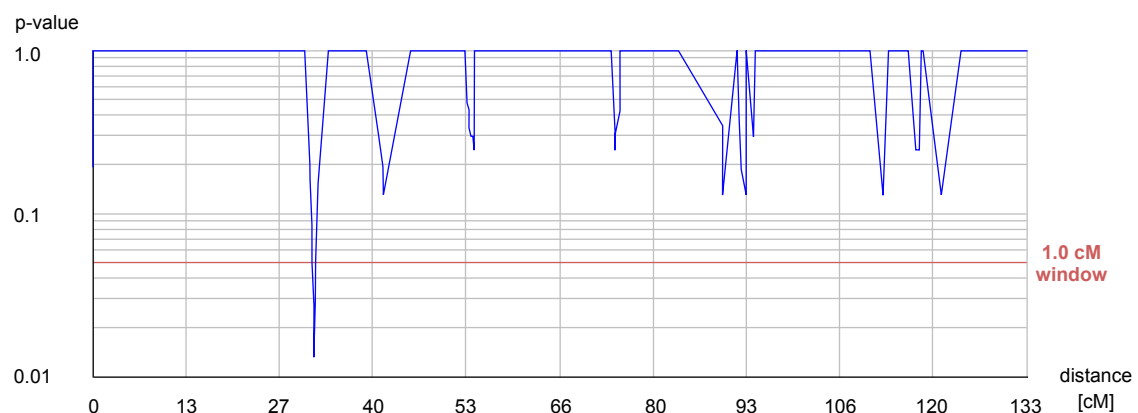
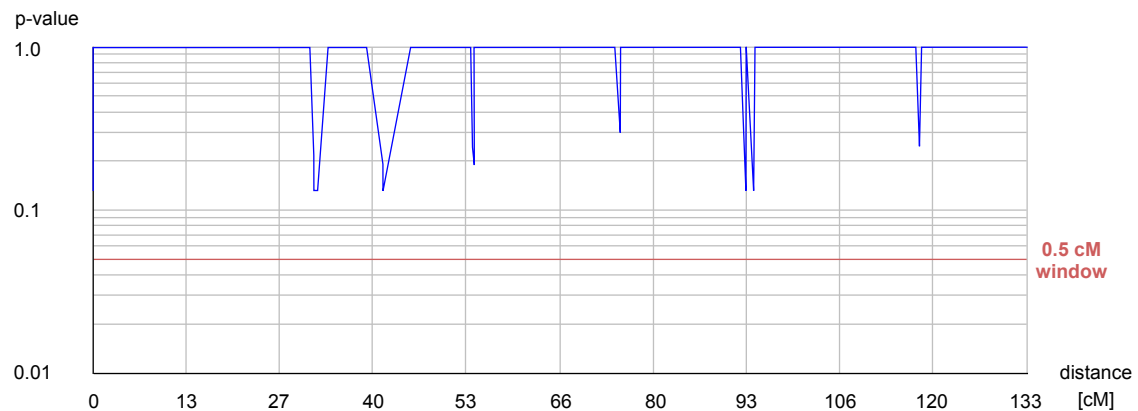


windows size → 2.0		
Selected Windows	p-value	Significative Markers
position (cM)		
51.546 - 53.546	0.0456	D16S769 D16S3100
52.270 - 54.270	0.0030	D16S769 D16S3100 D16S3093
52.579 - 54.579	8.0E-4	D16S769 D16S3100 D16S3093
53.429 - 55.429	0.0086	D16S3100 D16S3093

windows size → 2.5		
Selected Windows	p-value	Significative Markers
position (cM)		
51.546 - 54.046	0.0069	D16S769 D16S3100
52.270 - 54.770	0.0030	D16S769 D16S3100 D16S3093
52.579 - 55.079	8.0E-4	D16S769 D16S3100 D16S3093
53.429 - 55.929	0.0086	D16S3100 D16S3093

windows size → 3.0		
Selected Windows	p-value	Significative Markers
position (cM)		
51.268 - 54.268	0.0129	D16S769 D16S3100
51.546 - 54.546	0.0069	D16S769 D16S3100 D16S3093
52.270 - 55.270	0.0030	D16S769 D16S3100 D16S3093
52.579 - 55.579	8.0E-4	D16S769 D16S3100 D16S3093
53.429 - 56.429	0.0086	D16S3100 D16S3093

Chromosome 17



windows size → 0.5

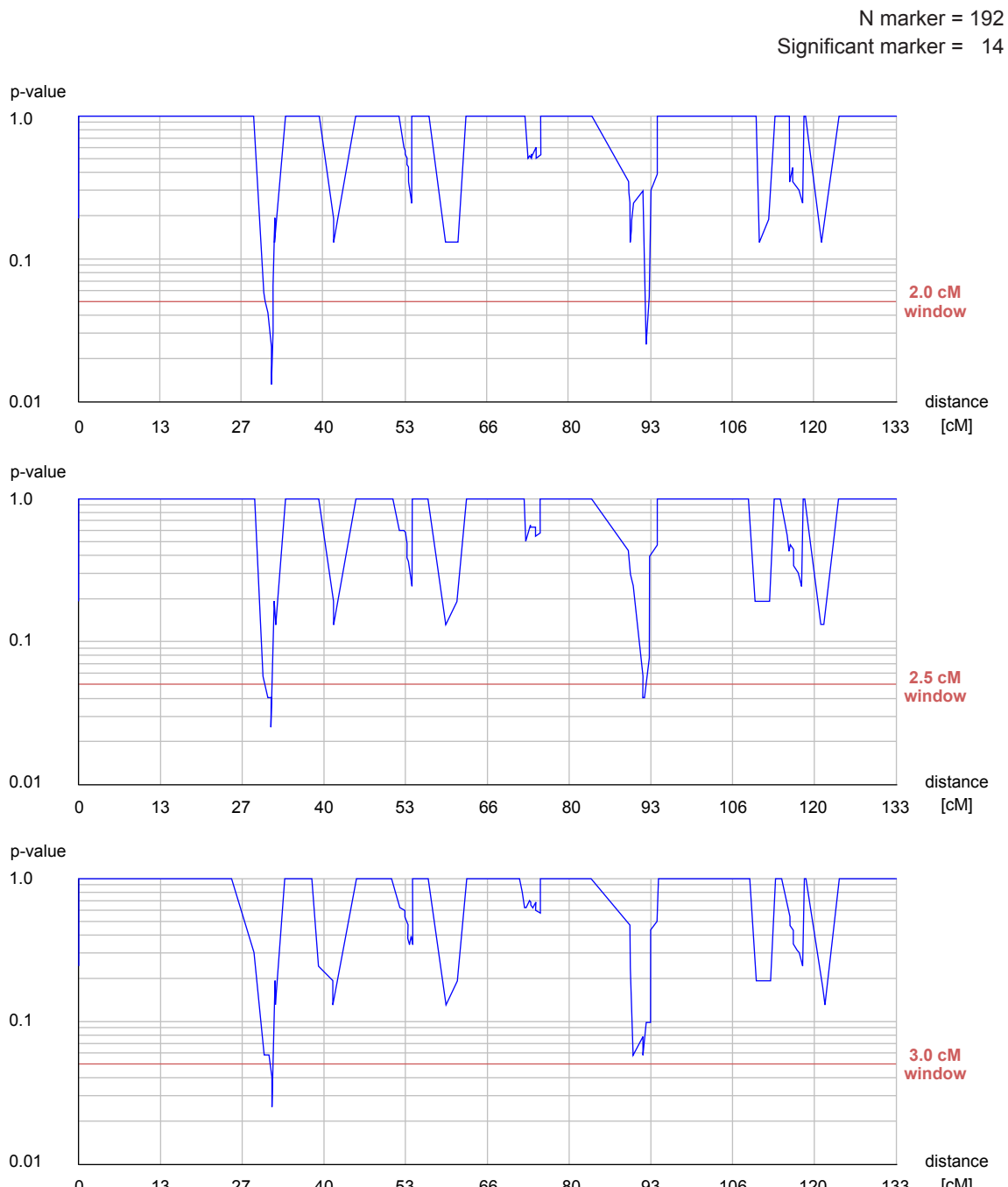
Selected Windows	p-value	Significative Markers
position (cM)		
31.499 - 32.499	0.0253	D17S974 D17S1303
31.506 - 32.506	0.0133	D17S974 D17S1303

windows size → 1.0

Selected Windows	p-value	Significative Markers
position (cM)		
31.499 - 32.499	0.0253	D17S974 D17S1303
31.506 - 32.506	0.0133	D17S974 D17S1303

windows size → 1.5

Selected Windows	p-value	Significative Markers
position (cM)		
30.961 - 32.461	0.0403	D17S974 D17S1303
31.499 - 32.999	0.0253	D17S974 D17S1303
31.506 - 33.006	0.0133	D17S974 D17S1303
93.058 - 94.558	0.0253	D17S917 D17S808

**windows size → 2.0**

<u>Selected Windows</u>	<u>p-value</u>	<u>Significative Markers</u>
<u>position (cM)</u>		
30.961 - 32.961	0.0403	D17S974 D17S1303
31.499 - 33.499	0.0253	D17S974 D17S1303
31.506 - 33.506	0.0133	D17S974 D17S1303
92.299 - 94.299	0.0253	D17S917 D17S808

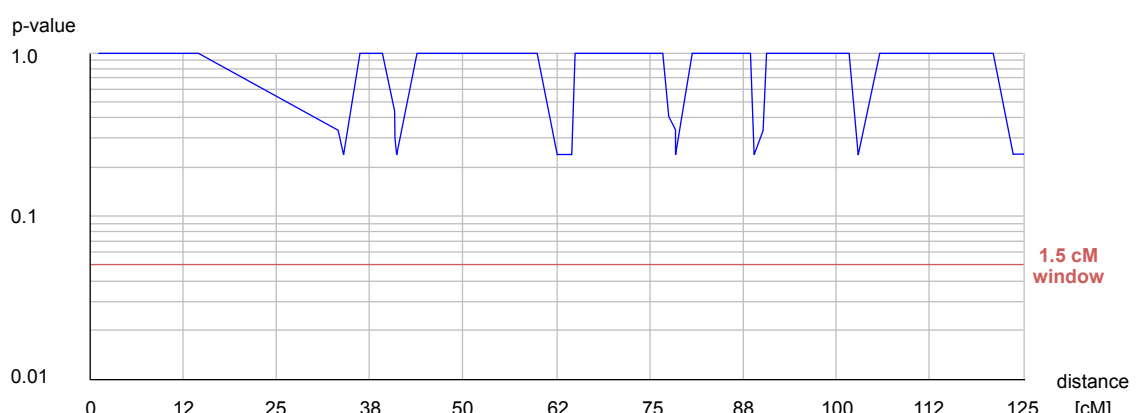
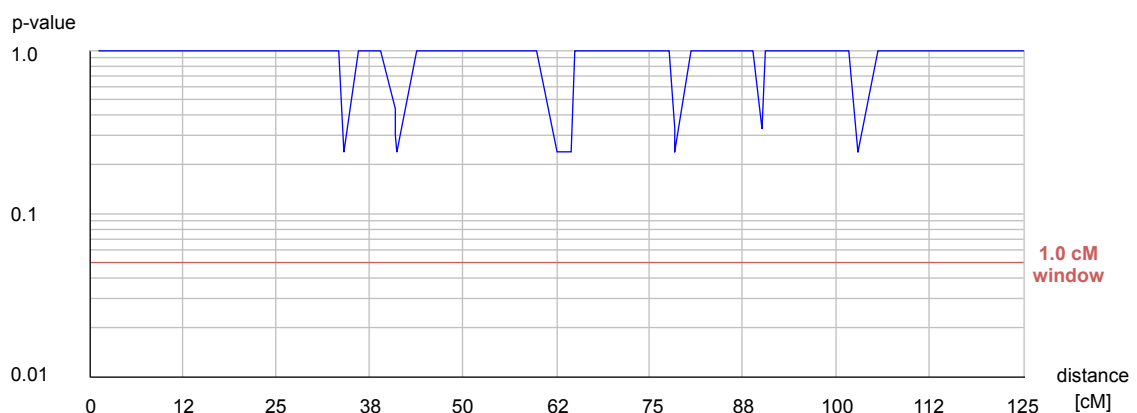
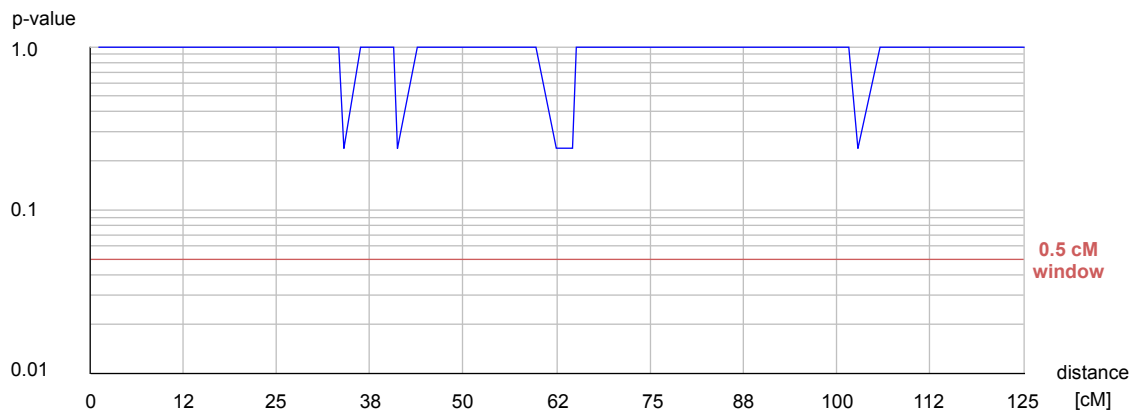
windows size → 2.5

<u>Selected Windows</u>	<u>p-value</u>	<u>Significative Markers</u>
<u>position (cM)</u>		
30.961 - 33.461	0.0403	D17S974 D17S1303
31.499 - 33.999	0.0403	D17S974 D17S1303
31.506 - 34.006	0.0253	D17S974 D17S1303
91.829 - 94.329	0.0403	D17S917 D17S808
92.299 - 94.799	0.0403	D17S917 D17S808

windows size → 3.0

<u>Selected Windows</u>	<u>p-value</u>	<u>Significative Markers</u>
<u>position (cM)</u>		
31.499 - 34.499	0.0403	D17S974 D17S1303
31.506 - 34.506	0.0253	D17S974 D17S1303

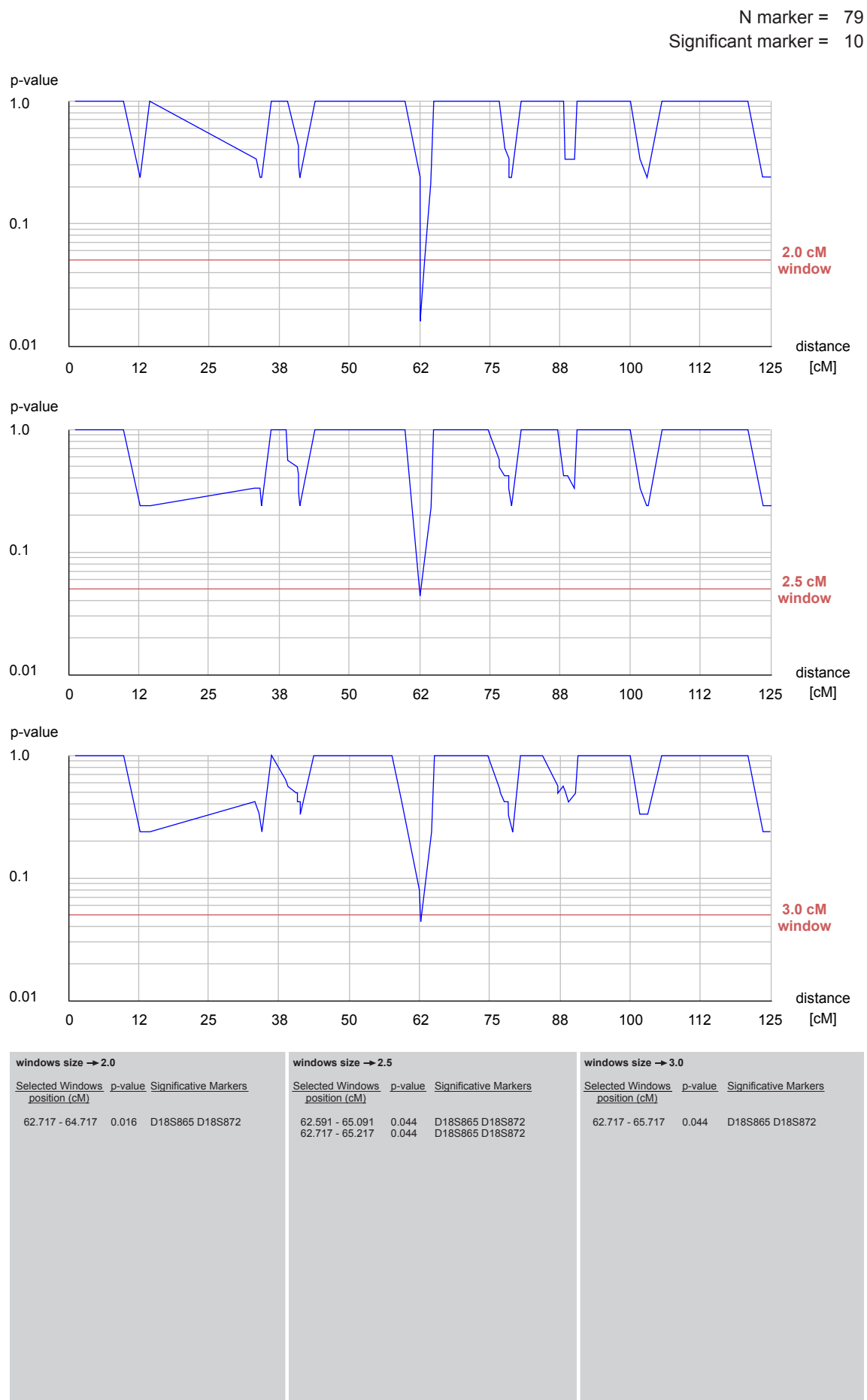
Chromosome 18



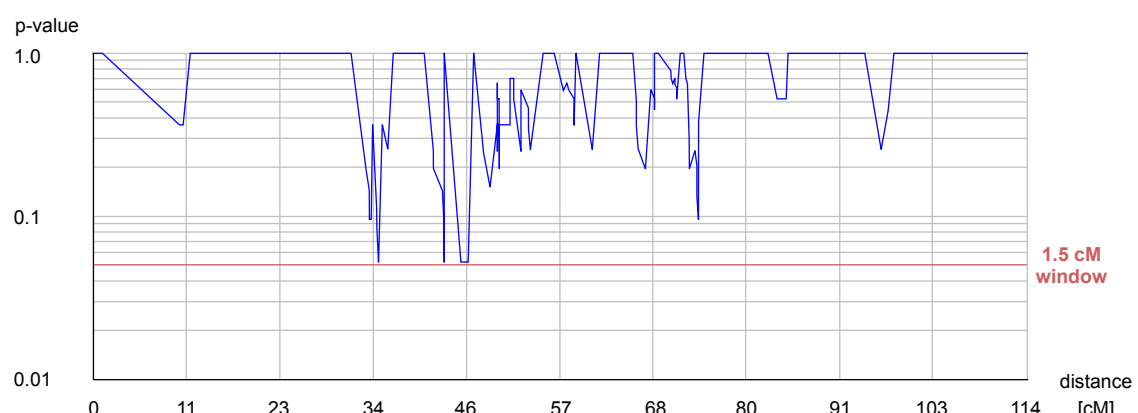
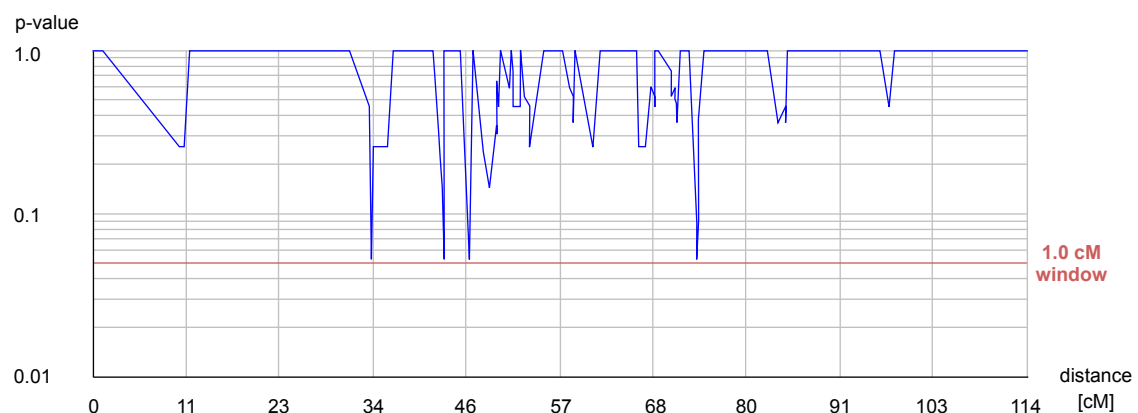
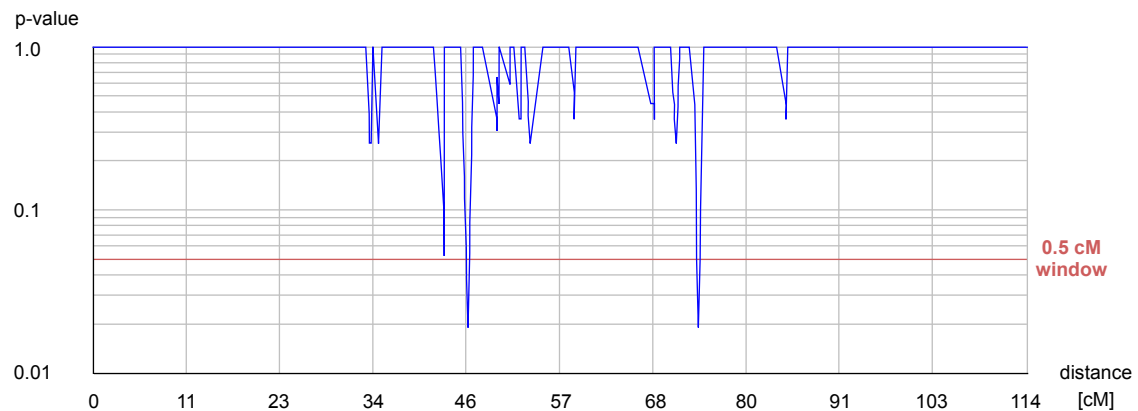
windows size → 0.5
Selected Windows p-value Significative Markers
position (cM)

windows size → 1.0
Selected Windows p-value Significative Markers
position (cM)

windows size → 1.5
Selected Windows p-value Significative Markers
position (cM)



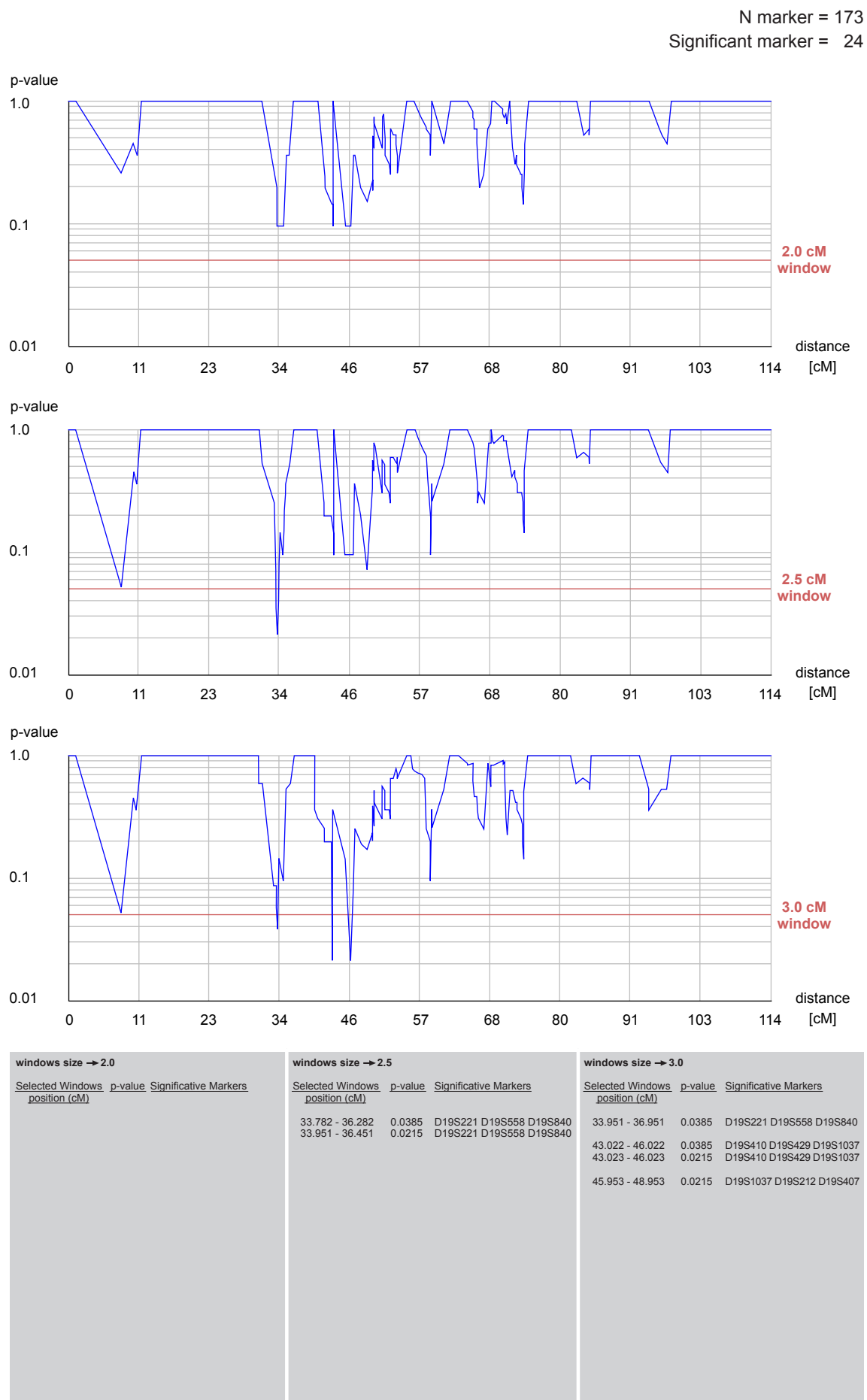
Chromosome 19



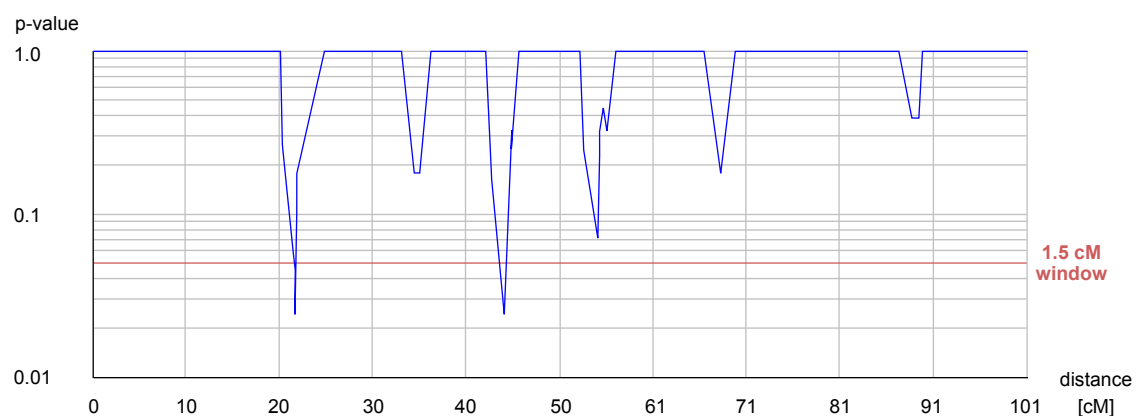
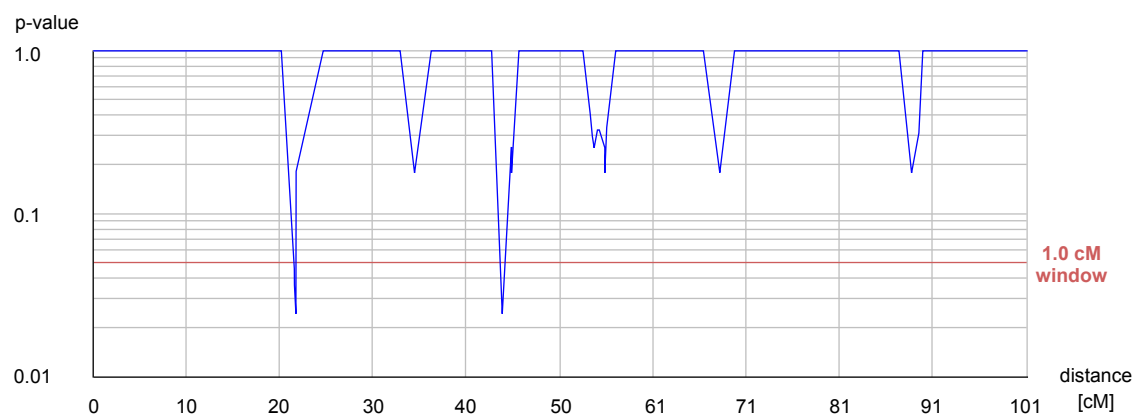
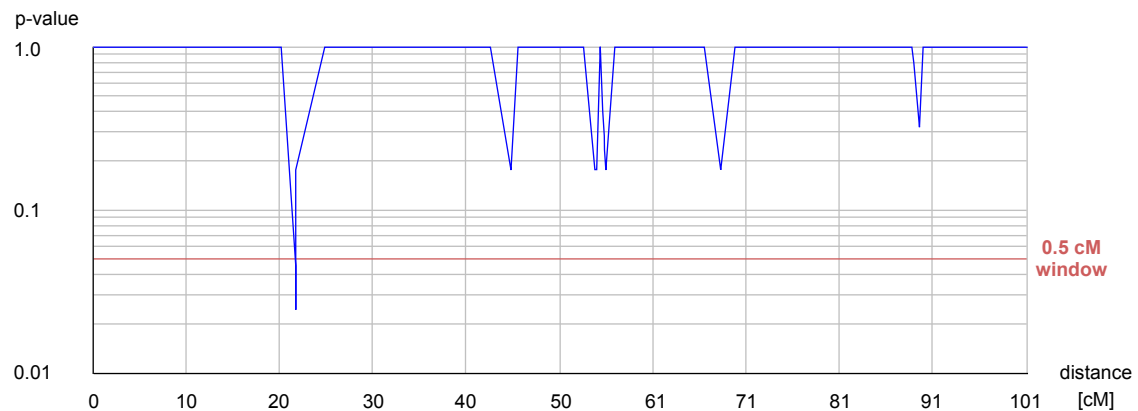
windows size → 0.5		
Selected Windows	p-value	Significative Markers
position (cM)		
45.953 - 46.453	0.0192	D19S1037 D19S212
73.920 - 74.420	0.0192	APOC2 D19S918

windows size → 1.0		
Selected Windows	p-value	Significative Markers
position (cM)		

windows size → 1.5		
Selected Windows	p-value	Significative Markers
position (cM)		



Chromosome 20

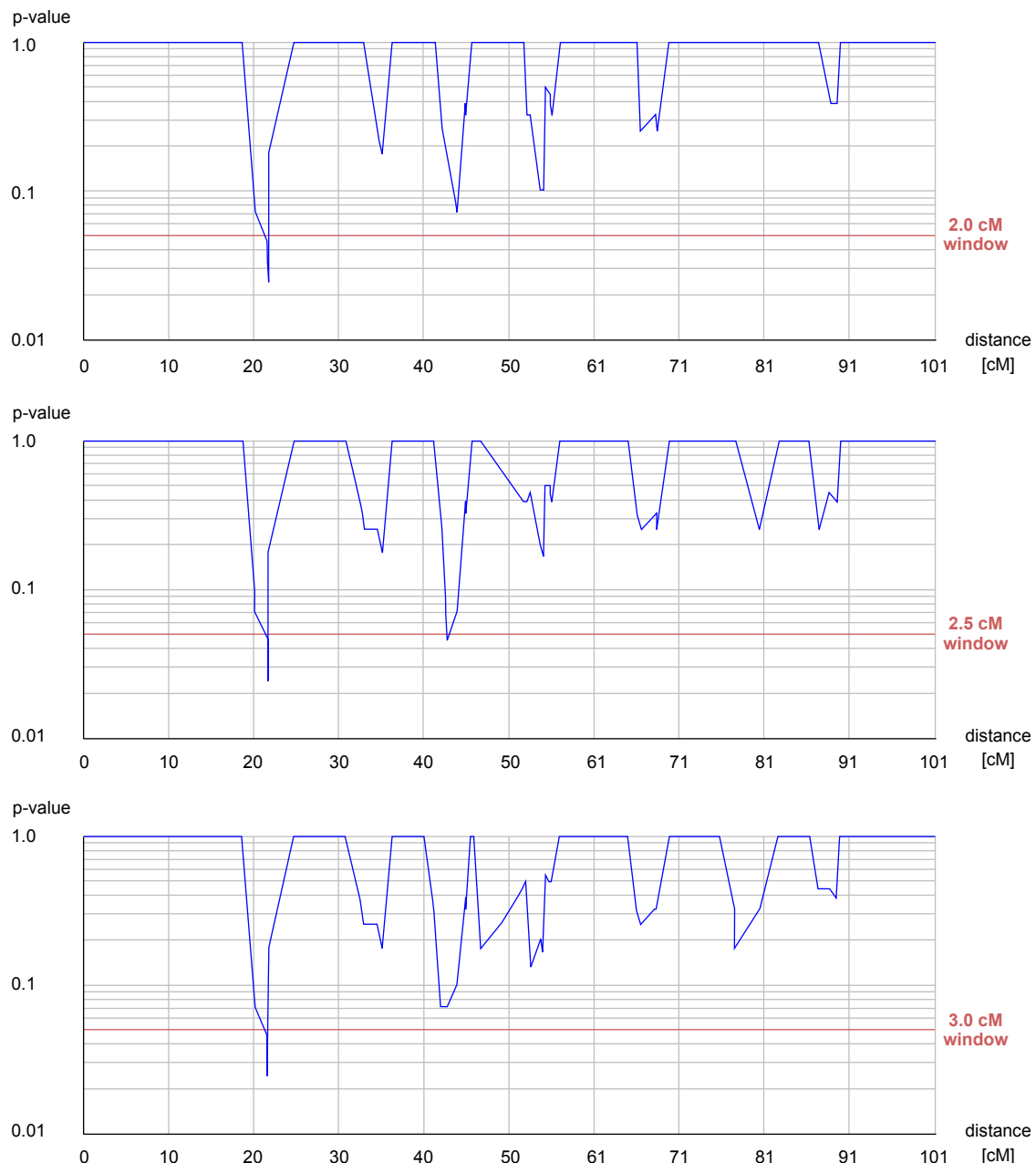


windows size → 0.5		
Selected Windows	p-value	Significative Markers
position (cM)		
21.933 - 22.433	0.0459	D20S603 D20S846
21.940 - 22.440	0.0244	D20S603 D20S846

windows size → 1.0		
Selected Windows	p-value	Significative Markers
position (cM)		
21.933 - 22.933	0.0459	D20S603 D20S846
21.940 - 22.940	0.0244	D20S603 D20S846
44.450 - 45.450	0.0244	D20S875 D20S112

windows size → 1.5		
Selected Windows	p-value	Significative Markers
position (cM)		
21.933 - 23.433	0.0459	D20S603 D20S846
21.940 - 23.440	0.0244	D20S603 D20S846
44.450 - 45.950	0.0244	D20S875 D20S112

N marker = 118
 Significant marker = 12



windows size → 2.0		
Selected Windows	p-value	Significative Markers
position (cM)		
21.933 - 23.933	0.0459	D20S603 D20S846
21.940 - 23.940	0.0244	D20S603 D20S846

windows size → 2.5		
Selected Windows	p-value	Significative Markers
position (cM)		
21.933 - 24.433	0.0459	D20S603 D20S846
21.940 - 24.440	0.0244	D20S603 D20S846
43.174 - 45.674	0.0459	D20S875 D20S112

windows size → 3.0		
Selected Windows	p-value	Significative Markers
position (cM)		
21.933 - 24.933	0.0459	D20S603 D20S846
21.940 - 24.940	0.0244	D20S603 D20S846

Chromosome 21



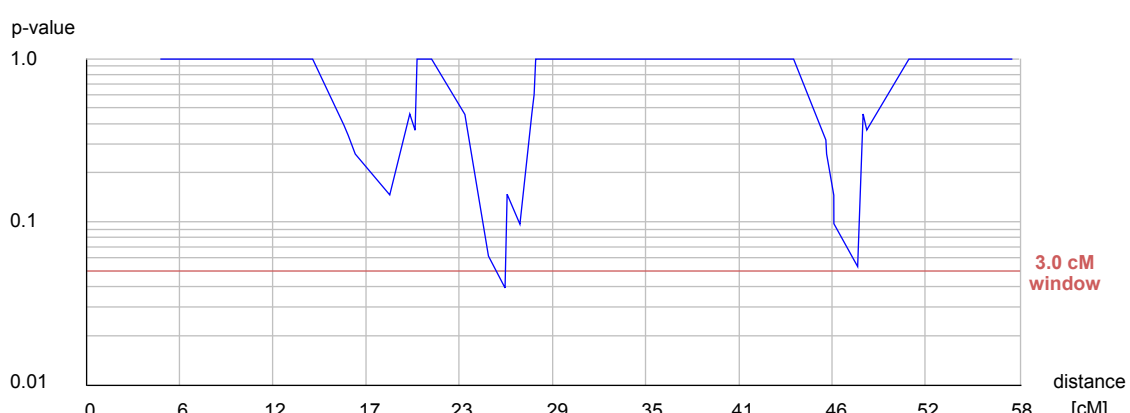
windows size → 0.5
Selected Windows p-value Significative Markers
position (cM)

windows size → 1.0
Selected Windows p-value Significative Markers
position (cM)

26.914 - 27.914 0.0196 D21S1443 D21S1435

windows size → 1.5
Selected Windows p-value Significative Markers
position (cM)

N marker = 50
Significant marker = 7

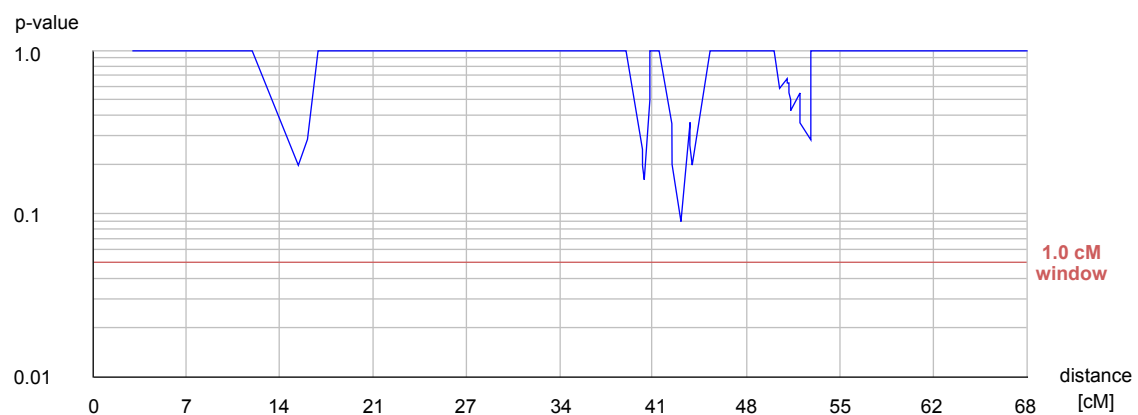
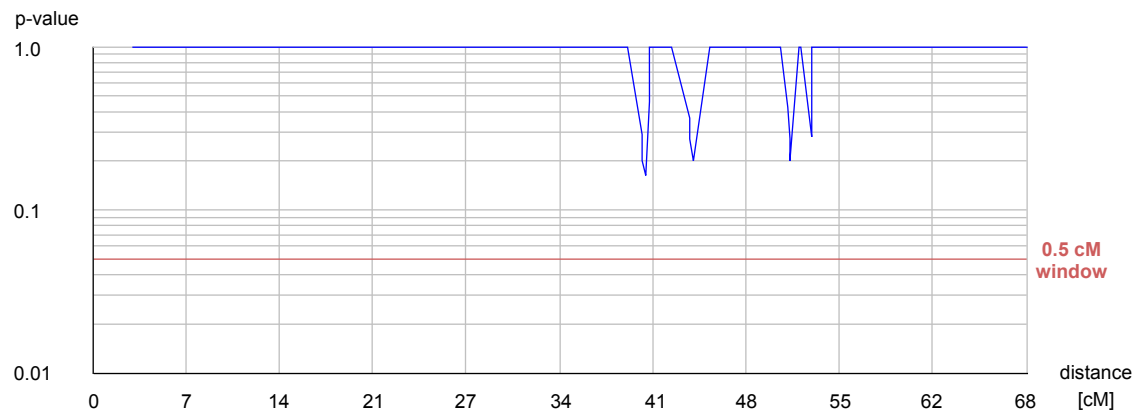


windows size → 2.0		
Selected Windows	p-value	Significative Markers
position (cM)		
26.069 - 28.069	0.0395	D21S367 D21S1443 D21S1435

windows size → 2.5		
Selected Windows	p-value	Significative Markers
position (cM)		
26.069 - 28.569	0.0395	D21S367 D21S1443 D21S1435

windows size → 3.0		
Selected Windows	p-value	Significative Markers
position (cM)		
26.069 - 29.069	0.0395	D21S367 D21S1443 D21S1435

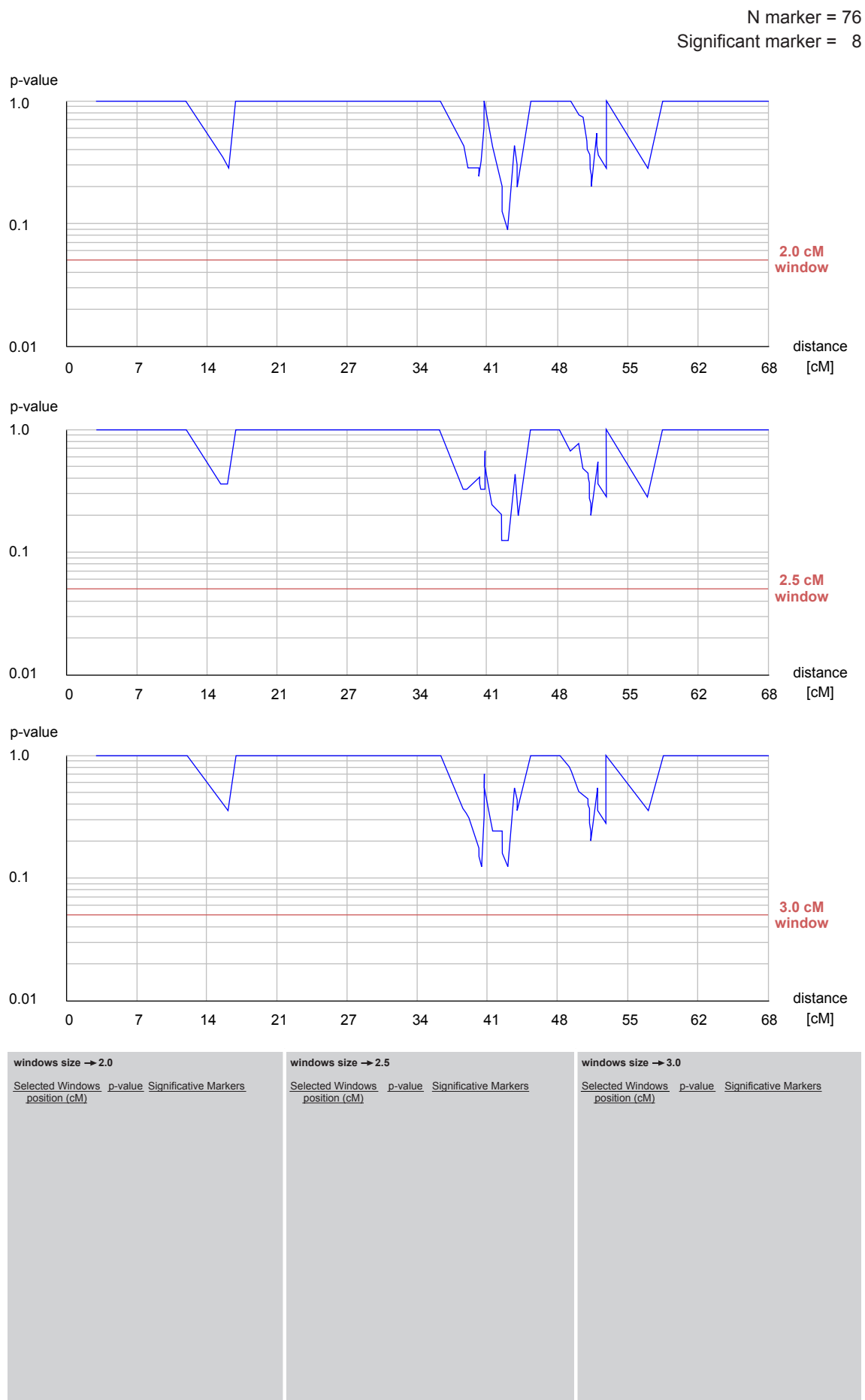
Chromosome 22



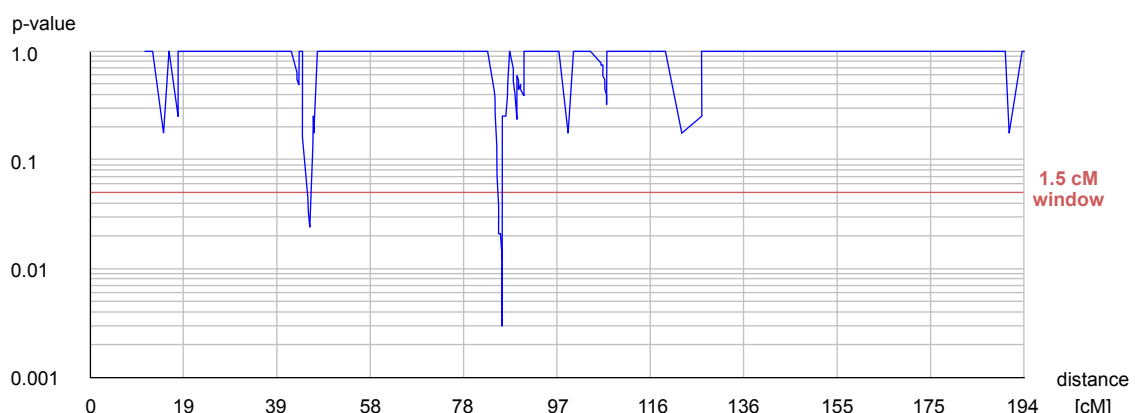
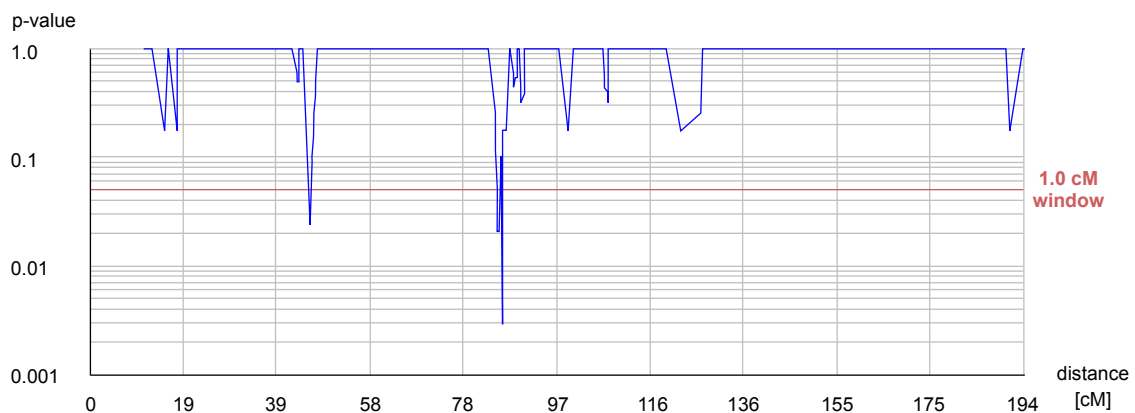
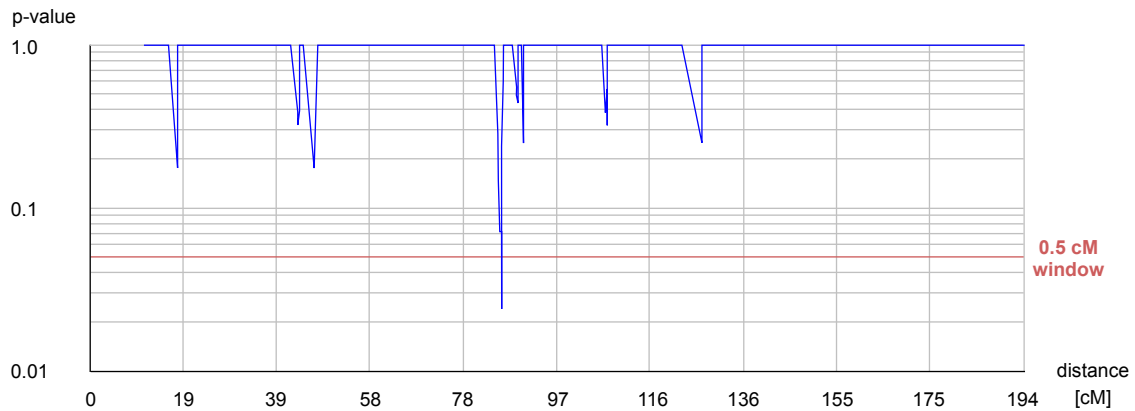
windows size → 0.5
Selected Windows p-value Significative Markers
position (cM)

windows size → 1.0
Selected Windows p-value Significative Markers
position (cM)

windows size → 1.5
Selected Windows p-value Significative Markers
position (cM)



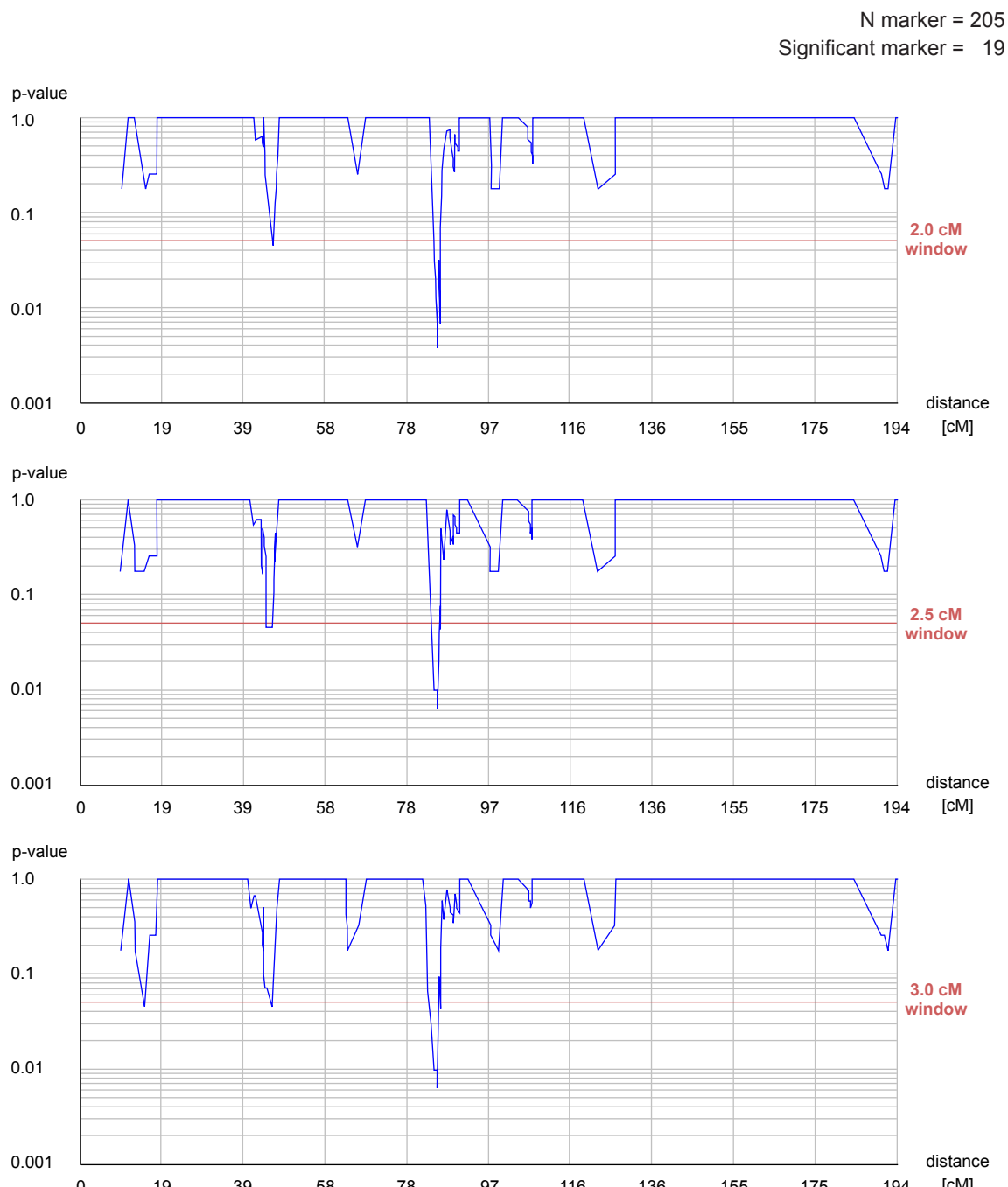
Chromosome X



windows size → 0.5		
Selected Windows	p-value	Significative Markers
position (cM)		
85.732 - 86.232	0.0454	DXS339 DXS8031
85.744 - 86.244	0.0242	DXS339 DXS8031

windows size → 1.0		
Selected Windows	p-value	Significative Markers
position (cM)		
45.818 - 46.818	0.0242	DXS1218 DXS8049
84.912 - 85.912	0.0209	DXS981 DXS339 DXS8031
84.996 - 85.996	0.0209	DXS981 DXS339 DXS8031
85.720 - 86.720	0.0128	DXS339 DXS8031 DXS8052
85.732 - 86.732	0.0069	DXS339 DXS8031 DXS8052
85.744 - 86.744	0.0030	DXS339 DXS8031 DXS8052
85.745 - 86.745	0.0242	DXS8031 DXS8052

windows size → 1.5		
Selected Windows	p-value	Significative Markers
position (cM)		
45.818 - 47.318	0.0242	DXS1218 DXS8049
84.912 - 86.412	0.0312	DXS981 DXS339 DXS8031
84.996 - 86.496	0.0209	DXS981 DXS339 DXS8031
85.301 - 86.801	0.0209	DXS339 DXS8031 DXS8052
85.720 - 87.220	0.0128	DXS339 DXS8031 DXS8052
85.732 - 87.232	0.0069	DXS339 DXS8031 DXS8052
85.744 - 87.244	0.0030	DXS339 DXS8031 DXS8052
85.745 - 87.245	0.0242	DXS8031 DXS8052



windows size → 2.0		
<u>Selected Windows</u>	<u>p-value</u>	<u>Significative Markers</u>
<u>position (cM)</u>		
45.818 - 47.818	0.0454	DXS1218 DXS8049
84.227 - 86.227	0.0437	DXS981 DXS339 DXS8031
84.912 - 86.912	0.0063	DXS981 DXS339 DXS8031
		DXS8052
84.996 - 86.996	0.0038	DXS981 DXS339 DXS8031
		DXS8052
85.301 - 87.301	0.0312	DXS339 DXS8031 DXS8052
85.720 - 87.720	0.0209	DXS339 DXS8031 DXS8052
85.732 - 87.732	0.0128	DXS339 DXS8031 DXS8052
85.744 - 87.744	0.0069	DXS339 DXS8031 DXS8052
85.745 - 87.745	0.0454	DXS8031 DXS8052

windows size → 2.5		
<u>Selected Windows</u>	<u>p-value</u>	<u>Significative Markers</u>
<u>position (cM)</u>		
44.469 - 46.969	0.0454	DXS1218 DXS8049
45.818 - 48.318	0.0454	DXS1218 DXS8049
84.227 - 86.727	0.0098	DXS981 DXS339 DXS8031
		DXS8052
84.912 - 87.412	0.0098	DXS981 DXS339 DXS8031
		DXS8052
84.996 - 87.496	0.0063	DXS981 DXS339 DXS8031
		DXS8052
85.301 - 87.801	0.0312	DXS339 DXS8031 DXS8052
85.744 - 88.244	0.0437	DXS339 DXS8031 DXS8052

windows size → 3.0		
<u>Selected Windows</u>	<u>p-value</u>	<u>Significative Markers</u>
<u>position (cM)</u>		
15.566 - 18.566	0.0454	DXS1283E DXS8051
45.818 - 48.818	0.0454	DXS1218 DXS8049
82.907 - 85.907	0.0437	DXS981 DXS339 DXS8031
84.227 - 87.227	0.0098	DXS981 DXS339 DXS8031
		DXS8052
84.912 - 87.912	0.0098	DXS981 DXS339 DXS8031
		DXS8052
84.996 - 87.996	0.0063	DXS981 DXS339 DXS8031
		DXS8052
85.744 - 88.744	0.0437	DXS339 DXS8031 DXS8052

Appendix D – Genes of interest derived from sliding windows

142 potential candidate genes contained in significant genomic windows that derive from STR-genotyping data of a pooled DNA approach with MS patients and controls.

CHR, n	Candidate genes	Gene symbol
1; 8	H3 histone, family 3A Acyl-Coenzyme A binding domain containing 3 Mix1 homeobox-like 1 (<i>Xenopus laevis</i>) TGS2 Fibromodulin Proline arginine-rich end leucine-rich repeat protein Opticin Hypothetical protein DKFZp686K08109	H3F3A ACBD3 MIXL1 TGS2 FMOD PRELP OPTC ATP2B4
2; 3	Succinate-CoA ligase, GDP-forming, alpha subunit NADH dehydrogenase (ubiquinone) 1 beta subcomplex, 3, 12kDa Low density lipoprotein-related protein 1B	SUCLG1 NDUFB3 LRP1B
3; 2	APG7L protein Ribosomal protein L32	APGL7 RPLR32
4; 6	Scrapie-responsive protein 1 precursor Heart- and neural crest derivatives-expressed protein 2 Mortality factor 4 Latrophilin 3 precursor Hypothetical protein DKFZp686C0686 Hypothetical protein FLJ43569	SCRG1 HAND2 MORF4 LPHN3 EPHA5 MMRN1
5; 4	Monogenic, audiogenic seizure susceptibility 1 homolog Dmx-like 1 Hydroxysteroid (17-beta) dehydrogenase 4 5-methyltetrahydrofolate-homocysteine methyltransferase reductase	MASS1 DMXL1 HSD17B4 MTRR
6; 29	Apolipoprotein M Casein kinase 2, beta polypeptide G6b-A protein precursor Dimethylarginine dimethylaminohydrolase 2 Chloride intracellular channel 1 LSM2 homolog, U6 small nuclear RNA associated Chromosome 6 open reading frame 48 Sialidase 1 DOM3Z protein Chromosome 6 open reading frame 31 Palmitoyl-protein thioesterase 2 NG3 protein 1-acylglycerol-3-phosphate O-acyltransferase 1 Ring finger protein 5 Advanced glycosylation end product-specific receptor Pre-B-cell leukemia transcription factor 2 Bromodomain containing 2 Collagen, type XI, alpha 2 Hydroxysteroid (17-beta) dehydrogenase 8 Vacuolar protein sorting 52 40S ribosomal protein S18 Chromosome 6 open reading frame 11	APOM CSNK2B C6orf25 DDAH2 CLIC1 LSM2 C6orf48 NEU1 DOM3Z C6orf31 PPT2 EGFL8 AGPAT1 RNF5 AGER PBX2 BRD2 COL11A2 HSD17B8 VPS52 RPS18 C6orf11

	Ral guanine nucleotide dissociation stimulator-like 2	RGL2
	Kinesin family member C1	KIFC1
	PHD finger protein 1	PHF1
	Synaptic Ras GTPase activating protein 1	SYNGAP1
	Zinc finger and BTB domain containing protein 9	ZBTB9
	Fucosyltransferase 9	FUT9
	F-box and leucine-rich repeat protein 4	FXL4
7; 9	LSM8 homolog, U6 small nuclear RNA associated Ankyrin repeat domain 7 Distal-less homeo box 5 Neuronal pentraxin II Smad ubiquitination regulatory factor 1 Growth factor receptor-bound protein 10 Dopa decarboxylase Zuotin related factor 1 Prestin	LSM8 ANKRD7 DLX5 NPTX2 SMURF1 GRB10 DDC ZRF1 PRES
8; 7	Extracellular sulfatase Sulf-1 precursor Solute carrier organic anion transporter family, member 5A1 PR domain containing 14 nuclear receptor coactivator 2 Translocation associated membrane protein 1 Eyes absent homolog 1 V-yes-1 Yamaguchi sarcoma viral related oncogene homolog	SULF1 SLCO5A1 PRDM14 NCOA2 TRAM1 EYA1 LYN
9; 1	BA438B23.1 (Neuronal leucine-rich repeat protein)	NM_152570
10; 5	Neuropeptide FF receptor 1 (G protein-coupled receptor 147) Nodal homolog inter-alpha (globulin) inhibitor H2 KIN, antigenic determinant of recA protein homolog ATP synthase, H+ transporting, mitochondrial F1 complex, gamma polypeptide 1	GPR147 NODAL ITIH2 KIN ATP5C1
11; 7	Doublecortin domain-containing protein 1 Reticulocalbin 1, EF-hand calcium binding domain Wilms tumor 1 F-box protein 3 LIM domain only 2 Jerky homolog-like Olfactory receptor, family 6, subfamily X	DCD1 RCN1 WT1 FBXO3 LMO2 JRK1 OR6X1
12; 13	Low density lipoprotein receptor-related protein 6 MANSC domain containing protein 1 precursor (UNQ316/PRO361) Retinoic acid induced 3 protein (G protein-coupled receptor family C group 5 member A) G protein-coupled receptor, family C, group 5, member D Heme-binding protein Epithelial membrane protein 1 DYRK2 protein Nuclear protein double minute 1 Ras-related protein Rap-1b (GTP-binding protein smg p21B) Nuclear pore complex protein Nup107 MDS023 (MRPS35 protein) Myosin binding protein C, slow type ADP-ribosylation factor-like 1	LRP6 MANSC1 GPCR5A GPR5CD HEBP1 EMP1 DYRK2 MDM1 RAP1B NUP107 MRPS35 MYBPC1 ARL1
13; 8	Component of oligomeric golgi complex 6 Forkhead box O1A (rhabdomyosarcoma) Mitochondrial ribosomal protein S31 Solute carrier family 25 (mitochondrial carrier; ornithine transporter) member 15 WW domain binding protein 4 (formin binding protein 21)	COG6 FOXO1A MRPS31 SLC25A15 WBP4

	Kelch repeat and BTB domain containing protein 6	KBTBD6
	Kelch repeat and BTB domain containing protein 7	KBTBD7
	Mitochondrial translational release factor 1	MTRF1
14; 2	Olfactory receptor, family 4, subfamily E	OR4E2
	Pellino homolog 2	PELI2
15; 4	Ribosomal protein L4	RPL4
	SMAD, mothers against DPP homolog 6	SMAD6
	Ceroid-lipofuscinosis, neuronal 6, late infantile, variant	CLN6
	Integrin, alpha 11	ITA11
16; 3	Transition protein 2 (during histone to protamine replacement)	TNP2
	Protamine 2	PRM2
	Protamine 1	PRM1
17; 5	Myosin, heavy polypeptide 3, skeletal muscle, embryonic	MYH3
	BRCA1 interacting protein C-terminal helicase 1	BRIP1
	Thyroid hormone receptor-associated protein complex 240 kDa component	THRAP
	Methyltransferase-like protein 2 (HSPC266)	METL2
	Serine/threonine-protein kinase tousled-like 2 (PKU-alpha)	TLK2
19; 14	Mannosidase, alpha, class 2B, member 1	MAN2B1
	Deoxyhypusine synthase	DHPS
	Transportin 2 (importin 3, karyopherin beta 2b)	TNPO2
	ArsA arsenite transporter, ATP-binding	ASNA1
	Nuclear factor I/X (CCAAT-binding transcription factor)	NFIX
	Probable N(2),N(2)-dimethylguanosine tRNA methyltransferase	TRM1
	Syntaxin 10	STX10
	phosphoinositide-3-kinase, regulatory subunit 2 (p85 beta)	PIK3R2
	Phosphodiesterase 4C, cAMP-specific	PDE4C
	Mitochondrial ribosomal protein L34	MRPL34
	6-phosphogluconolactonase	PGLS
	Ribosomal protein L18a	RPL18A
	Solute carrier family 5 (sodium iodide symporter), member 5	SLC5A5
	Apolipoprotein C-II	APOC2
20; 2	Bone morphogenetic protein 2	BMP2
	PCSK2 protein	PCSK2
21; 3	ATP synthase, H ⁺ transporting, mitochondrial F0 complex, subunit F6	ATP5J
	GA binding protein transcription factor, alpha subunit 60kDa	GABPA
	Cysteine and tyrosine-rich 1	CYYR1
X; 7	Pyrimidinergic receptor P2Y4	P2RY4
	Arrestin 3, retinal (X-arrestin)	ARR3
	Kinesin family member 4A	KIF4A
	Testis protein TEX11	TEX11
	Variable charge, X-linked	VCX
	GS2 protein (DXS1283E)	PNPLA4
	Variable charge X-linked protein 2 (VCX-B protein)	VCX2

$$\Sigma = 142$$

Appendix E – Allele and genotype frequency distributions and corresponding statistics

Data derived from 16 tested SNPs on 572 individuals

* not significant when subjected to Sequential Bonferroni correction (correction for multiple testing was enabled when stratification was performed).

^a deviating from Hardy-Weinberg Equilibrium (HWE)

Table E1 | Allele and genotype frequency distribution VGGL4; MS vs. Controls

		MS patients (n = 287)	Controls (n = 285)	p -value	Odds ratio	95% CI
SNP 24	Allele					
	A	69 (12.1%)	68 (12.0%)	0.945		
	G	501 (87.9%)	500 (88.0%)			
	Genotype					
	AA	3 (1.1%)	3 (1.1%)	1.000		
	AG	63 (22.1%)	62 (21.8%)	0.937		
SNP 9	Allele					
	A	264 (46.0%)	278 (48.8%)	0.347		
	G	310 (54.0%)	292 (51.2%)			
	Genotype					
	AA	68 (23.7%)	61 (21.4%)	0.512		
	AG	128 (44.6%)	156 (54.7%)	0.015	0.67	0.48 – 0.93
SNP 20	Allele					
	A	517 (90.1%)	522 (91.6%)	0.377		
	C	57 (9.9%)	48 (8.4%)			
	Genotype					
	AA	232 (80.8%)	241 (84.6%)	0.239		
	AC	53 (18.5%)	40 (14.0%)	0.151		
	CC	2 (0.7%)	4 (1.4%)	0.449		

Table E2 | Allele and genotype frequency distribution VGGL4; RRMS vs Controls

		RRMS (n = 192)	Controls (n = 285)	p-value	Odds ratio	95% CI
SNP 24	Allele					
	A	42 (11.0%)	68 (12.0%)	0.645		
	G	340 (89.0%)	500 (88.0%)			
	Genotype					
	AA	2 (1.0%)	3 (1.1%)	1.000		
	AG	38 (19.9%)	62 (21.8%)	0.612		
SNP 9	Allele					
	A	186 (48.4%)	278 (48.8%)	0.919		
	G	198 (51.6%)	292 (51.2%)			
	Genotype					
	AA	52 (27.1%)	61 (21.4%)	0.152		
	AG	82 (42.7%)	156 (54.7%)	0.010	0.62	0.43 – 0.89
SNP 20	Allele					
	A	347 (90.4%)	522 (91.6%)	0.519		
	C	37 (9.6%)	48 (8.4%)			
	Genotype					
	AA	156 (81.3%)	241 (84.6%)	0.342		
	AC	35 (18.2%)	40 (14.0%)	0.217		
	CC	1 (0.5%)	4 (1.4%)	0.653		

Table E3 | Allele and genotype frequency distribution VGGL4; PPMS vs Controls

		PPMS (n = 95)	Controls (n = 285)	p-value	Odds ratio	95% CI
SNP 24	Allele					
	A	27 (14.4%)	68 (12.0%)			
	G	161 (85.6%)	500 (88.0%)	0.392		
	Genotype					
	AA	1 (1.1%)	3 (1.1%)	1.000		
	AG	25 (26.6%)	62 (21.8%)	0.341		
	GG	68 (72.3%)	219 (77.1%)	0.348		
SNP 9	Allele					
	A	78 (41.0%)	278 (48.8%)			
	G	112 (59.0%)	292 (51.2%)	0.065	0.73	0.53 – 1.02
	Genotype					
	AA	16 (16.8%)	61 (21.4%)	0.338		
	AG	46 (48.4%)	156 (54.7%)	0.285		
	GG	33 (34.7%)	68 (23.9%)	0.038*	1.70	1.03 – 2.81
SNP 20	Allele					
	A	170 (89.5%)	522 (91.6%)			
	C	20 (10.5%)	48 (8.4%)	0.379		
	Genotype					
	AA	76 (80.0%)	241 (84.6%)	0.301		
	AC	18 (18.9%)	40 (14.0%)	0.249		
	CC	1 (1.1%)	4 (1.4%)	1.000		

Table E4 | Allele and genotype frequency distribution VGGL4; PPMS vs RRMS

		PPMS (n = 95)	RRMS (n = 192)	p-value	Odds ratio	95% CI
SNP 24	Allele					
	A	27 (14.4%)	42 (11.0%)			
	G	161 (85.6%)	340 (89.0%)	0.247		
	Genotype					
	AA	1 (1.1%)	2 (1.0%)	1.000		
	AG	25 (26.6%)	38 (19.9%)	0.200		
	GG	68 (72.3%)	151 (79.1%)	0.206		
SNP 9	Allele					
	A	78 (41.0%)	186 (48.4%)			
	G	112 (59.0%)	198 (51.6%)	0.095	0.74	0.52 – 1.05
	Genotype					
	AA	16 (16.8%)	52 (27.1%)	0.055	0.55	0.29 – 1.02
	AG	46 (48.4%)	82 (42.7%)	0.360		
	GG	33 (34.7%)	58 (30.2%)	0.438		
SNP 20	Allele					
	A	170 (89.5%)	347 (90.4%)	0.737		
	C	20 (10.5%)	37 (9.6%)			
	Genotype					
	AA	76 (80.0%)	156 (81.3%)	0.800		
	AC	18 (18.9%)	35 (18.2%)	0.883		
	CC	1 (1.1%)	1 (0.5%)	0.553		

Table E5 | Allele and genotype frequency distribution PRF1; MS vs. Controls

		MS patients (n = 287)	Controls (n = 285)	p-value	Odds ratio	95% CI
SNP 16	Allele					
	A	320 (56.1%)	348 (61.1%)			
	G	250 (43.9%)	222 (38.9%)	0.092	0.82	0.65 – 1.03
	Genotype					
	AA	95 (33.3%)	110 (38.6%)	0.190		
	AG	130 (45.6%)	128 (44.9%)	0.866		
SNP 1	Allele					
	A	213 (37.2%)	179 (31.4%)			
	G	359 (62.8%)	391 (68.6%)	0.038	1.30	1.01 – 1.66
	Genotype					
	AA	40 (14.0%)	31 (10.9%)	0.260		
	AG	133 (46.5%)	117 (41.1%)	0.189		
	GG	113 (39.5%)	137 (48.1%)	0.039	0.71	0.51 – 0.98

Table E6 | Allele and genotype frequency distribution PRF1; RRMS vs Controls

		RRMS (n = 192)	Controls (n = 285)	p-value	Odds ratio	95% CI
SNP 16	Allele					
	A	212 (55.2%)	348 (61.1%)			
	G	172 (44.8%)	222 (38.9%)	0.072	0.79	0.61 – 1.02
	Genotype					
	AA	61 (31.8%)	110 (38.6%)	0.127		
	AG	90 (46.9%)	128 (44.9%)	0.673		
SNP 1	Allele					
	A	145 (37.8%)	179 (31.4%)			
	G	239 (62.2%)	391 (68.6%)	0.042*	1.33	1.01 – 1.74
	Genotype					
	AA	28 (14.6%)	31 (10.9%)	0.228		
	AG	89 (46.4%)	117 (41.1%)	0.252		
	GG	75 (39.1%)	137 (48.1%)	0.052	0.69	0.48 – 1.00

Table E7 | Allele and genotype frequency distribution PRF1; PPMS vs Controls

		PPMS (n = 95)	Controls (n = 285)	p-value	Odds ratio	95% CI
SNP 16	Allele					
	A	108 (58.1%)	348 (61.1%)			
	G	78 (41.9%)	222 (38.9%)	0.470		
	Genotype					
	AA	34 (36.6%)	110 (38.6%)	0.725		
	AG	40 (43.0%)	128 (44.9%)	0.749		
SNP 1	Allele					
	A	68 (36.2%)	179 (31.4%)			
	G	120 (63.8%)	391 (68.6%)	0.227		
	Genotype					
	AA	12 (12.8%)	31 (10.9%)	0.617		
	AG	44 (46.8%)	117 (41.1%)	0.328		
	GG	38 (40.4%)	137 (48.1%)	0.197		

Table E8 | Allele and genotype frequency distribution PRF1; PPMS vs RRMS

		PPMS (n = 95)	RRMS (n = 192)	p-value	Odds ratio	95% CI
SNP 16	Allele					
	A	108 (58.1%)	212 (55.2%)	0.519		
	G	78 (41.9%)	172 (44.8%)			
	Genotype					
	AA	34 (36.6%)	61 (31.8%)	0.421		
	AG	40 (43.0%)	90 (46.9%)	0.539		
SNP 1	Allele					
	A	68 (36.2%)	145 (37.8%)	0.712		
	G	120 (63.8%)	239 (62.2%)			
	Genotype					
	AA	12 (12.8%)	28 (14.6%)	0.677		
	AG	44 (46.8%)	89 (46.4%)	0.942		
	GG	38 (40.4%)	75 (39.1%)	0.825		

Table E9 | Allele and genotype frequency distribution ADAMTS14; MS vs. Controls

		MS patients (n = 287)	Controls (n = 285)	p-value	Odds ratio	95% CI
SNP 6	Allele					
	C	152 (26.6%)	127 (22.3%)	0.091	1.26	0.96 – 1.66
	T	420 (73.4%)	443 (77.7%)			
	Genotype					
	CC	19 (6.6%)	14 (4.9%)	0.375		
	CT	114 (39.9%)	99 (34.7%)	0.206		
SNP 19 ^a	Allele					
	A	206 (36.5%)	194 (34.5%)	0.482	0.76	0.54 – 1.05
	G	358 (63.5%)	368 (65.5%)			
	Genotype					
	AA	61 (21.6%)	54 (19.2%)	0.477		
	AG	84 (29.8%)	86 (30.6%)	0.833		
SNP 8 ^a	Allele					
	C	208 (36.2%)	218 (38.3%)	0.482	0.71	0.51 – 1.00
	G	366 (63.8%)	352 (61.8%)			
	Genotype					
	CC	28 (9.8%)	50 (17.5%)	0.007	0.51	0.31 – 0.83
	CG	152 (53.0%)	118 (41.4%)	0.006	1.59	1.15 – 2.22
SNP 23	Allele					
	A	69 (12.1%)	92 (16.2%)	0.048	0.71	0.51 – 1.00
	G	501 (87.9%)	476 (83.8%)			
	Genotype					
	AA	4 (1.4%)	8 (2.8%)	0.241		
	AG	61 (21.4%)	76 (26.8%)	0.135		
SNP 10	Allele					
	A	148 (25.8%)	134 (23.6%)	0.066	1.42	0.98 – 2.07
	G	426 (74.2%)	434 (76.4%)			
	Genotype					
	AA	17 (5.9%)	15 (5.3%)	0.739		
	AG	114 (39.7%)	104 (36.6%)	0.446		
SNP 21	Allele					
	C	530 (92.7%)	500 (88.0%)	0.008	1.72	1.15 – 2.57
	T	42 (7.3%)	68 (12.0%)			
	Genotype					
	CC	246 (86.0%)	221 (77.8%)	0.011	1.75	1.13 – 2.71
	CT	38 (13.3%)	58 (20.4%)	0.023	0.60	0.38 – 0.93
SNP 12	Allele					
	A	295 (51.9%)	303 (53.5%)	0.590		
	G	273 (48.1%)	263 (46.5%)			
	Genotype					
	AA	71 (25.0%)	79 (27.9%)	0.431		
	AG	153 (53.9%)	145 (51.2%)	0.530		
	GG	60 (21.1%)	59 (20.8%)	0.935		

SNP 22	Allele					
	A	229 (40.2%)	214 (37.5%)	0.362		
Genotype	T	341 (59.8%)	356 (62.5%)			
	AA	40 (14.0%)	45 (15.8%)	0.557		
Genotype	AT	149 (52.3%)	124 (43.5%)	0.036	1.42	1.02 – 1.98
	TT	96 (33.7%)	116 (40.7%)	0.083	0.74	0.53 – 1.04

Table E10 | Allele and genotype frequency distribution ADAMTS14; RRMS vs Controls

		RRMS (n = 192)	Controls (n = 285)	p-value	Odds ratio	95% CI
SNP 6	Allele					
	C	103 (26.8%)	127 (22.3%)	0.108		
Genotype	T	281 (73.2%)	443 (77.7%)			
	CC	15 (7.8%)	14 (4.9%)	0.194		
SNP 19 ^a	Allele					
	A	122 (32.3%)	194 (34.5%)	0.475		
Genotype	G	256 (67.7%)	368 (65.5%)			
	AA	34 (18.0%)	54 (19.2%)	0.738		
SNP 8 ^a	Allele					
	C	135 (35.2%)	218 (38.3%)	0.332		
Genotype	G	249 (64.8%)	352 (61.8%)			
	CC	19 (9.9%)	50 (17.5%)	0.020*	0.52	0.29 – 0.91
SNP 23	Allele					
	A	46 (12.0%)	92 (16.2%)	0.075	0.71	0.48 – 1.04
Genotype	G	336 (88.0%)	476 (83.8%)			
	AA	3 (1.6%)	8 (2.8%)	0.376		
SNP 10	Allele					
	A	105 (27.3%)	134 (23.6%)	0.190		
Genotype	G	279 (72.7%)	434 (76.4%)			
	AA	11 (5.7%)	15 (5.3%)	0.833		
SNP 21	Allele					
	C	357 (93.5%)	500 (88.0%)	0.006*	1.94	1.20 – 3.13
Genotype	T	25 (6.5%)	68 (12.0%)			
	CC	167 (87.4%)	221 (77.8%)	0.008*	1.98	1.19 – 3.31
SNP 12	Allele					
	A	194 (50.5%)	303 (53.5%)	0.362		
Genotype	G	190 (49.5%)	263 (46.5%)			
	AA	45 (23.4%)	79 (27.9%)	0.276		
SNP 22	Allele					
	A	147 (38.7%)	214 (37.5%)	0.723		
Genotype	T	233 (61.3%)	356 (62.5%)			
	AA	24 (12.6%)	45 (15.8%)	0.339		
	AT	99 (52.1%)	124 (43.5%)	0.066	1.41	0.98 – 2.04
	TT	67 (35.3%)	116 (40.7%)	0.233		

Table E11 | Allele and genotype frequency distribution ADAMTS14; PPMS vs Controls

		PPMS (n = 95)	Controls (n = 285)	p-value	Odds ratio	95% CI
SNP 6	Allele					
	C	49 (26.1%)	127 (22.3%)	0.287		
	T	139 (73.9%)	443 (77.7%)			
	Genotype					
	CC	4 (4.3%)	14 (4.9%)	0.795		
	CT	41 (43.6%)	99 (34.7%)	0.122		
	TT	49 (52.1%)	172 (60.4%)	0.161		
SNP 19 ^a	Allele					
	A	84 (45.2%)	194 (34.5%)	0.009*	1.56	1.12 – 2.19
	G	102 (54.8%)	368 (65.5%)			
	Genotype					
	AA	27 (29.0%)	54 (19.2%)	0.046*	1.72	1.01 – 2.94
	AG	30 (32.3%)	86 (30.6%)	0.765		
	GG	36 (38.7%)	141 (50.2%)	0.055	0.63	0.39 – 1.01
SNP 8 ^a	Allele					
	C	73 (38.4%)	218 (38.3%)	0.966		
	G	117 (61.6%)	352 (61.8%)			
	Genotype					
	CC	9 (9.5%)	50 (17.5%)	0.060	0.49	0.23 – 1.04
	CG	55 (57.9%)	118 (41.4%)	0.005	1.95	1.22 – 3.12
	GG	31 (32.6%)	117 (41.1%)	0.145		
SNP 23	Allele					
	A	23 (12.2%)	92 (16.2%)	0.190		
	G	165 (87.8%)	476 (83.8%)			
	Genotype					
	AA	1 (1.1%)	8 (2.8%)	0.334		
	AG	21 (22.3%)	76 (26.8%)	0.395		
	GG	72 (76.6%)	200 (70.4%)	0.248		
SNP 10	Allele					
	A	43 (22.6%)	134 (23.6%)	0.787		
	G	147 (77.4%)	434 (76.4%)			
	Genotype					
	AA	6 (6.3%)	15 (5.3%)	0.703		
	AG	31 (32.6%)	104 (36.6%)	0.482		
	GG	58 (61.1%)	165 (58.1%)	0.613		
SNP 21	Allele					
	C	173 (91.1%)	500 (88.0%)	0.253		
	T	17 (8.9%)	68 (12.0%)			
	Genotype					
	CC	79 (83.2%)	221 (77.8%)	0.267		
	CT	15 (15.8%)	58 (20.4%)	0.322		
	TT	1 (1.1%)	5 (1.8%)	0.632		
SNP 12	Allele					
	A	101 (54.9%)	303 (53.5%)	0.748		
	G	83 (45.1%)	263 (46.5%)			
	Genotype					
	AA	26 (28.3%)	79 (27.9%)	0.949		
	AG	49 (53.3%)	145 (51.2%)	0.736		
	GG	17 (18.5%)	59 (20.8%)	0.623		
SNP 22	Allele					
	A	82 (43.2%)	214 (37.5%)	0.169		
	T	108 (56.8%)	356 (62.5%)			
	Genotype					
	AA	16 (16.8%)	45 (15.8%)	0.809		
	AT	50 (52.6%)	124 (43.5%)	0.122		
	TT	29 (30.5%)	116 (40.7%)	0.077	0.64	0.39 – 1.05

Table E12 | Allele and genotype frequency distribution ADAMTS14; PPMS vs RRMS.

		PPMS (n = 95)	RRMS (n = 192)	p-value	Odds ratio	95% CI
SNP 6	Allele					
	C	49 (26.1%)	103 (26.8%)			
	T	139 (73.9%)	281 (73.2%)	0.847		
	Genotype					
	CC	4 (4.3%)	15 (7.8%)	0.319		
	CT	41 (43.6%)	73 (38.0%)	0.364		
	TT	49 (52.1%)	104 (54.2%)	0.745		
SNP 19 ^a	Allele					
	A	84 (45.2%)	122 (32.3%)			
	G	102 (54.8%)	256 (67.7%)	0.003	1.73	1.21 – 2.48
	Genotype					
	AA	27 (29.0%)	34 (18.0%)	0.034*	1.87	1.04 – 3.34
	AG	30 (32.3%)	54 (28.6%)	0.525		
	GG	36 (38.7%)	101 (53.4%)	0.020*	0.55	0.33 – 0.91
SNP 8 ^a	Allele					
	C	73 (38.4%)	135 (35.2%)			
	G	117 (61.6%)	249 (64.8%)	0.444		
	Genotype					
	CC	9 (9.5%)	19 (9.9%)	1.000		
	CG	55 (57.9%)	97 (50.5%)	0.239		
	GG	31 (32.6%)	76 (39.6%)	0.252		
SNP 23	Allele					
	A	23 (12.2%)	46 (12.0%)			
	G	165 (87.8%)	336 (88.0%)	0.947		
	Genotype					
	AA	1 (1.1%)	3 (1.6%)	1.000		
	AG	21 (22.3%)	40 (20.9%)	0.787		
	GG	72 (76.6%)	148 (77.5%)	0.866		
SNP 10	Allele					
	A	43 (22.6%)	105 (27.3%)			
	G	147 (77.4%)	279 (72.7%)	0.225		
	Genotype					
	AA	6 (6.3%)	11 (5.7%)	0.797		
	AG	31 (32.6%)	83 (43.2%)	0.084	0.64	0.38 – 1.07
	GG	58 (61.1%)	98 (51.0%)	0.109		
SNP 21	Allele					
	C	173 (91.1%)	357 (93.5%)			
	T	17 (8.9%)	25 (6.5%)	0.299		
	Genotype					
	CC	79 (83.2%)	167 (87.4%)	0.326		
	CT	15 (15.8%)	23 (12.0%)	0.460		
	TT	1 (1.1%)	1 (0.5%)	1.000		
SNP 12	Allele					
	A	101 (54.9%)	194 (50.5%)			
	G	83 (45.1%)	190 (49.5%)	0.329		
	Genotype					
	AA	26 (28.3%)	45 (23.4%)	0.380		
	AG	49 (53.3%)	104 (54.2%)	0.886		
	GG	17 (18.5%)	43 (22.4%)	0.449		
SNP 22	Allele					
	A	82 (43.2%)	147 (38.7%)			
	T	108 (56.8%)	233 (61.3%)	0.304		
	Genotype					
	AA	16 (16.8%)	24 (12.6%)	0.335		
	AT	50 (52.6%)	99 (52.1%)	0.933		
	TT	29 (30.5%)	67 (35.3%)	0.425		

Table E13 | Allele and genotype frequency distribution C10orf27; MS vs. Controls

		MS patients (n = 287)	Controls (n = 285)	p-value	Odds ratio	95% CI	
SNP 13	Allele						
		A 439 (76.8%)	384 (67.4%)				
	Genotype	G 133 (23.2%)	186 (32.6%)	0.0004	1.60	1.23 – 2.08	
		AA 170 (59.4%)	127 (44.6%)	0.0004	1.82	1.31 – 2.54	
		AG 99 (34.6%)	130 (45.6%)	0.007*	0.63	0.45 – 0.88	
	Allele	GG 17 (5.9%)	28 (9.8%)	0.085	0.58	0.31 – 1.09	
SNP 17		C 67 (11.7%)	75 (13.2%)				
		T 505 (88.3%)	495 (86.8%)	0.460			
Genotype	CC 0 (-)	4 (1.4%)		0.109			
	CT 67 (23.4%)	67 (23.5%)		0.982			
	TT 219 (76.6%)	214 (75.1%)		0.678			
Allele	A 191 (33.3%)	181 (31.8%)					
	C 383 (66.7%)	389 (68.2%)		0.583			
	AA 29 (10.1%)	31 (10.9%)		0.763			
SNP 18	Genotype	AC 133 (46.3%)	119 (41.8%)		0.269		
		CC 125 (43.6%)	135 (47.4%)		0.360		

Table E14 | Allele and genotype frequency distribution C10orf27; RRMS vs Controls

		RRMS (n = 192)	Controls (n = 285)	p-value	Odds ratio	95% CI
SNP 13	Allele					
		A 299 (77.9%)	384 (67.4%)			
	Genotype	G 85 (22.1%)	186 (32.6%)	0.0004	1.70	1.27 – 2.30
		AA 117 (60.9%)	127 (44.6%)	0.0005	1.94	1.34 – 2.82
		AG 65 (33.9%)	130 (45.6%)	0.010*	0.61	0.42 – 0.89
SNP 17	Allele	GG 10 (5.2%)	28 (9.8%)	0.068	0.50	0.24 – 1.06
		C 56 (14.6%)	75 (13.2%)			
		T 328 (85.4%)	495 (86.8%)	0.530		
	Genotype	CC 0 (-)	4 (1.4%)		0.152	
		CT 56 (29.2%)	67 (23.5%)		0.166	
		TT 136 (70.8%)	214 (75.1%)		0.303	
SNP 18	Allele					
		A 125 (32.6%)	181 (31.8%)			
		C 259 (67.4%)	389 (68.2%)		0.796	
	Genotype	AA 19 (9.9%)	31 (10.9%)		0.731	
		AC 87 (45.3%)	119 (41.8%)		0.442	
		CC 86 (44.8%)	135 (47.4%)		0.580	

Table E15 | Allele and genotype frequency distribution C10orf27; PPMS vs Controls

		PPMS (n = 95)	Controls (n = 285)	p-value	Odds ratio	95% CI
SNP 13	Allele					
	A	140 (74.5%)	384 (67.4%)			
	G	48 (25.5%)	186 (32.6%)	0.068	1.41	0.97 – 2.05
	Genotype					
	AA	53 (56.4%)	127 (44.6%)	0.047*	1.61	1.01 – 2.57
	AG	34 (36.2%)	130 (45.6%)	0.109		
SNP 17	Allele					
	C	11 (5.9%)	75 (13.2%)			
	T	177 (94.1%)	495 (86.8%)	0.005	0.41	0.21 – 0.79
	Genotype					
	CC	0 (-)	4 (1.4%)	0.576		
	CT	11 (11.7%)	67 (23.5%)	0.014*	0.43	0.22 – 0.86
SNP 18	Allele					
	A	66 (34.7%)	181 (31.8%)			
	C	124 (65.3%)	389 (68.2%)	0.447		
	Genotype					
	AA	10 (10.5%)	31 (10.9%)	0.924		
	AC	46 (48.4%)	119 (41.8%)	0.256		
	CC	39 (41.1%)	135 (47.4%)	0.285		

Table E16 | Allele and genotype frequency distribution C10orf27; PPMS vs RRMS

		PPMS (n = 95)	RRMS (n = 192)	p-value	Odds ratio	95% CI
SNP 13	Allele					
	A	140 (74.5%)	299 (77.9%)			
	G	48 (25.5%)	85 (22.1%)	0.366		
	Genotype					
	AA	53 (56.4%)	117 (60.9%)	0.461		
	AG	34 (36.2%)	65 (33.9%)	0.699		
SNP 17	Allele					
	C	11 (5.9%)	56 (14.6%)			
	T	177 (94.1%)	328 (85.4%)	0.002	0.37	0.19 – 0.71
	Genotype					
	CC	0 (-)	0 (-)			
	CT	11 (11.7%)	56 (29.2%)	0.001	0.32	0.16 – 0.65
SNP 18	Allele					
	A	66 (34.7%)	125 (32.6%)			
	C	124 (65.3%)	259 (67.4%)	0.601		
	Genotype					
	AA	10 (10.5%)	19 (9.9%)	0.868		
	AC	46 (48.4%)	87 (45.3%)	0.619		
	CC	39 (41.1%)	86 (44.8%)	0.548		

Appendix F – Haplotype and haplotype pair frequency distributions and corresponding statistics

Chi-square-test: no Yates correction; P-value estimation: 2-tail, 1 degree of freedom; OR = odds ratio; 95% CI = 95% confidence interval; MAF = Minor Allele frequency.

1) VGLL-4

SNP #24: A/G; MAF(A) = 0.12

SNP #9: A/G; MAF(A) = 0.47

SNP #20: A/C; MAF(C) = 0.09

Haplotype frequencies VGLL-4

#	Haplotype	MS (n)	%	HC (n)	%	RRMS (n)	%	PPMS (n)	%
H1	GAA	261	45.8	277	48.8	183	47.9	78	41.5
H2	GGA	183	32.1	175	30.8	120	31.4	63	33.5
H3	AGA	68	11.9	68	12.0	41	10.7	27	14.4
H4	GGC	56	9.8	47	8.3	36	9.4	20	10.6
H5	GAC	1	0.2	1	0.2	1	0.3	0	–
H6	AAA	1	0.2	0	–	1	0.3	0	–
Σ		570		568		382		188	

Haplotype frequency comparison VGLL-4

#	Haplotype	Groups	P	OR	95% CI
H1	GAA	MS	HC	0.314	
		RR	HC	0.794	
		PP	HC	0.083	0.75 0.53 - 1.04
		PP	RR	0.148	
H2	GGA	MS	HC	0.638	
		RR	HC	0.844	
		PP	HC	0.490	
		PP	RR	0.614	
H3	AGA	MS	HC	0.983	
		RR	HC	0.557	
		PP	HC	0.392	
		PP	RR	0.209	
H4	GGC	MS	HC	0.362	
		RR	HC	0.538	
		PP	HC	0.374	
		PP	RR	0.647	
H5	GAC	MS	HC	1.000	
		RR	HC	1.000	
		PP	HC	1.000	
		PP	RR	1.000	
H6	AAA	MS	HC	1.000	
		RR	HC	0.402	
		PP	RR	1.000	

2) *PRF1*

SNP#16: A/G; MAF(G) = 0.41

SNP#1: A/G; MAF(A) = 0.34

Haplotype frequencies *PRF1*

#	Haplotype	MS (n)	%	HC (n)	%	RRMS (n)	%	PPMS (n)	%
H1	AG	320	56.1	347	60.9	212	55.2	108	58.1
H2	GA	213	37.4	178	31.2	145	37.8	68	36.6
H3	GG	37	6.5	44	7.7	27	7.0	10	5.4
H4	AA	0	-	1	0.2	0	-	0	-
Σ		570		570		384		186	

Haplotype frequency comparisons *PRF1*

#	Haplotype	Groups		P	OR	95% CI
H1	AG	MS	HC	0.105		
		RR	HC	0.081	0.79	0.61 - 1.03
		PP	HC	0.496		
		PP	RR	0.519		
H2	GA	MS	HC	0.029	1.31	1.03 - 1.68
		RR	HC	0.037	1.34	1.02 - 1.75
		PP	HC	0.178		
		PP	RR	0.781		
H3	GG	MS	HC	0.420		
		RR	HC	0.691		
		PP	HC	0.328		
		PP	RR	0.587		
H4	AA	MS	HC	1.000		
		RR	HC	1.000		
		PP	HC	1.000		

Haplotype pair frequencies *PRF1*

HapPair	MS (n)	%	HC (n)	%	RRMS (n)	%	PPMS (n)	%
1/1	95	33.3	109	38.2	61	31.8	34	36.6
1/2	113	39.6	102	35.8	76	39.6	37	39.8
1/3	17	6.0	26	9.1	14	7.3	3	3.2
1/4	0	-	1	0.4	0	-	0	-
2/2	40	14.0	31	10.9	28	14.6	12	12.9
2/3	20	7.0	14	4.9	13	6.8	7	7.5
3/3	0	-	2	0.7	0	-	0	-
Σ	285		285		192		93	

Haplotype pair frequency comparisons *PRF1*

HapPair	MS	%	HC	%	P	OR	95% CI
1/1	95	33.3	109	38.2	0.221		
1/2	113	39.6	102	35.8	0.342		
1/3	17	6.0	26	9.1	0.154		
1/4	0	–	1	0.4	1.000		
2/2	40	14.0	31	10.9	0.254		
2/3	20	7.0	14	4.9	0.289		
3/3	0	–	2	0.7	0.499		
Σ	285		285				

HapPair	RRMS	%	HC	%	P	OR	95% CI
1/1	61	31.8	109	38.2	0.148		
1/2	76	39.6	102	35.8	0.401		
1/3	14	7.3	26	9.1	0.479		
1/4	0	–	1	0.4	1.000		
2/2	28	14.6	31	10.9	0.228		
2/3	13	6.8	14	4.9	0.389		
3/3	0	–	2	0.7	0.518		
Σ	192		285				

HapPair	PPMS	%	HC	%	P	OR	95% CI
1/1	34	36.6	109	38.2	0.771		
1/2	37	39.8	102	35.8	0.488		
1/3	3	3.2	26	9.1	0.073	0.33	0.10 - 1.12
1/4	0	–	1	0.4	1.000		
2/2	12	12.9	31	10.9	0.577		
2/3	7	7.5	14	4.9	0.433		
3/3	0	–	2	0.7	1.000		
Σ	93		285				

HapPair	PPMS	%	RRMS	%	P	OR	95% CI
1/1	34	36.6	61	31.8	0.421		
1/2	37	39.8	76	39.6	0.974		
1/3	3	3.2	14	7.3	0.285		
2/2	12	12.9	28	14.6	0.856		
2/3	7	7.5	13	6.8	0.808		
Σ	93		192				

3a) ADAMTS14

SNP#19: A/G; MAF(A) = 0.36

SNP#8: C/G; MAF(C) = 0.37

SNP#23: A/G; MAF(A) = 0.14

SNP#21: C/T; MAF(T) = 0.10

SNP#22: A/T; MAF(A) = 0.39

Haplotype frequencies ADAMTS14

#	Haplotype	MS	%	HC	%	RRMS	%	PPMS	%
H1	GGGCT	145	29.5	144	29.0	108	32.5	37	23.1
H2	ACGCA	118	24.0	121	24.4	77	23.2	41	25.6
H3	GGGCA	52	10.6	45	9.1	35	10.5	17	10.6
H4	GCGCT	29	5.9	33	6.7	25	7.5	4	2.5
H5	GGACT	28	5.7	32	6.5	21	6.3	7	4.4
H6	ACGCT	30	6.1	30	6.0	14	4.2	16	10.0
H7	AGGCT	40	8.1	26	5.2	23	6.9	17	10.6
H8	GGATT	12	2.4	26	5.2	7	2.1	5	3.1
H9	GCGTT	8	1.6	15	3.0	5	1.5	3	1.9
H10	GGATA	2	0.4	6	1.2	0	–	2	1.3
H11	AGGCA	14	2.8	5	1.0	8	2.4	6	3.8
H12	GGACA	6	1.2	5	1.0	4	1.2	2	1.3
H13	GCGCA	1	0.2	4	0.8	1	0.3	0	–
H14	GGGTT	6	1.2	4	0.8	4	1.2	2	1.3
H15	ACATT	1	0.2	0	–	0	–	1	0.6
Σ		492		496		332		160	

Haplotype frequency comparisons ADAMTS14

#	Haplotype	Groups		P	OR	95%CI
H1	GGGCT	MS	HC	0.879		
		RR	HC	0.284		
		PP	HC	0.146		
		PP	RR	0.032	0.62	0.41 - 0.96
H2	ACGCA	MS	HC	0.880		
		RR	HC	0.691		
		PP	HC	0.754		
		PP	RR	0.554		
H3	GGGCA	MS	HC	0.429		
		RR	HC	0.483		
		PP	HC	0.538		
		PP	RR	0.978		
H4	GCGCT	MS	HC	0.623		
		RR	HC	0.628		
		PP	HC	0.049	0.36	0.13 - 1.03
		PP	RR	0.025	0.31	0.11 - 0.92

H5	GGACT	MS	HC	0.617		
		RR	HC	0.942		
		PP	HC	0.442		
		PP	RR	0.533		
H6	ACGCT	MS	HC	0.974		
		RR	HC	0.250		
		PP	HC	0.108		
		PP	RR	0.012	2.52	1.20 - 5.31
H7	AGGCT	MS	HC	0.069	1.60	0.96 - 2.67
		RR	HC	0.314		
		PP	HC	0.026	2.15	1.13 - 4.07
		PP	RR	0.160		
H8	GGATT	MS	HC	0.022	0.45	0.22 - 0.91
		RR	HC	0.029	0.39	0.17 - 0.91
		PP	HC	0.391		
		PP	RR	0.538		
H9	GCGTT	MS	HC	0.205		
		RR	HC	0.247		
		PP	HC	0.583		
		PP	RR	0.719		
H10	GGATA	MS	HC	0.287		
		RR	HC	0.087	0.11	0.01 - 2.02
		PP	HC	1.000		
		PP	RR	0.105		
H11	AGGCA	MS	HC	0.039	2.88	1.03 - 8.05
		RR	HC	0.153		
		PP	HC	0.029	3.83	1.15 - 12.7
		PP	RR	0.399		
H12	GGACA	MS	HC	0.772		
		RR	HC	1.000		
		PP	HC	0.680		
		PP	RR	1.000		
H13	GCGCA	MS	HC	0.374		
		RR	HC	0.653		
		PP	HC	0.577		
		PP	RR	1.000		
H14	GGGTT	MS	HC	0.545		
		RR	HC	0.720		
		PP	HC	0.637		
		PP	RR	1.000		
H15	ACATT	MS	HC	0.498		
		RR	HC			
		PP	HC	0.244		
		PP	RR	0.325		

Haplotype pair frequencies ADAMTS14

HapPair	MS (n)	%	HC (n)	%	RRMS (n)	%	PPMS (n)	%
1/1	22	8.9	27	10.9	16	9.6	6	7.5
1/2	24	9.8	22	8.9	18	10.8	6	7.5
1/3	25	10.2	20	8.1	19	11.4	6	7.5
1/4	17	6.9	10	4.0	15	9.0	2	2.5
1/5	11	4.5	13	5.2	9	5.4	2	2.5
1/6	10	4.1	4	1.6	6	3.6	4	5.0
1/7	4	1.6	3	1.2	3	1.8	1	1.3
1/8	5	2.0	10	4.0	2	1.2	3	3.8
1/9	1	0.4	5	2.0	1	0.6	0	-
1/14	4	1.6	3	1.2	3	1.8	1	1.3
2/2	6	2.4	14	5.6	6	3.6	0	-
2/3	9	3.7	8	3.2	5	3.0	4	5.0
2/4	8	3.3	8	3.2	6	3.6	2	2.5
2/5	11	4.5	10	4.0	6	3.6	5	6.3
2/6	6	2.4	11	4.4	3	1.8	3	3.8
2/7	23	9.3	11	4.4	14	8.4	9	11.3
2/8	6	2.4	8	3.2	5	3.0	1	1.3
2/9	3	1.2	2	0.8	1	0.6	2	2.5
2/10	2	0.8	1	0.4	0	-	2	2.5
2/11	11	4.5	5	2.0	5	3.0	6	7.5
2/12	3	1.2	4	1.6	2	1.2	1	1.3
2/13	0	0.0	3	1.2	0	-	0	-
3/3	5	2.0	6	2.4	3	1.8	2	2.5
3/9	3	1.2	2	0.8	2	1.2	1	1.3
3/10	0	0.0	2	0.8	0	-	0	-
3/12	2	0.8	0	-	1	0.6	1	1.3
3/13	1	0.4	0	-	1	0.6	1	1.3
3/14	2	0.8	1	0.4	1	0.6	0	-
4/4	1	0.4	3	1.2	1	0.6	0	-
4/5	1	0.4	4	1.6	1	0.6	0	-
4/6	1	0.4	3	1.2	1	0.6	0	-
4/9	0	0.0	2	0.8	0	-	0	-
5/5	2	0.8	0	-	2	1.2	0	-
5/6	0	0.0	2	0.8	0	-	0	-
5/8	0	0.0	2	0.8	0	-	0	-
5/12	1	0.4	1	0.4	1	0.6	0	-
6/6	2	0.8	1	0.4	0	-	2	2.5
6/7	8	3.3	7	2.8	3	1.8	5	6.3
6/9	1	0.4	1	0.4	1	0.6	0	-
7/7	2	0.8	2	0.8	1	0.6	1	1.3
7/8	0	0.0	1	0.4	0	-	0	-
7/11	1	0.4	0	-	1	0.6	0	-
8/8	0	0.0	1	0.4	0	-	0	-
8/9	0	0.0	2	0.8	0	-	0	-
8/10	0	0.0	1	0.4	0	-	0	-
8/15	1	0.4	0	-	0	-	1	1.3
9/13	0	0.0	1	0.4	0	-	0	-
10/10	0	0.0	1	0.4	0	-	0	-
11/11	1	0.4	0	-	1	0.6	0	-
Σ	246		248		166		80	

Haplotype pair frequency comparisons ADAMTS14; MS vs. HC

HapPair	MS	%	HC	%	P	OR	95%CI
1/1	22	8.9	27	10.9	0.470		
1/2	24	9.8	22	8.9	0.735		
1/3	25	10.2	20	8.1	0.418		
1/4	17	6.9	10	4.0	0.159		
1/5	11	4.5	13	5.2	0.691		
1/6	10	4.1	4	1.6	0.112		
1/7	4	1.6	3	1.2	0.724		
1/8	5	2.0	10	4.0	0.294		
1/9	1	0.4	5	2.0	0.216		
1/14	4	1.6	3	1.2	0.724		
2/2	6	2.4	14	5.6	0.108		
2/3	9	3.7	8	3.2	0.811		
2/4	8	3.3	8	3.2	1.000		
2/5	11	4.5	10	4.0	0.809		
2/6	6	2.4	11	4.4	0.324		
2/7	23	9.3	11	4.4	0.031	2.22	1.06 - 4.67
2/8	6	2.4	8	3.2	0.788		
2/9	3	1.2	2	0.8	0.685		
2/10	2	0.8	1	0.4	0.623		
2/11	11	4.5	5	2.0	0.136		
2/12	3	1.2	4	1.6	1.000		
2/13	0	0.0	3	1.2	0.249		
3/3	5	2.0	6	2.4	1.000		
3/9	3	1.2	2	0.8	0.685		
3/10	0	0.0	2	0.8	0.499		
3/12	2	0.8	0	-	0.248		
3/13	1	0.4	0	-	0.498		
3/14	2	0.8	1	0.4	0.623		
4/4	1	0.4	3	1.2	0.624		
4/5	1	0.4	4	1.6	0.373		
4/6	1	0.4	3	1.2	0.624		
4/9	0	0.0	2	0.8	0.499		
5/5	2	0.8	0	-	0.248		
5/6	0	0.0	2	0.8	0.499		
5/8	0	0.0	2	0.8	0.499		
5/12	1	0.4	1	0.4	1.000		
6/6	2	0.8	1	0.4	0.623		
6/7	8	3.3	7	2.8	0.800		
6/9	1	0.4	1	0.4	1.000		
7/7	2	0.8	2	0.8	1.000		
7/8	0	0.0	1	0.4	1.000		
7/11	1	0.4	0	-	0.498		
8/8	0	0.0	1	0.4	1.000		
8/9	0	0.0	2	0.8	0.499		
8/10	0	0.0	1	0.4	1.000		
8/15	1	0.4	0	-	0.498		
9/13	0	0.0	1	0.4	1.000		
10/10	0	0.0	1	0.4	1.000		
11/11	1	0.4	0	-	0.498		
Σ	246		248				

Haplotype pair frequency comparisons ADAMTS14; RRMS vs. HC

HapPair	RRMS	%	HC	%	P	OR	95%CI
1/1	16	9.6	27	10.9	0.683		
1/2	18	10.8	22	8.9	0.506		
1/3	19	11.4	20	8.1	0.248		
1/4	15	9.0	10	4.0	0.036	2.36	1.04 - 5.40
1/5	9	5.4	13	5.2	1.000		
1/6	6	3.6	4	1.6	0.209		
1/7	3	1.8	3	1.2	0.688		
1/8	2	1.2	10	4.0	0.135		
1/9	1	0.6	5	2.0	0.409		
1/14	3	1.8	3	1.2	0.688		
2/2	6	3.6	14	5.6	0.484		
2/3	5	3.0	8	3.2	1.000		
2/4	6	3.6	8	3.2	1.000		
2/5	6	3.6	10	4.0	1.000		
2/6	3	1.8	11	4.4	0.174		
2/7	14	8.4	11	4.4	0.094	1.98	0.88 - 4.49
2/8	5	3.0	8	3.2	1.000		
2/9	1	0.6	2	0.8	1.000		
2/10	0	-	1	0.4	1.000		
2/11	5	3.0	5	2.0	0.531		
2/12	2	1.2	4	1.6	1.000		
2/13	0	-	3	1.2	0.277		
3/3	3	1.8	6	2.4	0.746		
3/9	2	1.2	2	0.8	1.000		
3/10	0	-	2	0.8	0.519		
3/12	1	0.6	0	-	0.401		
3/13	1	0.6	0	-	0.401		
3/14	1	0.6	1	0.4	1.000		
4/4	1	0.6	3	1.2	0.652		
4/5	1	0.6	4	1.6	0.652		
4/6	1	0.6	3	1.2	0.652		
4/9	0	-	2	0.8	0.519		
5/5	2	1.2	0	-	0.160		
5/6	0	-	2	0.8	0.519		
5/8	0	-	2	0.8	0.519		
5/12	1	0.6	1	0.4	1.000		
6/6	0	-	1	0.4	1.000		
6/7	3	1.8	7	2.8	0.750		
6/9	1	0.6	1	0.4	1.000		
7/7	1	0.6	2	0.8	1.000		
7/8	0	-	1	0.4	1.000		
7/11	1	0.6	0	-	0.401		
8/8	0	-	1	0.4	1.000		
8/9	0	-	2	0.8	0.519		
8/10	0	-	1	0.4	1.000		
9/13	0	-	1	0.4	1.000		
10/10	0	-	1	0.4	1.000		
11/11	1	0.6	0	-	0.401		
Σ	166		248				

Haplotype pair frequency comparisons ADAMTS14; PPMS vs. HC

HapPair	PPMS	%	HC	%	P	OR	95%CI
1/1	6	7.5	27	10.9	0.522		
1/2	6	7.5	22	8.9	0.821		
1/3	6	7.5	20	8.1	1.000		
1/4	2	2.5	10	4.0	0.737		
1/5	2	2.5	13	5.2	0.537		
1/6	4	5.0	4	1.6	0.103		
1/7	1	1.3	3	1.2	1.000		
1/8	3	3.8	10	4.0	1.000		
1/9	0	-	5	2.0	0.340		
1/14	1	1.3	3	1.2	1.000		
2/2	0	-	14	5.6	0.026	0.10	0.01 - 1.70
2/3	4	5.0	8	3.2	0.496		
2/4	2	2.5	8	3.2	1.000		
2/5	5	6.3	10	4.0	0.374		
2/6	3	3.8	11	4.4	1.000		
2/7	9	11.3	11	4.4	0.055	2.73	1.09 - 6.86
2/8	1	1.3	8	3.2	0.694		
2/9	2	2.5	2	0.8	0.251		
2/10	2	2.5	1	0.4	0.149		
2/11	6	7.5	5	2.0	0.028	3.94	1.17 - 13.3
2/12	1	1.3	4	1.6	1.000		
2/13	0	-	3	1.2	1.000		
3/3	2	2.5	6	2.4	1.000		
3/9	1	1.3	2	0.8	0.569		
3/10	0	-	2	0.8	1.000		
3/12	1	1.3	0	-	0.244		
3/14	1	1.3	1	0.4	0.429		
4/4	0	-	3	1.2	1.000		
4/5	0	-	4	1.6	1.000		
4/6	0	-	3	1.2	1.000		
4/9	0	-	2	0.8	1.000		
5/6	0	-	2	0.8	1.000		
5/8	0	-	2	0.8	1.000		
5/12	0	-	1	0.4	1.000		
6/6	2	2.5	1	0.4	0.149		
6/7	5	6.3	7	2.8	0.174		
6/9	0	-	1	0.4	1.000		
7/7	1	1.3	2	0.8	0.569		
7/8	0	-	1	0.4	1.000		
8/8	0	-	1	0.4	1.000		
8/9	0	-	2	0.8	1.000		
8/10	0	-	1	0.4	1.000		
8/15	1	1.3	0	-	0.244		
9/13	0	-	1	0.4	1.000		
10/10	0	-	1	0.4	1.000		
Σ	80		248				

Haplotype pair frequency comparisons ADAMTS14; PPMS vs. RRMS

HapPair	PPMS	%	RRMS	%	P	OR	95%CI
1/1	6	7.5	16	9.6	0.643		
1/2	6	7.5	18	10.8	0.496		
1/3	6	7.5	19	11.4	0.378		
1/4	2	2.5	15	9.0	0.064	0.26	0.06 - 1.16
1/5	2	2.5	9	5.4	0.511		
1/6	4	5.0	6	3.6	0.732		
1/7	1	1.3	3	1.8	1.000		
1/8	3	3.8	2	1.2	0.333		
1/9	0	-	1	0.6	1.000		
1/14	1	1.3	3	1.8	1.000		
2/2	0	-	6	3.6	0.181		
2/3	4	5.0	5	3.0	0.477		
2/4	2	2.5	6	3.6	1.000		
2/5	5	6.3	6	3.6	0.344		
2/6	3	3.8	3	1.8	0.394		
2/7	9	11.3	14	8.4	0.489		
2/8	1	1.3	5	3.0	0.667		
2/9	2	2.5	1	0.6	0.248		
2/10	2	2.5	0	0.0	0.105		
2/11	6	7.5	5	3.0	0.184		
2/12	1	1.3	2	1.2	1.000		
3/3	2	2.5	3	1.8	0.661		
3/9	1	1.3	2	1.2	1.000		
3/12	1	1.3	1	0.6	0.546		
3/13	0	-	1	0.6	1.000		
3/14	1	1.3	1	0.6	0.546		
4/4	0	-	1	0.6	1.000		
4/5	0	-	1	0.6	1.000		
4/6	0	-	1	0.6	1.000		
5/5	0	-	2	1.2	1.000		
5/12	0	-	1	0.6	1.000		
6/6	2	2.5	0	0.0	0.105		
6/7	5	6.3	3	1.8	0.117		
6/9	0	-	1	0.6	1.000		
7/7	1	1.3	1	0.6	0.546		
7/11	0	-	1	0.6	1.000		
8/15	1	1.3	0	0.0	0.325		
11/11	0	-	1	0.6	1.000		
Σ	80		166				

3b) ADAMTS14

SNP#19: A/G; MAF(A) = 0.36

SNP#8: C/G; MAF(C) = 0.37

SNP#23: A/G; MAF(A) = 0.14

SNP#10: A/G; MAF(A) = 0.25

SNP#21: C/T; MAF(T) = 0.10

Haplotype frequencies *ADAMTS14*

#	Haplotype	MS	%	HC	%	RRMS	%	PPMS	%
H1	ACGGC	146	26.9	152	28.5	90	24.5	56	31.8
H2	GGGAC	145	26.7	127	23.8	102	27.7	43	24.4
H3	GGGGC	78	14.3	79	14.8	59	16.0	19	10.8
H4	GGAGC	45	8.2	45	8.4	32	8.7	13	7.4
H5	GCGGC	41	7.5	42	7.9	32	8.7	9	5.1
H6	GGAGT	17	3.1	39	7.3	10	2.7	7	4.0
H7	AGGGC	55	10.1	29	5.4	31	8.4	24	13.6
H8	GCGGT	8	1.5	12	2.2	6	1.6	2	1.1
H9	GGGGT	7	1.3	3	0.6	5	1.4	2	1.1
H10	AGGAC	1	0.2	4	0.7	1	0.3	0	–
H11	AGGGT	1	0.2	2	0.4	0	–	1	0.6
Σ		544		534		368		176	

Haplotype frequency comparisons *ADAMTS14*

#	Haplotype	Groups		P	OR	95% CI
H1	ACGGC	MS	HC	0.553		
		RR	HC	0.173		
		PP	HC	0.378		
		PP	RR	0.062	1.46	0.98 - 2.16
H2	GGGAC	MS	HC	0.249		
		RR	HC	0.145		
		PP	HC	0.899		
		PP	RR	0.343		
H3	GGGGC	MS	HC	0.832		
		RR	HC	0.595		
		PP	HC	0.209		
		PP	RR	0.094	0.63	0.36 - 1.09
H4	GGAGC	MS	HC	0.930		
		RR	HC	0.870		
		PP	HC	0.750		
		PP	RR	0.623		
H5	GCGGC	MS	HC	0.840		
		RR	HC	0.643		
		PP	HC	0.243		
		PP	RR	0.166		

H6	GGAGT	MS	HC	0.002	0.41	0.23 - 0.73
		RR	HC	0.003	0.36	0.18 - 0.72
		PP	HC	0.157		
		PP	RR	0.441		
H7	AGGGC	MS	HC	0.004	1.96	1.23 - 3.12
		RR	HC	0.074	1.61	0.95 - 2.72
		PP	HC	0.0004	2.73	1.54 - 4.82
		PP	RR	0.066	1.69	0.96 - 2.98
H8	GCGGT	MS	HC	0.375		
		RR	HC	0.632		
		PP	HC	0.535		
		PP	RR	1.000		
H9	GGGGT	MS	HC	0.342		
		RR	HC	0.282		
		PP	HC	0.603		
		PP	RR	1.000		
H10	AGGAC	MS	HC	0.214		
		RR	HC	0.654		
		PP	HC	0.577		
		PP	RR	1.000		
H11	AGGGT	MS	HC	0.621		
		RR	HC	0.517		
		PP	HC	1.000		
		PP	RR	0.326		

Haplotype pair frequencies ADAMTS14

HapPair	MS (n)	%	HC (n)	%	RRMS (n)	%	PPMS (n)	%
1/1	13	4.8	26	9.7	8	4.4	5	5.7
1/2	40	14.7	32	12.0	27	14.7	13	14.8
1/3	3	1.1	2	0.8	2	1.1	1	1.1
1/4	14	5.1	16	6.0	8	4.4	6	6.8
1/5	8	2.9	14	5.2	6	3.3	2	2.3
1/6	8	2.9	9	3.4	5	2.7	3	3.4
1/7	42	15.4	22	8.2	22	12.0	20	22.7
1/8	4	1.5	3	1.1	2	1.1	2	2.3
1/10	1	0.4	1	0.4	1	0.5	0	-
1/11	0	-	2	0.8	0	-	0	-
2/2	17	6.3	11	4.1	11	6.0	6	6.8
2/3	30	11.0	36	13.5	23	12.5	7	8.0
2/4	10	3.7	10	3.8	8	4.4	2	2.3
2/5	14	5.1	7	2.6	10	5.4	4	4.5
2/6	7	2.6	7	2.6	5	2.7	2	2.3
2/7	2	0.7	2	0.8	1	0.5	1	1.1
2/8	3	1.1	4	1.5	3	1.6	0	-
2/9	6	2.2	3	1.1	4	2.2	2	2.3
2/10	0	-	3	1.1	0	-	0	-
3/3	6	2.2	6	2.2	5	2.7	1	1.1
3/4	14	5.1	9	3.4	9	4.9	5	5.7
3/5	16	5.9	8	3.0	13	7.1	3	3.4

3/6	1	0.4	11	4.1	0	–	1	1.1
3/7	2	0.7	1	0.4	2	1.1	0	–
4/4	3	1.1	1	0.4	3	1.6	0	–
4/5	1	0.4	4	1.5	1	0.5	0	–
4/6	0	–	4	1.5	0	–	0	–
5/5	1	0.4	3	1.1	1	0.5	0	–
5/8	0	–	3	1.1	0	–	0	–
6/6	0	–	3	1.1	0	–	0	–
6/8	0	–	2	0.8	0	–	0	–
7/7	4	1.5	2	0.8	3	1.6	1	1.1
7/11	1	0.4	0	–	0	–	1	1.1
8/9	1	0.4	0	–	1	0.5	0	–
Σ	272		267		184		88	

Haplotype pair frequency comparisons ADAMTS14; MS vs. HC

HapPair	MS (n)	%	HC (n)	%	P	OR	95% CI
1/1	13	4.8	26	9.7	0.026	0.47	0.23 - 0.93
1/2	40	14.7	32	12.0	0.353		
1/3	3	1.1	2	0.8	1.000		
1/4	14	5.1	16	6.0	0.669		
1/5	8	2.9	14	5.2	0.197		
1/6	8	2.9	9	3.4	0.810		
1/7	42	15.4	22	8.2	0.010	2.01	1.21 - 3.49
1/8	4	1.5	3	1.1	1.000		
1/10	1	0.4	1	0.4	1.000		
1/11	0	–	2	0.8	0.245		
2/2	17	6.3	11	4.1	0.265		
2/3	30	11.0	36	13.5	0.385		
2/4	10	3.7	10	3.8	1.000		
2/5	14	5.1	7	2.6	0.181		
2/6	7	2.6	7	2.6	1.000		
2/7	2	0.7	2	0.8	1.000		
2/8	3	1.1	4	1.5	0.723		
2/9	6	2.2	3	1.1	0.504		
2/10	0	–	3	1.1	0.121		
3/3	6	2.2	6	2.2	1.000		
3/4	14	5.1	9	3.4	0.395		
3/5	16	5.9	8	3.0	0.143		
3/6	1	0.4	11	4.1	0.003	0.1	0.0 - 0.7
3/7	2	0.7	1	0.4	1.000		
4/4	3	1.1	1	0.4	0.624		
4/5	1	0.4	4	1.5	0.213		
4/6	0	–	4	1.5	0.060	0.1	0.0 - 2.0
5/5	1	0.4	3	1.1	0.369		
5/8	0	–	3	1.1	0.121		
6/6	0	–	3	1.1	0.121		
6/8	0	–	2	0.8	0.245		
7/7	4	1.5	2	0.8	0.686		
7/11	1	0.4	0	–	1.000		
8/9	1	0.4	0	–	1.000		
Σ	272		267				

Haplotype pair frequency comparisons *ADAMTS14*; RRMS vs. HC

HapPair	RRMS (n)	%	HC (n)	%	P	OR	95% CI
1/1	8	4.4	26	9.7	0.033	0.42	0.19 - 0.95
1/2	27	14.7	32	12.0	0.405		
1/3	2	1.1	2	0.8	1.000		
1/4	8	4.4	16	6.0	0.526		
1/5	6	3.3	14	5.2	0.360		
1/6	5	2.7	9	3.4	0.788		
1/7	22	12.0	22	8.2	0.191		
1/8	2	1.1	3	1.1	1.000		
1/10	1	0.5	1	0.4	1.000		
1/11	0	–	2	0.8	0.516		
2/2	11	6.0	11	4.1	0.382		
2/3	23	12.5	36	13.5	0.761		
2/4	8	4.4	10	3.8	0.809		
2/5	10	5.4	7	2.6	0.137		
2/6	5	2.7	7	2.6	1.000		
2/7	1	0.5	2	0.8	1.000		
2/8	3	1.6	4	1.5	1.000		
2/9	4	2.2	3	1.1	0.451		
2/10	0	–	3	1.1	0.274		
3/3	5	2.7	6	2.2	0.764		
3/4	9	4.9	9	3.4	0.468		
3/5	13	7.1	8	3.0	0.067	2.46	1.00 - 6.07
3/6	0	–	11	4.1	0.004	0.06	0.00 - 1.03
3/7	2	1.1	1	0.4	0.570		
4/4	3	1.6	1	0.4	0.309		
4/5	1	0.5	4	1.5	0.653		
4/6	0	–	4	1.5	0.149		
5/5	1	0.5	3	1.1	0.649		
5/8	0	–	3	1.1	0.274		
6/6	0	–	3	1.1	0.274		
6/8	0	–	2	0.8	0.516		
7/7	3	1.6	2	0.8	0.402		
8/9	1	0.5	0	–	0.408		
Σ	184		267				

Haplotype pair frequency comparisons *ADAMTS14*; PPMS vs. HC

HapPair	PPMS (n)	%	HC (n)	%	P	OR	95% CI
1/1	5	5.7	26	9.7	0.284		
1/2	13	14.8	32	12.0	0.467		
1/3	1	1.1	2	0.8	0.576		
1/4	6	6.8	16	6.0	0.800		
1/5	2	2.3	14	5.2	0.375		
1/6	3	3.4	9	3.4	1.000		
1/7	20	22.7	22	8.2	0.0009	3.28	1.69 - 6.35
1/8	2	2.3	3	1.1	0.601		
1/10	0	–	1	0.4	1.000		
1/11	0	–	2	0.8	1.000		
2/2	6	6.8	11	4.1	0.386		
2/3	7	8.0	36	13.5	0.191		
2/4	2	2.3	10	3.8	0.737		

2/5	4	4.6	7	2.6	0.476
2/6	2	2.3	7	2.6	1.000
2/7	1	1.1	2	0.8	0.576
2/8	0	–	4	1.5	0.576
2/9	2	2.3	3	1.1	0.601
2/10	0	–	3	1.1	1.000
3/3	1	1.1	6	2.2	1.000
3/4	5	5.7	9	3.4	0.348
3/5	3	3.4	8	3.0	0.737
3/6	1	1.1	11	4.1	0.307
3/7	0	–	1	0.4	1.000
4/4	0	–	1	0.4	1.000
4/5	0	–	4	1.5	0.576
4/6	0	–	4	1.5	0.576
5/5	0	–	3	1.1	1.000
5/8	0	–	3	1.1	1.000
6/6	0	–	3	1.1	1.000
6/8	0	–	2	0.8	1.000
7/7	1	1.1	2	0.8	0.576
7/11	1	1.1	0	–	0.248
Σ	88		267		

Haplotype pair frequency comparisons ADAMTS14; PPMS vs. RRMS

HapPair	PPMS (n)	%	RRMS (n)	%	P	OR	95% CI
1/1	5	5.7	8	4.4	0.762		
1/2	13	14.8	27	14.7	1.000		
1/3	1	1.1	2	1.1	1.000		
1/4	6	6.8	8	4.4	0.391		
1/5	2	2.3	6	3.3	1.000		
1/6	3	3.4	5	2.7	0.716		
1/7	20	22.7	22	12.0	0.022	2.17	1.11 - 4.23
1/8	2	2.3	2	1.1	0.597		
1/10	0	–	1	0.5	1.000		
2/2	6	6.8	11	6.0	0.793		
2/3	7	8.0	23	12.5	0.307		
2/4	2	2.3	8	4.4	0.508		
2/5	4	4.6	10	5.4	1.000		
2/6	2	2.3	5	2.7	1.000		
2/7	1	1.1	1	0.5	0.543		
2/8	0	–	3	1.6	0.553		
2/9	2	2.3	4	2.2	1.000		
3/3	1	1.1	5	2.7	0.668		
3/4	5	5.7	9	4.9	0.775		
3/5	3	3.4	13	7.1	0.282		
3/6	1	1.1	0	–	0.324		
3/7	0	–	2	1.1	1.000		
4/4	0	–	3	1.6	0.553		
4/5	0	–	1	0.5	1.000		
5/5	0	–	1	0.5	1.000		
7/7	1	1.1	3	1.6	1.000		
7/11	1	1.1	0	–	0.324		
8/9	0	–	1	0.5	1.000		
Σ	88		184				

4) C10orf27

SNP#13: A/G; MAF(G) = 0.28

SNP#17: C/T; MAF(C) = 0.13

SNP#18: A/C; MAF(A) = 0.33

Haplotype frequencies *C10orf27*

#	Haplotype	MS (n)	%	HC (n)	%	RRMS (n)	%	PPMS (n)	%
H1	ATC	215	41.3	200	38.6	144	42.4	71	39.4
H2	ATA	164	31.5	136	26.3	105	30.9	59	32.8
H3	GTC	94	18.1	130	25.1	53	15.6	41	22.8
H4	GCA	10	1.9	27	5.2	9	2.6	1	0.6
H5	ACC	32	6.2	21	4.1	26	7.6	6	3.3
H6	GTA	4	0.8	2	0.4	2	0.6	2	1.1
H7	GCC	0	–	2	0.4	0	–	0	–
H8	ACA	1	0.2	0	–	1	0.3	0	–
Σ		520		518		340		180	

Haplotype frequency comparisons *C10orf27*

#	Haplotype	Groups	P	OR	95% CI
H1	ATC	MS	HC	0.368	
		RR	HC	0.274	
		PP	HC	0.843	
		PP	RR	0.522	
H2	ATA	MS	HC	0.060	1.29
		RR	HC	0.140	0.99 - 1.69
		PP	HC	0.093	1.37
		PP	RR	0.658	0.95 - 1.98
H3	GTC	MS	HC	0.006	0.66
		RR	HC	0.0009	0.55
		PP	HC	0.533	0.49 - 0.89
		PP	RR	0.043	1.60
H4	GCA	MS	HC	0.004	0.36
		RR	HC	0.081	0.50
		PP	HC	0.003	0.10
		PP	RR	0.176	0.23 - 1.07
H5	ACC	MS	HC	0.124	
		RR	HC	0.024	1.96
		PP	HC	0.824	1.08 - 3.54
		PP	RR	0.056	0.42
H6	GTA	MS	HC	0.687	0.17 - 1.03
		RR	HC	0.651	
		PP	HC	0.275	
		PP	RR	0.612	

H7	GCC	MS	HC	0.249				
		RR	HC	0.521				
		PP	HC	1.000				
H8	ACA	MS	HC	1.000				
		RR	HC	0.396				
		PP	RR	1.000				

Haplotype pair frequencies *C10orf27*

HapPair	MS (n)	%	HC (n)	%	RRMS (n)	%	PPMS (n)	%
1/1	48	18.5	43	16.6	33	19.4	15	16.7
1/2	65	25.0	47	18.1	41	24.1	24	26.7
1/3	39	15.0	56	21.6	24	14.1	15	16.7
1/5	15	5.8	11	4.2	13	7.6	2	2.2
2/2	23	8.8	17	6.6	15	8.8	8	8.9
2/3	30	11.5	34	13.1	17	10.0	13	14.4
2/4	3	1.2	11	4.2	2	1.2	1	1.1
2/5	17	6.5	8	3.1	13	7.6	4	4.4
2/6	2	0.8	2	0.8	1	0.6	1	1.1
2/8	1	0.4	0	–	1	0.6	0	–
3/3	8	3.1	14	5.4	2	1.2	6	6.7
3/4	7	2.7	11	4.2	7	4.1	0	–
3/6	2	0.8	0	0.0	1	0.6	1	–
3/7	0	–	1	0.4	0	–	0	–
4/4	0	–	1	0.4	0	–	0	–
4/5	0	–	2	0.8	0	–	0	–
4/7	0	–	1	0.4	0	–	0	–
Σ	260		259		170		90	

Haplotype pair frequency comparisons *C10orf27*

HapPair	MS (n)	%	HC (n)	%	P	OR	95% CI
1/1	48	18.5	43	16.6	0.578		
1/2	65	25.0	47	18.1	0.058	1.50	0.99 - 2.30
1/3	39	15.0	56	21.6	0.051	0.64	0.41 - 1.00
1/5	15	5.8	11	4.2	0.427		
2/2	23	8.8	17	6.6	0.330		
2/3	30	11.5	34	13.1	0.582		
2/4	3	1.2	11	4.2	0.033	0.26	0.07 - 0.96
2/5	17	6.5	8	3.1	0.099	2.20	0.93 - 5.18
2/6	2	0.8	2	0.8	1.000		
2/8	1	0.4	0	–	1.000		
3/3	8	3.1	14	5.4	0.200		
3/4	7	2.7	11	4.2	0.350		
3/6	2	1	0	–	0.499		
3/7	0	–	1	0.4	0.499		
4/4	0	–	1	0.4	0.499		
4/5	0	–	2	0.8	0.249		
4/7	0	–	1	0.4	0.499		
Σ	260		259				

HapPair	RRMS (n)	%	HC (n)	%	P	OR	95% CI
1/1	33	19.4	43	16.6	0.456		
1/2	41	24.1	47	18.1	0.134		
1/3	24	14.1	56	21.6	0.051	0.60	0.35 - 1.01
1/5	13	7.6	11	4.2	0.134		
2/2	15	8.8	17	6.6	0.384		
2/3	17	10.0	34	13.1	0.328		
2/4	2	1.2	11	4.2	0.086	0.27	0.06 - 1.23
2/5	13	7.6	8	3.1	0.040	2.60	1.05 - 6.41
2/6	1	0.6	2	0.8	1.000		
2/8	1	0.6	0	–	0.396		
3/3	2	1.2	14	5.4	0.034	0.21	0.05 - 0.93
3/4	7	4.1	11	4.2	1.000		
3/6	1	0.6	0	–	0.396		
3/7	0	–	1	0.4	1.000		
4/4	0	–	1	0.4	1.000		
4/5	0	–	2	0.8	0.520		
4/7	0	–	1	0.4	1.000		
Σ	170		259				

HapPair	PPMS (n)	%	HC (n)	%	P	OR	95% CI
1/1	15	16.7	43	16.6	1.000		
1/2	24	26.7	47	18.1	0.084	1.64	0.93 - 2.88
1/3	15	16.7	56	21.6	0.364		
1/5	2	2.2	11	4.2	0.528		
2/2	8	8.9	17	6.6	0.479		
2/3	13	14.4	34	13.1	0.724		
2/4	1	1.1	11	4.2	0.310		
2/5	4	4.4	8	3.1	0.515		
2/6	1	1.1	2	0.8	1.000		
3/3	6	6.7	14	5.4	0.609		
3/4	0	–	11	4.2	0.073	0.12	0.01 - 2.05
3/6	1	1.1	0	–	0.258		
3/7	0	–	1	0.4	1.000		
4/4	0	–	1	0.4	1.000		
4/5	0	–	2	0.8	1.000		
4/7	0	–	1	0.4	1.000		
Σ	90		259				

HapPair	PPMS (n)	%	RRMS (n)	%	P	OR	95% CI
1/1	15	16.7	33	19.4	0.587		
1/2	24	26.7	41	24.1	0.652		
1/3	15	16.7	24	14.1	0.584		
1/5	2	2.2	13	7.6	0.095	0.28	0.06 - 1.25
2/2	8	8.9	15	8.8	1.000		
2/3	13	14.4	17	10.0	0.311		
2/4	1	1.1	2	1.2	1.000		
2/5	4	4.4	13	7.6	0.432		
2/6	1	1.1	1	0.6	1.000		
2/8	0	–	1	0.6	1.000		
3/3	6	6.7	2	1.2	0.022	6.00	1.19 - 30.4
3/4	0	–	7	4.1	0.100		
3/6	1	1.1	1	0.6	1.000		
Σ	90		170				

5) Inter-genic Haplotype combination

a) ***ADAMTS14*: SNP #19 A/G; MAF(A) = 0.36**

***C10orf27*: SNP #17 C/T; MAF(C) = 0.13**

Haplotype frequencies *ADAMTS14 – C10orf27*

#	Haplotype	MS (n)	%	HC	%	RRMS	%	PPMS	%
H1	GT	306	58.4	306	57.1	213	61.6	93	52.2
H2	AT	170	32.4	168	31.3	93	26.9	77	43.3
H3	GC	33	6.3	49	9.1	27	7.8	6	3.4
H4	AC	15	2.9	13	2.4	13	3.8	2	1.1
Σ		524		536		346		178	

Haplotype frequency comparisons *ADAMTS14 – C10orf27*

#	Haplotype	Groups		P	OR	95% CI
H1	GT	MS	HC	0.666		
		RR	HC	0.188		
		PP	HC	0.260		
		PP	RR	0.041	0.68	0.47 - 0.98
H2	AT	MS	HC	0.701		
		RR	HC	0.156		
		PP	HC	0.0037	1.67	1.18 - 2.37
		PP	RR	0.00015	2.07	1.42 - 3.03
H3	GC	MS	HC	0.083	0.67	0.42 - 1.06
		RR	HC	0.489		
		PP	HC	0.014	0.35	0.15 - 0.82
		PP	RR	0.057	0.41	0.17 - 1.02
H4	AC	MS	HC	0.657		
		RR	HC	0.254		
		PP	HC	0.380		
		PP	RR	0.102		

Haplotype pair frequencies *ADAMTS14 – C10orf27*

HapPair	MS (n)	%	HC (n)	%	RRMS (n)	%	PPMS (n)	%
1 / 1	104	39.7	97	36.2	74	42.8	30	33.7
1 / 2	65	24.8	72	26.9	38	22.0	27	30.3
1 / 3	33	12.6	41	15.3	27	15.6	6	6.7
2 / 2	45	17.2	42	15.7	21	12.1	24	27.0
2 / 4	15	5.7	12	4.5	13	7.5	2	2.2
3 / 3	0	0	3	1.1	0	0	0	0
3 / 4	0	0	1	0.4	0	0	0	0
Σ	262		268		173		89	

Haplotype pair frequency comparisons *ADAMTS14 – C10orf27*

HapPair	MS	%	HC	%	P	OR	95% CI
1 / 1	104	39.7	97	36.2	0.406		
1 / 2	65	24.8	72	26.9	0.589		
1 / 3	33	12.6	41	15.3	0.369		
2 / 2	45	17.2	42	15.7	0.640		
2 / 4	15	5.7	12	4.5	0.514		
3 / 3	0	0	3	1.1	0.249		
3 / 4	0	0	1	0.4	1.000		
Σ	262		268				

HapPair	RRMS	%	HC	%	P	OR	95% CI
1 / 1	74	42.8	97	36.2	0.166		
1 / 2	38	22.0	72	26.9	0.246		
1 / 3	27	15.6	41	15.3	0.930		
2 / 2	21	12.1	42	15.7	0.301		
2 / 4	13	7.5	12	4.5	0.178		
3 / 3	0	0	3	1.1	0.283		
3 / 4	0	0	1	0.4	1.000		
Σ	173		268				

HapPair	PPMS	%	HC	%	P	OR	95% CI
1 / 1	30	33.7	97	36.2	0.671		
1 / 2	27	30.3	72	26.9	0.526		
1 / 3	6	6.7	41	15.3	0.046	0.40	0.16 - 0.98
2 / 2	24	27.0	42	15.7	0.017	1.99	1.12 - 3.52
2 / 4	2	2.2	12	4.5	0.531		
3 / 3	0	0	3	1.1	0.577		
3 / 4	0	0	1	0.4	1.000		
Σ	89		268				

HapPair	PPMS	%	RRMS	%	P	OR	95% CI
1 / 1	30	33.7	74	42.8	0.155		
1 / 2	27	30.3	38	22.0	0.137		
1 / 3	6	6.7	27	15.6	0.049	0.39	0.16 - 0.99
2 / 2	24	27.0	21	12.1	0.0026	2.67	1.39 - 5.14
2 / 4	2	2.2	13	7.5	0.097	0.28	0.06 - 1.28
Σ	89		173				

b) ADAMTS14: SNP #21 A/G; MAF(A) = 0.10**C10orf27: SNP #13 C/T; MAF(C) = 0.28**

Haplotype frequencies ADAMTS14 – C10orf27

#	Haplotype	MS (n)	%	HC (n)	%	RRMS (n)	%	PPMS (n)	%	
H1	CA	400	73.3	328	63.8	273	74.2	127	71.3	
H2	CG	117	21.4	145	28.2	77	20.9	40	22.5	
H3	TA	25	4.6	27	5.3	17	4.6	8	4.5	
H4	TG	4	0.7	14	2.7	1	0.3	3	1.7	
		Σ		546		514		368		178

Haplotype frequency comparisons ADAMTS14 – C10orf27

#	Haplotype	Groups		P	OR	95% CI
H1	CA	MS	HC	0.0009	1.55	1.20 - 2.02
		RR	HC	0.001	1.63	1.21 - 2.19
		PP	HC	0.068	1.41	0.97 - 2.05
		PP	RR	0.483		
H2	CG	MS	HC	0.011	0.69	0.52 - 0.92
		RR	HC	0.014	0.67	0.49 - 0.92
		PP	HC	0.136		
		PP	RR	0.679		
H3	TA	MS	HC	0.612		
		RR	HC	0.182		
		PP	HC	0.843		
		PP	RR	1.000		
H4	TG	MS	HC	0.016	0.26	0.09 - 0.81
		RR	HC	0.006	0.10	0.01 - 0.74
		PP	HC	0.580		
		PP	RR	0.104		

Haplotype pair frequencies ADAMTS14 – C10orf27

HapPair	MS (n)	%	HC (n)	%	RRMS (n)	%	PPMS (n)	%	
1 / 1	146	53.5	103	40.1	100	54.3	46	51.7	
1 / 2	87	31.9	100	38.9	58	31.5	29	32.6	
1 / 3	21	7.7	22	8.6	15	8.2	6	6.7	
2 / 2	13	4.8	18	7.0	9	4.9	4	4.5	
2 / 4	4	1.5	9	3.5	1	0.5	3	3.4	
3 / 3	2	0.7	1	0.4	1	0.5	1	1.1	
3 / 4	0	0.0	3	1.2	0	0	0	0	
4 / 4	0	0	1	0.4	0	0	0	0	
	Σ		273		257		184		89

Haplotype pair frequency comparisons *ADAMTS14 – C10orf27*

HapPair	MS	%	HC	%	P	OR	95% CI
1 / 1	146	53.5	103	40.1	0.002	1.72	1.22 - 2.43
1 / 2	87	31.9	100	38.9	0.090	0.73	0.51 - 1.05
1 / 3	21	7.7	22	8.6	0.715		
2 / 2	13	4.8	18	7.0	0.272		
2 / 4	4	1.5	9	3.5	0.164		
3 / 3	2	0.7	1	0.4	1.000		
3 / 4	0	0.0	3	1.2	0.113		
4 / 4	0	0.0	1	0.4	0.485		
Σ	273		268				

HapPair	RRMS	%	HC	%	P	OR	95% CI
1 / 1	100	54.3	103	40.1	0.003	1.78	1.21 - 2.61
1 / 2	58	31.5	100	38.9	0.111		
1 / 3	15	8.2	22	8.6	0.879		
2 / 2	9	4.9	18	7.0	0.424		
2 / 4	1	0.5	9	3.5	0.051	0.15	0.02 - 1.20
3 / 3	1	0.5	1	0.4	1.000		
3 / 4	0		3	1.2	0.269		
4 / 4	0		1	0.4	1.000		
Σ	184		268				

HapPair	PPMS	%	HC	%	P	OR	95% CI
1 / 1	46	51.7	103	40.1	0.057	1.60	0.99 - 2.6 2
1 / 2	29	32.6	100	38.9	0.288		
1 / 3	6	6.7	22	8.6	0.660		
2 / 2	4	4.5	18	7.0	0.614		
2 / 4	3	3.4	9	3.5	1.000		
3 / 3	1	1.1	1	0.4	0.449		
3 / 4	0		3	1.2	0.572		
4 / 4	0		1	0.4	1.000		
Σ	89		268				

HapPair	PPMS	%	RRMS	%	P	OR	95% CI
1 / 1	46	51.7	100	54.3	0.679		
1 / 2	29	32.6	58	31.5	0.860		
1 / 3	6	6.7	15	8.2	0.811		
2 / 2	4	4.5	9	4.9	1.000		
2 / 4	3	3.4	1	0.5	0.103		
3 / 3	1	1.1	1	0.5	0.547		
Σ	89		184				